

**Dissecting the Telomere-Independent Pathways  
Underlying Human Cellular Senescence**

By

**Emilie Marie Isabelle Rovillain**

A thesis submitted to the University College of London  
for the degree of Doctor of Philosophy

Department of Neurodegenerative diseases  
Institute of Neurology  
UCL  
Queen Square  
London WC1 3BG

**2010**

## **ABSTRACT**

Cellular senescence is an irreversible program of cell cycle arrest triggered in normal somatic cells in response to a variety of intrinsic and extrinsic stimuli including telomere attrition, DNA damage, physiological stress and oncogene activation.

Finding that inactivation of the pRB and p53 pathways by SV40-LT antigen cooperates with hTERT to immortalize cells has allowed us to use a thermolabile mutant of SV40-LT to develop human fibroblasts where the cells are immortal if grown at 34°C but undergo an irreversible growth arrest within 5 days at 38°C. When these cells cease dividing, senescence-associated- $\beta$ -galactosidase (SA- $\beta$ -Gal) activity is induced and the growth-arrested cells have many features of senescent cells.

Since these cells growth-arrest in a synchronous manner, I have used Affymetrix expression profiling to identify the genes differentially expressed upon senescence. This identified 816 up- and 961 down-regulated genes whose expression was reversed when growth arrest was abrogated. I have shown that senescence was associated with activation of the NF- $\kappa$ B pathway and up-regulation of a number of senescence-associated-secretory-proteins including IL6. Perturbation of NF- $\kappa$ B signalling either by direct silencing of NF- $\kappa$ B subunits or by upstream modulation overcame growth-arrest indicating that activation of NF- $\kappa$ B signalling has a causal role in promoting senescence.

I also applied a retroviral shRNA screen covering ~10,000 genes to the same cell model. Overlapping with the microarray data revealed particularly interesting targets, such as LTBP3 and Layilin. Finally, I profiled micro-rna expression. 15 of the top micro-rnas down-regulated upon senescence were chosen to express in the HMF3A system. 6 of them were able to bypass the growth-arrest.

In conclusion, my work has uncovered novel markers involved in senescence as well as identifying that both activation of p53 and pRb pathway result in activation of NF- $\kappa$ B signalling which promotes senescence. Both results lead to a better understanding of senescence and its pathways.

## **TABLE OF CONTENTS**

ABSTRACT.....	2
TABLE OF CONTENTS .....	3
LIST OF FIGURES.....	14
LIST OF TABLES .....	17
LIST OF ABBREVIATIONS.....	18
ENCLOSED UNBOUND MATERIAL.....	22
STATEMENT CONCERNING COLLABORATIONS .....	22
ACKNOWLEDGEMENTS.....	22
1 INTRODUCTION.....	24
1.1 REPLICATIVE SENESCENCE DISCOVERY .....	24
1.2 DEFINITION OF SENESCENCE .....	25
1.3 TELOMERE INDUCED SENESCENCE .....	25
1.3.1 Telomeres .....	25
1.3.2 Telomeres and DDR.....	27
1.3.3 hTERT.....	29
1.3.4 Telomerase and tumourigenesis.....	30
1.4 DNA DAMAGE INITIATED SENESCENCE.....	30
1.5 ONCOGENE-INDUCED SENESCENCE .....	32
1.6 CANCER AND SENESCENCE .....	33
1.7 AGEING AND SENESCENCE.....	33
1.8 PATHWAYS OF SENESCENCE.....	34
1.8.1 The p53 pathway.....	34
1.8.1.1 TP53 gene and p53 protein .....	35
1.8.1.2 Functions of the p53 protein .....	35
1.8.1.3 Regulation of p53 activity.....	36
1.8.1.4 p19 <sup>Arf</sup> protein.....	38
1.8.1.5 Oncogenic Ras .....	40
1.8.1.6 p21 <sup>WAF1/Cip1/Sdi1</sup> .....	40
1.8.1.7 p53 family: p63 and p73 proteins.....	41
1.8.2 The pRb pathway .....	42
1.8.2.1 Cell cycle, cyclins and CDKs .....	42

1.8.2.2	CDK inhibitors.....	42
1.8.2.3	CDKs and E2F .....	43
1.8.2.4	Rb family of proteins.....	43
1.8.2.5	pRb gene .....	44
1.8.2.6	pRb discovery .....	44
1.8.2.7	pRb function.....	45
1.8.2.8	E2F .....	47
1.8.3	Common pathways.....	48
1.8.3.1	INK4A Locus .....	48
1.8.3.2	p16 <sup>INK4a</sup> .....	49
1.8.3.3	p14 <sup>ARF</sup> .....	50
1.9	DNA TUMOUR VIRUSES .....	52
1.9.1	SV40.....	52
1.9.2	LT.....	53
1.9.3	Adenovirus Type 5.....	55
1.9.3.1	E1A.....	55
1.9.3.2	E1B.....	56
1.9.4	HPV Type 16 .....	56
1.9.4.1	E7 .....	57
1.9.4.2	E6 .....	58
1.10	SASP: SENESCENCE-ASSOCIATED SECRETORY PHENOTYPE AND ROS: REACTIVE OXYGEN SPECIES .....	58
1.11	NF-κB PATHWAY .....	60
1.11.1	Introduction .....	60
1.11.2	NF-κB family.....	61
1.11.3	Activation .....	62
1.11.4	Inhibition .....	63
1.11.4.1	The IκB family .....	63
1.11.4.2	IκB kinase: IKK.....	63
1.11.5	Canonical NF-κB pathway .....	65
1.11.6	Non-canonical pathway.....	66
1.11.7	NF-κB and cancer .....	68
1.11.8	NF-κB, senescence and ageing.....	68
1.12	MICRO-RNAS .....	69

1.12.1	Introduction .....	69
1.12.2	MiRNA and siRNA.....	70
1.12.3	Biogenesis.....	71
1.12.4	Mechanism of MiRNA regulation .....	71
1.12.5	Micro-RNAs and cancer.....	73
1.12.6	Micro-RNA and senescence .....	74
1.13	MODEL OF STUDY: HMF3A CELLS .....	75
1.13.1	Reconstitution of WT LT activity in the HMF3A system alone .....	76
1.13.2	Refinement of the HMF3A system by introduction of the murine ecotropic receptor .....	78
1.14	ABROGATION OF THE P53 PATHWAY .....	78
1.15	ABROGATION OF THE PRB PATHWAY .....	78
1.15.1	Inactivation of the INK4A Locus .....	79
1.15.1.1	Knockdown of p14 <sup>ARF</sup> by ShRNA .....	79
1.15.1.2	Knockdown of p16 <sup>INK4a</sup> by ShRNA .....	79
1.15.1.3	Constitutive Expression of Bmi-1 .....	80
1.16	AIM OF THE THESIS.....	80
2	MATERIAL AND METHODS .....	83
2.1	MAMMALIAN CELL CULTURE .....	83
2.1.1	Cell lines and Culture.....	83
2.1.2	Cell media.....	83
2.1.3	Cell Culture Conditions.....	83
2.1.4	Sub-Culturing of Cells .....	84
2.1.5	Preservation of Cells .....	84
2.1.6	Recovery of Frozen Cells .....	84
2.2	RETROVIRAL AND LENTIVIRAL INFECTIONS .....	85
2.2.1	Retroviral and Lentiviral constructs.....	85
2.2.2	Viral Packaging and infections .....	86
2.2.2.1	Packaging of Retroviral Constructs.....	86
2.2.2.2	Packaging of Lentiviral Constructs .....	87
2.2.2.3	Infection with viral supernatant and selection .....	87
2.3	DNA MANIPULATION.....	88

2.3.1	Plasmid DNA Preparation .....	88
2.3.1.1	Small Scale Plasmid Preparation .....	88
2.3.1.2	Large Scale Plasmid Preparation .....	89
2.3.2	DNA Quantification .....	90
2.3.3	DNA-Agarose Gel Electrophoresis.....	90
2.3.4	DNA Sequencing .....	90
2.3.5	Cloning of PCR Products .....	90
2.4	RNA MANIPULATION.....	91
2.4.1	RNA Isolation .....	91
2.4.2	RNA Quantification .....	91
2.5	PROTEIN ANALYSIS .....	92
2.5.1	Preparation of Total Protein Extracts.....	92
2.5.2	Determination of Protein Concentration .....	92
2.5.3	Sodium-Dodecyl-Sulphate-Polyacrylamide-Gel-Electrophoresis .....	93
2.5.4	Western Blotting of SDS-PAGE.....	93
2.5.5	Antibodies Used.....	94
2.6	GROWTH CURVES .....	95
2.6.1	Cell line .....	95
2.6.2	Protocol .....	95
2.7	IRREVERSIBILITY ASSAYS .....	95
2.7.1	Cell line .....	95
2.7.2	Protocol .....	96
2.8	GROWTH COMPLEMENTATION ASSAYS .....	96
2.8.1	Cell line .....	96
2.8.2	Complementation experiment.....	96
2.9	SENESCENCE SPECIFIC EXPRESSION PROFILING .....	97
2.9.1	Cell line .....	97
2.9.2	RNA preparation.....	97
2.9.3	RNA expression profiling.....	98
2.10	SENESCENCE SPECIFIC MIRNA EXPRESSION PROFILING .....	98

2.10.1	Cell line .....	98
2.10.2	Tissue culture.....	98
2.10.3	RNA preparation.....	99
2.10.4	Quality Control of RNA Samples and shipping to LC sciences.....	100
2.10.5	Microarray analysis.....	100
2.10.5.1	Pairwise Comparisons for micro-rna Microarray Analysis .....	100
2.10.5.2	Expression analysis and normalization.....	101
2.10.6	Individual miRNA validation in vitro .....	101
2.10.6.1	Candidates miR-Vec Clones .....	102
2.10.6.2	Preparation of clones and sequence checking .....	102
2.10.6.3	HMF3A Growth Complementation Assay in plates .....	102
2.11	SHRNA SCREENING.....	103
2.11.1	Cell line .....	103
2.11.2	RNAi library .....	103
2.11.3	Virus packaging .....	103
2.11.4	Sensitivity of the model.....	104
2.11.5	Titration of Phoenix Eco viral Supernatants.....	104
2.11.6	Experiment planning for each plasmids pools.....	105
2.11.7	Confidence intervals.....	105
2.11.8	Genomic DNA extraction.....	106
2.11.9	TOPO cloning and sequencing .....	107
2.12	PRIMARY CELLS IMMORTALIZATION.....	108
3	CELL MODEL AND GROWTH COMPLEMENTATION .....	109
3.1	CREATION OF CLONAL CELL LINES DERIVED FROM HMF3A CELLS AND GROWTH COMPLEMENTATION ASSAYS.....	109
3.1.1	Objectives .....	109
3.1.2	Refinement of the HMF3A cells by clonal selection .....	109
3.1.2.1	Growth curves .....	110
3.1.2.2	Complementation with E7 and E1A.....	112
3.1.2.3	Irreversibility.....	115
3.1.3	Reconstitution of WT LT antigen in HMF3A <sup>EcoR</sup> and CL3 <sup>EcoR</sup> cells .....	122
3.1.4	Abrogation of the p53 pathway in HMF3A <sup>EcoR</sup> and CL3 <sup>EcoR</sup> cells.....	126
3.1.5	Abrogation of the pRb pathway in HMF3A <sup>EcoR</sup> and CL3 <sup>EcoR</sup> cells .....	128

3.1.5.1	Constitutive Expression of Ad 5 E1A and HPV16 E7 .....	131
3.1.5.2	Constitutive ectopic expression of E2F-DB mutant.....	136
3.2	DISCUSSION.....	138
3.2.1	Cellular senescence is p53-dependant process in the HMF3A cells.....	139
3.2.2	Senescence is a p21 <sup>CIP1/WAF1/Sdi1</sup> -Dependent Process in the HMF3A Cells	141
3.2.3	Inactivation of the pRb pathway in the HMF3A cells .....	142
3.2.3.1	p16 <sup>INK4a</sup> inactivation in the HMF3A Cells .....	142
3.2.3.2	Bmi-1 Activity in the HMF3A Cells.....	143
3.2.3.3	Ectopic Expression of E1A and E7 .....	143
3.2.3.4	Possible Mechanisms by which E1A and E7 Bypass the Conditional HMF3A Growth Defect .....	144
3.2.3.5	p14 <sup>ARF</sup> is not necessary between the p16-pRb and p21-p53 Pathways..... .....	145
3.2.3.6	E2F-DB bypass the conditional growth arrest by repressing the pRb pathway .....	146
3.2.4	p16-pRb does not always act downstream of p53-p21 to induce senescence ... .....	147
4	ACTIVATION OF THE NF-κB SIGNALLING PROMOTES CELLULAR SENESCENCE .....	148
4.1	SENESCENCE SPECIFIC GENE EXPRESSION RESULTS .....	148
4.1.1	Objectives .....	148
4.1.2	Why use Microarray Analysis?.....	149
4.1.3	Which Microarray Technology?.....	151
4.1.4	Microarray Strategy .....	152
4.1.5	Microarray procedure.....	156
4.1.6	Microarray results .....	156
4.1.7	Validation of Microarray Data.....	162
4.1.7.1	Why Validate?.....	162
4.1.7.2	Real time validation of expression data using the BioTrove Open Arrays .....	162
4.1.8	Comparison of genes differentially expressed upon senescence with the meta-signature of genes over-expressed in cancer .....	165
4.2	BIOLOGICAL VALIDATION BY LENTIVIRAL SILENCING OR ECTOPIC EXPRESSION.....	167
4.2.1	Objectives .....	167



4.2.2	Up-regulated genes upon senescence: Does Silencing bypass the growth arrest?	167
4.2.2.1	CLCA2 silencing bypassed senescence at a low level	168
4.2.2.2	AK3L1 silencing bypassed senescence	169
4.2.2.3	TRIB2 silencing bypassed senescence	169
4.2.2.4	CDKN2A silencing bypassed senescence	171
4.2.2.5	DAPK1 silencing was not sufficient to bypass senescence	172
4.2.2.6	BLCAP silencing bypassed senescence at a low level	172
4.2.2.7	RUNX1 bypassed senescence	173
4.2.2.8	GRAMD3 silencing bypassed senescence	173
4.2.2.9	SCN2A silencing was not sufficient to bypass senescence	174
4.2.3	Down-regulated genes upon senescence: Does ectopic expression bypass the growth arrest?	174
4.2.3.1	HMGB2	176
4.2.3.2	DEPDC1	176
4.2.3.3	BUB1B	177
4.2.3.4	NEK2	179
4.2.3.5	MELK	180
4.2.3.6	MLF1-IP two splice forms 88 and 401	181
4.2.3.7	DBF4, CDKN2C (p18) and PLK4	182
4.2.3.8	FOXM1	182
4.3	NF- $\kappa$ B PATHWAY ACTIVATION UPON SENESENCE IS CAUSAL TO SENESENCE	189
4.3.1	Objectives	189
4.3.2	NF- $\kappa$ B pathway is activated upon senescence at the mRNA level	189
4.3.2.1	Transcription factor motif matrix module	191
4.3.2.2	NF- $\kappa$ B targets gene expression modulation	191
4.3.3	Is the NF- $\kappa$ B pathway also activated at a protein level?	195
4.3.4	Is phosphorylation of RelA/p65 also induced?	195
4.3.5	What happens if the NF- $\kappa$ B complex is inactivated?	197
4.3.5.1	RNAi mediated silencing of NF- $\kappa$ B subunits abrogates senescence growth arrest	197
4.3.6	Modulation of the NF- $\kappa$ B pathway overcomes senescence growth arrest	200
4.3.6.1	TMEM9B and BCL2L1 silencing bypass senescence	200
4.3.6.2	Silencing of cEBP $\beta$ , BTG2 and TXNIP silencing bypass senescence	202
4.3.6.3	Ectopic expression of IKB-SR bypasses senescence	202
4.3.6.4	Ectopic expression of SIRT1 bypasses senescence	207
4.3.7	NF- $\kappa$ B Activation is Causal to Senescence	207

4.4	DISCUSSION.....	209
4.4.1	SASP: Senescence-Associated Secretory Phenotype .....	209
4.4.2	Senescence Down-Regulated Genes .....	210
4.4.3	Ectopic expression of down regulated genes rescues the growth arrest .....	211
4.4.4	NF-κB Pathway Activation upon Senescence is causal to Senescence .....	214
4.4.4.1	Senescence Up-Regulated Genes .....	215
4.4.4.2	Silencing of over-expressed genes bypasses the growth arrest .....	216
4.4.4.3	Senescence expression profile reveals links with Cancer expression profile	217
4.4.4.4	NF-κB pathway is activated upon senescence .....	218
5	AN RNA INTERFERENCE SCREEN IDENTIFIES DOWNSTREAM EFFECTORS OF THE P53-P21 AND P16-PRB PATHWAYS.....	222
5.1	RNAI INTERFERENCE SCREEN.....	222
5.1.1	Objectives .....	222
5.1.2	The Open Access RNAi project at UCL .....	223
5.1.3	Which viral delivery system? Which library? .....	223
5.1.4	ShRNA Screening Strategy .....	228
5.1.5	Sensitivity of the model.....	228
5.1.6	Confidence intervals.....	230
5.1.7	Titration of Phoenix Eco viral Supernatants.....	232
5.1.8	Primary screen in the HMF3A: Procedure .....	232
5.1.9	ShRNA constructs sequence recovery .....	239
5.1.10	Results of the primary screen .....	240
5.2	<i>IN VITRO</i> VALIDATION OF THE SCREENING .....	247
5.2.1	Overlap of the candidates of the shRNA screen with microarray data for genes up-regulated upon senescence in CL3 <sup>EcoR</sup> cells.....	247
5.2.2	Optimisation of the GIPZ lentiviral library .....	247
5.2.3	Secondary screen using lentiviral shRNA silencing .....	248
5.3	DISCUSSION.....	256
5.3.1	Sensitivity, Stringency and Saturation .....	256
5.3.2	Positive hits of the primary HMF3A retroviral shRNA screen .....	258
5.3.3	Overlap with the microarray up-regulated genes reveals new targets .....	259

5.3.4	<i>In vitro</i> validation of ATXN10, LAYN, LTBP3, SGBT and TMEM9B silencing .....	259
5.3.4.1	TMEM9B.....	259
5.3.4.2	LTBP3 .....	261
5.3.4.3	ATXN10 .....	264
5.3.4.4	LAYN .....	265
5.3.4.5	SGBT .....	265
5.3.4.6	TAOK1, RAS4A and ARMCX2.....	267
6	ROLE OF MICRO-RNAS IN CELLULAR SENESCENCE.....	270
6.1	SENESCENCE SPECIFIC MICRO-RNA DIFFERENTIAL EXPRESSION.....	270
6.1.1	Objectives .....	270
6.1.2	Background to micro-RNA Expression Profiling Technology .....	270
6.1.3	HMF3AEcoR: miRNA expression profiling experimental design.....	271
6.1.4	Quality Control of RNA Samples .....	273
6.1.5	miRNAs senescence specific differential expression .....	273
6.1.6	Up-regulated micro-RNAs .....	283
6.1.7	Down-regulated micro-RNAs.....	283
6.2	BIOLOGICAL VALIDATION BY GROWTH COMPLEMENTATION ASSAY IN THE HMF3A CELLS .....	283
6.2.1	Objectives .....	283
6.2.2	Validation by ectopic expression .....	284
6.2.2.1	miR Vec clones .....	284
6.2.2.2	Sequencing of the MiRVec clones .....	287
6.2.3	Complementation assay with the miR-Vec clones .....	287
6.2.3.1	MiR-18a, miR-130b, miR-372, miR-373 and Let7a.....	288
6.2.3.2	MiR-92b, miR-15a, miR-16, miR-195 and miR-25.....	288
6.2.3.3	MiR-195, miR-218, miR-20b, miR-29b, miR-186 and miR-25 .....	291
6.2.3.4	MiR-128, miR-423-5p and Let7g.....	291
6.2.4	Overlapping with the microarray data and the shRNA screen .....	294
6.2.4.1	MiR-25.....	294
6.2.4.2	MiR-195.....	297
6.2.4.3	MiR-218.....	297
6.2.4.4	MiR-193b.....	297
6.2.4.5	MiR-186.....	298
6.2.4.6	MiR-423-5p.....	298

6.3	EXPRESSION PROFILING OF HMF3A CELLS IN WHICH GROWTH ARREST WAS OVERCOME BY ECTOPIC EXPRESSION OF MIRS .....	298
6.3.1	Objectives .....	298
6.3.2	Microarray Strategy .....	299
6.3.3	Microarray procedure.....	301
6.3.4	MiR-186 .....	301
6.3.5	MiR-195 .....	301
6.3.6	MiR-25 .....	302
6.3.7	MiR-218 .....	302
6.3.8	MiR-423-5p .....	303
6.3.9	MiR-372 .....	303
6.4	RAS INDUCED PREMATURE SENESCENCE.....	303
6.4.1	Objectives .....	303
6.4.2	Strategy.....	304
6.4.3	Procedure.....	305
6.5	DISCUSSION.....	307
6.5.1	Up-regulated micro-RNAs .....	307
6.5.1.1	MiR-34a.....	308
6.5.1.2	MiR-146a.....	309
6.5.2	Down-regulated micro-RNAs.....	310
6.5.2.1	MiR-25.....	310
6.5.2.2	MiR-195.....	312
6.5.2.3	MiR-218.....	313
6.5.2.4	MiR-193b.....	314
6.5.2.5	MiR-186.....	315
6.5.2.6	MiR-423-5p.....	315
6.5.3	Expression profiling of HMF3A cells in which senescence has been bypassed by ectopic expression of miRs .....	316
6.5.4	Expression of the miRs in 226L cells .....	317
6.5.5	RAS transformation of primary cells .....	318
6.5.6	Further work .....	322
7	SUMMARY AND FINAL DISCUSSION.....	324
7.1	SUMMARY OF RESULTS.....	325

7.2	FUTURE DIRECTIONS.....	326
7.2.1	Saturation of shRNA screen in CL3 <sup>EcoR</sup> .....	326
7.2.2	Secondary shRNA screen .....	327
7.2.3	Ectopic expression validation by protein analysis .....	327
7.2.4	FOXM1 .....	328
7.2.4.1	Which spliceform is important?.....	328
7.2.4.2	Which kinases regulate the activation of FOXM1? .....	329
7.2.4.3	What is the mechanism of action of FOXM1? .....	330
7.2.4.4	What causes the decreased expression of FOXM1 in cell senescence?.... .....	330
7.3	FINAL REMARKS .....	331
8	REFERENCES .....	332

## LIST OF FIGURES

<b>Figure 1.1:</b>	Replicative Senescence.....	27
<b>Figure 1.2:</b>	Telomere shortening .....	29
<b>Figure 1.3:</b>	Causes and consequences of cellular senescence .....	32
<b>Figure 1.4:</b>	The p53 signalling pathway.....	38
<b>Figure 1.5:</b>	The pRb signaling pathway.....	40
<b>Figure 1.6:</b>	NF-κB: the canonical pathway.....	65
<b>Figure 1.7:</b>	NF-κB: the non canonical pathway .....	68
<b>Figure 1.8:</b>	Micro-RNAs biogenesis.....	73
<b>Figure 1.9:</b>	Engineering of the CL3 <sup>EcoR</sup> cells.....	78
<b>Figure 3.1:</b>	Clonal cell lines growth rates.....	112
<b>Figure 3.2:</b>	Growth complementation assay in the clonal cell lines.....	114
<b>Figure 3.3:</b>	Growth complementation assay in the clonal cell lines repeat... ..	115
<b>Figure 3.4:</b>	Irreversibility HMF3A <sup>EcoR</sup> and CL3 <sup>EcoR</sup> cells: Photos.....	117
<b>Figure 3.5:</b>	Irreversibility HMF3A <sup>EcoR</sup> and CL3 <sup>EcoR</sup> cells: Growth assays and staining.....	120
<b>Figure 3.6:</b>	Induction of SA-β-galactosidase.....	122
<b>Figure 3.7:</b>	Complementation HMF3A <sup>EcoR</sup> by ectopic expression and RNAi silencing.....	124
<b>Figure 3.8:</b>	Complementation CL3A <sup>EcoR</sup> by ectopic expression and RNAi silencing .....	125
<b>Figure 3.9:</b>	Expression of LT in the HMF3A <sup>EcoR</sup> cells .....	126
<b>Figure 3.10:</b>	Expression of p53 in the HMF3A <sup>EcoR</sup> cells .....	130
<b>Figure 3.11:</b>	Expression of p21 <sup>CIP1/WAF1/Sdi1</sup> in the HMF3A <sup>EcoR</sup> cells.....	131
<b>Figure 3.12:</b>	Conserved regions of the DNA tumour Viruses.....	133
<b>Figure 3.13:</b>	Expression of pRb in the HMF3A <sup>EcoR</sup> cells.....	135
<b>Figure 3.14:</b>	Expression of E7 in the HMF3A <sup>EcoR</sup> cells.....	136
<b>Figure 3.15:</b>	Expression of E2F-DB in the HMF3A <sup>EcoR</sup> cells.....	138
<b>Figure 4.1:</b>	Cancer: a multistep process.....	151
<b>Figure 4.2:</b>	HMF3A <sup>EcoR</sup> Microarray strategy.....	154

<b>Figure 4.3:</b>	Microarray Strategy for the complementations.....	156
<b>Figure 4.4:</b>	Validation of microarray data by real time qPCR.....	165
<b>Figure 4.5:</b>	<i>In vitro</i> validation of up-regulated microarray targets by silencing constructs .....	171
<b>Figure 4.6:</b>	Silencing of GRAMD3 and SCN2A.....	176
<b>Figure 4.7:</b>	<i>In vitro</i> validation of down-regulated microarray targets by ectopic expression.....	179
<b>Figure 4.8:</b>	FOXM1.....	184-185
<b>Figure 4.9:</b>	FOXM1 protein expression.....	188
<b>Figure 4.10:</b>	Ectopic expression of FOXM1 WT, FOXM1 $\Delta$ N $\Delta$ KEN and FOXM1-6K.....	189
<b>Figure 4.11:</b>	FOXM1 protein expression in cells expressing FOXM1 WT, FOXM1 $\Delta$ N $\Delta$ KEN and FOXM1-6K .....	191
<b>Figure 4.12:</b>	Secretion of IL8 and IL6 by senescent cells.....	197
<b>Figure 4.13:</b>	Increase in phosphorylation of RelA (Ser536) in senescent cells..	199
<b>Figure 4.14:</b>	Silencing of NF- $\kappa$ B transcription factor subunits.....	200
<b>Figure 4.15:</b>	Silencing of TMEM9B and BCL2L1.....	202
<b>Figure 4.16:</b>	Silencing of cEBP $\beta$ .....	204
<b>Figure 4.17:</b>	Silencing of BTG2 and TXNIP.....	205
<b>Figure 4.18:</b>	Silencing of secreted proteins CCI26, IGFBP7, GDF15 and IL32	206
<b>Figure 4.19:</b>	Ectopic expression of IKB-SR.....	207
<b>Figure 4.20:</b>	Ectopic expression of SIRT1.....	209
<b>Figure 5.1:</b>	Mir-30 adapted shRNAmiR transcript design.....	225
<b>Figure 5.2:</b>	pSM2 retroviral plasmid: design and features.....	227
<b>Figure 5.3:</b>	pGIPZ lentiviral plasmid: design and features .....	228
<b>Figure 5.4:</b>	shRNA screen strategy.....	230
<b>Figure 5.5:</b>	Screen sensitivity test.....	232
<b>Figure 5.6:</b>	Silencing of TMEM9B (mix).....	251
<b>Figure 5.7:</b>	Silencing of TMEM9B (individual).....	252
<b>Figure 5.8:</b>	Silencing of LTBP3.....	253
<b>Figure 5.9:</b>	Silencing of ATXN10.....	254

<b>Figure 5.10:</b>	Silencing of SGTB and LAYN.....	256
<b>Figure 6.1:</b>	miRs microarray profiling strategy .....	273
<b>Figure 6.2:</b>	Differential miRs upon growth arrest and quiescence.....	281
<b>Figure 6.3:</b>	Ectopic expression of miR-18a, miR-130b, miR-373 and miR-372	290
<b>Figure 6.4:</b>	Ectopic expression of miR-25, miR-92b, miR-195, miR-15a and miR-16a .....	291
<b>Figure 6.5:</b>	Ectopic expression of miR-29b, miR-20, miR-186, miR-193b and miR- 218.....	293
<b>Figure 6.6:</b>	Ectopic expression of miR-423-5p, miR-128, and Let7g.....	294
<b>Figure 6.7:</b>	Ectopic expression of miR-423-5p, miR-218 and miR-19.....	296
<b>Figure 6.8:</b>	Ectopic expression of miR-423-5p, miR-186, miR-20b, miR-193b, miR- 29b, miR25, miR-195 and miR-218.....	297
<b>Figure 6.9:</b>	Microarray profiling strategy of cells expressing miR-218, miR195, miR- 193b, miR-423-5p and miR-25 .....	301
<b>Figure 6.10:</b>	Edctopic expression of micro-RNAs in human breast epithelial cells	320



## **LIST OF TABLES**

<b>Table 4.1:</b>	Senescence specific changes in gene expression.....	158-159
<b>Table 4.2:</b>	Senescence specific changes in gene expression with complementation.....	161-162
<b>Table 4.3:</b>	Results of comparison Affymetrix with OpenArray™.....	167
<b>Table 4.4:</b>	Metasignatures of neoplastic transformation and undifferentiated cancer.....	167
<b>Table 4.5:</b>	Transcription factor motifs.....	193
<b>Table 4.6:</b>	Senescence specific changes in NF-κB target genes expression with complementation.....	194-195
<b>Table 5.1:</b>	shRNA screen confidence.....	232
<b>Table 5.2:</b>	Virus pools titration and supernatant volume used.....	234
<b>Table 5.3:</b>	Reseeding densities and number of growing colonies obtained after growth complementation assay .....	236-239
<b>Table 5.4:</b>	Results of the screen .....	242-246
<b>Table 5.5:</b>	Senescence specific changes with complementation for ATXN10, LAYN, LTBP3, SGTB and TMEM9B .....	261
<b>Table 6.1:</b>	Dual hybridization Analysis.....	275
<b>Table 6.2:</b>	Raw microarray results upon growth arrest.....	277-278
<b>Table 6.3:</b>	Raw microarray results upon quiescence.....	279-280
<b>Table 6.4:</b>	Up-regulated micro-RNAs upon senescence .....	282
<b>Table 6.5:</b>	Down-regulated micro-RNAs upon senescence .....	283
<b>Table 6.6:</b>	Layout of of the primary BJ cells immortalization experiment	307

## **LIST OF ABBREVIATIONS**

<b>2D-DIGE</b>	two-dimensional difference gel electrophoresis
<b>3D</b>	three-dimensional
<b>6-FAM</b>	6-carboxyfluorescein
<b>aa</b>	amino acid
<b>AEBSF</b>	4-(2-aminoethyl) benzenesulphonyl fluoride
<b>Ago</b>	Argonaute
<b>ALT</b>	alternate lengthening of telomeres
<b>amp<sup>R</sup></b>	ampicillin resistance gene
<b>APC</b>	anaphase-promoting complex
<b>APS</b>	ammonium persulphate
<b>ARF</b>	alternate reading frame
<b>ATP</b>	adenosine triphosphate
<b>ATCC</b>	American type culture collection
<b>B-Gal</b>	β-galactosidase
<b>bHLH</b>	basic helix-loop-helix
<b>BLAST</b>	Basic Local Alignment Search Tool
<b>blast<sup>R</sup></b>	blasticidin resistance gene
<b>bp</b>	base pair
<b>BrdU</b>	bromo-deoxyuridine
<b>BSA</b>	bovine serum albumin
<b>CaCl<sub>2</sub></b>	calcium chloride
<b>CDK</b>	cyclin-dependent kinase
<b>CDKI</b>	cyclin-dependent kinase inhibitor
<b>cDNA</b>	complementary deoxyribonucleic acid
<b>Cfu</b>	colony forming units
<b>ChIP</b>	chromatin immunoprecipitation
<b>CIP</b>	calf intestinal alkaline phosphatase
<b>CR</b>	conserved region
<b>C-terminal</b>	carboxy-terminal
<b>DAPI</b>	4'-6-diamidino-2-phenylindole
<b>dd</b>	double-distilled
<b>DDR</b>	DNA damage response
<b>DEPC</b>	diethyl pyrocarbonate
<b>DK</b>	cyclin D1-CDK4 <sup>R24C</sup> fusion construct
<b>DMEM</b>	Dulbecco's modified Eagle medium
<b>DMSO</b>	dimethyl sulphoxide
<b>DNA</b>	deoxyribonucleic acid
<b>dNTP</b>	deoxyribonucleotide triphosphate
<b>DSB</b>	double strand break
<b>dsRNA</b>	double-stranded ribonucleic acid
<b>DTT</b>	dithiothreitol
<b>EBV</b>	Epstein Barr Virus
<b>ECL</b>	enhanced chemiluminescence

<b>Eco<sup>R</sup></b>	murine ecotropic receptor
<b>EDTA</b>	ethylenediaminetetraacetic acid
<b>ES</b>	embryonic stem
<b>FBS</b>	foetal bovine serum
<b>FCS</b>	foetal calf serum
<b>FDR</b>	false-discovery rate
<b>G<sub>0</sub></b>	quiescence
<b>G<sub>1</sub></b>	first gap phase
<b>G<sub>2</sub></b>	second gap phase
<b>GFP</b>	green fluorescent protein
<b>GPI</b>	glycosylphosphatidylinositol
<b>GSE</b>	genetic suppressor element
<b>GTP</b>	guanine triphosphate
<b>HAT</b>	histone acetylase
<b>HCl</b>	hydrochloric acid
<b>hCMV</b>	human cytomegalovirus
<b>HDAC</b>	histone deacetylase
<b>HDF</b>	human diploid fibroblast
<b>HEK293</b>	human embryonic kidney 293
<b>HEPES</b>	4-(2-hydroxyethyl)-1-piperazineethanesulphonic acid
<b>HGPS</b>	Hutchinson-Gilford Progeria Syndrome
<b>HMF</b>	Human mammary fibroblast
<b>HPV</b>	Human Papilloma Virus
<b>hr</b>	hour
<b>HRP</b>	horseradish peroxidase
<b>hTERT</b>	catalytic component of human telomerase
<b>IE</b>	immediate early promoter
<b>IL</b>	interleukin
<b>IPTG</b>	isopropyl- $\beta$ -D-thiogalactopyranoside
<b>IR</b>	ionizing radiation
<b>IRES</b>	internal ribosomal entry site
<b>kb</b>	kilobase
<b>KCl</b>	potassium chloride
<b>kDa</b>	kilodalton
<b>KOD</b>	<i>Thermococcus kodakaraensi</i> DNA polymerase
<b>LB</b>	luria broth base
<b>Liquid N<sub>2</sub></b>	liquid nitrogen
<b>LOWESS</b>	locally weighted linear regression
<b>LT</b>	SV40 large T antigen
<b>LTR</b>	long terminal repeat
<b>M</b>	molar
<b>M1</b>	mortality stage I
<b>M2</b>	mortality stage II
<b>mM</b>	millimolar
<b>M phase</b>	mitosis phase
<b>MCS</b>	multiple cloning site

<b>MEF</b>	mouse embryo fibroblast
<b>MgCl<sub>2</sub></b>	magnesium chloride
<b>MgSO<sub>4</sub></b>	magnesium sulphate
<b>min</b>	minute
<b>miR</b>	micro ribonucleic acid
<b>miRNA</b>	micro ribonucleic acid
<b>micro-RNA</b>	micro ribonucleic acid
<b>MoMuLV</b>	Moloney Murine Leukaemia Virus
<b>MoMuSV</b>	Moloney Murine Sarcoma Virus
<b>MOPS</b>	3 – [N-morpholino] propanesulphonic acid
<b>MPF</b>	maturation promoting factor
<b>mRNA</b>	messenger ribonucleic acid
<b>N</b>	ploidy
<b>N<sub>2</sub></b>	nitrogen
<b>NaCl</b>	sodium chloride
<b>NaOH</b>	sodium hydroxide
<b>NES</b>	nuclear export signal
<b>(NH<sub>4</sub>)<sub>2</sub>SO<sub>4</sub></b>	ammonium sulphate
<b>NHEJ</b>	non-homologous end-joining
<b>NKI</b>	Netherland Cancer Institute
<b>NLS</b>	nuclear localisation signal
<b>nt</b>	nucleotide
<b>N-terminus</b>	amino-terminus
<b>OD</b>	optical density
<b>ORF</b>	open reading frame
<b>P</b>	phosphorylation
<b>PAGE</b>	polyacrylamide gel electrophoresis
<b>PBS</b>	phosphate buffered saline
<b>PcG</b>	polycomb group
<b>PCR</b>	polymerase chain reaction
<b>PD</b>	population doubling
<b>PMT</b>	photomultiplier tube
<b>PNK</b>	polynucleotide kinase
<b>PTGS</b>	post-translational gene silencing
<b>puro<sup>R</sup></b>	puromycin resistance gene
<b>R</b>	restriction point
<b>REF</b>	rat embryo fibroblast
<b>RIPA</b>	radioimmunoprecipitation
<b>RISC</b>	ribonucleic acid -induced silencing complex
<b>RITS</b>	ribonucleic acid -induced transcriptional silencing
<b>RNA</b>	ribonucleic acid
<b>RNAse</b>	ribonuclease
<b>RNAi</b>	ribonucleic acid interference
<b>ROS</b>	reactive oxygen species
<b>rpm</b>	revolutions per minute
<b>RT</b>	reverse transcription

<b>RT-PCR</b>	reverse transcription-polymerase chain reaction
<b>S phase</b>	deoxyribonucleic acid synthesis phase
<b>SA</b>	senescence-associated
<b>SAHF</b>	senescence-associated heterochromatic foci
<b>SAM</b>	significance analysis of microarrays
<b>SA-<math>\beta</math>-Gal</b>	Senescence associated $\beta$ galactosidase
<b>SCF</b>	Skp1/Cullin/F-box protein
<b>SDS</b>	sodium dodecyl sulphate
<b>sec</b>	second
<b>shRNA</b>	short hairpin ribonucleic acid
<b>SIPS</b>	stress-induced premature senescence
<b>siRNA</b>	short-interfering ribonucleic acid
<b>SNP</b>	single nucleotide polymorphism
<b>STASIS</b>	stress or aberrant signalling-induced senescence
<b>SV40</b>	Simian Virus 40
<b>TAE</b>	Tris-acetate-EDTA
<b>TEMED</b>	N,N,N',N' tetraethylenemethyldiamine
<b>TERC</b>	catalytic ribonucleic component of human telomerase
<b>TKO</b>	triple knockout
<b>T-OLA</b>	telomere oligonucleotide ligation assay
<b>ts</b>	temperature sensitive
<b>Ub</b>	ubiquitination
<b>UNG</b>	uracil-N-glycosylase
<b>UTR</b>	untranslated region
<b>UV</b>	ultraviolet radiation
<b>UVP</b>	dual intensity ultraviolet trans-illuminator
<b>V</b>	Volt
<b>v/v</b>	volume per volume
<b>w/v</b>	weight per volume
<b>WS</b>	Werner Syndrome
<b>wt</b>	wildtype
<b>X-gal</b>	5-bromo-4-chloro-3-indolyl- $\beta$ -D-galactopyranoside

## **ENCLOSED UNBOUND MATERIAL**

Supplementary figures and tables are on a CD (in the cover).

## **STATEMENT CONCERNING COLLABORATIONS**

The work presented in this thesis is the work of the author unless otherwise indicated.

## **ACKNOWLEDGEMENTS**

I would like to thank Parmjit Jat for his fantastic support throughout my PhD. He has been a precious help in guiding me through the various projects undertaken for this thesis and helping me to link them all in one story. His patience for my “frenchism” was most appreciated.

Also, I owe many thanks to the great people that I worked with in the Jat Lab: Tim Szeto for his great humour in the lab, Nunu namely Parineeta Aurora for her consistent support and friendliness, Kat namely Katharina Wanek for being my best chatting buddy during the long hours in the tissue culture lab, Louise Mansfield for getting me started with all the project and for being the most organized person I’ve known so far, Annika Alexopoulou for being a model of dedication and work, and Mark, James and Catia, the three undergrad students we received in our lab during that period, for being fresh, interested and great fun.

I am also grateful to Mike O’Hare, Anita Grigoradis, Ray Young and Holger Hummerich for their helpful discussions, practical advice and participation in treating the data. A special thank to Jess for being a great friend within the unit and keeping me in a good mood whenever needed.

I would also like to extend my thanks to the Wellcome Trust to permit me financially to undertake that big project.

For provision of reagents, I would like to thank Reuven Agami, Ole Gjoerup, Gregory Hannon, Ed Harlow, Scott Lowe, Karl Munger, John Sedivy, Andrew Fry Leicester, David Glover, Jesus Gil, Pascal Meier, Rene Medema, Xin Lu, Greg Towers and Didier Trono, Andrei Gudkov, Julian Downward and Jay Morgenstern.

Finally, this project would not have been completed without the amazing support of both my family and friends. So, I would like to thank Steven and Paula for their support during the writing of the thesis. In particular, I would like to thank my parents, Christine and Jean, Camille, my sister, and Chris, my boyfriend; I dedicate this work to them.

# **1 INTRODUCTION**

## **1.1 REPLICATIVE SENEESCENCE DISCOVERY**

The first “immortal” cells, discovered in a tissue culture laboratory, in 1951, were HeLa cells, from the name of a patient, Mrs. Henrietta Lacks, from whom the biopsy was extracted (Finkel, Serrano et al. 2007). This mother of five underwent a biopsy at John Hopkins hospital for a suspicious cervical mass which was then identified as an undifferentiated epidermoid carcinoma in the cervix. A portion of that biopsy also went to George and Martha Gey’s research laboratory. Unfortunately, Mrs. Lacks local lesion could never be eradicated, and she died within six months of disseminated cancer. The laboratory was more fortunate, however. This peculiar tumour grew very well in the laboratory and because it could be transferred from generation to generation, it was established as a perpetual cell line. At that point, scientists thought they had discovered true immortal cells. They, however, quickly established that there was a limit to cell division and that the cells would stop dividing and become specialised after a certain number of divisions. Moorhead and Hayflick, more than 40 years ago, discovered that normal human diploid fibroblasts stop dividing after 60-80 population doubling in culture. In 1961, they proved that this growth arrest wasn’t due to anything present in the culture medium as they took early passage cells and transferred them into the conditioned media without any changes but was due to some intrinsic factors, “Hayflick factors” (Hayflick and Moorhead 1961). These factors would accumulate inside the cells until they senesced.

Today this proliferative limit named replicative is considered to be triggered largely by erosion of the telomeres but also by various intrinsic and extrinsic factors such as DNA damage, structure alteration, activation of certain oncogenes and physiological stress.



## 1.2 DEFINITION OF SENESENCE

Cellular senescence was described for the first time in 1961 by Hayflick and Moorhead as an irreversible growth arrest of human diploid cells that had lost their ability to divide after a certain number of divisions (Figure 1.1) (Hayflick and Moorhead 1961).

Senescent cells are viable almost indefinitely, at least *in vitro*, even if they have stopped dividing and synthesising DNA. They typically undergo dramatic morphological and functional changes and acquire a very distinct gene and protein expression profile. For instance, these cells acquire increased adhesion to the extracellular matrix and a flattened and much enlarged phenotype with a vacuolated morphology (Chang, Broude et al. 1999; Serrano and Blasco 2001; Narita, Nunez et al. 2003). A biochemical assay has even been developed to detect senescent cells based on the increased senescence-associated- $\beta$ -galactosidase (SA- $\beta$ -Gal) (Dimri, Lee et al. 1995; Shelton, Chang et al. 1999; Pascal, Debacq-Chainiaux et al. 2005). Confidence in the SA- $\beta$ -Gal assay, however, has been eroded by findings that its expression can be induced in some immortalized cells and even reversed under some conditions (Herbig, Jobling et al. 2004). Another assay was developed as an alternative to test the senescence status using three biomarkers (telomere dysfunction, activation of the ATM DNA-damage response, and heterochromatinization of the nuclear genome).

Nevertheless, no precise link between these morphological and functional changes and senescent signalling has been established so far and the senescence pathways outline has yet to be defined.

## 1.3 TELOMERE INDUCED SENESENCE

### 1.3.1 Telomeres

Telomeres are DNA-protein complexes at the ends of linear eukaryotic chromosomes. Mammalian telomeres are composed of tandem repeats of a TTAGGG patterns of DNA associated with proteins (Moyzis, Buckingham et al. 1988; Wellinger and Sen 1997).

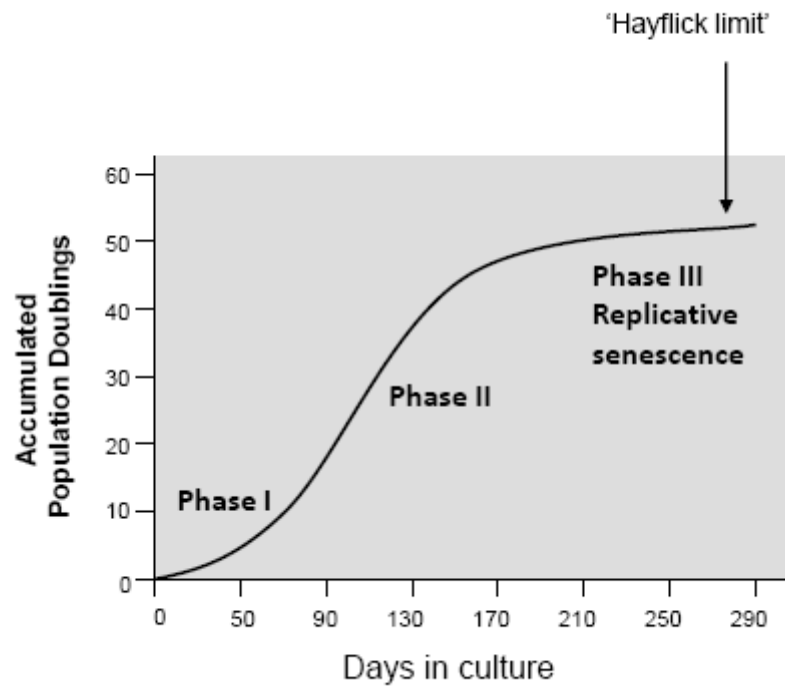


**Figure 1.1: Replicative Senescence**

Hayflick and Moorhead [Hayflick and Moorhead, 1961] analysed primary HDFs sub-cultivated in vitro and demonstrated that these cells exhibited a finite proliferative potential; after approximately 50 PDs, at a point termed the 'Hayflick limit', the cultures failed to expand, and the cells were considered senescent.

They were first discovered by Barbara McClintock and Herman Muller in the 1930's and are capping structures that enclose and protect the ends of all eukaryotic linear chromosomes from degradation (d'Adda di Fagagna, Teo et al. 2004).

The telomere induced senescence is the first molecular mechanism identified capable of inducing irreversible cell growth arrest. The study of telomere length regulation revealed that cells lose 50-200 base pairs of telomeric DNA with every single cell division during S-phase and therefore progressively shortening their telomeres (Harley, Futcher et al. 1990; Blasco 2005). The human telomeres are around 8 to 12 kb at birth. Eventually, telomeres reach a critical dysfunctional length that activates the p53 tumour suppressor factor resulting in the cell senescence or apoptosis (de Lange 2005; von Zglinicki, Saretzki et al. 2005). Only one or a few such telomere erosions are necessary to trigger senescence (Martens, Chavez et al. 2000; Hemann, Rudolph et al. 2001).

### 1.3.2 Telomeres and DDR

In humans, several studies have shown a correlation between telomeres length, age and aging diseases in a wide range of tissues (Cawthon, Smith et al. 2003; Panossian, Porter et al. 2003; Ogami, Ikura et al. 2004; Canela, Vera et al. 2007). A large amount of evidence demonstrated that telomere erosion was contributing to genome instability (Maser and DePinho 2002) by initiating DNA damage response (DDR) (Figure 1.2). However, mouse models with competent p53 pathways have recently shown that telomere shortening could act as a tumour suppressor by promoting replicative senescence (Figure 1.2). In opposition, in cells with mutant p53, the telomere induced DDR triggers genome instability and tumourigenesis (Blasco, Lee et al. 1997; Cosme-Blanco, Shen et al. 2007).

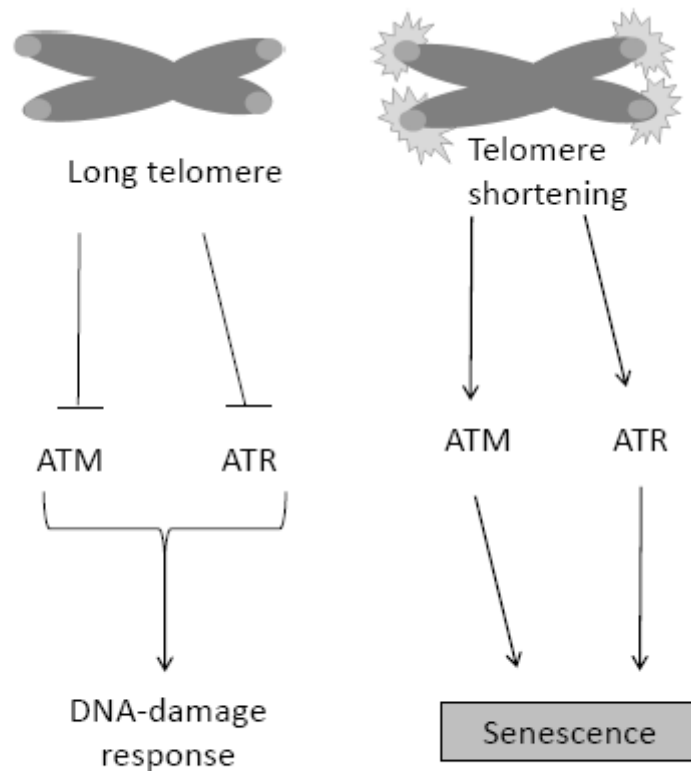


**Figure 1.2: Telomeres shortening**

In cells that do not express telomerase, telomeres become shorter with each cycle of cell division. **a**, Long telomeres ensures that telomere ends, which are similar in chemical composition to broken DNA sequences within chromosomes, are not mistaken for sites of DNA damage by the ATM- and ATR-mediated DNA-repair machinery. **b**, When telomeres become critically short, they induce cellular senescence. Such short telomeres were known to activate ATM and ATR kinases, which mediate the DNA-damage response. Lazzarini Denchi and de Lange now identify structural changes that lead to the activation of ATM and ATR at telomeres.

### 1.3.3 hTERT

Telomeres have a DNA damage repair system necessary for their maintenance through the action of telomerases. Telomerase are ribonucleoproteins, with a catalytic DNA polymerase activity called telomerase reverse transcriptase (TERT), which are in charge of elongating telomeres (Greider and Blackburn 1985). There are two major components of the telomerase holoenzyme: the telomerase reverse transcriptase (TERT) protein subunit that catalyzes the enzymatic reaction of DNA synthesis and the telomerase RNA (TR) component that serves as a template for the addition of deoxyribonucleotides to the ends of chromosomes. The catalytic RNA is constitutive. TERT is generally turned off in somatic cells. Although other proteins are associated with the holoenzyme, these two components are essential and sufficient for telomerase activity and telomere lengthening (Ishikawa 1997; Weinrich, Pruzan et al. 1997). However, most human adult tissues express telomerase at levels not high enough to maintain the telomeres length intact and this attrition results in aging (Collins and Mitchell 2002). The use of a telomerase depleted mouse model helped to prove that the telomerase is the main cellular activity responsible in the telomere maintenance (Blasco, Lee et al. 1997). This explains why germ-line cells and cancer cells express TERT at high levels. Correspondingly, ectopic expression of telomerase *in vitro* alone can contribute to the creation of immortalized human fibroblast cell line from primary cells in particular cases (Bodnar, Ouellette et al. 1998).

Fundamentally, all human cancer cells have developed a mechanism to maintain telomeres, essentially through an induction of telomerase activity (Stewart and Weinberg 2006). Alternatively, another mechanism exists, known as ALT for alternative lengthening of telomeres, which involves inter telomeres homologous recombination (Muntoni and Reddel 2005).

#### 1.3.4 Telomerase and tumourigenesis

Consequently to these conclusions, the telomerase is often described as a tumourigenic and an anti-aging factor. For example, it has been proven that mice deficient in telomerase activity are cancer resistant while wild type mice would develop normally tumours following various genetic alteration or carcinogenic treatments (Gonzalez-Suarez, Samper et al. 2000; Blasco 2005). These mice also display a shortened lifespan, even from the first generation, which decreases with every new generation of deficient mice (Blasco, Lee et al. 1997; Lee, Russo et al. 1998; Garcia-Cao, Garcia-Cao et al. 2006). Mice over-expressing telomerase, on the contrary, are prone to tumour development (Gonzalez-Suarez, Samper et al. 2000; Canela, Martin-Caballero et al. 2004; Gonzalez-Suarez, Geserick et al. 2005) and an increased lifespan has been shown in the few telomerase transgenic mice that do not develop cancer (Gonzalez-Suarez, Geserick et al. 2005). However, it is important to note that telomerase induction cannot prevent senescence caused by non-telomeric DNA damage or other inducers (Chen, Prowse et al. 2001) as telomere shortening is only one of the causes of cellular senescence.

### **1.4 DNA DAMAGE INITIATED SENESCENCE**

All cells must protect their genomic integrity in order to guarantee a proper transfer of the genetic information during the cell division. Cells respond to genotoxic stress including DNA double strand breaks (DSBs) by activating a signalling cascade known as DNA damage response (DDR). The DDR is a complex cascade of reactions regulated by multiple and various DNA repair factors and cell cycle regulators, which seems to converge on only one protein preferentially, p53, which is a key factor in the timely execution of cell fate decisions. In addition, P53 is also downstream of telomere shortening.

It is well established that DNA damage, especially DSBs, contribute to trigger senescence (Di Leonardo, Linke et al. 1994; Parrinello, Samper et al. 2003) (Figure 1.3).

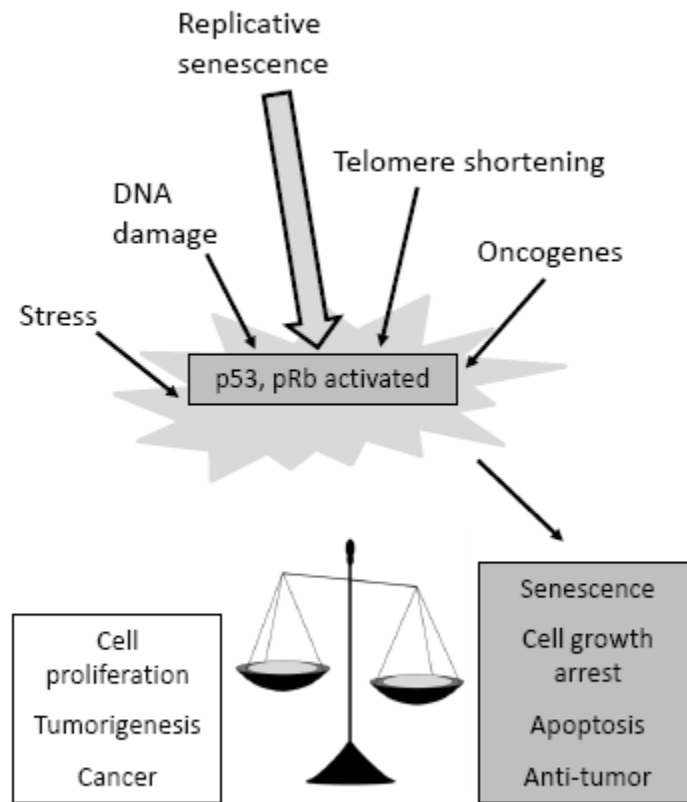


**Figure 1.3: Causes and consequences of cellular senescence**

Cellular senescence is triggered in response to a variety of intrinsic and extrinsic stimuli including progressive shortening of telomeres, changes in telomeric structure at the ends of chromosomes or other forms of genotoxic stress such as oncogene activation, DNA damage or oxidative stress resulting in a DNA damage response and growth arrest via activation of the p53-p21 pathway (Ben-Porath and Weinberg, 2004; Campisi and d’Adda di Fagagna, 2007). When cellular senescence occurs, cellular proliferation is lost, and the balance is tipped toward apoptosis and cell cycle arrest.

Recent data even suggest that DNA damage could be just a general common cause underlying various different forms of cellular senescence such as oncogene-induced and telomere-induced senescence (d'Adda di Fagagna, Reaper et al. 2003; Bartkova, Rezaei et al. 2006; Di Micco, Amitrano et al. 2006) (Figure 1.3). *In vitro* cultured cells undergo irreversible growth arrest when subject to various forms of DNA damage (te Poele, Okorokov et al. 2002; Parrinello, Samper et al. 2003). The age-dependant accumulation of DNA damage seems to be also a contributing factor to cellular senescence (Vijg 2000) therefore leading to an accumulation of senescent cells in aging tissues as well as depletion in the number/function of stem cells.

## 1.5 ONCOGENE-INDUCED SENESCENCE

Oncogene-induced senescence (OIS) is a protective mechanism to avoid tumour formation. The first human oncogene identified was Ras in 1982 and was found to be able to transform immortalized rodent cells (Der, Krontiris et al. 1982; Parada, Tabin et al. 1982) but needed additional DNA damage or genetic attrition to assist in transforming primary cells (Land, Chen et al. 1986). In 1997, the accumulation of Ras in wild type cells was proved to trigger proliferation followed by an irreversible growth arrest accompanied by the accumulation of p53 and p16<sup>INK4A</sup> proteins (Serrano 1997). This Ras-induced senescence was also found to be bypassed by the inactivation *in vitro* of pRb and p53 pathways, suggesting similarities to tumour suppressor mechanisms.

The proof of oncogene-induced senescence has since then been demonstrated *in vivo* in human tumour and mouse tumour models (Braig, Lee et al. 2005; Chen, Trotman et al. 2005; Collado, Gil et al. 2005; Michaloglou, Vredeveld et al. 2005; Courtois-Cox, Genter Williams et al. 2006; Dankort, Filenova et al. 2007) (Figure 1.3). Furthermore, mutations in K-ras, B-raf, PTEN and NF1 have been observed to trigger cellular senescence *in vivo*. Senescence occurs in benign but not in advanced tumours, supporting the first *in vitro* observation that activation of these pathways lead to an initial burst of proliferation before causing cellular senescence (Courtois-Cox, Jones et al. 2008).



## **1.6 CANCER AND SENESCENCE**

Senescence can compromise tissue repair and regeneration and contribute to tissue and organismal ageing due to depletion of stem/progenitor cell compartments. It could also lead to removal of defective and potentially cancerous cells from the proliferating pool thereby limiting tumour development (Campisi and d'Adda di Fagagna 2007; Collado, Blasco et al. 2007) (Figure 1.3). In contrast to normal somatic cells, cancer cells have the potential to proliferate indefinitely and this acquisition of an infinite proliferative potential was proposed to be one of the six key events required for malignant transformation (Hanahan and Weinberg 2000). The underlying mechanisms that control cellular senescence, the signal transduction pathways involved and how the diverse signals that result in senescence are all integrated remain poorly defined.

There are a lot of common key regulation checkpoints and very subtle differences between tumourigenesis and senescence pathways and the balance between one another is a fine line (Figure 1.3). For instance, both can be triggered, in different situations, by DNA damage as results of DNA repair mechanisms activation (Bartkova, Rezaei et al. 2006; Halazonetis, Gorgoulis et al. 2008; Wang, Sengupta et al. 2008)

## **1.7 AGEING AND SENESCENCE**

Several studies implicate a role for p53 and pRb in establishing senescence but also a potential role as a regulator of organismal ageing (Tyner, Venkatachalam et al. 2002; Maier, Gluba et al. 2004; Dumble, Moore et al. 2007). Although a physiological role for p53 in ageing is controversial because it is supposed to extend lifespan by reducing the occurrence of cancer, studies with different mouse models indicate a delicate balance between tumour suppressive and age promoting functions of p53, under particular circumstances. While pRb null mice are lethal, p53 null mice are viable but highly cancer prone (Donehower, Harvey et al. 1992; Vooijs and Berns 1999).

On the other hand, Donehower has also described a mouse with a mutant p53 allele that appears to enhance overall p53 activity, resulting in enhanced cancer resistance accompanied by premature aging phenotypes and reduced longevity (Tyner, Venkatachalam et al. 2002). Another lab also generated a p53 hypermorphic transgenic mouse which displays even more dramatic accelerated aging (Maier, Gluba et al. 2004).

## **1.8 PATHWAYS OF SENESENCE**

Two pathways, p53 and pRb, are of particular importance concerning senescence and have been (although never fully understood) extensively described in the literature. One of the tasks this thesis is focusing on is to use the model to identify downstream effectors of p53 and pRb and then investigate in normal cells whether they also are relevant in these.

### **1.8.1 The p53 pathway**

p53 is the quintessential tumour suppressor. p53, also named the “guardian of the genome” is primordial in maintaining the genomic integrity of the cells (Lane 1992; Vogelstein, Lane et al. 2000). The importance of a functional p53 protein for a normal cell cycle is emphasized by the fact that the p53 protein does not function correctly in nearly half of all human cancers. In about half of these tumours, p53 is inactivated directly as a result of mutations in the p53 gene. In many others, it is inactivated indirectly through binding to viral proteins, or as a result of alterations in genes whose products interact with p53 or transmit information to or from p53 (Vogelstein, Lane et al. 2000). It has also been shown that p53-deficient mice show a very high incidence of multiple, spontaneous tumours at an early age (Donehower, Harvey et al. 1992; Donehower, Godley et al. 1995).

### *1.8.1.1 TP53 gene and p53 protein*

P53 was first described in 1979 by its interaction with the viral protein SV40 LT antigen and the adenovirus E1B 58K (DeLeo, Jay et al. 1979; Lane and Crawford 1979; Linzer and Levine 1979). It was initially considered to be an oncogene but was subsequently identified to be a tumour suppressor (Linzer and Levine 1979). The TP53 human gene is located on chromosome 17 and possesses 11 exons whereas the mouse gene also containing the same number of exons is situated on chromosome 11 (Soussi and May 1996). The human protein is ~53kDa (Hainaut, Soussi et al. 1997).

### *1.8.1.2 Functions of the p53 protein*

The general assumption is that the p53 is normally present at low level partly as a result of its degradation by the specific ubiquitin ligase MDM2, through the ubiquitinylation-proteasome pathway but can be activated in cells as a response to various signals such as DNA damage, stress, anoxia or depletion of the nucleotide pools. The tumour suppressor ARF helps to stabilize p53 by binding and inhibiting MDM2. In response to stress signals (perhaps the best studied of which is the response to DNA damage) p53 becomes functionally active and triggers either a transient cell cycle arrest, cell death (apoptosis) or permanent cell cycle arrest (senescence).

Both cellular senescence (Sionov and Haupt 1999) and apoptosis (Heinrichs and Deppert 2003) are potent tumour suppressor mechanisms that irreversibly prevent damaged cells from going under neoplastic transformation. As a matter of fact, they also were some of the first explored functions of p53. Later on, other important functions, such as DNA repair (Albrechtsen, Dornreiter et al. 1999) and inhibition of angiogenesis (Vogelstein, Lane et al. 2000), were discovered. p53 promotes longevity by reducing somatic mutation and/or abnormal cell growth and consequently reducing the occurrence of cancer (Campisi 2003; Vijg, Busuttil et al. 2005). Recent evidence suggests that an increased p53 activity can, at least under some circumstances, promote

organismal ageing (Tyner, Venkatachalam et al. 2002; Dumble, Gatzka et al. 2004; Maier, Gluba et al. 2004).

p53 is a sequence-specific transcription factor that binds to target consensus sites and affects the transcription of its target genes (el-Deiry 1998). p53 regulates these genes either by transcriptional activation (Murphy, Ahn et al. 1999) or by modulating other protein activities by direct binding (Guimaraes and Hainaut 2002).

#### *1.8.1.3 Regulation of p53 activity*

The regulation of p53 activity can happen at various levels: p53 transcription, for example, is effectively increased by DNA damage (Lu, Pochampally et al. 2000). It is generally believed, though, that the principal mechanisms governing the activity of p53 occur at the protein level. These include post-translational modifications, regulation of the stability of p53 protein, and control of its sub-cellular localization (Woods and Vousden 2001). Of the post-translational modifications of p53, the most widely studied and best-known so far is phosphorylation. After DNA damage induced by ionizing radiation or UV light, phosphorylation takes place mostly at the N-terminal domain of p53 (Appella and Anderson 2001). Another important modification is acetylation, which (Ito, Adachi et al. 2001). In response to DNA damage, the p53 protein is also modified by conjugation to SUMO-1, a ubiquitin-like protein (Gostissa, Hengstermann et al. 1999). Many proteins able to interact with p53 may also play a role in p53 regulation (Vousden and Lu 2002).

Mdm2-mediated degradation regulates the stability of p53 (Figure 1.4). Mdm2 was originally identified as a dominant transforming oncogene (Fakharzadeh, Trusko et al. 1991) and has been found to be amplified in human cancers (Momand, Jung et al. 1998). Deletion of the *mdm2* gene in mice is embryonically lethal, probably due to increased accumulation of p53, but this lethality can be counter-acted by deletion of the TP53 gene (Jones, Roe et al. 1995; Montes de Oca Luna, Wagner et al. 1995).

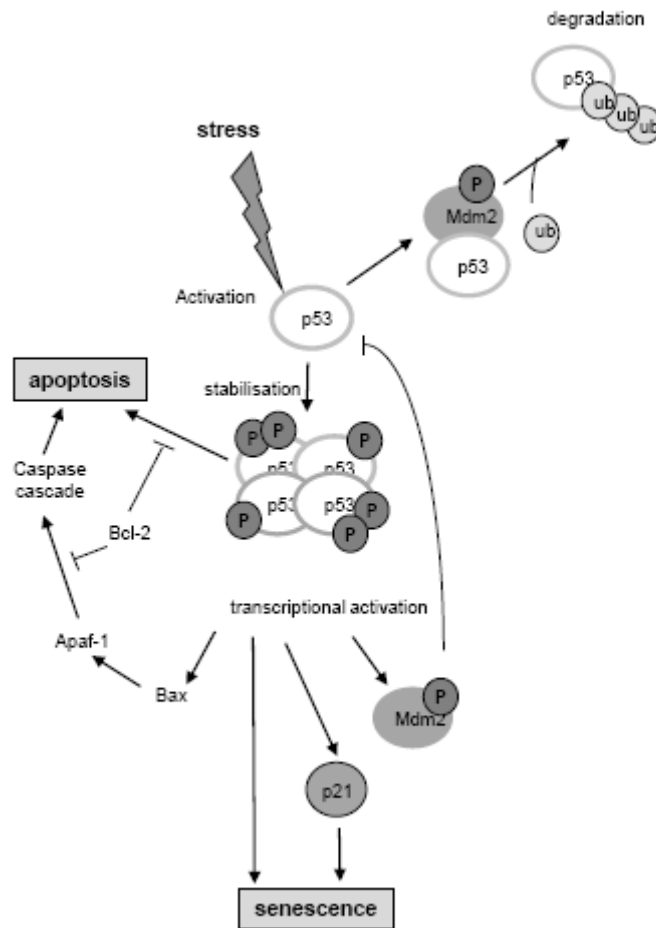


**Figure 1.4: The p53 Signalling Pathway**

Schematic diagram of the p53 signalling pathways that is involved in regulating progression through the cell cycle in response to genotoxic stress or oncogenic signals. Ub: ubiquitin; P: phosphorylation.

The mdm2 protein regulates the activity of the p53 protein with many mechanisms such as blocking the transcriptional activity of the p53 protein, exporting p53 from the nucleus to the cytoplasm and promoting the degradation of p53 (Tao and Levine 1999; Alarcon-Vargas and Ronai 2002). The p53-mdm2 relationship is vital in the regulation of cell growth and death.

#### *1.8.1.4 p19<sup>ARF</sup> protein*

p19<sup>Arf</sup> (ARF, Alternative Reading Frame) is a protein capable of interacting with mdm2 (Kamijo, Weber et al. 1998) and interfering with the autoregulatory feedback loop between the p53 and mdm2 proteins (Figure 1.5), thus increasing the amount of p53. The gene that encodes the p19<sup>Arf</sup> protein also encodes p16<sup>INK4a</sup>. However, the p19<sup>Arf</sup> protein is expressed by a separate promoter (Mao, Merlo et al. 1995). Both p16<sup>INK4a</sup> and p19<sup>Arf</sup> are tumour suppressors (Zhang & Xiong 2001). The p19<sup>Arf</sup> protein is exclusively localized in the nucleolus (Weber, Taylor et al. 1999) where it can bind to the central or C-terminal portion of the mdm2 protein (Zhang, Xiong et al. 1998). There are currently three competing theories about how p19<sup>Arf</sup> inhibits mdm2-mediated p53 degradation. The first possibility is that the p19<sup>Arf</sup> protein sequesters the mdm2 protein into the nucleolus, thus releasing p53 (Tao and Levine 1999; Weber, Taylor et al. 1999). The second model suggests that nucleolar p19<sup>ARF</sup> is relocalized by mdm2 to the nucleoplasm and forms a ternary complex with mdm2 and p53, thus blocking the nuclear export of both mdm2 and p53 (Zhang, Xiong et al. 1998). Additionally, p19<sup>Arf</sup> has been shown to bind the p53 protein directly, indicating that it can, in addition to mdm2, recruit p53 into ternary complexes (Kamijo, Weber et al. 1998). The third model proposes that, because the p19<sup>Arf</sup> protein is able to bind to the mdm2 protein and inhibit its ubiquitin ligase activity, p19<sup>Arf</sup> might prevent p53 nuclear export by blocking the ubiquitination of p53 (Honda and Yasuda 1999). It was shown by Weber and coworkers (Weber, Jeffers et al. 2000) that triple knock-out mice lacking functional p53, mdm2 and p19<sup>Arf</sup> proteins develop tumours at a greater frequency than mice lacking p53 and mdm2 or p53 alone. This suggests that p19<sup>Arf</sup> is a tumour suppressor independent of mdm2 and p53.

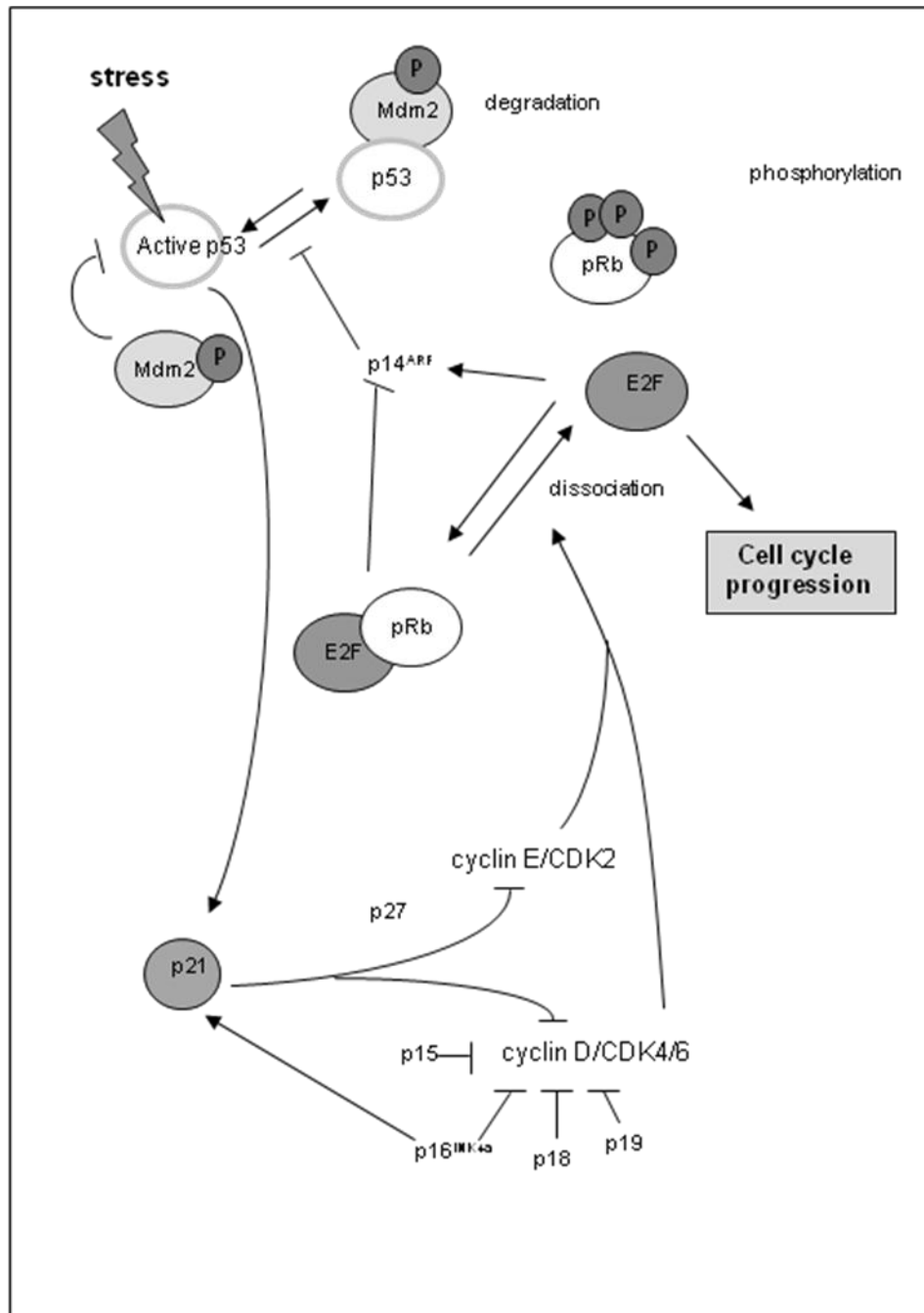


**Figure 1.5: The pRb Signalling Pathway**

Schematic diagram of the pRb signalling pathway involved in the cell cycle regulation in response to genotoxic stress or oncogenic signals.

P: phosphorylation.

The p19<sup>Arf</sup> protein itself is regulated primarily at the transcriptional level. Both Myc and E1A oncoproteins have been shown to induce the synthesis of p19<sup>Arf</sup> (de Stanchina, McCurrach et al. 1998; Zindy, Eischen et al. 1998). In summary, these three proteins form a system that regulates their localization, amount and function.

#### *1.8.1.5 Oncogenic Ras*

Mammalian ras genes are considered crucial in the regulation of cell proliferation (Bos 1989; Johnson, Greenbaum et al. 1997). In mammals, the Ras family consists of three genes located on different chromosomes, encoding the homologous 21 kDa proteins H-Ras, N-Ras and K-Ras. It has been estimated that 30% of all human cancers express mutated forms of ras (McMahon and Woods 2001). Ras can have either negative or positive effects on cell growth, differentiation and death (Frame and Balmain 2000). The signal is subsequently transmitted by a cascade of kinases, which results in the activation of MAPK. The Ras-MAPK pathway is apparently involved in the regulation of basal and induced levels of p53 (Fukasawa and Vande Woude 1997; Serrano, Lin et al. 1997). In vascular smooth muscle cells, benzo(a)pyrene treatment has been shown to cause an increase in Ras mRNA levels (Kerzee and Ramos 2000). Ras, in turn, induces p19<sup>Arf</sup> in murine fibroblasts (Groth, Weber et al. 2000; Ferbeyre, de Stanchina et al. 2002). There are also data that support a linear model from Ras through the induction of p19<sup>Arf</sup> to p53. Palmero (Palmero, Pantoja et al. 1998) showed that an oncogenic form of Ras protein increases significantly p19<sup>Arf</sup> mRNA. In ARF<sup>-/-</sup> mouse embryonic fibroblasts (MEF), the p53 level is not affected by oncogenic Ras. In an earlier work on wild-type MEFs, the p53 level increased after oncogenic Ras (Serrano, Lin et al. 1997). It can thus be concluded that p19<sup>Arf</sup> is required for oncogenic Ras-induced accumulation of p53.

#### *1.8.1.6 p21<sup>WAF1/Cip1/Sdi1</sup>*

The p21<sup>CIP1/WAF1/Sdi1</sup> protein was the first cyclin-dependent kinase inhibitor (CDKI) identified (el-Deiry, Tokino et al. 1993; Harper, Adami et al. 1993; Noda, Ning et al. 1994). The p21<sup>CIP1/WAF1/Sdi1</sup> protein has multiple functions. El-Deiry (1993) named this



gene WAF1 and found it to code a protein that mediates p53-induced growth arrest of the cell cycle, and thus functions as a regulator of cell cycle progression at G1. Almost simultaneously, another group showed it to be a regulator of CDK activity by its interaction with a CDK (Harper, Adami et al. 1993). Yet another group demonstrated its gene expression to be induced in relation to cellular senescence (Noda, Ning et al. 1994). It has been shown that p21<sup>CIP1/WAF1/Sdi1</sup> can inhibit all CDK-cyclin activities (Boulaire, Fotedar et al. 2000), directly inhibit DNA replication (Li, Waga et al. 1994; Shivji, Grey et al. 1994; Chen, Jackson et al. 1995) and at low level, act as an assembly factor for CYD/CDK4,6 (LaBaer, Garrett et al. 1997; Cheng, Olivier et al. 1999).

The gene is transcriptionally up-regulated by wild-type p53 (el-Deiry, Tokino et al. 1993). The activation of p53 causes induction, directly downstream, of p21<sup>CIP1/WAF1/Sdi1</sup>, which thanks to its promiscuous nature can, in turn, inhibit all CDK-cyclin complexes and arrests the cell at different stages of the cell cycle (Gartel, Serfas et al. 1996; Colman, Afshari et al. 2000; Taylor and Stark 2001) (Figure 1.4). This gives time for DNA repair before replication or mitosis and thus links p21<sup>CIP1/WAF1/Sdi1</sup> directly to the tumour suppressor function of p53.

#### *1.8.1.7 p53 family: p63 and p73 proteins*

Two genes notably similar to the TP53 gene seem to be of importance in the cell cycle. One of these genes is called p63, p51 or KET, (Schmale and Bamberger 1997; Osada, Ohba et al. 1998; Yang, Kaghad et al. 1998) and the other p73 (Kaghad, Bonnet et al. 1997). They encode proteins that share high sequence similarity and conserved functional domains with p53 and can exert p53-like functions, such as transactivation of p53 target genes and induction of apoptosis (Yang, Kaghad et al. 2002). Both give rise to differentially spliced mRNAs and then, respectively, to several different proteins homologous to p53 (Levrero, De Laurenzi et al. 2000). There are at least three different forms of the p63 protein differing at the C-terminal end ( $\alpha$ ,  $\beta$  and  $\gamma$ ) that may also differ within the transactivation domain (p63TA and p63 $\Delta$ DN) and six different variants of the p73 protein, p73-. The p73 protein, like p53, accumulates in response to DNA damage,

and it is noteworthy that different types of inducers of DNA damage seem to affect p73 in different ways (Levrero, De Laurenzi et al. 2000). Both p63 and p73 take part in the regulation of normal cell development and apoptosis (Lohrum and Vousden 2000). Different forms of p63 protein can act in a dominant-negative manner towards p53 (Yang, Kaghad et al. 1998), but whether p63 dysregulation has a role in tumourigenesis remains to be seen. p73, on the other hand, has been suggested to be a tumour suppressor protein (Levrero, De Laurenzi et al. 2000), although opposite opinions have also been presented (Irwin and Kaelin 2001). The function of p63 or p73 as a tumour suppressor still remains unclear (Michael and Oren 2002).

## 1.8.2 The pRb pathway

### *1.8.2.1 Cell cycle, cyclins and CDKs*

Senescence is by definition an irreversible arrest of the cell cycle; therefore, it is no surprise that cell cycle and senescence share an intricate web of their respective pathways. Cyclins were the first discovered cell cycle regulators, their expression levels increasing before mitosis and decreasing during cytokinesis (Evans, Rosenthal et al. 1983). They are divided into different categories each sporting a specific role in the cell cycle sequence. Cyclins A have been associated with Mitosis and the S-phase (DNA synthesis phase) of the cycle whereas cyclins B were only associated with the mitosis and cyclins E with the S-phase. Cyclins D were linked to the G1-phase (Roberts 1999). Cyclins function by activating cyclin-dependant kinases (CDK) through binding. These CDKs, in opposition, conserve stable expression levels throughout all the cell cycle.

### *1.8.2.2 CDK inhibitors*

The Cyclin-CDK activity is also regulated by CDK inhibitors (CDKIs). These CDKI have proven to be of great importance and have been classified into 2 families, namely the INK4A family and the Cip/Kip family.

- INK4A family

The INK4A family consists of p16<sup>INK4a</sup>, p15<sup>INK4b</sup>, p18<sup>INK4c</sup> and p19<sup>INK4d</sup>. INK4A family members function by inhibiting the kinase activity of CDK4 and CDK6 (Serrano, Hannon et al. 1993) (Figure 1.5). p16<sup>INK4a</sup> and p15<sup>INK4b</sup> are known to be associated with tumour suppression while p18<sup>INK4c</sup> and p19<sup>INK4d</sup> are highly expressed during development (Zindy, Soares et al. 1997).

- Cip/Kip family

The Cip/Kip family consists of family members p21<sup>CIP1/WAF1/Sdi1</sup>, p27 and p57 (Sherr and Roberts 1999). All the members of this family bind and inactivate CDK2 complexes; however, the mechanism by which they inactivate the complexes varies between them. The Cip/Kip family also functions as both positive and negative regulators of the CDK4/6 complexes; p21<sup>CIP1/WAF1/Sdi1</sup>, for example, acts as an assembly factor for CDK4/6 complexes at low levels but turns into an inactivator while its levels increase.

### *1.8.2.3 CDKs and E2F*

During G<sub>0</sub> (quiescence) and early G<sub>1</sub> (first gap phase) of the cell cycle, a combination of low levels of cyclins and high CDKI activity ensures pRb remains bound to the E2F transcription factor (Figure 1.5). Then, in response to extracellular signals, such as mitogens, D-type cyclins start to accumulate and to increase the cyclin D-CDK4/6 activity. This results in the phosphorylation pRb and the subsequent release of E2F. This permits transcriptional activation of E2F-responsive genes required for S-phase (Weinberg 1995; Bartek, Bartkova et al. 1996).

### *1.8.2.4 Rb family of proteins*

One of the major targets of the cyclin-CDK kinases is the Rb family of proteins. The Rb family is defined by the possession of a bipartite pocket region and is comprised of three members, pRb, p107 and p130. The pocket region consists of two conserved domains that are separated by a spacer region. In the case of pRb, this region encompasses aa

379-928 (Lee, Shew et al. 1987; Hannon, Demetrick et al. 1993; Mayol, Grana et al. 1993; Zhu, van den Heuvel et al. 1993).

The fact that Rb family members exhibit a high level of sequence homology results in some level of functional redundancy; for example, Rb family members share common activities in the regulation of cell proliferation, differentiation and apoptosis (Claudio, De Luca et al. 1996). However, functional specificity of individual family members has also been described; for example, p107 is the predominant family member that remains bound to E2F-responsive promoters; p130 is the predominant family member that remains bound during G<sub>1</sub> phase (Takahashi, Rayman et al. 2000; Rayman, Takahashi et al. 2002), whereas pRb is commonly expressed in both proliferating and non-proliferating cells.

#### *1.8.2.5 pRb gene*

The *RB1* gene encodes pRb, a ubiquitously expressed 105 kilodalton (kDa) protein. The fact that pRb is ubiquitously expressed and regulated in a cell cycle-dependent manner is consistent with it functioning as a general regulator of the cell cycle (Lee, Shew et al. 1987; Buchkovich, Duffy et al. 1989; DeCaprio, Ludlow et al. 1989; Cobrinik, Dowdy et al. 1992). Its primary function is to inactivate the E2F family of transcription factors during G<sub>1</sub>/S phase transition of the cell cycle, yet over 100 other pRb-binding proteins have been described (Morris and Dyson 2001). These include cell cycle regulated proteins such as Mdm2 (Xiao, Chen et al. 1995), PML (Alcalay, Tomassoni et al. 1998) or helix-loop-helix proteins involved in differentiation (Iavarone, Garg et al. 1994; Alani, Young et al. 2001).

#### *1.8.2.6 pRb discovery*

RB1 was the first tumour suppressor gene to be cloned in humans and originally formed the basis of Knudson's two-hit hypothesis (Knudson 1971), a hypothesis that was supported by evidence derived from analysis of patients with hereditary and non-

hereditary forms of retinoblastoma, a rare tumour of the eye; Knudson showed that individuals with the hereditary form of retinoblastoma often developed bilateral tumours whereas individuals with the non-hereditary form usually developed unilateral tumours. This led Knudson to hypothesize that two mutational events were required to inactivate the gene responsible for retinoblastoma, but, in individuals that inherited a mutation in the retinoblastoma gene, only one mutational event was required to inactivate the remaining functional allele. RB1 was subsequently identified as the gene that was causal to this process and it has since been shown that most human cancers harbour mutations that directly or indirectly compromise pRb function (Murphree and Benedict 1984; Sellers and Kaelin 1997); as an example, inactivating mutations frequently occur in RB1 itself, in addition to the mutation of upstream regulators of pRb, such as the homozygous deletion of p16<sup>INK4a</sup> or amplification of the CDK4 locus. Significantly, most tumour-associated RB1 mutations occur in the pocket protein domain (Hu, Dyson et al. 1990; Huang, Wang et al. 1990; Classon and Dyson 2001).

pRb was also found to be sequestered and thereby inactivated by SV40 LT antigen, Polyoma LT antigen, Adenovirus E1A protein, HPV 16/18 E7 protein (DeCaprio, Ludlow et al. 1988; Dyson and Harlow 1992; Moran 1993; Mymryk and Bayley 1994; Eckner, Ludlow et al. 1996).

#### *1.8.2.7 pRb function*

During G<sub>0</sub> and early G<sub>1</sub>, the C-terminal domain of pRb is hypophosphorylated (Knudsen and Wang 1996; Bonetto, Fanciulli et al. 1999). This enables pRb to bind directly to and inactivate (Figure 1.5) E2F in two ways; firstly, by binding to an 18 amino acid motif within the E2F transactivation domain, pRb directly blocks the ability of E2F to form a transcriptionally active complex (Flemington, Speck et al. 1993; Helin, Harlow et al. 1993). Secondly, pRb recruits repressive complexes such as histone deacetylase (HDAC) complexes and histone methyltransferases to the promoter regions of these genes to actively repress E2F transcription (Brehm, Miska et al. 1998; Luo, Postigo et al. 1998; Zhang, Postigo et al. 1999; Chen and Wang 2000; Dahiya, Gavin et al. 2000; He, Cook et al. 2000; Lai, Kennedy et al. 2001; Frolov and Dyson 2004). pRb also binds to a heterochromatic protein, HP1, via its LXCXE motif to promote the binding of HP1

to modified histones. HP1 uses its chromodomain to directly bind to modified histones, in addition to adjacent histone tails, thereby spreading the transcriptional silencing signal to nearby nucleosomes (Bannister, Zegerman et al. 2001; Lachner, O'Carroll et al. 2001; Nielsen, Schneider et al. 2001). This activity leads to the formation of a compact DNA structure that is inaccessible to transcription factors.

Evidence to support the role of pRb in transcriptional silencing includes the fact that, during G<sub>1</sub> phase, pocket proteins can be detected in peri-nucleolar foci that also contain E2Fs and histone desacetylases (Kennedy, Barbie et al. 2000).

During mid G<sub>1</sub> phase, pRb is phosphorylated by the activity of cyclin D1-CDK4/6 (Figure 1.5). At R and late G<sub>1</sub> phase, pRb is further phosphorylated by the activity of cyclin E-CDK2 (Adams 2001) (Figure 1.5). Hyperphosphorylation of pRb in the C-terminal domain peaks during late G<sub>1</sub> phase and causes pRb to dissociate from E2F (Weinberg 1995; Knudsen and Wang 1996; Bonetto, Fanciulli et al. 1999). This is supported by evidence that loss of Rb family repressor complexes at E2F-responsive promoters enables E2F to induce expression of S phase genes required for DNA synthesis (Takahashi, Rayman et al. 2000; Rayman, Takahashi et al. 2002; Taubert, Gorrini et al. 2004). pRb is maintained in its hyperphosphorylated form until emergence from M phase (Weinberg 1995), when it is dephosphorylated by PP1, a type 1 serine/threonine phosphatase (Nelson, Krucher et al. 1997).

In addition to regulating cell cycle progression, pRb also plays a role in senescence, differentiation and apoptosis. During senescence, pRb interacts with HP1 and histone methyltransferases such as SUV39H1 to specifically repress E2F-responsive promoters and maintain the senescent state. However, experimental data is limiting due to the difficulty of obtaining good immunofluorescence data from compact chromatin (Narita, Nunez et al. 2003). In contrast, differentiation requires the direct interaction of pRb with tissue specific transcription factors to induce the differentiation of many different cell lineages, including adipogenesis, myogenesis and haematopoiesis (Gu, Schneider et al. 1993; Dunaief, Strober et al. 1994; Condorelli, Testa et al. 1995; Condorelli and

Giordano 1997). pRb activity is essential for this process (Lee, Chang et al. 1992), and this is shown by the inability of cells from mice deficient in pRb activity to differentiate both *in vitro* and *in vivo* (Maione, Fimia et al. 1994; Slack, Skerjanc et al. 1995; Lipinski and Jacks 1999; Thomas, Carty et al. 2001; Classon and Harlow 2002; de Bruin, Maiti et al. 2003). There is also some evidence to indicate that pRb can inhibit apoptosis; for example, reconstitution of pRb in Saos-2 cells (a p53- and pRb- null osteosarcoma cell line) is sufficient to bypass apoptosis induced by exposure to ionizing radiation (IR) (Haas-Kogan, Kogan et al. 1995). Moreover, functional pRb activity is sufficient to inhibit IFN  $\gamma$ -induced apoptosis (Berry, Lu et al. 1996).

#### 1.8.2.8 E2F

The predominant function of Rb family members is to negatively regulate E2F activity. Consequently, E2F plays a critical role in the cell cycle regulation and this is shown by the fact that E2F activity is commonly abrogated during tumorigenesis; for example, deregulation of the E2F family occurs in almost all cancers (Phillips and Vousden 2001), whereas over-expression of E2F1 induces senescence in primary HDFs (Dimri, Itahana et al. 2000).

E2F functions as a transcriptional regulator by forming a heterodimer with its cognate partner DP. Two DP proteins have been identified, namely DP1 and DP2, their heterodimerisation enhances both E2F transactivational activity, and the ability of Rb family members to bind to and negatively regulate E2F. Seven E2F family members have been described to date and these can be sub-divided into transcriptional activators (E2Fs 1-3a) and transcriptional repressors (E2Fs 3b-7). The lack of transactivation and pocket protein-binding domains in E2F6 (Cartwright, Muller et al. 1998; Gaubatz, Wood et al. 1998; Trimarchi, Fairchild et al. 1998) is thought to render this particular E2F as a repressor as it prevents activator E2Fs from binding to the DNA and/or recruits polycomb group (PcG) proteins to target genes (Trimarchi, Fairchild et al. 2001). E2F7 represents a recently identified E2F family member that is likely to function as a transcriptional repressor, as determined by sequence analysis (de Bruin, Maiti et al. 2003).

### 1.8.3 Common pathways

#### *1.8.3.1 INK4A Locus*

The *INK4A* locus situated on human chromosome 9p21 is amongst the most frequent sites of genetic loss in human cancer and constitutes a unique feature in eukaryotes in the fact that it results in two splice variants that both encode tumour suppressor proteins, namely p16<sup>INK4a</sup> and p14<sup>ARF</sup>. These proteins share no sequence homology at the protein level and differ in their functional activity, yet both function to negatively regulate distinct pathways that are critical for cell cycle progression: p16<sup>INK4a</sup> regulates the pRb pathway whereas p14<sup>ARF</sup> regulates the p53 pathway. Both p16<sup>INK4a</sup> and p14<sup>ARF</sup> share common regulatory mechanisms since they are both induced in response to aberrant growth or oncogenic stress, and both can be induced upon senescence. Yet, whilst there is substantial evidence to associate functional inactivation of p16<sup>INK4a</sup> with tumourigenesis, evidence to link p14<sup>ARF</sup> inactivation to tumourigenesis is less clear. This is due to the fact that p14<sup>ARF</sup> promoter methylation and missense mutations specific to p14<sup>ARF</sup> are rare and p14<sup>ARF</sup> has not been as extensively analysed as p16<sup>INK4a</sup> in the context of human cancer.

Moreover, p14<sup>ARF</sup> activity is often lost concomitantly with p16<sup>INK4a</sup> and/or p15<sup>INK4b</sup>; for example, p15<sup>INK4b</sup> is located only 10 Kilobases (kb) from the first exon of p14<sup>ARF</sup>, therefore, co-deletion of p14<sup>ARF</sup> with p15<sup>INK4b</sup> frequently occurs. It is likely that p16<sup>INK4a</sup> and p14<sup>ARF</sup> evolved by selection of a common function and this hypothesis is supported by their common ability to function as tumour suppressive proteins, their ability to be expressed under similar conditions and co-regulated by molecules such as Bmi-1, CBX7 and TBX2 (Jacobs, Kieboom et al. 1999; Jacobs, Keblusek et al. 2000; Gil, Bernard et al. 2004).



### 1.8.3.2 p16<sup>INK4a</sup>

The role of p16<sup>INK4a</sup> as a tumour suppressor was first indicated by studies of familial melanoma that showed that incidences of melanoma segregated with missense mutations in p16<sup>INK4a</sup> (Hussussian, Struewing et al. 1994; Holland, Beaton et al. 1995; Liu, Lassam et al. 1995; Zuo, Weger et al. 1996). It has since been shown that p16<sup>INK4a</sup> is inactivated by deletion, point mutation and promoter methylation in many primary tumours and derived cell lines. However, the fact that humans homozygous for a severely truncated form of p16<sup>INK4a</sup> may remain tumour free for several decades indicates that loss of p16<sup>INK4a</sup> activity is not sufficient to induce tumourigenesis. More likely, p16<sup>INK4a</sup> cooperates with other events (Gruis, Weaver-Feldhaus et al. 1995; Pavel, Smit et al. 2003).

p16<sup>INK4a</sup> functions by specifically inactivating cyclin D-containing CDK complexes; p16<sup>INK4a</sup> binds to and induces a conformational change in CDK4/CDK6 that results in the inhibition of adenosine triphosphate (ATP) -binding and thereby disrupts the interaction with D-type cyclins. This activity prevents CDK4/6 from phosphorylating pRb (Alcorta, Xiong et al. 1996; Hara, Smith et al. 1996; Serrano 1997; Kiyono, Foster et al. 1998; Zhu, Woods et al. 1998; Ohtani, Zebedee et al. 2001; Schmitt, Fridman et al. 2002). Evidence to support this includes the fact that loss of pRb and p16<sup>INK4a</sup> activity generally occurs as mutually exclusive events in non-small cell lung cancer (Otterson, Kratzke et al. 1994; Shapiro, Park et al. 1995). Moreover, p16<sup>INK4a</sup> expression cannot efficiently arrest pRb-deficient cell lines (Lukas, Parry et al. 1995).

p16<sup>INK4a</sup> is positively regulated at the transcriptional level by Ets-1, a transcriptional activator that is activated by phosphorylation via ERK and p38 in response to Ras signalling. This pathway is subject to negative regulation; for example Wip-1 phosphatase negatively regulates p38 (Bulavin, Phillips et al. 2004) and other negative regulators of p16<sup>INK4a</sup> include Bmi-1 (B lymphoma Moloney Murine Leukaemia Virus (MoMuLV) insertion region 1; (Itahana, Zou et al. 2003; Park, Morrison et al. 2004), and Id1 (Inhibitor of DNA-binding 1) (Zheng, Wang et al. 2004).

P16<sup>INK4a</sup> also represents one of the few genes up-regulated upon replicative senescence and maintained at a high level in senescent cells. This up-regulation correlates with the constitutive hypo-phosphorylation of pRb in senescent cells (Alcorta, Xiong et al. 1996; Hara, Smith et al. 1996; Zindy, Soares et al. 1997; Stein, Drullinger et al. 1999). In contrast, inactivation of p16<sup>INK4a</sup> is sufficient to enable some human cell types to become immortalised in conjunction with reconstitution of telomerase activity; for example, human mammary epithelial cells and keratinocytes (Kiyono, Foster et al. 1998; Rheinwald, Hahn et al. 2002).

### 1.8.3.3 p14<sup>ARF</sup>

p14<sup>ARF</sup> was originally identified as a splice variant of the *INK4A* locus and is also known as ARF (Alternate ReadinG Frame), p14<sup>ARF</sup> in humans, or p19<sup>Arf</sup> in mice. p14<sup>ARF</sup> has its own promoter and differs to p16<sup>INK4a</sup> by the inclusion of an alternative first exon (Quelle, Zindy et al. 1995). This results in the translation of p14<sup>ARF</sup> in an alternate reading frame to p16<sup>INK4a</sup>, so that it exhibits no amino acid homology to p16<sup>INK4a</sup>. The first indication that p14<sup>ARF</sup> functioned as a tumour suppressor came from the observation that mice lacking the first exon of p14<sup>ARF</sup> were prone to spontaneous and carcinogen-induced tumours (Serrano, Lee et al. 1996). Loss of p14<sup>ARF</sup> activity was subsequently shown to render p53 inactivation surplus for immortalisation of MEFs, both *in vitro* (Kamijo, Zindy et al. 1997) and in tumours *in vivo* (Chin, Pomerantz et al. 1997), and could inhibit transformation of MEFs by Mdm2. Yet, this activity did not occur in cells lacking *p53* (Pomerantz, Schreiber-Agus et al. 1998). This indicated that p14<sup>ARF</sup> functioned upstream of p53 in a linear pathway. p14<sup>ARF</sup> specific mutations have since been reported in incidences of familial melanoma and astrocytoma (Randerson-Moor *et al*, 2001; Rizos *et al*, 2001). Moreover, promoter methylation of p14<sup>ARF</sup>, but not p16<sup>INK4a</sup> was implicated in some incidences of colon cancer (Esteller, Tortola et al. 2000; Esteller, Gonzalez et al. 2001; Sato, Harpaz et al. 2002), and the finding that TBX2 and Pokemon, two transcriptional repressors of p14<sup>ARF</sup> (Jacobs, Keblusek et al. 2000; Maeda, Hobbs et al. 2005), are both aberrantly over-expressed in a subset of human breast cancers and lymphomas indirectly links p14<sup>ARF</sup> to human cancer.

p14<sup>ARF</sup> functions by sequestering Mdm2 to the nucleolus, thereby impairing the ability of Mdm2 activity to promote the degradation of p53 by ubiquitin-mediated proteolysis (Pomerantz, Schreiber-Agus et al. 1998; Zhang, Xiong et al. 1998; Sherr 2000; Sherr and DePinho 2000). This activity enables p14<sup>ARF</sup> to indirectly stabilise p53 (Weber, Taylor et al. 1999; Sherr and Weber 2000; Lowe and Sherr 2003). The N-terminal 25 aa are critical for p14<sup>ARF</sup> functional activity, and this region is encoded entirely by exon 1 $\beta$  (Quelle, Zindy et al. 1995). It has also been shown that p14<sup>ARF</sup> can inhibit cell proliferation by p53-independent pathways (Cleveland and Sherr 2004)

p14<sup>ARF</sup> expression is repressed under normal cellular conditions but is activated in response to aberrant signalling; for example, in response to oncogenic signals such as c-Myc, E2F-1, oncogenic Ras, v-abl, DMP1 and  $\beta$ -Catenin (DeGregori, Leone et al. 1997; Dimri, Itahana et al. 2000; Inoue, Wen et al. 2000; Inoue, Zindy et al. 2001; Sherr 2001).

The p19<sup>Arf</sup>-p53 pathway is the major pathway that induces senescence in mice (Lowe and Sherr 2003; Sharpless and DePinho 2005) since p19<sup>Arf</sup> expression correlates with the onset of senescence in MEFs and since cells that lack p19<sup>Arf</sup> do not senesce in culture (Kamijo, Zindy et al. 1997; Zindy, Soares et al. 1997). Moreover, p19<sup>Arf</sup>-null mice are prone to develop spontaneous tumours (Kamijo, Zindy et al. 1997; Kamijo, Bodner et al. 1999). There is also evidence to suggest that over-expression of E2F1 induces p14<sup>ARF</sup>, thereby negatively regulating Mdm2 activity and stabilising p53 (DeGregori, Leone et al. 1997; Prives 1998; Sherr and DePinho 2000). This activity indirectly links the pRb and p53 pathway, and also links E2F activity to the induction of senescence (Zhu, Woods et al. 1998). However, the significance of this pathway in humans is unclear; for example, despite the fact that p14<sup>ARF</sup> over-expression can induce cell cycle arrest or senescence (Quelle, Zindy et al. 1995; Kamijo, Zindy et al. 1997; Dimri, Itahana et al. 2000; Wei, Hemmer et al. 2001), it has been argued that p14<sup>ARF</sup> activity is not critical for these processes (Munro, Stott et al. 1999; Wei, Hemmer et al. 2001; Rheinwald, Hahn et al. 2002; Sharpless and DePinho 2005). Moreover, p14<sup>ARF</sup> expression levels rise only in some HDF strains upon replicative senescence (Dimri, Itahana et al. 2000).

## 1.9 DNA TUMOUR VIRUSES

SV40, Adenovirus, and Human Papilloma Virus (HPV) are three examples of DNA tumour viruses. The natural hosts of DNA tumour viruses are differentiated cells, therefore, these viruses have evolved mechanisms to enable them to replicate in a non-proliferative cellular environment. The mitogenic properties include the ability to alter the cellular transcription machinery to promote the expression of proteins that are required for viral replication, to overcome the finite proliferative potential and to block cellular defences against viral intrusion. Consequently, some of the viral proteins encoded by the DNA tumour viruses are able to inactivate the major control pathways regulating the cell cycle and are therefore implicated in the induction of tumourigenesis; for example, SV40 LT, HPV Type 16 E6 and E7 and Adenovirus Type 5 E1A and E1B all function as potent viral oncoproteins to induce immortalisation and transformation of many cell types (Braithwaite, Cheetham et al. 1983; Caporossi and Bacchetti 1990; Chang, Ray et al. 1997; Duensing and Munger 2002). This has led to the extensive use of these viruses as molecular tools to delineate many signalling pathways in mammals. Importantly, these viral oncoproteins were the first to reveal the critical roles of p53 and pRb in the regulation of the cell cycle.

### 1.9.1 SV40

SV40 is a member of the papovavirus family of small icosahedral DNA viruses. SV40 was first linked to tumourigenesis by its ability to stably transform a proportion of hamster and rodent cell lines infected with this virus. Infection of newborn hamsters with SV40 induced the formation of tumours (Hilleman 1998). Unlike the natural lytic lifecycle of SV40 in its natural hosts (rhesus monkey or African green monkey cells), human or hamster cells are semi-permissive to infection with SV40; infection of these cells is sufficient for early SV40 genes to be expressed in a transient manner and survive infection. Moreover, a small proportion of infected cells permit viral replication. In contrast, mouse cells can be infected with SV40 but are non-permissive for viral replication and do not produce progeny virus particles.

### 1.9.2 LT

Three antigens are expressed from the SV40 early region by differential splicing of the same messenger RNA (mRNA) transcript; namely, large T (LT) antigen, small t antigen and 17 kT antigen. The 708 aa LT protein alone is responsible for many of the functions of SV40 that are required for it to complete its lifecycle. LT is also involved in promoting the immortalisation of many cell types; for example, LT activity is sufficient to bypass replicative senescence in rat embryo fibroblasts (Jat and Sharp 1989). Moreover, LT activity is required to maintain these cells in an immortalised state since inactivation of LT results in a rapid and irreversible arrest in either G<sub>1</sub> or G<sub>2</sub> phase (Jat and Sharp 1989). This indicates that the endogenous senescence machinery remains intact during this process. In accordance with this finding, MEFs become dependent upon LT for maintaining growth only when their normal mitotic lifespan has elapsed (Ikram, Norton et al. 1994).

LT possesses multifunctional activity; for example, it possesses both DNA and RNA helicase activity (Scheffner, Knippers et al. 1989), ATPase activity (Tjian and Robbins 1979), RNA-binding activity (Carroll, Samad et al. 1988), DNA-binding activity (Carroll, Hager et al. 1974) and transcriptional regulation activity (Alwine, Reed et al. 1977; Hansen, Tenen et al. 1981; Mitchell, Wang et al. 1987; Saffer, Jackson et al. 1990; Zhu, Rice et al. 1991; Gilinger and Alwine 1993; Gruda, Zabolotny et al. 1993; Rice and Cole 1993; Rushton, Jiang et al. 1997). LT can also impair the activities of many host cell proteins such as p53 (Lane and Crawford 1979; Linzer and Levine 1979), pRb (DeCaprio, Ludlow et al. 1988), p107 (Dyson, Buchkovich et al. 1989; Ewen, Ludlow et al. 1989), p130 (Hannon, Demetrick et al. 1993), CBP, BUB1 (Cotsiki, Lock et al. 2004; Williams, Roberts et al. 2007), p300 (Avantaggiati, Carbone et al. 1996; Eckner, Ludlow et al. 1996) and TBP (Martin, Subler et al. 1993). Nuclear localisation is mediated the N-terminal region of LT (Soule and Butel 1979; Kalderon, Richardson et al. 1984).

LT shares significant sequence homology to the conserved region 2 (CR2) domain of E1A and E7 protein between amino acid residues 103-107. However, within SV40 LT,

there is a CR2 domain that has LXCXE which can be functionally swapped. This region contains the canonical LXCXE-binding motif that mediates stable Rb family binding (DeCaprio, Ludlow et al. 1988; Moran 1988; Munger, Werness et al. 1989). LT only binds to the hypophosphorylated and therefore active form of Rb family members (Ludlow, DeCaprio et al. 1989; Ludlow, Shon et al. 1990). Consequently, LT promotes the release of E2F, enabling it to activate transcription from E2F-responsive promoters. This activity is critical for immortalisation as mutants defective for pRb-binding exhibit a reduced ability to immortalise rodent cells (DeCaprio, Ludlow et al. 1988; Powell, Darmon et al. 1999). There is evidence to suggest that pRb-binding is important for the ability of LT to transform cells since some pRb-binding LT mutants are defective for transformation (Ali and DeCaprio 2001).

P53 was originally identified as a LT-binding protein (Lane and Crawford 1979; Linzer and Levine 1979) and binding to p53 is mediated by a bipartite region located towards the C-terminus of the protein between amino acid residues 351-450 and 533-626. LT interaction with p53 occurs via direct binding of LT to the sequence-specific DNA-binding domain of p53, as mutants of p53 that are impaired in sequence-specific DNA-binding activity are unable to bind to LT. The interaction of LT with p53 leads to abrogation of p53 activity since p53 is unable to transcriptionally regulate its target genes. This interaction stabilises p53 as both the half-life and steady-state levels of p53 are increased (Oren and Levine 1981; Deppert, Haug et al. 1987). It has also been suggested that the association of p300 and Mdm2 with p53 in a LT-binding complex contributes to this activity (Brown, Deb et al. 1993; Henning, Rohaly et al. 1997; Grossman, Perez et al. 1998). The ability of LT to impair p53 activity appears to be critical for the immortalisation of MEFs (Conzen and Cole 1995). This is in contrast to data derived from rat embryo fibroblasts since LT mutants that lack the C-terminal p53 bipartite binding domain are able to immortalise (Powell, Darmon et al. 1999). This indicates that additional activities of LT may be able to inactivate downstream effectors of p53, and this may be mediated via Rb family binding (Quartin, Cole et al. 1994; Rushton, Jiang et al. 1997). P300 and CBP binding sites are also present in both the N-

terminal and C-terminal domains of LT (Eckner 1996; Lill, Grossman et al. 1997), although their interactions may occur indirectly via p53-binding.

### 1.9.3 Adenovirus Type 5

Adenoviridae are double-stranded DNA viruses, 51 different serotypes have been identified. They primarily infect host epithelial tissues in the lung or enteric system and have been associated with the development of acute respiratory diseases. Adenovirus type 12 was the first serotype to be identified as being associated with tumourigenesis in rodents (Trentin, Yabe et al. 1962), but there is no evidence to indicate that adenovirus can induce tumourigenesis in humans. Transcription of the adenovirus genome is regulated by virus-encoded regulatory factors and two of the genes to be transcribed are E1A and E1B.

#### *1.9.3.1 E1A*

E1A represents a major regulatory protein expressed very early during adenovirus infection that is capable of activating transcription from a variety of viral and cellular promoters and notably all the other genes encoded within the viral genome. Like LT, E1A exhibits multifunctional activity and can directly bind to multiple cellular proteins required for cell proliferation to mediate this activity. Indeed, Rb family members, cyclin A, p300 and others were originally identified by their interaction with E1A (Whyte, Buchkovich et al. 1988; Faha, Ewen et al. 1992). E1A is synthesised almost immediately after infection and two of the most abundant products are the 13S and 12S E1A splice variants (Perricaudet, le Moullec et al. 1980).

The conserved CR2 motif defines the region in E1A where Rb family members bind (Harlow, Whyte et al. 1986; Whyte, Buchkovich et al. 1988; Whyte, Williamson et al. 1989). However, residues in conserved region 1 (CR1) of E1A are also involved in this process (Whyte, Williamson et al. 1989). This interaction disrupts pRb-E2F complexes and enables E2F to promote entry into S phase (Sherr 1996). E1A is localised to the nucleus by virtue of a highly basic pentapeptide signal sequence located at the extreme

C-terminus. E1A, like LT, can also bind to p300 (Dorsman, Hagmeyer et al. 1995; Wang, Moran et al. 1995; Goodman and Smolik 2000), and this promotes the formation of a pRb/p300/E1A complex that may both stabilise the E1A-pRb interaction (Barbeau, Charbonneau et al. 1994) and promote acetylation of pRb at the C-terminus (Chan, Krstic-Demonacos et al. 2001). This activity is important for E1A-induced cell cycle progression and transformation (Egan *et al*, 1989; Whyte *et al*, 1989). CtBP, a putative HDAC recruitment protein, binds to a region in the C-terminus (Goodman and Smolik 2000). Other known cellular binding partners include cyclin A, p400, CDK2, BS69, TBP and various components of the TFIID complex.

#### 1.9.3.2 E1B

E1A can induce apoptosis through the stabilisation of the p53 tumour suppressor protein during oncogenic transformation (White, Sabbatini et al. 1992; Lowe and Ruley 1993; White, Chiou et al. 1994), additional factor(s) are required to abrogate p53 and prevent the induction of apoptosis. In adenovirus, this activity is performed by E1B. The ability of adenovirus to segregate pRb and p53-abrogation activities between two different viral oncoproteins is in contrast to the combined functional activity of LT. Moreover, multiple proteins are encoded by adenovirus to inhibit p53-dependent apoptosis; E1B-55kDa and E4orf directly bind to and inactivate p53 (Yew, Liu et al. 1994; Nevels, Rubenwolf et al. 1997), whereas E1B-19kDa blocks apoptosis by mimicking the anti-apoptotic activity of Bcl2 (Rao, Debbas et al. 1992).

#### 1.9.4 HPV Type 16

HPV type 16 is a member of the small double-strand DNA tumour virus family that specifically infects squamous epithelial cells. The lifecycle of HPVs are linked to the differentiation program of the host epithelial cells since HPVs infect undifferentiated, basal keratinocytes, but most of the viral lifecycle occurs in the differentiated upper epithelial strata where virus particles are shed. Papilloma viruses can be divided into mucosal or cutaneous growth tropism groups and further subdivided in respect to their



propensity for malignant progression, namely high or low risk. HPV type 16 represents the most prevalent mucosal high risk HPV type and two proteins encoded by HPV function in an analogous manner to both LT and E1A and E1B, namely E6 and E7. E6 and E7 are stably expressed in HPV-positive cervical cancers and cancer-derived cell lines (Schwarz, Freese et al. 1985), and they are essential to maintain the transformed state of HPV-positive cells (Alvarez-Salas, Cullinan et al. 1998).

#### *1.9.4.1 E7*

E7 has been identified in approximately 90% of all human cervical cancers (zur Hausen 2001) and 20% of oral cancers (Gillison, Koch et al. 2000). E7 is a small multifunctional protein of 98 aa encoded by the early region of HPV and is responsible for the ability of this virus in overcoming G1 phase arrest induced by loss of cell adhesion, growth factor withdrawal, DNA damage and differentiation signals. Similar to LT and E1A, E7 possesses the canonical LXCXE motif of Rb family binding in CR2 that facilitates the targeted binding of hypophosphorylated pRb (Gage, Meyers et al. 1990) and other members of the Rb family (Dyson and Harlow 1992; Davies, Hicks et al. 1993). In addition to the LXCXE motif, E7 also shares sequence homology with LT and E1A in a small region of CR1. E7 exhibits a high turnover rate of approximately 2 hours (hrs), mediated by ubiquitin-mediated proteolysis.

A number of additional E7-interacting proteins have been described; for example, E7 can bind to two CDKIs, namely p21<sup>CIP1/WAF1/Sdi1</sup> and p27<sup>kip1</sup>. In addition, it has been suggested that p21<sup>CIP1/WAF1/Sdi1</sup> inactivation is critical for the ability of E7 to promote viral DNA replication during keratinocyte differentiation, in addition to overriding the cytostatic effect of TNF- $\alpha$  in these cells. E7 has also been shown to associate indirectly with cell cycle regulators such as cyclin A, cyclin E and CDK2 via p107 to promote their aberrant expression and activity. There is also evidence that E7 can inhibit p53 transcriptional activity (Massimi and Banks 2000); in this model, Casein kinase II (CKII) activity may be required to phosphorylate E7 and stimulate the ability of E7 to complex with TBP and form a tripartite complex with p53. This activity is similar to the tripartite complex proposed for E1A, p53 and TBP.

#### 1.9.4.2 E6

Like adenovirus, the activity of a second viral oncoprotein is required to directly bind to and inactivate p53 to inhibit the induction of apoptosis. In HPV-16, E6, a small protein of 151 aa mediates this activity (Scheffner, Munger et al. 1992). Unlike LT and E1B however, E6 destabilises p53 by association with the ubiquitin ligase E6AP to promote p53 degradation by the ubiquitination pathway (Huibregtse, Scheffner et al. 1991; Scheffner, Huibregtse et al. 1993; Rapp and Chen 1998). This activity impairs the ability of p53 to induce apoptosis or growth arrest; for example, the majority of human cervical cancers exhibit wt p53 activity, yet its activity is functionally neutralised by the activity of E6 (Thomas, Pim et al. 1999). The oncogenic activity of E6 has also been demonstrated by its ability to transform established MEFs and to confer resistance to terminal differentiation of human keratinocytes (Mantovani and Banks 2001). Its ability to transcriptionally activate the catalytic component of human telomerase (hTERT) in some cell types (Gewin and Galloway 2001; Oh, Kyo et al. 2001; Veldman, Horikawa et al. 2001) is important for it to function as an oncoprotein. In addition to inactivating p53, E6 can impair the activity of many other cellular proteins; for example, E6 down-regulates p21<sup>CIP1/WAF1/Sdi1</sup> in many normal cell types (Burkhart, Alcorta et al. 1999) and interacts with the pro-apoptotic Bak, TNFR-1, and DNA repair proteins MGMT and XRCC1 (Mantovani and Banks 2001; Filippova, Song et al. 2002), amongst others. The fact that both pro- and anti-apoptotic activities for E6 have been described is difficult to reconcile but may be cell context-dependent; for example, in HDFs, E6 expression inhibits oxidant-induced apoptosis within 24 hrs but sensitises cells to apoptosis after prolonged incubation (Chen and Wang 2000).

#### 1.10 SASP: SENESCENCE-ASSOCIATED SECRETORY PHENOTYPE AND ROS: REACTIVE OXYGEN SPECIES

It has long been known within the field that the culture medium of senescent cells is enriched with secreted proteins (Shelton, Chang et al. 1999; Krtolica and Campisi 2002). The SASP concept was first proposed by the Campisi group, when they realized that

secreted factors from senescent fibroblasts promote the transformation of pre-malignant, but not of normal, mammary epithelial cells. This initial observation of SASP indicated that senescence might not simply be a tumour suppressor mechanism, but rather a double-edged sword within the tumour microenvironment. What remained unclear, however, were the functional effects of SASP on the senescence phenotype itself. A series of recent papers (Acosta, O'Loughlen et al. 2008; Coppe, Patil et al. 2008; Kuilman, Michaloglou et al. 2008; Wajapeyee, Serra et al. 2008; Augert, Payre et al. 2009), have added various new members involved in SASP and notably IL-6 and IL-8 which are also up-regulated upon senescence in the HMF3A system described within this thesis, and collectively reinforced the idea that senescence is both regulated by and regulates the extracellular environment. Senescence bypass screening is a powerful tool to identify new components of the senescence machinery. Some of these factors might be potential tumour suppressors, whereas others could be 'context-dependent' tumour suppressors or even oncogenes.

Senescence is clearly more complex than CDKI-mediated growth arrest or extrinsic secretion signalling. Senescent cells express hundreds of genes differentially (Shelton, Chang et al. 1999), prominent among these being pro-inflammatory secretory genes (Coppe, Patil et al. 2008) and marker genes for a retrograde response induced by mitochondrial dysfunction (Passos, Saretzki et al. 2007). Recent studies showed that activated chemokine receptor CXCR2 (Acosta, O'Loughlen et al. 2008), insulin-like growth factor binding protein 7 (Wajapeyee, Serra et al. 2008), IL6 receptor (Kuilman, Michaloglou et al. 2008) or down-regulation of the transcriptional repressor HES1 (Sang, Collier et al. 2008) may be required for the establishment and/or maintenance of the senescent phenotype in various cell types. A signature pro-inflammatory secretory phenotype takes 7–10 days to develop under DDR (Coppe, Patil et al. 2008; Rodier, Coppe et al. 2009). Together, these data suggest that senescence develops quite slowly from an initiation stage (e.g. DDR-mediated cell cycle arrest) towards fully irreversible, phenotypically complete senescence. It is the intermediary steps that define the establishment of senescence, which are largely unknown with respect to kinetics and governing mechanisms (Passos, Nelson et al. 2010).

Reactive oxygen species (ROS) are likely to be involved in establishment and stabilization of senescence. Elevated ROS levels are associated with both replicative (telomere-dependent) and stress- or oncogene-induced senescence (Saretzki 2003; Ramsey and Sharpless 2006; Passos, Saretzki et al. 2007; Lu and Finkel 2008). ROS also accelerate telomere shortening and can damage DNA directly and thus induce DDR and senescence (Chen, Jackson et al. 1995; Lu and Finkel 2008; Rai, Phadnis et al. 2008). Conversely, activation of the major downstream effectors of the DDR/senescence checkpoint can induce ROS production (Polyak, Xia et al. 1997; Macip, Igarashi et al. 2002; Macip, Igarashi et al. 2003).

Recently, a novel mechanism has been described for senescence; the existence of a dynamic feedback loop that is triggered by a DNA damage response (DDR) and, which after a delay of several days, locks the cell into an actively maintained state of 'deep' cellular senescence. The essential feature of the loop is that long-term activation of p21<sup>CIP1/WAF1/Sdi1</sup> induces mitochondrial dysfunction and production of reactive oxygen species (ROS) through serial signalling including GADD45-MAPK14 (p38MAPK)-GRB2-TGFBR2-TGF $\beta$ . These ROS in turn replenish short-lived DNA damage foci and maintain an ongoing DDR. This loop was shown to be both necessary and sufficient for the stability of growth arrest during the establishment of the senescent phenotype.

## **1.11 NF- $\kappa$ B PATHWAY**

### **1.11.1 Introduction**

NF- $\kappa$ B was first discovered in the lab of Nobel Prize laureate David Baltimore via its interaction with an 11-base pair sequence in the immunoglobulin Kappa light-chain enhancer in B cells and plasma cells but not pre B-cells (Sen and Baltimore 1986).

Later, it was demonstrated that NF- $\kappa$ B DNA binding activity was induced by a variety of extrinsic factors, and that this activation is independent from de-novo protein

synthesis. NF- $\kappa$ B has been detected in most cell types, and specific NF- $\kappa$ B binding sites have been identified in promoters and enhancers of a high number of inducible genes.

NF- $\kappa$ B proteins comprise a family of structurally-related eukaryotic transcription factors that are involved in the control of a large number of normal cellular and organismal processes, such as immune and inflammatory responses, stress and injury. Some examples are the induction of IL-2, TAP1 and MHC molecules and involvement in many aspects of the inflammatory response, such as induction of IL-1 (alpha and beta), TNF-alpha and leukocyte adhesion molecules (E-selectin, VCAM-1 and ICAM-1). NF- $\kappa$ B is also involved in many aspects of cell growth, differentiation, proliferation and apoptosis via the induction of certain growth and transcription factors (e.g. c-myc, ras and p53). In addition, these transcription factors are persistently active in a number of disease states, including cancer, arthritis, chronic inflammation, asthma, neurodegenerative diseases, and heart disease.

#### 1.11.2 NF- $\kappa$ B family

There are five proteins in the mammalian NF- $\kappa$ B family (Nabel and Verma 1993): RelA, RelB, c-Rel, NFKB1 and NFKB2. All NF- $\kappa$ B family members share structural homology with the retroviral oncoprotein v-Rel, resulting in their classification as NF- $\kappa$ B / Rel proteins (Gilmore 2006). RelA, RelB, and c-Rel all have a transactivation domain in their C-terminus. In contrast, the NFKB1 and NFKB2 proteins are synthesized as large precursors, p105, and p100, which undergo processing to generate the mature NF- $\kappa$ B subunits, p50 and p52, respectively. The processing of p105 and p100 is mediated by the ubiquitin/proteasome pathway and involves selective degradation of their C-terminal region containing ankyrin repeats. Whereas the generation of p52 from p100 is a tightly-regulated process, p50 is produced by constitutive processing of p105 (Karin and Ben-Neriah 2000; Senftleben, Cao et al. 2001).

### 1.11.3 Activation

Part of NF- $\kappa$ B's importance in regulating cellular responses is that it belongs to the category of "rapid-acting" primary transcription factors, i.e., transcription factors that are present in cells in an inactive state and do not require new protein synthesis to be activated (other members of this family include transcription factors such as c-Jun, STATs, and nuclear hormone receptors). This allows NF- $\kappa$ B to act as a "first responder" to harmful cellular stimuli. Stimulation of a wide variety of cell-surface receptors, such as RANK, TNFR, leads directly to NF- $\kappa$ B activation and fairly rapid changes in gene expression (Gilmore 2006)

NF- $\kappa$ B can be induced by stimuli such as pro-inflammatory cytokines and bacterial toxins (e.g. LPS, exotoxin B) and a number of viruses/viral products (e.g. HIV-1, HTLV-I, HBV, EBV, Herpes simplex) as well as pro-apoptotic and necrotic stimuli (oxygen free radicals, UV light, gamma-irradiation). Many bacterial products, as an example, can activate NF- $\kappa$ B. The identification of Toll-like receptors (TLRs) as specific pattern recognition molecules and the finding that stimulation of TLRs leads to activation of NF- $\kappa$ B improved our understanding of how different pathogens activate NF- $\kappa$ B. For example, studies have identified TLR4 as the receptor for the LPS component of Gram-Negative bacteria (Doyle and O'Neill 2006). TLRs are key regulators of both innate and adaptive immune responses (Hayden, West et al. 2006).

Unlike RelA, RelB, and c-Rel, the p50 and p52 NF- $\kappa$ B subunits do not contain transactivation domains in their C terminal halves. Nevertheless, the p50 and p52 NF- $\kappa$ B members play critical roles in modulating the specificity of NF- $\kappa$ B function. Although homodimers of p50 and p52 are, in general, repressors of NF- $\kappa$ B site transcription; both p50 and p52 participate in target gene transactivation by forming heterodimers with RelA, RelB, or c-Rel (Li and Verma 2002). In addition, p50 and p52 homodimers also bind to the nuclear protein Bcl-3, and such complexes can function as transcriptional activators (Franzoso, Bours et al. 1992; Bours, Franzoso et al. 1993; Fujita, Nolan et al. 1993).

#### 1.11.4 Inhibition

In unstimulated cells, the NF- $\kappa$ B dimers are sequestered in the cytoplasm by a family of inhibitors, called I $\kappa$ Bs (Inhibitor of  $\kappa$ B), which are proteins that contain multiple copies of ankyrin. By virtue of their ankyrin repeat domains, the I $\kappa$ B proteins mask the nuclear localization signals (NLS) of NF- $\kappa$ B proteins and keep them sequestered in an inactive state in the cytoplasm (Jacobs and Harrison 1998).

##### *1.11.4.1 The I $\kappa$ B family*

To date seven I $\kappa$ B s have been identified: I $\kappa$ B $\alpha$ , I $\kappa$ B $\beta$ , I $\kappa$ B $\gamma$ , I $\kappa$ B $\epsilon$  and Bcl-3 but the best-studied and major I $\kappa$ B protein is I $\kappa$ B $\alpha$ . Due to the presence of ankyrin repeats in their C-terminal halves, p105 and p100 also function as I $\kappa$ B proteins. I $\kappa$ B $\gamma$  is unique in that it is synthesized from the NFKB1 gene using an internal promoter, thereby resulting in a protein that is identical to the C-terminal half of p105 (Inoue, Kerr et al. 1992). The c-terminal half of p100, that is often referred to as I $\kappa$ B $\delta$ , also functions as an inhibitor (Dobrzanski, Ryseck et al. 1995; Basak, Kim et al. 2007).

##### *1.11.4.2 I $\kappa$ B kinase: IKK*

Activation of the NF- $\kappa$ B is initiated by the signal-induced degradation of I $\kappa$ B proteins: signals that induce NF- $\kappa$ B activity cause the phosphorylation of I $\kappa$ Bs, their dissociation and subsequent degradation, allowing NF- $\kappa$ B proteins to enter the nucleus and induce gene expression.

This occurs primarily via activation of a kinase called the I $\kappa$ B kinase (IKK). IKK is composed of a heterodimer of the catalytic IKK-alpha and IKK-beta subunits and a "master" regulatory protein termed NEMO (NF- $\kappa$ B essential modulator) or IKK-gamma (Figure 1.6). When activated by signals, usually coming from the outside of the cell, the I $\kappa$ B kinase phosphorylates two serine residues located in an I $\kappa$ B regulatory domain (serines 32 and 36 in human I $\kappa$ B $\alpha$ ) leading to the ubiquitinylation of the I $\kappa$ B inhibitor molecules and their degradation by the proteasome.

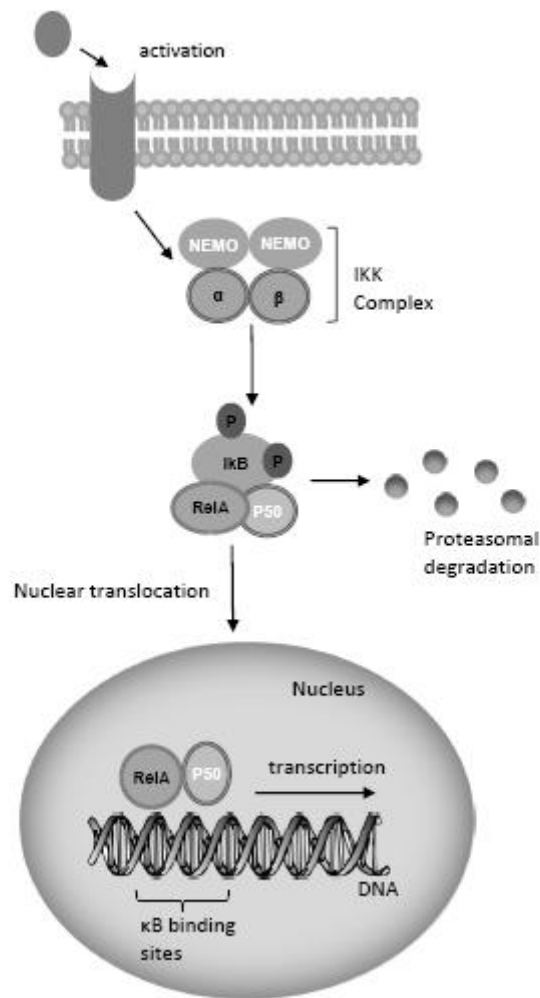


**Figure 1.6: NF-κB: The canonical pathway**

The binding of ligand to a receptor leads to the recruitment and activation of an IKK complex comprising IKK alpha and/or IKK beta catalytic subunits and two molecules of NEMO. The IKK complex then phosphorylates IκB leading to its degradation by the proteasome. NFκB then translocates to the nucleus to activate target genes regulated by κB sites.



With the degradation of the I $\kappa$ B inhibitor, the NF- $\kappa$ B complex is then free to enter the nucleus where it can 'turn on' the expression of specific genes that have DNA-binding sites for NF- $\kappa$ B. The activation of these genes by NF- $\kappa$ B then leads to the given physiological response, for example, an inflammatory or immune response, a cell survival response, or cellular proliferation.

IKK-alpha knockout mice die shortly after birth and exhibit developmental abnormalities such as shortened and truncated limbs, ears, heads and snouts due to a defect of differentiation of skin epidermal cells (keratinocytes). In general, IKK-alpha seems to be involved in skeletal development. Interestingly, IL-1 and TNF-alpha still can activate NF- $\kappa$ B in cells from IKK-alpha  $-/-$  mice.

IKK-beta knockout mice-embryos die from excessive loss of hepatocytes due to apoptosis. Apoptosis appears to be induced by TNF-alpha since IKK-beta and TNFR1 double knockout mice are not affected by hepatocyte apoptosis and embryonic death. Additionally, fibroblasts from IKK-beta  $-/-$  mice undergo apoptosis in response to TNF-alpha, presumably due to a missing "survival" signal usually provided by NF- $\kappa$ B activation (May and Gosh, 1999).

#### 1.11.5 Canonical NF- $\kappa$ B pathway

There are two signalling pathways leading to the activation of NF- $\kappa$ B known as the canonical pathway (or classical) and the non-canonical pathway (or alternative pathway) (Karin 1999; Gilmore 2006; Scheidereit 2006; Tergaonkar 2006). The common regulatory step in both of these cascades is activation of an I $\kappa$ B kinase (IKK) complex consisting of catalytic kinase subunits (IKKa and/or IKKb) and the regulatory non-enzymatic scaffold protein NEMO (NF-kappa B essential modulator also known as IKKg) (Figure 1.6). Activation of NF- $\kappa$ B dimers is due to IKK-mediated phosphorylation-induced proteasomal degradation of the I $\kappa$ B inhibitor enabling the active NF- $\kappa$ B transcription factor subunits to translocate to the nucleus and induce target

gene expression. NF- $\kappa$ B activation leads to the expression of the I $\kappa$ B $\alpha$  gene, which consequently sequesters NF- $\kappa$ B subunits and terminates transcriptional activity unless a persistent activation signal is present.

In the canonical signalling pathway, binding of ligand such as IL-1 or TNF $\alpha$  to a cell surface receptor such as a member of the Toll-like receptor super-family leads to the recruitment of adaptors (such as TRAF) to the cytoplasmic domain of the receptor (Figure 1.6). These adaptors, in turn, recruit the IKK complex comprising IKK alpha and/or IKK beta catalytic subunits and two molecules of NEMO. This leads to the phosphorylation and degradation of the I $\kappa$ B inhibitor. The canonical pathway activates NF- $\kappa$ B dimers comprising of RelA, c-Rel, RelB and p50.

#### 1.11.6 Non-canonical pathway

In this alternative NF- $\kappa$ B activation pathway, activation of NIK (NF- $\kappa$ B inducing kinase) upon receptor ligation leads to the phosphorylation and subsequent proteasomal processing of the NFKB2 precursor protein p100 into mature p52 subunit (Figure 1.7). Then p52 dimerizes with RelB to appear as a nuclear RelB/p52 DNA binding activity and regulate a distinct class of genes (Bonizzi, Bebien et al. 2004). In contrast to the canonical signalling that relies upon NEMO-IKK mediated degradation of I $\kappa$ B $\alpha$ , - $\beta$ , - $\epsilon$ , the non-canonical signalling critically depends on NIK mediated processing of p100 into p52. This pathway utilizes an IKK complex that comprises two IKK $\alpha$  subunits, but not NEMO. Given their distinct regulations, these two pathways were thought to be independent of each other. However, recent analyses revealed that synthesis of the constituents of the non-canonical pathway, RelB and p52, is controlled by the canonical IKK-I $\kappa$ B-RelA/p50 signalling (Basak, Shih et al. 2008). This suggests that an integrated NF- $\kappa$ B system network underlies activation of both RelA and RelB containing dimer and that a malfunctioning canonical pathway will lead to an aberrant cellular response also through the non-canonical pathway.

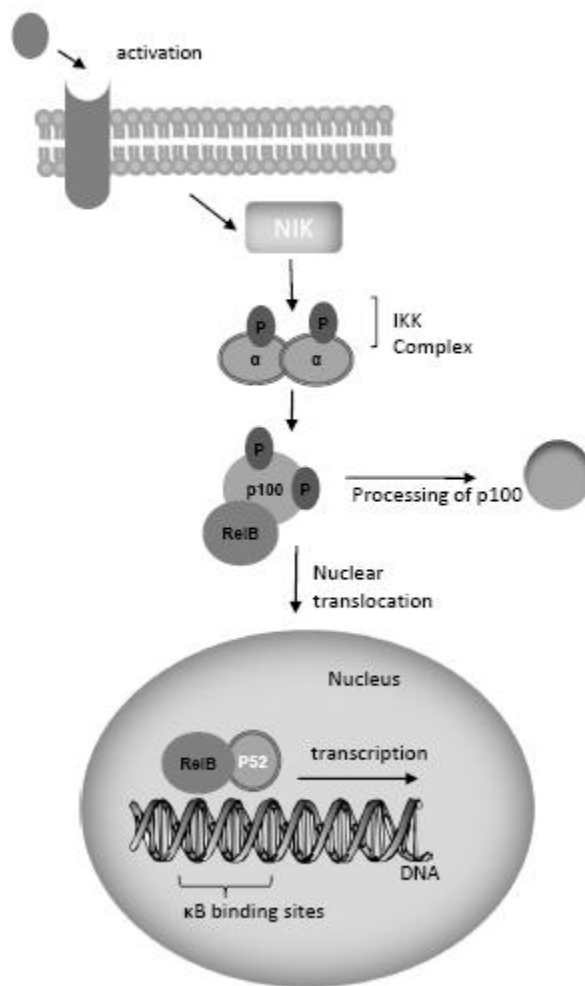


**Figure 1.7: NF-κB: The non canonical pathway**

Receptor binding leads to the activation of NIK, which phosphorylates and activates an IKK alpha complex that in turn phosphorylates the IκB domain of p100 leading to the liberation of p52/RelB. This heterodimer subsequently translocates to the nucleus to activate target genes regulated by κB sites.

#### 1.11.7 NF- $\kappa$ B and cancer

In many cancer cells (including breast cancer, colon cancer, prostate cancer, lymphoid cancers, and probably many others; see Diseases link) NF- $\kappa$ B is constitutively active and located in the nucleus. In some cancers, this is due to chronic stimulation of the IKK pathway, while in other cases (such as some Hodgkin's and diffuse large B-cell lymphoma cells) the gene encoding I $\kappa$ B can be mutated and defective. Moreover, several human lymphoid cancer cells have mutations or amplifications of genes encoding Rel / NF- $\kappa$ B transcription factors (REL in human B-cell lymphoma) and many multiple myelomas have mutations in genes encoding NF- $\kappa$ B signaling regulatory proteins that lead to constitutive activation of NF- $\kappa$ B. It is thought that continuous nuclear Rel / NF- $\kappa$ B activity protects cancer cells from apoptosis and in some cases stimulates their growth. Therefore, many current anti-tumour therapies seek to block NF- $\kappa$ B activity as a means to inhibit tumour growth or to sensitize the tumour cells to more conventional therapies, such as chemotherapy.

#### 1.11.8 NF- $\kappa$ B, senescence and ageing

The NF- $\kappa$ B family of ubiquitously transcription factors is widely known as key regulators of inflammatory and immune response. However, more recently they have been shown to function as regulators of diverse cellular processes such as cell proliferation and differentiation and the response to stresses such as oxidative, physical and chemical stress. Activation of NF- $\kappa$ B also blocks apoptosis and promotes cell survival.

A previous study in our lab suggested that the loss of proliferative potential in the HMF3A conditionally immortal fibroblasts may involve the activation of the NF- $\kappa$ B pathway (Hardy, Mansfield et al. 2005). NF- $\kappa$ B has also been shown to be associated

with growth arrest in the study of Penzo (Penzo, Massa et al. 2009) who has shown that acute activation of NF- $\kappa$ B in murine embryo fibroblasts results in growth arrest. The growth arrest was associated with repression of 20 genes essential for cell cycle progression that are known targets of either E2F or FOXM1.

In addition, Adler (Adler, Sinha et al. 2007) using a systematic bioinformatic approach to identify combinatorial cis-regulatory motifs showed that NF- $\kappa$ B activity controlled cell cycle exit and was continually required to enforce many features of ageing in a tissue specific manner. Moreover activation of NF- $\kappa$ B with age is consistent with elevated levels inflammatory markers and a pro-inflammatory phenotype associated with many age related diseases. Factors that mediate NF- $\kappa$ B and inflammation include the insulin/IGF pathway, SIRT1, FOXO, PDC-1 and PPAR (Salminen, Ojala et al. 2008). Expression of relA was found to be lower in senescent cells (Helenius, Hanninen et al. 1996) whereas c-Rel was elevated (Bernard, Gosselin et al. 2004). Kriete (Kriete, Mayo et al. 2008) showed that there was a constitutive activation of NF- $\kappa$ B in older human subjects compared to young donors.

## **1.12 MICRO-RNAS**

### **1.12.1 Introduction**

Micro-RNAs are a class of post-transcriptional regulators (Kusenda, Mraz et al. 2006; Vasudevan, Russell et al. 2007; Place, Li et al. 2008). They are short ~22 nucleotide RNA sequences that bind to fully or partially complementary sequences in the 3' UTR of multiple target mRNAs, usually resulting in their silencing (Bartel 2004). Micro-rnas have been predicted to target ~60% of all genes (Friedman, de Jong et al. 2007), are abundantly present in all human cells (Lim, Lau et al. 2003) and are able to repress hundreds of targets (Brennecke, Stark et al. 2005).

Micro-rnas were first discovered in 1993 by Victor Ambros, Rosalind Lee and Rhonda Feinbaum during a study into development in the nematode *C. elegans* regarding the gene *lin-14* (Lee, Feinbaum et al. 1993). This screen led to the discovery that the gene *lin-14* was able to be regulated by a short RNA product from *lin-4* itself, a gene that transcribed a 61 nucleotide precursor that matured to a 22 nucleotide mature RNA which contained sequences partially complementary to multiple sequences in the 3' UTR of the *lin-14* mRNA. This complementarity was sufficient and necessary to inhibit the translation of *lin-14* mRNA. Since then, over 10,000 miRNAs have been discovered in all studied multicellular eukaryotes including mammals, fungi and plants. More than 700 miRNAs have so far been identified in humans ([www.miRbase.com](http://www.miRbase.com)) and over 800 more are predicted to exist (Bentwich, Avniel et al. 2005).

Due to their abundant presence and far-reaching potential, miRNAs have all sorts of functions in physiology, from cell differentiation, proliferation, apoptosis (Brennecke, Hipfner et al. 2003) to the endocrine system (Poy, Eliasson et al. 2004), haematopoiesis (Chen, Li et al. 2004), fat metabolism (Wilfred, Wang et al. 2007). They display different expression profiles from tissue to tissue (Lagos-Quintana, Rauhut et al. 2002), reflecting the diversity in cellular phenotypes and as such suggest a role in tissue differentiation and maintenance.

#### 1.12.2 MiRNA and siRNA

Micro-rna are similar to, but distinct from, another type of short RNA, known as small interfering RNA (siRNA). Although miRNA and siRNA both have gene regulation functions, there are subtle differences. MiRNA may be slightly shorter than siRNA (which has 20 to 25 nucleotides). MiRNA is single-stranded, while siRNA is formed from two complementary strands. The two kinds of RNA are encoded slightly differently. siRNA are usually synthesised *in vitro* and introduced by transfection but can also be generated from shRNA or from miRNAs. The mechanism by which they regulate genes is also slightly different.

### 1.12.3 Biogenesis

Micro-RNA genes reside in regions of the genome as distinct transcriptional units as well as in clusters of polycistronic units - carrying the information of several micro-rnas (Lagos-Quintana, Rauhut et al. 2001; Lau, Lim et al. 2001; Reinhart, Weinstein et al. 2002). Studies suggest that approximately half of known micro-RNA reside in non-protein coding RNAs (intron and exon) or within the intron of protein coding genes (Rodriguez, Griffiths-Jones et al. 2004), generally within the 3'UTR. Micro-rna (miRNA) genes are generally transcribed by RNA Polymerase II (Pol II) in the nucleus to form large primary micro-rna transcripts (pri-miRNA) (Figure 1.8), which are capped and polyadenylated (Kim 2005). These pri-miRNA transcripts are then processed into micro-rna precursor (pre-miRNA) by the microprocessor complex Drosha–DGCR8 (Pasha) in the nucleus. The resulting precursor hairpin, the pre-miRNA, is exported from the nucleus by Exportin-5–Ran-GTP. In the cytoplasm, the RNase Dicer in complex with the double-stranded RNA-binding protein TRBP cleaves the pre-miRNA hairpin to its mature length. The functional strand of the mature miRNA is loaded together with Argonaute (Ago2) proteins into the RNA-induced silencing complex (RISC), where it guides RISC to silence target mRNAs through mRNA cleavage, translational repression or deadenylation, whereas the passenger strand (black) is degraded.

### 1.12.4 Mechanism of MiRNA regulation

Once incorporated into a RISC, the mature micro-rna binds to the mRNA target to negatively regulate gene expression in one of two ways that depend on the degree of complementarity between the miRNA and its target:

- miRNAs that bind to their mRNA targets with perfect (or nearly perfect) complementarity induce target-mRNA direct cleavage and destruction of the mRNA (Rhoades, Reinhart et al. 2002; Chen and Meister 2005) most usually in plants. miRNAs using this mechanism bind to miRNA complementary sites that are generally found in the coding sequence or ORF of the mRNA target.

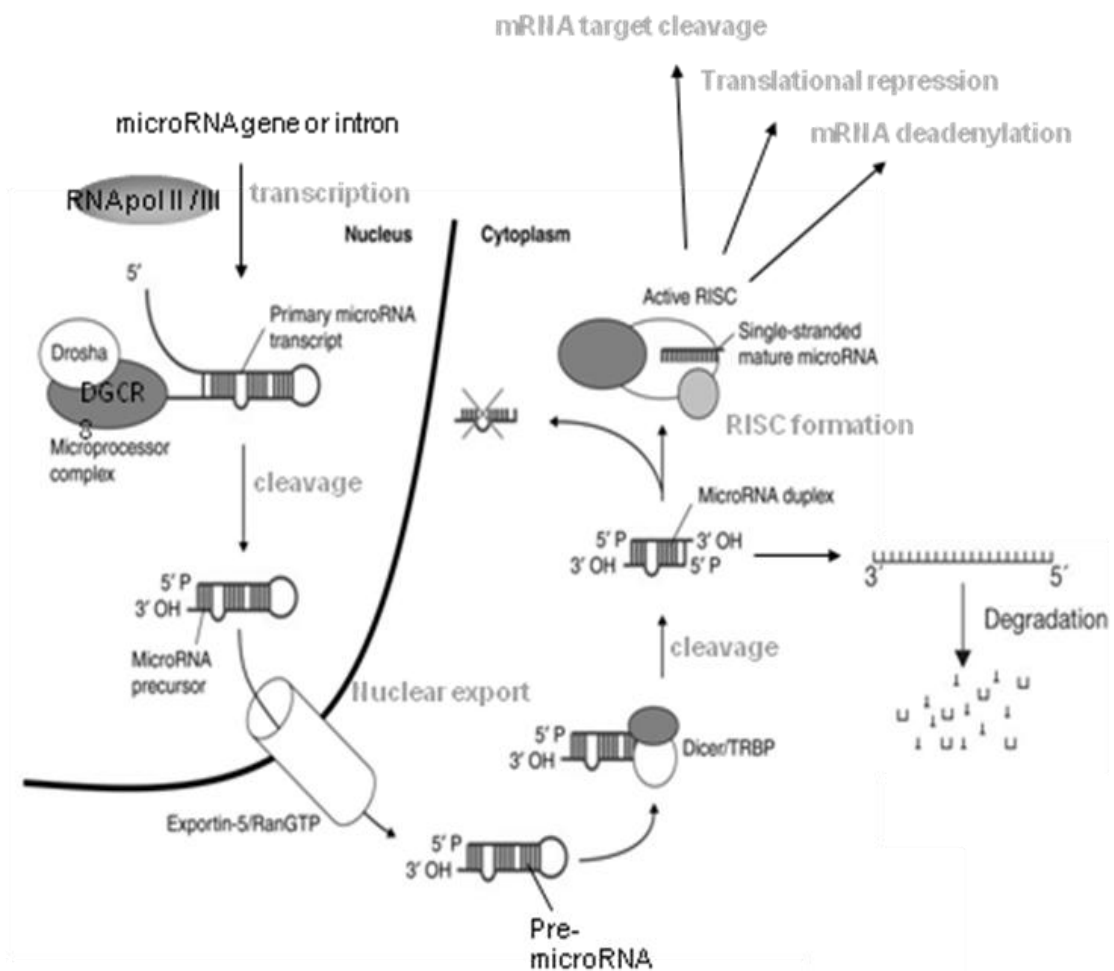


**Figure 1.8: Micro-RNAs biogenesis**

MicroRNA (miRNA) genes are generally transcribed by RNA Polymerase II (Pol II) in the nucleus to form large primary microRNA transcripts (pri-miRNA, which are capped and polyadenylated). These pri-miRNA transcripts are then processed into microRNA precursor (pre-miRNA) by the microprocessor complex Drosha–DGCR8 (Pasha) in the nucleus. The resulting precursor hairpin, the pre-miRNA, is exported from the nucleus by Exportin-5–Ran-GTP. In the cytoplasm, the RNase Dicer in complex with the double-stranded RNA-binding protein TRBP cleaves the pre-miRNA hairpin to its mature length. The functional strand of the mature miRNA is loaded together with Argonaute (Ago2) proteins into the RNA-induced silencing complex (RISC), where it guides RISC to silence target mRNAs through mRNA cleavage, translational repression or deadenylation, whereas the passenger strand (black) is degraded.



- In contrast, nearly all animal miRNAs studied so far are not usually exactly complementary to their mRNA targets, and seem to inhibit protein synthesis while retaining the stability of the mRNA target (Ambros 2004). miRNAs that bind to mRNA targets with imperfect complementarity block target gene expression at the level of protein translation. Recent evidence indicates that miRNAs might also affect mRNA stability. Complementary sites for miRNAs using this mechanism are generally found in the 3' untranslated regions (3' UTRs) of the target mRNA genes.

It has been suggested that transcripts may be regulated by multiple miRNAs and that an individual miRNA may target numerous transcripts if their sequences have similarities. It all depends on the seed sequence which is formed by seven or eight nucleotides of the mature miRNA, starting from the first or second nucleotide, and is most crucial for interaction between the miRNA and its target.

#### 1.12.5 Micro-RNAs and cancer

The relevance of miRNAs to cancer was suggested by changes in their expression patterns (Iorio, Ferracin et al. 2005; Volinia, Calin et al. 2006) and recurrent amplification and deletion of miRNA genes in tumours (Akao, Nakagawa et al. 2006; Dews, Homayouni et al. 2006).

Several miRNAs have emerged as candidate components of oncogene and tumour-suppressor networks. The miR-17-92 cluster (He, Thomson et al. 2005; O'Donnell, Wentzel et al. 2005; Dews, Homayouni et al. 2006), miR-372/373 (Voorhoeve, le Sage et al. 2006) and miR-155/BIC (Tam and Dahlberg 2006) have been implicated as proto-oncogenes in B-cell lymphomas and testicular cancers. On the other hand, miR-15-16 is frequently deleted in patients with chronic lymphocytic leukaemia (CLL) (Calin, Dumitru et al. 2002; Mraz, Pospisilova et al. 2009). Expression studies and functional studies have also revealed the potential tumour-suppressive roles of let-7 in various

cancers (Johnson, Grosshans et al. 2005; Mayr, Hemann et al. 2007), possibly owing to its ability to repress key oncogenic components, including Ras and HMGA2.

A study of mice altered to produce excess c-myc — a protein implicated in several cancers — shows that miRNA has an effect on the development of cancer. Mice engineered to produce a surplus of types of miRNA namely the cluster mir-17–92 found in lymphoma cells developed the disease within 50 days and died two weeks later. In contrast, mice without the surplus miRNA lived over 100 days (Cui, Li et al. 2007). Another study found that two types of miRNA (miR 17-5p and miR-20b) inhibit the E2F1 protein, which regulates cell proliferation. miRNA appears to bind to messenger RNA before it can be translated to proteins that switch genes on and off (O'Donnell, Wentzel et al. 2005).

Consistent with this, the suppression of key components of the miRNA biogenesis machinery in cancer cells has been reported to promote transformation both *in vitro* and *in vivo* (Kumar, Lu et al. 2007). The true extent to which the disruption of miRNA pathways has a role in tumorigenesis remains to be determined. However, early indications are that this family of genes is intimately integrated into the regulatory processes that are normally disrupted during transformation. Moreover, the placement of several miRNAs into known oncogenic and tumour-suppressor networks is beginning to solve longstanding mysteries of how the circuitry of these pathways is wired.

#### 1.12.6 Micro-RNA and senescence

Several studies have started linking micro-RNA regulation and cellular senescence but the exact mechanisms of this relation remains to be specified.

The ability of miRNAs to regulate a variety of target genes allows them to induce changes in multiple pathways and processes such as development, apoptosis, proliferation and differentiation. MiRNAs could therefore facilitate the complex cellular changes required to establish the senescent phenotype. Identification of the mRNA

sequences that miRNAs regulate is mainly derived using bioinformatics techniques. The mirBase sequence database is the main repository for miRNA sequence and target information and contains 695 human miRNA sequences, each with the potential to regulate on average 1000 gene targets. It is this large number of potential targets across different biological pathways that could give miRNAs the power to potentially induce complex cell phenotypes, like senescence.

Several studies highlight a number of senescence-associated micro-rnas such as Let-7f, miR-499, miR-371 (Wagner, Horn et al. 2008), miR-372, miR-373 (Voorhoeve, le Sage et al. 2006), miR-34a (He, He et al. 2007; Tazawa, Tsuchiya et al. 2007), miR-34b and miR-34c (Kumamoto, Spillare et al. 2008), miR-20b (Poliseno, Pitto et al. 2008) In addition, tumour-suppressive miR-34a expression induced senescence-like growth arrest through modulation of the E2F pathway in human colon cancer cells (Tazawa, Tsuchiya et al. 2007).

### **1.13 MODEL OF STUDY: HMF3A CELLS**

One of the main stumbling blocks in studying the molecular pathways that underlie the finite proliferative life span has been the absence of suitable model systems for study because of the asynchrony of this process in heterogeneous cell populations that are typically used for serial sub-cultivation. Studies with human cells are further complicated by the genetic, epigenetic and proliferative variation that can exist between different donors as well as phenotypic differences between cells within the cultures. To simplify this process many investigators study oncogene-induced senescence (OIS) with the expression of activated oncogenes such as RASV12, RAF, BRAF or E600 since it occurs prematurely without telomere attrition and can be induced acutely in a variety of cell types (Serrano, Lin et al. 1997; Michaloglou, Vredeveld et al. 2005; Collado and Serrano 2010).

A different approach was taken by making use of the finding that reconstitution of telomerase activity by introduction of the catalytic subunit of human telomerase (hTERT) alone was incapable of immortalising all human somatic cells (Bodnar,

Ouellette et al. 1998; Vaziri, Ni et al. 1998), but inactivation of the p16-pRb and p53-p21 pathways were required in addition (Counter, Meyerson et al. 1998; Kiyono, Foster et al. 1998). It was found that expressing LT, a viral oncoprotein that binds and inhibits the activity of several proteins, including p53 and Rb (Ali and DeCaprio 2001), together with expressing hTERT, can immortalize human primary mammary fibroblasts by preventing cellular senescence (O'Hare, Bond et al. 2001) (Figure 1.9).

This observation permitted the use a thermolabile mutant (U19tsA58) of LT antigen to develop a line of conditionally immortalised human mammary fibroblasts (HMF3A) that remain stringently temperature sensitive and show no sign of transformation in >300 population doublings (Figure 1.9). These cells are immortal if grown at 34°C but undergo an irreversible growth arrest within 5 days upon shift up to 38°C when the thermolabile T antigen is inactivated (O'Hare, Bond et al. 2001). When these cells cease dividing, SA- $\beta$ -Gal activity is induced and the growth-arrested cells have features and express genes in common with senescent cells (Hardy, Mansfield et al. 2005). Since these cells growth arrest in a synchronous manner they are potentially an excellent starting point for dissecting the pathways that underlie cellular senescence and act downstream of p16-pRb and p53-p21.

For these reasons, the conditionally immortalised HMF3A system represented a potential system with which to dissect telomere-independent cellular senescence pathways by determining target genes ability to complement the growth of these cells under non permissive conditions.

#### 1.13.1 Reconstitution of WT LT activity in the HMF3A system alone

The conditionally immortalised phenotype of the HMF3A system is critically dependent upon the activity of U19tsA58 LT (Hardy *et al*, 2005; O'Hare *et al*, 2001). Dr. Louise Mansfield has shown in her thesis that reconstitution of wt LT activity into these cells by amphotropic retroviral infection was sufficient to overcome conditional senescence in a stable manner.

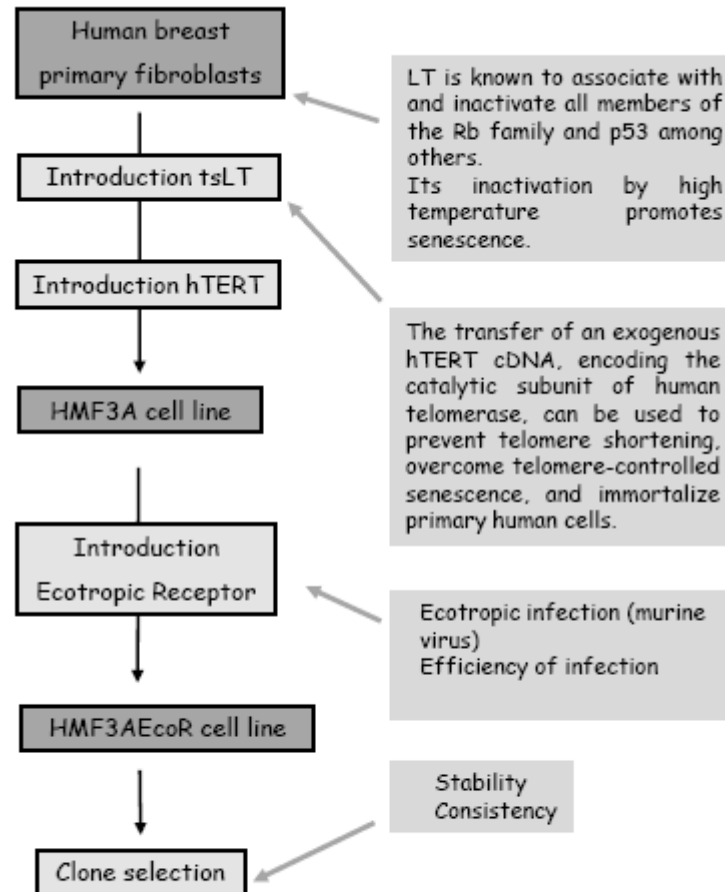


**Figure 1.9: Engineering of the CL3<sup>EcoR</sup> cells**

CL3<sup>EcoR</sup> cells were engineered by using a thermolabile mutant (U19tsA58) of LT antigen along with expressing the human catalytic subunit of human telomerase (hTERT) to develop a line of conditionally immortalized human mammary fibroblasts (HMF3A). In a second time, the HMF3A was refined by expressing a murine ecotropic receptor in a stable manner. Finally, after introduction of the receptor, the cells have also been cloned to produce a consistent and homogenous population.

### 1.13.2 Refinement of the HMF3A system by introduction of the murine ecotropic receptor

The HMF3A system was initially refined by Dr. Louise Mansfield by engineering the HMF3A cells to express a murine ecotropic receptor so that they become infectable with ecotropic retroviruses. This step has increased the cell transduction efficiency and the safety of the manipulations due to the fact that ecotropic viruses, unlike amphotropic viruses, cannot infect human cells.

## 1.14 ABROGATION OF THE P53 PATHWAY

Louise Mansfield also showed that abrogation of the p53 pathway into the mixed population of HMF3A<sup>EcoR</sup> by ecotropic retroviral delivery of either p21<sup>CIP1/WAF1/Sdi1</sup> shRNA, p53 GSE or p53 shRNA was sufficient to bypass the conditional growth defect.

## 1.15 ABROGATION OF THE PRB PATHWAY

Similarly to p53, Dr Louise Mansfield tried to target the pRb pathway for inactivation. Louise Mansfield showed that abrogation of the pRb pathway into the mixed population of HMF3AEcoR by ecotropic retroviral expression of E1A or E7 was sufficient to bypass the conditional growth defect.

However, the induction could not be attributed to pRb alone as both expression constructs used, namely E7 and E1A, could have used their multifunctional activity to abrogate other pathways as well as the pRb pathway. As a consequence, Dr. Mansfield tried to inactivate the pRb pathway using other reagents. The results of this investigation are presented here briefly for further understanding of the research strategy detailed in the thesis.

### 1.15.1 Inactivation of the INK4A Locus

In addition to E7 and E1A, and in order to investigate whether the abrogation of the Rb pathway specifically was sufficient to bypass the growth arrest, Dr. Louise Mansfield tried to inactivate the INK4A locus. Two splice variants are encoded by the *INK4A* locus; the cyclin-dependent kinase inhibitor p16<sup>INK4a</sup> and p14<sup>ARF</sup>. Both of these splice variants represent components of the pRb pathway: p16<sup>INK4a</sup> negatively regulates pRb functional activity by inhibiting cyclin D-CDK4/6 complexes, whereas p14<sup>ARF</sup> function downstreams of pRb to negatively regulate pRb effector signalling in an E2F-dependent process. Furthermore, p14<sup>ARF</sup> acts as a link between the pRb and p53 pathways as it stabilises p53 by binding to the Mdm2 protein.

Therefore, it was anticipated that abrogation of either, or even both, of these components would functionally inactivate the pRb pathway. Dr Louise Mansfield performed these experiments in the HMF3AEcoR cells.

#### *1.15.1.1 Knockdown of p14<sup>ARF</sup> by ShRNA*

Knockdown of p14<sup>ARF</sup> was performed by Dr. Louise in the HMF3A system with a construct found to silence p14<sup>ARF</sup> in HDF (Berns, Hijmans et al. 2004). The complementation did not work in this case compared to the positive control, p53 shRNA. This indicated that p14<sup>ARF</sup> knockdown was insufficient to overcome the HMF3A conditional growth arrest.

#### *1.15.1.2 Knockdown of p16<sup>INK4a</sup> by ShRNA*

In a similar manner, p16<sup>INK4a</sup> knockdown by shRNA was investigated by Dr. Louise Mansfield with two constructs that were previously shown to work and to be insufficient alone to bypass the induction of senescence in other cell types(Wei, Herbig et al. 2003; Reynolds, Leake et al. 2004), but in the HMF3A, only a small reduction or no reduction

in p16<sup>INK4a</sup> protein levels could be observed by Western blot analysis. Consequently, the level of p16<sup>INK4a</sup> knockdown was not considered significant.

p16<sup>INK4a</sup> knockdown was also proved insufficient to overcome conditional growth arrest in BJ cells constitutively expressing hTERT and a temperature sensitive mutant of LT (BJ-TERT-tsLT cells); (Berns, Hijmans et al. 2004).

#### *1.15.1.3 Constitutive Expression of Bmi-1*

Since RNAi could not effectively knock down p16<sup>INK4a</sup> at the protein level, an alternative method to inactivate the INK4A locus was sought by Dr. Louise Masfield. Bmi-1 is a transcriptional repressor of the PcG family that promotes stable, epigenetic gene silencing through chromatin modifications mediated by histone methylation (van der Lugt, Domen et al. 1994). Its constitutive expression leads to the inactivation of the INK4A locus. Bmi-1 has been shown to be significantly down-regulated upon replicative senescence in primary HDFs, but not in quiescent HDFs, whereas its over-expression was sufficient to extend the replicative lifespan of some HDF strains (Jacobs, Kieboom et al. 1999; Itahana, Zou et al. 2003). A Bmi-1 retroviral expression construct, pBabepuro-Bmi-1 was introduced into HMF3A<sup>EcoR</sup> cells by Dr. Louise Mansfield and assessed for its ability to complement the conditional growth defect of these cells. Not only did the complementation not work but Western blot analysis also revealed that ectopic expression of Bmi-1 did not affect the steady-state levels of p16<sup>INK4a</sup> protein.

### **1.16 AIM OF THE THESIS**

Due to the asynchronous nature of the growth arrest, senescence is a difficult process to study in serially sub-cultivated primary human cells. Therefore, a conditionally immortalised human mammary fibroblast cell line was developed in the JAT laboratory by retroviral transduction of early passage, adult interlobular mammary fibroblasts with a temperature sensitive (ts), non-DNA-binding mutant SV40 LT,



namely U19tsA58, and hTERT (O'Hare, Bond et al. 2001). The HMF3A cells have been modified by the stable expression of an ecotropic receptor allowing more efficient and safe use of ecotropic virus supernatants in the cells. After introduction of the receptor, the cells have also been cloned to produce a consistent and homogenous population. This represented a good model in which to study cellular senescence.

The aims of the thesis were the following:

1. Validation of the HMF3A<sup>EcoR</sup> clone 3 or CL3<sup>EcoR</sup>

It was important to specify the senescence model and test the sensitivity of the complementation assay in the mixed population of HMF3A<sup>EcoR</sup> cells and the clonal model, CL3<sup>EcoR</sup>, to compare their sensitivity, consistency and representativity. Another big objective was to optimise the complementation assay to be more standardised and with a minimal background.

2. Validation of the complementation assay using p53 and pRb abrogation alone

Here, I wanted to confirm that abrogation of either the p53 pathway alone or the pRb alone were both sufficient to bypass the conditional growth arrest in both cell models.

3. To identify the changes in gene expression triggered by senescence by expression profiling and validate NF- $\kappa$ B involvement in senescence

Since these cells growth-arrest in a synchronous manner, Affymetrix expression profiling was used to identify the genes differentially expressed specifically upon senescence. I also wanted to validate some of the identified targets *in vitro*. Hardy *et al* have shown previously, thanks to an *in silico* promoter analysis that cEBPbeta and NF- $\kappa$ B might be activated upon senescence (Hardy, Mansfield et al. 2005). I wanted to validate that this activation was real in this model both by the expression profiling and *in vitro* validation.

4. To look for new targets by using a shRNA functional screen using complementation assay

Since a complementation assay was optimised and validated in these cells and had permitted successfully to check the importance of several genes from the pRb or p53 pathway, the next step was to widen this principle to a gene library in order to identify new senescence key effectors, not necessarily already described as such in the literature. I wanted to apply a retroviral shRNA screen covering ~10,000 genes with the same cell model by complementation assay.

5. To identify the changes in micro-rnas expression triggered by senescence by expression profiling

At the beginning of the thesis, the literature was submerged by articles about the new forefront micro-RNAs represented in gene expression modulation responsible of various cellular mechanism and diseases. I consequently planned to profile micro-RNAs expression upon senescence in the model thanks to MiRNA microarray technology (LC Sciences). I also wanted to validate the identified targets *in vitro*.

6. Identify miRs targets and effect *in vitro*

I then wanted to see what effect these validated micro-rnas targets had on the transcriptome by expression profiling and *in silico* analysis and whether these new data would overlap with previous data obtained within this thesis.

## **2 MATERIAL AND METHODS**

### **2.1 MAMMALIAN CELL CULTURE**

#### **2.1.1 Cell lines and Culture**

HEK293T, Phoenix Eco and Phoenix Ampho were obtained from the ATCC. HMF3A and HMF3A<sup>ECoR</sup> cells were a proprietary cell line (O'Hare, Bond et al. 2001). BJ primary cells were obtained from ATCC.

#### **2.1.2 Cell media**

Tissue culture media and cell culture reagents were purchased from Invitrogen. All HMF3A and primary cells were maintained in Dulbecco's Modified Eagle Medium (DMEM) supplemented with 2 millimolar (mM) glutamine, 100 units/ml penicillin, 100 µg/ml streptomycin and 10% volume per volume (v/v) heat inactivated foetal calf serum (FCS).

Primary cells, after infection with RAS, were maintained in the same medium but phenol free and the FCS was replaced by heat inactivated charcoal stripped FBS (fetal bovine serum).

#### **2.1.3 Cell Culture Conditions**

All cell lines were maintained in a 5% CO<sub>2</sub> and 20% oxygen atmosphere.  $\phi$  amphotropic and  $\phi$  ecotropic cell lines were maintained at 37°C. The HMF3A cell line and HMF3AEco<sup>R</sup> cells were maintained at 34°C  $\pm$ 0.5°C, a temperature at which the cells

proliferated continuously due to the functional activity of U19tsA58 LT. HMF3A temperature shift experiments were performed at  $38^{\circ}\text{C} \pm 0.5^{\circ}\text{C}$ , a temperature at which U19tsA58 LT was inactivated and the cells became senescent within a period of 5 days (O'Hare *et al*, 2001). Primary cells were maintained at  $37^{\circ}\text{C} \pm 0.5^{\circ}\text{C}$ .

#### 2.1.4 Sub-Culturing of Cells

Cells were grown until a sub-confluent state was reached (approximately 80% confluence). Media was then removed and the monolayer of cells was washed twice with PBS. The monolayer was detached using 1x trypsin-EDTA (1 ml/T75 cm<sup>2</sup> flask) for 5 mins at  $34^{\circ}\text{C}$  and the trypsin-EDTA was inactivated by adding 10 ml of complete media. Cells were then plated at a defined ratio (e.g. 1 in 8 of the total cells), or counted using a haemocytometer and plated at the required density.

#### 2.1.5 Preservation of Cells

Cells from a sub-confluent T75 cm<sup>2</sup> flask were trypsinised, resuspended in complete media and spun down at 1200 revolutions per minute (rpm) for 2 mins to remove any traces of trypsin. Cells were resuspended in FCS supplemented with 10% dimethyl sulphoxide (DMSO; BDH). 2x 1 ml aliquots were then transferred to cryotubes and frozen at  $-70^{\circ}\text{C}$  wrapped in several layers of tissue for insulation. Tubes were transferred into liquid nitrogen (N<sub>2</sub>) after 24 hrs.

#### 2.1.6 Recovery of Frozen Cells

Cells were removed from liquid N<sub>2</sub> storage and thawed rapidly at  $37^{\circ}\text{C}$ . 9 ml of complete media was added to the cells in a 15 ml falcon tube and cells were pelleted at 1200 rpm for 2 mins to remove DMSO-containing media. The cell pellet was resuspended in 10 ml of complete media, transferred to a T25 cm<sup>2</sup> flask and incubated at

the appropriate temperature in a 5% CO<sub>2</sub> and 20% oxygen atmosphere until sub-confluence was reached. Cells were then sub-cultured, as described above.

## 2.2 RETROVIRAL AND LENTIVIRAL INFECTIONS

### 2.2.1 Retroviral and Lentiviral constructs

Retroviral vector pBabepuro-wt LT cDNA and pRetroSuper were provided by O. Gjoerup, University of Pittsburg, USA; pLPC-12SE1AORI was from S. Lowe, Cold Spring Harbor Laboratory, USA; pBabePuro HPV16 E7 was provided by K. Munger, Harvard Medical School, USA; pLXIPGSEp53 was provided by A. Gudkov, Roswell Park Cancer Institute, USA; pWZLpuro $\epsilon$ -EcoR was from J. Downward, CRUK, UK; pWZL-BlastF was from J. Morgenstern, Millenium Inc., USA; pYESir2-puro was from Addgene and pLPCX was purchased from BD Biosciences. pLPCX-E2F-DB was constructed by subcloning the E2F-DB gene from pCMV-DB provided by Xin Lu (LICR, UK) into pLPCX.

The following Foxm1 constructs were obtained from Rene Medema:

pWPT-GFP: lentiviral empty vector (expressing GFP as a control for infection)

pWPT- FoxM1 wt : lentiviral human FoxM1c full-length (aa 1-763)

pWPT- FoxM1  $\Delta$ N/ $\Delta$ KEN : lentiviral human FoxM1c N-terminal deleted (aa 210-763)  
constitutively active and non-degradable (Laoukili et al., Cell Cycle 7:2720-26, 2008)

pWPT- FoxM1 6K-R : lentiviral human FoxM1c K201, 218, 356, 460, 478, 495R)  
Sumoylation-defective mutant (not published)

The FOXM1 constructs were then cloned into pLPCX by Catia Caetano.

DEPDC1, HMGB2 and MLF1-IP two splice forms Clone ID: 8860370- BC141854 (renamed 88 here) and Clone ID: 40108113- BC131556 (renamed 401 here) constructs were purchased from geneservice and cloned into pLPCX by Parmjit Jat.

DBF4 (ASK) was obtained as a cDNA clone from UCL cloned into pGEM-T. It was then subcloned into pLPCX by Parmjit Jat.

NEK2 was obtained as a cDNA clone from Andrew Fry Leicester in pGEM-3Zf(-)- 2 kb insert and cloned into pLPCX by Parmjit Jat.

PLK4 cDNA clone was obtained from David Glover who obtained it from GeneService and cloned into pLPCX by Parmjit Jat.

hBub1 was obtained as HA-BUB1 in pLB(N)CX blasticidin resistance vector from Ole Gjoerup.

CDKN2C (p18) and MELK were purchased from geneservice and cloned into pLPCX by Parmjit Jat.

LNCX-ER: RAS was kindly provided by Jesus Gil (Barradas et al, 2009).

The miR expressing vectors were purchased from Gene Service.

Lentiviral vector encoding tetracycline inducible expression of IKB-SR was provided by P. Meier, The Breakthrough Toby Robins Breast Cancer Research Centre, UK. Lentiviral shRNAmir silencing constructs derived from the Open Biosystems human GIPZ lentiviral shRNAmir library, were provided by the UCL shRNA library core facility. Lentiviral Gag/Pol expression vector p8.9 and pMDG, VSV-G viral envelope expression vector were provided by G. Towers (UCL, UK) and D. Trono (University of Geneva, Switzerland).

## 2.2.2 Viral Packaging and infections

### 2.2.2.1 Packaging of Retroviral Constructs

$\phi$  amphotropic and  $\phi$  ecotropic retroviral packaging cells were plated at  $1 \times 10^6$  cells/10 cm plate the day prior to transfection. Cells were transfected the following day (at approximately 30% confluence) with 10 or 20  $\mu$ g (for the micro-rna experiment) of retroviral vector DNA and 12  $\mu$ l of FuGENE 6 Transfection reagent (ROCHE), according to manufacturer's instructions. 24 hrs post-transfection, media was changed

using 10 ml fresh media per plate. 48 hrs post-transfection, the retroviral supernatant was harvested, filtered through a 0.45  $\mu\text{m}$  filter, and either used immediately or quickly frozen at  $-80^{\circ}\text{C}$ .

A second harvest was made when needed by re-adding 10 ml of media into the harvested plates and harvesting the supernatant in a similar way the next day. Frozen aliquots of retroviral supernatant were thawed rapidly at  $37^{\circ}\text{C}$  before use.

#### *2.2.2.2 Packaging of Lentiviral Constructs*

HEK293T packaging cells were plated at  $1 \times 10^6$  cells/10cm plate the day prior to transfection. Cells were transfected the following day (at approximately 80% confluence) with 1.5 $\mu\text{g}$  of lentiviral pGIPZ DNA vector mixed with 1 $\mu\text{g}$  p8.91 (gag-pol expressor) and 1 $\mu\text{g}$  pMDG.2 (VSV-G expressor) and 10  $\mu\text{l}$  of FuGENE 6 Transfection reagent (ROCHE): First 200 $\mu\text{l}$  of medium were mixed with the fucose then after an incubation of 5 min, the DNA mix was added and then after an incubation of 15 min, the mix medium/fucose/DNA was added to the cells. 24 hrs post-transfection, media was changed using 10 ml fresh media per plate. 48 hrs post-transfection, the retroviral supernatant was harvested, filtered through a 0.45  $\mu\text{m}$  filter, and either used immediately or quickly frozen at  $-80^{\circ}\text{C}$ .

A second harvest was made when needed by re-adding 10 ml of media into the harvested plates and harvesting the supernatant in a similar way the next day. Frozen aliquots of retroviral supernatant were thawed rapidly at  $37^{\circ}\text{C}$  before use.

#### *2.2.2.3 Infection with viral supernatant and selection*

Cells utilized for infection were seeded at  $5 \times 10^5$  cells/T75  $\text{cm}^2$  flask or  $1 \times 10^6$  cells/T175  $\text{cm}^2$  flasks. The following day (at approximately 30% confluence), media was aspirated, and cells were infected with retroviral or lentiviral supernatant in the presence of 8 $\mu\text{g}/\text{ml}$  polybrene. The volume of retroviral supernatant used for the infection varied for each experiment according to the viral titre. Cells were then incubated at  $34^{\circ}\text{C}$  for 24 hrs.

The following day, media was replaced with 10ml (for T-75 cm<sup>2</sup> flasks) or 15 ml (for T-175 cm<sup>2</sup> flasks) fresh media then, 4 days post-infection, antibiotic selection was added (2 µg/ml puromycin for retroviral infection or 6 µg/ml puromycin for lentiviral infection or 5 µg/ml blasticidin, for the amphotropic constructs; Invitrogen), and media (including antibiotic) was changed every 3-4 days.

## **2.3 DNA MANIPULATION**

### **2.3.1 Plasmid DNA Preparation**

All plasmid preparations (both small scale and large scale preparations) were carried out using QIAGEN kits and following the manufacturer's instructions.

#### *2.3.1.1 Small Scale Plasmid Preparation*

Bacterial stocks were kept at -70°C in LB medium containing 15% glycerol. Liquid cultures of bacteria picked from single colonies were grown in a bacterial shaker (vigorous shaking) overnight at 37°C in 5 ml of LB medium with the appropriate antibiotic. 1.5 ml of culture was then transferred to a 1.5 ml microfuge tube and spun at 13000 rpm for 30 sec. The cell pellet was resuspended in 250 µl of solution P1 (50 mM Tris/hydrochloric acid (HCl), pH 8.0, 10 mM EDTA and 100 mg/ml RNase A). 250 µl of solution P2 (200 mM sodium hydroxide (NaOH) and 1% sodium dodecyl sulphate (SDS)) was added and gently mixed by inverting the 1.5 ml microfuge tube 4-6 times. To the same 1.5 ml microfuge tube, 350 µl of solution N3 (3.0 M sodium acetate, pH 5.5) was added and immediately mixed by inverting the 1.5 ml microfuge tube 4-6 times. The mixture was then spun in a microfuge for 10 mins at 13000 rpm and the supernatant transferred to a QIAprep column. The column was centrifuged for 30 sec at 13000 rpm then the flow-through was discarded. The column was then washed with 0.5 ml of PB buffer (QIAprep Spin Miniprep kit, QIAGEN) and then 0.75 ml of PE buffer



(QIAprep Spin Miniprep kit, QIAGEN). DNA was then eluted with 50  $\mu$ l of ddH<sub>2</sub>O. All solutions used were from the QIAfilter Plasmid Mini kit, QIAGEN.

### *2.3.1.2 Large Scale Plasmid Preparation*

200 ml of LB medium containing the appropriate antibiotic was inoculated with an overnight culture of bacteria and grown overnight at 37°C with vigorous shaking. Bacteria were harvested at 6100 rpm for 15 mins at 4°C using an SLA 1500 rotor and Sorvall RC5C centrifuge. The cell pellet was resuspended in 10 ml of resuspension buffer P1 (50 mM Tris-HCl pH 8.0, 10 mM EDTA and 100  $\mu$ g/ml RNase A, stored at 4°C). 10 ml of lysis buffer P2 (200 mM NaOH and 1% SDS) was added and, after a 5 mins incubation step at room temperature, 10 ml of ice-cold neutralisation buffer P3 (3mM potassium acetate pH 5.5) was added and the mixture was directly applied to a QIAfilter Cartridge. The QIAfilter Cartridge was incubated at room temperature for 10 mins before the cell lysate was filtered and directly applied to a previously equilibrated QIAGEN-tip 500 column (equilibration buffer QBT: 750 mM NaCl, 50 mM MOPS (3 – (N-morpholino) propanesulphonic acid) pH 7.0, 15% ethanol (v/v) and 0.15% Triton X-100) and allowed to enter the resin by gravity. The column was washed twice with 30 ml of wash buffer QC (1 M NaCl, 50 mM MOPS pH 7.0 and 15% ethanol). DNA was then eluted with 15 ml of elution buffer QF (1.25 M sodium chloride (NaCl), 50 mM Tris-HCl pH 8.5 and 15% ethanol) and precipitated in 10.5 ml of isopropanol at room temperature. Centrifugation was performed at 11000 rpm for 30 mins at 4°C using the SS34 rotor and Sorvall RC5C centrifuge. The DNA pellet was washed with 70% ethanol then centrifuged again at 11000 rpm for 5 mins. The supernatant was removed and the DNA pellet was air dried for 5 mins. DNA was resuspended in 200  $\mu$ l ddH<sub>2</sub>O in a 1.5 ml microfuge tube. All solutions used were from the QIAfilter Plasmid Maxi kit, QIAGEN.

### 2.3.2 DNA Quantification

To determine DNA concentration, the OD of the solution was measured at 260 nm ( $OD_{260}$ ) using a Nanodrop 1000 from Thermo scientific. DNA concentration was calculated using the relationship: 1 OD unit at 260 nm = 50  $\mu$ g/ml DNA.

### 2.3.3 DNA-Agarose Gel Electrophoresis

DNA fragments were loaded with 1x DNA loading buffer (2.5% Ficoll, 0.04% (w/v) bromophenol blue and 0.04% Xylene) and fractionated by electrophoresis on 1% (w/v) agarose (Invitrogen) gels, prepared in 1x TAE (40 mM Tris-acetate and 2 mM EDTA) with 1  $\mu$ g/ml ethidium bromide (BDH). Electrophoresis in 1x TAE was carried out in electrophoresis tanks and DNA fragments were separated at a constant voltage of 100 Volts (V) for a minimum of 20 mins. Samples were loaded alongside 5  $\mu$ l 1kb+ DNA ladder (Invitrogen). Ethidium bromide stained DNA fragments were then visualised on a UVP (Dual intensity UV trans-illuminator), and an image was produced and printed with a Sony video graphic printer.

### 2.3.4 DNA Sequencing

For the miniprep DNA samples, DNA sequencing was outsourced to a sequencing service in the Institute of Neurology, Prion Unit.

### 2.3.5 Cloning of PCR Products

The cloning of the constructs used for complementation was the work of Dr. Louise Mansfield or Prof. Parmjit Jat.

## 2.4 RNA MANIPULATION

### 2.4.1 RNA Isolation

CL3<sup>EcoR</sup> and HMF3A cultures grown in T-75 cm<sup>2</sup> flasks were fed with fresh media the day prior to RNA extraction and were harvested at no greater than 80% confluence on the day of RNA extraction. Media was removed and the cells were washed twice with 1x PBS. 2.5 ml of TRIzol (Life Technologies) was then added to each T75 cm<sup>2</sup> flask and cells were left to lyse for 5 mins at room temperature. Cell lysates were then passed several times through a 5 ml pipette, after which the samples were incubated for 5 mins at room temperature. 0.2 ml of chloroform (per 1 ml of TRIzol used) was then added, and the samples were vigorously shaken by hand for 15 sec, followed by a 5 mins incubation step at room temperature. Samples were then centrifuged at 11000 rpm for 15 mins at 4°C using a SS34 rotor and Sorvall RC5C centrifuge. Following centrifugation, the aqueous phase of the mixture was transferred to a fresh tube and RNA precipitated with propan-2-ol (0.5 ml for each 1 ml of TRIzol used). Samples were incubated at room temperature for 10 mins then centrifuged at 10000 rpm for 10 mins at 4°C. Supernatant was removed and the pellet was washed once with ethanol diluted to 75% in DEPC (diethyl pyrocarbonate) treated H<sub>2</sub>O (0.1% DEPC dissolved in ddH<sub>2</sub>O; 1 ml of ethanol for each 1 ml of TRIzol used). The RNA pellet was briefly air-dried then resuspended in 50-100 µl of DEPC treated H<sub>2</sub>O and incubated at room temperature for at least 30 mins to ensure it was completely resuspended.

### 2.4.2 RNA Quantification

After RNA extraction, optical density of the solution was measured at 260nm (OD<sub>260</sub>) using a Bio-Rad spectrophotometer (Bio-Rad Smart Spec<sup>TM</sup> 3000 Spectrophotometer). RNA concentration was calculated using the relationship:

1OD unit at 260 nm = 40 µg/ml RNA

## 2.5 PROTEIN ANALYSIS

### 2.5.1 Preparation of Total Protein Extracts

HMF3A cultures grown in T75 cm<sup>2</sup> flasks were fed with fresh media the day prior to lysis and were harvested at no greater than 80% confluence on the day of lysis. For lysis, cells were washed twice with cold 1x PBS, and 0.5 ml of 1x radioimmunoprecipitation (RIPA) lysis buffer (150 mM NaCl, 1% Triton-X-100, 0.5% sodium deoxycholate, 0.1% SDS and 50 mM Tris pH 8.0) was added to each T75 cm<sup>2</sup> flask. 2 µl of Protease Inhibitor Cocktail (2 mM 4-[2-aminoethyl] benzenesulphonyl fluoride [AEBSF], 1 mM EDTA, 130 µM Bestatin, 14 µM E-64, 1 µM Leupeptin and 0.3 µM Aprotinin; Sigma) was added per 1 ml of lysis buffer used. Cells were incubated on ice for 30 mins then scraped and transferred to a 1.5 ml microfuge tube. Lysates were passed three times through a 21-gauge needle to shear the DNA then centrifuged at 10000 rpm for 30 mins at 4°C. The supernatant from each lysis reaction was transferred to a fresh 1.5 ml microfuge tube, aliquoted then stored at -20°C.

### 2.5.2 Determination of Protein Concentration

Protein concentrations were determined using the Bio-Rad protein assay (Bio-Rad Laboratories), a protein assay based on the Bradford assay [Bradford, 1976]. The dye reagent was diluted 1:5 in PBS. A BSA standard curve was established with protein dilutions ranging from 1-15 µg/ml. 2 µl of each sample were mixed with 1 ml of freshly diluted dye and incubated at room temperature for 5 mins. OD595 was measured (Bio-Rad Smart Spec™ 3000 Spectrophotometer) and plotted against protein concentration of standards. The regression coefficient was calculated and the unknown sample concentrations determined.

### 2.5.3 Sodium-Dodecyl-Sulphate-Polyacrylamide-Gel-Electrophoresis

8 % Sodium dodecyl sulphate-polyacrylamide gel electrophoresis (SDS-PAGE) gels were prepared from a 30% (w/v) acrylamide stock solution (containing a ratio of 29.2 acrylamide: 0.8 N,N'-methylenebisacrylamide; Genomic Solutions) in 375 mM Tris-HCl pH 8.8 and 0.1% (w/v) SDS. Gels were polymerised by addition of ammonium persulphate (APS) (0.1% [w/v] final; Bio-Rad) and TEMED (N,N,N',N' tetraethylenemethyldiamine, 0.0006% [w/v] final; BDH Laboratory). For 10, 12 and 15% SDS-PAGE gels, quantities of the polymerising agents were adjusted accordingly.

30 µg of each cell lysate (unless otherwise stated) was heated at 90°C for 5 mins with 2x Laemmli sample buffer (8% SDS, 40% glycerol, 20% 2-mercaptoethanol, 0.008% bromophenol blue and 0.260 mM Tris-HCl, pH 6.8) and fractionated by SDS-PAGE. Electrophoresis was carried out at a constant voltage of 100-150 V during the day (or 40 V overnight) in running buffer (25 mM Tris, 190 mM Glycine, 0.1% [w/v] SDS). Proteins were stacked through 2 cm of stacking gel (5% polyacrylamide, 125 mM Tris-HCl pH 6.8 and 0.1% [w/v] SDS, polymerised by addition of APS and TEMED, as before). Proteins were fractionated alongside broad-range pre-stained SDS-PAGE standards (Bio-Rad Laboratories).

### 2.5.4 Western Blotting of SDS-PAGE

Following separation via SDS-PAGE, proteins were transferred to a nitrocellulose membrane, Hybond-c extra (Amersham Life Science) by electrophoretic transfer in a wet tank blotting system (Bio-Rad Laboratories Trans-Blot cell). The transfer was carried out in transfer buffer (25 mM Tris, 190 mM glycine and 20% [v/v] methanol) for 4 hrs at a constant voltage of 60 V at 4°C or, alternatively, overnight at a constant voltage of 20 V (4°C).

The nitrocellulose membrane was then blocked by incubation in 5% (w/v) skimmed milk powder (Marvel, Premier Brands) and 0.005% (v/v) Tween-20 (BDH Laboratory) in 0.5x PBS (PBS/Marvel) at room temperature for 1 hr or overnight at 4°C. The filter was then incubated for 1 hr at room temperature, or overnight at 4°C with the primary antibody diluted in PBS/Marvel at the indicated dilutions (as described below). The filter was then washed three times (15 mins each at room temperature) in 0.05% (v/v) Tween 20 and 0.5x PBS (PBS/Tween) prior to incubation with horseradish peroxidase (HRP) conjugated secondary antibody (Amersham Life Sciences enhanced chemiluminescence [ECLTM] western blotting analysis system) diluted 1:2000 in PBS/Tween for 1 hr. Following three further washes (15 mins each at room temperature) in PBS/Tween, the filters were developed in HRP detection reagents for 90 sec, according to manufacturer's instructions (ECL<sup>TM</sup>, Amersham Pharmacia Biotech). The membrane was then wrapped with Saran-wrap and exposed to an auto-radiographic film for times varying from 10 sec to 2 hrs (Fujifilm Super RX X-ray film). Films were developed with an AGFA X-ray film processor.

#### 2.5.5 Antibodies Used

Anti-HPV16 E7 mouse monoclonal antibody (clone 8C9) was purchased from Zymed Laboratories Inc, anti-cyclin D1 mouse monoclonal (clone A12), was purchased from Santa Cruz Biotechnology; anti- $\beta$  Actin mouse monoclonal (clone AC-40) and anti- $\beta$ -Tubulin mouse monoclonal antibodies (clone 2-28-33) were purchased from Sigma; anti-p21 mouse monoclonal antibody (clone SX118) was a kind gift from X. Lu (LICR, London); anti-E1A mouse monoclonal antibodies (clone M3 and M73) were a kind gift from E. Harlow (Massachusetts General Hospital Cancer Center, Charlestown); The antibodies were diluted for Western blot analysis as follows: p21<sup>CIP1/WAF1/Sdi1</sup> (SX118) 1:500;  $\beta$ -Actin (AC-40) 1:2000;  $\beta$ -Tubulin 1:2000; cyclin D1 (A12) 1:1000; E7 1:100; and HRP-conjugated secondary antibodies 1:2000; E1A mouse monoclonal antibody M73 was used at 1:50.

## **2.6 GROWTH CURVES**

### **2.6.1 Cell line**

The cells used for this experiment are HMF3A cells. These are a conditionally immortalized human mammary fibroblast cell line constitutively expressing U19 tsA58 LT and hTERT (O'Hare, Bond et al. 2001). These cells exhibit an immortalized phenotype at 34°C but undergo an irreversible growth arrest after 5 days at 38°C. These cells were also engineered to express the murine ecotropic receptor in order to infect them with ecotropic viruses. Cells from a HMF3A<sup>EcoR</sup> mixed population and 6 different clonal cell lines were used: clone #2, #3, #10, #27, #32, #33.

### **2.6.2 Protocol**

Cells were seeded at 5000 cells per well in a 6-well plate format at day minus 1 and grown at three different temperatures: 34°C, 37°C and 38°C for 12 days. These cultures were in duplicates for each condition (cell line and temperature) and for each time point (126 wells in total). The numbers of cells were counted at day 0, day 5, day 7 and day 12 at these 3 growth temperatures with the cells.

## **2.7 IRREVERSIBILITY ASSAYS**

### **2.7.1 Cell line**

The cells used for this experiment are HMF3A<sup>EcoR</sup> cells from both the mixed population and clonal cell line: clone #3. The passage used at the beginning of the experiment for the mixed population is p22+11 and for the clone #3 is p22 +12 (11 and 12 passages respectively after EcoR introduction and clone selection).

### 2.7.2 Protocol

Cells were seeded at  $0.3 \times 10^6$  in T-75cm<sup>2</sup> flasks at day -1 and grown at three different temperatures: 34°C, 37°C and 38°C for 7 days then at 34°C for another 2 weeks. The numbers of cells were counted at day 0, day 7, day 14 and day 21 at these 3 growth temperatures with the cells being reseeded each time at  $2 \times 10^5$  per T-75 cm<sup>2</sup> flask at day 7 and 14. The reason for this reseeded is to eliminate the cooperative bias due to the cell density. Each growth condition for each time point was represented in triplicate for counting. Duplicate cultures were seeded at 1, 3, 5, 10, 15 and 20,000 cells per well in 6-well plates and incubated at 34°C or 38°C for 7 days and then shifted back to 34°C for 14 days. Cells were stained after 3 weeks with 2% (w/v) methylene blue in 50% (v/v) ethanol and each condition for each time point was photographed by phase-contrast microscopy.

## 2.8 GROWTH COMPLEMENTATION ASSAYS

### 2.8.1 Cell line

The cells used for this experiment are HMF3A<sup>EcoR</sup> and CL3<sup>EcoR</sup> used at p22+11 and p22+12 respectively.

### 2.8.2 Complementation experiment

The cells were seeded at  $1 \times 10^6$  cells per 175 cm<sup>2</sup> flask. The cells were then infected with 10ml of Phoenix Ampho packaged virus supernatant for: 10µg of pLPCX, 10µg of pLPC LT WT, 10µg of pLPC E2F-DB, 10µg of pLPC 12S E1A, 10µg of pLPC E7, 10µg of pRS Lamin A/C, 10µg of pRS p53 RNAi, 10µg of pRS p21<sup>CIP1/WAF1/Sdi1</sup> RNAi and 10 µg of pLXIP GSE p53 individually and 20ml of Phoenix Ampho packaged virus supernatant for 10µg of pLPC E7 (two harvests). The cells were incubated at 34°C



overnight and the media was changed the next day. On day 4, puromycin selection at 2 $\mu$ g/ml was applied for 7 days. The culture were then washed with PBS, trypsinated, counted and seeded at either 1K, 3K, 5K, 10K, 30K and 50K per well in 6-well plates whenever possible in duplicate or at  $0.5 \cdot 10^5$  in T-75 cm<sup>2</sup> flasks whenever possible in triplicate. The plates or flasks were incubated at 34°C overnight and the next day, the media was replaced by fresh media (2ml in wells or 10 ml in T-75 cm<sup>2</sup> flasks) before the cells were shifted to 38°C for 3 weeks.

At week 1, 2 and 3, the cells were photographed under a microscope and at week 3, the cells were stained with methylene blue and photographed.

## **2.9 SENESCENCE SPECIFIC EXPRESSION PROFILING**

### 2.9.1 Cell line

The cells used for this experiment were CL3E<sup>coR</sup> at the passage p22+6 (6 passages after EcoR introduction and clone selection).

### 2.9.2 RNA preparation

To perform the microarray procedure, total RNA was extracted from CL3<sup>EcoR</sup> cells incubated at 34°C for 7days to prepare the reference RNA sample or at 38°C for 7 days with the various constructs described in chapter one (PLPCX, PLPC E7, PLPC E1A, PLPC E2F-DB, PLXIP GSE p53, pRS Lamin A/C shRNA, pRS p21 shRNA and pRS p53 shRNA) to prepare the different conditions samples to analyse. Additional total RNA was extracted from quiescent CL3<sup>EcoR</sup> cells and HMF3S cells to prepare the quiescence and heat shock samples. RNA was extracted from biological triplicate cultures using Trizol (Invitrogen), frozen and sent for Analysis to the Memorial Sloan-Kettering Cancer Center in New York.

### 2.9.3 RNA expression profiling

Expression profiling was carried out by the Memorial Sloan-Kettering Cancer Center Core facility using Affymetrix U133 plus 2 chips. The raw expression profiling data was then analysed by Holger Hummerich averaged and normalised using the RMA algorithm (Irizarry, Hobbs et al. 2003). Differentially expressed genes were identified using Linear Models for Microarray Analysis (LIMMA). LIMMA applies a modified t-test to each probe set employing an empirical Bayes approach for estimating sample variances. The P-values were corrected for multiple-testing using the Benjamini-Hochberg correction and a corrected P-value threshold of  $10^{-5}$  was used to identify significantly differentially expressed genes.

## **2.10 SENESCENCE SPECIFIC MIRNA EXPRESSION PROFILING**

### 2.10.1 Cell line

The cells used for this experiment are HMF3A<sup>EcoR</sup> mixed population cells with murine ecotropic expression used at p22 +10.

### 2.10.2 Tissue culture

The cells have been cultured either at 34°C for 2 days (namely 34 samples) or at 38°C for 7 days (namely 38 samples) DMEM supplemented with 2 mM glutamine, 100 units/ml penicillin, 100 µg/ml streptomycin and only 10% v/v heat inactivated FCS or serum-starved at 34°C for 7 days (namely 34°C quiescent samples) in DMEM supplemented with 2 mM glutamine, 100 units/ml penicillin, 100 µg/ml streptomycin and only 0.25% v/v heat inactivated FCS.

For the 34°C samples and the 34°C quiescent samples the cells were seeded at  $1 \times 10^6$  cells per plate in six individual 10cm plates. For the 38°C samples the cells were seeded at  $4 \times 10^5$  cells per plate in six individual 10cm plates. The cells were then grown at the temperature, in the medium required and for the required time, as described above, before the RNA was extracted. Each condition was grown in 6 plates to enable to pool 2 plates for 3 triplicates.

### 2.10.3 RNA preparation

The RNA, 9 samples in total, from the 3 condition each in triplicate was extracted, from the 10 cm plates using miRNeasy Mini Kit from Qiagen as recommended by LC Sciences (catalogue number 217004).

Cells from 10 cm plates were lysed directly on the plates by aspirating the cell-culture medium, washing the cells with PBS and then adding 700µl QIAzol Lysis Reagent (miRNeasy Mini Kit, Qiagen). The lysate was collected into a microcentrifuge tube and vortexed to mix and ensure that no cell clumps were visible. Tubes were then frozen at -20°C until all ready to be processed together. When ready, tubes were thawed at room temperature (15 to 25°C) for 15min and 140 µl chloroform was added to each of the tubes containing the homogenate. The tube were shaken vigorously for 15 s and incubated for 2-3min at room temperature. The tubes were then centrifuged for 15 min at 12,000 g at 4°C. After centrifugation, the samples separate into 3 phases: an upper, colourless, aqueous phase containing RNA; a white interphase; and a lower, red, organic phase. The upper aqueous phases were each transferred to new reaction tubes and 1 volume of 70% ethanol was added and mixed thoroughly by vortexing. The mixes were transferred into an RNeasy Mini spin columns (miRNeasy Mini Kit, Qiagen) placed in a 2 ml collection tube. The tubes were centrifuged at 8000 g for 15s at room temperature (15–25°C). The flow-throughs were then transferred into a 2 ml reaction tube and 450 µl of 100% ethanol (0.65 volumes) were added and mixed thoroughly by vortexing. The samples were transferred into an RNeasy MinElute spin columns (miRNeasy Mini Kit,

Qiagen) placed in a 2 ml collection tube. The tubes were centrifuged for 15 s at 8000 g at room temperature (15–25°C). The flow-throughs were discarded. 500 µl of Buffer RPE (miRNeasy Mini Kit, Qiagen) was added into the RNeasy MinElute spin columns and the tubes were centrifuged for 15 s at 8000 g. The flow-throughs were discarded. 500 µl of 80% ethanol was added to the RNeasy MinElute spin columns and the tubes were centrifuged for 15 s at 8000g. The flow-throughs were discarded. RNeasy MinElute spin columns were placed into new 2 ml collection tubes and a last spin to rinse completely the wash buffer was performed for 5 min at 8000g. The RNeasy MinElute spin column were placed into new 1.5 ml collection tubes and the miRNA-enriched fractions were eluted by adding 14 µl RNase-free water and centrifuging for 1 min at 8000 g to elute.

#### 2.10.4 Quality Control of RNA Samples and shipping to LC sciences

The 260 nm/230 nm ratio of each sample was analyzed by Nanodrop. The ratio should be greater than 1.0 and the 260 nm/280 nm ratio should be above 1.8. Prior to shipping, the total RNA was stabilised by adding 1/10th volume of 3M NaOAc, pH 5.2, then 3 volumes of 100% ethanol. The samples were then stocked at -80C until shipment. Samples were shipped on dry ice in 1.5 ml eppendorfs.

#### 2.10.5 Microarray analysis

##### *2.10.5.1 Pairwise Comparisons for micro-rna Microarray Analysis*

Dual hybridisation is used in the LC Sciences microarray set-up so the experiment was designed to make pairwise comparisons of the samples, whilst minimising the number of chips required (Chapter 6, Table 6.1).

This service is offered by LC Sciences as ‘Total RNA to Data Service – Dual sample option’. In this process, the total RNA samples are enriched for miRNAs and then labelled with Cy3 or Cy5 fluorescent dyes before hybridizing them to the same chip.

#### 2.10.5.2 *Expression analysis and normalization*

This analysis is designed to identify senescence-specific miR expression by determining which miRs are differentially expressed upon the shift from 34°C to 38°C but do not change significantly upon quiescence or by heat shock.

The microarrays were analyzed by LC sciences: the quality of the triplicates was checked and a normalization of the results was performed. In brief, the background is subtracted and then signals are normalized using a LOWESS filter (Bolstad, Irizarry et al. 2003). For the two-Cy3 and 5 dye experiments, the ratio of the two sets of detected signals (log<sub>2</sub> transformed, balanced) and p-value of the t-tests are calculated. Differentially detected signals are those with p-values less than 0.01. The differential expression between 34°C samples and 38°C samples (comparison A), and 34° and quiescent (comparison B) was analyzed and the selection of miRNAs differential for the comparison A but not B was achieved to create a list.

#### 2.10.6 Individual miRNA validation in vitro

GeneService provides a micro-rna library of miRs cloned into a retroviral expression vector and placed under control of a CMV promoter. The clones were generated in the Netherland Cancer Institute (NKI) and made publically available by GeneService (Voorhoeve, le Sage et al. 2006). These clones were cloned as ~500bp fragments from several tumour cell lines. Therefore, clusters of miRNAs may be represented in an individual miR clone (named miR-VEC).

### 2.10.6.1 *Candidates miR-Vec Clones*

16 MiR-Vec clones were obtained for candidate miR-18a, miR-130b, miR-372, miR-373, miR-92b, miR-15a, miR16, miR-25 miR-195, mir-218, mir-20b, mir-29b, mir-186, MiR-128, Let-7g, MiR-423-5p. In addition, hsa-let-7a1 was obtained as a negative control. Note, hsa-miR-373 and hsa-miR-372 clones were also obtained due to the cell transformation effects observed by Voorhoeve et al (2006).

### 2.10.6.2 *Preparation of clones and sequence checking*

Clones were ordered from Gene Service, streaked onto an Ampicillin LB Agar plate and a single colony was prepped up to Maxiprep level. Each maxiprep was sequenced using T7 promoter (this sequencing was performed by MWG service as internal sequencing was unable to read through the complex secondary structure).

### 2.10.6.3 *HMF3A Growth Complementation Assay in plates*

20 µg of each of the 16 plasmids was packaged in 10 cm plates (in duplicate) using Phoenix Amphi cells. Two constructs were known to be interesting candidates in cell transformation (Voorhoeve, le Sage et al. 2006): MirVec hsa-miR-372 and MirVec hsa-miR-373. A negative control, MirVec hsa-let-7a, (its expression doesn't vary between 34°C, 38°C or quiescence) and a positive control, pRS p21F, were also packaged for the same experiment.

HMF3A cells (at passage p26) were infected with 50 ml of each amphotropic retrovirus (5 harvests) then selected with 5 µg/ml blasticidin for 15 days or puromycin at 2 µg/ml for 4 days (for the p21<sup>CIP1/WAF1/Sdi1</sup> RNAi construct). Cells were reseeded in a 6-well-plate format with 1, 3, 5, 10, 30 and 50K cells (in duplicate, when possible) or at 0.5x10<sup>5</sup> or 1x10<sup>5</sup> or 1.2x10<sup>5</sup> (in triplicate when possible), then shifted to 38°C for 3 weeks.

The cultures of each condition were stained at the end of the 3 weeks with methylene blue dye (2% (w/v) methylene blue in 50% ethanol and ddH<sub>2</sub>O) and photographed to be analysed.

## **2.11 SHRNA SCREENING**

### 2.11.1 Cell line

The cells used for this experiment were CL3E<sup>coR</sup> at the passage p22+6 (6 passages after EcoR introduction and clone selection).

### 2.11.2 RNAi library

The RNAi library consists of 100 tubes of plasmids pools each containing between 150 to 200 different shRNA plasmids. Each gene is represented by 1 to 3 shRNA plasmids and each plasmid is complementary to a different region of the target gene. Multiple shRNA plasmids per gene are used in order to increase the likelihood of achieving maximum efficiency of gene knockdown. The library represents 20,000 constructs to test or 10,000 genes targeted.

### 2.11.3 Virus packaging

Cells were seeded at  $1 \times 10^6$  in 10cm plates (day 0) and transfected the next day (day 1). For the transfection, 12 $\mu$ l Fugene transfection reagent was added into 100 $\mu$ l media and the mix was incubated at room temperature for 5 minutes. Then, 10 $\mu$ g of plasmid DNA pool was added to the mix, and mixed gently by tapping. The mix was incubated at room temperature for 15-30 minutes. Prior to addition to the cells, the mix was pipetted up and

down to mix. It was then added dropwise over the cells. The media was changed on day 2 (12ml) and the supernatant was harvested the next day (day 3). The supernatant was then filtered through a 0.45µm membrane to remove any cells and aliquoted into 2x 1ml for virus titration and 10ml for the screen. Virus supernatants were frozen at -70°C or used immediately. 12ml of media was added to the cells for a second harvest the next day (day 4), as described above.

#### 2.11.4 Sensitivity of the model

A mixture was created by mixing a quantity of positive pRS p21F RNAi constructs at 1/200 with negative pRS Lamin A/C constructs. This spiked mix was packaged in Phoenix Eco cells and used to infect CL3<sup>EcoR</sup> at  $0,5 \times 10^6$  in a T-75 cm<sup>2</sup> flask (day 0). Along with it, a positive control, P21F RNAi and a negative, Lamin A/C constructs were each packaged and used to infect a flask of cells. The media was changed the next day and puromycin selection at 2µg/ml was added on day 4. At day 8, the cells were trypsinated and reseeded at  $8,5 \times 10^4$  per 15cm plate or  $0,5 \times 10^4$  per well in 6-wells plates. The next day (day 9) the media was changed and cells were shifted to 38°C for 3 weeks. At that point, the cells were stained using methylene blue dye.

#### 2.11.5 Titration of Phoenix Eco viral Supernatants

Cells were seeded at  $6 \times 10^4$  cells per well in 6-well plates (day 0) and infected the next day (day 1) with different volumes (from 0.5 ml to  $1 \times 10^{-4}$  ml of each virus pool in presence of 8µg/ml polybrene. The media was changed on day 2 and puromycin selection at 2 µg/ml was added on day 4. After 2 weeks, puromycin selection at 34°C, the cells were stained with methylene blue and the number of colonies counted. The volume required to obtain approximately 10,000 infectious events was determined.



Unfortunately, because the amount of DNA available to us was limited, for the pools with a low titer, the volume of viral supernatant used was set at 10 ml (maximum amount harvested).

#### 2.11.6 Experiment planning for each plasmids pools

Cells were seeded at  $0.5 \times 10^6$  per T-75 cm<sup>2</sup> flask on day 0 and infected on day 1 with the determined volume of virus supernatant in presence of 8µg/ml polybrene. Accompanying every experiment, a positive control, P21F RNAi construct virus supernatant, and a negative control, Lamin A/C construct virus supernatant, were each used to infect a flask of cells. The media was changed on day 2 and puromycin selection at 2µg/ml was added on day 4. At day 8, the cells were trypsinated and reseeded at  $5.3 \times 10^4$  per T-75cm<sup>2</sup> flasks or  $1.8 \times 10^4$  per T-25cm<sup>2</sup> flask. The next day the media was changed and cells were shifted to 38°C.

#### 2.11.7 Confidence intervals

Using the formula:  $\ln(1-0.95) / \ln(1-1/(\text{Library Size}))$ , recommended for genetic screens by Nolan labs (see <http://www.stanford.edu/group/nolan/screens/screens.html>), it is possible to calculate the number of essays needed depending on the size of the library and the confidence interval wanted (Chapter 4, Table 4.1).

If the interval of confidence chosen was 99%, the number of essays would have to be superior or equal to 43,254 for my library of 9393 genes. In the shRNA screen process, the number of cells reseeded after puromycin selection was  $5.3 \times 10^4$  which is superior to 43,254 so the confidence in the results are superior or equal to 99%.

### 2.11.8 Genomic DNA extraction

After 3 weeks at 38°C, the cells were trypsinised and reseeded in the same T-75cm<sup>2</sup> flask and grown to confluency. When confluency was reached, the cells were passaged once more. When cell numbers were sufficient (90% confluency), the genomic DNA was extracted from a near confluent T75 cm<sup>2</sup> culture using the QIAamp DNA Mini kit (Qiagen). Media was removed from the culture and the cell monolayer was washed once with 1x trypsin-EDTA (0.25% (v/v) trypsin and 0.03% (w/v) EDTA). The monolayer was then detached, using 1x trypsin-EDTA (0.5 ml/T25 cm<sup>2</sup> flask) for 5 mins at 34°C), and the trypsin-EDTA was then inactivated by adding 1 ml of complete media. Cells were transferred to a 1.5 ml microfuge tube and centrifuged for 5 mins at 3000 rpm. The supernatant was discarded and the cell pellet was resuspended in 1x PBS (Phosphate Buffered Saline (without CaCl<sub>2</sub> or MgCl<sub>2</sub>)) to a final volume of 200 µl, before 20 µl of QIAGEN Protease (QIAamp DNA Mini Kit, Qiagen) was added. 200 µl Buffer AL (QIAamp DNA Mini Kit, Qiagen) was then added and mixed by pulse-vortexing for 15 sec, followed at incubation at 56°C for 10 mins. The 1.5 ml microfuge tube was centrifuged briefly then 200 µl ethanol (96-100%) was added, followed by pulse-vortexing for 15 sec. The mixture was then applied to a QIAamp Spin Column (QIAamp DNA Mini Kit, Qiagen) and centrifuged at 8000 rpm for 1 min. The QIAamp Spin Column was placed in a clean 2 ml collection tube, washed with 500 µl Buffer AW1 (QIAamp DNA Mini Kit, Qiagen) and then centrifuged at 8000 rpm for 1 min. The QIAamp Spin Column was placed in a clean 2 ml collection tube then washed with 500 µl Buffer AW2 (QIAamp DNA Mini Kit, Qiagen) and centrifuged at 1300 rpm for 3 mins. The QIAamp Spin Column was then placed in a clean 1.5 ml microfuge tube and 200 µl Buffer AE (QIAamp DNA Mini Kit, Qiagen) was added. Following incubation at room temperature for 1 min, the 1.5 ml microfuge tube was centrifuged at 8000 rpm for 1 min. The DNA concentration was determined on Nanodrop using 1.5 µl. The DNA was then used for TOPO cloning before sequencing.

### 2.11.9 TOPO cloning and sequencing

200 ng genomic DNA was used in a 50  $\mu$ l PCR reaction that contained 1  $\mu$ l of 6.6  $\mu$ M primers pSM2 longF and 6.6  $\mu$ M pSM2 longR, 1  $\mu$ l KOD Hot Start DNA Polymerase (Novagen), 3  $\mu$ l 25 mM MgSO<sub>4</sub> (Novagen) and 5  $\mu$ l 2 mM dNTPs (Novagen). An initial denaturation step at 95°C for 2 mins was performed before PCR amplification. PCR amplification parameters were denaturation at 95°C for 20 sec; annealing at 60°C for 10 sec; extension at 70°C for 30 sec, and a final extension of 10 mins at 70°C after the last cycle. 40 cycles were used in total. The DNA was generally not visible after this first round of PCR so a second round of amplification using a set of nested primers, namely pSM2 F and pSM2 R, that were internal to the first set of primers was used to amplify the inserts in the same condition than previously (5 $\mu$ l of PCR product used) before TOPO-cloning. This time analysis by electrophoresis of 5 $\mu$ l of PCR product revealed a product of 424 bp in all samples that corresponded to the expected insert sequence, but not in a negative control sample where water was substituted for template DNA.

A PCR reaction containing 100 ng pSM2 scrambled was used as the positive control for PCR amplification, and a PCR reaction that contained no template was used as the negative control to check for contamination of the reaction mixture. 15 $\mu$ l of the amplified product were then resolved alongside 5  $\mu$ l 1kb+ DNA ladder (Invitrogen) on a 3% agarose gel to check for the generation of 438 bp PCR products that could be visualised on a UVP.

4  $\mu$ l of each PCR product was directly cloned into pCR2.1-TOPO vector (Invitrogen) using the TOPO TA Cloning Kit (Invitrogen), as described above. 4  $\mu$ l of the cloning reaction was transformed onto LB-agar plates containing 50  $\mu$ g/ml final concentration ampicillin and 80  $\mu$ l of 20 mg/ml X-gal and incubated at 37°C overnight. Blue/white selection was used to identify positive clones that were picked and prepped using the

QIAprep Spin Miniprep kit (QIAGEN), as described above. Positive clones were sequenced using M13R primer.

## 2.12 PRIMARY CELLS IMMORTALIZATION

First, viral supernatant was packaged using Phoenix Ampho cells for each of the following constructs: MiR-25, Mir-372, MiR-218, Mir-193b, MiR-423-5p, Mir-195, WT LT, p53 shRNA, p21 shRNA. 20 µg of each of the miRs constructs were packaged for 10µg of the others constructs. The construct ER-RAS was also packaged with 10µg DNA in Phoenix Ampho cells. hTERT viral supernatant was prepared from TEFLYA TERT producer cells (O'Hare *et al*, 2001).

The BJ cells were infected with 10 ml viral supernatant for hTERT and 40 ml of miR viral supernatant. The cells were then selected with hygromycin at 50 µg/ml (for hTERT alone) for at least 10 days and then with blastocidin at 2.5 µg/ml (for mir cultures) for at least 8 days, for WT LT, p53 shRNA and p21 shRNA. The selection was done with puromycin at 1µg/ml for at least 6 days. Control cells submitted to puromycin, blastocidin or hygromycin died in respectively 4, 7 and 9 days.

Upon completion of selection, all cultures were infected with 10 ml of ER-RAS and selected with geneticin (G418) at 0.75 mg per ml for 10 days. Control cells submitted to G418 died in 9 days.

To ensure that ER-RAS was not activated, cells immediately after infection, were transferred into phenol-red free medium supplemented with charcoal-stripped FBS, because a lipophilic impurity contained in the phenol red has been described as a weak estrogen agonist (Berthois *et al*, 1986).

### **3 CELL MODEL AND GROWTH COMPLEMENTATION**

#### **3.1 CREATION OF CLONAL CELL LINES DERIVED FROM HMF3A CELLS AND GROWTH COMPLEMENTATION ASSAYS**

##### 3.1.1 Objectives

My objectives were to specify the senescence model and test the sensitivity of the complementation assay in the mixed population of HMF3A<sup>EcoR</sup> cells. It was also to create a refined clonal model, CL3<sup>EcoR</sup>, to assess the sensitivity of this model, its consistency compared to the mixed population and to confirm whether complementation of the growth arrest with abrogation of either the p53 or the pRb pathway was able to bypass cellular senescence in the mixed population cells. Another main objective was to design protocols and optimise conditions to develop a more standardised assay that results in a minimal background. In addition, investigation of a new expression construct, namely E2F-DB, as an alternative method to abrogate the pRb pathway was tried.

##### 3.1.2 Refinement of the HMF3A cells by clonal selection

The nature of the complementation experiment requires a reproducible cell response in order to be able to compare complementation with different constructs. For that purpose, the mixed HMF3A cells were infected with a retrovirus transducing the murine ecotropic receptor and then, after antibiotic selection, single cell clone colonies were picked and a total of 35 different clones were selected. After growing the 35 clones, 6 fast growing clones were selected for further evaluation. The evaluation was performed by comparing the growth rates and the irreversibility of all the clones to the mixed population. As cellular senescence is an irreversible growth arrest, it was important for the new clonal model to reflect this property. In addition, similar growth

complementation assays were performed with the clones and with the most sensitive constructs to assess the accuracy of the model.

### *3.1.2.1 Growth curves*

In order to choose a clone for the experiments, the growth rate of the mixed population was compared to those of 6 different clonal cell lines of the HMF3AEcoR cells: clone #2, #3, #10, #27, #32, #33 were chosen from among approximately 35 clones as they were the fastest growing.

Cells were each grown at three different temperatures: 34°C, 37°C and 38°C for 12 days. The numbers of cells were counted at day 0, day 5, day 7 and day 12 in triplicate. Each culture was seeded at day -1 at a similar density of 5000 cells per well. The cultures at 34 °C do not have a day 12 value as the cultures were overgrown by that point and were starting to detach. The cell numbers were very similar between the cells growing at 37°C and at 38°C (Figure 3.1). On this Figure, the two temperatures 37°C and 38°C do not seem to have different effects on the cell growth rate. The cell numbers are relatively similar between clones and mixed population. However, when comparing the numbers on a same scale, it appears that there are three categories: slow growth clones (clones 2, 10 and 33) with numbers hardly reaching 20,000 cells after 7 days; medium pace growth clones (clones 27 and 32 and the mixed population) with numbers around 30,000 cells and one quick growth clone: clone 3. Clone #3 seems to be the clonal line with the best growth rate at 34°C reaching numbers of 45,000 cells at day 7. It is also possible to note that all the clonal cells lines undergo growth arrest at both 37°C and 38°C from day 5 (Figure 3.1).

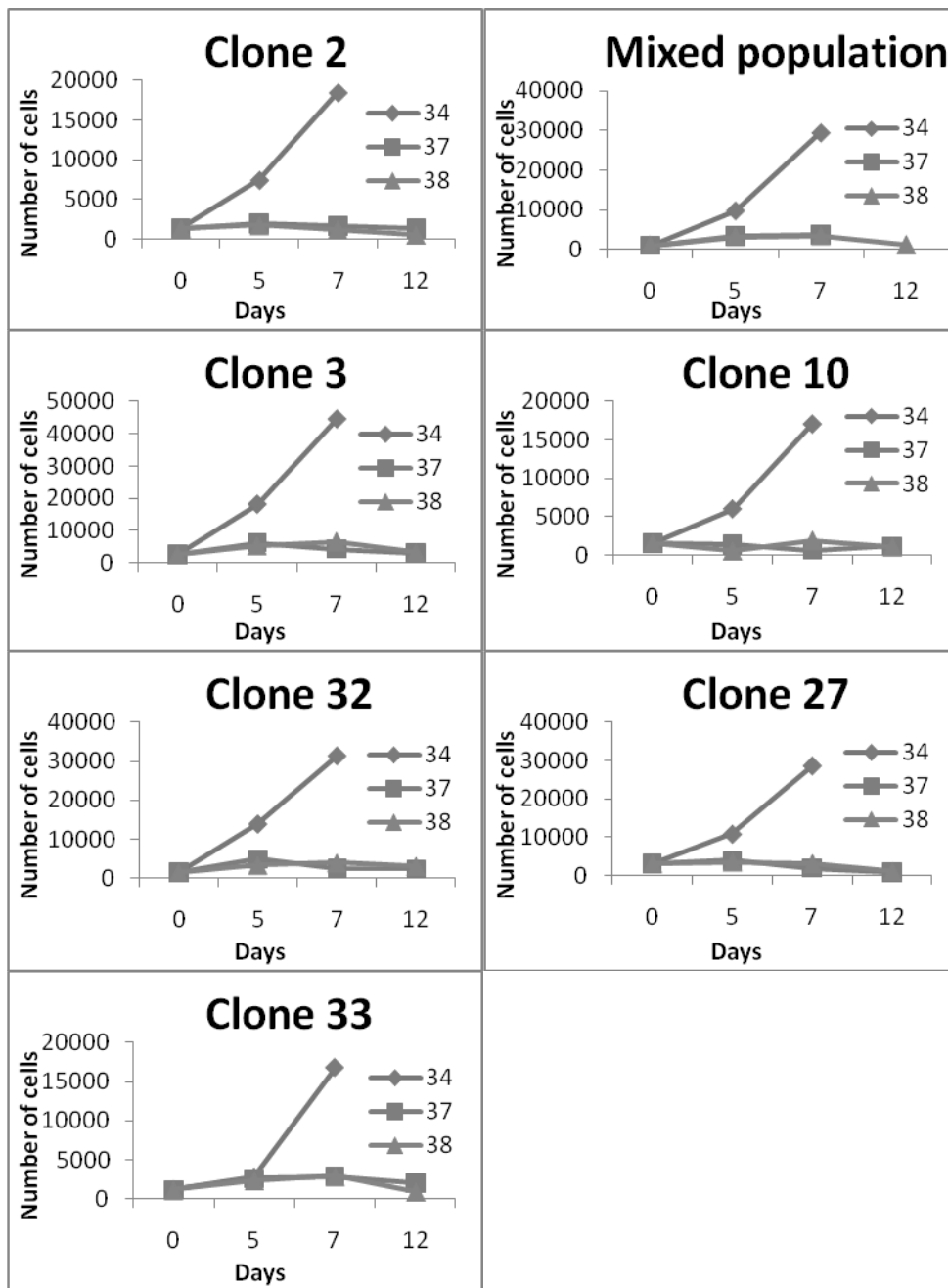


**Figure 3.1: Clonal cell lines growth rates**

The growth rate of the mixed population was compared to those of 6 different clonal cell lines of the HMF3A<sup>EcoR</sup> cells: clone #2, #3, #10, #27, #32 and #33. Cells were each grown at three different temperatures: 34°C, 37°C and 38°C for 12 days. The numbers of cells were counted at day 0, day 5, day 7 and day 12 in triplicate. Each culture was seeded at day -1 at a similar density of 5000 cells per well.

### 3.1.2.2 Complementation with E7 and E1A

Dr. Louise Mansfield had shown that senescence growth arrest in the HMF3A cells can be abrogated by ectopic expression of a certain number of genes and Ad E1A and HPV E7 represented the least efficient. I wanted to ensure that the clonal cell line could also be complemented by HPV E7 ectopic expression. This test would be a good evaluation of the clonal representativity and sensitivity.

It was important to make sure that both the mixed population and the clonal cell lines in parallel experiment could be rescued with these constructs. The first step was to infect the cells with ecotropic retroviral supernatant of pLPCX alone and pLPC-Ad E1A, pLPC-HPV E7, pRS p21 shRNA and p53GSE. The cells were reseeded after antibiotic selection at 1000, 5000, 10,000, 15,000 and 20,000 cells per well in 6-well-plates and grown at 38°C for 3 weeks before being stained (Figure 3.2). Only the three higher densities results are shown here as they are more significant numbers to compare and as in the lower ones almost no rescuants were observed. For these reasons, the experiment was repeated with slightly higher densities of 15,000, 20,000, and 30,000 cells per well (Figure 3.3).

The results show almost no background for the mixed cell culture nor for the clonal cell lines in both experiments (Figure 3.2A and 3.3A). The results in the mixed population cells with the E7 constructs show rescue at the higher densities of 20,000 or 30,000 cells per well (Figure 3.2D and 3.3E) although at a very low level compared to the positive control p21 shRNA or p53GSE (Figure 3.2C and 3.3B and C). The results are generally better in flasks probably because there could be more stress on cells plated in 6-well plates. The only 2 clonal lines to reproduce the mixed population results were clone #3 and clone #10, although, with clone #3, the cells rescue at a much higher level as it is possible to see stained colonies at 15,000 cells per well (Figure 3.2D and 3.3E).



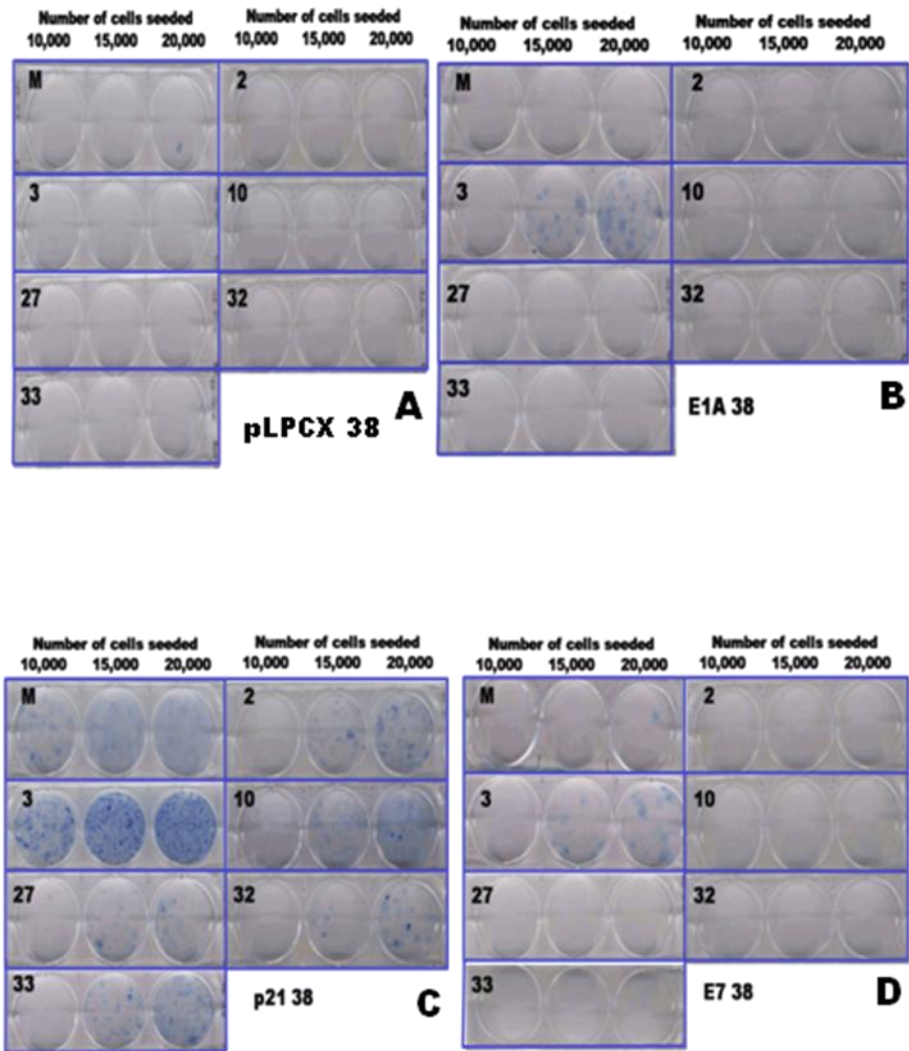


**Figure 3.2: Growth complementation assay in the clonal cell lines**

The mixed population and the clonal cell lines #2, #3, #10, #27, #32 and #33 were tested for growth complementation in parallel experiment. The cells were infected with ecotropic retroviral supernatant of pLPCX alone and pLPC-Ad E1A, pLPC-HPV E7, pRS p21 shRNA and p53GSE. The cells were reseeded after antibiotic selection at 1000, 5000, 10,000, 15,000 and 20,000 cells per well in 6-well-plates and grown at 38°C for 3 weeks before being stained

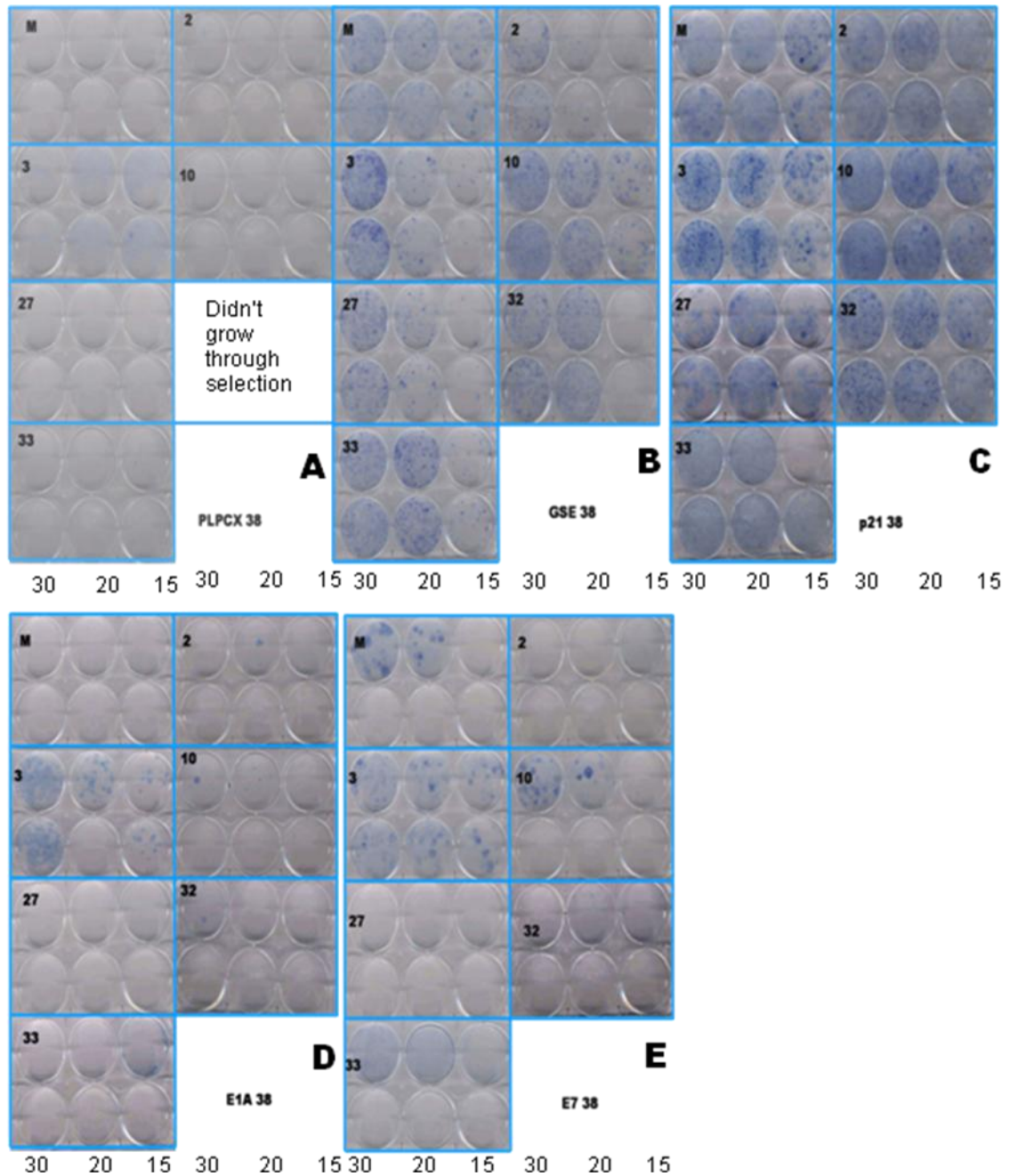


**Figure 3.3: Growth complementation assay in the clonal cell lines repeat**

The mixed population and the clonal cell lines #2, #3, #10, #27, #32 and #33 were tested for growth complementation in parallel experiment. The cells were infected with ecotropic retroviral supernatant of pLPCX alone and pLPC-Ad E1A, pLPC-HPV E7, pRS p21 shRNA and p53GSE. The cells were reseeded after antibiotic selection at 15000, 20000, and 30,000 cells per well in 6-well-plates and grown at 38°C for 3 weeks before being stained

The results with E1A show very similar results: the mixed population displays rescued colonies but very few and only at the higher reseeded density of 20,000 cells per well (Figure 3.2B and 3.3D), while the only clonal cell line to rescue significantly was clone #3 and at the densities of 15,000, 20,000 and 30,000 cells per well (Figure 3.2D and 3.3E).

The decision was made to test and validate clone #3 ( $CL3^{EcoR}$ ) as the model for this conditional senescence system. Since  $CL3^{EcoR}$  grew the best, growth arrested at 37 and 38°C and also rescued with both HPV E7 and Ad E1A, I chose to take it forward for testing.

### *3.1.2.3 Irreversibility*

Since cellular senescence is an irreversible growth arrest, it was very important to show that  $CL3^{EcoR}$  and the mixed population were undergoing an irreversible growth arrest and that the  $CL3^{EcoR}$  cells were representative of the HMF3A mixed population.

At the same time testing the irreversibility would permit the choice of temperature conditions that would eliminate reversible growth arrest.

#### ➤ Microscopical observation

Senescent cells display an increase in cell size and a flattened phenotype. To confirm if the  $HMF3A^{EcoR}$  mixed population and  $CL3^{EcoR}$  displayed these morphologic characteristics, senescence was triggered in the conditional model and the cells were observed microscopically. The conditionality of the mixed  $HMF3A^{EcoR}$  cells was tested by growing the cells at 34°C, 37°C or 38°C for 7 days and then back at 34°C for another 14 days after which the cells were observed and photographed under phase contrast microscope (Figure 3.4). The cells were also reseeded at an identical density after each photograph at day 7 and 14 to eliminate the density bias. I observed that a high density helped the cell growth while a low density slowed down the growth.

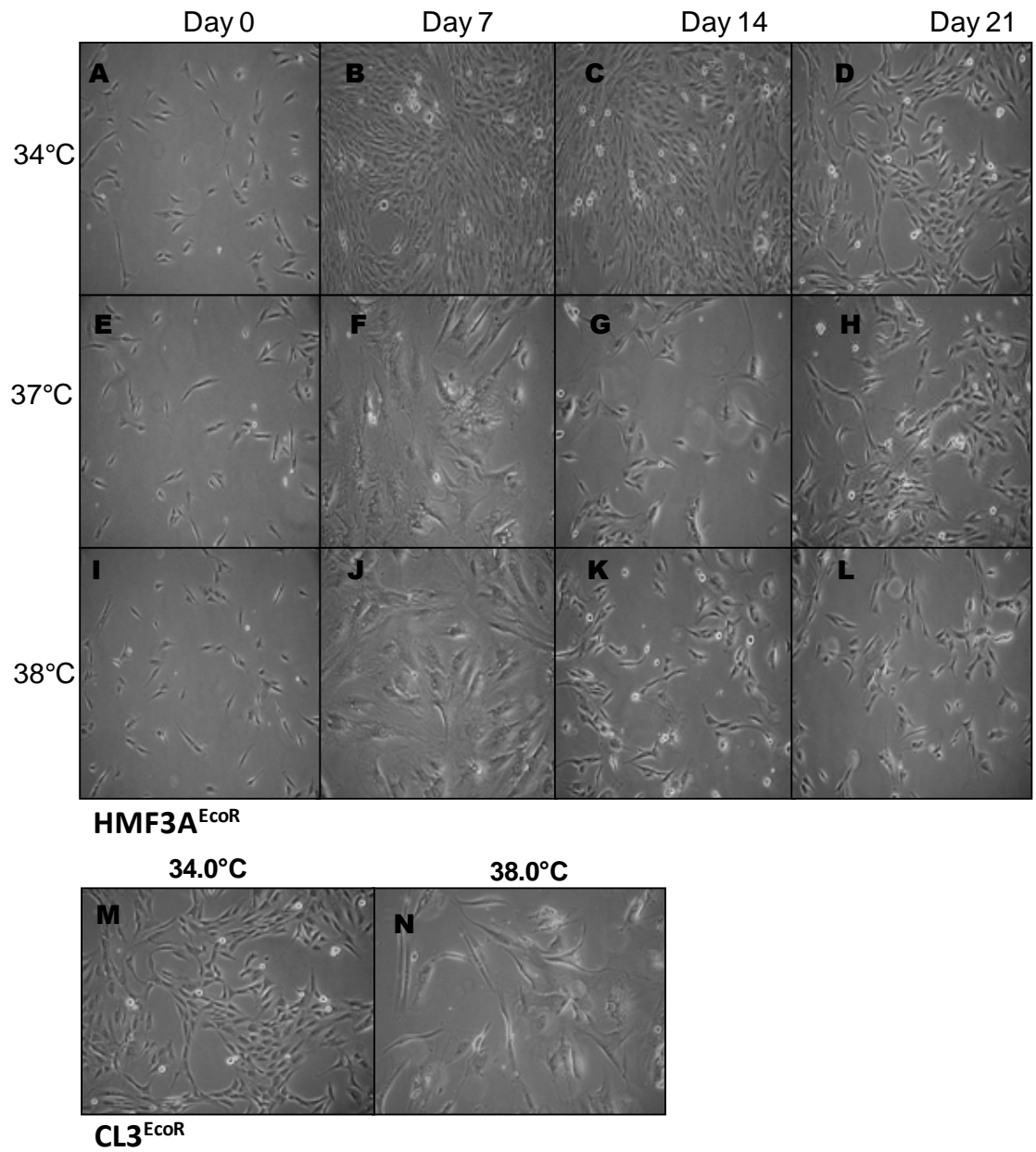


**Figure 3.4: Irreversibility HMF3A<sup>EcoR</sup> (A-L) and CL3<sup>EcoR</sup> (M-N) cells: Photos**

Irreversibility was tested in 6-well plates by incubating cells at 34°C or 38°C for 7 days and then shifting them back to 34°C for 14 days before photographing the cells under phase contrast microscope.

This density effect has also been previously described in the literature (Piedimonte, Borghetti et al. 1982). Cells all clearly display a flattened phenotype after 7 days at 37°C or 38°C (Figure 3.4, F and J). After shifting the cells back to 34°C, however, although the growth does not restart, the cells all display again a much smaller size and lose their flattened senescent phenotype (Figure 3.4, G-H and K-L). It is also possible to note that the density is much greater in the cells grown at 34°C all along (Figure 3.4, A-D) indicating a growth arrest with minimal background at the higher temperatures (Figure 3.4, E-L). The growth rate at 34°C seemed consistent all the way through. The cells at day 21 when grown at 34°C appeared slightly less dense on the photograph (Figure 3.4 D); however, the culture had similar cell numbers than the other days and the visual difference was only due to which area was photographed on the flask. There was no visible differences between the cells grown at 37°C or at 38°C for 7 days (Figure 3.4, F and J), however, after shifting them back to 34°C, it appeared that the cells grown at 37°C started growing again (Figure 3.4, G and H) when compared to the ones grown at 38°C (Figure 3.4, K and L). These results suggested that 37°C was not stringent enough to trigger an irreversible arrest and for that reason, I chose to perform the complementation assays at 38°C.

In addition, the growth arrest of Clone #3 (CL3<sup>EcoR</sup>) was tested by growing the cells for 7 days at either 34°C or 38°C. Microscopical observation showed healthy growing cells at 34°C and arrested cells with a similar flattened phenotype to the one of the mixed population at 38°C (Figure 3.4, M-N).

➤ Do Cell numbers confirm microscopical observation?

The mixed population of HMF3A<sup>EcoR</sup> cells were each plated at  $0.3 \times 10^6$  per T-75 cm<sup>2</sup> flask (day 0) and grown at 34°C or 38°C for 7 days (day 7) and then at 34°C for another 14 days (day 14 and 21). The numbers of cells were determined at day 0, day 7, day 14 and day 21 at these 3 growth temperatures with the cells being reseeded at  $2 \times 10^5$  per T-75 cm<sup>2</sup> flask at day 7 and 14. Reseeding eliminates the potential bias due to different cell densities in cultures. Each growth condition for each time point was represented in

triplicate. These cells numbers were represented as the accumulated relative growth at each time point (Figure 3.5A). The cells at 34°C for 3 weeks showed a growth rate just above 20 divisions per week. The cells grown at 38°C on the other hand seemed to have their growth arrested. Even when the cells were shifted back to 34°C for 2 weeks, the growth remains very poor as their relative growth is only around 5 divisions per week. This residual growth when the cells were shifted back to 34°C could be due to a low number of reversions, even though very little background is observed when the cells are maintained at 38°C. Together, these data suggest that the cells undergo irreversible growth arrest. Before concluding that this growth arrest was a senescence growth arrest, more tests were performed.

#### ➤ Cell staining

To confirm the microscopic results, HMF3A<sup>EcoR</sup> and CL3<sup>EcoR</sup> cells were plated at different densities in 6-well plates and grown at 34°C or 38°C for 7 days and then at 34°C for another 14 days. Cells were then stained with methylene blue and the plates scanned (Figure 3.5, B and C). The methylene blue dye used here stains healthy growing cells as dark blue. The flattened cells are stained in a much lighter shade. Cells from both HMF3A<sup>EcoR</sup> and CL3<sup>EcoR</sup> cultures show a greater intensity of staining for the 34°C samples than the 38°C ones, indicating no growing healthy cells at 38°C. This suggested the HMF3A<sup>EcoR</sup> and CL3<sup>EcoR</sup> cells undergo growth arrest at 38°C that is essentially irreversible. It is interesting to note that at the density of 10,000 cells or lower, there is very little background suggesting an appropriate density to use for the complementation assay.

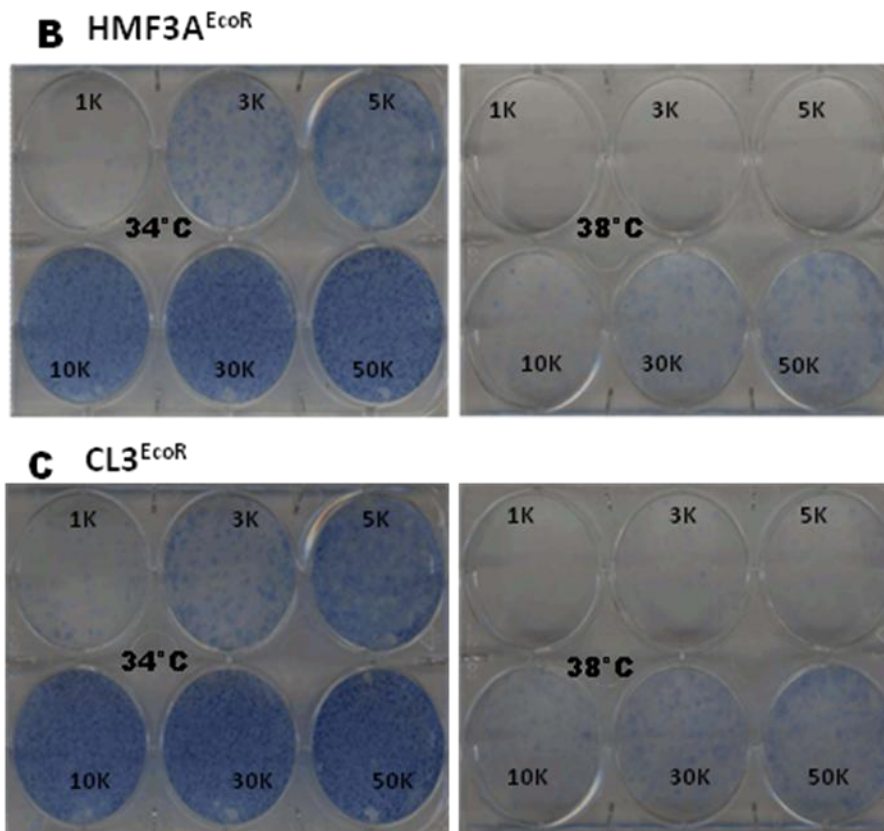
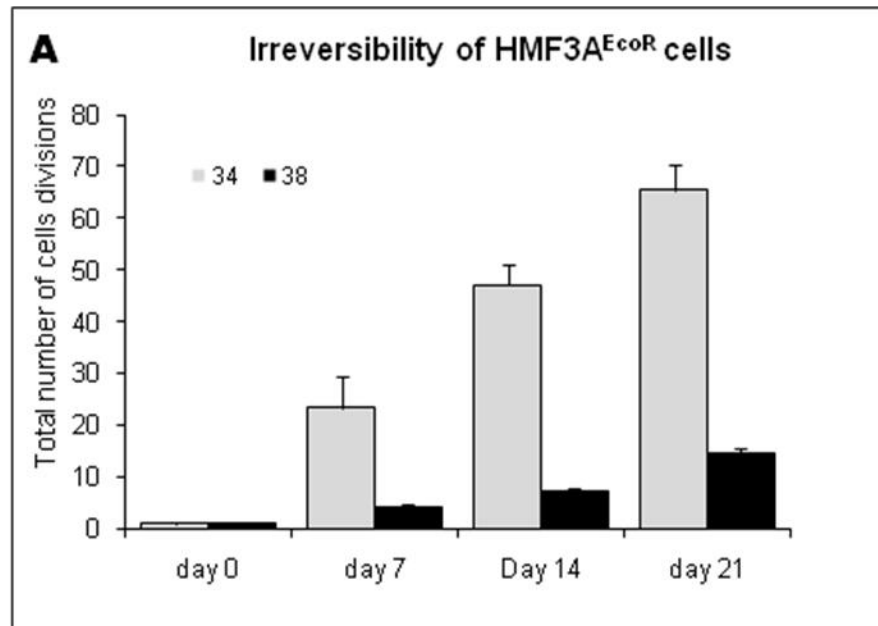


**Figure 3.5: Irreversibility HMF3A<sup>EcoR</sup> (A and B) and CL3<sup>EcoR</sup> (C) cells: Growth assay and staining**

Irreversibility was tested in 6-well plates by incubating cells at 34°C or 38°C for 7 days and then shifting them back to 34°C for 14 days before staining (B and C). It was also determined by counting HMF3A<sup>EcoR</sup> cells numbers achieved after culturing cells at 34°C or 38°C for 7 days and then at 34°C for another 14 days (A).

➤ SA-β-Gal activity

Senescence represents an arrested state in which the cells remain viable, but are not stimulated to divide by serum or passage in culture. Senescent cells display increase of cell size which has been confirmed by microscopy but also display activation of senescence-associated expression of β-galactosidase (SA-β-Gal) activity and altered patterns of gene expression. The SA-β-Gal activity is detectable by a histochemical reaction only in senescent cells and is not found in pre-senescent, quiescent or immortal cells. In order to assess whether the CL3<sup>EcoR</sup> cells were undergoing senescence upon growth arrest, cells were plated in 6 well plates at 5000 cells per well and grown at 34 or 38°C for 7 days. The cells were then stained for SA-β-galactosidase activity (Figure 3.6, C and D). The same experiment was performed in parallel with HMF3S cells. The HMF3S cells were derived from the same batch of primary human breast fibroblasts by immortalisation with hTERT and wild type SV40 U19 LT antigen and thus did not undergo growth arrest upon shift of temperature (Figure 3.6, A and B).

The results showed no blue colouration and healthy growing phenotype of the HMF3S cells at 34°C and 38°C (Figure 3.6, A and B). There is no blue colouration either of the CL3<sup>EcoR</sup> cells at 34°C (Figure 3.6C). At 38°C, the CL3<sup>EcoR</sup> cells show an intense blue colouration situated in the cytoplasm of the cells (Figure 3.6D). The cells were flattened and displayed a senescent phenotype. Thus, CL3<sup>EcoR</sup> cells undergo irreversible growth arrest at 38°C. This growth arrest at 38°C was stringent, essentially irreversible and turned on SA-β-Gal activity, a marker of senescence.

Complementation assays by abrogation of the pRb and the p53 pathways were performed in the CL3<sup>EcoR</sup> cells and the mixed population.



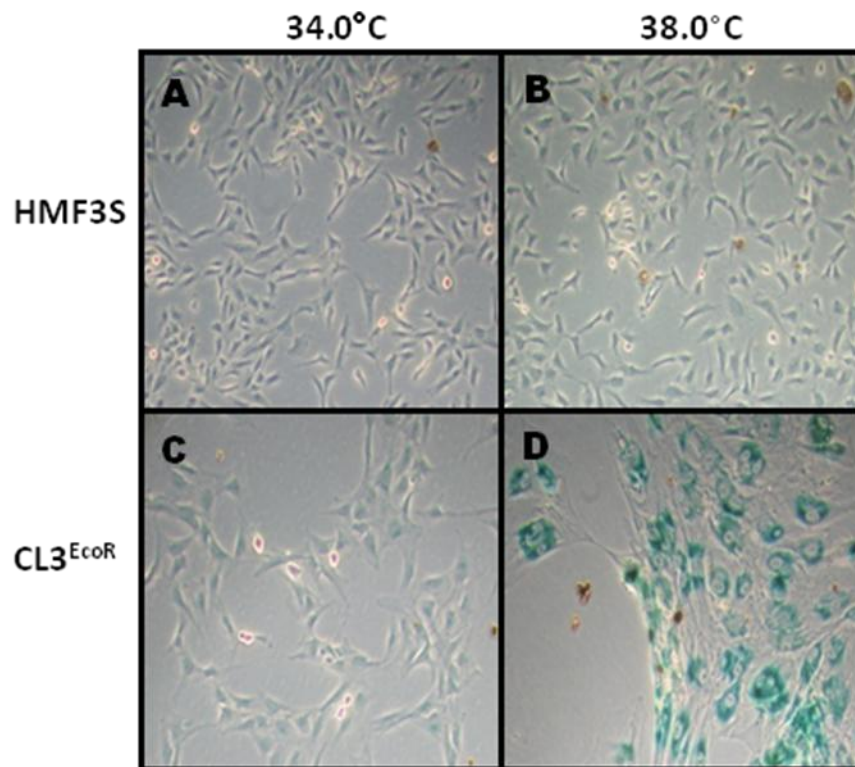


**Figure 3.6: Induction of SA-β-Gal**

CL3<sup>EcoR</sup> and HMF3S cells were incubated at either 34°C or 38°C for 7 days and were stained for SA-β-Gal activity. HMF3S cells which do not undergo growth arrest at 38°C were analysed as a temperature control.

### 3.1.3 Reconstitution of WT LT antigen in HMF3A<sup>EcoR</sup> and CL3<sup>EcoR</sup> cells

Reconstitution of WT LT activity in HMF3A cells by infection with amphotropic viruses had been shown by Dr. Louise Mansfield to be sufficient to abrogate growth arrest. This experiment was carried out in the new conditions with ecotropic virus in the CL3<sup>EcoR</sup> and the mixed population HMF3A<sup>EcoR</sup> Cells.

10 µg of pLPC WT LT and empty pLPCX VECTOR were packaged, using the  $\phi$  ecotropic cells. 10ml of the retroviral supernatant was used to infect CL3<sup>EcoR</sup> and HMF3A<sup>EcoR</sup> cultures seeded at  $5 \times 10^5$  cells in duplicate T75 cm<sup>2</sup> flasks in the presences of 8 µg/ml polybrene. Following incubation at 34°C for 4 days, 2 µg/ml puromycin was added to the culture medium and, after completion of 4 days of drug treatment, no viable cells remained in a non-infected culture, whereas multiple puromycin-resistant clones were observed in all infected cultures. Selection was removed and the cells were reseeded in 6 well-plates at 1000, 3000, 5000, 10,000, 30,000 and 50,000 cells per well before being shifted to 38°C for a further 14 days before fixing and staining with 2% (w/v) methylene blue (Figure 3.7 and 3.8).

The staining result showed no or very little background with the pLPCX empty vector (Figure 3.7A and 3.8A) which meant that the cells were unable to overcome growth arrest on their own but showed growth with the WT LT vector (Figure 3.7B and 3.8B) at all densities confirming that reconstitution of WT LT was sufficient to overcome the growth arrest in the CL3<sup>EcoR</sup> and HMF3A<sup>EcoR</sup> cells in a similar manner.

Western blot analysis of WT LT expressing mixed population HMF3A<sup>EcoR</sup> cells by western blot with p21<sup>CIP1/WAF1/Sdi1</sup> antibody showed a decrease in the expression of p21<sup>CIP1/WAF1/Sdi1</sup> (Figure 3.9B). Indeed, LT is known to bind and inactivate several proteins including pRb and p53 and p53 is directly upstream of p21<sup>CIP1/WAF1/Sdi1</sup>. Therefore, the inactivation of p53 by LT should trigger a decrease in the p21<sup>CIP1/WAF1/Sdi1</sup> proteins levels (Figure 3.9A).

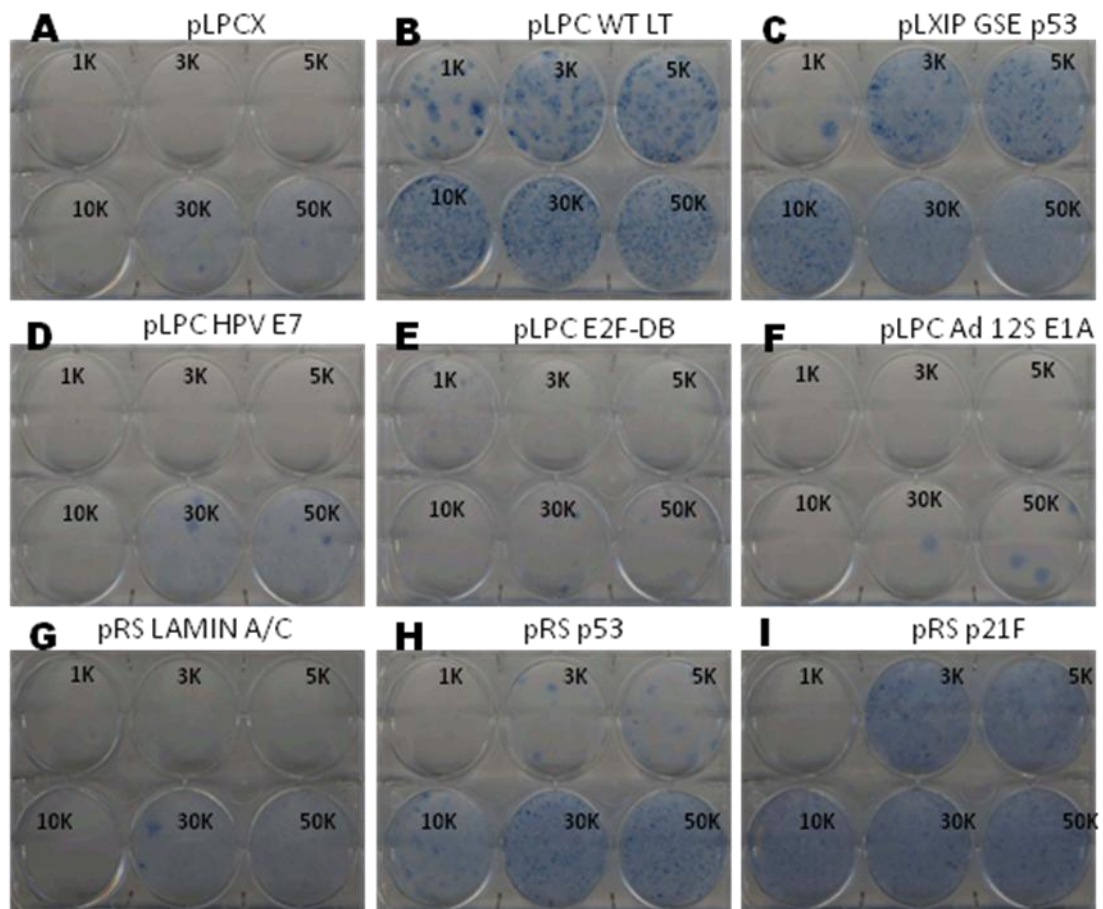


**Figure 3.7: Complementation HMF3A<sup>EcoR</sup> by ectopic expression and RNAi silencing**

Cells stably transduced with the retroviruses corresponding to pRS Lamin A/C (control gene), pRS p53 shRNA, pRS p21F shRNA, HPV-E7, E2F-DB, 12S E1A, PLPCX, WT LT and p53 GSE were seeded in 6-well plates at 1000, 3000, 5000, 10000, 30000 and 50000 and incubated at 38°C for 21 days before staining. Constructs able to overcome growth arrest yielded dark blue colonies of densely growing cells.

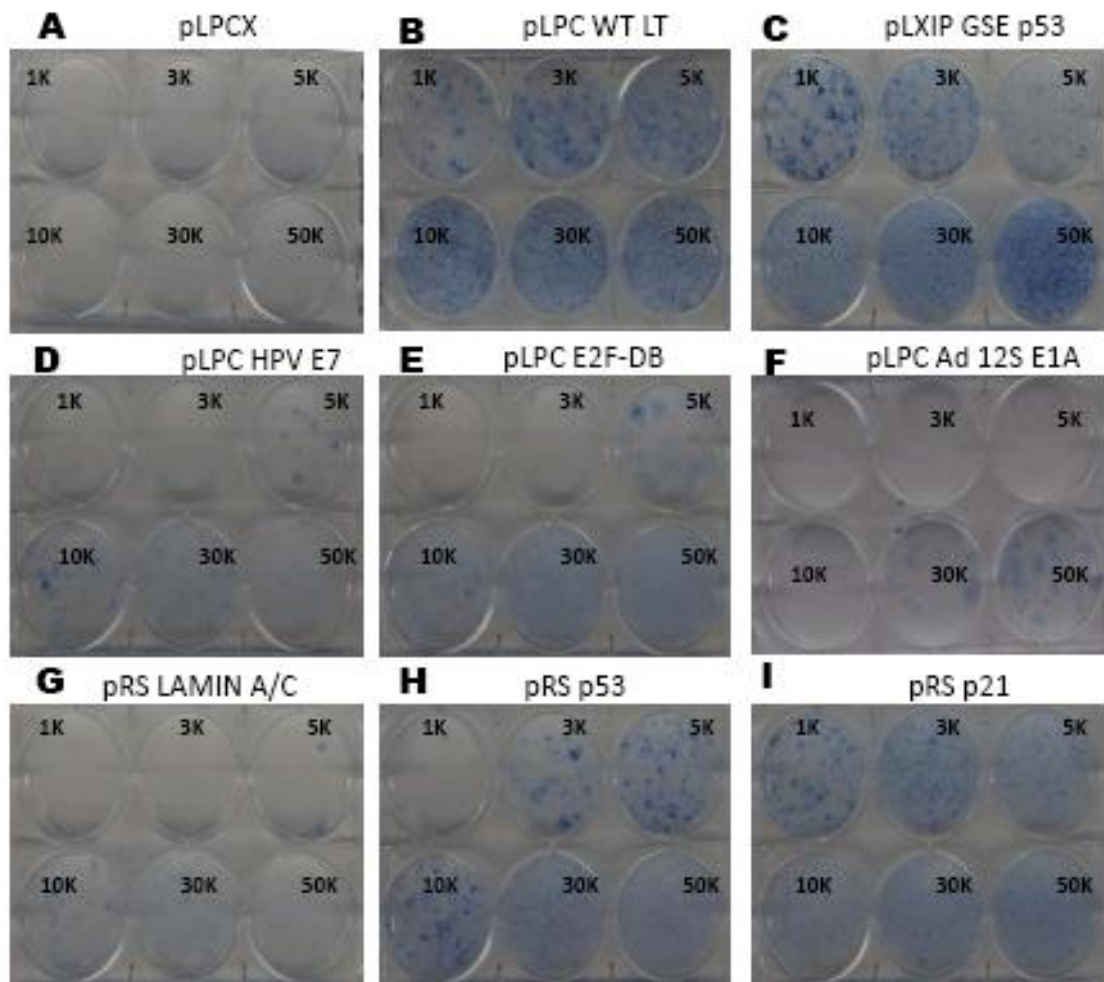


**Figure 3.8: Complementation  $CL3^{EcoR}$  by ectopic expression and RNAi silencing**

Cells stably transduced with the retroviruses corresponding to pRS Lamin A/C (control gene), pRS p53 shRNA, pRS p21F shRNA, HPV-E7, E2F-DB, 12S E1A, PLPCX, WT LT and p53 GSE were seeded in 6-well plates at 1000, 3000, 5000, 10000, 30000 and 50000 and incubated at 38°C for 21 days before staining. Constructs able to overcome growth arrest yielded dark blue colonies of densely growing cells.

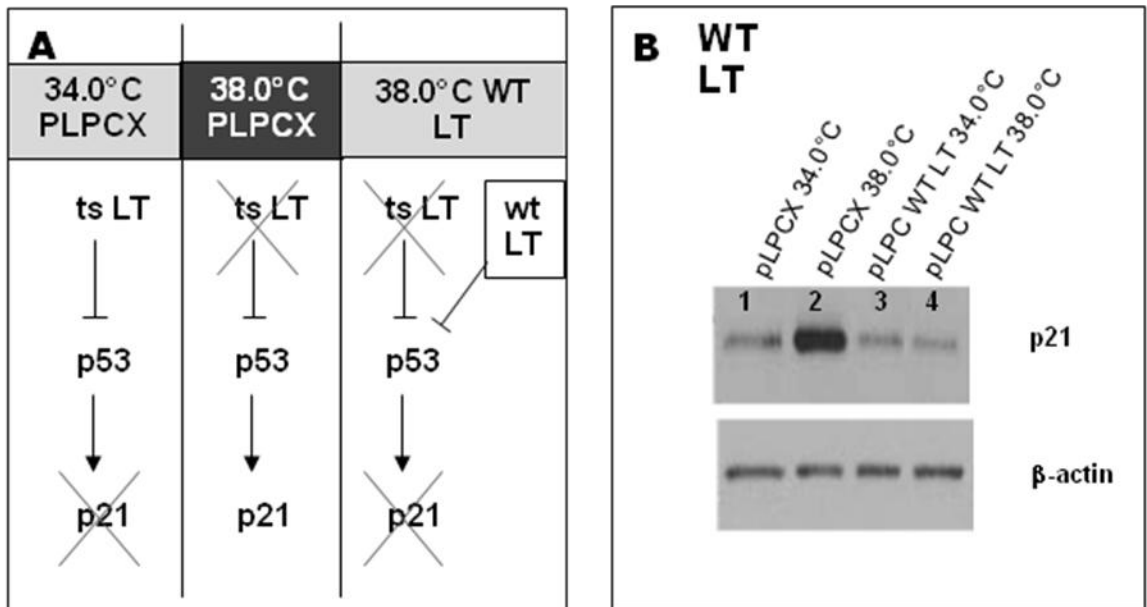


**Figure 3.9: Expression of LT in the HMF3A<sup>EcoR</sup> cells**

At 38°C, the thermolabile LT is inactivated, p53 gets activated leading to the increase of p21<sup>CIP1/WAF1/Sdi1</sup> expression directly downstream (A). If LT expression is reintroduced, p53 is inactivated and p21<sup>CIP1/WAF1/Sdi1</sup> expression levels stay low (A) The expression of p21<sup>CIP1/WAF1/Sdi1</sup> protein was analyzed by Western blot in cells transfected with either PLPCX or WT LT at 34 and 38°C (B).

### 3.1.4 Abrogation of the p53 pathway in HMF3A<sup>EcoR</sup> and CL3<sup>EcoR</sup> cells

Louise Mansfield had also shown that abrogation of the p53 pathway in the mixed population of HMF3A cells by ecotropic retroviral delivery was sufficient to bypass the conditional growth defect.

This experiment was repeated in the new conditions with the CL3<sup>EcoR</sup> and HMF3A<sup>EcoR</sup> cells to confirm a similar response. To inactivate the p53 pathway, three different reagents were used, one by ectopic expression and two by shRNA silencing; namely pLXIP GSE p53, pRS p21 shRNA and pRS p53 shRNA.

GSE p53 is a dominant-negative peptide of p53 that was originally identified in a GSE screen. It corresponds to a region in the oligomerisation domain of p53 (amino acids 273-368 in rat) (Ossovskaya, Mazo et al. 1996) and functions as a dominant-negative peptide of p53 by promoting the accumulation of endogenous p53 protein into a functionally inactive form. However, the high level of sequence conservation exhibited in the oligomerisation domain between p53 and the p53 family members p63 and p73 (Levrero, De Laurenzi et al. 2000), suggests that GSE p53 probably interacts with all three members of the p53 family. Therefore, RNAi represented a second, more specific method to abrogate p53 activity.

A p53 shRNA construct, pRetroSuper-p53, had previously been shown to efficiently knockdown p53 in HDFs (Berns, Hijmans et al. 2004). Therefore, the same shRNA construct was reconstructed by Dr. Louise Mansfield by cloning the p53 RNAi target sequence into the pRetroSuper retroviral expression vector.

p21<sup>CIP1/WAF1/Sdi1</sup>, directly downstream of p53, has been shown to be up-regulated upon replicative senescence in a number of cell types (Schwarze, Shi et al. 2001; Wagner, Hampel et al. 2001; Tang, Gordon et al. 2002; Hardy, Mansfield et al. 2005). Furthermore, over-expression of p21<sup>CIP1/WAF1/Sdi1</sup> in HDFs was shown to induce

premature senescence (McConnell, Starborg et al. 1998) and SAHF (senescence associated heterochromatin foci) (Chan, Narita et al. 2005), whereas knockdown of p21<sup>CIP1/WAF1/Sdi1</sup> by shRNA was sufficient to bypass the conditional growth arrest in an analogous conditionally immortalised HDF system, namely BJ-TERT-tsLT cells. This indicated that p21<sup>CIP1/WAF1/Sdi1</sup> should be functionally analysed in the HMF3A system. A number of p21<sup>CIP1/WAF1/Sdi1</sup> shRNA constructs were designed by Dr. Louise Mansfield using the criteria outlined by Reynolds and colleagues (Reynolds, Leake et al. 2004) to find one that worked best in the HMF3A cells to silence p21<sup>CIP1/WAF1/Sdi1</sup>;pRetroSuper-p21F.

10 µg of pRetroSuper-p53, pRetroSuper-p21, pRetroSuper Lamin A/C control vector, pLPC-GSEp53 and empty pLPCX vector each were packaged, using the φ ecotropic cells. The complementation assay was performed as described previously for WT LT and the cells were stained with 2% (w/v) methylene blue (Figure 3.7 and 3.8).

Whereas no growing colonies could be observed in the control-infected cultures pLPCX and pRS Lamin A/C shRNA (Figure 3.7 and 3.8, A and G), multiple colonies could be observed with a blue colouration in the p53 shRNA, p21 shRNA and GSE p53-infected cultures incubated at 38°C for 21 days, incubated under the same conditions (Figure 3.7 and 3.8, C, H, I) for both HMF3A<sup>EcoR</sup> and CL3<sup>EcoR</sup> cells. This indicated that down-regulation of p53 or p21<sup>CIP1/WAF1/Sdi1</sup> was sufficient to complement the growth of these cells under non-permissive conditions.

It is interesting to note that the efficiency of p53GSE to abrogate growth arrest was superior to p53 shRNA for both HMF3A<sup>EcoR</sup> and CL3<sup>EcoR</sup> cells which could be due to the contributing effects of the potential inactivation of p63 and p73. Additionally, the p21 shRNA also abrogated growth arrest more efficiently than p53GSE and p53 shRNA in both HMF3A<sup>EcoR</sup> and CL3<sup>EcoR</sup> cells. This could be explained by either a better knockdown of p21<sup>CIP1/WAF1/Sdi1</sup> by the shRNA than the p53. Similar complementation results were obtained in a duplicate experiment.

Protein lysates of each condition were analysed by western blot with a p21<sup>CIP1/WAF1/Sdi1</sup> antibody to assess whether the expression of p53 GSE, p53 shRNA and p21 shRNA would affect the proteins levels of p21<sup>CIP1/WAF1/Sdi1</sup>.

p53 is situated directly upstream of p21<sup>CIP1/WAF1/Sdi1</sup> and its inactivation by either p53 GSE (Figure 3.10A) or p53 shRNA (Figure 3.10C) brings p21<sup>CIP1/WAF1/Sdi1</sup> proteins levels down. Similarly, p21 shRNA also brings the p21<sup>CIP1/WAF1/Sdi1</sup> proteins levels down (Figure 3.11A).

The results show endogenous expression of p21<sup>CIP1/WAF1/Sdi1</sup> protein in the cells with the empty vector pLPCX or the control shRNA Lamin A/C and, as expected, an increase in p21<sup>CIP1/WAF1/Sdi1</sup> protein levels at 38°C compared to 34°C (Figure 3.10B and D, and Figure 3.11B lane 1 and 2). When the cells express either p53 GSE or p53 RNAi, or the p21 RNAi, the p21<sup>CIP1/WAF1/Sdi1</sup> protein levels are considerably reduced at both 34 and 38°C (Figure 3.10B and D, and Figure 3.11B, lane 3 and 4).

### 3.1.5 Abrogation of the pRb pathway in HMF3A<sup>EcoR</sup> and CL3<sup>EcoR</sup> cells

Similarly to p53, the pRb gene and genes that operate in the pRb pathway are frequently inactivated in most types of human cancer, either by direct mutation of pRb itself, or by mutation of an upstream regulator (Sherr 1996; Sellers and Kaelin 1997; Nevins 2001; Hahn and Weinberg 2002; Ortega, Malumbres et al. 2002). However, targeting pRb for inactivation is complicated by the problem of functional redundancy resulting from both the multiplicity of both Rb family members and potential pRb-binding partners.

The viral oncoproteins adenovirus type 5 E1A and HPV type 16 E7 represent two reagents commonly used to inactivate this pathway and Dr. Louise Mansfield showed that abrogation of the pRb pathway with either E1A or E7 expression could bypass the senescence growth arrest.



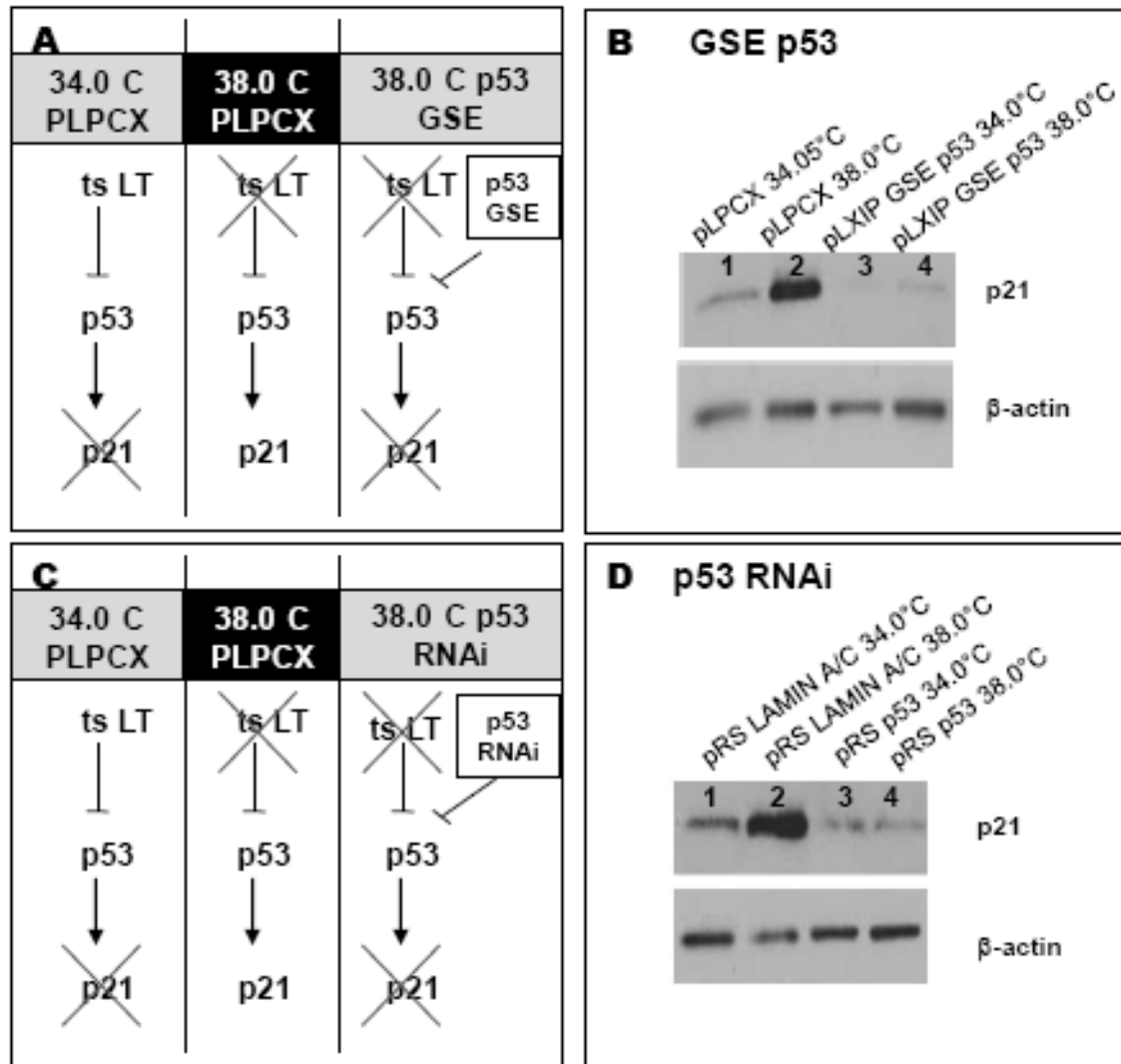


**Figure 3.10: Expression of p53 in the HMF3A<sup>EcoR</sup> cells**

At 38°C, the thermolabile LT is inactivated, leading to an increase of p53 and therefore the increase of p21<sup>CIP1/WAF1/Sdi1</sup> expression directly downstream (A-C). If p53 is repressed (A) or silenced (C), p21<sup>CIP1/WAF1/Sdi1</sup> expression levels stay low (B-D). The expression of p21<sup>CIP1/WAF1/Sdi1</sup> protein was analyzed by Western blot in cells transfected with either PLPCX, p53 shRNA or p53 GSE at 34 and 38°C (B-D).

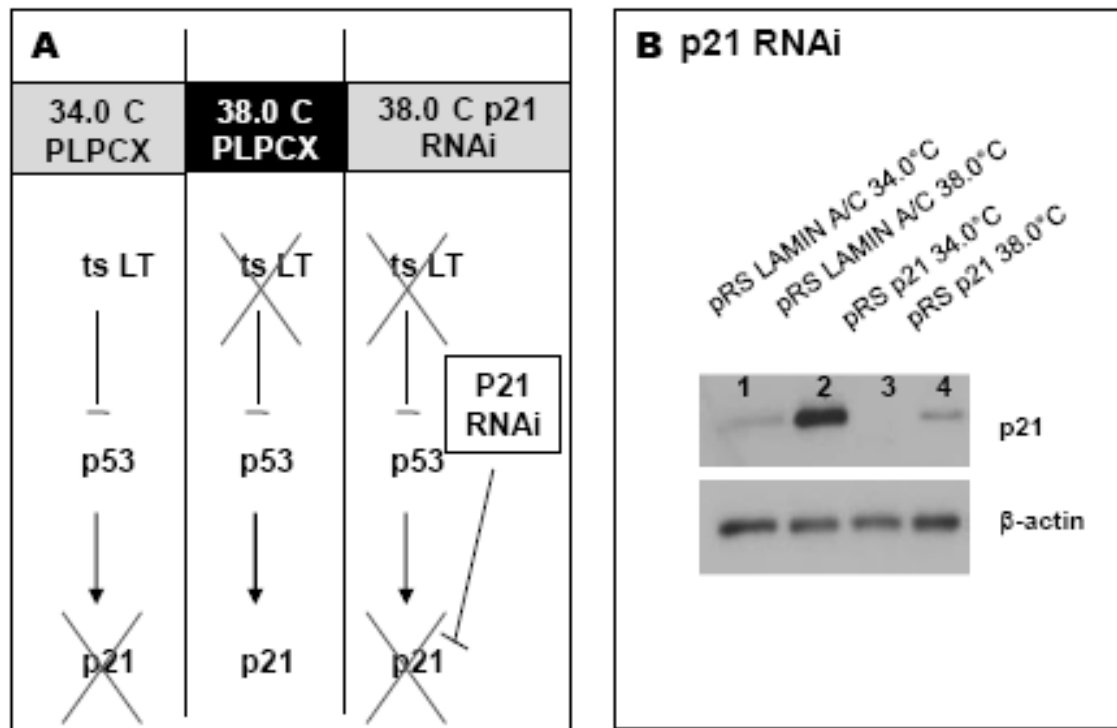


**Figure 3.11: Expression of p21<sup>CIP1/WAF1/Sdi1</sup> in the HMF3A<sup>EcoR</sup> cells**

At 38°C, the thermolabile LT is inactivated, leading to an increase of p53 and therefore the increase of p21<sup>CIP1/WAF1/Sdi1</sup> expression directly downstream (A). If p21 is silenced (A), p21 expression levels stay low (B). The expression of p21<sup>CIP1/WAF1/Sdi1</sup> protein was analyzed by Western blot in cells transfected with either PLPCX or p21 shRNA at 34 and 38°C (B-D).

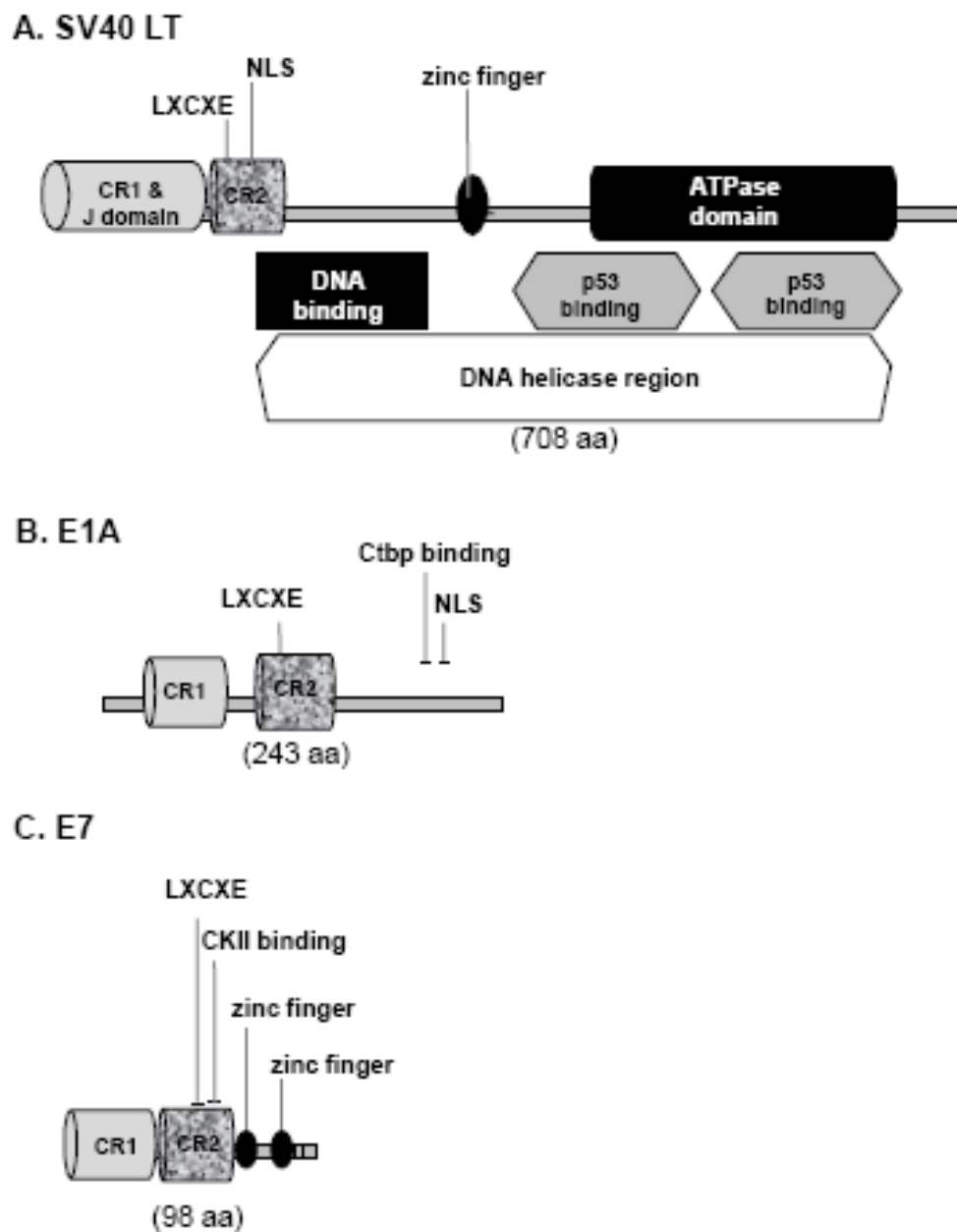
However, the induction could not be attributed to pRb alone as both E7 and E1A proteins possess a multifunctional activity able to abrogate other pathways as well as the pRb pathway.

In addition, Dr. Louise Mansfield had found that p14<sup>ARF</sup> knockdown was insufficient to overcome the HMF3A conditional growth arrest. She also tried to knockdown the p16<sup>INK4a</sup> but did not manage to get sufficient knockdown of p16<sup>INK4A</sup> protein levels despite trying two different shRNA construct namely pRetroSuper-p16#2 utilised by Wei and colleagues, and pRetroSuper-p16A (Reynolds, Leake et al. 2004).

Ectopic expression of E1A and E7 were tested in both HMF3A<sup>EcoR</sup> and CL3<sup>ECoR</sup> cells. However, because of E7 and E1A proteins multifunctional activity, a more specific reagent to inactivate the pRb pathway was also investigated; ectopic expression of E2F-DB, a mutant of E2F-1 shown to be functionally equivalent to the specific inactivation of the pRb family, was tested.

#### *3.1.5.1 Constitutive Expression of Ad 5 E1A and HPV16 E7*

E1A and E7 both possess a similar LxCxE-binding motif to LT (Figure 3.12A, B and C) which gives them the ability to bind to and inactivate the Rb family members. E1A retroviral expression construct, pLPC-12SE1AORI (gift from S. Lowe) and an E7 retroviral expression construct, pLPC-E7 (prepared by Dr. Louise Mansfield) were introduced into the CL3<sup>EcoR</sup> and HMF3A<sup>EcoR</sup> cells and assessed for their ability to complement the conditional growth defect of these cells.



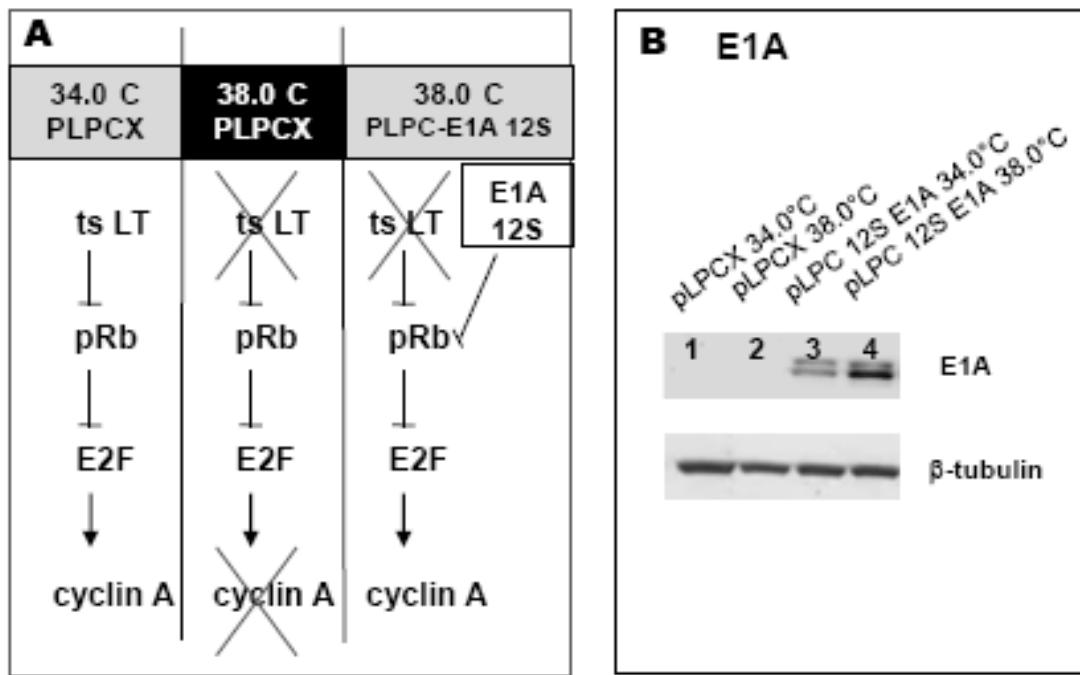
**Figure 3.12: Conserved Regions of the DNA Tumour Viruses**

Diagram of: **A:** SV40 LT; **B:** Adenovirus type 5 12S E1A; and **C:** HPV type 16 E7. NLS: Nuclear Localisation Signal; CR1: Conserved Region 1; CR2: Conserved Region 2; LXCXE: Rb family binding motif.

10 µg of pLPCX-12S E1A, pLPCX and pLPCX-E7 each were packaged, using the  $\phi$  ecotropic cells. The complementation assay was performed as described previously for WT LT and the cells were stained with 2% (w/v) methylene blue (Figure 3.7 and 3.8). In both cases, multiple healthy, growing colonies were observed in the E1A and E7-infected CL3<sup>EcoR</sup> (Figure 3.8, D and F) and HMF3A<sup>EcoR</sup> (Figure 3.7, D and F) cultures, but not the control-infected CL3<sup>EcoR</sup> (Figure 3.8A) and HMF3A<sup>EcoR</sup> (Figure 3.7A) cultures. As observed previously while selecting which clone to take forward, CL3<sup>EcoR</sup> cells displayed a higher efficiency to bypass growth arrest with these two constructs than HMF3A<sup>EcoR</sup> (Figure 3.7 and 3.8, D and F)

Protein lysates of each condition were analysed by western blot with an E1A or Cyclin A antibody to assess whether the ectopic expression of pLPC-12S E1A and E7 was efficient. E1A expression was detected by the E1A antibody (Figure 3.13A) and Cyclin A antibody should detect if expression of E7 was efficient in inactivating the pRb pathway (Figure 3.14A). Inactivation of the pRb function, generally by phosphorylation, induces E2F release and the subsequent expression of E2F-dependent proteins, such as CDC2 and Cyclin A (Jarrard, Sarkar et al. 1999). RT-PCR was performed with E7 specific primers on the RNA from the cells expressing E7. The results for E1A showed no endogenous expression in the cells with the empty vector (Figure 3.13B lanes 1 and 2) but a good expression of E1A in the cells with E1A vector at both 34°C and 38°C represented by an intense band (Figure 3.13B, lanes 3 and 4). The Western blot results for E7 showed the endogenous expression of Cyclin A at 34°C and its inactivation at higher temperature (Figure 3.14B, lanes 3 and 4). The RT-PCR results showed expression of E7 mRNA only in the cells expressing the E7 vector (Figure 3.14C, lane 3) compared to the controls (Figure 3.14C, lanes 1 and 2).

Constitutive expression of either E1A or E7 was sufficient to overcome the HMF3A conditional growth arrest at 38°C. By extension therefore, abrogation of the pRb pathway was sufficient to this bypass. However, it is still not possible to attribute this activity to the specific inactivation of one member of the pRb family as E1A and E7 function does not distinguish between Rb, p107 and p130.



**Figure 3.13: Expression of pRb in the HMF3A<sup>EcoR</sup> cells**

At 38°C, the thermolabile LT is inactivated, leading to an increase of pRb and therefore the repression of E2F which fail to activate the transcription of Cyclin A (A). If E1A is expressed, the pRb family is inactivated and cyclin A get transcribed (A). The expression of E1A protein was analyzed by Western blot in cells transfected with either PLPCX or plpC-E1A at 34 and 38°C (B).

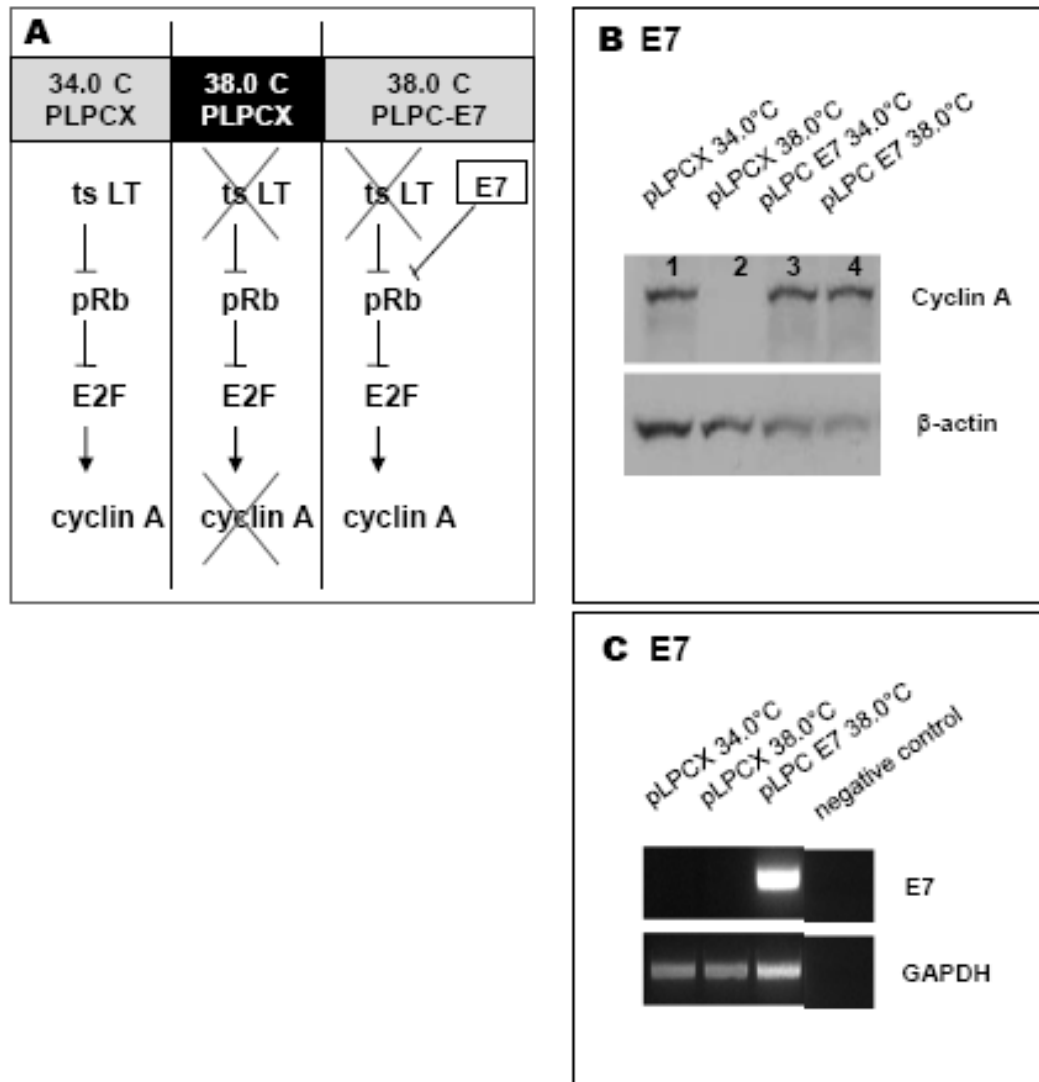


**Figure 3.14: Expression of E7 in the HMF3A<sup>EcoR</sup> cells**

At 38°C, the thermolabile LT is inactivated, leading to an increase of pRb and therefore the repression of E2F which fail to activate the transcription of cyclin A (A). If E7 is expressed, the pRb family is inactivated and cyclin A get transcribed (A). The expression of cyclin A protein was analyzed by Western blot (B) and E7 expression was checked by RT-PCR (C) in cells transfected with either PLPCX or plpC-E1A at 34 and 38°C.

### 3.1.5.2 Constitutive ectopic expression of E2F-DB mutant

The pRb family controls cell cycle progression by associating with E2Fs which suggest a great importance of the E2Fs factors in the induction of senescence. More observations also suggest a possible role for E2F in its regulation: the levels of various E2Fs decrease during the onset of senescence (Dimri, Hara et al. 1994; Haddad, Xu et al. 1999), and overexpressed E2F-1 induces both ARF (DeGregori, Leone et al. 1997; Bates, Phillips et al. 1998; Dimri, Itahana et al. 2000) and premature senescence (Dimri *et al*, 2000).

In addition, in primary MEFs, the use of a mutant of E2F-1, namely E2F-DB, which lacks both the C-terminal transactivation and the pRb binding domains but can still bind to DNA in heterodimeric complex with DP-1, was shown to rescue both p19<sup>Arf</sup> and p16<sup>INK4a</sup> induced growth arrest in mice (Zhang, Postigo et al. 1999). Studies in human cell systems are limited but one study involving IMR90 human fibroblasts has been described (Young and Longmore 2004). This paper provided detailed evidence that, like in the MEFs, E2F-DB can bind to E2F-responsive promoters and displace endogenous E2Fs in human fibroblasts. Sebastian (Sebastian, Malik et al. 2005) also showed that expression of E2F-DB was functionally equivalent to pRb family inactivation in MEFs. Therefore, the hypothesis was that E2F-DB, in the CL3<sup>EcoR</sup> and HMF3A<sup>EcoR</sup> cells, would inactivate the pRb pathway and activate Cyclin A expression (Figure 3.15A).

Therefore, an E2F-DB retroviral expression construct, was constructed by cloning the E2F-DB open reading frame (gift from Pr. Xin Lu) into the pLPCX vector, and introduced into the CL3<sup>EcoR</sup> and HMF3A<sup>EcoR</sup> cells.

10 µg of pLPC-E2F-DB and pLPCX retroviral expression constructs each were packaged, using the  $\phi$  ecotropic cells. The complementation assay was performed as described previously for WT LT and the cells were stained with 2% (w/v) methylene blue (Figure 3.7 and 3.8). In addition, duplicate cultures of HMF3A<sup>EcoR</sup> expressing pLPCX-E2F-DB and pLPCX were kept at 34°C for protein and RNA extraction. The protein lysates were analysed by Western blot with a cyclin A antibody (Figure 3.15B).



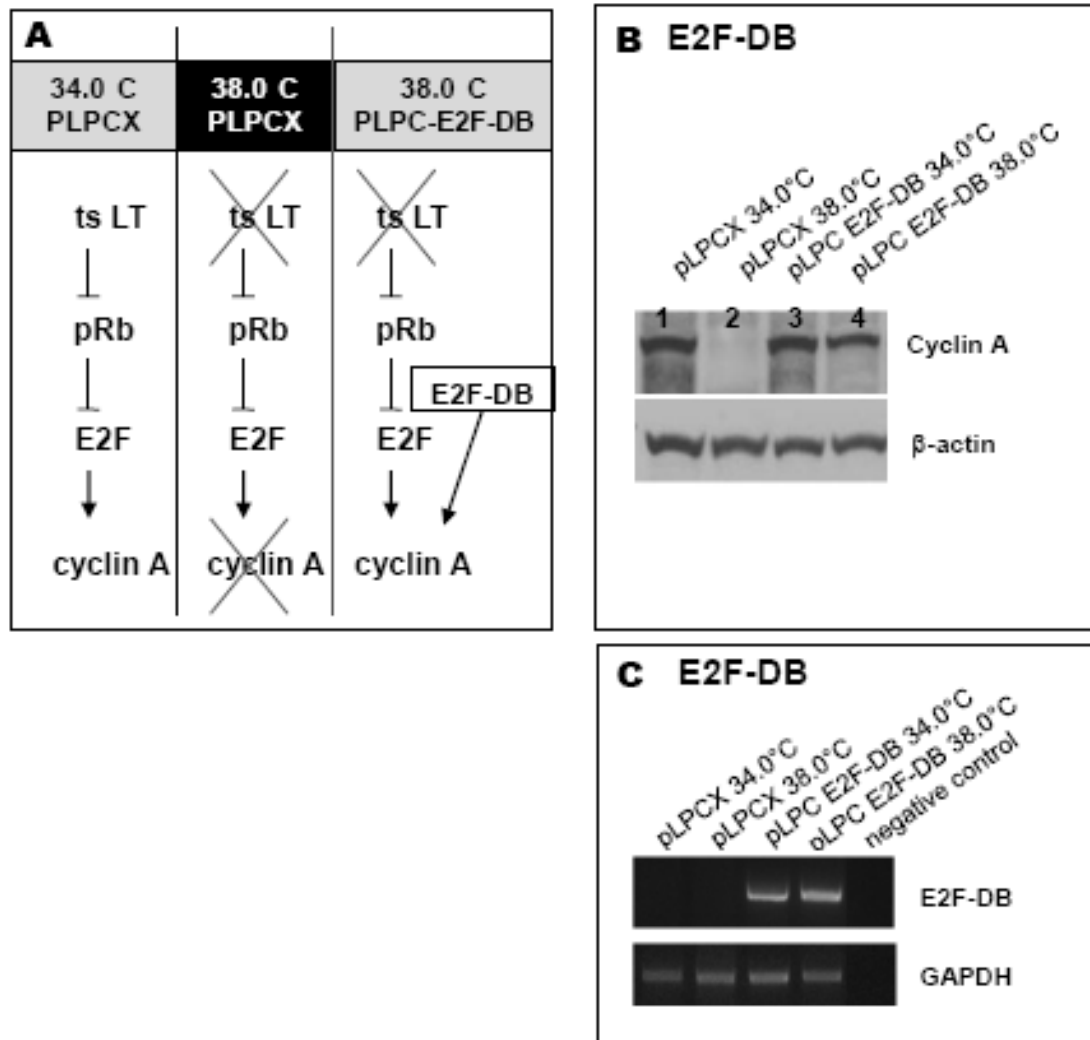


**Figure 3.15: Expression of E2F-DB in the HMF3A<sup>EcoR</sup> cells**

At 38°C, the thermolabile LT is inactivated, leading to an increase of pRb and therefore the repression of E2F which fail to activate the transcription of cyclin A (A). If E2F-DB is expressed, the pRb pathway is inactivated and cyclin A get transcribed (A). The expression of cyclin A protein was analyzed by Western blot (B and E7 expression was checked by RT-PCR (C) in cells transfected with either PLPCX or plpC-E1A at 34 and 38°C.

The RNA extracts were analysed by RT-PCR with E2F-DB construct specific primers (Figure 3.15C).

The results of the western blotting analysis showed endogenous expression of cyclin A protein in the cells with the empty vector, showing a decrease in cyclin A expression at 38°C compared to 34°C (Figure 3.15B, lane 1 and 2). The non permissive temperature leads to LT inactivation, activation of the pRb pathway, binding of the E2F transcription factor and loss of cyclin A expression. When the cells express E2F-DB, as demonstrated by the RT-PCR analysis (Figure 3.15C, lane 3 and 4), the cyclin A protein levels are considerably increased, as E2F is released, especially at 38°C where the levels are now almost equivalent to the ones at 34°C (Figure 3.15B, lane 3 and 4).

The E2F-DB infected culture complementation experiment showed a clear rescue by displaying multiple growing colonies (Figure 3.7 and 3.8, E), but not the control-infected HMF3A culture (Figure 3.7 and 3.8, A).

Since E2F-DB expression and therefore activation of E2F can both inactivate the pRb pathway and rescue the cells from senescence, and since E2F is a major downstream target of pRb, p107 and p130, I can hypothesize that inactivation of the pRb pathway going through E2F is critical for senescence growth arrest.

### 3.2 DISCUSSION

Reconstitution of WT LT activity as well as abrogation of either the pRb or the p53 pathway by ectopic expression of WT LT, E1A, E7, E2F-DB, GSE p53 or shRNA targeting p53 or p21<sup>CIP1/WAF1/Sdi1</sup> were shown to be sufficient to complement the conditional growth arrest at the non permissive temperature in both HMF3A<sup>EcoR</sup> and CL3<sup>EcoR</sup> cells. This validated the CL3<sup>EcoR</sup> cells to be representative of the mixed population to use to dissect the telomere-independent senescence pathways.

Abrogation of p53 or p21<sup>CIP1/WAF1/Sdi1</sup> permitted bypass of senescence in the all the clonal cell lines derived from HMF3A cells. In addition, most cells would form growing colonies after the p53-p21 pathway was abrogated. In comparison, not all clonal cell lines could be rescued by the abrogation of the pRb pathways and only a minor component of the HMF3A cells would form growing colonies as a result of the pRb pathway inactivation.

In addition, it was also concluded that abrogation of either the p53 pathway alone or the pRb pathway alone, were both sufficient to form growing colonies in both HMF3A<sup>EcoR</sup> and CL3<sup>EcoR</sup>.

### 3.2.1 Cellular senescence is p53-dependant process in the HMF3A cells

Our findings that abrogation of the p53 pathway alone was sufficient to bypass senescence in the HMF3A were in agreement with several studies on HDFs indicating a role of p53 in the induction of senescence (Shay, Pereira-Smith et al. 1991; Brown, Wei et al. 1997; Wei, Hemmer et al. 2001; Berns, Hijmans et al. 2004). Moreover, loss of p53 activity alone was reported to be sufficient to impair senescence and promote tumour progression in an *in vivo* model of prostate cancer (Chen, Trotman et al. 2005). Additional data showed that inactivation of the p53 pathway alone was sufficient to bypass senescence in MEFs (Dirac and Bernards 2003); (Harvey, McArthur et al. 1993) and HDFs (Wei, Herbig et al. 2003). In the HDFs, not only Rb<sup>-/-</sup> clones bypassed senescence but the same phenotype was documented for p21<sup>CIP1/WAF1/Sdi1</sup> and p53 heterozygous cells, indicating that loss of function of all three genes results in failure to establish senescence. By contrast, in that study, the abolition of p16<sup>INK4A</sup> function by the expression of a p16<sup>INK4A</sup>-insensitive cyclin-dependent kinase 4 protein or siRNA-mediated knockdown provided only minimal lifespan extension that was terminated by senescence (Wei, Herbig et al. 2003).

However, the results described were not in agreement with studies that utilised a TRF2 inhibition model; de Lange and colleagues have used over-expression of a dominant-negative form of TRF2 (TRF2<sup>ΔBΔM</sup>) to study a process known as ‘sudden telomere deprotection’, where senescence occurs in the absence of telomere shortening (Karlseder, Broccoli et al. 1999; Stansel, de Lange et al. 2001; Smogorzewska and de Lange 2002). In addition to showing that WT LT expression was sufficient to bypass senescence induced in the TRF2 inhibition model, De Lange *et al* showed that p16<sup>INK4a</sup> functioned as a fail-safe mechanism for p53 induced senescence in the absence of a functional p53 pathway (Smogorzewska and de Lange 2002; Jacobs and de Lange 2004).

This is in agreement with the Campisi group finding that in human fibroblasts and mammary epithelial cells, expression of telomerase alone does not suffice to reverse senescence, while p53 inactivation in cells with low levels of p16<sup>INK4A</sup> (BJ cells) resumed robust growth. In contrast, cells with high levels of p16<sup>INK4A</sup> (Wi-38 cells) failed to proliferate upon p53 inactivation. Therefore, in that case, p16<sup>INK4A</sup> provided a dominant second barrier to the unlimited growth of human cells (Beausejour, Krtolica et al. 2003).

Therefore, the demonstration that abrogation of p53 activity alone was sufficient to complement the conditional HMF3A growth defect, was contradictory to the Campisi and de Lange data that implied that both the p53 and pRb pathways must be inactivated.

The fact that endogenous p16<sup>INK4a</sup> expression was readily detectable in the HMF3A cells suggests that, in this context, abrogation of senescence by inactivation of either pathway happens in spite of p16<sup>INK4A</sup> expression. The fact that HMF3A cells were originally derived from adult breast cells may be significant in terms of cell context.

The fact that the TRF2<sup>ΔBΔM</sup> inhibition model represents a telomere-dependent system, unlike the HMF3A system, may help to reconcile the differences observed between these two systems. Moreover, different methods were used to measure the effects of p53

abrogation upon the induction of senescence which may also be an important consideration.

To validate these findings, both hTERT and the p53 shRNA construct should be introduced directly into adult mammary fibroblasts and assessed for their ability to bypass the finite proliferative potential of these cells; it is hypothesised that hTERT and p53 inactivation will be sufficient to bypass this process, in a similar manner to the combined activities of hTERT and LT (O'Hare *et al*, 2001).

As a limitation, however, it is possible that ectopic expression of hTERT and p53 may not be sufficient to bypass cellular senescence in this context, since there may be fundamental differences between immortalisation in primary cells, and maintenance of the immortal state (such as HMF3A cells grown under permissive conditions); for example, expression of an amino terminal LT mutant that retains p53-binding activity (*d11135*), was sufficient to complement the growth of rat *tsa14* cells, but was not able to immortalise (Powell, Darmon *et al*. 1999). This indicated that LT functional activities, in addition to abrogation of p53, were required to initiate this process. It is important to remember that activities required for initiation may not be required for maintenance.

### 3.2.2 Senescence is a p21<sup>CIP1/WAF1/Sdi1</sup>-Dependent Process in the HMF3A Cells

The fact that down-regulation of p21<sup>CIP1/WAF1/Sdi1</sup>, like p53, by shRNA was sufficient to bypass the HMF3A conditional growth defect was in accordance other studies of HDFs (Brown, Wei *et al*. 1997; Wei, Herbig *et al*. 2003; Berns, Hijmans *et al*. 2004). Moreover, microarray analysis has shown that ectopic expression of p21<sup>CIP1/WAF1/Sdi1</sup> in human fibrosarcoma cells is sufficient to induce changes that are known to occur in senescent cells, such as the up-regulation of PAI-1 and other extracellular matrix components and secreted proteases (Chang, Watanabe *et al*. 2000), whereas down-regulation of a large number of genes involved in DNA replication, repair and mitosis by

ectopic p21<sup>CIP1/WAF1/Sdi1</sup> expression has also been described (Harvat, Wang et al. 1998; Chang, Watanabe et al. 2000).

In the HMF3A cells, it was likely that p21<sup>CIP1/WAF1/Sdi1</sup> functioned in a p53-dependent process to induce the irreversible growth arrest, since p21<sup>CIP1/WAF1/Sdi1</sup> levels were significantly down-regulated in HMF3AEco<sup>R</sup> cells complemented for growth at 38°C by the introduction of either p53 shRNA or GSE p53. However, the possibility that senescence occurred in a p53-independent process could not be excluded. Chen and colleagues (Chen, Trotman et al. 2005) used two immortalised human models that lacked functional p53 activity to demonstrate that up-regulation of p21<sup>CIP1/WAF1/Sdi1</sup> in response to Chk2 induction was sufficient to induce senescence.

### 3.2.3 Inactivation of the pRb pathway in the HMF3A cells

Unlike p53, inactivation of the pRb pathway was technically difficult to achieve in the HMF3A cells due to the existence of multiple pRb family members and the possibility that they exhibit functional redundancy. Consequently, a variety of reagents were used to determine the functional role of this pathway in the induction of the HMF3A growth arrest.

#### 3.2.3.1 p16<sup>INK4a</sup> inactivation in the HMF3A Cells

ShRNA targeting has been used previously to impair the negative regulatory activity of p16<sup>INK4a</sup>, a CDKI that functions upstream of pRb. Unfortunately, efficient p16<sup>INK4a</sup> knockdown could not be obtained by shRNA-targeting in the HMF3A cells despite trying two different shRNA construct using identical, if not overlapping, target sequences for p16<sup>INK4a</sup> that had successfully achieved p16<sup>INK4a</sup> knockdown in the literature (Brookes, Rowe et al. 2002; Narita, Nunez et al. 2003; Wei, Herbig et al. 2003; Berns, Hijmans et al. 2004; Bond, Jones et al. 2004). As a result of efficient

p16<sup>INK4a</sup> knockdown, these studies had concluded that down-regulation of p16<sup>INK4a</sup> was not sufficient to prevent the induction of senescence.

The utilisation of alternative, more effective p16<sup>INK4a</sup> shRNA targets could have addressed this problem. However, only a limited region of the *INK4A* locus can be used to design shRNA constructs to specifically down-regulate p16<sup>INK4a</sup>, but not p14<sup>ARF</sup>, which renders this form of analysis not usable in the HMF3A cells.

### 3.2.3.2 *Bmi-1 Activity in the HMF3A Cells*

Bmi-1 ectopic expression was hypothesised to reduce expression from the *INK4A* locus, as demonstrated in other HDF strains such as WI-38 HDFs (Itahana, Zou et al. 2003). However, ectopic Bmi-1 expression had no effect upon p16<sup>INK4a</sup> expression in the HMF3A cells. This supports the hypothesis that human fibroblasts differ in their sensitivity to Bmi-1, an oncogene that extends the replicative lifespan of fibroblasts by repressing p16<sup>INK4A</sup>, apparently because they differ in the level of p16<sup>INK4A</sup> they express at senescence (Itahana, Zou et al. 2003; Jacobs and de Lange 2004). This raises the possibility that human cell strains also differ in the mechanisms that maintain the senescence state.

### 3.2.3.3 *Ectopic Expression of E1A and E7*

Introduction of E1A or E7 into the HMF3A complementation assay was sufficient to complement the growth of these cells. These findings are consistent with the demonstration that E1A expression is sufficient to bypass cellular senescence in primary IMR-90 HDFs (Serrano, Lin et al. 1997; Narita, Nunez et al. 2003). However, the efficiency of abrogation by E7 and E1A expression was much lower than abrogation of the p53 pathway with only a few cells leading to healthily growing colonies, indicating that the pathways must be parallel and not linear. In addition, expression of E7 and E1A did not function to reverse senescence in all the clones tested while abrogation of p53 or

p21<sup>CIP1/WAF1/Sdi1</sup> yielded growing colonies with all clones and the mixed population. This indicated that the pRb pathway may have a lesser importance in the senescence mechanism functioning as an alternative secondary pathway to activate the growth arrest.

This hypothesis is in contradiction with that of Wei and colleagues (Wei, Herbig et al. 2003) who used gene targeting of p53, p21<sup>CIP1/WAF1/Sdi1</sup> and pRb, in addition to ectopic expression of DK and p16<sup>INK4A</sup> RNAi, to conclude that p53, p21<sup>CIP1/WAF1/Sdi1</sup> and pRb acted in a linear genetic pathway (with pRb acting downstream of p53) to regulate entry into replicative senescence, and that p16<sup>INK4A</sup> formed a branch that entered at the level of pRb (Wei, Herbig et al. 2003). It should be noted that this model is also contradictory with the senescence induction model proposed by Sharpless and DePinho (Sharpless and DePinho 2005).

#### *3.2.3.4 Possible Mechanisms by which E1A and E7 Bypass the Conditional HMF3A Growth Defect*

It is possible that both E1A and E7 could have targeted a number of additional cellular proteins, in addition to pRb and/or p300, to bypass senescence. The mechanism by which E1A and E7 could have achieved this is unknown, yet the observation that the HMF3A growth arrest was bypassed by inactivation of p53 and/or p21<sup>CIP1/WAF1/Sdi1</sup> suggested that inactivation of the p53 pathway could have been involved. This conclusion was in agreement with data derived from the immortalisation of REFs with a temperature sensitive mutant of p53 (Vousden, Vojtesek et al. 1993); Vousden and colleagues showed that both E1A and E7 were able to bypass the conditional growth arrest of these cells and they suggested that E1A and E7 were able to do so by modulating the activity of p53, without altering its conformation or stability. Quartin and colleagues also showed that activities mediated by the N-terminal region of LT could bypass the same conditional growth arrest (Quartin, Cole et al. 1994).

Neither E1A, nor E7 are known to bind directly to p53, yet there is evidence to suggest that they are both able to inactivate downstream components of this pathway. As an



example, E7 has been shown to bind to and inactivate p21<sup>CIP1/WAF1/Sdi1</sup> (Helt, Funk et al. 2002). Conversely, there is no evidence of a similar interaction between p21<sup>CIP1/WAF1/Sdi1</sup> and E1A. However, p300/CBP, as described above, is a good candidate for this activity since it is involved in many transcriptional regulation processes by virtue of its endogenous HAT activity; for example LT, E1A and E7 have all been shown to interact with p300/CBP, and it has been implicated in the regulation of both p53 phosphorylation and acetylation status (Pearson, Carbone et al. 2000; Webley, Bond et al. 2000; Pedoux, Sengupta et al. 2005).

However, the fact that expression of E2F-DB, a repressor of the pRb pathway, is sufficient alone to bypass senescence in the HMF3A cells indicates that inactivation of the pRb pathway alone is sufficient to overcome senescence. This does not mean that there is no interaction between the pRb and the p53 pathways but only that these are not essential to senescence.

### *3.2.3.5 p14<sup>ARF</sup> is not necessary between the p16-pRb and p21-p53 Pathways*

E2F has been shown to directly activate p14<sup>ARF</sup> in response to various oncogenic stimuli (DeGregori, Leone et al. 1997; Bates, Phillips et al. 1998; Zhu, DeRyckere et al. 1999; Parisi, Pollice et al. 2002; Aslanian, Iaquina et al. 2004). Since p14<sup>ARF</sup> binds to Mdm2 and impairs the ability of Mdm2 to negatively regulate p53 activity, p14<sup>ARF</sup> provides a link between the pRb and p53 pathways (Dimri *et al*, 2000). However, evidence from the HMF3A model indicated that p14<sup>ARF</sup> did not act upstream of p53 to mediate bypass of the growth arrest as a functional p14<sup>ARF</sup> shRNA construct was insufficient to complement the growth of these cells as Dr. Louise Mansfield has shown in her thesis. Therefore, the link between the pRb and p53 pathways via E2F and p14<sup>ARF</sup> was probably not significant in the HMF3A cells. This conclusion is in accordance with the findings of both Brookes and colleagues (Brookes *et al*, 2002) and Wei and colleagues (Wei *et al*, 2001). Wei and colleagues showed that in HDFs, Ras induced expression of both p21<sup>CIP1/WAF1/Sdi1</sup> and p16<sup>INK4A</sup>, but not p14<sup>ARF</sup>; therefore, the induction of p21<sup>CIP1/WAF1/Sdi1</sup> appeared to be p14<sup>ARF</sup>-independent. However, these findings were not

in agreement with those of Dimri and colleagues (Dimri *et al.*, 2000) who showed that HDFs deficient in p14<sup>ARF</sup> did not undergo senescence. The fact that p14<sup>ARF</sup> has been detected at very low levels in normal human cells may have precluded, to some extent, accurate analysis of p14<sup>ARF</sup> activity in these studies.

The HMF3A data was also in contrast to the substantial evidence linking the activity of p19<sup>Arf</sup> to the induction of senescence in mice; for example, the p19<sup>Arf</sup>-p53 pathway has been shown to play a critical role in the induction of senescence in MEFs (Harvey, McArthur *et al.* 1993; Kamijo, Zindy *et al.* 1997) and a functional screen showed that down-regulation of p19<sup>Arf</sup> was sufficient to rescue premature senescence (Shvarts, Brummelkamp *et al.* 2002). Conversely, enforced expression of p19<sup>Arf</sup> was sufficient to induce cell cycle arrest in MEFs (Quelle, Zindy *et al.* 1995). Therefore, the differential activities of p14<sup>ARF</sup> in humans and p19<sup>Arf</sup> in mice may be species- and/or cell type-specific (Brookes, Rowe *et al.* 2002). General consensus is that ARF is more important in mice whereas p16<sup>INK4A</sup> is more important in humans.

It was also possible that, upon the HMF3A temperature shift, E2F activity was able to induce p53 activation in the absence of p14<sup>ARF</sup> induction, similar to the activation of E2F in response to DNA damage and apoptosis (Tolbert, Lu *et al.* 2002; Lindstrom and Wiman 2003). It has been indeed shown that the cyclin A-binding domain of E2F1 can directly interact with and stabilise p53 in response to DNA damage (Nip, Strom *et al.* 2001; Hsieh, Yap *et al.* 2002; Rogoff, Pickering *et al.* 2002). Such possibilities require further investigation in the HMF3A cells.

#### *3.2.3.6 E2F-DB bypass the conditional growth arrest by repressing the pRb pathway*

E2F, by its interaction to the pRb protein, form a repressor complex that directly binds to the DNA of downstream targets. A mutant form of E2F-1, namely E2F-DB, lacks the pRb-interacting domain as well as the transactivation domain, but is still capable of binding DNA and displacing endogenous E2F-1/pRb complexes from their binding sites.

Sebastian *et al* (2005) used the E2F-DB construct to mimic pRb family inactivation and showed that expression of E2F-DB was functionally equivalent to pRb family inactivation in MEFs.

It has been demonstrated that E2F-DB mutant protein prevents P16<sup>INK4A</sup>-mediated growth arrest and allows cells to proliferate at a normal rate, even with a high level of the P16<sup>INK4A</sup> inhibitor (Zhang, Postigo et al. 1999). Additional data shows that E2F-DB can rescue cell cycle arrest induced by ectopic p19<sup>Arf</sup> expression in MEFs (Rowland, Denissov et al. 2002). E2F-DB was also able to rescue the proliferative potential of M33-null MEFs to a normal rate, whereas they were impaired in the progression into the S phase of the cell cycle in spite of P16<sup>INK4A</sup> and p19<sup>Arf</sup> accumulation (Core, Joly et al. 2004). These results are in agreement with the finding that in the HMF3A cells expression of E2F-DB is sufficient to bypass senescence, suggesting that inactivation of the pRb alone is sufficient to bypass senescence.

#### 3.2.4 p16-pRb does not always act downstream of p53-p21 to induce senescence

The development of a conditionally immortal system of human mammary fibroblasts (HMF3A) cells enabled to define the relative contributions of the p16-pRb and p53-p21 pathways towards senescence, by developing a complementation assay to abrogate each of these pathways by ectopic expression of various constructs or shRNA mediated silencing.

Together, these results indicated that in these conditionally immortalised human mammary fibroblasts, the predominant pathway that induces the irreversible growth arrest was the p53-p21 pathway since it was most efficiently abrogated when this pathway was inactivated. Inactivation of the p16-pRb pathway also overcomes the growth arrest but much less efficiently and in a much smaller number of cells compared to p53. This indicates that pRb does not always act downstream of p53-p21 but may support the idea of parallel pathways.

## **4 ACTIVATION OF THE NF- $\kappa$ B SIGNALLING PROMOTES CELLULAR SENESENCE**

### **4.1 SENESENCE SPECIFIC GENE EXPRESSION RESULTS**

#### 4.1.1 Objectives

Genome wide expression profiling technologies have been extensively employed to identify genes that are differentially expressed in a wide variety of cell types, cancers and other disease processes. They have also been used to systematically analyse a variety of cellular processes such as quiescence, stress, replicative and oncogene-induced senescence and identify the downstream targets of the E2F and p53 pathways.

Previously, cDNA microarrays representing approximately 6000 genes were used to identify genes that are differentially expressed when the conditionally immortal mammary fibroblasts undergo irreversible growth arrest, upon activation of the p16-pRb and p53-p21 pathways. It was discovered that the transcriptional changes that occurred upon the conditional HMF3A model growth arrest directly correlated with the transcriptional changes that occurred upon replicative senescence (Hardy, Mansfield et al. 2005). It appeared that three pathways associated with the induction of replicative senescence, namely, the p53, pRb and ERK signalling pathways, were also important regulators of the conditional HMF3A growth arrest. In addition, *in silico* analysis of the promoters of genes known to be differential in senescence indicated that NF- $\kappa$ B and C-EBP transcription factors may be activated upon senescence.

To investigate further how exactly these pathways affect the genes expression and furthermore which group of genes preferentially have their expression affected upon senescence and also to identify novel genes and signaling pathways causal to the induction of cellular senescence, an extended genome wide microarray expression profiling analysis (complete coverage of the Human Genome for analysis of over 47,000

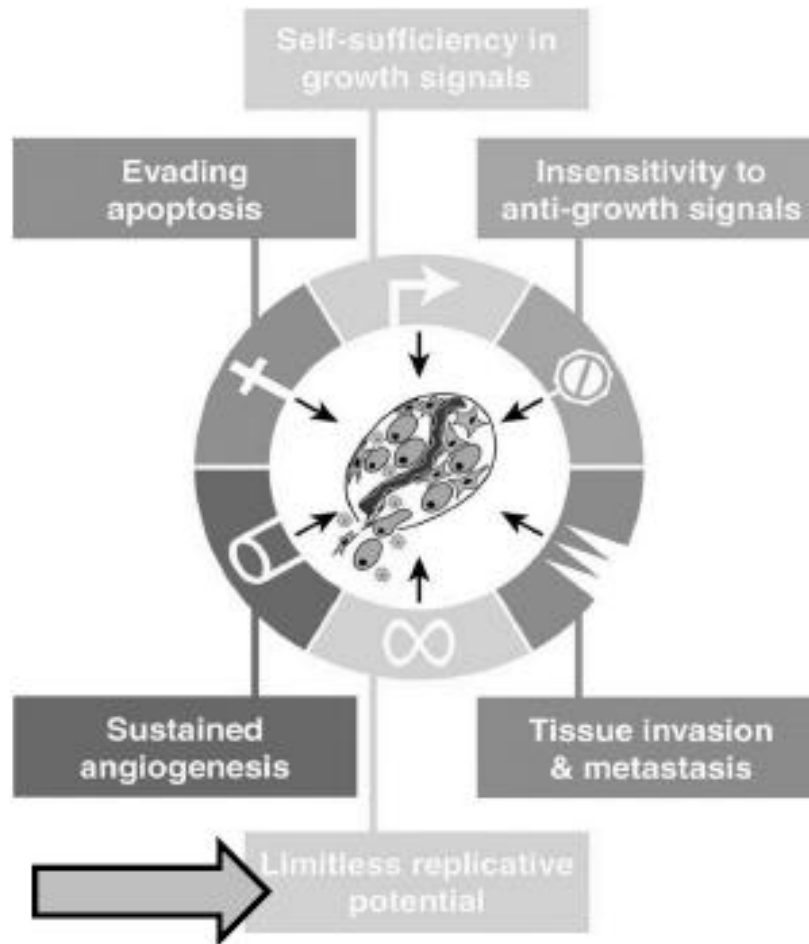
transcripts) was performed. It was hypothesised that the activity of critical mediators of senescence would be abrogated in all cells in which the process had been abrogated. Consequently, I developed a clonal derivative of HMF3A called CL3<sup>EcoR</sup> which behave like HMF3A cells. I first identified changes that were specific for growth arrest by eliminating changes due to the temperature shift and also identified changes in expression that could be caused by quiescence.

From there, the study was broadened by overcoming senescence in these cells by individually abrogating the p53-p21 (with p53 shRNA, p21 shRNA or p53 GSE) and p16-pRb (with E7, E1A or E2F-DB) pathways as previously described in chapter 1 and profiling the resultant cells. Upon verification of the expression data by quantitative real-time PCR, the functional activity of the candidate gene was further analysed using the HMF3A complementation assay to validate the biological effects of the regulated genes.

#### 4.1.2 Why use Microarray Analysis?

The onset of tumourigenesis is a complex mechanism hypothesised to be involving a limited, but essential set of alterations necessary for tumour development (Hanahan and Weinberg 2000); namely, self-sufficiency in growth signals, insensitivity to anti-growth signals, evading of apoptosis, limitless replicative potential, sustained angiogenesis, and tissue invasion and metastasis (Figure 4.1). The authors state that most, if not all, cancers will have acquired these capabilities during their development; yet different genes may be inactivated in different ways, to achieve the same endpoint.

Bypassing senescence represents an example of one of the possible mechanisms utilised by the cells to acquire limitless replicative potential, making the HMF3A conditional cells an excellent *in vitro* model to investigate the signalling pathways that underline senescence. HMF3A cultures in which senescence has been bypassed by expression of wt LT, E1A, E7, E2F-DB, p53 shRNA and GSE p53 represented valuable resources with which to investigate the downstream signalling pathways that induce senescence.



from Hanahan and Weinberg, 2000.

**Figure 4.1: Cancer: A multistep process**

Figure from Hanahan and Weinberg, 2000.

In contrast to normal somatic cells, cancer cells have the potential to proliferate indefinitely and the acquisition of this limitless replicative potential has been proposed to be one of the six key events required for malignant transformation .

Many experimental techniques were applicable for this investigation, but the rapid evolution in the development of microarray platform technologies over recent years and the unbiased nature of the analysis meant that gene expression profiling represented an attractive approach with which to assess the putative role of many novel genes in this process. There are many previous examples of the application of this technique in studies involving senescent HDFs (Cristofalo and Tresini 1998; Shelton, Chang et al. 1999).

A major advantage in applying microarray analysis to the HMF3A system, unlike these other studies, however, was the rapid and synchronous nature of the conditional growth arrest. Additionally, previous study by Hardy et al (2005) has shown that genes expressed upon HMF3A conditional senescence directly correlated with the transcriptional changes that occurred upon natural replicative senescence.

#### 4.1.3 Which Microarray Technology?

Advances in sequence selection, sequence clustering, probe modelling, probe selection, analysis algorithms, and array manufacturing enabled the release of the Human Genome U133 Set in 2001. In addition, this design incorporated the first complete draft of the human genome. The GeneChip® Human Genome U133 Plus 2.0 microarray, the latest iteration of the human expression arrays, developed by Affymetrix, was utilised. Enhancements in array manufacturing, new scanner technology and improvements in data acquisition allowed better accuracy. The Human Genome U133 Plus 2.0 Array contained over 54,000 probe sets representing approximately 38,500 genes on a single array. This increase in feature density allows the expression of all known transcripts of an organism to be analyzed on a single array. The sequences from which these probe sets were derived were selected from GenBank®, dbEST, and RefSeq.

#### 4.1.4 Microarray Strategy

It was important to address the issue of variability in the design of the microarray experiment in order to obtain biologically relevant and reproducible microarray data.

The clonal nature of the CL3<sup>EcoR</sup> limited, to some extent, the experimental error that could have occurred as a result of biological variability. However, to further minimise sources of technical variability, each experimental condition was analyzed using biological triplicates. Specifically, three cultures were processed in parallel and RNA was extracted from each culture, as suggested by Lee and colleagues (Lee, Kuo et al. 2000). Assays were performed as systematically as possible to minimise experimental variation and all samples were processed simultaneously.

It was also important to utilise an appropriate experimental design to ensure the maximum amount of information was obtained from the microarray data (Larkin, Frank et al. 2005).

To identify the changes in gene expression that occur upon irreversible growth arrest, (GA) triplicate independent biological samples of RNA extracted from CL3<sup>EcoR</sup> cells growing at 34°C or after growth arrest at 38°C for 7 days were analysed by expression profiling (Figure 4.2). These changes also included gene expression changes that were non-specific to senescence induction as they could be due to heat shock triggered by the temperature shift (HS).

To eliminate changes in gene expression due to the temperature shift (HS), two methods could have been used: Firstly, irreversibly arrested CL3<sup>EcoR</sup> cells incubated at 38°C for 7 days can be compared to irreversibly arrested CL3<sup>EcoR</sup> cells shifted back down to 34°C for 7 days. However, there is a possibility that irreversibly arrested CL3<sup>EcoR</sup> cells will exhibit an altered pattern of gene expression of heat-shock genes when compared to proliferating cells. In addition, some genes may even be turned back on, even though the cells do not divide. Consequently, a second method utilising the



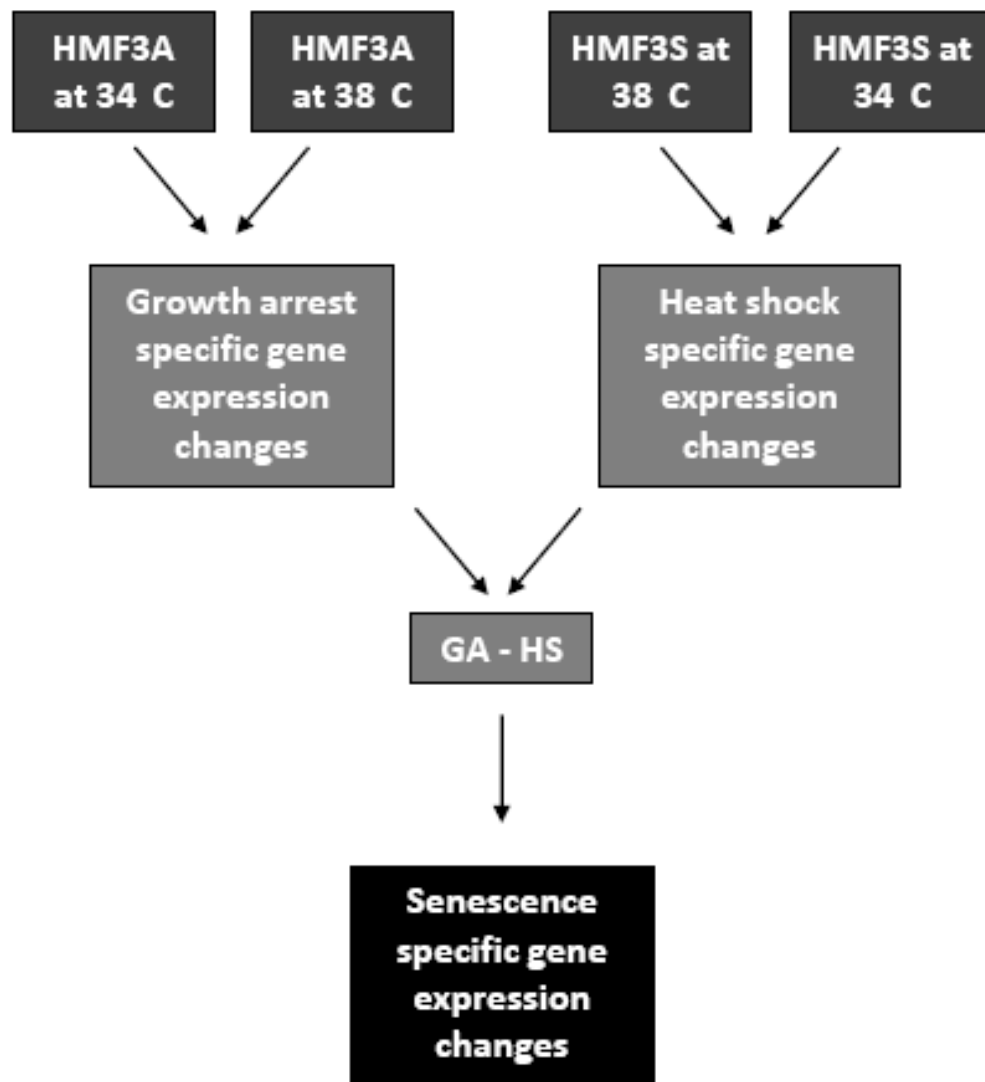


**Figure 4.2: HMF3A<sup>EcoR</sup> Microarray strategy**

To identify the changes in gene expression that occur upon irreversible growth arrest (GA) and heat shock (HS) triplicate independent biological samples of RNA extracted from CL3<sup>EcoR</sup> (GA) or HMF3S cells (HS) cells growing at 34°C or at 38°C for 7 days were analysed by expression profiling.

HMF3S cell line was chosen (Figure 4.2). Triplicate independent RNA samples extracted from HMF3S cells grown at 34°C and after shift up to 38°C for 7 days were analysed. HMF3S cells were immortalised from the same batch of primary human mammary fibroblasts, using a wild type U19 LT antigen not sensitive to temperature in conjunction with hTERT, and do not growth arrest upon shift at 38°C but continue to divide and do not express SA-β-Gal. Each condition was processed in biological triplicate.

To identify genes that were differential due to the irreversible growth arrest of CL3<sup>EcoR</sup> cells, all changes detected upon shift up of HMF3S cells were eliminated (Figure 4.2). Genes were considered growth arrest specific when the difference of Log<sub>2</sub> Fold Change in the gene expression between “CL3<sup>EcoR</sup> 38 versus 34” and “HMF3S 38 versus 34” was >1 or < -1 (equivalent to a 2 fold up- or down-regulation).

In order to identify genes whose expression may also be altered by serum starvation resulting in quiescence, a state of reversible growth arrest, CL3<sup>EcoR</sup> cells were serum starved for 7 days at 34°C, triplicate independent RNA samples extracted and compared to profiles of CL3<sup>EcoR</sup> cells cultured at 34°C; shown schematically in Figure 4.3.A.

If changes in gene expression are specific for the senescence growth arrest, they should be reversed upon its abrogation. To identify if changes in gene expression would be reversed, triplicate independent cultures of CL3<sup>EcoR</sup> cells after complementation of the growth defect with SV40 LT antigen, Ad5 E1A 12S, HPV16 E7, E2F-DB, p53GSE, p53shRNA and p21shRNA were derived and profiled. The data for each rescued culture was averaged, compared to its appropriate control cells to obtain the set of differential genes which were then compared to the differential GA data set (shown schematically in Figure 4.3B).

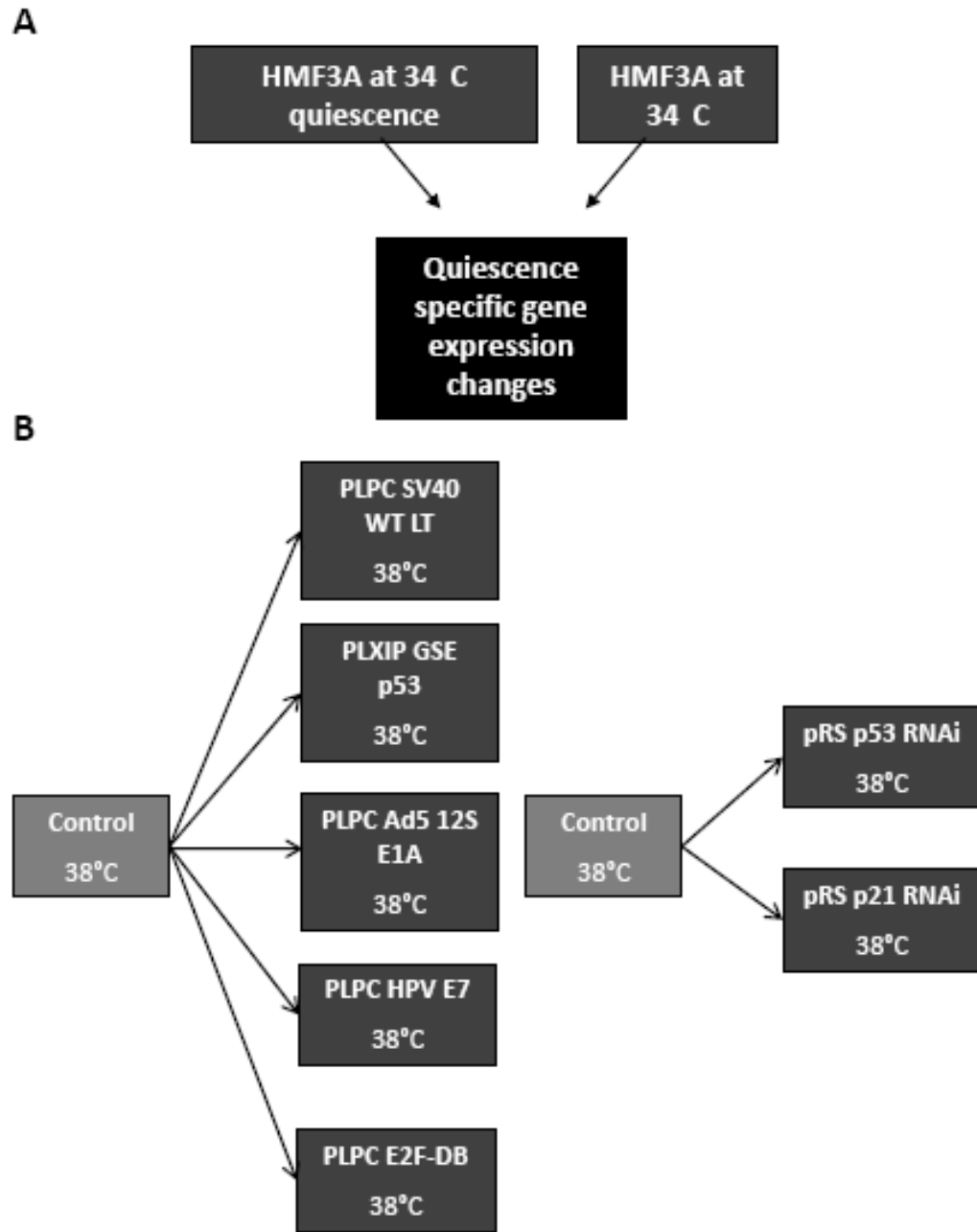


**Figure 4.3: Microarray strategy for the complementations**

To identify the changes in gene expression that occur upon quiescence (Q) triplicate independent biological samples of RNA extracted from CL3<sup>EcoR</sup> cells growing at 34°C in a normal media or in a FCS depleted media (quiescence) for 7 days were analysed by expression profiling (A). To identify if changes in gene expression would be reversed, triplicate independent cultures of CL3<sup>EcoR</sup> cells after complementation of the growth defect with SV40 LT antigen, Ad5 E1A 12S, HPV16 E7, E2F-DB, p53GSE, p53shRNA and p21shRNA were derived and profiled (B).

#### 4.1.5 Microarray procedure

To perform the microarray procedure, total RNA was extracted from CL3<sup>EcoR</sup> cells incubated at 34 and 38°C to prepare the reference RNA samples (Figure 4.2 and 4.3A and B) or at 38°C with the various constructs described in chapter one (PLPCX, PLPC E7, PLPC E1A, PLPC E2F-DB, PLXIP GSE p53, pRS Lamin A/C shRNA, pRS p21 shRNA and pRS p53 shRNA) to prepare the different conditions samples to analyse. Additional total RNA was extracted from quiescent CL3<sup>EcoR</sup> cells and HMF3S cells to prepare the heat shock and quiescence samples. RNA was extracted from biological triplicate cultures using Trizol (Invitrogen), frozen and sent for analysis at the Memorial Sloan Kettering Cancer Center Microarray facility.

#### 4.1.6 Microarray results

Application of the strategy outlined in Figure 4.2 identified 3059 up-regulated transcripts of which 816 were up-regulated >2 fold and 5005 were down-regulated, 961 of which were down-regulated >2 fold. The top 24 up- and down-regulated transcripts ranked according to log<sub>2</sub> Fold Change are shown in Table 4.1 A and B; the complete lists are in Supplementary Tables S4.1 and S4.2 (supplementary on a CD). Three of the top four most highly down-regulated transcripts (NUF2, SLC25 and NDC80) are all components of the NDC80 kinetochore complex; NUF2 was decreased 23 fold (P-value 1.88E-23), SPC25 18 fold (P-value 1.39E-24) and NDC80 17 fold (P-value 1.12E-21) respectively. All of the top down-regulated transcripts yielded highly significant p-values. Four of the top five most highly up-regulated transcripts correspond to the same gene, CLCA family member 2, chloride channel regulator. This was due to the gene being present in four different locations on the chips. It also validates the accuracy of the microarray if the same gene represented by different oligos gives similar results. The fold increase in expression of CLCA2 was 28 (P-value 1.87E-12), 23 (P-value 5.62E-13), 19 (P-value 6.25E-12) and 15 (P-value 1.85E-12) respectively.

# A

Probe	Symbol	Description	logFC GA	P.val	logFC HS	P.Val	logFC Q	P.Val
217528_at	CLCA2	CLCA family member 2, chloride channel regulator	4.79	1.9E-12	0.18	8.0E-01	0.89	8.1E-02
206165_s_at	CLCA2	CLCA family member 2, chloride channel regulator	4.51	5.6E-13	-0.08	9.0E-01	0.67	1.5E-01
209821_at	IL33	interleukin 33	4.24	8.0E-10	2.58	4.1E-05	3.06	9.5E-07
206166_s_at	CLCA2	CLCA family member 2, chloride channel regulator	4.22	6.3E-12	-0.16	8.1E-01	0.09	8.7E-01
206164_at	CLCA2	CLCA family member 2, chloride channel regulator	3.87	1.9E-12	-0.10	8.6E-01	0.57	1.7E-01
243036_at	RP4-692D3.1	hypothetical protein LOC728621	3.75	3.5E-12	-0.18	7.4E-01	1.55	2.0E-04
225895_at	SYNPO2	synaptopodin 2	3.74	3.0E-10	0.45	4.5E-01	-1.62	9.3E-04
203158_s_at	GLS	glutaminase	3.53	8.5E-16	-0.62	4.8E-02	1.35	7.9E-06
220518_at	ABI3BP	ABI gene family, member 3 (NESH) binding protein	3.52	1.0E-13	0.07	8.8E-01	3.95	4.3E-15
205433_at	BCHE	butyrylcholinesterase similar to ankyrin repeat domain 20 family, member A1	3.51	2.9E-07	1.65	1.3E-02	0.54	4.1E-01
237737_at	LOC727770		3.51	1.5E-08	-0.46	4.9E-01	-0.34	5.6E-01
223734_at	OSAP	ovary-specific acidic protein	3.44	1.8E-14	0.96	3.7E-03	-0.76	1.4E-02
201860_s_at	PLAT	plasminogen activator, tissue	3.42	1.2E-17	1.71	9.9E-09	0.45	6.2E-02
210118_s_at	IL1A	interleukin 1, alpha	3.42	1.7E-10	0.22	7.0E-01	3.82	1.1E-11
226757_at	IFIT2	interferon-induced protein with tetratricopeptide repeats 2	3.39	8.7E-08	0.34	6.4E-01	1.62	4.3E-03
220115_s_at	CDH10	cadherin 10, type 2 (T2-cadherin)	3.37	9.1E-12	1.77	2.5E-05	-1.77	9.8E-06
205067_at	IL1B	interleukin 1, beta	3.33	1.9E-08	0.06	9.4E-01	3.54	5.2E-09
229331_at	SPATA18	spermatogenesis associated 18 homolog (rat)	3.31	1.3E-15	0.09	8.2E-01	-0.38	1.6E-01
238733_at			3.29	1.0E-16	0.18	5.7E-01	1.13	1.5E-05
39402_at	IL1B	interleukin 1, beta	3.29	7.2E-09	0.38	5.4E-01	3.43	3.2E-09
228128_x_at	PAPPA	pregnancy-associated plasma protein A, pappalysin 1	3.25	2.2E-11	1.69	4.8E-05	2.77	1.1E-09
203159_at	GLS	glutaminase	3.23	4.1E-18	-0.65	5.1E-03	1.42	1.6E-08
223395_at	ABI3BP	ABI gene family, member 3 (NESH) binding protein	3.2	1.6E-09	0.87	7.8E-02	3.39	4.2E-10
225720_at	SYNPO2	synaptopodin 2	3.16	1.5E-15	-0.05	9.0E-01	-1.02	1.3E-04

## B

Probe	Symbol	Description	logFC GA	P.val	logFC HS	P.Val	logFC Q	P.Val
223381_at	NUF2	NUF2, NDC80 kinetochore complex component, homolog (S. cerevisiae)	-4.52	1.9E-23	0.46	4.1E-02	-0.40	5.4E-02
203764_at	DLGAP5	discs, large (Drosophila) homolog-associated protein 5	-4.21	3.0E-26	0.28	8.3E-02	-0.72	4.4E-06
209891_at	SPC25	SPC25, NDC80 kinetochore complex component, homolog (S. cerevisiae)	-4.20	1.4E-24	-0.13	5.5E-01	-0.37	3.7E-02
204162_at	NDC80	NDC80 homolog, kinetochore complex component (S. cerevisiae)	-4.08	1.1E-21	0.43	6.9E-02	-0.05	8.4E-01
202870_s_at	CDC20	cell division cycle 20 homolog (S. cerevisiae)	-4.06	1.3E-25	-0.06	7.8E-01	-1.34	1.1E-11
219918_s_at	ASPM	asp (abnormal spindle) homolog, microcephaly associated (Drosophila)	-3.99	3.0E-22	0.52	1.5E-02	-0.17	4.2E-01
204641_at	NEK2	NIMA (never in mitosis gene a)-related kinase 2	-3.97	1.3E-25	0.24	1.5E-01	-0.43	4.2E-03
232238_at	ASPM	asp (abnormal spindle) homolog, microcephaly associated (Drosophila)	-3.97	2.1E-22	0.84	7.7E-05	-0.11	5.9E-01
232278_s_at	DEPDC1	DEP domain containing 1	-3.77	2.3E-22	0.90	1.5E-05	-0.28	1.4E-01
219148_at	PBK	PDZ binding kinase	-3.71	5.3E-26	-0.10	5.6E-01	-0.50	2.3E-04
215942_s_at	GTSE1	G-2 and S-phase expressed 1	-3.62	3.9E-19	0.38	1.4E-01	-0.15	5.5E-01
222039_at	KIF18B	kinesin family member 18B	-3.57	2.8E-22	-0.01	9.8E-01	-0.38	3.1E-02
228323_at	CASC5	cancer susceptibility candidate 5	-3.56	9.9E-23	0.04	8.8E-01	-0.36	3.5E-02
204962_s_at	CENPA	centromere protein A	-3.52	6.3E-25	0.46	2.5E-03	-0.06	6.9E-01
201291_s_at	TOP2A	topoisomerase (DNA) II alpha 170kDa	-3.44	1.4E-24	0.51	9.1E-04	0.02	9.1E-01
1552619_a_a	ANLN	anillin, actin binding protein	-3.42	7.2E-25	-0.20	2.0E-01	-1.01	1.4E-09
207165_at	HMMR	hyaluronan-mediated motility receptor (RHAMM)	-3.39	1.1E-23	0.71	2.0E-05	-0.06	7.2E-01
218755_at	KIF20A	kinesin family member 20A	-3.39	1.1E-22	0.66	1.9E-04	-0.98	9.6E-08
236641_at	KIF14	kinesin family member 14	-3.37	2.5E-23	0.71	2.6E-05	-0.04	8.3E-01
203755_at	BUB1B	BUB1 budding uninhibited by benzimidazoles 1 homolog beta (yeast)	-3.36	3.1E-25	0.18	2.5E-01	-0.30	2.2E-02
204318_s_at	GTSE1	G-2 and S-phase expressed 1	-3.36	1.1E-22	0.36	4.1E-02	-0.29	7.5E-02
202240_at	PLK1	polo-like kinase 1 (Drosophila)	-3.35	1.5E-26	0.14	3.1E-01	-1.04	3.7E-12
204444_at	KIF11	kinesin family member 11	-3.34	1.3E-23	-0.08	6.7E-01	-0.50	8.5E-04
218009_s_at	PRC1	protein regulator of cytokinesis 1	-3.33	2.4E-25	0.24	9.0E-02	-0.59	1.2E-05

**Table 4.1: Senescence specific changes in gene expression**

Log<sub>2</sub> fold changes in gene expression that occur upon irreversible growth arrest are indicated as GA, upon shift up of HMF3S cells from 34°C to 38°C are indicated as HS and upon serum starvation are indicated as Q. Up-regulated transcripts are indicated in green whereas down-regulated transcripts are in red. Results for the top 24 up- (A) and down-regulated (B) transcripts upon growth arrest, heat shock and quiescence are shown.

The P-values for the up-regulated transcripts were lower than those for the down-regulated transcripts but were still highly significant and less than E-07.

To refine the differential gene expression data set, several comparisons were carried out including identifying genes associated with quiescence (Figure 4.3A). This control is designed to identify whether gene expression is also altered upon quiescence, namely, serum-starvation.

The results are also presented in Table 4.1 A and B as  $\log_2$  FC Q for the top 24 up- and down-regulated transcripts. Interestingly, many of the top 24 up-regulated genes were also highly up-regulated upon serum starvation (Table 4.1A); for example IL33, ABI3P, IL1A, IL1B, and PAPPA.

The results obtained after rescue with the various constructs for the top 24 up- and down-regulated genes upon irreversible growth are shown in Table 2A&B; the complete data sets are in Supplementary Tables S4.1 and S4.2 (on CD).

The results showed that when growth arrest was overcome, differential expression was reversed; down-regulated genes (red) were up-regulated (green) whereas up-regulated genes (green) were suppressed (red). The global reversion, for the quasi-totality of the genes, upon complementation by abrogation of the pRb pathway or the p53 pathway, is impressive and further reinforces the involvement of these genes in the senescence mechanisms. However, the fold change was not always the same across the different complementations eg. for CLCA2 (Table 4.2A), the fold suppression upon rescue with Ad5 E1A 12S, p53shRNA and GSE53 was about 30 fold whereas with HPV16 E7, E2F-DB and p21shRNA, the fold change was 4 fold. Although these differences may be due to level of expression of the complementing gene, they are more likely to reflect the rescuing pathways as illustrated by the changes in expression of MDM2 (HMD2, Table 4.2C) which is an E3 ubiquitin ligase that associates with p53 and maintains it at a low level; up-regulation of p53 results in up-regulation of MDM2. When CL3<sup>EcoR</sup> cells undergo growth arrest MDM2 was up-regulated; expression of all three MDM2 features was increased.

# A

Symbol	Description	logFC GA	log FC HS	logFC Q	logFC wt_LT	logFC GSE_p53	logFC pRS_p53	logFC pRS_p21	logFC E1A	logFC E7	logFC E2F-DB
CLCA2	CLCA family member 2, chloride channel regulator	4.79	0.18	0.89	-4.70	-5.46	-6.13	-2.51	-5.59	-1.97	-1.83
CLCA2	CLCA family member 2, chloride channel regulator	4.51	-0.08	0.67	-4.45	-5.26	-5.94	-2.49	-5.08	-1.76	-1.86
IL33	interleukin 33	4.24	2.58	3.06	-6.75	-5.33	-2.33	-2.83	-7.10	-4.14	-3.66
CLCA2	CLCA family member 2, chloride channel regulator	4.22	-0.16	0.09	-3.87	-4.48	-5.21	-2.29	-4.46	-1.60	-1.89
CLCA2	CLCA family member 2, chloride channel regulator	3.87	-0.10	0.57	-3.18	-3.37	-4.41	-2.58	-3.45	-1.61	-1.52
RP4-692D3.1	hypothetical protein LOC728621	3.75	-0.18	1.55	-4.26	-2.96	-2.19	-2.63	-4.59	-2.85	-2.98
SYNPO2	synaptopodin 2	3.74	0.45	-1.62	-1.39	-0.55	-2.68	-2.73	-3.41	-2.20	-3.13
GLS	glutaminase	3.53	-0.62	1.35	-1.84	-0.78	-0.82	-1.23	-1.82	-1.64	-1.24
ABI3BP	ABI gene family, member 3 (NESH) binding protein	3.52	0.07	3.95	-2.32	-1.84	-1.64	-1.29	-2.75	-1.13	-0.88
BCHE	butyrylcholinesterase	3.51	1.65	0.54	-1.55	-1.73	-1.60	-1.67	0.48	-1.55	-0.36
LOC727770	similar to ankyrin repeat domain 20 family, member A1	3.51	-0.46	-0.34	-4.08	-4.32	-3.71	1.17	-2.83	-1.35	0.01
OSAP	ovary-specific acidic protein	3.44	0.96	-0.76	-0.50	-0.68	-1.12	-1.60	0.48	-0.76	-0.11
PLAT	plasminogen activator, tissue	3.42	1.71	0.45	-1.54	-1.12	-1.10	-1.92	-2.69	-1.57	-1.67
IL1A	interleukin 1, alpha	3.42	0.22	3.82	-4.36	-3.28	-0.70	-0.26	-5.18	-1.05	-0.04
IFIT2	interferon-induced protein with tetratricopeptide repeats 2	3.39	0.34	1.62	-0.70	-1.67	-0.53	-1.42	-3.47	-0.86	-2.46
CDH10	cadherin 10, type 2 (T2-cadherin)	3.37	1.77	-1.77	-2.78	-2.39	-3.19	-0.50	-0.97	-1.24	-1.65
IL1B	interleukin 1, beta	3.33	0.06	3.54	-4.60	-4.13	-1.41	-1.48	-5.44	-1.98	-0.86
SPATA18	spermatogenesis associated 18 homolog (rat)	3.31	0.09	-0.38	-1.78	-3.10	-2.79	-0.19	-0.28	-0.91	-1.63
238733_at		3.29	0.18	1.13	-2.10	-2.94	-3.22	0.47	2.08	-0.35	0.14
IL1B	interleukin 1, beta	3.29	0.38	3.43	-4.58	-3.83	-1.31	-1.37	-5.89	-1.82	-0.80
PAPPA	pregnancy-associated plasma protein A, pappalysin 1	3.25	1.69	2.77	-3.90	-1.92	-1.80	-0.16	-5.56	-1.76	-1.35
GLS	glutaminase	3.23	-0.65	1.42	-1.60	-0.26	-1.01	-1.18	-1.68	-1.63	-1.26
ABI3BP	ABI gene family, member 3 (NESH) binding protein	3.2	0.87	3.39	-3.68	-2.11	-1.16	-1.20	-7.66	-1.70	-1.52
SYNPO2	synaptopodin 2	3.16	-0.05	-1.02	-0.97	-0.73	-2.04	-2.08	-1.67	-1.16	-1.59



## B

Symbol	Description	logFC GA	logFC HS	logFC Q	logFC wt_LT	logFC GSE_p 53	logFC pRS_p5 3	logFC pRS_p2 1	logFC E7	logFC E1A	logFC E2F-DB
NUF2	NUF2, NDC80 kinetochore complex component, homolog (S. cerevisiae)	-4.52	0.46	-0.40	4.60	4.15	3.77	3.21	3.71	4.79	3.93
DLGAP5	discs, large (Drosophila) homolog-associated protein 5	-4.21	0.28	-0.72	4.11	3.54	3.41	3.19	3.36	4.30	3.66
SPC25	SPC25, NDC80 kinetochore complex component, homolog (S. cerevisiae)	-4.20	-0.13	-0.37	3.43	3.22	3.21	2.93	2.96	3.63	3.14
NDC80	NDC80 homolog, kinetochore complex component (S. cerevisiae)	-4.08	0.43	-0.05	3.97	4.29	3.50	2.95	3.13	3.39	2.98
CDC20	cell division cycle 20 homolog (S. cerevisiae)	-4.06	-0.06	-1.34	3.73	3.41	3.54	3.03	3.38	3.53	3.59
ASPM	asp (abnormal spindle) homolog, microcephaly associated (Drosophila)	-3.99	0.52	-0.17	4.66	4.19	3.93	3.40	3.94	5.11	4.29
NEK2	NIMA (never in mitosis gene a)-related kinase 2	-3.97	0.24	-0.43	3.99	3.57	3.22	3.06	3.42	3.99	3.71
ASPM	asp (abnormal spindle) homolog, microcephaly associated (Drosophila)	-3.97	0.84	-0.11	4.30	3.91	3.62	3.09	3.41	4.81	3.86
DEPDC1	DEP domain containing 1	-3.77	0.90	-0.28	3.99	3.73	3.53	3.06	3.41	3.89	3.82
PBK	PDZ binding kinase	-3.71	-0.10	-0.50	3.34	3.45	2.93	2.81	3.02	3.27	3.17
GTSE1	G-2 and S-phase expressed 1	-3.62	0.38	-0.15	3.16	2.68	2.39	2.15	2.37	3.11	2.39
KIF18B	kinesin family member 18B	-3.57	-0.01	-0.38	3.35	3.47	3.09	2.69	2.83	3.18	2.90
CASC5	cancer susceptibility candidate 5	-3.56	0.04	-0.36	3.62	3.30	3.08	2.91	2.76	3.50	3.09
CENPA	centromere protein A	-3.52	0.46	-0.06	3.56	3.35	2.98	2.44	2.76	3.80	2.89
TOP2A	topoisomerase (DNA) II alpha 170kDa	-3.44	0.51	0.02	3.39	3.51	2.80	2.56	2.81	3.52	2.94
ANLN	anillin, actin binding protein	-3.42	-0.20	-1.01	3.54	3.34	3.08	2.69	2.95	3.15	3.32
HMMR	hyaluronan-mediated motility receptor (RHAMM)	-3.39	0.71	-0.06	3.17	3.04	3.08	2.88	3.06	2.78	3.21
KIF20A	kinesin family member 20A	-3.39	0.66	-0.98	3.78	3.37	2.89	2.78	3.11	3.64	3.06
KIF14	kinesin family member 14	-3.37	0.71	-0.04	3.62	3.03	3.13	2.70	2.80	3.91	3.13
BUB1B	BUB1 budding uninhibited by benzimidazoles 1 homolog beta (yeast)	-3.36	0.18	-0.30	3.21	3.03	2.81	2.41	2.60	3.22	2.72
GTSE1	G-2 and S-phase expressed 1	-3.36	0.36	-0.29	3.30	2.87	2.36	2.17	2.53	3.36	2.61
PLK1	polo-like kinase 1 (Drosophila)	-3.35	0.14	-1.04	2.96	2.24	2.61	2.21	2.46	2.61	2.58
KIF11	kinesin family member 11	-3.34	-0.08	-0.50	3.19	2.87	2.37	2.07	2.46	3.14	2.43
PRC1	protein regulator of cytokinesis 1	-3.33	0.24	-0.59	3.14	2.81	2.58	2.25	2.66	3.33	2.69

## C

Log FC	GA	P. Val	Q	P. Val	HS	P. Val	wt LT	P. Val	GSE p53	P. Val	P53 RNAi	P. Val	P21 RNAi	P. Val	E1A	P. Val	E7	P. Val	E2F DB	P. Val
MDM2	1.91	7.E-10	0.28	3.E-01	-0.08	8.E-01	-1.60	5.E-08	-2.78	7.E-14	-2.41	7.E-12	0.79	4.E-03	1.49	8.E-08	0.11	8.E-01	0.73	6.E-03
MDM2	1.70	4.E-11	-0.10	6.E-01	-0.10	7.E-01	-1.27	4.E-08	-2.42	5.E-15	-2.20	1.E-13	0.73	9.E-04	1.59	8.E-11	0.24	3.E-01	0.60	4.E-03
MDM2	1.42	8.E-09	-0.26	2.E-01	0.33	2.E-01	-1.14	9.E-07	-1.68	2.E-10	-1.73	2.E-10	0.47	4.E-02	1.39	5.E-09	0.09	8.E-01	0.52	2.E-02

**Table 4.2: Senescence specific changes in gene expression with complementation**

Log<sub>2</sub> fold changes in gene expression that occur upon irreversible growth (GA), upon shift up of HMF3S cells from 34°C to 38°C (HS) and upon serum starvation (Q). If changes in gene expression are specific for the senescence growth arrest, they should be reversed upon its abrogation. Up-regulated transcripts are indicated in green whereas down-regulated transcripts are in red. Results for the top 24 up- (A) and down-regulated (B) transcripts after complementation with the indicated constructs as well as the changes in expression of the three MDM2/HDM2 features (C) are shown.

When growth arrest was abrogated using WT LT antigen, p53GSE or p53shRNA that directly inhibit p53 activity, MDM2 expression was reversed for all three features. However when growth arrest was abrogated with Ad5 E1A 12S, HPV16 E7 and E2F-DB or p21shRNA, none of which are known to directly act on p53, MDM2 expression levels remained up-regulated, although the fold up-regulation was reduced by HPV16 E7 and E2F-DB or upon silencing of p21<sup>CIP1</sup>.

#### 4.1.7 Validation of Microarray Data

##### *4.1.7.1 Why Validate?*

The fact that considerable inconsistencies have been observed between different microarray studies in terms of the different platform technologies, methodologies, protocols and analyses (Bammler, Beyer et al. 2005; Irizarry, Warren et al. 2005; Larkin, Frank et al. 2005), emphasised the need to independently verify the microarray data. A number of techniques were available to facilitate this, including semi-quantitative RT-PCR, real-time PCR, northern blot and ribonuclease protection assay. However, due to the number of genes to verify and the short time scale left to do so, I collaborated with Biotrove Inc. to use their signal transduction panel of ~600 genes for real time PCR analysis. I provided Biotrove with the mRNA, Dr Elen Ortenberg did the Q-PCR analysis and the initial data analysis.

##### *4.1.7.2 Real time validation of expression data using the BioTrove Open Arrays*

To confirm the expression profiling data, the OpenArray Pathways Human Signal Transduction Panel Analysis developed by Biotrove was utilised. Duplicate RNA samples that had been used for the profiling studies extracted from CL3<sup>EcoR</sup> cells grown at 34°C and after shift to 38°C for 7 days or HMF3S cells grown at 34°C and 7 days after shift to 38°C were used. The 630 genes comprising the Signal Transduction panel are presented in Supplementary Table S4.3 (supplementary on a CD). Ct values were

normalised using the geomean of 18 housekeeping genes.  $\Delta$ Cts were calculated for each sample and averaged for each group. The biological replicates were highly reproducible (Figure 4.4A); the average standard deviation in  $\Delta$ Ct between biological replicates was  $<0.3$ Ct. First, filtering of growth arrest genes whose expression was very low (Ct  $>22$ ) and genes whose Ct confidence  $<300$  was applied. In addition, fluidics filters were applied too with ROX  $>1500$  and SYBR  $>400$ . The differences in the  $\Delta$ Ct ( $\Delta\Delta$ Ct) were then calculated for the 318 remaining genes and used to determine the fold change in expression ( $FC = 2^{\Delta\Delta Ct}$ ).

The results of the Biotrove Real Time qPCR Openarray were plotted against the Affymetrix array data for both growth arrest and heat shock (Figure 4.4B). Comparison of the  $\log_2$  fold changes in expression show a plot concentrated around a linear regression trend line with a coefficient of correlation of respectively 0.62 and 0.59 for the totality of the points. This correlation coefficient was not entirely satisfactory in terms of statistics to confidently validate the correlation between the two techniques. However, both techniques are known to be very variable and therefore the threshold of the correlation coefficient to be expected for confirmation of the method has to be lowered. In addition, if you remove only 4 points (out of 318) that seem to be aberrant results on the graph, the coefficients of correlation climb to 0.80 for the growth arrest and 0.72 for the heat shock, which validates more than satisfactorily the microarray results. It could be that these 4 points are false as correct clone annotation was not assessed for each of the differentially expressed genes against Basic Local Alignment Search Tool (BLAST) so correct clone sequence for each spot cannot be guaranteed. Another possibility could be that the microarray chip itself and the individual spots on it could have been subject to cross contamination.

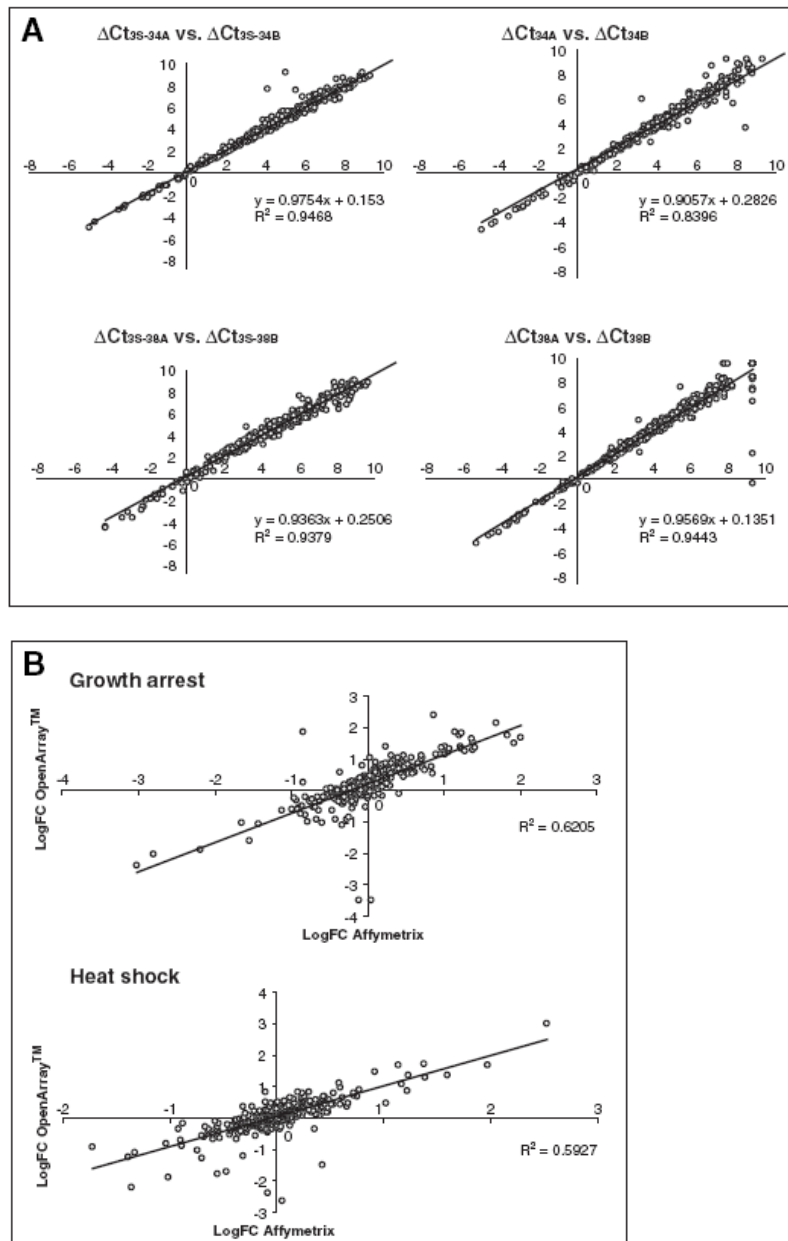


**Figure 4.4: Validation of microarray data by real-time qPCR**

**(A) Reproducibility between samples:** RNA samples used for expression profiling were analysed by real time qPCR using the OpenArray™ Pathways Human Signal Transduction panel. Ct values were normalised using the geomean of 18 house keeping genes.  $\Delta$ Cts were calculated for each sample and averaged for each group. The graphs show that the duplicate RNA samples were highly reproducible. **(B) Comparison of Affymetrix with OpenArray™:** Comparison of the log<sub>2</sub>fold changes in expression obtained using the Affymetrix U133 Plus2 chips versus real time qPCR for growth arrest (CL3<sup>EcoR</sup> at 34°C and 38°C) and heat shock (HMF3S at 34°C and 38°C). Genes whose expression level was very low (Ct>22) and whose Ct confidence was <300 were not considered. The fluidics filters ROX>1500 and SYBR>400 were also applied.

Nearly 80% of the genes show concordant direction changes in expression between the two methods, for both growth arrest (79.9%) and heat shock (78.6%) (Table 4.3A), which confirms the microarray data. However, the actual values of the log-fold changes detected by real time qPCR or by hybridisation analysis were different (full results of the Biotrove experiment for both HMF3S and CL3<sup>ECoR</sup> cells are presented in Supplementary Table S4.4 and S4.5 (Supplementary on a CD). When looking only at the genes that are up-regulated on the Affymetrix chip (Table 4.3B); the results are much better with a concordance of 93.7% and 90.3% respectively for growth arrest and heat shock. Similarly, when looking at the genes down-regulated on the Affymetrix chip (Table 4.3C), the results are not as good with a concordance of 66.0% and 67.7% only respectively for growth arrest and heat shock. This would mean that up-regulated results are more trustworthy than the down-regulated ones and that there is a bias in one or both of the methods when genes are down-regulated.

#### 4.1.8 Comparison of genes differentially expressed upon senescence with the meta-signature of genes over-expressed in cancer

To determine if any of the senescence growth arrest genes have previously been identified to be important for cancer development, the growth arrest data set was overlapped with the meta-signatures of genes over-expressed upon neoplastic transformation and in undifferentiated cancer (Rhodes, Yu et al. 2004). The neoplastic transformation meta-signature comprises 67 over-expressed genes presented in Supplementary Table S4.6 (on a CD); 33 of these were found to be down-regulated and 10 were up-regulated upon growth arrest in CL3<sup>ECoR</sup> cells (Table 4.4 and Supplementary Table S 4.6). The meta-signature of genes over-expressed in undifferentiated cancer comprises 69 genes of which 5 were up-regulated and 46 were down-regulated upon growth arrest in CL3<sup>ECoR</sup> cells (Table 4.4 and Supplementary Table S4.6). This indicated that 49% and 67% of the genes over-expressed upon neoplastic transformation and in undifferentiated cancer were also down-regulated upon senescence.

A	growth arrest		heat shock		
	gene expression regulation on affymetrix chip and real time	No of oligos	in percent	No of oligos	in percent
	same direction	254	79.9	250	78.6
	opposite direction	64	20.1	68	21.4

B	UP Affy		growth arrest		heat shock	
	gene expression regulation on affymetrix chip and real time	No of oligos	in percent	No of oligos	in percent	
	same direction	149	93.7	139	90.3	
	opposite direction	10	6.3	15	9.7	

C	Down Affy		growth arrest		heat shock	
	gene expression regulation on affymetrix chip and real time	No of oligos	in percent	No of oligos	in percent	
	same direction	105	66.0	111	67.7	
	opposite direction	54	34.0	53	32.3	

**Table 4.3: Results of comparison Affymetrix with OpenArray™**

(A)**Concordance total results:** Numbers of concordant direction changes in expression between the two methods, for both growth arrest and heat shock. (B)**Concordance results of up-regulated genes upon senescence by Affymetrix:** Numbers of concordant direction changes in expression between the two methods, for both growth arrest and heat shock. (C)**Concordance results of down-regulated genes upon senescence by Affymetrix:** Numbers of concordant direction changes in expression between the two methods, for both growth arrest and heat shock .

Number of genes up-regulated in :	Up -regulated in Senescence in CL3 <sup>EooR</sup>	Down regulated in Senescence in CL3 <sup>EooR</sup>	Total genes
Neoplastic Transformation	10 (15%)	33 (49%)	67
Undifferentiated Cancer	5 (7%)	46 (67%)	69

**Table 4.4: Metasignatures of neoplastic transformation and undifferentiated cancer**

The growth arrest differential data set was overlapped with the meta-signatures of genes over-expressed upon neoplastic transformation and undifferentiated cancer (Rhodes *et al* 2004). The results of the overlap are shown both in number of genes and percentage of the the total number of genes studied in the Rhodes paper.

This further validates a definite correlation between cancer expression changes and senescence expression changes making these results interesting to study further to understand the importance of senescence in the cancer mechanisms and the roles played by these changing targets. I believe this is the first time an overlap was made between senescence and cancer expression data. The metasignatures of genes that are up-regulated upon neoplastic transformation or undifferentiated cancer show that nearly 50% of these genes were down-regulated upon senescence which highlights the importance of this barrier to cancer development.

## **4.2 BIOLOGICAL VALIDATION BY LENTIVIRAL SILENCING OR ECTOPIC EXPRESSION**

### 4.2.1 Objectives

To biologically validate the results of the microarray and to check whether up-and down-regulation of genes were causal to senescence or merely a consequence of it, *in vitro* validation was designed.

Genes down-regulated upon senescence can be tested by ectopic expression to define whether this down-regulation was essential to senescence. Up-regulated genes can be tested by silencing expression. The silencing strategy chosen to validate the micro-array results was Lentiviral shRNA silencing using pGIPZ lentiviral shmiRs from Open Biosystems.

### 4.2.2 Up-regulated genes upon senescence: Does Silencing bypass the growth arrest?

Genes up-regulated upon senescence that possessed some link to the cell cycle or to cancer in the literature were chosen. Silencing of these genes were performed either by

multiple individual constructs or by a mix of several constructs and were tested by complementation assay in the CL3<sup>EcoR</sup> cells to assess whether their silencing would bypass the growth arrest and therefore would place them as key effectors in the senescence pathways.

#### *4.2.2.1 CLCA2 silencing bypassed senescence at a low level*

CLCA2 belongs to the calcium sensitive chloride conductance protein family. It is expressed predominantly in trachea and lung and suggested to play a role in the complex pathogenesis of cystic fibrosis. It may also serve as an adhesion molecule for lung metastatic cancer cells, mediating vascular arrest and colonization, and furthermore, it has been implicated to act as a tumour suppressor gene for breast cancer. CLCA2 was the most up-regulated target upon senescence with 4 oligos coming up in the top 5 up-regulated genes.

In addition, all four members of the human CLCA gene family cluster on the short arm of chromosome 1 at 1p31, a region that is frequently deleted in breast cancer (Hoggard, Brintnell et al. 1995; Nagai, Negrini et al. 1995; Tsukamoto, Ito et al. 1998; Su, Roberts et al. 1999; Sossey-Alaoui, Kitamura et al. 2001). However, only CLCA2 gene expression was shown to be down-regulated in breast cancer and was suggested to act as a tumour suppressor (Gruber and Pauli 1999; Li, Cowell et al. 2004). Interestingly, Elble and colleagues have shown that acute expression of CLCA2 induces a senescence like growth arrest (Walia, Ding et al. 2009).

For these reasons, it was interesting to see whether the level expression of CLCA2 and its potential tumour suppressor activity would have an effect on senescence in the CL3<sup>EcoR</sup> cells.

A complementation assay was performed in CL3<sup>EcoR</sup> cells with a mix of 3 lentiviral GIPZ CLCA2 silencing constructs namely: human GIPZ lentiviral shMiR



V2LHS\_197853, human GIPZ lentiviral shMiR V2LHS\_197750 and human GIPZ lentiviral shMiR V2LHS\_199854.

The cells were stained after 3 weeks at 38°C. The results show in Figure 4.5 that CLCA2 silencing with a mix of 3 constructs permits rescue, at a low level, when compared to the negative control. A repeat of this experiment (data not shown) showed an even lower level of rescue.

#### *4.2.2.2 AK3L1 silencing bypassed senescence*

AK3L1 has been described as a gene over-expressed in fibroblasts undergoing replicative senescence (Binet, Ythier et al. 2009). It also appears that AK3L1 is a predicted target of miR-195, according to Targetscan and miRanda, two miR target prediction softwares with miR-195 being a micro-RNA that attracted my interest in Chapter 4. The results of the complementation assay with a mix of 2 silencing constructs for AK3L1, namely human GIPZ lentiviral shMiR V2LHS\_59300 and human GIPZ lentiviral shMiR V2LHS\_59298 show a rescue compared to the negative control (Figure 4.5) and at a slightly higher level than the one with silencing CLCA2. A repeat experiment showed a rescue at an even higher level, with approximately 30% more growing colonies.

#### *4.2.2.3 TRIB2 silencing bypassed senescence*

Tribbles homolog 2 (Trib2) was up-regulated upon senescence in this study but was previously identified as a down-regulated transcript in leukemic cells undergoing non-senescence growth arrest. In mechanistic studies, Trib2 was identified as an oncogene with pro-proliferation properties in prostate cancer progression and acute myeloid leukemia, the latter effect being mediated through regulation of the C/EBP family of proteins and notably inactivation of cEBPalpha and cEBPbeta (Keeshan, He et al. 2006; Naiki, Saijou et al. 2007). This is not in agreement with my finding that TRIB2 was up-regulated upon senescence and that this up-regulation was accompanying the growth arrest suggesting anti-growth properties rather than proliferative properties in the CL3<sup>EcoR</sup> cells.

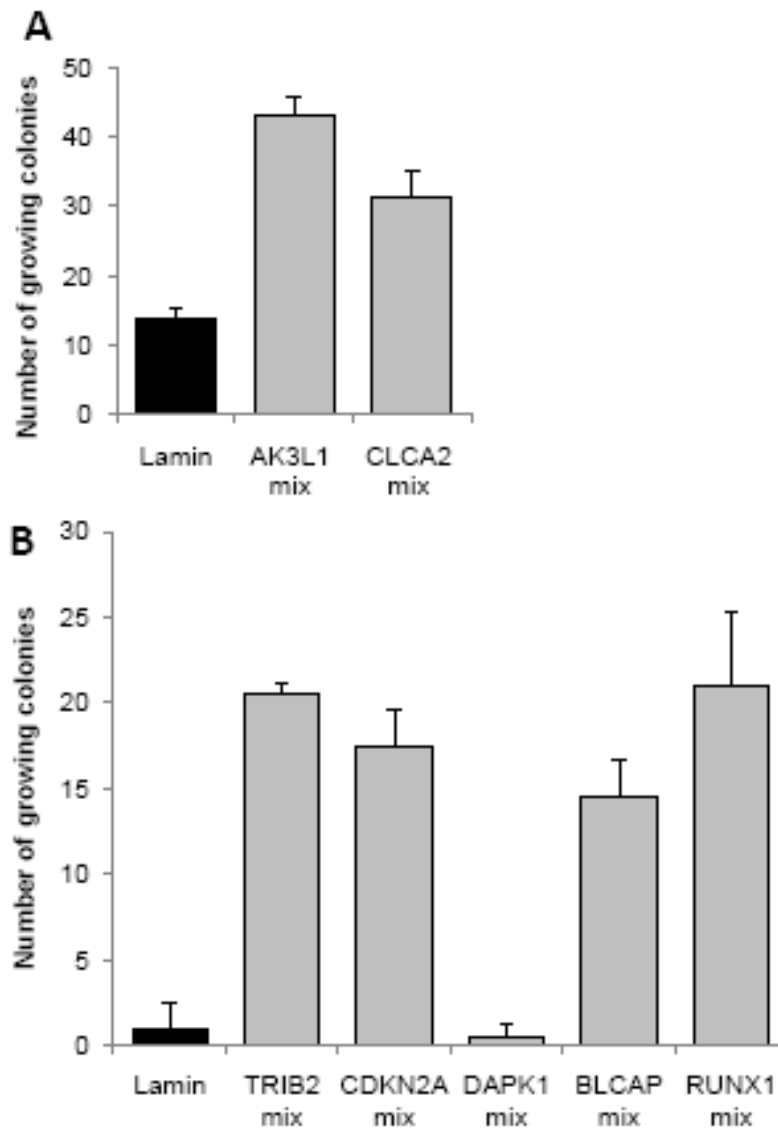


**Figure 4.5: In vitro validation of up-regulated microarray targets by silencing constructs**

(A) **Silencing of AK3L1 and CLCA2:** CL3<sup>EcoR</sup> cells were infected in triplicate with a mix of lentiviruses shRNAmir silencing constructs expressing AK3L1 (V2LHS\_59300 and V2LHS\_59298) and CLCA2 (V2LHS\_197853, V2LHS\_197750 and V2LHS\_199854) and assayed for growth complementation at 38°C. After 3 weeks the number of growing colonies were counted. (B) **Silencing of TRIB2, CDKN2A, DAPK1, BLCAP and RUNX1:** CL3<sup>EcoR</sup> cells were infected in triplicate with a mix of lentiviruses shRNAmir silencing constructs expressing TRIB2 (V2LHS\_200999 and V2LHS\_200588), CDKN2A (V2LHS\_195839, V2LHS\_200698 and V2LHS\_200168), DAPK1 (V2LHS\_62089, V2LHS\_62085 and V2LHS\_62084), BLCAP(V2LHS\_90065 and V2LHS\_90063) and RUNX1(V2LHS\_150257, V2LHS\_150259 and V2LHS\_150256) and assayed for growth complementation at 38°C. After 3 weeks the number of growing colonies were counted.

In addition, I found that although TRIB2 was up-regulated, not only cEBPalpha and beta expression were not down-regulated but cEBPbeta was actually up-regulated upon senescence.

The results of the complementation assay with a mix of 2 lentiviral silencing constructs for TRIB2 namely human GIPZ lentiviral shMiR V2LHS\_200999 and human GIPZ lentiviral shMiR V2LHS\_200588 permitted the rescue from senescence of the cells when compared to the negative control (Figure 4.5).

#### *4.2.2.4 CDKN2A silencing bypassed senescence*

CDKN2A or p16<sup>INK4A</sup> has been linked tightly to the senescence pathways (see introduction chapter). This gene is known to be an important tumour suppressor gene capable of inducing cell cycle arrest. The transcript of p16<sup>INK4A</sup> contains an alternate open reading frame (ARF) that functions as a stabilizer of the tumour suppressor protein p53 as it can bind with MDM2 and blocks its nucleo-cytoplasmic shuttling by sequestering it in the nucleolus which end up blocking MDM2-induced degradation of p53 thereby enhancing p53-dependent transactivation and apoptosis. ARF can also trigger G2 growth arrest and apoptosis in a p53-independent manner by preventing the activation of cyclin B1/CDC2 complexes.

CDKN2A was found here to be up-regulated upon senescence in the HMF3A. However, it is important to note that we previously failed in silencing CDKN2A with various different silencing constructs (see introduction chapter) and the expression has not been checked on this occasion. Nevertheless, the potential silencing of p16<sup>INK4A</sup> with a mix of 3 lentiviral silencing constructs namely human GIPZ lentiviral shMiR V2LHS\_195839, human GIPZ lentiviral shMiR V2LHS\_200698 and human GIPZ lentiviral shMiR V2LHS\_200168 seem to have a rescuing effect here at a level equivalent to TRIB2 (Figure 4.5).

#### 4.2.2.5 *DAPK1* silencing was not sufficient to bypass senescence

Death-associated protein kinase 1 is a positive mediator of gamma-interferon induced programmed cell death (Deiss, Feinstein et al. 1995; Shohat, Shani et al. 2002; Bialik and Kimchi 2004). It is a unique multidomain kinase acting both as a tumour suppressor and an apoptosis inducer. TCR-induced NF- $\kappa$ B activation was also shown to be activated as a target of DAPK (Chuang, Fang et al. 2008).

It was also up-regulated in my data, and therefore was tested in a complementation assay using a mix of 3 lentiviral silencing constructs of DAPK1.

Here, the complementation assay was not a success and DAPK1 silencing with a mix of 3 lentiviral silencing constructs for DAPK1 namely human GIPZ lentiviral shMiR V2LHS\_62089, human GIPZ lentiviral shMiR V2LHS\_62085 and human GIPZ lentiviral shMiR V2LHS\_62084 was not able to bypass the conditional cell cycle arrest (Figure 4.5).

#### 4.2.2.6 *BLCAP* silencing bypassed senescence at a low level

BLCAP was identified as a tumour suppressor protein that reduces cell growth by stimulating apoptosis. HeLa cells expressing BLCAP show reduced cell growth compared to vector-transfected cognate cells and this expression also led to growth arrest and significantly enhanced apoptosis *in vitro* and reduced tumour formation *in vivo* (Zuo, Zhao et al. 2006). Over-expressed BLCAP resulted in growth inhibition of a human tongue cancer cell line Tca8113 *in vitro*, accompanied by S phase cell cycle arrest and apoptosis. Taken together, BLCAP may play a role not only in regulating cell proliferation but also in coordinating apoptosis and cell cycle via a novel way independent of p53 and NF- $\kappa$ B (Yao, Duan et al. 2007).

BLCAP is up-regulated upon senescence-like growth arrest and it was therefore not surprising that its up-regulation was linked to growth inhibition in the literature. For these reasons, BLCAP silencing was investigated in a complementation assay.

A mix of 2 lentiviral silencing constructs of BLCAP, namely human GIPZ lentiviral shMiR V2LHS\_90065 and human GIPZ lentiviral shMiR V2LHS\_90063 was used for complementation assay and showed a rescue of the cells from senescence when compared to the negative control (Figure 4.5).

#### *4.2.2.7 RUNX1 bypassed senescence*

All three family members: RUNX1, 2 and 3 possess the ability to induce senescence-like growth arrest in primary murine fibroblasts (Linggi, Muller-Tidow et al. 2002; Wotton, Blyth et al. 2004; Kilbey, Blyth et al. 2007). An analogous role was suggested for Runx1 in hematopoietic progenitors by the failure of NRAS- induced growth suppression in cells lacking Runx1 (Motoda, Osato et al. 2007).

For these reasons and because RUNX1 was also up-regulated upon senescence, RUNX1 silencing was tested with a mix of 3 lentiviral silencing constructs namely human GIPZ lentiviral shMiR V2LHS\_150257, human GIPZ lentiviral shMiR V2LHS\_150259 and human GIPZ lentiviral shMiR V2LHS\_150256 in a complementation assay in the CL3<sup>ECOR</sup> cells. The results show a rescue compared to the negative control (Figure 4.5).

#### *4.2.2.8 GRAMD3 silencing bypassed senescence*

GRAMD3 is one of the genes up-regulated upon senescence. It also appears that GRAMD3, according to Targetscan and miRanda, two miR target prediction softwares, is a potential target of miR-195 and miR-25, two of the micro-RNA studied in chapter 4. No literature was available for GRAMD3. However, its silencing by 2 individual lentiviral silencing constructs namely Human GIPZ lentiviral shRNAmiR V2LHS\_235566 and Human GIPZ lentiviral shRNAmiR V2LHS\_135659 showed to

bypass the growth arrest in a reproducible manner and at a level with a number of colonies stained after 3 weeks above 100 (Figure 4.6). This experiment was repeated with the same results.

#### *4.2.2.9 SCN2A silencing was not sufficient to bypass senescence*

SCN2A stands for sodium channel, voltage-gated, type II, alpha subunit. Voltage-gated sodium channels (NaV) are responsible for action potential initiation and propagation in excitable cells, including nerve, muscle, and neuroendocrine cell types. They are also expressed at low levels in non-excitable cells, where their physiological role is unclear. SCN2A was one of the 20 top up-regulated genes upon senescence.

Its silencing was tested with 2 individual silencing constructs namely human GIPZ lentiviral shMiR V2LHS\_202838 and human GIPZ lentiviral shMiR V2LHS\_203129. The results show a weak rescue but with a number of colonies higher above the Lamin background. The experiment was repeated with similar results (Figure 4.6). This result was not considered conclusive enough.

#### 4.2.3 Down-regulated genes upon senescence: Does ectopic expression bypass the growth arrest?

James Robinson, a BSc rotation student, tried to obtain antibodies to verify the expression for all these proteins, namely HMGB2, DEPDC1, NEK2 and MLF1-IP 88 and 401, and to carry out Western blotting but none of the available antibodies except for MELK and FOXM1 worked.

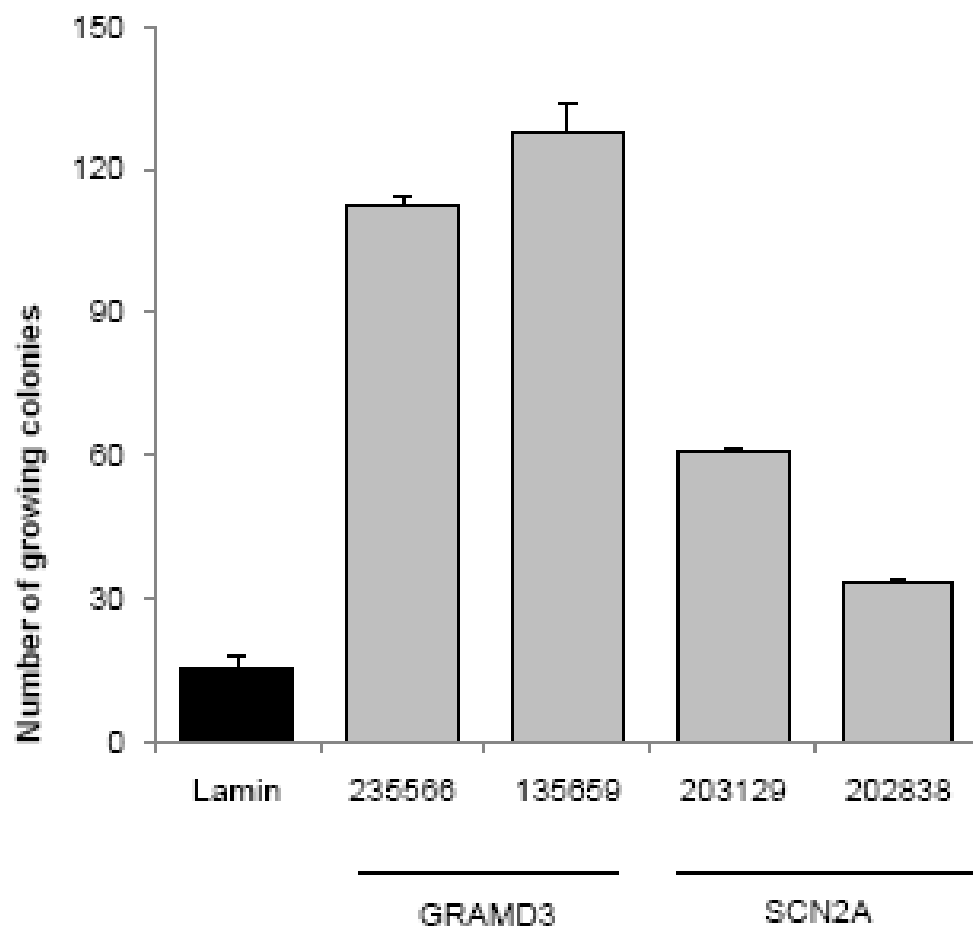


**Figure 4.6: Silencing of GRAMD3 and SCN2A**

CL3<sup>EcoR</sup> cells were infected in triplicate with lentiviruses expressing the indicated shRNAmir silencing constructs and assayed for growth complementation at 38°C. After 3 weeks the number of growing colonies were counted.

#### 4.2.3.1 HMGB2

HMGB2 encodes for a member of the non-histone chromosomal high mobility group protein family. *In vitro* studies have demonstrated that this protein is able to efficiently bend DNA and form DNA circles. Previous reports have shown that architectural DNA-bending/looping chromosomal proteins HMGB1 and HMGB2 (formerly known as HMG1 and HMG2), which function in a number of biological processes including transcription and DNA repair, interact *in vitro* with p53 and stimulate p53 binding to DNA containing p53 consensus sites (Jayaraman, Moorthy et al. 1998; Brickman, Adam et al. 1999; Imamura, Izumi et al. 2001). HMGB1 and 2 were also shown to physically interact with two splicing variants of p73, alpha and beta and stimulate p73 binding to different p53-responsive elements and therefore modulate its activity (Stros, Ozaki et al. 2002).

HMGB2 was also strongly down regulated upon senescence; therefore, it was chosen to be tested by complementation assay.

PLPC-HMGB2, a full length expression construct for HMGB2, was packaged with ecotropic phoenix cells to produce retroviral supernatant which was used for complementation assay in the CL3<sup>EcoR</sup> cells. After selection, cells were reseeded as usual and placed at 38°C for 3 weeks. The cells did not rescue above the background (plpcx empty vector) (data not shown). A repeat of this experiment showed the same result. However, because the expression of HMGB2 was not verified, it is not possible to conclude on the actual efficiency of its ectopic expression.

#### 4.2.3.2 DEPDC1

DEPDC1 was shown to be up-regulated in bladder cancer cells. In addition, suppression of DEPDC1 expression with small-interfering RNA significantly inhibited growth of bladder cancer cells (Kanehira, Harada et al. 2007). It was also represented 3 times (3



different oligos corresponding to the same gene) in the top 25 down-regulated targets upon senescence.

For these reason, ectopic expression of this gene was also tested by complementation assay with retroviral expression of PLPC-DEPDC1, a full length expression construct for DEPDC1.

The results showed rescue compared to the negative control (Figure 4.7). However, these results were not reproducible at a satisfactorily level of rescue with very weak rescue for some of the cultures tested. The effect of DEPDC1 on senescence growth arrest remains, therefore, to be confirmed. In addition, the expression of DEPDC1 was not verified and therefore, the actual efficiency of its ectopic cannot be assessed.

#### 4.2.3.3 *BUB1B*

Bub1 is a kinase believed to function primarily in the mitotic spindle checkpoint. Mutation or aberrant Bub1 expression is associated with chromosomal instability, aneuploidy, and human cancer (Cahill, Lengauer et al. 1998). Bub1 expression was reported to be low in cells undergoing replicative senescence. It was also described that targeting Bub1 by RNAi or simian virus 40 (SV40) large T antigen in normal human diploid fibroblasts results in premature senescence.

Premature senescence caused by lower Bub1 levels was dependant on p53 as senescence induction was blocked by dominant negative p53 expression or depletion of p21<sup>CIP1/WAF1/Sdi1</sup>, a p53 target (Gjoerup, Wu et al. 2007; Gao, Ponte et al. 2009).

Since BUB1 was in the top 25 down regulated targets upon senescence in the CL3<sup>EcoR</sup> cells with two different oligos, highlight the quality of the microarray and the importance of BUB1 in the senescence processes. All together, this makes BUB1 a perfect target to ectopically express in the conditional system.

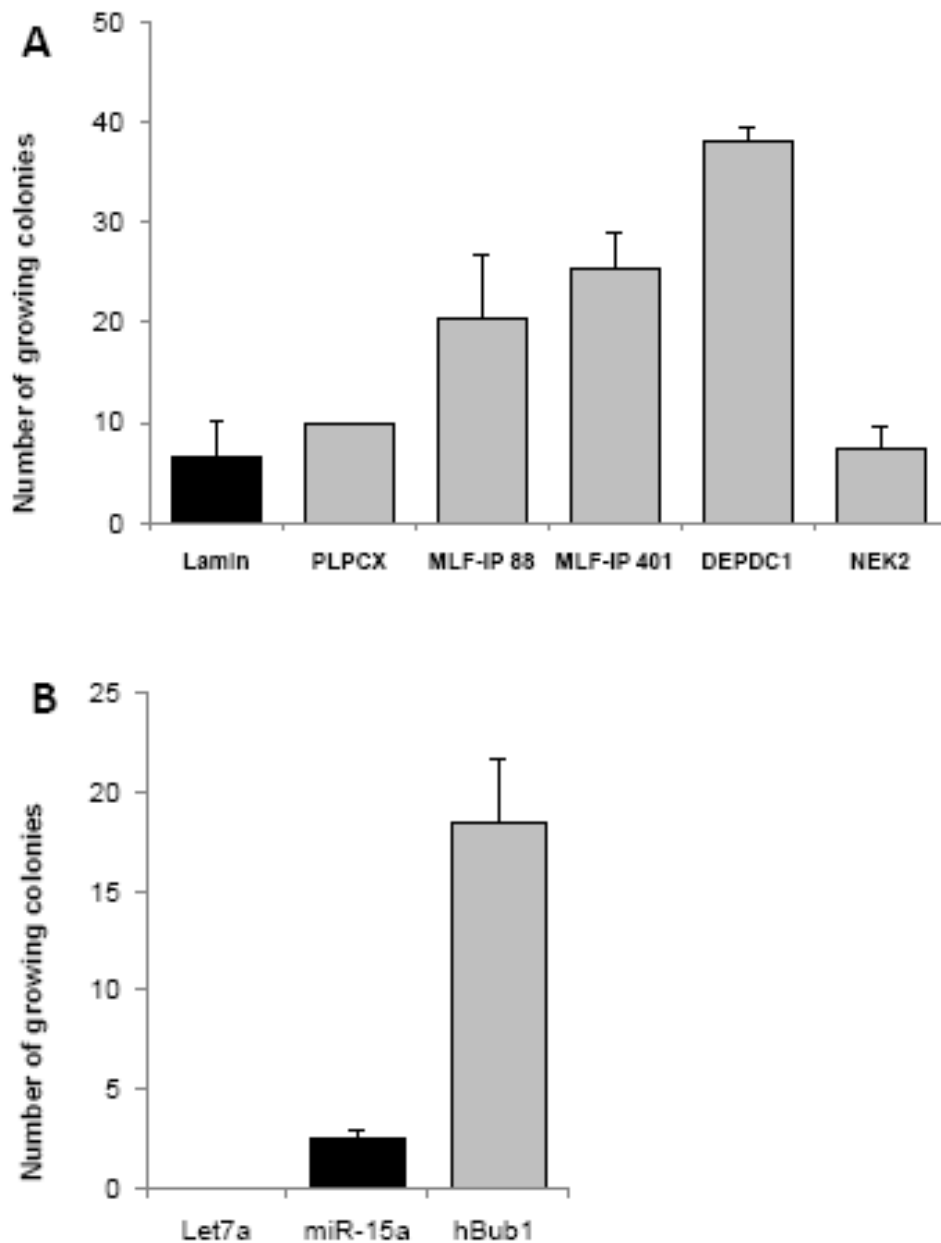


**Figure 4.7: *In vitro* validation of microarray down-regulated targets by ectopic expression**

**(A) Ectopic expression of MLF-IP88, MLF-IP401, DEPDC1 and NEK2:** CL3<sup>EcoR</sup> cells were infected in triplicate with retroviruses expressing the indicated PLPC expression constructs and assayed for growth complementation at 38°C. After 3 weeks the number of growing colonies were counted. **(B) Ectopic expression of hBUB1:** CL3<sup>EcoR</sup> cells were infected in triplicate with retroviruses expressing the indicated PLPC expression constructs and assayed for growth complementation at 38°C. After 3 weeks the number of growing colonies were counted

pLB(N)C- HA-BUB1 was packaged into amphotropic phoenix cells and used to infect the HMF3A cells. After blastocidin selection for 15 days, the cells were reseeded at  $0.5 \times 10^5$  in T-75 cm<sup>2</sup> and shifted to 38C for 3 weeks before being stained as described previously. The results show a clear rescue of the cells, although at a low level, compared to the negative control.

In addition, because HA-BUB1B expression had previously been shown by Ole Gjoerup to be functional, I was confident that the expression construct of BUB1B worked and therefore that BUB1B was causal to senescence escape.

#### 4.2.3.4 *NEK2*

Nek2 is a cell-cycle-regulated protein kinase that localizes to the centrosome and is likely to be involved in regulating centrosome structure at the G(2)/M transition. Nek2 is expressed as two splice variants. These isoforms, designated Nek2A and Nek2B, are detected in primary blood lymphocytes as well as adult transformed cells (Hames and Fry 2002). Expression levels of the Nek2 kinase in human cancer cell lines and primary tumours revealed that Nek2 protein is elevated 2- to 5-fold in cell lines derived from a range of human tumours including those of cervical, ovarian, breast, prostate, and leukemic origin (Hayward, Clarke et al. 2004). More recently, NEK2 was also reported by the same group to be abnormally expressed in a wide variety of human cancers (Hayward and Fry 2006).

NEK2 was also down-regulated in the HMF3A conditional system and its ectopic expression was chosen to be tested by complementation assay using a full length expression construct.

The results show that NEK2 expression was unable to rescue the cells from senescence (Figure 4.7). However, again its ectopic expression was not confirmed so no conclusion can be made on its actual efficiency to bypass senescence.

#### 4.2.3.5 MELK

Several studies found a correlation between MELK expression and the malignancy of several cancers. MELK has been shown to be over-expressed by at least a 5-fold increase in invasive glioblastoma multiforme (GBM). In addition, in the examination of more than 100 tumours of the central nervous system, progressively higher expression of MELK was found to correlate with astrocytoma grade. Similar level of over-expression was also observed in medulloblastoma. Furthermore, MELK knockdown in malignant astrocytoma cell lines caused a reduction in proliferation and anchorage-independent growth in *in vitro* assays (Marie, Okamoto et al. 2008). Melk was also found highly expressed in murine neural stem cells and regulated their proliferation and correlated with pathologic grade of brain tumours. In primary cultures from human glioblastoma and medulloblastoma, MELK knockdown by siRNA results resulted in inhibition of the proliferation and survival of these tumours (Nakano, Masterman-Smith et al. 2008).

Using accurate genome-wide expression profiles of breast cancers, another study found MELK to be significantly over-expressed in the great majority of breast cancer cells. Suppression of MELK expression by small interfering RNA significantly inhibited growth of human breast cancer cells (Lin, Park et al. 2007). Altogether, these results suggested a critical role for MELK in cell proliferation and tumourigenesis.

For these reasons, MELK ectopic expression was tested by complementation assay and the results (data not shown) showed that introduction of MELK in the HMF3A cells was not sufficient to bypass the conditional senescence. However, western blotting analysis was performed by James Robinson with a MELK antibody (data not shown) revealed that MELK was not expressed at a sufficient level in these cells and therefore since the expression of MELK in these cells was not confirmed, I could not conclude on the effect of MELK expression itself on the growth arrest.

The ectopic expression of MELK would be definitely worth investigating further perhaps with a different expression construct but, in reason of the short time scale was dropped.

#### 4.2.3.6 *MLF1-IP two splice forms 88 and 401*

The myelodysplasia/myeloid leukemia factor 1-interacting protein MLF1-IP is a novel gene which encodes for a putative transcriptional repressor. MLF1-IP has been shown to be over-expressed in human and rat glioblastoma (GBM) especially in the tumour core where it was co-localized with MLF1 and nestin (Hanissian, Teng et al. 2005).

In biological studies, there have been several observations suggesting that MLF1 is physiologically involved in a tumour suppressor pathway. MLF1 has been found to be over-expressed in more than 25% of myelodysplastic syndromes (MDS) -associated cases of AML, in the malignant transformation phase of MDS, and in lung squamous cell carcinoma (Matsumoto, Yoneda-Kato et al. 2000; Sun, Zhang et al. 2004). The aberrant over-expression is usually related to mutations and to inactivation of p53 in various cell lines (Yoneda-Kato, Tomoda et al. 2005). It was also reported that MLF1 is a negative regulator of cell cycle progression that functions upstream of the tumour suppressor p53 (Dornan, Wertz et al. 2004). The introduction of NPM-MLF1 into early-passage murine embryonic fibroblasts allowed the cells to escape from cellular senescence at a markedly earlier stage and induced neoplastic transformation in collaboration with the oncogenic form of Ras (Yoneda-Kato and Kato 2008). MLF1-IP also happened to be down-regulated upon senescence.

For this reason, MLF1-IP was a good target to try and express ectopically in a complementation assay. The cDNA was cloned in LPCX after amplification by Pr. Parmjit Jat and these were used for the complementation as described previously. Colonies numbers and phenotype were not convincing enough to indicate a significant bypass of senescence with either isoform expressions (Figure 4.7A). In addition, the expression of MLF1-IP was not verified making its actual efficiency impossible to assess.

#### 4.2.3.7 *DBF4, CDKN2C (p18) and PLK4*

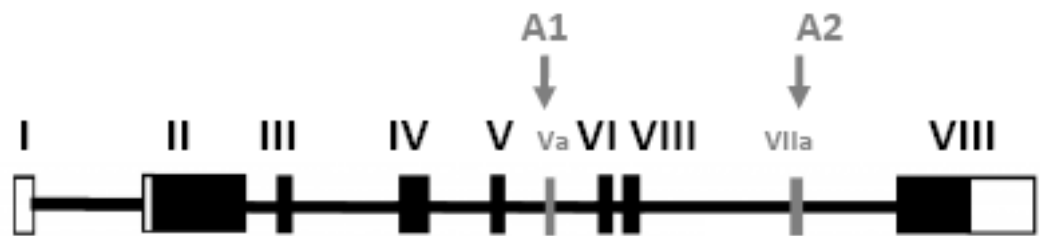
DBF4, CDKN2C (p18) and PLK4 were the other targets chosen due to their involvement in cell proliferation and their down-regulation upon senescence. Full length ectopic expression constructs were generated but, these did not yield sufficient number of puromycin resistant clones. So after a few tries and due to the timescale, their investigation was dropped.




#### 4.2.3.8 *FOXM1*

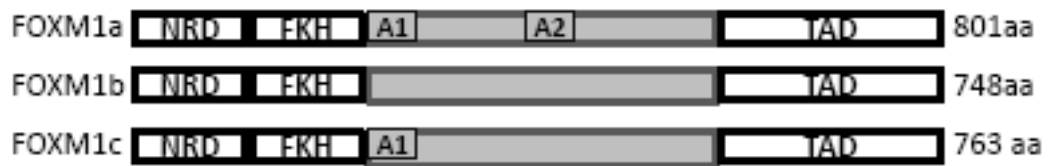
FOXM1 is a transcription factor that belongs to the evolutionarily conserved Forkhead family comprising more than 50 transcription factors that share a conserved Forkhead or Winged-helix DNA-binding domain (Laoukili, Stahl et al. 2007; Myatt and Lam 2007; Wierstra and Alves 2007). In humans, there are 17 Fox gene subfamilies (FOXA-R) with at least 41 different genes. Despite the highly conserved Forkhead DNA binding domain (DBD), the function and regulation of the FOX proteins varies considerably between the different families probably due to sequence variations outside the DBD allowing for functional diversity and regulation. FOX protein family members play a role in a wide variety of biological processes such as development, differentiation, proliferation, apoptosis, migration, invasion and ageing; some such as FOXM1 have even been linked to cancer (Myatt and Lam 2007).

Human FOXM1 exists as three splice variants: FOXM1 a, b and c (A, B, C in Figure 4.8A). All three isoforms bind to the same DNA sequences but only FOXM1b and FOXM1c are transactivators. Disruption of the transactivation domain but retention of the DBD in FOXM1a indicates that it has the potential to be a naturally occurring dominant negative variant (Figure 4.8A).

**A**



-  Untranslated region
-  Coding region
-  Alternative spiced exons



NRD: N-terminal repressor domain  
FKH: Forkhead winged helix DNA binding domain  
TAD: Transactivation domain

**B**

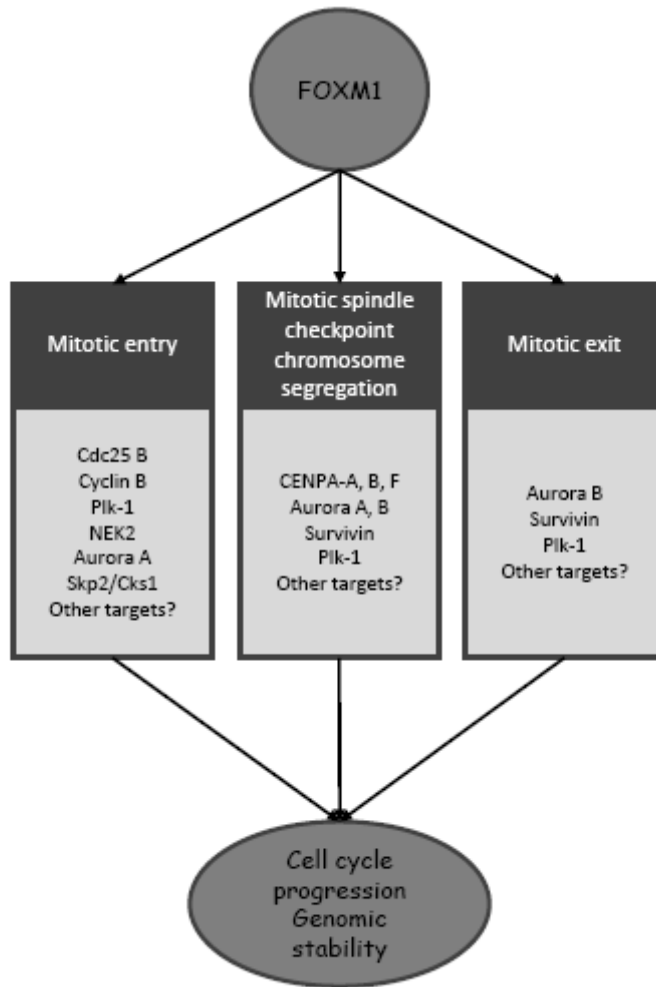


**Figure 4.8: FOXM1**

(A) **FOXM1 splice variants:** DNA gene containing 10 exons, 2 of which being splicing exons Va (A1) and VIIa (A2) that originates 3 different splice variants, encoding for 3 FOXM1 protein isoforms: FOXM1a, containing both alternative exons, FOXM1b, not containing any alternative exons and FOXM1c only containing exon Va. (B) **Involvement of the FoxM1-regulatory gene network in the regulation of cell cycle progression and maintenance of the genomic stability (from Laoukili, 2007).** Several microarray analyses studies have revealed numerous FoxM1 target genes. The most significant of these genes can be clustered in function of their role in the regulation of the cell cycle, more specifically of the G2/M-phases of the cell cycle: mitotic entry, mitotic spindle checkpoint and/or chromosome segregation, and cytokinesis and mitotic exit. The proper coordination of the expression of these genes in space and time participates to proper cell cycle progression and maintenance of the genomic stability.



FOXM1 exhibits a proliferation-specific expression pattern (Wierstra and Alves 2007). It is highly expressed in the developing embryo but is turned off upon terminal differentiation. In the adult expression is limited to proliferating cell types and self-renewing tissues such as thymus, testis, small intestine and colon that contain proliferative cells; significantly lower levels are found in ovary, spleen and lung. FOXM1 expression also decreases upon ageing. FOXM1 expression has been detected in all proliferating cells but is not expressed in quiescent or terminally differentiated cells. However FOXM1 is readily induced when quiescent cells re-enter the cell cycle upon stimulation. The increase in FOXM1 expression is initiated in late G1 at the onset of S phase reaching a maximal level which is maintained throughout G2 and mitosis. However the transcriptional activity of FOXM1 is only maximal during G2 and correlates with its increased phosphorylation. During exit from mitosis, FOXM1 is actively degraded by the anaphase-promoting complex (Laoukili, Alvarez-Fernandez et al. 2008; Park, Wang et al. 2008).

FOXM1 contains an N-terminal auto-repressor domain that inhibits transactivation by an intramolecular interaction with the C-terminal transactivation domain (TAD) (Wierstra and Alves 2007; Park, Wang et al. 2008). This repression can be relieved by phosphorylation of multiple cdk sites within the TAD; cyclinA/cdk2 has been suggested to be essential for phosphorylation of these sites (Laoukili, Alvarez-Fernandez et al. 2008). Phosphorylation by cyclinE/cdk2 and PLK1 has also been suggested to be important for regulating FOXM1 activity. CyclinD/cdk4, 6 may activate FOXM1 indirectly by relieving its inhibition by the retinoblastoma protein. Phosphorylation by MAPK has been proposed to be required for translocation of FOXM1 to the nucleus (Ma, Tong et al. 2005). Expression studies have indicated that FOXM1 regulates expression of the G2-specific gene expression signature of mammalian cells (Laoukili, Kooistra et al. 2005; Wang, Chen et al. 2005; Mooi and Peeper 2006). This comprises Cyclin B, Polo-like-kinase 1 (PLK1), Aurora B, Cdc25B, CENP-F, NEK2 and many other regulators of cell cycle progression and genomic stability (Figure 4.8B).

Since many of these genes as well as FOXM1 are down-regulated in our HMF3A cells when they undergo senescence, we initiated a collaboration with Rene Medema to determine if FOXM1 has a causative role in this process. They provided us with lentiviral expression constructs for full length FOXM1c (FOX WT), a sumoylation-defective inactive mutant (FOX 6K, not published) and a constitutively active, non-degradable, N-terminal deleted FOXM1c (FOX $\Delta$ N $\Delta$ KEN, comprising amino acids 210-763; Laoukili *et al*, 2008).

To confirm the microarray, the levels of FOXM1 were analysed by Western blot by James Robinson with an anti-FOXM1 antibody in either growing cells after 7 days at 34°C or in senescent cells shifted to 38°C for one week. The western blot membrane was scanned and the intensity was calculated for each of the bands. The absolute intensity was then calculated by the ratio FOXM1/B2-microglobulin. The results show a decrease in the level of FOXM1 protein in senescent cells in all three experiments although the exact level of expression of FOXM1 varied (Figure 4.9). These results corroborate the microarray analysis and confirm a decrease of FOXM1 levels in senescent cells.

The FOXM1 inserts within the three lentiviral constructs were excised and recloned into PLPCX by Catia Caetano and these were used in a complementation assay. The staining result (Figure 4.10) showed that constitutively active FOXM1 (FOXM1 $\Delta$ N $\Delta$ KEN) abrogates senescence in our HMF3A cells upon temperature shift whereas full length FOXM1 (FOXM1) or the mutant (FOXM1-6K) were unable to rescue even when highly expressed. The experiment was repeated with similar results although with a lower number of growing colonies.

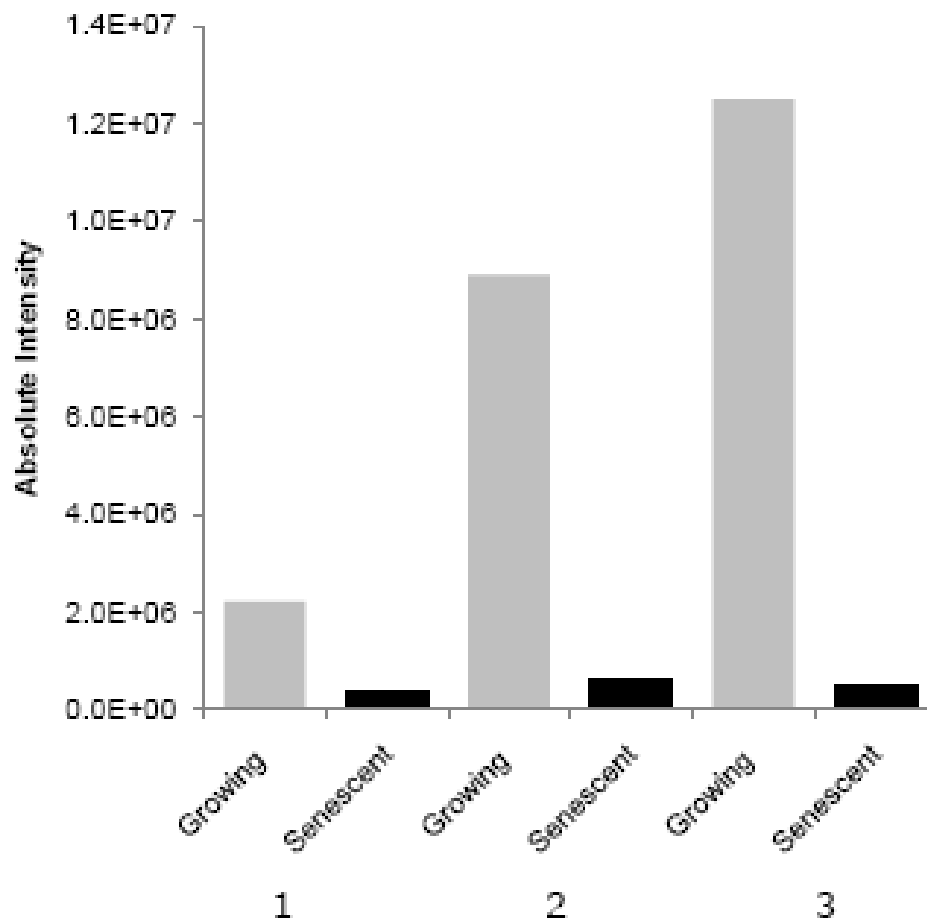


**Figure 4.9: FOXM1 protein expression**

The levels of FOXM1 were analysed by Western blot with an anti-FOXM1 antibody in either growing cells after 7days at 34°C or in senescent cells shifted to 38°C for 3 weeks. The western blot membrane was scanned and the intensity was calculated for each of the bands. The absolute intensity was then calculated by the ratio FOXM1/B2-microglobulin. This Figure represents 3 Western Blot repeats.

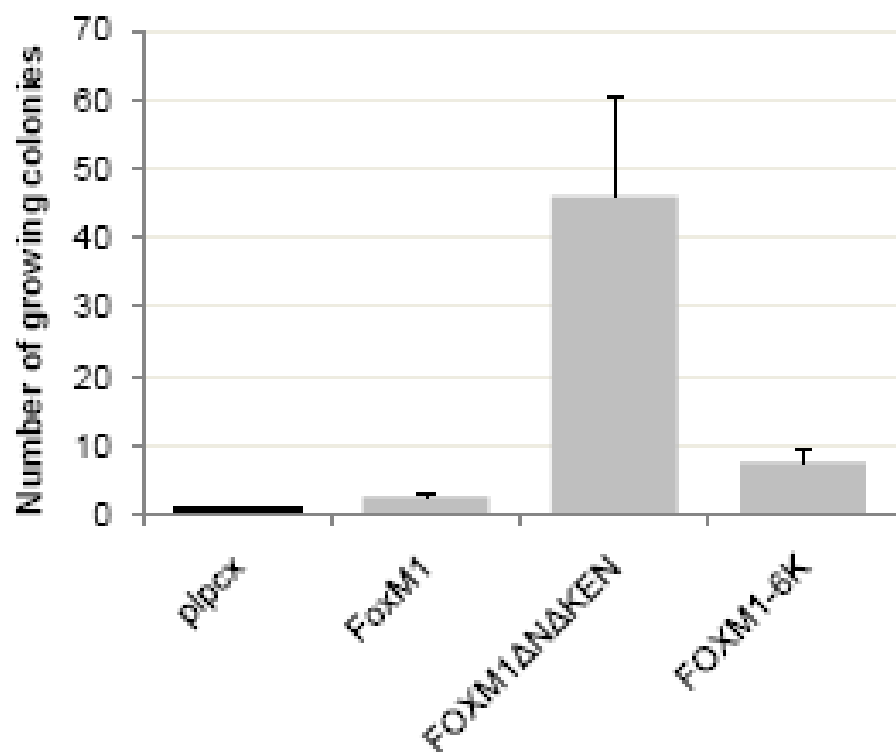


**Figure 4.10: Ectopic expression of FOXM1 WT, FOXM1ΔNAKEN and FOXM1-6K :** CL3<sup>EcoR</sup> cells were infected in triplicate with retroviruses expressing the indicated PLPC expression constructs and assayed for growth complementation at 38°C. After 3 weeks the number of growing colonies were counted.

In addition, duplicate cultures expressing the three different FOXM1 constructs as well as a negative control, PLPCX, were grown at 34°C and analysed by western blot with an anti-FOXM1 antibody. The results showed an expression of FOXM1 in the three conditions (Figure 4.11, lane 1, 2 and 3) but not in the negative control (Figure 4.11, lane 4). It is possible to note that the constitutively active mutant of FOXM1, FOX $\Delta$ N $\Delta$ KEN, show a lower band at 75KDa, corresponding to the size of the truncated protein (Figure 4.11, lane 2).

### **4.3 NF- $\kappa$ B PATHWAY ACTIVATION UPON SENESCENCE IS CAUSAL TO SENESCENCE**

#### 4.3.1 Objectives

*In silico* promoter analysis of differentially expressed genes upon senescence suggested that the NF- $\kappa$ B pathway may be activated upon irreversible growth arrest (Hardy, Mansfield et al. 2005). Additionally, simple observation of the microarray data suggested similar conclusions. The objectives in this section were to investigate further the involvement of NF- $\kappa$ B pathway in senescence and use different approaches to validate *in vitro* my initial hypothesis.

#### 4.3.2 NF- $\kappa$ B pathway is activated upon senescence at the mRNA level

Microarray analysis can provide very useful information on pathways and pattern. To determine whether the NF- $\kappa$ B pathway was actually involved in senescence, two methods were employed: The first one was to analyse the 4 transcription factor motifs of NF- $\kappa$ B in all the differential gene data set, the second was to extract all the genes that are known targets of NF- $\kappa$ B from the differential gene data set and to look at their modulation.

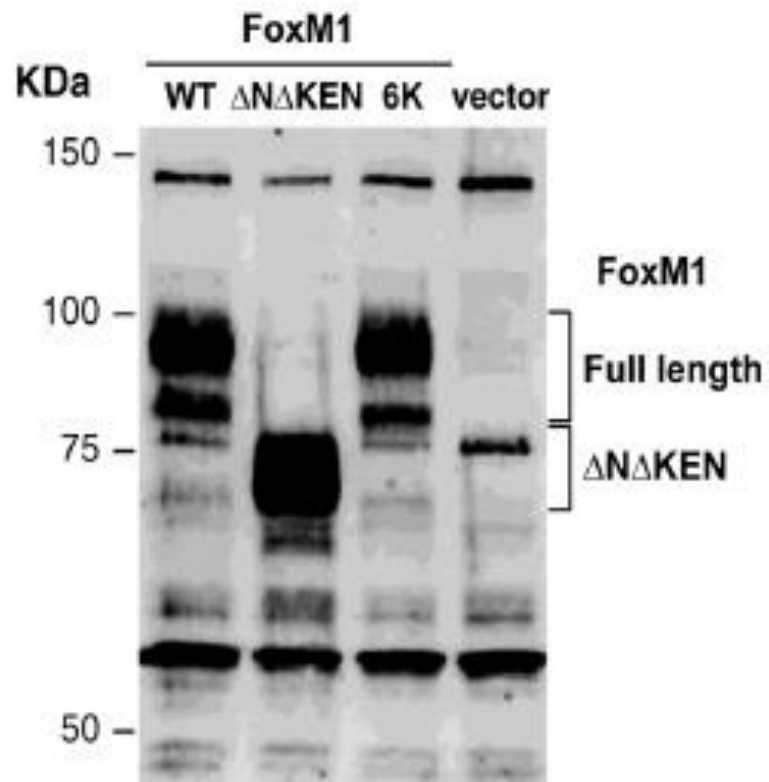


**Figure 4.11: FOXM1 protein expression in cells expressing FOXM1 WT, FOXM1 $\Delta N\Delta KEN$  and FOXM1-6K**

The levels of FOXM1 were analyzed by Western blot with an anti-FOXM1 antibody in the cells expressing the indicated PLPC expression constructs.

#### *4.3.2.1 Transcription factor motif matrix module*

To determine if the differentially expressed genes contained binding sites for the family of NF- $\kappa$ B transcription factors, this expression dataset was compared with a motif module map comprising a matrix of 12,254 genes and 2,394 known transcription factors (<http://motifmap.googlepages.com>) (Adler, Lin et al. 2006). All four NF- $\kappa$ B factor motifs were found to be present within the promoters of the up- and down-regulated genes (Table 4.5). In the up-regulated genes the NF- $\kappa$ B motifs were present within the promoters of 200, 134, 124 and 114 genes, ranking them in the top 3%, 5.7%, 6.4% and 7.4% abundant motifs respectively. In the down-regulated genes, the NF- $\kappa$ B motifs were present within the promoters of 217, 175, 144 and 116 genes, ranking them in the top 4.2%, 5.9%, 7.5% and 10.3% abundant motifs respectively.

#### *4.3.2.2 NF- $\kappa$ B targets gene expression modulation*

To determine if the differential GA gene set comprised known NF- $\kappa$ B targets, the list of differentially expressed genes was compared to the set of 960 putative NF- $\kappa$ B targets proposed by Gilmore (<http://www.nf-kb.org>). 93 NF- $\kappa$ B targets were found to be differentially expressed; 67 of these were up-regulated (Table 4.6A and Supplementary Table S4.7 (supplementary on a CD)) whereas 26 were down-regulated (Table 6B and Supplementary Table S4.7). IL1A and IL1B were the most highly up-regulated genes. The senescence-associated secretory phenotype (SASP) cytokine IL6 was also up-regulated. The other SASP cytokines IL8 and IGFBP7 were also up-regulated (Table 4.6C) but since the adjusted P-values were greater than 0.00001, they were not identified as significant. Interestingly IL6 expression was up-regulated to a greater extent by serum starvation. Almost all of the top NF- $\kappa$ B targets found to be up-regulated upon senescence growth arrest were also up-regulated upon serum starvation including IL1A and B, the most highly up-regulated NF- $\kappa$ B targets; generally the modulation by serum starvation was greater than with senescence growth arrest.

UP	No_of_genes	Position out of 2394 TF	Rank by percent
V_NFKB_Q6_01.wtmx	200	73	3.0
V_NFKAPPAB65_01.wtmx	134	136	5.7
V_NFKAPPAB_01.wtmx	124	154	6.4
V_NFKAPPAB50_01.wtmx	114	178	7.4
DOWN	No_of_genes	Position out of 2394 TF	Rank by percent
V_NFKB_Q6_01.wtmx	217	100	4.2
V_NFKAPPAB65_01.wtmx	175	142	5.9
V_NFKAPPAB_01.wtmx	144	180	7.5
V_NFKAPPAB50_01.wtmx	116	246	10.3

**Table 4.5: Transcription factor motifs**

The differential expression dataset was compared with a motif module map comprising a matrix of 12,254 genes and 2,394 known transcription factors (Adler et al. 2006). All four NF- $\kappa$ B factor motifs were found to be present within the promoters of the up- and down-regulated genes. In the up-regulated genes the NF- $\kappa$ B motifs were present within the promoters of 200, 134, 124 and 114 genes, ranking them in the top 3%, 5.7%, 6.4% and 7.4% abundant motifs respectively. In the down-regulated genes, the NF- $\kappa$ B motifs were present within the promoters of 217, 175, 144 and 116 genes, ranking them in the top 4.2%, 5.9%, 7.5% and 10.3% abundant motifs respectively.



**A**

Symbol	logFC GA	logFC Q	logFC HS	logFC wt_LT	logFC GSE_p53	logFC E1A	logFC E7	logFC E2F-DB	logFC pRS_p53	logFC pRS_p21
IL1A	3.42	3.82	0.22	-4.36	-3.28	-5.18	-1.05	-0.04	-0.70	-0.26
IL1B	3.33	3.54	0.06	-4.60	-4.13	-5.44	-1.98	-0.86	-1.41	-1.48
IL1B	3.29	3.43	0.38	-4.58	-3.83	-5.89	-1.82	-0.80	-1.31	-1.37
BMP2	2.64	4.73	0.24	-5.09	-3.59	-4.51	-3.45	-2.96	-1.45	-1.91
BMP2	2.25	4.80	0.24	-5.00	-3.18	-4.42	-3.51	-3.20	-1.47	-1.80
SOD2	2.10	3.04	0.72	-2.27	-2.00	-2.83	-0.92	-0.63	-0.71	-0.87
40118	2.04	2.14	-0.56	-2.97	-2.23	-2.96	-1.84	-1.41	-1.74	-1.71
IL6	2.01	4.16	0.13	-3.37	-2.65	-5.35	-2.64	-1.97	-1.24	-1.93
AKR1C1	2.01	3.30	-0.65	-2.44	-0.82	-4.22	-1.2	-1.19	0.46	-0.12
TNFAIP3	1.96	2.42	0.32	-3.27	-3.30	-4.35	-1.64	-1.60	-1.68	-1.74
IL32	1.96	0.78	0.17	-1.42	-1.23	-0.26	-0.99	-0.36	-0.86	-1.11
40118	1.93	2.10	-0.38	-2.89	-2.36	-2.67	-1.79	-1.34	-1.67	-1.76
40118	1.92	1.96	-0.61	-2.74	-2.13	-2.52	-1.53	-1.11	-1.55	-1.51
CCL2	1.92	3.55	0.62	-1.14	-1.75	-5.25	-1.06	-1.65	-1.05	-1.26
TNFAIP3	1.90	2.53	0.31	-3.58	-3.42	-4.90	-1.74	-1.77	-1.68	-1.90
CCL20	1.84	3.63	0.16	-2.96	-3.49	-2.34	-2.02	-1.37	-2.07	-2.61
CSF2	1.81	2.97	-0.29	-3.41	-3.31	-3.97	-0.77	0.94	-1.07	-1.23
AKR1C1	1.79	4.57	-0.28	-3.22	-1.47	-4.07	-2.14	-2.19	0.12	-0.94
AKR1C1	1.78	3.16	-0.38	-2.03	-0.73	-2.80	-1.11	-1.12	0.50	-0.08
FTH1	1.75	1.30	-0.01	-1.28	-0.62	-2.96	-0.64	-0.65	-0.65	-0.44
SOD2	1.69	3.53	0.85	-2.12	-2.49	-2.84	-0.91	-0.72	-0.54	-0.83
CDKN1A	1.68	0.73	-0.66	-1.54	-2.65	-0.40	-0.39	-0.35	-1.95	-1.17
GCLC	1.66	1.86	-0.68	-1.58	-1.42	-1.36	-1.35	-1.5	-1.55	-1.71
ANGPT1	1.64	-1.04	0.06	-0.98	0.48	-5.61	-1.03	-1.88	-0.02	-0.13

**B**

Symbol	logFC GA	logFC Q	logFC HS	logFC wt_LT	logFC GSE_p53	logFC E1A	logFC E7	logFC DB	logFC pRS_p53	logFC pRS_p21
BRCA2	-2.20	0.32	0.05	1.88	1.08	2.04	1.56	1.98	1.9	1.65
DPYD	-1.50	-2.15	-0.16	0.25	0.39	0.04	0.58	0.19	0.53	0.27
BRCA2	-1.42	0.63	-0.10	1.15	1.09	1.19	0.99	1.37	0.88	0.73
UCP2	-1.33	-0.67	-0.02	1.38	0.65	1.82	0.73	1.39	-0.05	0.04
S100A10	-1.18	-0.25	-0.37	0.99	0.23	1.73	0.63	0.90	0.38	0.47
TWIST1	-1.03	0.46	0.28	1.51	1.45	0.48	0.65	0.41	0.8	0.46
CD44	-0.99	0.49	-0.73	0.66	0.65	-1.08	0.44	0.44	0.65	0.78
PPP5C	-0.98	-0.04	-0.33	0.56	0.42	0.54	0.13	0.18	0.45	0.33
HOXA9	-0.98	-0.26	-0.40	0.74	1.29	1.78	0.16	0.08	0.49	0.78
HOXA9	-0.91	-0.16	-0.35	0.77	1.36	1.85	0.11	0.15	0.46	0.68
TNC	-0.79	0.36	-0.09	-0.20	0.10	-3.97	-0.51	-1.37	-0.22	-0.25
EGFR	-0.79	-0.40	-0.33	-0.12	0.34	-0.83	-0.27	-0.12	0.25	-0.08
PIM1	-0.76	0.56	0.34	1.18	0.99	0.38	0.36	-0.05	0.46	0.27
AHCTF1	-0.74	0.35	0.04	0.39	0.90	0.26	0.12	0.43	0.47	0.32
AHCTF1	-0.73	-0.02	-0.07	0.61	0.53	0.67	0.43	0.59	0.49	0.41
EGFR	-0.72	-0.06	-0.34	-0.02	0.59	-1.09	-0.41	-0.29	0.10	-0.28
BMI1	-0.70	-0.28	-0.18	0.18	0.43	0.89	0.27	0.31	0.17	0.18
NR3C1	-0.69	-0.14	-0.02	-0.07	0.32	-0.19	-0.29	-0.49	0	0.02
UBE2M	-0.69	0.01	-0.22	0.18	0.15	0.10	-0.09	0.09	0.03	0.17
GNB2L1	-0.65	0.25	0	0.61	0.50	1.09	0.44	0.44	0.35	0.30
PTEN	-0.60	-0.32	-0.25	0.57	0.46	0.48	0.49	0.40	0.56	0.58
HMGN1	-0.57	-0.12	0.03	0.63	0.63	0.82	0.58	0.64	0.43	0.36
DPYD	-0.55	-1.22	-0.29	0.12	-0.01	0.04	0.53	0.22	0.46	0.25
AHCTF1	-0.55	-0.10	-0.10	0.58	-0.01	0.77	0.61	0.72	0.65	0.70

**Table 4.6: Senescence specific changes in NF- $\kappa$ B target genes expression with complementation** Log<sub>2</sub> fold changes in gene expression that occur upon growth arrest (GA), heat shock (HS) and upon serum starvation (Q). If changes in gene expression are specific for the senescence growth arrest, they should be reversed upon its abrogation. Up-regulated transcripts are indicated in green whereas down-regulated transcripts are in red. Results for the top 24 up- (A) and down-regulated (B)

**C**

ID	Symbol	logFC GA	logFC Q	logFC HS	logFC wt LT	logFC pRS p53	logFC GSE-p53	logFC pRS p21	logFC E1A	logFC E2F-DB	logFC E7
201783_s_at	RELA	-0.37	0.08	-0.33	-0.09	-0.27	0.06	-0.52	-0.31	-0.44	-0.34
230202_at	RELA	0.1	-0.16	-0.21	-0.07	-0.19	-0.02	-0.1	-0.4	-0.14	-0.13
209878_s_at	RELA	-0.43	-0.03	-0.34	0.1	0.1	-0.1	-0.1	-0.08	-0.27	-0.1
205205_at	RELB	0.29	1.45	0.33	-0.77	-0.56	-1.01	-0.58	-0.81	-0.47	-0.6
209239_at	NFKB1	-0.35	1.17	0.23	-0.01	-0.03	-0.14	-0.26	0.24	0.34	0.14
207535_s_at	NFKB2	0.45	1.15	0.19	-0.4	0.08	-0.55	-0.08	-0.28	-0.01	-0.09
209636_at	NFKB2	0.39	0.9	0.14	-0.48	-0.05	-0.73	-0.21	-0.33	0.06	0.02
211524_at	NFKB2	-0.08	-0.1	-0.15	0.12	0.09	-0.11	0.17	0.18	0.06	0.18
212312_at	BCL2L1	0.65	-0.24	-0.49	-1.24	-0.89	-1.2	-0.02	-1.19	-0.12	-0.49
206665_s_at	BCL2L1	0.59	-0.24	-0.62	-0.81	-0.68	-0.6	0.01	-1.21	0.02	-0.4
215037_s_at	BCL2L1	0.6	-0.54	-0.47	-0.91	-0.54	-1.05	0.17	-1.03	0.14	-0.12
231228_at	BCL2L1	-0.04	0.02	-0.13	-0.14	-0.11	-0.4	0.04	-0.18	0.22	0.14
201236_s_at	BTG2	1.83	0.22	-0.2	-1.37	-2.2	-1.92	0.46	0.01	0.01	-0.09
201235_s_at	BTG2	0.73	-0.05	-0.05	-0.41	-0.64	-0.26	0.37	0.03	0.12	-0.07
223710_at	CCL26	1.81	-0.1	0.19	-0.43	0.54	0.59	-0.37	-2.4	-0.07	0.25
212501_at	CEBPB	0.6	1.82	0.13	-1.31	-0.41	-0.73	-0.41	-3.12	-0.59	-0.8
221577_x_at	GDF15	2.93	0.4	0.13	-4.55	-3.49	-4.88	-0.68	-5.63	-0.77	-2
201162_at	IGFBP7	1.26	-0.27	0.34	-3.28	-1.06	-2.72	-1.08	-1.79	-1.36	-1.85
201163_s_at	IGFBP7	1.01	-0.27	0.27	-3.26	-0.83	-2.21	-0.84	-1.77	-1.05	-1.78
213910_at	IGFBP7	0.22	0.22	-0.14	-0.48	-0.11	-0.93	-0.23	-0.49	-0.36	-0.35
210118_s_at	IL1A	3.42	3.82	0.22	-4.36	-0.7	-3.28	-0.26	-5.18	-0.04	-1.05
208200_at	IL1A	0.04	0.41	-0.07	0.13	0.16	-0.29	0.26	0.74	0.33	0.12
205067_at	IL1B	3.33	3.54	0.06	-4.6	-1.41	-4.13	-1.48	-5.44	-0.86	-1.98
39402_at	IL1B	3.29	3.43	0.38	-4.58	-1.31	-3.83	-1.37	-5.89	-0.8	-1.82
203828_s_at	IL32	1.96	0.78	0.17	-1.42	-0.86	-1.23	-1.11	-0.26	-0.36	-0.99
205207_at	IL6	2.01	4.16	0.13	-3.37	-1.24	-2.65	-1.93	-5.35	-1.97	-2.64
211506_s_at	IL8	1.14	2.56	1.7	-5	-2.15	-5.77	-2.21	-7.47	-1.26	-2.03
202859_x_at	IL8	0.66	1.1	1.06	-3.26	-1.01	-4.13	-1.01	-5.89	-0.53	-1
218878_s_at	SIRT1	-1.2	0.52	-0.19	0.98	0.34	0.85	0.37	0.85	0.69	0.72
218065_s_at	TMEM9B	0.44	-0.27	-0.11	-0.43	-0.33	-0.29	-0.38	-0.13	-0.18	-0.2
222507_s_at	TMEM9B	0.39	-0.29	-0.19	-0.35	-0.28	-0.29	-0.34	0.11	-0.07	-0.12
201010_s_at	TXNIP*	2.45	0.5	0.24	-2.3	-0.41	-1.36	-0.89	-1.46	-1.78	-1.55
201008_s_at	TXNIP*	2.42	0.22	0.29	-2.51	-0.36	-1.58	-0.95	-1.45	-1.87	-1.54
201009_s_at	TXNIP*	1.54	0.13	0.27	-1.65	-0.35	-1.22	-0.71	-1.22	-1.39	-1.25

**Table 4.6: Senescence specific changes in NF- $\kappa$ B target genes expression with complementation** NFKB targets after complementation with the indicated constructs are shown as well as the changes in expression of all the NFKB targets examined in more details in this study (C).

However they were not affected by heat shock. Moreover up-regulation of these NF- $\kappa$ B targets was reversed when growth arrest was overcome by abrogating the p53-p21 or p16-pRb pathways. In addition to IL1A and B and IL6, a number of other secreted protein genes were found to be up-regulated including IL15, IL32, IL33, CCL2, CCL20, CCL26, BMP2, GDF15, LIF, IGFBP4 and IGFBP5.

#### 4.3.3 Is the NF- $\kappa$ B pathway also activated at a protein level?

To determine if the increase in RNA expression of the NF- $\kappa$ B targets was associated with increases in protein expression and secretion particularly of the SASP cytokines, the levels of IL6 and IL8 were determined in 12 hour culture supernatants collected from CL3<sup>EcoR</sup> cells at 34°C and after a 3 week growth arrest at 38°C; culture supernatants from HMF3S cells growing at 34°C and 38°C were used as controls for the temperature shift. Growth arrest was associated with a very large increase in the level of IL6 which was not due to the temperature shift (Figure 4.12A). IL8 levels were also increased upon growth arrest but not to the same extent as IL6 (Figure 4.12B).

Together these results show that in these conditionally immortal cells senescence growth arrest results in altered expression of many targets of the NF- $\kappa$ B pathway and up-regulation of a number of SASP proteins.

#### 4.3.4 Is phosphorylation of RelA/p65 also induced?

Activation of NF- $\kappa$ B signalling is habitually associated with increased phosphorylation of RelA. To determine if RelA phosphorylation was increased upon growth arrest, lysates prepared from CL3<sup>EcoR</sup> cells grown at 34°C and after 7 days at 38°C were analysed by Western blot using in parallel an antibody specific for total RelA or RelA phosphorylated on Serine 536. Protein extracts prepared from HMF3S cells grown at 34°C and 38°C were used as temperature controls.

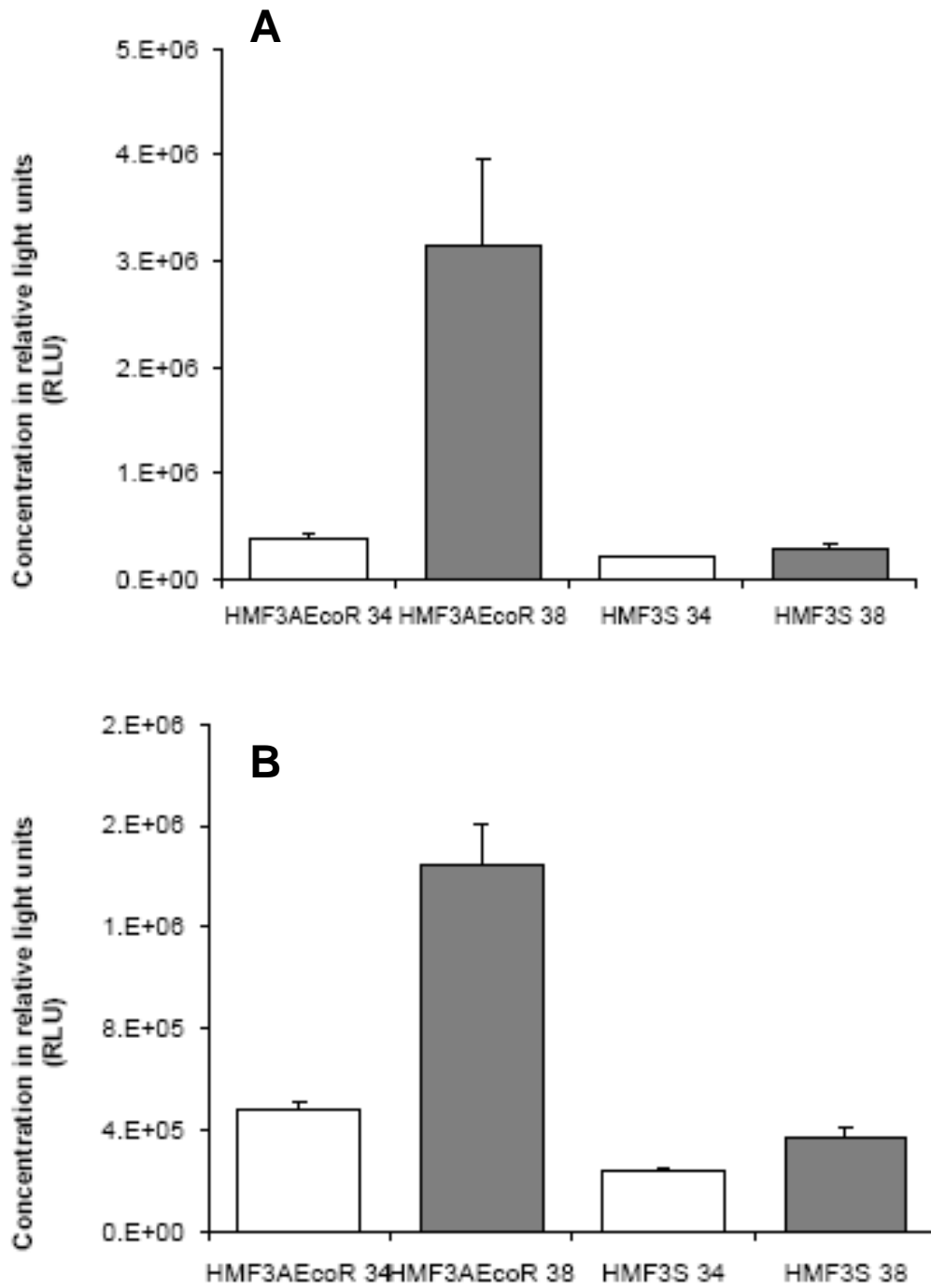


**Figure 4.12: Secretion of IL6 (A) and IL8 (B) by senescent cells**

12 hour supernatants harvested from cells grown at 34°C or at 38°C for 21 days were analysed by Quantiglo ELISAs from R&D Systems. All measurements are from independent biological triplicates.

Phosphorylation of RelA was increased upon growth arrest (Figure 4.13) in accordance with the finding that the NF- $\kappa$ B pathway was activated upon growth arrest.

#### 4.3.5 What happens if the NF- $\kappa$ B complex is inactivated?

##### *4.3.5.1 RNAi mediated silencing of NF- $\kappa$ B subunits abrogates senescence growth arrest*

Since the NF- $\kappa$ B pathway was activated upon growth arrest of CL3<sup>EcoR</sup> cells, I determined whether this activation has a causative role by determining if growth arrest would be overcome upon individual silencing of the various components of the NF- $\kappa$ B transcription factor complex. The silencing strategy chosen here was to use silencing constructs from the Open Biosystems human GIPZ lentiviral shRNAmiR library. Silencing constructs corresponding to RelA, RelB, NFKB1 and NFKB2 subunits were individually transduced into CL3<sup>EcoR</sup> cells after packaging as lentiviruses in HEK cells. Stably infected cells were selected in puromycin at 6  $\mu$ g per ml, pooled and assayed for complementation. Selection of the infected cells at 6  $\mu$ g per ml puromycin enriches for the transduced cells that have the highest levels of shRNAmiR expression. All experiments were carried out in triplicate and numbers of densely growing colonies of cells determined after 3 weeks at 38°C.

Although none of the NF- $\kappa$ B silencing constructs were as efficient as silencing p21<sup>CIP1/WAF1/Sdi1</sup>, silencing of the NF- $\kappa$ B subunits was clearly able to overcome growth arrest (Figure 4.14). Some constructs yielded more colonies than others but at least two constructs for each subunit yielded growing colonies. The numbers of growing colonies obtained after silencing NF- $\kappa$ B components were very similar or slightly higher than obtained upon inactivation of the p16-Rb pathway with HPV16 E7 or E2F-DB protein and the growing phenotype of the obtained was very clear cut.

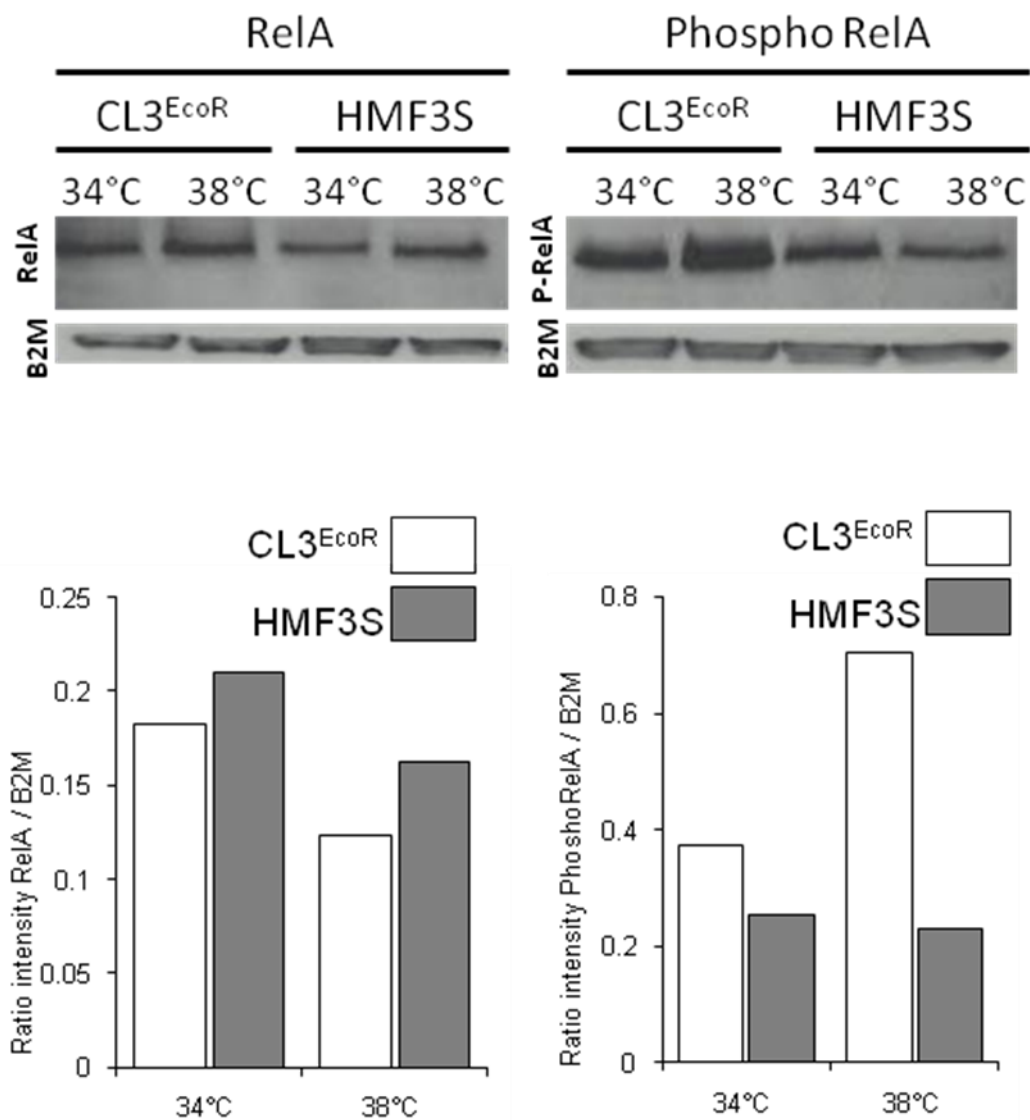


**Figure 4.13: Increase in phosphorylation of RelA (Ser536) in senescent cells**

Nuclear proteins extracted from cells grown at 34°C or 38°C for 12 days were analysed by western blotting using Phospho- NF-κB p65 (Ser536) (93H1) and NF-κB p65 (C22B4; Cell Signalling).

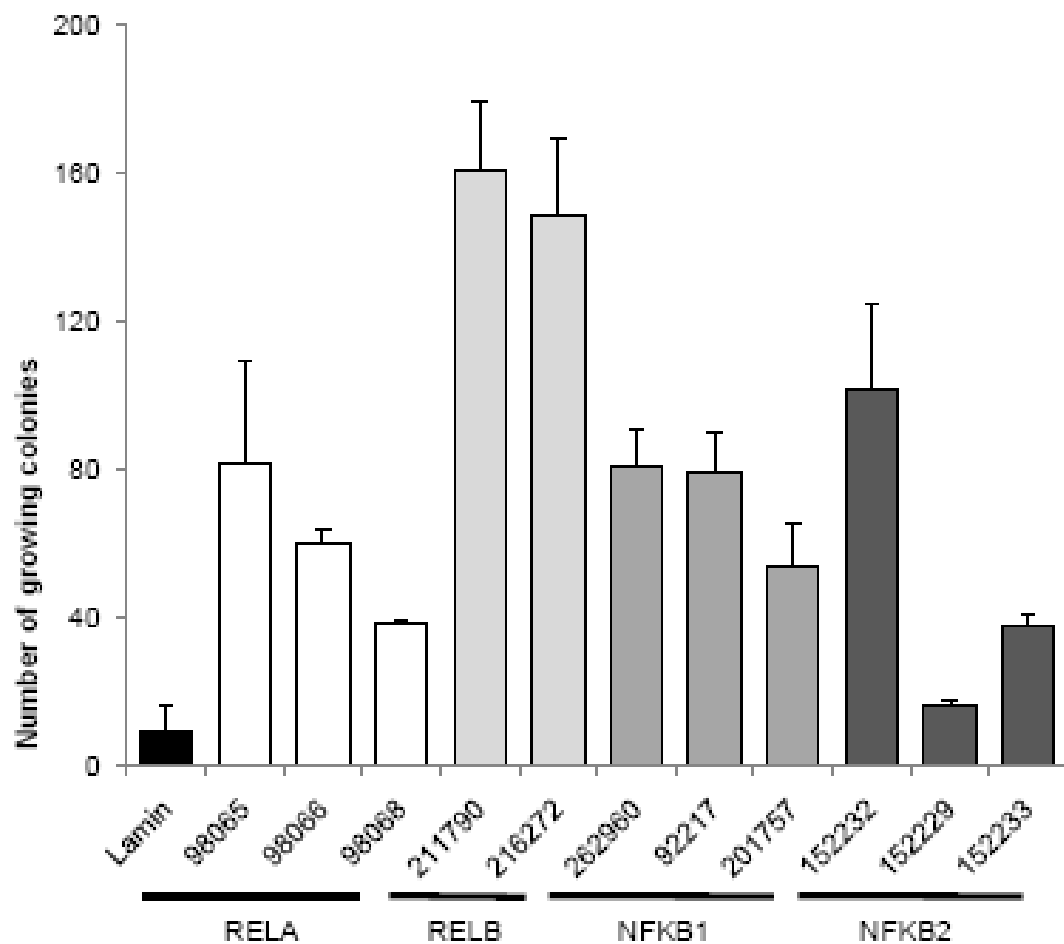


**Figure 4.14: Silencing of NF-κB transcription factor subunits**

CL3<sup>EcoR</sup> cells were infected in duplicate with lentiviruses expressing the indicated GIPZ shRNA mir silencing constructs. After puromycin selection,  $0.5 \times 10^5$  stably transduced cells were seeded in triplicate, incubated at 38°C for 21 days and stained. Densely growing colonies were counted after microscopic examination.

#### 4.3.6 Modulation of the NF- $\kappa$ B pathway overcomes senescence growth arrest

To confirm that the NF- $\kappa$ B pathway has a causative role in senescence, it was modulated both positively and negatively by RNAi mediated silencing and ectopic gene expression.

##### *4.3.6.1 TMEM9B and BCL2L1 silencing bypass senescence*

In a parallel project, an RNA interference screen has been used to identify genes whose suppression overcomes growth arrest of CL3<sup>EcoR</sup> cells (ER, LM and PSJ, manuscript in preparation, see next chapter). One of the shRNAs isolated corresponded to TMEM9B. TMEM9B was up-regulated 1.3 fold (P-value 1.47E-07, Table 4D) upon growth arrest which was reversed when growth arrest was overcome. Since TMEM9B has been shown to activate NF- $\kappa$ B dependent reporter constructs (Matsuda, Suzuki et al. 2003; Dodeller, Gottar et al. 2008), silencing its expression should suppress the NF- $\kappa$ B pathway resulting in abrogation of senescence growth arrest. Four lentiviral shmiRs targeting TMEM9B from the Open Biosystems human genome wide GIPZ library were introduced individually into CL3<sup>EcoR</sup> cells and the transduced cells analysed by the growth complementation assay. Densely growing colonies were obtained after 3 weeks growth at 38°C (Figure 4.15). Another gene identified by the RNA interference screen was BCL2L1, a member of the BCL2 family of proteins that is dependant and act downstream of NF- $\kappa$ B. BCL2L1 was up-regulated 1.57 fold (P-value 9.24E-04, Table 4D) upon growth arrest which was reversed totally upon complementation with either p53 or pRb abrogation. Silencing of BCL2L1 also overcame growth arrest (Figure 4.15) with 3 lentiviral shmiRs constructs out of 3 tested.



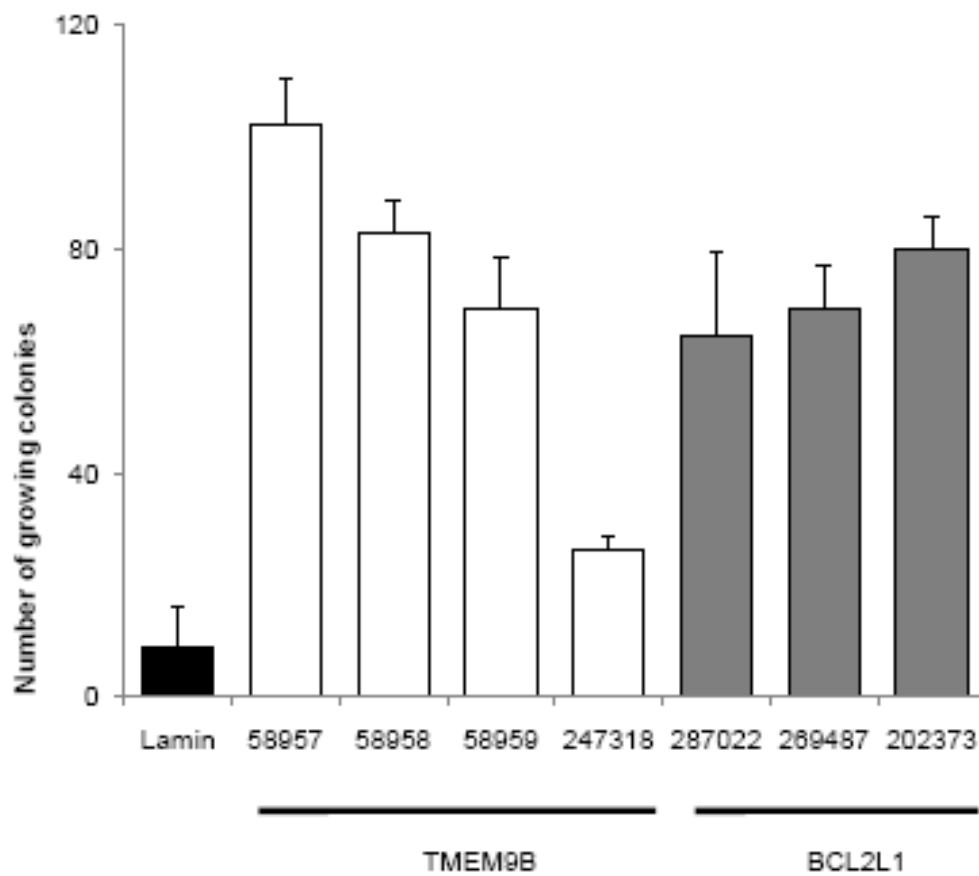


**Figure 4.15: Silencing of TMEM9B and BCL2L1**

CL3<sup>EcoR</sup> cells were infected in duplicate with lentiviruses expressing the indicated pGIPZ shRNA mir silencing constructs and assayed for growth complementation at 38°C. The number of growing colonies were counted after 3 weeks.

#### *4.3.6.2 Silencing of cEBP $\beta$ , BTG2 and TXNIP silencing bypass senescence*

Silencing of C/EBP $\beta$ , a transcription factor, previously proposed to be up-regulated in these conditional cells and linked to NF- $\kappa$ B activity also abrogated growth arrest (Figure 4.16) with two silencing constructs out of two tested. Silencing of BTG2, an NF- $\kappa$ B responsive gene (Kawakubo, Carey et al. 2004) and TXNIP, another member of the NF- $\kappa$ B pathway, as well as the secreted proteins CCL26, GDF15, IGFBP7 and IL32 were also able to complement growth (Table 4.6C and Figure 4.17 and 4.18).

#### *4.3.6.3 Ectopic expression of I $\kappa$ B-SR bypasses senescence*

NF- $\kappa$ B activity can also be suppressed by ectopic expression of a non-phosphorylatable, dominant negative form of I $\kappa$ B $\alpha$ , the super-repressor of NF- $\kappa$ B (I $\kappa$ B-SR). A tetracycline inducible lentiviral expression construct for I $\kappa$ B-SR was introduced into CL3<sup>EcoR</sup> cells and the stably transduced cells assayed by the complementation assay upon doxycycline induction. Expression of I $\kappa$ B-SR overcame growth arrest further indicating that activation of NF- $\kappa$ B activity has a causative role in the growth arrest (Figure 4.19).

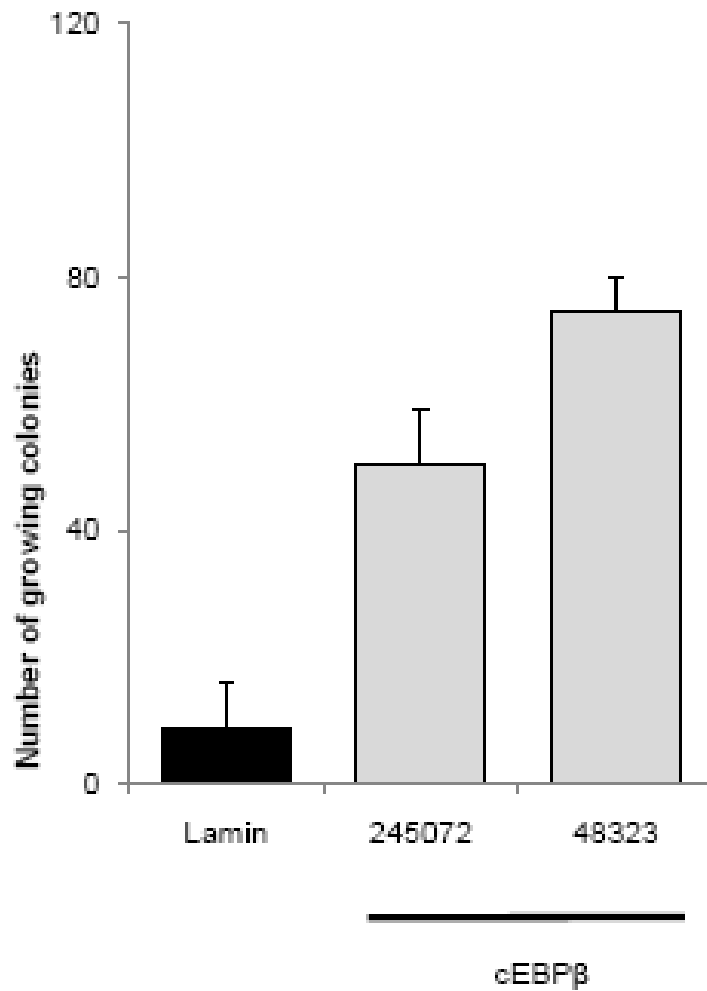


**Figure 4.16: Silencing of C/EBP $\beta$**

CL3<sup>EcoR</sup> cells were infected in duplicate with lentiviruses expressing the indicated pGIPZ shRNAmir silencing constructs and assayed for growth complementation at 38°C. The number of growing colonies was counted after 3 weeks.

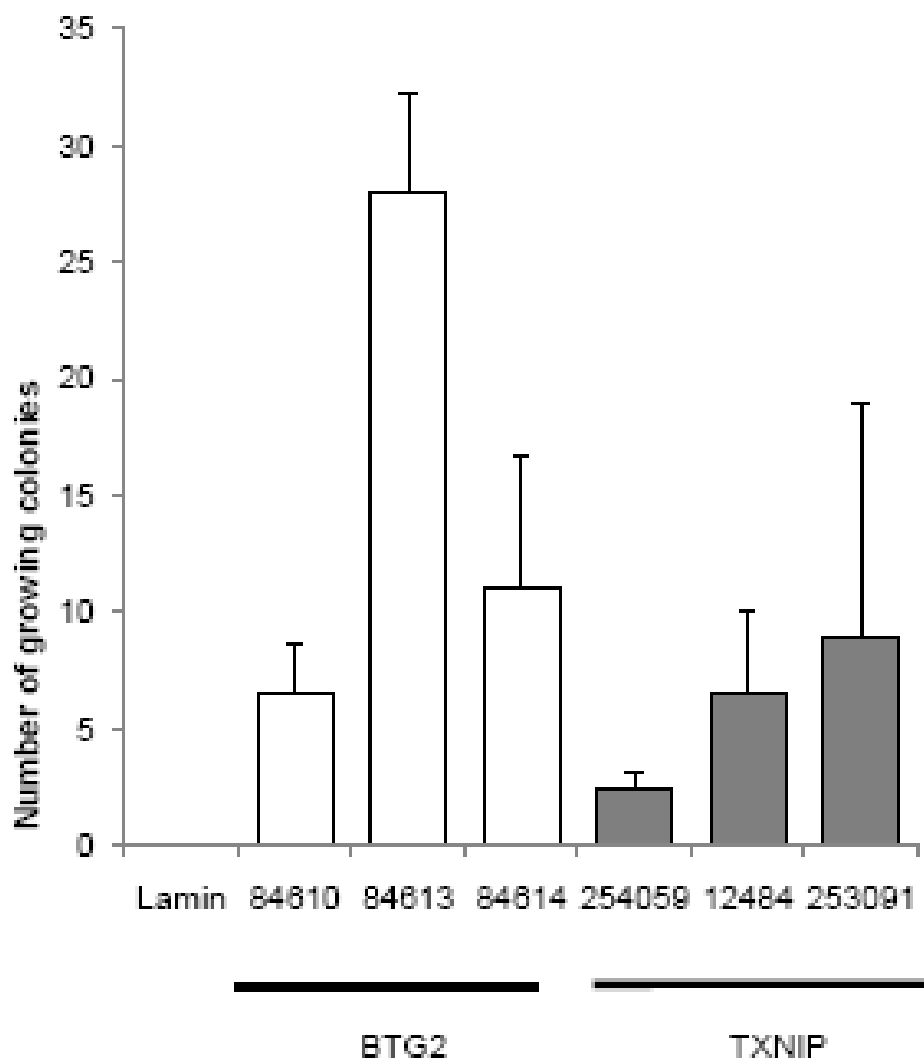


**Figure 4.17: Silencing of BTG2 and TXNIP**

CL3<sup>EcoR</sup> cells were infected in duplicate with lentiviruses expressing the indicated pGIPZ shRNA mir silencing constructs and assayed for growth complementation at 38°C. The number of growing colonies was counted after 3 weeks.

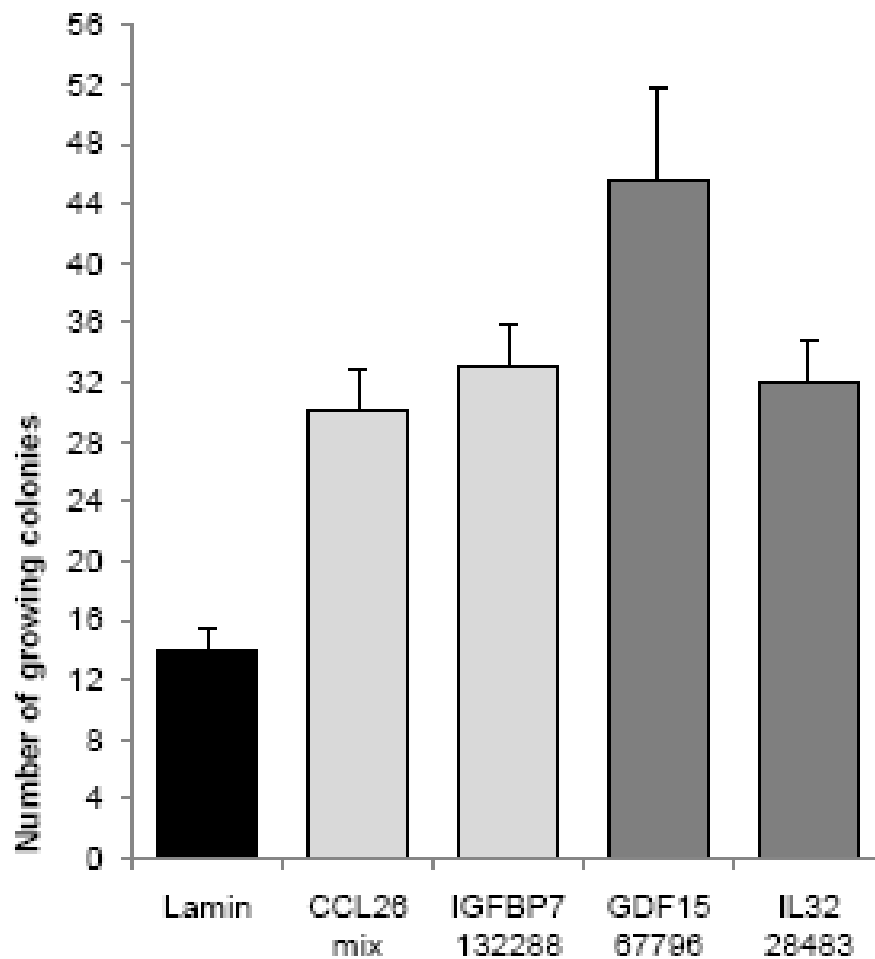


**Figure 4.18: Silencing of secreted proteins CCL26, IGFBP7, GDF15 and IL32**

CL3<sup>EcoR</sup> cells were infected in duplicate with lentiviruses expressing a mix of shMIRS silencing constructs for CCL26 (V2LHS\_70279, V2LHS\_70276 and V2LHS\_70275 ) or the indicated pGIPZ shRNA mir silencing constructs and assayed for growth complementation at 38°C. The number of growing colonies was counted after 3 weeks.

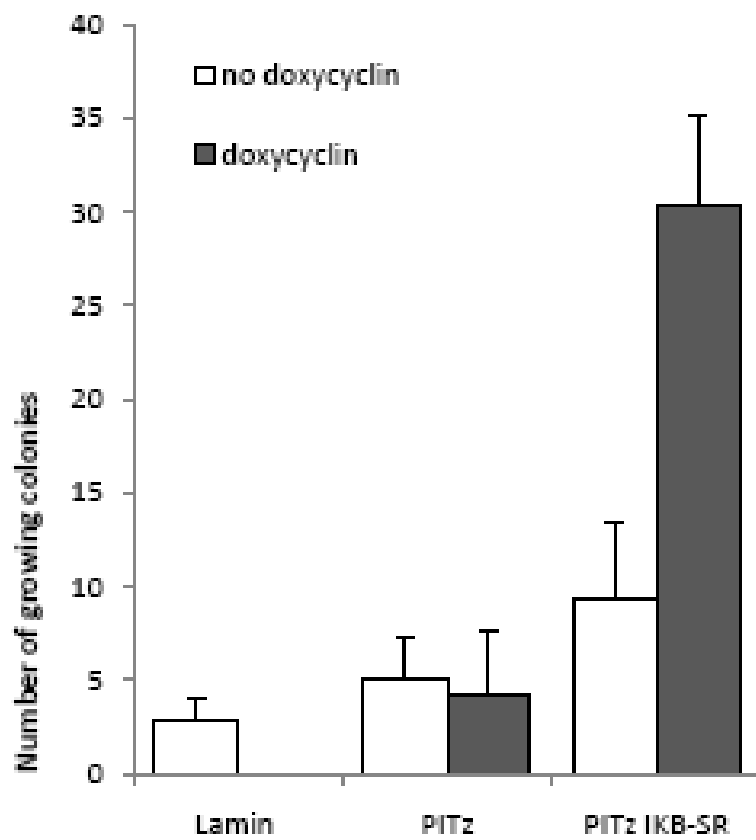


**Figure 4.19: Ectopic expression of IKB-SR**

CL3<sup>EcoR</sup> cells were infected in duplicate with lentiviruses expressing Lamin A/C shRNA, pTIPz Ikb-SR or an empty pTIPz vector. Stably transduced cells were assayed for growth complementation at 38°C with or without doxycycline. The number of growing was counted after 3 weeks.

#### 4.3.6.4 *Ectopic expression of SIRT1 bypasses senescence*

To further confirm the role of NF- $\kappa$ B activity, ectopic expression of SIRT1 was used to suppress NF- $\kappa$ B. SIRT1, the human homologue of Sir2, is a histone deacetylase that has been shown to suppress NF- $\kappa$ B activity (Yeung, Hoberg et al. 2004). SIRT1 expression was down-regulated 2.3 fold (P-value 9.22E-12; Table 4.6C) upon growth arrest which was reversed upon complementation. Ectopic expression of SIRT1 promoted growth in the complementation assay (Figure 2.20) and initial experiments suggest that this is dependent upon the deacetylation function of SIRT1. However as SIRT1 also negatively regulates p53 activity (Langley, Pearson et al. 2002), it may be overcoming growth arrest by inactivating p53 rather than suppressing NF- $\kappa$ B activity or acting on both.

#### 4.3.7 NF- $\kappa$ B Activation is Causal to Senescence

Together the results show that the senescence growth arrest in these conditionally immortalised fibroblasts involves activation of the NF- $\kappa$ B pathway and that suppression of this pathway by either direct silencing of NF- $\kappa$ B subunits or by upstream modulation can overcome growth arrest. Involvement of the NF- $\kappa$ B pathway was further indicated by silencing of BCL2L1, BTG2 and TXNIP that act downstream of NF- $\kappa$ B and C/EBP $\beta$  that may act in concert with NF- $\kappa$ B to regulate gene expression.

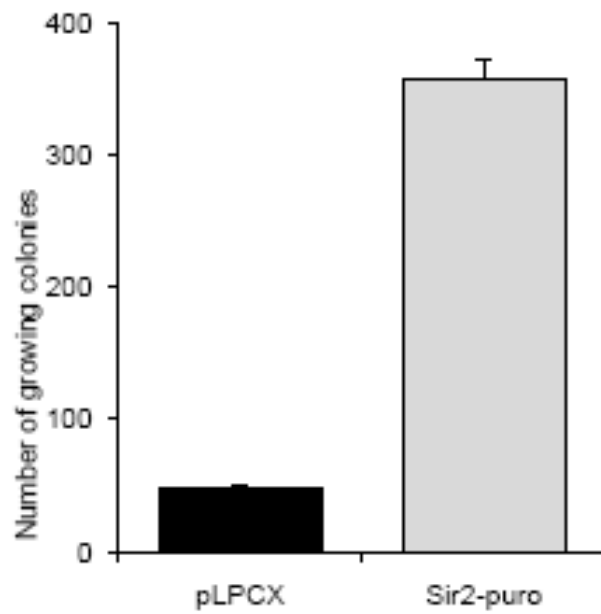


**Figure 4.20: Ectopic expression of SIRT1**

CL3<sup>EcoR</sup> cells infected in duplicate with retroviruses pYESir2-puro and pLPCX were assayed for growth complementation at 38°C.



## 4.4 DISCUSSION

One of the major stumbling blocks in dissecting the molecular pathways that underlie cell senescence has been the asynchrony of this process in heterogeneous cell populations used for serial sub-cultivation. The finding that HMF3A cells undergo an essentially synchronous growth arrest within 7 days of shift up to 38°C and that this can be readily overcome has enabled us to combine genome wide expression profiling with genetic complementation to identify genes that are differentially expressed when the cells undergo proliferation arrest. This identified 961 genes which were down-regulated >2 fold and 816 genes that were up-regulated >2 fold. Moreover when growth arrest was abrogated by complementation, the differential expression was reversed; down-regulated genes were up-regulated whereas up-regulated genes were suppressed.

Some of the genes identified, such as MAN1C1, PERP, DAB2, GM2A and PRNP have previously been shown to be induced upon senescence (Wagner, Horn et al. 2008). Many of the other up-regulated genes encode metalloproteinases and collagenases and other extra-cellular matrix degrading enzymes that are involved in collagen turnover and are hallmarks of a senescent cell microenvironment; for example, ADAMST1, cadherin2, CD36, MT1F, MT1X, MMP10, MMP12 and TIMP1 (West, Pereira-Smith et al. 1989; Millis, McCue et al. 1992; Yoon, Kim et al. 2004). Another large subset of up-regulated genes included those that encode for secreted factors, including NRG1, FGF2, VEGFC, CSF1, DAF, CD59, IL15, IL32, IL33, CCL2, CCL20, CCL26, BMP2, GDF15, LIF, IGFBP4 and IGFBP5.

### 4.4.1 SASP: Senescence-Associated Secretory Phenotype

It has long been known within the field that the culture medium of senescent cells is enriched with secreted proteins (Shelton, Chang et al. 1999; Krtolica and Campisi 2002). The SASP concept was first proposed by the Campisi group, when they realized that

secreted factors from senescent fibroblasts promote the transformation of pre-malignant, but not of normal, mammary epithelial cells. This initial observation of SASP implies that senescence might not simply be a tumour suppressor mechanism, but rather a double-edged sword within the tumour microenvironment. What remained unclear; however, were the functional effects of SASP on the senescence phenotype itself. A series of recent papers (Acosta, O'Loughlen et al. 2008; Coppe, Patil et al. 2008; Kuilman, Michaloglou et al. 2008; Wajapeyee, Serra et al. 2008; Augert, Payre et al. 2009), have identified various new members involved in SASP and notably IL-6 and IL-8 which are also up-regulated upon senescence in the HMF3A cells, and collectively reinforced the idea that senescence is both regulated by and regulates the extracellular environment.

#### 4.4.2 Senescence Down-Regulated Genes

Many of the other down-regulated genes including those that are required for cell cycle progression, cell proliferation and mitosis, were similarly identified in the original HMF3A microarray study (Hardy, Mansfield et al. 2005), such as CDK4, CDC2, CDC25B, CDC25C, BUBR1, PRC1, FOXM1 and UBE2C. Down-regulation of a number of genes that encode proteosomal subunit components was also noted, namely PSMB1, PSMB4, PSMB7, PSMB6, and this finding was in accordance with that of Chondrogianni and colleagues (Chondrogianni, Stratford et al. 2003) who identified a reduction in the expression level of catalytic subunits of the 20S proteasome and subunits of the 19S regulatory complex upon the induction of senescence.

Many of the down-regulated genes are associated with the cell cycle and are generally not affected by serum starvation (Table 4.2B). Three of the top four most highly down-regulated transcripts (NUF2, SLC25 and NDC80) are all components of the NDC80 kinetochore complex. The down-regulated transcripts also comprise genes that are necessary for the transition from G1 to S phase (Cdc6 and Cdc25B) and G2 to M phase (AurkB, Bub1 and Kif20a) as well as Polo like kinase 1 and MCM 4, 5 and 7. Many of these are known to be direct targets of the E2F and FoxM1 transcription factors suggesting that they are co-ordinately regulated by them. The association of the down-

regulated genes with the control of the cell cycle is consistent with the observed loss of proliferative potential when cells undergo senescence. Moreover when HMF3A cells cease dividing they undergo growth arrest in G1 phase in a manner analogous to senescent cells that also predominantly arrest in G1 phase. Since no cells arrest in S phase, it indicates that cells are unable to undergo the G1 to S transition consistent with the finding that genes involved in the G1 to S transition were down-regulated. The down-regulation of genes related to G2 phase is particularly interesting because DNA synthesis can be induced in senescent cells by exposure to fresh mitogens or by super-infection with DNA tumour viruses but the cells will not undergo mitosis suggesting there may also be block in the G2 phase in senescence (Gorman and Cristofalo 1985). Using a rodent model of senescence we have previously proposed that senescence involves a growth arrest in both G1 and G2 and that the block in G2 may actually be the cause of the irreversible loss of proliferative potential (Gonos, Burns et al. 1996).

#### 4.4.3 Ectopic expression of down regulated genes rescues the growth arrest

Out of six down-regulated genes chosen to be tested, two permitted rescue in a significant manner, namely BUB1B and FOXM1, when the other four did not give convincing rescue. However, since the failing constructs expression was not confirmed by western blot analysis, it is not possible to draw conclusion on their actual efficiency on bypassing senescence. Another three genes did not yield sufficient number of puro resistant clones and therefore could not be tested appropriately.

We have noted previously that in the HMF3A complementation assay, the density of the cells was an essential parameter to keep in consideration as a low density could cause a stress which would not permit the rescue from senescence.

HMGB2 and NEK2 did not yield growing colonies; however, their expression was not confirmed and therefore their efficiency to rescue cannot be assessed.

DEPDC1 was able to bypass cellular senescence at a very low level but with very variable results and therefore was not considered significant enough. It was previously reported that silencing of DEPDC1 was able to inhibit growth of bladder cancer cells (Kanehira, Harada et al. 2007), therefore it seemed possible that its expression would permit the growth in the conditional fibroblasts. This should be investigated further in the future.

BUB1 was a potential target to test in our system as it was believed to function as a growth enhancer protein in several other models (Cahill, Lengauer et al. 1998; Gjoerup, Wu et al. 2007; Gao, Ponte et al. 2009). It was then expected that its expression in the CL3<sup>EcoR</sup> cells would bypass senescence. Its ectopic expression permitted the bypass of the growth by yielding healthily growing colonies at a level above background.

MELK was one of the targets, that I thought most promising in the context of breast cancer and brain cancer as its expression was found to be directly linked to the malignancy of several cancers including breast cancer and as its silencing was also linked to growth suppression (Lin, Park et al. 2007; Marie, Okamoto et al. 2008; Nakano, Masterman-Smith et al. 2008). However, the results did not show a bypass of senescence. Moreover, Catia Caetano blotted the cells with a MELK antibody and could not detect any protein expression so no comment about MELK ectopic expression effect on senescence can be made. It would be worth investigating MELK further perhaps with a new expression construct.

MLF1-IP was a potential target to test in this context as its expression has been previously linked to several cancers malignancy and the escape from senescence in murine embryonic fibroblasts (Matsumoto, Yoneda-Kato et al. 2000; Dornan, Wertz et al. 2004; Sun, Zhang et al. 2004; Hanissian, Teng et al. 2005; Yoneda-Kato, Tomoda et al. 2005; Yoneda-Kato and Kato 2008). However, the level of rescue was considered too low to be of interest. In addition, the expression of MLF-IP was not confirmed and therefore no conclusion could be made about its efficiency to bypass senescence.

Transcriptionally active FOXM1 was sufficient to bypass senescence and was shown to have a causative role in cellular senescence but further studies are required to confirm and extend these findings to which isoform(s) are differentially expressed, how they are activated, what causes their expression to be down-regulated and what is their mechanism of action.

Indeed, I have found that senescence in CL3<sup>EcoR</sup> cells can be abrogated by the constitutively active FOXM1c but not the wild type protein. This indicates a requirement for the actual activation of FOXM1. The N-terminus of FOXM1 contains an auto-repressor domain that inhibits transactivation by an intramolecular interaction with the C-terminal TAD (Figure 4.8A). This repression can be relieved by phosphorylation of multiple cdk sites within the TAD by cyclinA/cdk2 or possibly by cyclinE/cdk2; PLK1 and PLK4 may also play a role. The expression profiling data indicates that cdk2 and cyclinE expression are unaffected upon growth arrest whereas cyclinA expression is down-regulated about 20 fold, PLK1 30 fold and PLK4 12 fold respectively.

Unfortunately, when PLK4 was ectopically expressed to be tested here, it did not yield a sufficient number of puro-resistant cells, and therefore could not be tested. Maybe a different expression system should be used.

Another important question would be to determine what causes the down-regulation of FOXM1 upon cell senescence. Although it was recently suggested that that Stress-activated kinase p38 (p38SAPK) is capable of inhibiting FoxM1 expression (Adam *et al*, 2009), the transcription profiling data indicates that this unlikely to be the mechanism, since expression of the three isoforms  $\alpha$  (MAPK14),  $\beta$  (MAPK11) and  $\gamma$  (MAPK13) of p38SAPK present in HMF3A cells, is unaffected upon growth arrest.

Previously it was suggested that in Basal Cell Carcinomas, FOXM1 was a downstream target of Gli1, which is transcriptionally up-regulated by Sonic hedgehog (Shh)-signalling (Teh, Wong *et al*. 2002). Gli1 is a member of the Gli family of three transcription factors Gli1, 2 and 3. Gli 1 and 2 are activators whereas Gli3 is a repressor.

The expression profiling data shows that all three Gli proteins are expressed in proliferating CL3<sup>EcoR</sup> cells but upon growth arrest Gli2 and 3 are down-regulated whereas Gli1 may be slightly up-regulated. This could be another explanation for the down-regulation of FOXM1 upon senescence.

In conclusion, many of the down-regulated genes are associated with the cell cycle (Table 4.1B and Supplementary Table S4.2). They comprise genes necessary for the transition from G1 to S phase (CDC6 and E2F1), G2 phase (CDC22, TOP2A and cyclinA) and G2 to M phase (AURKB, BUB1 and KIF20A) as well as Polo like kinase 1 and MCM 4, 5 and 7 (Whitfield, Sherlock et al. 2002). Many of these are direct targets of E2F and FOXM1 suggesting they are likely to be co-ordinately regulated by them. This is supported by my finding that constitutively active FOXM1 abrogated senescence. The association of these down-regulated genes with cell cycle control is consistent with the loss of proliferative potential when cells undergo senescence growth arrest mostly in G1. However, the down-regulation of genes related to G2 is interesting because DNA synthesis can be induced in senescent cells by exposure to fresh mitogens or by super-infection with DNA tumour viruses but the cells do not undergo mitosis suggesting there may also be block in G2 in senescence (Gorman and Cristofalo 1985). Using a rodent model of senescence, Pr Parmjit Jat had previously proposed that senescence involves growth arrest in both G1 and G2 and that the block in G2 may actually be the cause of the irreversible loss of proliferative potential (Gonos, Burns et al. 1996).

#### 4.4.4 NF- $\kappa$ B Pathway Activation upon Senescence is causal to Senescence

An *in silico* analysis of our differential data set and previous data suggested a potential activation of NF- $\kappa$ B upon senescence (Hardy, Mansfield et al. 2005). I investigated further the involvement of NF- $\kappa$ B pathway in senescence and used different approaches to validate *in vitro* my initial hypothesis.

#### 4.4.4.1 Senescence Up-Regulated Genes

In contrast to the down-regulated genes which are unaffected by serum starvation, many of the up-regulated genes were significantly up-regulated by serum starvation (IL33, ABI3BP, IL1A, IL1B and PAPPA amongst the top 24 up-regulated genes). Four of the top five most highly up-regulated transcripts correspond to CLCA family member 2, chloride channel regulator. The Chloride Channel Accessory (CLCA) family of proteins has four members in humans, are widely expressed in variety of cell types and encode 900 amino acid proteins that have been shown to produce a novel Cl<sup>-</sup> current that can be activated by calcium and inhibited by Cl<sup>-</sup> channel inhibitors. Elble and colleagues have recently shown that hCLCA2 is a direct downstream target of p53 and its acute expression results in a senescence like cell cycle arrest or apoptosis depending upon the cell context (Walia, Ding et al. 2009); Elble, personal communication).

The up-regulated genes also comprises a number of secreted proteins such as IL1A and B, IL6, IL15, IL32, IL33, CCL2, CCL20, CCL26, BMP2, GDF15, LIF, IGFBP4 and IGFBP5; IL8 and IGFBP7 were also up-regulated but since the adjusted P-values were greater than 0.0001 they were not identified as significant. IL6 and IL8 were also shown to be secreted into the medium. IL6, IL8 and IGFBP7 have been found to be secreted by senescent cells and act cell autonomously to induce and reinforce senescence (Acosta, O'Loughlen et al. 2008; Coppe, Patil et al. 2008; Kuilman, Michaloglou et al. 2008; Wajapeyee, Serra et al. 2008; Adams 2009; Augert, Payre et al. 2009; Kuilman and Peeper 2009; Orjalo, Bhaumik et al. 2009). Kuilman *et al* (2008) have further suggested that induction of these SASP proteins was specific to oncogene-induced senescence and not affected by quiescence. The results (Table 6C) indicate that these secreted proteins are also strongly up-regulated by serum starvation. Acosta *et al* (2008) have shown that activation of these secreted chemokines was regulated by the NF- $\kappa$ B and C/EBP $\beta$  transcription factors; the results discussed below are in accordance with these findings. Orjalo *et al* (2009) have suggested that IL1A, one of the most highly up-regulated genes was an essential cell-autonomous regulator of the senescence-associated IL6/8 cytokine network. In addition to IL6, IL8 and IGFBP7, I have found that a number of other secretory proteins were up-regulated. Moreover silencing expression of CCL26, IL32

and GDF15 was capable of abrogating growth arrest indicating that they may also have a role in promoting and reinforcing senescence. However, it remains to be demonstrated whether CCL26, GDF15 and IL32 play a similar role in promoting senescence in primary fibroblasts and whether the other up-regulated cytokines have a similar role.

#### *4.4.4.2 Silencing of over-expressed genes bypasses the growth arrest*

Out of nine genes up-regulated upon senescence chosen to be tested, six permitted the bypass of the conditional growth arrest, two gave a weak rescue and one did not rescue at all. This highlights the importance of mRNA expression regulation in the senescence mechanisms.

AK3L1, CLCA2, SCN2A, GRAMD3, TRIB2, p16<sup>INK4A</sup>, BLCAP and RUNX1 silencing all permitted the rescue of the cells from senescence using a mix of silencing constructs or individual silencing constructs. Interestingly, rescue by silencing of TRIB2 is contradictory to the literature as it was reported to be able to inactivate cEBPalpha and beta (Naiki, Saijou et al. 2007) which are not only known to be involved in senescence. In addition, cEBPbeta silencing permitted rescue in the HMF3A cells.

CDKN2A or p16<sup>INK4A</sup> silencing also permitted to bypass the growth arrest; this further reinforces the hypothesis that abrogation of the pRb alone was sufficient to bypass the conditional growth arrest.

RUNX1 silencing did permit the bypass of senescence in the HMF3A system. This was in accordance to several studies where RUNX1 was able to induce senescence-like growth arrest in primary murine fibroblasts (Linggi, Muller-Tidow et al. 2002; Wotton, Blyth et al. 2004; Kilbey, Blyth et al. 2007). This senescence-inducing effect is spared in cells lacking expression of p19<sup>Arf</sup>, an inducer of the p53 pathway (Linggi, Muller-Tidow et al. 2002). More recently another study suggested that this senescence inducing effect was actually happening through pathways independent to the one of replicative



senescence. Indeed, RUNX1 induced early growth stasis with only low levels of DNA damage signalling and a lack of chromatin condensation, a normal marker of irreversible growth arrest. In human fibroblasts, RUNX1 also induced p53 in the absence of detectable p14<sup>ARF</sup> but not in the absence of p16<sup>INK4A</sup> (Wolynec, Wotton et al. 2009).

BLCAP silencing did not permit rescue in the HMF3A model even if its ectopic expression was linked to growth inhibition in several cell line and models (Zuo, Zhao et al. 2006; Yao, Duan et al. 2007).

GRAMD3 permitted the bypass of senescence and represent a totally novel target to study in the context of the cell cycle and senescence. In addition, the fact that its expression seems regulated by two of the miRs whose expression can overcome senescence in chapter 4 makes it an even more credible target in the senescence pathway.

SCN2A and CLCA2 silencing both showed rescue at a low level and each of the repeat experiment showed the same results. This suggests a role, even minor, for these two genes both involved in ion conductance. Kriete and Mayo (2009) have proposed that mobilisation of calcium stored within the endoplasmic reticulum in conjunction with increases in reactive oxygen species from the mitochondria activates NF-κB signalling. The involvement of calcium in senescence is intriguing since the most highly up-regulated gene I identified was CLCA2. CLCA2, a chloride channel regulator was also found to be able to induce a senescence-like growth arrest upon acute expression (Walia *et al*, 2009; Elble, personal communication).

#### *4.4.4.3 Senescence expression profile reveals links with Cancer expression profile*

Overlay of the differential data set with the meta-signatures of genes that are up-regulated upon neoplastic transformation or undifferentiated cancer (Rhodes, Yu et al. 2004) showed that nearly 50% of these genes were down-regulated when HMF3A cells undergo growth arrest. Hanahan and Weinberg (2000) have proposed that six

independent events are required for malignant transformation and the acquisition of an infinite proliferative potential is one of these events. The results indicate that even though overcoming senescence may only be one of the six events, 50% of the genes are related to it and thus it must be an important barrier in cancer development.

#### *4.4.4.4 NF- $\kappa$ B pathway is activated upon senescence*

Our previous study suggested that the loss of proliferative potential in these conditionally immortal fibroblasts may involve activation of the NF- $\kappa$ B pathway (Hardy, Mansfield et al. 2005). I therefore analysed the promoters of the differentially expressed genes and found that NF- $\kappa$ B motifs were amongst the top 10% of most abundant motifs in both the up- and down-regulated genes.

A role for NF- $\kappa$ B activation was further highlighted by the finding that 67 NF- $\kappa$ B targets were up-regulated against 26 that were down-regulated significantly upon growth arrest (Table 4B and C); this included the increased expression of SASP proteins, including IL6, IL8 and IGFBP7 that are known to promote and reinforce senescence. Expression of other NF- $\kappa$ B targets was also differential but since the P-values were greater than 0.00001, they were not considered to be significant. In contrast to the down-regulated genes almost all of the up-regulated NF- $\kappa$ B targets were also up-regulated upon serum starvation.

Moreover, the increased expression, including the SASP proteins was reversed upon abrogation of the growth arrest by almost all constructs; even though expression of the down-regulated genes was also reversed it was not as clear cut. Although NF- $\kappa$ B is generally suggested to promote growth, my finding that it may be associated with growth arrest is in accordance with the study of Penzo *et al* (2008) who have shown that acute activation of NF- $\kappa$ B in murine embryo fibroblasts results in growth arrest in association with repression of 20 genes essential for cell cycle progression that are known targets of either E2F or FOXM1. Comparison of these genes with the differential GA set indicates that all of these genes except CDC5A were significantly repressed upon growth arrest (Supplementary Table S4.2). FOXM1 and E2F were down-regulated 6.23

and 1.8 fold respectively upon senescence growth arrest and the down-regulation was reversed when senescence was overcome (Supplementary Table S4.2). Moreover constitutively active FOXM1 ( $\Delta$ NAKEN) and E2F-DB overcome senescence growth arrest suggesting that transcriptionally active forms of these transcription factors may have a causative role in senescence.

➤ Diversity of the NF- $\kappa$ B function

The NF- $\kappa$ B family of ubiquitously transcription factors are widely known as key regulators of inflammatory and immune response. More recently they have been shown to function as regulators of diverse cellular processes such as cell proliferation and differentiation and the response to stresses such as oxidative, physical and chemical stress. Activation of NF- $\kappa$ B also blocks apoptosis and promotes cell survival. This family of transcription factors consists of five proteins, RelA (p65), RelB, c-Rel, NFKB1 (p105/p52) and NFKB2 (p100/p52) that are related through the Rel homology (RH) domain, a highly conserved DNA-binding and dimerisation domain. They associate to form homo- and heterodimers and regulate transcription by binding to  $\kappa$ B motifs within flanking DNA sequences. In unstimulated cells, the complexes are retained within the cytoplasm by binding to a member of the I $\kappa$ B family of inhibitory proteins that bind to and mask the nuclear transport sequence. Upon stimulation, the I $\kappa$ B protein is phosphorylated resulting in its ubiquitination and degradation leading to liberation of the NF- $\kappa$ B complex, translocation to the nucleus and binding to target DNA. The I $\kappa$ B proteins are phosphorylated by the I $\kappa$ B kinases which consist of three subunits: the catalytic subunits IKK $\alpha$  and IKK $\beta$  and the regulatory subunit IKK $\gamma$  (NEMO). Each of the above components is integrated into a complex signalling network central to the control of NF- $\kappa$ B activity.

➤ NF- $\kappa$ B and ageing

Since my initial finding that NF- $\kappa$ B activity may be associated with senescence, Adler *et al* (2007) using a systematic bioinformatic approach to identify combinatorial cis-

regulatory motifs showed that NF- $\kappa$ B activity controlled cell cycle exit and was continually required to enforce many features of ageing in a tissue specific manner. Moreover activation of NF- $\kappa$ B with age is consistent with elevated levels inflammatory markers and a pro-inflammatory phenotype associated with many age related diseases. For instance, factors that mediate NF- $\kappa$ B and inflammation include the insulin/IGF pathway, SIRT1, FOXO, PDC-1 and PPAR $\gamma$ . NF- $\kappa$ B is also constitutively activated in older human subjects compared to young donors (Kriete, Mayo et al. 2008). Moreover, RelA has been proposed to maintain cellular senescence by promoting DNA repair and genomic stability (Wang, Jacob et al. 2009).

The recent findings that senescence is associated with secretion of SASP proteins including the inflammatory cytokines IL6 and IL8, further suggest a role for NF- $\kappa$ B activation for inducing and reinforcing senescence.

#### ➤ NF- $\kappa$ B Causal Role in Senescence

Our study shows that NF- $\kappa$ B has a direct causal role in senescence. The expression profiling results in Table 4.6C show that the NF- $\kappa$ B transcription factor subunits are themselves not differentially expressed upon senescence growth arrest. Their expression was also not consistently modulated upon abrogation of senescence by the different constructs. However, I have shown that silencing of NF- $\kappa$ B transcription factor subunits by RNA interference clearly abrogated growth arrest upon activation of the p16-pRb and p53-p21 pathways (Figure 4.7).

In addition, my RNA interference growth promotion screen has identified TMEM9B a known upstream activator of NF- $\kappa$ B (ER, LM and PSJ, manuscript in preparation, see Chapter 5). Here, I show that TMEM9B was up-regulated upon growth arrest (Table 4.6) and that shRNA mediated silencing of TMEM9B can overcome growth arrest in the CL3<sup>EcoR</sup> cells (Figure 4.15). Silencing of BCL2L1, a direct downstream mediator of NF- $\kappa$ B and C/EBP $\beta$ , a transcription factor linked to NF- $\kappa$ B also overcomes growth

arrest. Moreover constitutive expression of I $\kappa$ B-SR, the super-repressor of NF- $\kappa$ B, also abrogated growth arrest suggesting that NF- $\kappa$ B activation is likely to be via the canonical pathway. Activation of the canonical NF- $\kappa$ B pathway was also indicated by the increased phosphorylation of RelA-Serine 536 upon growth arrest (Figure 4.13).

Kriete and Mayo (2009) have proposed another potential mechanism for NF- $\kappa$ B activation in ageing, the atypical pathway. They proposed that mobilisation of calcium stored within the endoplasmic reticulum in conjunction with increases in reactive oxygen species from the mitochondria activates NF- $\kappa$ B signalling. The involvement of calcium in senescence is intriguing since the most highly up-regulated gene I identified was CLCA2, a chloride channel regulator and CLCA2 can induce senescence like growth arrest upon acute expression (Walia, Ding et al. 2009); Elble, personal communication).

Our study has clearly delineated a central role for NF- $\kappa$ B activity in cellular senescence irrespective of whether it is induced via the p53-p21 or the p16-pRb tumour suppressor pathway. It indicates that senescence growth arrest is associated with activation of the canonical signalling pathway resulting in up- and down-regulation of known target genes including the SASP cytokines IL6 and IL8 that can act cell autonomously to induce and reinforce senescence. Moreover, this activation could also down-regulate FOXM1 and E2F and their downstream targets that are critical for cell cycle progression particularly the G2 phase. Although it is not clear how activation of the p53-p21 or p16-pRb pathways results in activation of NF- $\kappa$ B signalling, one possibility is SIRT1, a deacetylase that can suppress NF- $\kappa$ B activity. SIRT1 expression was down-regulated upon senescence but reversed upon its abrogation. Another possibility is TMEM9B, a lysosomal transmembrane protein that can activate NF- $\kappa$ B dependent expression; TMEM9B was slightly up-regulated upon senescence and reversed when it was overcome. Although it remains to be demonstrated whether SIRT1 and TMEM9B are the signal and what causes their differential expression, this study shows that NF- $\kappa$ B activation has a causal role in promoting senescence and suggests a framework for dissecting the underlying signalling network.

## **5 AN RNA INTERFERENCE SCREEN IDENTIFIES DOWNSTREAM EFFECTORS OF THE P53-P21 AND P16-PRB PATHWAYS**

### **5.1 RNAI INTERFERENCE SCREEN**

#### 5.1.1 Objectives

The discovery of RNAi has revolutionized the way investigators approach the studies of gene expression, regulation and interactions, particularly as it relates to drug development. It is a powerful tool which has been widely utilised in a variety of cells lines to perform loss-of-function genetic screens and identify target genes involved in various cellular processes (Zender, Xue et al. 2008; Hu, Kim et al. 2009; Zhang, Binari et al. 2010). Here, the objective was to silence by RNAi 9,392 different cancer associated genes in the conditional HMF3A cells and see if that would abrogate senescence growth arrest by using a retroviral shRNA (short hairpin RNA) library specifically designed for application in mammalian systems (Berns, Hijmans et al. 2004; Paddison 2008).

I have shown previously that inactivation of the p53-p21, the p16-pRb or the NF- $\kappa$ B pathway individually were able to bypass growth arrest in this model but the signal transduction pathways involved and how these diverse signals that result in senescence are all integrated, remain poorly defined. These functional assays would allow the identification of any genes whose silencing overcome senescence growth arrest and therefore any genes involved in and causal to the growth arrest. Potential positives were confirmed by carrying out a secondary screen using either pools of lentiviral shmiris or individual lentiviral shmiris.

### 5.1.2 The Open Access RNAi project at UCL

RNA interference is a natural system that exists within living cells to control and regulate the levels of expression of genes at the mRNA level. There are two types of small RNA molecules which are miRNAs (micro-rnas) and siRNAs (small interfering RNA) utilized here as shRNA (short hairpin RNA).

The RNAi library that I used was originally developed by Greg Hannon (CSHL) and Steve Elledge (Harvard) as a retroviral library. I used the pSM2 library version 1.3 provided by Chris Lord and Alan Ashworth (Breakthrough breast cancer research center). This version was extended later to make it genome-wide and also cloned into the pGIPZ lentiviral shRNAmir vector which I used to validate the results from the first version. Clones forming this library were provided by the UCL RNAi consortium.

“Functional genomics is playing an ever important role in deciphering the roles of specific genes in cancer and developmental biology, as well as in neuro-sciences, infectious diseases and immunity. The Open Access RNAi program helped foster this collaboration between the UCL Cancer Institute, UCL Institutes for Child Health and Neurology, and Division of Infection and Immunity, enabling us to provide world-class scientists in central London access to the latest shRNA libraries for focused functional screens.” said Dr. Chris Boshoff, Director, UCL Cancer Institute.

### 5.1.3 Which viral delivery system? Which library?

The Open Biosystems Expression Arrest™ pSM2 retroviral shRNAmir Library is a whole genome RNAi resource for transient, stable and *in vivo* RNAi studies. The collection has several unique features that make it a very versatile and efficient tool for RNAi studies including large-scale screens (Paddison, Silva et al. 2004) and notably its human micro-rna-30 (miR30) adapted design (Figure 5.1) which increases knockdown specificity and efficiency (Boden, Pusch et al. 2004).

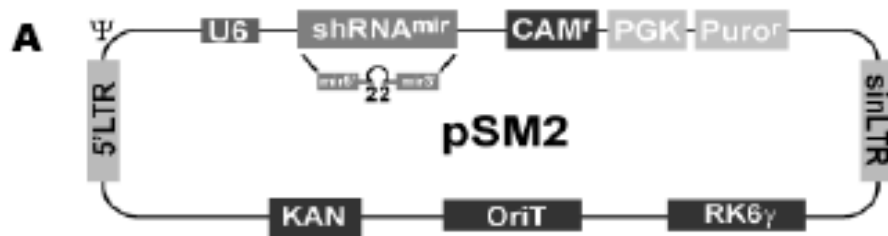




The pSM2 retroviral shRNA human library version 1.3 consisted of 100 pools numbered 1 to 100. The 100 tubes of plasmids pools each contains between 150 to 200 different shRNA constructs using the pSM2 plasmid (Figure 5.2). Each gene is represented by 1 to 3 shRNA plasmids and each plasmid is complementary to a different region of the target gene. Multiple shRNA plasmids per gene are used in order to increase the likelihood of achieving maximum efficiency of gene knockdown. The library version 1.3 contained 15,148 constructs representing 9,392 human genes targeted.

The fact that only 9,392 genes were analysed in this experiment with respect to the 22,500 estimated number of unique human genes (International Human Genome Sequencing Consortium, 2004) has to be taken into consideration. However, these 9392 genes were enriched for cancer-associated genes which make them very relevant to studying cell cycle disruption. This makes this screen a good tool to indentify new targets involved in senescence.

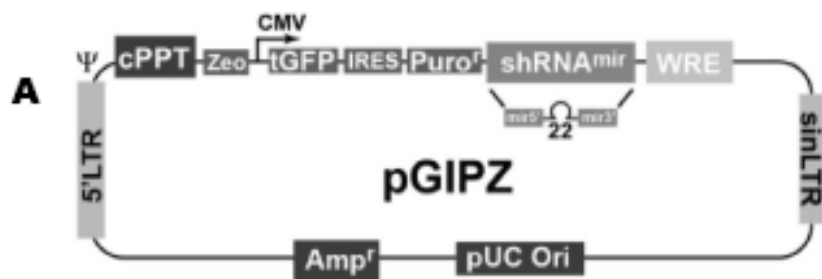
The pGIPZ was developed in a similar manner combining the design advantages of micro-rna-adapted shRNA (shRNAmir) with the pGIPZ lentiviral vector (Figure 5.3) to create a powerful RNAi trigger capable of producing RNAi in most cell types including primary and non-dividing cells. This library gives access to 44,602 lentiviral silencing constructs corresponding to 18,076 different human genes. Here, constructs from this library were used to validate the results of the primary screen by silencing genes individually rather than in pools.



**B**

Vector Element	Utility
U6 Promoter	RNA generated with four uridine overhangs at each 3' end
PGK	phosphoglycerate kinase eukaryotic promoter
puroR	Puromycin resistance for mamalian selection
5'LTR	5' long terminal repeat
SIN-LTR	3' self inactivating long terminal repeat
RK6g	Conditional origin of replication. Requires the expression of pir1 gene within the bacterial host to propogate
Kanr/CAMr	Bacterial selectable marker

**Figure 5.2: pSM2 retroviral plasmid : design (A) and features (B)**  
 (figure from OpenBiosystems literature).



**B**

Vector Element	Utility
CMV Promoter	RNA Polymerase II promoter
cPPT	Central Polypurine tract helps translocation into the nucleus of non-dividing cells
WRE	Enhances the stability and translation of transcripts
turbo GFP	Marker to track shRNAmir expression
Puro <sup>r</sup>	Mammalian selectable marker
AMP <sup>r</sup>	Ampicillin bacterial selectable marker
5'LTR	5' long terminal repeat
pUC ori	High copy replication and maintenance in e.coli
SIN-LTR	3' Self inactivating long terminal repeat
RRE	Rev response element
ZEO <sup>r</sup>	Bacterial selectable marker

**Figure 5.3: pGIPZ lentiviral plasmid : design (A) and features (B)**  
(figure from OpenBiosystems literature).

#### 5.1.4 ShRNA Screening Strategy

The screen was performed on the HMF3A conditional cells particularly using the CL3<sup>EcoR</sup> cells. The cells were infected with each of the 100 pools and reseeded (to avoid the density bias on cell growth) before being shifted to 38°C for 3 weeks. Because these cells have the particular properties to grow at 34°C but arrest at 38 °C when thermolabile LT is inactivated (Figure 5.4), the flasks showing growing colonies after 3 weeks of cultures would be considered to contain the candidate shRNAs of the primary screen (Figure 5.4).

The genomic DNA would then be extracted for these growing cells to identify the proviral shRNA inserts responsible for the growth arrest bypass and the corresponding involved gene. As it was difficult to ring clone colonies near each other and because there was very few colonies in some flasks, the total growing cultures were trypsinised and re-plated to enrich for growing cells. Owing to the presence of multiple inserts in the whole cultures and in order to identify each individual shRNA construct, an extra step of bacterial cloning was added before sequencing the inserts. All hits should have been analysed in a secondary screen to eliminate false positives; however, here, due to the limiting time scale, the microarray expression profiling data and literature were used to prioritise the order in which they were tested.

#### 5.1.5 Sensitivity of the model

Before starting the screen, it was important to get a proof of feasibility of an assay combining our HMF3A system and the shRNA pool format. It was also important to determine the sensitivity of the assay. Each of the pools contains between 150 and 200 shRNA constructs; consequently, it was necessary to test that a mix containing a positive control construct diluted 1/200 in a negative control was able to trigger a rescue and this was identifiable.

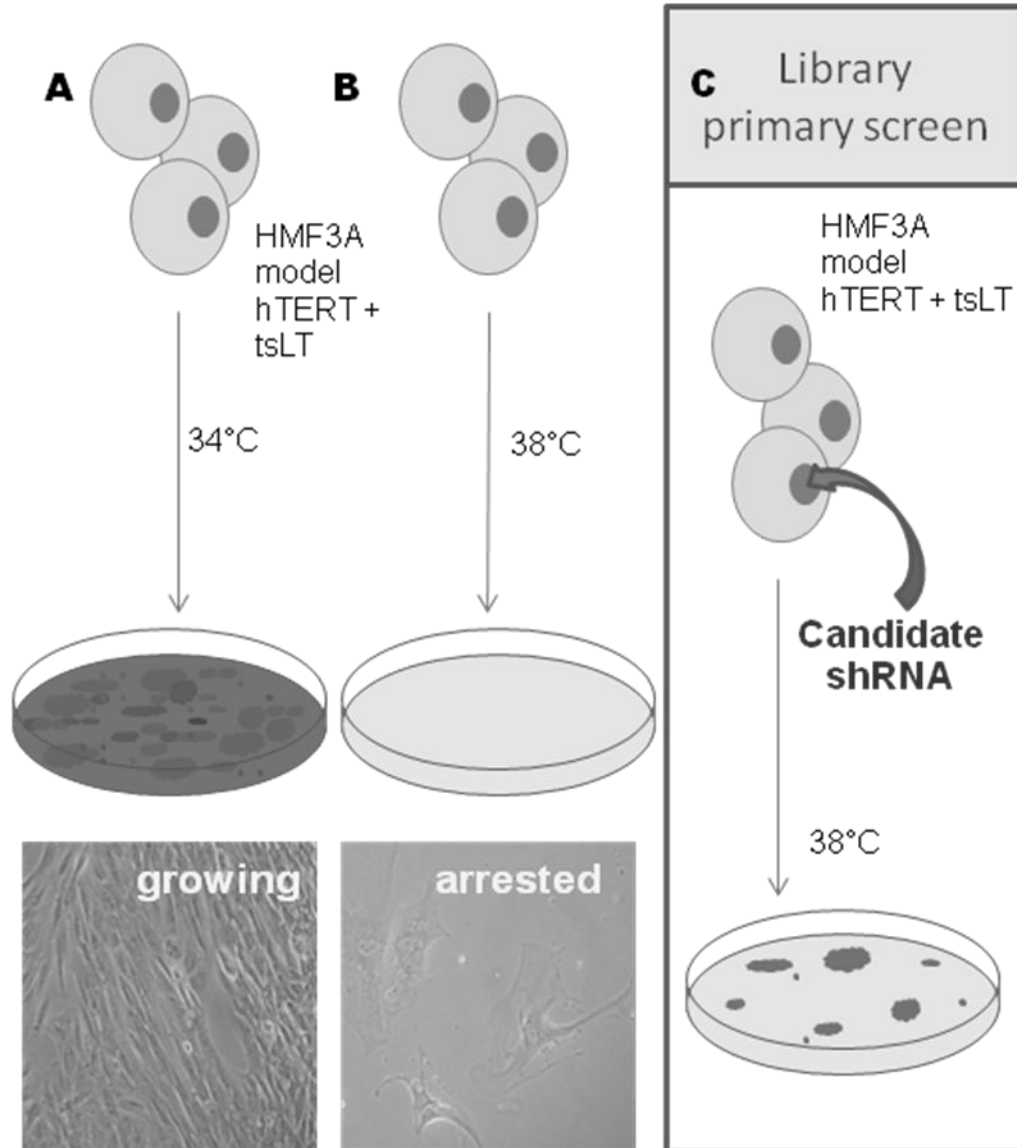


**Figure 5.4: ShRNA screen strategy**

The screening was performed on the conditional CL3<sup>EcoR</sup> cells. These cells have the particular properties to grow at 34°C (A) but arrest at 38 °C (B) when thermolabile LT is inactivated . The cells were infected with each of the 100 pools and reseeded before being shifted to 38°C for 3 weeks (C) ; The flasks showing growing colonies after 3 weeks of cultures would be considered containing the candidate shRNAs of the primary screen.

Therefore, a mixture was created by mixing a quantity of positive previously tested pRS p21F RNAi construct at 1/200 with negative pRS Lamin A/C construct. This spiked mix was packaged as described in Material and Method in Phoenix Ecotropic cells and used to infect CL3<sup>EcoR</sup> at  $0.5 \times 10^6$  in a T-75 cm<sup>2</sup> flask. Along with it, a positive control, p21F RNAi and a negative, Lamin A/C construct were each packaged and used to infect a flask of cells as above. After selection, the cells were trypsinised and reseeded at  $8.5 \times 10^4$  per 15cm plate or  $0.5 \times 10^4$  per well in 6-well plates. The next day the media was changed and cells were shifted to 38°C for 3 weeks. At that point, the cells were stained using methylene blue dye.

The Lamin negative control (Figure 5.5, A and D) showed very little background whereas the p21 positive control (Figure 5.5, B and E) produced a confluent monolayer. The spiked mixture Lamin/p21 exhibited numerous distinguishable growing colonies. These results suggest that the sensitivity of the test was sufficient to permit the identification of 1 construct in a mix of 200; therefore, the proof of concept of the model was verified. This test was performed with a batch of CL3<sup>EcoR</sup> from the passage p22+9 to make sure that cells from the exact same batch could be used for the screen itself.

#### 5.1.6 Confidence intervals

Using the formula:  $\ln(1-0.95) / \ln(1-1/(\text{Library Size}))$  which is recommended for genetic screens (see <http://www.stanford.edu/group/nolan/screens/screens.html>) by the Nolan lab, it is possible to calculate the number of infectious events that needed to be screened depending on the size of the library and the confidence interval required (Table 5.1). In that case, for a confidence interval of 99%, the number of infection events for the screening of our library of 9393 genes would have to be superior or equal to 43,254. This suggested that for each pool approximately 1000 independent infectious events would be sufficient for a 99% confidence that all shRNAs within a pool had been sampled.

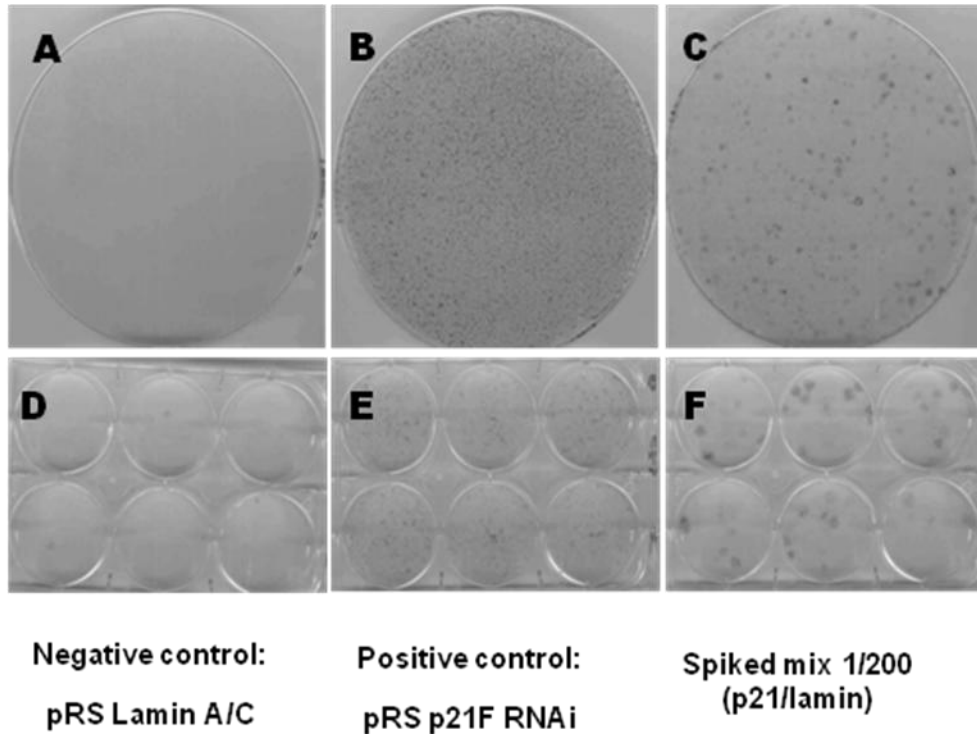


**Figure 5.5: Screen sensitivity test**

Cells were infected with either pRS Lamin A/C (A and D), either pRS p21F RNAi (B and E) or a mix 1/200 p21F/lamin (C and F). After puromycin selection, cells have been reseeded at  $8.5 \times 10^4$  per 15 cm plate (A, B and C) or  $0.5 \times 10^4$  per well in 6-wells plates (D, E and F) and shifted to 38°C for 3 weeks. The plates were then stained and photographed.

Confidence Interval (%)	9393 Genes	200 Genes
95%	28137	598
98%	36744	780
99%	43254	919

**Table 5.1: shRNA screen confidence intervals**

The table displays the number of infectious events required to be screened depending on the size of the library and the confidence interval.

In the shRNA screen, the number of cells reseeded after puromycin selection was  $5.3 \times 10^4$  which is really superior to 919 so the confidence in the results are superior or equal to 99%. However, to ensure that the screen would be saturating, virus sufficient to give rise to 10,000 infectious events was utilised for each pool (Table 5.2).

#### 5.1.7 Titration of Phoenix Eco viral Supernatants

CL3<sup>EcoR</sup> cells are very susceptible to cellular stress under low cell density growth conditions. As such, an experiment was performed to determine the quantity of titrated viral supernatant required to obtain approximately 10,000 infectious events for each pool.

Cells were seeded at  $6 \times 10^4$  cells per well in 6-well plates (day 0) and infected the next day (day 1) with different volumes (from 0.5ml to  $1 \times 10^{-4}$  ml) of each virus pool in presence of 8µg/ml polybrene. After 2 weeks puromycin selection at 34°C, the cells were stained with methylene blue and the number of colonies counted. The volume of virus required to produce approximately 10,000 infectious events was calculated for each pool (Table 5.2). Unfortunately, because the amount of DNA available to us was limited, for the pools with a low titer, the volume of viral supernatant used was set at 10 ml (maximum amount harvested).

#### 5.1.8 Primary screen in the HMF3A: Procedure

The screen was performed in successive waves of 10 pools. Cells were seeded at  $0.5 \times 10^6$  per T-75 cm<sup>2</sup> flask on day 0 and infected on day 1 with the determined volume of virus supernatant (Table 5.2) in presence of 8µg/ml polybrene. Each time, a positive control, pRS-p21F RNAi construct virus supernatant, and a negative control, pRS-Lamin A/C construct virus supernatant, were each used to infect a flask of cells.



DNA Pool	volume virus used (ml)	DNA Pool	volume virus used (ml)	DNA Pool	volume virus used (ml)	DNA Pool	volume virus used (ml)
1	9.0	25	10.0	51	10.0	75	10.0
2	9.0	26	10.0	52	10.0	76	10.0
p21	5.0	27	10.0	p21	1.3	77	10.0
lamin	5.0	28	10.0	lamin	1.3	78	10.0
3	8.0	29	10.0	53	10.0	79	10.0
4	8.0	30	10.0	54	8.7	80	10.0
5	8.0	31	10.0	55	10.0	81	10.0
6	2.0	32	10.0	56	10.0	82	10.0
7	8.0	p21	1.3	57	10.0	p21	5.0
8	8.0	lamin	1.3	58	6.8	lamin	5.0
9	8.0	33	10.0	59	7.7	83	10.0
10	8.0	34	10.0	60	8.6	84	10.0
11	8.0	35	10.0	61	9.6	85	10.0
12	8.0	36	10.0	62	10.0	86	10.0
p21	1.3	37	10.0	p21	1.3	87	10.0
lamin	1.3	38	10.0	lamin	1.3	88	10.0
13	10.0	39	10.0	63	10.0	89	10.0
14	10.0	40	10.0	64	10.0	90	10.0
15	10.0	41	10.0	65	10.0	91	10.0
16	10.0	42	10.0	66	10.0	92	10.0
17	10.0	p21	1.3	67	10.0	p21	5.0
18	10.0	lamin	1.3	68	10.0	lamin	5.0
19	10.0	43	10.0	69	10.0	93	10.0
20	10.0	44	10.0	70	10.0	94	10.0
21	10.0	45	10.0	71	10.0	95	10.0
22	10.0	46	10.0	72	10.0	96	10.0
p21	1.3	47	10.0	p21	5.0	97	10.0
lamin	1.3	48	10.0	lamin	5.0	98	10.0
23	10.0	49	10.0	73	10.0	99	10.0
24	10.0	50	10.0	74	10.0	100	10.0

**Table 5.2: Virus pools titration and supernatant volume used**

The negative control permitted the evaluation of the level of background for each experiment and the positive control made sure that the complementation assay worked in these conditions. The media was changed on day 2 and puromycin selection at 2 µg/ml was added on day 4. On day 8, the cells were trypsinised, counted and reseeded at  $5.3 \times 10^4$  per T-75cm<sup>2</sup> flask or  $1.8 \times 10^4$  per T-25cm<sup>2</sup> flask in as many flasks as possible in order to screen a representative number of cells. The next day the media was changed and cells were shifted to 38°C for 3 weeks. After 3 weeks, multiple growing colonies were observed in the p21 shRNA-infected CL3<sup>EcoR</sup> cultures; however, minimal background was observed in the Lamin A/C shRNA-infected CL3<sup>EcoR</sup> cultures. The number of colonies for each pool was counted and each colony was checked under the microscope for a growing phenotype. The number of cells counted just before reseeding, the number of flasks reseeded and the number of colonies for each flask reseeded after 3 weeks at 38°C is shown in Table 5.3. The hits that were significantly above background (more and/or bigger colonies, all analysed for phenotype under the microscope) were reseeded (and are shown in red in Table 5.3). Occasionally, a background of growing colonies was observed. For these batches, only the flasks showing a growth above background were selected. The results show that 34 pools out of 100 yielded growing colonies at a level above background. Particularly, the pools 13, 78 and 82 gave colonies in a higher number and most importantly of a size superior to that of the other hits. Pools 16, 18, 19, 21 and 80 also yielded colonies but they were smaller. For each pool that contained growing colonies, 1 to 4 flasks containing the highest number of colonies were reseeded for extracting genomic DNA and resulted in a total of 81 sub-pools to analyse. Genomic DNA was extracted from 80% confluent T-75 cm<sup>2</sup> cultures. As a caveat, it should be noted that genomic DNA harvested from these cultures were representative of a heterogeneous population from multiples colonies and of many different shRNAs species, therefore, sequencing of multiple inserts was required to identify all shRNA target sequences. Nonetheless, a secondary growth complementation screen of CL3<sup>EcoR</sup> cells utilising the pure shRNA construct would permit identification of functional inserts. Moreover, the growing cells should predominate the culture and thus shMiRs isolated from the growing cells should be over-represented.

DNA Pool	Cells number after selection	number of T-75cm <sup>2</sup> flasks reseeded	number of T-25cm <sup>2</sup> flasks reseeded	colonies after 3 weeks in T-75	colonies after 3 weeks in T-25
3	3.75x10 <sup>5</sup>	7	none	0, 0, 1, <b>2, 3</b> , 0, 1	n/a
4	2.44x10 <sup>5</sup>	4	none	1, 1, 0, <b>3</b>	n/a
5	3.06x10 <sup>5</sup>	5	none	0, <b>2, 3</b> , 0, 0	n/a
6	1.22x10 <sup>5</sup>	2	none	0, 0	n/a
7	8.50x10 <sup>5</sup>	8	none	0, <b>2, 2, 3</b> , 1, 0, 1, 1	n/a
8	9.61x10 <sup>5</sup>	8	none	0, 1, 1, 0, 0, 0, 0, 0	n/a
9	9.61x10 <sup>5</sup>	8	none	<b>2, 3, 3</b> , 1, 0, 0, 1, 1	n/a
10	6.86x10 <sup>5</sup>	8	none	0, 0, 0, 0, 0, 0, 1, 1	n/a
11	5.11x10 <sup>5</sup>	8	none	0, 0, 2, 0, 0, 0, 1, 1	n/a
12	3.75x10 <sup>5</sup>	7	none	<b>2</b> , 1, 0, <b>4</b> , 1, 0, 0	n/a
<b>p21 lamin</b>	1.64x10 <sup>5</sup>	<b>1</b>	none	confluent	confluent
	3.39x10 <sup>5</sup>	<b>4</b>	none	0, 0, 1, 1	n/a
13	2.22x10 <sup>5</sup>	4	none	<b>6, 4, 8, 5</b>	n/a
14	2.28x10 <sup>5</sup>	4	none	1, 0, 2, 0	n/a
15	1.08x10 <sup>5</sup>	2	none	2, 1	n/a
16	1.22x10 <sup>5</sup>	2	none	<b>8, 11</b>	n/a
17	3.61x10 <sup>4</sup>	none	2	n/a	0, 0
18	6.10x10 <sup>4</sup>	1	none	<b>10</b>	n/a
19	1.03x10 <sup>5</sup>	2	none	<b>5, 6</b>	n/a
20	1.56x10 <sup>5</sup>	3	none	0, 1, 0	n/a
21	9.72x10 <sup>4</sup>	1	2	<b>5</b>	0, 0
22	1.94x10 <sup>4</sup>	none	1	n/a	0
<b>p21 lamin</b>	1.36x10 <sup>5</sup>	<b>2</b>	none	confluent	confluent
	4.11x10 <sup>5</sup>	<b>4</b>	none	3, 1, 3, 4	n/a
23	2.47x10 <sup>5</sup>	4	1	3, 0, 1, 1	0
24	4.08x10 <sup>5</sup>	7	1	2, 0, 0, 0, 1, 1, 0	0
25	3.42x10 <sup>5</sup>	6	none	0, 0, 0, 1, 1, 0	n/a
26	4.53x10 <sup>5</sup>	8	none	0, 0, 1, 3, 1, 4, 0, 0	n/a
27	1.50x10 <sup>5</sup>	2	2	4, 3	0, 1
28	2.31x10 <sup>5</sup>	4	none	1, 3, 1, 2	n/a
29	2.19x10 <sup>5</sup>	4	none	3, 0, 0, 1, 1	n/a
30	1.39x10 <sup>5</sup>	2	1	<b>2, 4</b>	1
31	2.44x10 <sup>5</sup>	4	1	1, 0, 0, 0	0
32	8.90x10 <sup>4</sup>	1	1	<b>3</b>	n/a
<b>p21 lamin</b>	5.44x10 <sup>5</sup>	<b>2</b>	none	confluent	confluent
	2.22x10 <sup>5</sup>	<b>2</b>	none	4, 1, 5, 6	0, 0, 0, 0

DNA Pool	Cells number after selection	number of T-75cm <sup>2</sup> flasks resseeded	number of T-75cm <sup>2</sup> flasks reseeded	colonies after 3 weeks in T-75	colonies after 3 weeks in T-25
33	1.40x10 <sup>4</sup>	none	1	n/a	0
34	2.31x10 <sup>5</sup>	4	1	1, 0, 0, 0	0
35	2.25x10 <sup>5</sup>	4	none	0, 1, 0, 0	n/a
36	4.81x10 <sup>5</sup>	9	none	0, 0, 0, 1, 0, 0, 0, 0, 0	n/a
37	1.89x10 <sup>5</sup>	3	1	0, 0, 1	0
38	2.19x10 <sup>5</sup>	4	none	0, 0, 0, 0	n/a
39	3.06x10 <sup>5</sup>	5	none	1, 0, 0, 0, 0	n/a
40	1.22x10 <sup>5</sup>	2	none	0, 0	n/a
41	1.83x10 <sup>5</sup>	3	1	2, 1, 1	0
42	3.25x10 <sup>5</sup>	6	none	0, 2, 0, 1, 0, 1	n/a
p21 lamin	2.05x10 <sup>5</sup>	2	none	confluent	n/a
	4.30x10 <sup>5</sup>	4	4	0, 0, 1, 0	0, 0, 0, 0
43	4.72x10 <sup>4</sup>	none	2	n/a	0, 0
44	7.20x10 <sup>4</sup>	1	1	0	0
45	7.20x10 <sup>4</sup>	1	1	2	0
46	7.50x10 <sup>4</sup>	1	1	0	2
47	8.05x10 <sup>4</sup>	1	1	3	0
48	1.65x10 <sup>4</sup>	none	1	n/a	0
49	1.35x10 <sup>4</sup>	none	1	n/a	0
50	5.80x10 <sup>4</sup>	none	3	n/a	0, 0, 0,
51	4.70x10 <sup>4</sup>	none	2	n/a	2, 0
52	4.72x10 <sup>4</sup>	none	2	n/a	1, 0
p21 lamin	1.67x10 <sup>5</sup>	2	none	confluent	confluent
	4.25x10 <sup>5</sup>	4	4	1, 1, 4, 6	0, 2, 0, 2
53	3.17x10 <sup>5</sup>	6	none	0, 1, 0, 0, 2, 7	n/a
54	5.61x10 <sup>5</sup>	9	none	2, 4, 1, 6, 1, 1, 0, 3	n/a
55	3.00x10 <sup>5</sup>	5	none	2, 2, 1, 1, 7	n/a
56	4.78x10 <sup>5</sup>	9	none	0, 5, 1, 2, 0, 6, 1, 2, 4	n/a
57	4.83x10 <sup>5</sup>	9	none	0, 0, 0, 0, 0, 0, 1, 0, 1	n/a
58	4.42x10 <sup>5</sup>	8	none	0, 0, 0, 1, 2, 1, 4, 9	n/a
59	3.74x10 <sup>5</sup>	7	none	0, 2, 3, 1, 1, 6, 2	n/a
60	4.08x10 <sup>5</sup>	7	none	0, 4, 3, 5, 6, 1	n/a
61	3.67x10 <sup>5</sup>	7	none	3, 1, 4, 0, 0, 1, 0	n/a
62	1.94x10 <sup>5</sup>	4	none	1, 0, 3, 1	n/a
p21 lamin	2.00x10 <sup>5</sup>	2	none	confluent	n/a
	6.92x10 <sup>5</sup>	4	4	6, 2, 2, 2	n/a

DNA Pool	Cells number after selection	number of T-75cm <sup>2</sup> flasks resseeded	number of T-75cm <sup>2</sup> flasks reseeded	colonies after 3 weeks in T-75	colonies after 3 weeks in T-25
63	8.60x10 <sup>4</sup>	1	2	2	0, 0
64	6.90x10 <sup>4</sup>	1	1	1	1
65	5.50x10 <sup>4</sup>	1	none	0	n/a
66	8.88x10 <sup>4</sup>	1	2	2	3, 3
67	1.33x10 <sup>5</sup>	2	1	0, 2	0
68	2.50x10 <sup>5</sup>	4	1	0, 0, 1, 1	0
69	1.00x10 <sup>5</sup>	2	none	0, 0	n/a
70	6.10x10 <sup>4</sup>	1	none	0	n/a
71	9.40x10 <sup>4</sup>	1	2	2	0, 1
72	1.03x10 <sup>5</sup>	2	none	0, 2	n/a
p21	8.75x10 <sup>5</sup>	4	4	confluent	confluent
lamin	1.13x10 <sup>6</sup>	4	4	1, 6, 7, 2	2, 0, 0, 0
73	2.86x10 <sup>5</sup>	5	1	1, 0, 2, 2, 7	0
74	2.24x10 <sup>5</sup>	4	none	4, 2, 2, 3 : pooled in 1	n/a
75	2.58x10 <sup>5</sup>	4	2	2, 3, 0, 4	0, 0
76	1.67x10 <sup>5</sup>	3	none	0, 1, 4	n/a
77	4.97x10 <sup>5</sup>	9	none	1, 3, 1, 3, 3, 3,	n/a
78	3.78x10 <sup>5</sup>	7	none	4, 2, 6	n/a
79	1.58x10 <sup>5</sup>	3	none	4, 3, 8, 3, 5, 6, 6	n/a
80	1.03x10 <sup>5</sup>	2	none	3, 5, 2	n/a
81	3.86x10 <sup>5</sup>	7	none	7, 12	n/a
82	3.50x10 <sup>5</sup>	6	1	0, 0, 3, 2, 2, 0, 3	n/a
p21	6.72x10 <sup>5</sup>	4	4	9, 3, 7, 3, 10, 11	4
lamin	1.25x10 <sup>6</sup>	1	4	confluent	confluent
83	1.25x10 <sup>5</sup>	2	1	1, 7, 1, 1	0, 1, 0, 1
84	1.03x10 <sup>5</sup>	2	none	0, 0	0
85	1.11x10 <sup>5</sup>	2	none	2, 1	n/a
86	1.06x10 <sup>5</sup>	2	none	0, 0	n/a
87	7.20x10 <sup>4</sup>	1	1	0, 0	n/a
88	1.39x10 <sup>5</sup>	2	1	0	0
89	1.96x10 <sup>5</sup>	3	2	0, 1	0
90	8.89x10 <sup>4</sup>	1	2	0, 0, 1	0, 1
91	1.69x10 <sup>5</sup>	3	none	0	0, 0
92	1.03x10 <sup>5</sup>	2	none	0, 0, 0	n/a
p21	1.20x10 <sup>6</sup>	1	4	0, 1	n/a
lamin	1.85x10 <sup>6</sup>	4	4	confluent	confluent
				0, 0, 0, 2	0, 0, 0, 0

DNA Pool	Cells number after selection	number of T-75cm <sup>2</sup> flasks resseeded	number of T-75cm <sup>2</sup> flasks reseeded	colonies after 3 weeks in T-75	colonies after 3 weeks in T-25
93	3.78x10 <sup>5</sup>	7	none	1, 1, 1, 0, 0, 0, 0	n/a
94	5.84x10 <sup>5</sup>	7	none	1, 1, 0, 0, 0, 0, 0	n/a
95	3.11x10 <sup>5</sup>	5	none	2, 0, 1, 1, 0	n/a
96	2.11x10 <sup>5</sup>	4	none	1, 4, 2, 2	n/a
97	2.19x10 <sup>5</sup>	4	none	1, 0, 1, 0	n/a
98	3.98x10 <sup>5</sup>	7	none	1, 0, 0, 0, 1, 1, 2	n/a
99	2.99x10 <sup>5</sup>	5	none	1, 0, 0, 0, 0	n/a
100	2.47x10 <sup>5</sup>	4	none	0, 0, 1, 0	n/a
1	1.08x10 <sup>5</sup>	2	none	0, 0	n/a
2	2.16x10 <sup>5</sup>	4	none	0, 0, 0, 0	n/a
p21	1.18x10 <sup>6</sup>	1	none	confluent	confluent
lamin	9.75x10 <sup>5</sup>	4	none	1, 1, 0, 1	n/a

Red: flasks reseeded for genomic DNA extraction, if they are from the same pool they would have been renamed pool X A, B, C, ect...

**Table 5.3: Reseeding densities and number of growing colonies obtained after growth complementation assay**

The table displays the pool number, the number of cells counted after puromycin selection, the number of T-75 and T-25cm<sup>2</sup> flasks reseeded and the number of growing colonies in each of them after 3 weeks at 38°C. The number in red indicate the flasks that were reseeded for genomic DNA extraction.

### 5.1.9 ShRNA constructs sequence recovery

Two distinct methods of target shRNA sequence retrieval were possible.

The first method uses a DNA barcoding system that was simultaneously developed by both Berns and colleagues (Berns, Hijmans et al. 2004) and Paddison and colleagues (Paddison, Silva et al. 2004). In the CSHL library, each shRNA construct was labelled with a unique 60-nucleotide (nt) sequence such that each construct could be detected in a process analogous to microarray analysis. This method was considered but would require chips as well as setting up the labelling and scanning procedures. In addition, we did not have much viral supernatant for extra optimisation, so this method was not selected.

The second method involved extracting genomic DNA from the growing CL3<sup>EcoR</sup> cells followed by PCR amplification using vector-specific primers that spanned the shRNA insert sequence and cloning into a TA-cloning vector. Sequencing of multiple colonies would allow determination of the identity of the functional shRNA species integrated within the cells.

200 ng of genomic DNA was used for PCR amplification with the pSM2 specific primers: pSM2 longF and pSM2 longR, and the separated by electrophoresis on a 3% agarose gel with ethidium bromide alongside a positive control for PCR, namely 5 µl of the PCR product generated from the amplification of 100 ng of pSM2 scrambled control vector. The DNA was generally not visible after this first round of PCR so a second round of amplification using a set of nested primers, namely pSM2 F and pSM2 R, that were internal to the first set of primers was used to amplify the inserts before TOPO-cloning. This time analysis by electrophoresis of 5µl of PCR product revealed a product of 424 bp in all samples that corresponded to the expected insert sequence, but not in a negative control sample where water was substituted for template DNA. The PCR product was cloned into pCR2.1-TOPO vector (Invitrogen) using the TOPO TA Cloning

Kit (Invitrogen). The resulting transformed *E. coli* were plated onto LB-agar plates containing 50 µg/ml final concentration ampicillin and 80 µl of 20 mg/ml X-gal and incubated at 37°C overnight. Blue/white selection was used to identify positive clones from which, plasmid DNA was subsequently extracted using the QIAprep Spin Miniprep kit (QIAGEN). This step insured that every bacterial clone picked would only contain one insert. Plasmid DNAs were sequenced by the MRC Prion Unit sequencing facility.

The sequencing was performed with M13R primer which is a primer specific for the pCR2.1-TOPO vector. Each DNA was sequenced to reveal the shRNAmir insert.

The insert was determined by searching for the miR-30 context and miR-30 loop (Figure 5.1) that are common to all inserts and frame the hairpins. The sequence of the hairpin was used to identify the gene by searching the pSM2 database provided by Open Biosystems but also by BLASTN analysis of the NCBI human genome database. The sequences that could not be linked back to the list of insert sequences in the Open Biosystems were not pursued and are not presented here.

#### 5.1.10 Results of the primary screen

The rescued shRNAmirs hairpins identified 111 different genes and another 30 inserts corresponding to unidentified loci. For each pool, the number of time sequences were obtained, the corresponding insert references and gene symbols are shown in Table 5.4. This table also shows in the last column if the insert recovered was a match to the inserts present in that particular pool (indicated by “match”) or an insert listed from another pool of the library (indicated by “listed in pool X”). 24 different inserts did not come up in the pool they were supposed to. Some inserts were detected several times in multiple other pools. For example, the insert V2HS\_119967 which was listed as an insert in pool 52 came up several times in pools 3a, 4, 7a, 9a and b, 12a and b, 30a and b, 59b, 60b and c, 64a, 71, 72, 74, 77, and 98d.



Pool	insert reference	gene names	gene symbol	number of sequences	
3a	V2HS_63142	keratin associated protein 5-9	KRTAP5-9	3	match
3a	V2HS_119967	LOC100287210	LOC100287210	4	listed in pool 52
3a	V2HS_56766	acyl-CoA synthetase medium-chain family member 3	ACSM3	1	match
3a	V2HS_95607	leucine rich repeat containing 37A	LRR37A	1	listed in pool 402
3b	V2HS_53974	PRO0255 protein	PRO0255	5	match
3b	V2LHS_63482	paired box 1	PAX1	2	match
4	V2HS_119967	LOC100287210	LOC100287210	2	listed in pool 52
4	V2HS_66751			4	match
4	V2HS_70011	serum amyloid A-like 1	SAAL1	2	match
4	V2HS_98079	human solute carrier family 22	SLC22	1	listed in pool 79
5a	V2HS_108647	human LOC349868	LOC349868	3	listed in pool 79
5a	V2HS_70473	polymerase (dna directed), mu	POLM	2	listed in pool 330
5a	V2HS_71958	human olfactory receptor, family 5, subfamily P, member 3	OR5P3	3	match
5b	V2HS_119967			7	match
5b	V2HS_66652	human protein phosphatase 3 (formerly 2B), catalytic	PPP3CB	1	match
5b	V2HS_70473	polymerase (dna directed), mu	POLM	4	listed in pool 330
7a	V2HS_112910	human cyclin-dependent kinase 8	CDK8	1	match
7a	V2HS_119967	LOC100287210	LOC100287210	1	listed in pool 52
7a	V2HS_64878	CD28 antigen	CD28	1	listed in pool 16
7a	V2HS_98079	solute carrier family 22 (extraneuronal monoamine transporter), member 3	SLC22A3	1	listed in pool 79
7a	V2LHS_97017	sterile alpha motif containing 4a	SAMD4	1	listed in pool 172
7b	v2HS_56367	human similar to progesterone receptor membrane component		6	match
7b	v2HS_69776	cytochrome P450, family 4, subfamily Z, polypeptide 2	CYP4Z2P	1	match
9a	V2HS_108647			1	listed in pool 79
9a	V2HS_119967	LOC100287210	LOC100287210	1	listed in pool 52
9a	V2HS_62506	family with sequence similarity 181, member B	FAM181B	1	match
9b	V2HS_55950	prostate stem cell antigen	PSCA	2	match
9b	V2HS_119967	LOC100287210	LOC100287210	3	listed in pool 52
9b	V2HS_70312	TRK-fused gene	TFG	4	match
9b	v2HS_71740	ataxin 10	ATXN10	1	
9b	V2HS_98079	solute carrier family 22 (extraneuronal monoamine transporter), member 3	SLC22A3	1	listed in pool 79
9c	V2HS_64384	amyloid beta (A4) precursor protein binding family A member 2	APBA2	1	match
9c	V2LHS_97017	sterile alpha motif containing 4a	SAMD4	1	listed in pool 172
12a	V2HS_119967	LOC100287210	LOC100287210	5	listed in pool 52
12a	V2HS_58950	human signal-regulatory protein beta 2	SIRPB2	3	match
12b	V2HS_57276	protein tyrosine phosphatase, non-receptor type 13	PTPN13	1	match
12b	V2HS_101484	doublecortin domain containing 2B	DCDC2B	4	listed in pool 74
12b	V2HS_119967	LOC100287210	LOC100287210	5	listed in pool 52
13a	V2HS_162164	iodotyrosine deiodinase	IYD	1	listed in pool 839
13a	V2HS_55731	phenylalanine-tRNA synthetase-like, beta subunit	FARSB	1	match

Pool	insert reference	gene names	gene symbol	number of sequences	
13a	V2HS_59258	dynein, light chain, roadblock-type 1	DYNLRB1	3	match
13a	V2HS_59891	TAO kinase 1	Taok1	5	match
13a	V2HS_71174	peroxisome proliferator-activated receptor gamma,coactivator 1 alpha	PPARGC1A	1	match
13b	V2HS_57692	human similar to peptidase (prosome, macropain) 26S subunit	LOC643766	2	match
13b	V2HS_68714	abl-interactor 1	ABI1	3	match
13c	V2HS_59653			1	match
13d	V2HS_55731	phenylalanyl-tRNA synthetase, beta subunit	FARSB	1	match
13d	V2HS_64320	Smith-Magenis syndrome chromosome region, candidate 7	SMCR7	1	match
13d	V2HS_71174	peroxisome proliferator-activated receptor gamma	PPARG	3	match
13d	V2HS_71453			2	match
16a	V2HS_64878	CD28 antigen	CD28	8	match
18	V2HS_59716			1	match
18	v2HS_63989	StAR-related lipid transfer (START) domain containing 6	STARD6	1	match
19a	V2HS_247318	TMEM9 domain family, member B	TMEM9B	4	match
19a	V2HS_57051	cDNA DKFZp564H0764	DKFZp564H0764	5	match
19a	VH2S_106158			1	listed in pool 82
19b	V2HS_59560	chromosome 13 open reading frame 15	c13orf15	10	match
21	v2HS_55310, v2HS_55312	glucosamine-phosphate N-acetyltransferase 1	GNPNAT1	6	match
21	V2HS_68437	cDNA FLJ30947	FLJ30947	2	match
30a	V2HS_119967	LOC100287210	LOC100287210	6	listed in pool 52
30a	V2HS_34338	human protein phosphatase 4, regulatory subunit 2	PPP4R2	7	match
30a	V2HS_114455	testis derived transcript (3 LIM domains)	TES	1	listed in pool 149
30b	V2HS_119967	LOC100287210	LOC100287210	1	listed in pool 52
30b	V2HS_34338	protein phosphatase 4, regulatory subunit 2	PPP4R2	1	match
30b	V2HS_36467	solute carrier family 33 (acetyl-CoA transporter), member 1	Slc33a1	8	match
30b	V2HS_46793	ubiquitin-activating enzyme E1C (UBA3 homolog, yeast)	UBA3	1	match
32	v2HS_42104	cDNA FLJ38187	FLJ38187	5	match
41	v2HS_48278	choline kinase-beta	CHKB	6	match
54a	V2HS_112629	basic transcription factor 3, like 1	BTF3L1	1	match
54a	V2HS_121153			2	match
54a	V2HS_125538			1	match
54b	V2HS_129527			6	match
54c	V2HS_112629	basic transcription factor 3, like 1	BTF3L1	2	match
54c	V2HS_129417			1	match
55a	v2HS_117465	SH3 domain binding glutamic acid-rich protein like 2	SH3BGR2	2	match
55a	V2HS_119051			1	match
55b	V2HS_116174	YTH domain containing 2	YTHDC2	1	listed in pool 58
55b	V2HS_119120	hypothetical protein FLJ20032	FLJ20032	6	
56a	V2HS_117914	similar to transketolase (DKFZP434L1717)	TKTL2	1	match
56b	v2HS_115231	rab23 member RAS oncogene family	RAB23	4	match

Pool	insert reference	gene names	gene symbol	number of sequences	
56b	V2HS_117914	similar to transketolase (DKFZP434L1717)	TKTL2	2	match
56c	V2HS_117239	human chromosome 9 open reading frame 58	C9orf58	3	match
56c	V2HS_120429			1	match
56c	V2HS_94458	arachidonate 15-lipoxygenase, type B	ALOX15B	2	listed in pool 146
58a	V2HS_116174	human FLJ21940 protein	FLJ21940	1	match
58a	v2HS_118722	layilin	LAYN	2	match
58b	v2HS_112838	ectonucleoside triphosphate diphosphohydrolase 3	ENTPD3	3	match
58b	V2HS_112982	human chromodomain helicase DNA binding protein 3	CHD3	1	match
58b	V2HS_116174	human FLJ21940 protein	FLJ21940	1	match
58c	v2HS_112838	ectonucleoside triphosphate diphosphohydrolase 3	ENTPD3	1	match
58c	V2HS_118254	WD repeat and FYVE domain containing 2	WDFY2	1	match
58c	V2HS_122548	ribosomal protein S3A	RPS3A	4	listed in pool 53
58c	V2HS_125075			1	match
59a	v2HS_111554	interleukine 2	IL2	8	match
59a	V2HS_176550	small glutamine-rich tetratricopeptide repeat (TPR)-containing, beta	SGTB	2	match
59b	V2HS_116377	TMEM135 domain family	TMEM135	1	match
59b	v2HS_117064	CD1e molecule	CD1E	3	match
59b	V2HS_119967	LOC100287210	LOC100287210	4	listed in pool 52
59b	V2HS_120757	olfactory receptor, family 8, subfamily K, member 1	OR8K1	1	match
59c	V2HS_108647			1	listed in pool 79
59c	v2HS_115544	DEAD (Asp-Glu-Ala-Asp) box polypeptide 47	DDX47	3	match
59c	V2HS_116833	intermediate filament protein syncoilin (SYNCOILIN),	SYNC	1	match
60a	V2HS_121585	dual specificity phosphatase 3	DUSP3	10	match
60b	V2HS_117903	glutamine rich 2	QRICH2	4	match
60b	V2HS_119967	LOC100287210	LOC100287210	1	listed in pool 52
60b	V2HS_121585	dual specificity phosphatase 3	DUSP3	2	match
60b	V2HS_128131			2	match
60b	V2HS_98079	solute carrier family 22 (extraneuronal monoamine transporter), member 3	SLC22A3	1	listed in pool 79
60c	V2HS_119967	LOC100287210	LOC100287210	8	listed in pool 52
60c	V2HS_121585	dual specificity phosphatase 3	DUSP3	2	match
64a	V2HS_119967			10	listed in pool 52
64b	V2HS_121013	plasma kallikrein-like protein 4	Kikbl4	3	match
66a	V2HS_117673	latent transforming growth factor beta binding protein 3	LTBP3	15	match
66b	V2HS_115659	three prime repair exonuclease 1	TREX1	5	match
66b	V2HS_117673	latent transforming growth factor beta binding protein 3	LTBP3	8	match
66c	V2HS_115659	three prime repair exonuclease 1	TREX1	1	match
71	V2HS_103818	LOC284804	LOC284804	2	listed in pool 78
71	V2HS_119967	LOC100287210	LOC100287210	9	listed in pool 52
71	V2HS_97891	melanoma antigen (LOC51152)	LOC51152	5	match
72	V2HS_106385	MGC30618	MGC30618	1	match

Pool	insert reference	gene names	gene symbol	number of sequences	
72	V2HS_119967	LOC100287210	LOC100287210	9	listed in pool 52
74	V2HS_119967	LOC100287210	LOC100287210	11	listed in pool 52
77	V2HS_119967	LOC100287210	LOC100287210	12	listed in pool 52
78a	V2HS_94763	paired related homeobox 1	PRRX1	1	match
78a	V2HS_99138	solute carrier family 25	SLC25A21	7	match
78b	V2HS_102207	TMEM63 domain family member B	TMEM63B	1	match
78b	V2HS_103818	LOC284804	LOC284804	4	match
78b	v2HS_95356	armadillo repeat containing, X-linked 2	ARMCX2	2	match
78b	v2HS_98650	mitochondrial ribosomal protein 63	MRP63	1	match
78c	V2HS_102155			1	match
78c	V2HS_108506			1	match
78c	V2HS_96236	zinc finger and BTB domain containing 1	ZBTB1	2	match
78d	V2HS_184999	eukaryotic initiation factor 4A isoform 1	EIF4A3	3	listed in pool 528
78d	V2HS_96236	zinc finger and BTB domain containing 1	ZBTB1	1	match
79a	V2HS_105974			3	match
79a	V2HS_184999	eukaryotic initiation factor 4A isoform 1	EIF4A3	3	listed in pool 528
79a	V2HS_98079	solute carrier family 22 (extraneuronal monoamine transporter), member 3	SLC22A3	4	match
79b	V2HS_108647			2	match
79b	V2HS_98079	solute carrier family 22 (extraneuronal monoamine transporter), member 3	SLC22A3	5	match
79c	V2HS_101943	anthrax toxin receptor-like	ANTXRL	1	match
79c	V2HS_105093	human solute carrier family 35, member F4	SLC35F4	2	match
79c	V2HS_106291			1	match
79c	V2HS_106472			1	match
79c	V2HS_107395			1	match
79c	v2HS_91777	nuclear receptor co-repressor 1	NCOR1	4	match
79c	V2HS_91794	olfactory receptor, family 5, subfamily D, member 3 pseudogen	OR5D3P	1	match
80a	v2HS_102441	adenylate cyclase 1	ADCY1	5	match
80a	V2HS_130882	glutamate receptor, metabotropic 3	GRM3	1	listed in pool 91
80a	v2hs_97368	yippee-like 5	YPEL5	2	match
80b	v2HS_102441	adenylate cyclase 1	ADCY1	5	match
80b	V2HS_106345			4	listed in pool 144
80b	v2HS_99202	similar to heterogeneous nuclear ribonucleoprotein A1		1	match
82a	V2HS_184999	eukaryotic initiation factor 4A isoform 1	EIF4A3	1	listed in pool 528
82a	V2HS_101845	human prickle-like 2 (Drosophila)	PRICKLE2	3	match
82a	V2HS_109096			1	listed in pool 84
82a	V2HS_99423	hypothetical protein DKFZp434K1172	DKFZp434K1172	1	match
82b	V2HS_109596			1	match
82b	V2HS_108399			3	match
82b	V2HS_146196	shisa homolog 7	shisa7	1	match
82b	v2HS_93536	human proteolipid protein 1	PLP1	5	match

Pool	insert reference	gene names	gene symbol	Number sequence	
82b	V2LHS_97017	sterile alpha motif domain containing 4A	SAMD4	1	listed in pool 172
82c	V2HS_106158			3	match
82c	v2HS_93615	p53	TP53	1	match
82c	v2HS_95112	RASp21 protein activator 4	RASA4	1	match
82c	V2HS_99526	BCL2 like 12	BCL2L12	1	match
82c	V2LHS_97017	sterile alpha motif domain containing 4A	SAMD4	4	listed in pool 172
82d	V2HS_94640	aryl hydrocarbon receptor nuclear translocator-like	ARNTL	3	listed in pool 411
82d	V2HS_100174	desmoglein 4	DSG4	2	listed in pool 145
82d	V2HS_96026	adnp homeobox2	ADNP2	3	match
82d	vhs_100819	Rho GTPase activating protein 20	ARHGAP20	2	match
84a	V2HS_106409			1	match
84a	v2HS_95019	zinc finger protein 16	ZNF16	9	match
84a	V2HS_97152	biquitin-conjugating enzyme E2, J1 (UBC6 homolog	UBE2J1	1	match
84b	v2HS_95019	zinc finger protein 16	ZNF16	10	match
94	V2HS_141495	zinc finger protein 454	ZNF454	7	listed in pool 96
94	V2HS_33370	leucine zipper protein 1	LUZP1	1	match
95a	V2HS_130457	radial spoke head 10 homolog B (Chlamydomonas)	RSPH10B	6	match
95a	V2HS_131154	KCNJ2, potassium inwardly-rectifying channel, subfamily J	KCNJ2	1	match
95c	V2HS_184999	eukaryotic initiation factor 4A isoform 1	EIF4A3	1	listed in pool 528
98a	V2HS_141367	cDNA FLJ37626	FLJ37626	10	match
98d	V2HS_100218	human deltex 3 homolog (Drosophila)	DTX3	4	listed in pool 78
98d	V2HS_119967	LOC100287210	LOC100287210	2	listed in pool 52
98d	V2HS_133299	human insulin-like growth factor binding protein 6	IGFBP6	3	match
98d	V2HS_135564	Homo sapiens chromosome X open reading frame 57	CXORF57	1	match
98d	V2HS_146491			1	match

**Table 5.4: Results of the screen**

The table displays the genes that were recovered by sequencing the genomic DNA extracted from the growing colonies. The columns represent the pool that gave rescue, the name and symbol of the genes recovered by sequencing from that pool, the number of time this sequence was recovered and their expected location in the library.

This suggested that there may have been cross-contamination of the library perhaps during replica plating. However, this was not a problem since the aim of this screen was to identify any shRNAmiRs that can bypass the growth arrest. Since this insert originally from pool 52 was isolated from so many pools, it could be that it was a strong positive or that it was highly represented within the library.

Pools 13, 78 and 82 that produced more colonies and colonies that were larger and healthier than others, identified the following genes:

Pool 13: IYD, DYNLRB, FARSB, PPARGC1A, Taok1, ABI1, LOC643766, FARSB, PPARG, SMCR7;

Pool 78: PRRX1, SLC25A21, ARM CX2, LOC284804, MRP63, TMEM63B, ZBTB1, EIF4A3, ZBTB1;

Pool 82: DKFZp434K1172, PRICKLE2, SAMD4, PLP1, shisa7, SAMD4, BCL2L12, RASA4, TP53, ARNTL, DSG4, ADNP2, ARHGAP20.

It is interesting to note that pool 82, one of the pools that gave the best rescue of the screen, contained the shmiRs targeting TP53, one of which (V2HS\_93615) was identified in the screen, thereby validating it. shRNAmirs targeting p21 were not present in this library.

Unfortunately the other shMIRs targeting TP53 were not isolated suggesting that either my screen was not saturating or that the other p53 shRNAmirs were unable to silence p53 at a level sufficient to bypass senescence in CL3<sup>EcoR</sup> cells.

## 5.2 *IN VITRO* VALIDATION OF THE SCREENING

### 5.2.1 Overlap of the candidates of the shRNA screen with microarray data for genes up-regulated upon senescence in CL3<sup>EcoR</sup> cells

To prioritise the 137 candidates identified from the primary screen for functional validation, they were compared to genes found to be up-regulated upon senescence and whose expression was reversed when senescence was abrogated (ER et al, submitted). This identified 5 common genes, ATXN10, LAYN, LTBP3, SGTB and TMEM9B. The microarray expression profiling data is presented in Table 2. They were all up-regulated upon senescence growth arrest: ATXN10 by 1.3 fold (p-value  $8.3 \times 10^{-4}$ ), LAYN by 2 fold (p-value  $1.8 \times 10^{-4}$ ), LTBP 3 by 1.32 (p-value  $8.6 \times 10^{-8}$ ) and 0.45 (p-value  $6.1 \times 10^{-5}$ ), SGTB by 1.3 fold (p-value  $8.8 \times 10^{-4}$ ) and TMEM9B by 1.4 (p-value  $1.4 \times 10^{-9}$ ) and 1.3 fold (p-value  $2.2 \times 10^{-4}$ ) respectively.

The identification of TMEM9B was particularly remarkable because the microarray analysis had suggested that senescence growth arrest in these cells was associated with activation of the NF- $\kappa$ B signalling pathway and TMEM9B had previously been shown to be able to activate NF- $\kappa$ B dependent reporter constructs (Matsuda, Suzuki et al. 2003; Dodeller, Gottar et al. 2008). TMEM9B is also essential for activation of NF- $\kappa$ B by TNF and acts downstream of RIP1 and upstream of MAPK and I $\kappa$ B kinases at the level of TAK1 (Dodeller, Gottar et al. 2008).

### 5.2.2 Optimisation of the GIPZ lentiviral library

The shmiRs from the pGIPZ and the pSM2 library are essentially similar, what is different is the vector system and how they are delivered to the cells. Moreover, it was observed that the pSM2 vectors were not stable in *E.coli* and that the lentiviral shmiRs

were much more stable. We chose to use lentiviral vectors since they were freely available to us through the RNAi consortium rather than the pSM2 library.

For the lentiviral supernatants to be used for the secondary screen, optimisation of the packaging and infection protocols was necessary. The packaging was done in HEK293 cells as suggested by protocols provided by the RNAi consortium. The infection itself, however, required optimisation as getting a level of silencing high enough to see a biological phenotype proved to be tricky.

Katharina Wanek had been working with the lentiviral shmiRNA library and found that selection at 2µg/ml puromycin for 4 days, failed to give a satisfactory expression of the vector, monitored by the level of GFP positive cells. In addition, even shmiRNAs targeting p21 could not yield rescue. What was more important is the pRS-p21F shRNA selected at 2µg/ml gave excellent rescue, therefore the problem laid with the shmiR vector.

However, she found that a higher level of puromycin, 6µg/ml enriched for infected cells in which the GIPZ vector was expressed at higher levels. Furthermore, maintaining selection upon shift to 38°C gave a lower level of background reversion. Others have found that enriching for the higher expression by GFP expression also yields higher levels of RNA knockdown.

### 5.2.3 Secondary screen using lentiviral shRNA silencing

In order to validate these 5 targets, the secondary screen was performed in two parts: First, complementation was attempted with a mix of multiple (as many as were available) silencing constructs from the Human GIPZ lentiviral shRNAmir library available for these genes. This was then repeated using each construct individually.

To determine if silencing of TMEM9B would bypass senescence, 4 GIPZ lentiviral silencing constructs (V2LHS\_247318, V2LHS\_58957, V2LHS\_58958 and



V2LHS\_58959) targeting TMEM9B were obtained, pooled and introduced into CL3<sup>EcoR</sup> cells after packaging as lentiviruses. Lentiviral human GIPZ LaminA/C shRNAmir (V2LHS\_62719) was used as a negative control. The transduced cells were selected with 6µg/ul of puromycin for 5 days and reseeded in triplicate at 0.5x10<sup>5</sup> in T-75 flasks. The cells were then shifted to 38°C for 3 weeks, stained with methylene blue and the number of colonies was counted. Silencing of TMEM9B was clearly able to overcome senescence (Figure 5.6). The result shows small background with the Lamin A/C constructs with an average of approximately 20 small colonies and a much larger number of healthy growing colonies with the mixed silencing constructs with an average of approximately 100 colonies. This confirmed the results for TMEM9B presented in the Chapter 4 and showed that it was possible to achieve silencing with the GIPZ lentiviral vector in the CL3<sup>EcoR</sup> cells. Moreover, each of the constructs was able overcome senescence arrest when introduced individually into CL3<sup>EcoR</sup> cells, with V2LHS\_58957 being the most efficient (Figure 5.7); it was interesting to note that the least efficient hairpin (247318), was the hair pin isolated by the shRNA screen.

Next, only individual shRNA inserts were used for the genes LTBP3, ATXN10, LAYN and SGTB.

The complementation assay for LTBP3 silencing show the results for only one silencing construct (V2HS\_34089) that was available at the time. The LTBP3 silencing construct (Figure 5.8) produced numerous healthy growing colonies in comparison to the Lamin shRNAmiRs which resulted in low level background.

ATX10 silencing was tested with 4 different silencing constructs namely V2HS\_71735, V2HS\_71736, V2HS\_71737 and V2HS\_71740. All four constructs gave a high level of rescue when compared to the negative control Lamin silencing construct (Figure 5.9).

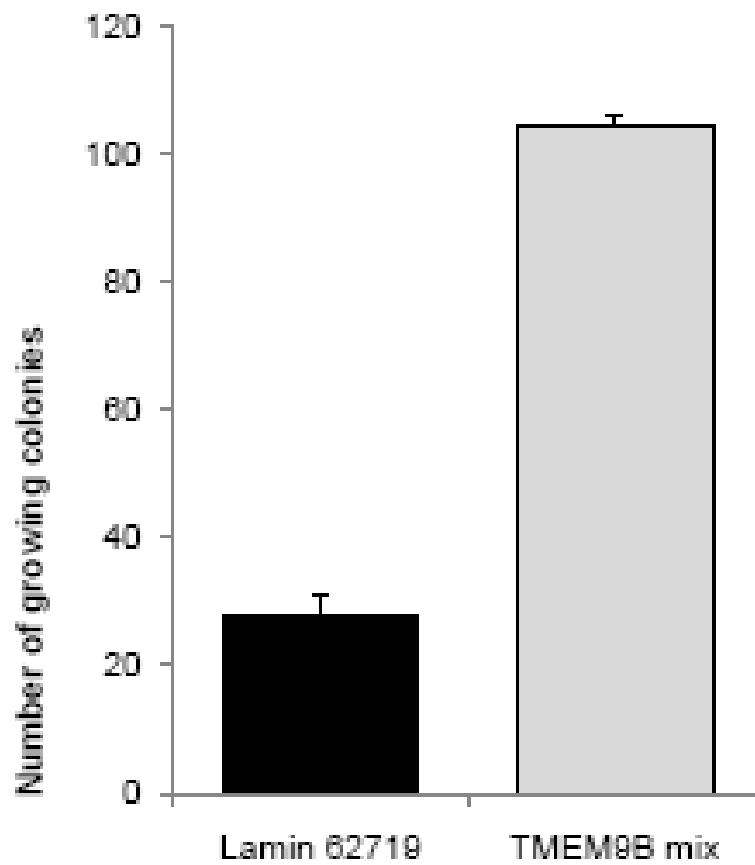


**Figure 5.6: Silencing of TMEM9B (mix)**

CL3<sup>EcoR</sup> cells were infected in triplicate with a mix of lentiviruses shRNAmir silencing constructs for TMEM9B (human GIPZ lentiviral shMIR V2LHS\_247318, V2LHS\_5895, V2LHS\_58958 and V2LHS\_58957) and assayed for growth complementation at 38°C. After 3 weeks the number of growing colonies were counted.

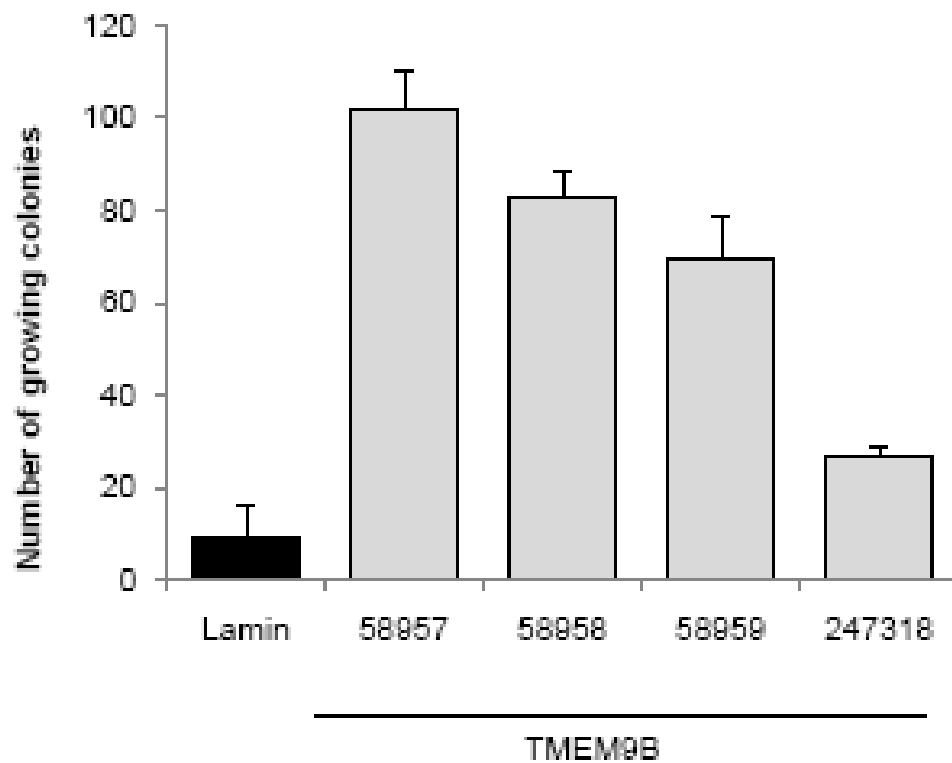


**Figure 5.7: Silencing of TMEM9B (individual)**

CL3<sup>EcoR</sup> cells were infected in triplicate with lentiviruses expressing the indicated shRNA mir silencing constructs and assayed for growth complementation at 38°C. After 3 weeks the numbers of growing colonies were counted.

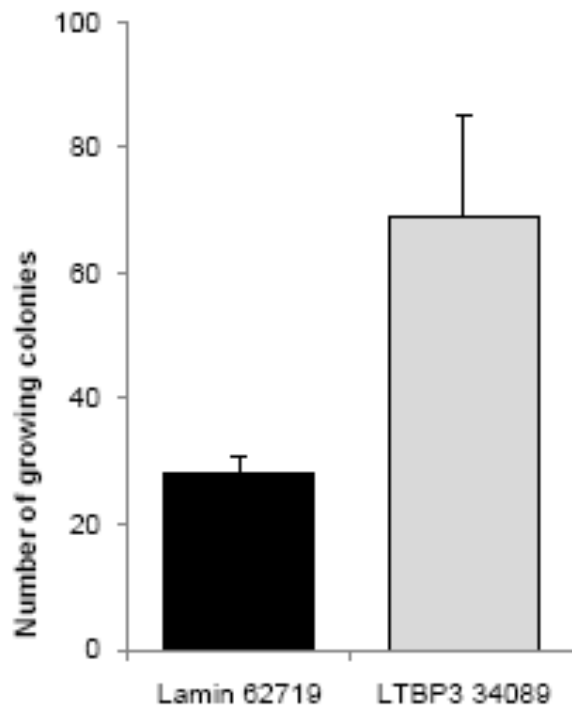


**Figure 5.8: Silencing of LTBP3**

CL3<sup>EcoR</sup> cells were infected in triplicate with lentiviruses expressing the indicated shRNAmir silencing constructs and assayed for growth complementation at 38°C. After 3 weeks the numbers of growing colonies were counted.

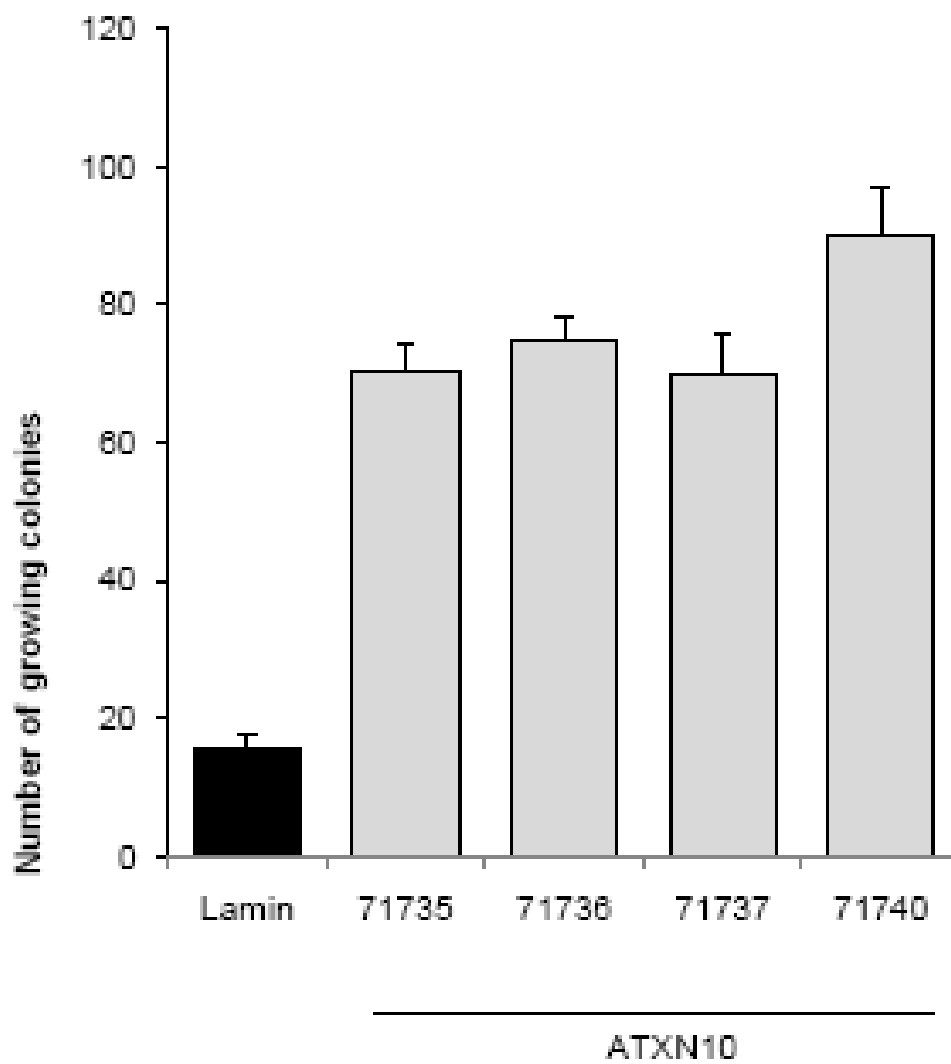


**Figure 5.9: Silencing of ATXN10**

CL3<sup>EcoR</sup> cells were infected in triplicate with lentiviruses expressing the indicated shRNAmir silencing constructs and assayed for growth complementation at 38°C. After 3 weeks the number of growing colonies were counted.

SGTB silencing was tested with 3 different silencing constructs namely V2HS\_176551, V2HS\_218863, and V2HS\_176555. Two out of three constructs gave a high level of rescue when compared to the negative control Lamin silencing construct (Figure 5.10). The last construct did not permitted bypass of the growth arrest significantly.

LAYN silencing was tested with 2 different silencing constructs namely V2HS\_265009, and V2HS\_118722. Both constructs yielded numerous growing healthy colonies when compared to the negative control Lamin silencing construct (Figure 5.10).

Taken together the results showed that silencing of TMEM9B, ATXN10, LAYN, LTBP3 and SGTB were able to bypass senescence in the conditionally immortal human fibroblasts.

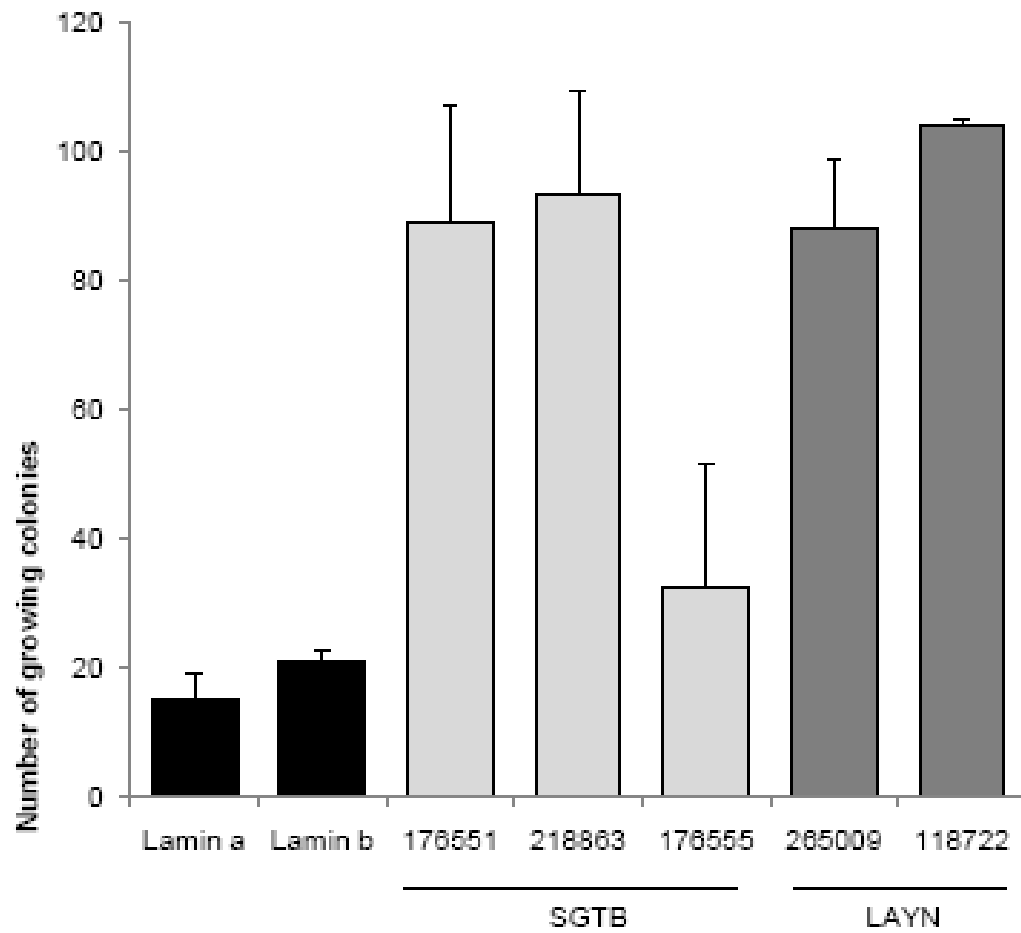


**Figure 5.10: Silencing of SGTB and LAYN**

CL3<sup>EcoR</sup> cells were infected in triplicate with lentiviruses expressing the indicated shRNA mir silencing constructs and assayed for growth complementation at 38°C. After 3 weeks the numbers of growing colonies were counted.

## 5.3 DISCUSSION

To directly identify the downstream effectors of the p53-p21 and p16-pRB pathways crucial for mediating entry into senescence, I have carried out a loss-of-function RNA interference screen in the conditionally immortal HMF3A human fibroblasts. These cells are immortal but undergo a rapid irreversible senescence arrest which can be readily bypassed upon inactivation of the p53-p21 and p16-pRB pathways. This screen identified 111 known genes and another 30 shRNAmirs corresponding to unidentified loci. Comparison of these known targets with genes up-regulated upon senescence in these cells identified 5 common genes TMEM9B, ATXN10, LAYN, LTBP3 and SGTB. Direct silencing of these 5 genes using lentiviral shRNAmirs bypasses senescence in the HMF3A cells. Although none of these five genes had previously been linked to cellular senescence, TMEM9B has been suggested to be an upstream positive modulator of NF- $\kappa$ B and I have found that activation of NF- $\kappa$ B signalling acts to promote senescence.

### 5.3.1 Sensitivity, Stringency and Saturation

The effectiveness of any screen is dependent upon its sensitivity; therefore, it was important to minimise the background levels of false-positive hits without losing information concerning the identity of all true positive hits. In this respect, optimal conditions for performing an RNAi screen in the HMF3A system had been previously determined by the development of the CL3<sup>EcoR</sup> complementation assay. The sensitivity of the screen itself was then tested successfully using complementation assay with a spiked mixture of positive shRNA construct namely pRS p21 shRNA into negative control namely pRS Lamin A/C, at a ratio of 1 in 200 (Figure 5.5). This demonstrated that the screen assay was sensitive enough to be able to discriminate the effects of a single shRNA constructs in a mix of 200. The stringency of the screen also proved satisfactory, with a low level of reversion (Figure 5.5, A and D).



siRNAs can have 'off-target' effects, which are often the result of partial homology to other transcripts (Jackson, Bartz et al. 2003; Semizarov, Frost et al. 2003). The Open Biosystems shRNA library was designed to avoid off-target effects by minimizing homology of shRNAs to other transcripts and by offering usually more than one constructs per gene to silence. It is very unlikely that two independent siRNAs against the same transcript target a common off-target transcript for suppression.

CL3<sup>EcoR</sup> complementation assay with p53 silencing was an easy way to validate the screen with a positive control. A shRNA for TP53 was present in pool 82. Infection of the cells with the viral supernatant containing constructs of the pool 82 gave a successful rescue from growth arrest compared to the negative control and the p53 shRNA hairpin was identified by sequencing, although only 1 insert for p53 was recovered. This result does reinforce the quality of the assay. I did not identify the shRNA for p21<sup>CIP1/WAF1/Sdi1</sup> in the genetic screen as it was not present in the RNAi library. The fact that only one shMiRs targeting p53 was isolated indicated that the first screen might not be saturating.

The screen is unlikely to be saturating since all the shRNA targeting the same gene were not always isolated from a positive pool. For example, for all the silencing constructs tested here, namely TMEM9B, SGTB, LAYN and ATX10 shRNAs, all shown to rescue in the CL3<sup>EcoR</sup> cells, only one hairpin each was recovered from sequencing out of 4, 3, 2 and 4 inserts respectively represented in their respective pools. This in accordance with that of Westbrook and colleagues (Westbrook, Stegmeier et al. 2005), who similarly raised concerns over the lack of saturation in shRNA screens.

These characteristics have to be taken into consideration when examining the results of the screen. The CL3<sup>EcoR</sup> system was suitable for the application of such an *in vitro* RNAi screen with the final aim of identifying novel genes that are downstream effector of the p53-p21 and p16-pRb pathways. Indeed, these cells were highly infectable, yielded low background and grew very well.

In addition, it is important to note here that these cells were thawed for each assay of 10 pools (infected on the same week) from a unique batch of frozen CL3<sup>EcoR</sup>. This minimised the background by limiting any potential reversion due to a long term *in vitro* culture. In fact, it was found in a first trial of the screen that when passaged extensively in stressing conditions (LT inactivated), the CL3<sup>EcoR</sup> cultures can acquire mutant cells that can become enriched upon cultivation and affect the outcome of the screen by increasing the background.

### 5.3.2 Positive hits of the primary HMF3A retroviral shRNA screen

The primary screen shows that a total of 34 pools out of 100 gave growing colonies at a level above background. Particularly, the pools 13, 78 and 82 gave a higher number of colonies and colonies of a larger size. For each pool considered as a hit, 1 to 4 flasks containing the highest number of colonies were reseeded for genomic DNA extraction resulting in a total of 81 sub-pools to analyse for proviral shRNAmiRs. Sequencing revealed a match for 111 different genes and another 30 unidentified loci.

A number of sequences were never matched to either the OpenBiosystems hairpin database or the NCBI genomic database. This could be due to the removal of the hairpin from the bank between the release of the pools and the sequence analysis or to a genetic mutation making the sequence impossible to recognize. Furthermore, short sequences are difficult to match against the all human genome and only one base mutation could render the sequence unrecognizable. The unknown sequences could also correspond to expression tags not yet documented as the library contain both known ESTs and unidentified expression tags.

Due to time limitation, it wasn't possible to run a complete secondary screen for the gene list since for each gene there were at least another 1 to 3 shMiRs available in the pGIPZ library. For this reason, a filtering was performed by overlapping the microarray up-regulated genes with the primary screen gene list.

### 5.3.3 Overlap with the microarray up-regulated genes reveals new targets

The list of candidates identified from the primary screen was overlapped with the microarray up-regulated genes whose expression was reversed upon complementation. The overlap was 5 genes: ATX10, LAYN, LTBP3, SGTB and TMEM9B. The list could be longer if the all microarray data was compared, however, for more consistency, only the differential data set containing ~8000 significantly differentially expressed genes as described in Chapter 4 was compared to the candidates. These five genes were then silenced in a secondary screen using lentiviral shRNAmirs and were able to bypass growth arrest.

### 5.3.4 *In vitro* validation of ATXN10, LAYN, LTBP3, SGTB and TMEM9B silencing

#### 5.3.4.1 *TMEM9B*

Pool 19 of the primary shRNA screen identified *TMEM9B* as a target which upon silencing would result in bypass of senescence arrest. *TMEM9B* was up-regulated 0.44 and 0.39 log<sub>2</sub> fold change (P value 1.47x10<sup>-7</sup> and 1.97x10<sup>-4</sup>, Table 5.5) upon growth arrest in the CL3<sup>EcoR</sup> cells which was reversed upon abrogation of the p53-p21 or the p16-pRB pathways. *TMEM9B* expression was unaffected by quiescence. A role for *TMEM9B* in inducing senescence was further supported by my finding that direct silencing of *TMEM9B* using 4 different lentiviral shRNAmirs either as a mix or individually bypasses senescence in the HMF3A cells (Figure 5.6 and 5.7).

Probe	Symbol	GA	Q	HS	wt_LT	GSE					E2F DB
						p53	pRS p53	pRS_p21	E1A	E7	
208832_at	ATXN10	0.36	-0.64	0.25	0.11	0.34	-0.18	-0.35	0.11	0.02	-0.23
228080_at	LAYN	1.04	-0.56	0.30	-0.84	-0.56	-0.95	-0.70	-1.56	-0.56	-0.11
219922_s_at	LTBP3	1.32	0.44	0.66	-0.43	-0.31	-1.04	-1.32	-1.02	-1.19	-1.41
227308_x_at	LTBP3	0.46	-0.14	0.03	-0.19	-0.12	-0.43	-0.57	-0.44	-0.28	-0.55
228745_at	SGTB	0.36	-1.02	0.29	-0.85	0.03	-0.42	-0.81	-0.75	-0.56	-0.69
218065_s_at	TMEM9B	0.44	-0.27	-0.11	-0.43	-0.29	-0.33	-0.38	-0.13	-0.20	-0.18
222507_s_at	TMEM9B	0.39	-0.29	-0.19	-0.35	-0.29	-0.28	-0.34	0.11	-0.12	-0.07

**Table 5.5: Senescence specific changes with complementation for ATXN10, LAYN, LTBP3, SGTB and TMEM9B**

Log<sub>2</sub> fold changes in gene expression (and their p-values) that occur upon irreversible growth arrest (GA), heat shock(HS), quiescence(Q) and the indicated complementation. Up-regulated transcripts are indicated in green whereas down-regulated transcripts are in red. Results for ATXN10, LAYN, LTBP3, SGTB and TMEM9B are shown .

TMEM9B is a glycosylated protein localized in membranes of the lysosome and partially in early endosomes. TMEM9B has also been shown to be an important component of TNF signalling and a module shared between the interleukin-1 and Toll-like receptor pathways. It was also shown to be essential for the TNF activation of both NF- $\kappa$ B and MAPK signalling pathways by acting downstream of RIP1 and upstream of the MAPK and I $\kappa$ B kinases at the level of the TAK1 complex (Dodeller, Gottar et al. 2008). It has also been identified by a large-scale characterization study to be one of the genes activating NF- $\kappa$ B and MAPK signalling pathways (Matsuda, Suzuki et al. 2003).

These results are all consistent with my finding that in the conditionally immortal HMF3A cells, senescence growth arrest is associated with an activation of NF- $\kappa$ B signalling and suppression of this pathway bypasses senescence (Chapter 4). These results also seem to suggest that TMEM9B up-regulation could be the cause of the NF- $\kappa$ B activation upon senescence.

The details of this activation are not known, nor are the ways in which the NF- $\kappa$ B pathway is involved in triggering senescence here. Investigating further the details of this involvement could include some expression analysis of the cells expressing the NF- $\kappa$ B signalling or not in order to determine which genes are affected and particularly whether the p16-pRb and p53-p21 pathways are affected by it.

#### 5.3.4.2 *LTBP3*

The latent TGF- $\beta$ -binding protein 3 (LTBP3) hairpin sequence was identified from two of the three pools of DNA derived from pool 66. LTBP3 was up-regulated 2.5 and 1.4 fold (p-value  $9.41 \times 10^{-8}$  and  $8.18 \times 10^{-5}$  respectively) upon growth arrest, which was reversed when growth arrest was overcome (Table 5.5). LTBP3 was also slightly up-regulated upon quiescence.

LTBPs are secreted proteins that were initially identified through their binding to the growth factor. Three of the four known LTBPs are able to associate covalently with the

small latent forms of TGF $\beta$  and may be involved in their assembly, secretion and targeting (Oklu and Hesketh 2000). LTBP3 in particular has been found to play an essential role in the secretion and targeting of TGF-beta1 (Penttinen, Saharinen et al. 2002).

This is not in agreement with the microarray data where TGFB1 was slightly down-regulated by -0.45 and -0.16 log<sub>2</sub> fold change (p-values of 5.2x10<sup>-4</sup> and 2.86x10<sup>-1</sup> respectively) upon senescence and up-regulated upon rescue by LT abrogating the p53 pathway in the CL3<sup>EcoR</sup> cells. This suggests that although LTBP3 was reported to help secretion of TGFB1, it might not act at the transcription level.

Interestingly, LTPB1 and LTBP2 are also up-regulated upon growth arrest indicating that most of the LTBP complexes are activated in the senescent cells and thereby may result in increased TGF $\beta$  secretion upon senescence. At the transcription level, TGFB2 and TGFB3 are both up-regulated upon growth arrest by an average of 0.5 and 0.25 log<sub>2</sub> respectively which suggest that regulation of these two other transforming growth factors follows a different mechanism than TGFB1.

LTBPs have subsequently been found to associate with the extracellular matrix. The close identity between LTBPs and members of the fibrillin family, mutations in which have been linked directly to Marfan's syndrome, suggests that anomalous expression of LTBPs may be associated with disease. The implication of TGF $\beta$  in such a wide range of biological responses suggests that it plays important roles in many normal cellular functions. Consistent with these multiple roles, anomalous regulation of TGF $\beta$  activity has been associated with the development of a number of diseases, most notably several forms of cancer (Kimchi, Wang et al. 1988).

Studies indicated that modulation of LTBP function, and hence of TGF $\beta$  activity, was associated with a variety of cancers (Oklu and Hesketh 2000). The contribution of transforming growth factor (TGF) beta to breast cancer as a regulator of cancer suppression and progression has been studied from a myriad of perspectives since

seminal studies more than two decades ago (Silberstein and Daniel 1987) and now exceeds a thousand papers.

It is now generally agreed that during early tumour outgrowth, elevated TGF $\beta$  levels suppress tumour formation (Massague 1990), whereas at later stages there is a switch towards malignant conversion and progression. Inactivation of tumour suppressor genes, the sequential acquisition of oncogenic mutations, and epigenetic changes within the cancer genome divert the canonical growth inhibitory arm of the TGF $\beta$  signalling pathway towards behaviours that increase motility, invasion and metastasis (Derynck, Akhurst et al. 2001).

Thus, if these LTBP proteins play critical roles in controlling and directing the activity of TGF $\beta$ s, it could suggest an indirect implication in the suppression and/or the development of cancer.

Since silencing of LTBP3 can bypass cellular senescence in CL3<sup>EcoR</sup> cells (Figure 5.8), it suggests that LTBP3 is definitely linked with the control of cell growth and may be playing a role in suppressing tumour progression. This is in accordance with the identification of TGF $\beta$  as the cellular senescence-inducing factor in the human lung adenocarcinoma cell line A549 (Katakura 2006). It is also in accordance with several other reports suggesting that TGF $\beta$ 1 is capable of inducing cellular senescence. For instance, stimulation of human diploid fibroblasts with TGF $\beta$ 1 triggers the appearance of biomarkers of cellular senescence such as SA- $\beta$ -Gal activity and increases steady state mRNA levels of senescence associated genes including Apo J, fibronectin, and M22 (Frippiat, Chen et al. 2001; Frippiat, Dewelle et al. 2002; Debacq, Heraud et al. 2005).

It is important to note that only one shRNA constructs was available at the time of the experiment from the Open Biosystems library. Although the experiment was successfully repeated twice with similar results, it would be valuable to use an

alternative silencing construct for this gene to prove that the biological consequences are not due to an off-target effect.

#### 5.3.4.3 *ATXN10*

The hair pin targeting ataxin 10 (*ATXN10*) was recovered from pool 9. This gene was slightly up-regulated (1.3 fold, p-value  $8.35 \times 10^{-4}$ ) upon senescence arrest which was reversed upon silencing of p53 and p21<sup>CIP1/WAF1/Sdi1</sup> or ectopic expression of the dominant negative E2F-DB protein (Table 5.5). Surprisingly, though, while p21<sup>CIP1/WAF1/Sdi1</sup> or p53 shRNA reverse the up-regulation to down-regulation, p53 GSE does not have any effect on *ATXN10* expression. WT LT, E1A and E7 expression also had very little effect on the *ATXN10* expression. However, it is difficult to conclude on this data because there was only one oligo representing *ATXN10*.

Spinocerebellar ataxia type 10 (*SCA10*) is a dominantly inherited disorder characterized by ataxia, seizures and anticipation caused by an intronic ATTCT pentanucleotide repeat expansion. The *ATXN10* gene encodes a novel protein, ataxin 10, known previously as E46L, which is widely expressed in the brain and belongs to the family of armadillo repeat proteins. Although clinical features of the disease are well characterized, nothing is known so far about the affected *SCA10* gene product, *ATXN10*. *ATXN10* knock down by RNAi has been shown recently to cause increased apoptosis in primary cerebellar cultures, thus implicated in *SCA10* pathogenesis (Marz, Probst et al. 2004; Waragai, Nagamitsu et al. 2006).

This is in contrast to my finding that silencing of *ATXN10* in HMF3A cells by four different shRNAmirs did not cause apoptosis but promoted growth and permitted a bypass of senescence growth arrest (Figure 5.9). This is not incompatible, the differences in the biological phenotype are probably due to the cell context, but it definitely underlines a regulating role of *ATXN10* in cell growth.



#### 5.3.4.4 LAYN

The Layilin (LAYN) shRNAmir was isolated from pool 58. LAYN was up-regulated by 2.0 fold upon senescence arrest (p-value  $1.81 \times 10^{-4}$ ) and this was reversed upon abrogation of the growth arrest by inactivation of either the p53-p21 or the p16-pRb pathways or both (Table 5.5).

Moreover, two different LAYN shRNAmirs were found to directly bypass senescence in CL3<sup>ECOR</sup> cells (Figure 5.10).

Layilin is a widely expressed integral membrane hyaluronan receptor, originally identified as a binding partner of talin located in membrane ruffles. Talin is responsible, along with its adaptor proteins, for maintaining the cytoskeleton-membrane linkage by binding to integral membrane proteins and to the cytoskeleton.

Recently, Layilin has been suggested to play a crucial role in lymphatic metastasis of lung carcinoma A549 cells (Chen, Zhuo et al. 2008). That study found that suppression of layilin expression by RNA interference significantly inhibited A549-cell invasion and migration *in vitro* and lymphatic metastasis *in vivo* and thereby resulted in the increased survival of tumour-bearing mice.

#### 5.3.4.5 SGBT

The shRNAmir corresponding to Small glutamine-rich tetratricopeptide (SGBT) was recovered from pool 59. SGBT expression was slightly up-regulated (1.3 fold, p-value  $8.79 \times 10^{-4}$ ) upon senescence growth arrest which was reversed upon abrogation of the p53-p21 and p16-pRB pathways.

SGBT or hSGT, also known as viral protein U-binding protein (UBP), was originally identified as a protein interacting with non-structural protein NS1 of parvovirus H-1 (Cziepluch, Lampel et al. 2000). SGBT has been reported to function as a molecular

chaperone that can associate with various cellular proteins such as the ubiquitous heat-shock proteins cognate Hsc70 and Hsp70 (Liu, 1999), regulate their ATPase activity (Tobaben, Thakur et al. 2001) and negatively influences their ability to refold denatured proteins (Wu, Liu et al. 2001).

hSGT was also shown to physically interact with myostatin in yeast cells which suggested a functional relationship between these proteins in skeletal muscle cells (Wang, Zhang et al. 2003).

It was proposed that hSGT may act as a molecular chaperone that assists in secretion and activation of myostatin together with other unidentified factors.

Myostatin is a member of the TGF $\beta$  superfamily and function as a negative regulator of skeletal muscle growth (Grobet, Martin et al. 1997; McPherron and Lee 1997). Myostatin shares all common features of TGF $\beta$  superfamily members. Like TGF $\beta$ , myostatin is also present in serum and circulates in the blood of adult mice in a biologically inactive form (Zimmers, Davies et al. 2002).

It has been suggested that assembly, secretion, and activation of TGF $\beta$  are regulated in part by its interacting proteins, such as latency-associated proteins (LAPs) and latent TGF $\beta$ -binding proteins (Koli, Saharinen et al. 2001).

Removal of LTBP is indispensable for TGF $\beta$  activation in cells as biological activity of TGF $\beta$  in circulation is tightly controlled by their existence as latent complexes with LTBPs. The regulation of TGF $\beta$  function by these proteins may have extremely important biological implications. Altered expression of LTBPs has been associated with development of human diseases such as cancer and atherosclerosis (Eklov, Funa et al. 1993; Mizoi, Ohtani et al. 1993) although the functional role of LTBPs in these diseases is largely unclear.

Although the functional consequences of the observed interactions of hSGT with myostatin remain unclear, it is conceivable that hSGT functions as LTBP3 to regulate myostatin secretion and thereby to determine its biological activity in skeletal muscle cells.

This corroborates the fact that along with SGTB (Figure 5.10), LTBP3 silencing also bypass senescence (Figure 5.8) and it is interesting that both SGTB and LTBP3 were two of the five targets identified by the shRNA screen. This reinforces the hypothesis that their functions are very similar and further validate their role in Cancer and Senescence, highlighting the importance of TGF $\beta$  in these processes.

#### 5.3.4.6 *TAOK1, RAS4A and ARM CX2*

An extra three targets from the primary screen were found to be of interest in the context of senescence. Since these genes were not up-regulated upon senescence, they were not silenced in the conditional system. However, according to the literature, they may be of interest.

Taok1 was a gene identified from pool 13. TAOK1 mRNA expression does not vary upon senescence however it is possible that its protein activity could be subject to variation upon senescence.

##### ➤ TAOK1

TAOK1 is known to activate the p38 MAP kinase pathway through the specific phosphorylation of MKK3. The p38 MAPK pathway is a complex pathway responsive to stress stimuli and involved in cell differentiation and apoptosis which has shown to have an important causative role in senescence. It is well known that oncogenic Ras, the constitutively active form of Ras, contributes to transformation-associated phenotypes in immortalized cells but senescence in normal cells (Katz and McCormick 1997; Serrano, Lin et al. 1997). It was shown that among the divergent downstream pathways of Ras,

the Erk MAPK pathway is responsible for the Ras-induced senescence (Lin, Barradas et al. 1998; Zhu, Woods et al. 1998). It was also reported that p38 MAPK activation is involved in this Ras-Erk MAPK-induced senescence (Wang, Chen et al. 2002).

This suggests that TAOK1 might be necessary to the activation of the p38 MAPK pathway which itself play a causative role in senescence.

TAOK1 has also been identified in a genomic screen to identify human kinases and phosphatases important for the regulation of mitotic progression. TAOK1 is a micro-tubule affinity-regulating kinase which is required for both chromosome congression and checkpoint-induced anaphase delay (Draviam, Stegmeier et al. 2007). It is known to interact with BUB1. The consequences of this interaction are not known. Interestingly, TAOK1 over-expression has been shown in breast cancer lines (Kao, Salari et al. 2009) and somatic mutation of TAOK1 has been described in several human cancer tissues including glioblastoma (Parsons, Jones et al. 2008), lung cancer (Davies, Hunter et al. 2005) and digestive tract squamous cell carcinoma.

#### ➤ RAS4A

This gene encodes a member of the GAP1 family of GTPase-activating proteins that has been identified to suppress the Ras/MAPK pathway in response to an elevation of  $\text{Ca}^{2+}$ . Stimuli that increase intracellular  $\text{Ca}^{2+}$  levels result in the translocation of this protein to the plasma membrane, where it activates Ras GTPase activity. Consequently, Ras is converted from the active GTP-bound state to the inactive GDP-bound state and no longer activates the downstream pathways that regulate gene expression, cell growth, and differentiation (Lockyer, Kupzig et al. 2001). RAS4A is not up-regulated upon senescence but its expression might be essential to some pathways that take place during senescence and that might be necessary to the trigger or the maintenance of the cell cycle arrest. Interestingly, K- ras4A was found to be over-expressed 2-to 3-fold higher in lung tumour cell lines (Wang and You 2001).

➤ ARM CX2 or ALEX2

This gene encodes a member of the ALEX family of proteins and may play a role in tumour suppression. The encoded protein contains a potential N-terminal transmembrane domain and a single Armadillo (arm) repeat. Other proteins containing the arm repeat are involved in development, maintenance of tissue integrity, and tumourigenesis. The genes encoding ALEX1, ALEX2 and ALEX3 co-localize to the same region in Xq21.33-q22.2. ALEX1 and Expression of ALEX1 and ALEX2 mRNA was found to be lost or significantly reduced in human lung, prostate, colon, pancreas, and ovarian carcinomas and also in cell lines established from different human carcinomas. These genes are, however, normally expressed in cell lines derived from other types of tumours, e.g., sarcomas, neuroblastomas, and gliomas. ALEX gene was suggested to play a role in suppression of tumours originating from epithelial tissue, i.e., carcinomas (Kurochkin, Yonemitsu et al. 2001).

ARM CX2 was up-regulated upon senescence when looking at the raw microarray data; it did not appear in the differential data set since it was also up-regulated in the heat shock control. Since it was found amongst the targets in the primary screen, it suggests that it may also potentially have a role in senescence which is in accordance with its down-regulation in some tumours.

## **6 ROLE OF MICRO-RNAS IN CELLULAR SENESENCE**

### **6.1 SENESENCE SPECIFIC MICRO-RNA DIFFERENTIAL EXPRESSION**

#### **6.1.1 Objectives**

Micro-RNAs have recently emerged as key regulators of gene expression in many developmental and cancer processes like cell proliferation, differentiation, cell cycle, apoptosis and metastasis. It is actually hypothesized that probably every cellular process is regulated at least partially by micro-RNAs, and an aberrant micro-RNA expression signature can be the hallmark of several diseases, including cancer (Iorio and Croce 2009).

An increasing number of studies have then demonstrated that micro-RNAs can function as potential oncogenes or tumour suppressor genes, depending on the cellular context and on the target genes they regulate. The Aim of this chapter was to analyse senescence-specific micro-RNAs expression in the HMF3A<sup>EcoR</sup> system in a similar way to the one used for the genome wide microarray in order to investigate the involvement of miRs in senescence and their potential as a tool to understand better the mechanism behind senescence pathways.

#### **6.1.2 Background to micro-RNA Expression Profiling Technology**

Genome-wide microarray gene expression analysis has been widely utilised to investigate human cancers and allowed the identification of important genes for both prognostic and therapeutics (Martin, Graner et al. 2001; Chung, Sung et al. 2002; Mohr, Leikauf et al. 2002; van 't Veer, Dai et al. 2002; Ramaswamy and Perou 2003). Recently, microarray analysis has been enriched by the development of platforms for the analysis of micro-RNA (miRNA) expression (Calin, Sevignani et al. 2004; Liu, Calin et

al. 2004). Investigation of over-expression and down-regulation of miRNAs in senescence would represent an innovative and efficient approach from a completely different perspective to study the senescence mechanisms. Previous studies have demonstrated that there is a large number of deregulated miRNAs in human breast cancer. Different miRNA expression signatures (Iorio, Ferracin et al. 2005; Mertens-Talcott, Chintharlapalli et al. 2007; Ma and Weinberg 2008) have also been correlated with different prognostic parameters such as tumour size, nodal involvement, vascular invasiveness and chemotherapy resistance (Yan, Zhou et al. 2009; Zhao, Yang et al. 2009). Here, using micro-RNA expression profiling within the HMF3A<sup>EcoR</sup> cells could bring new answers to the understanding of cellular senescence.

One of the first microarrays to become available and used by the Massague lab was from LC Sciences (Tavazoie, Alarcon et al. 2008) and represented a human genome-wide miRNA array, based upon the latest release (10.1) from the Sanger miRBase Sequence Database (catalogue number MRA-1001) and corresponds to 723 unique mature miRNA probes.

### 6.1.3 HMF3A<sup>EcoR</sup>: miRNA expression profiling experimental design

My aim was to identify any significant changes in miRNA expression between HMF3A<sup>EcoR</sup> cells incubated at 34°C and HMF3A<sup>EcoR</sup> cells incubated at 38°C for 7 days, and to identify changes that occur due to quiescence (Figure 6.1). The quiescence specific signal was determined by comparing the signal from HMF3A<sup>EcoR</sup> cells incubated at 34°C with serum starved (0.5%FCS) HMF3A<sup>EcoR</sup> cells incubated at 34°C for a week.

Each chip contained multiple redundant miRNA probe regions required to detect miRNA transcripts ([www.sanger.ac.uk/Software/Rfam/mirna/](http://www.sanger.ac.uk/Software/Rfam/mirna/)) listed in Sanger miRBase Release 10.1. Furthermore, multiple control probes were also present on each chip as quality controls for production, sample labelling and assay conditions.

Because of the possibility of sample variation, biological triplicates were used.

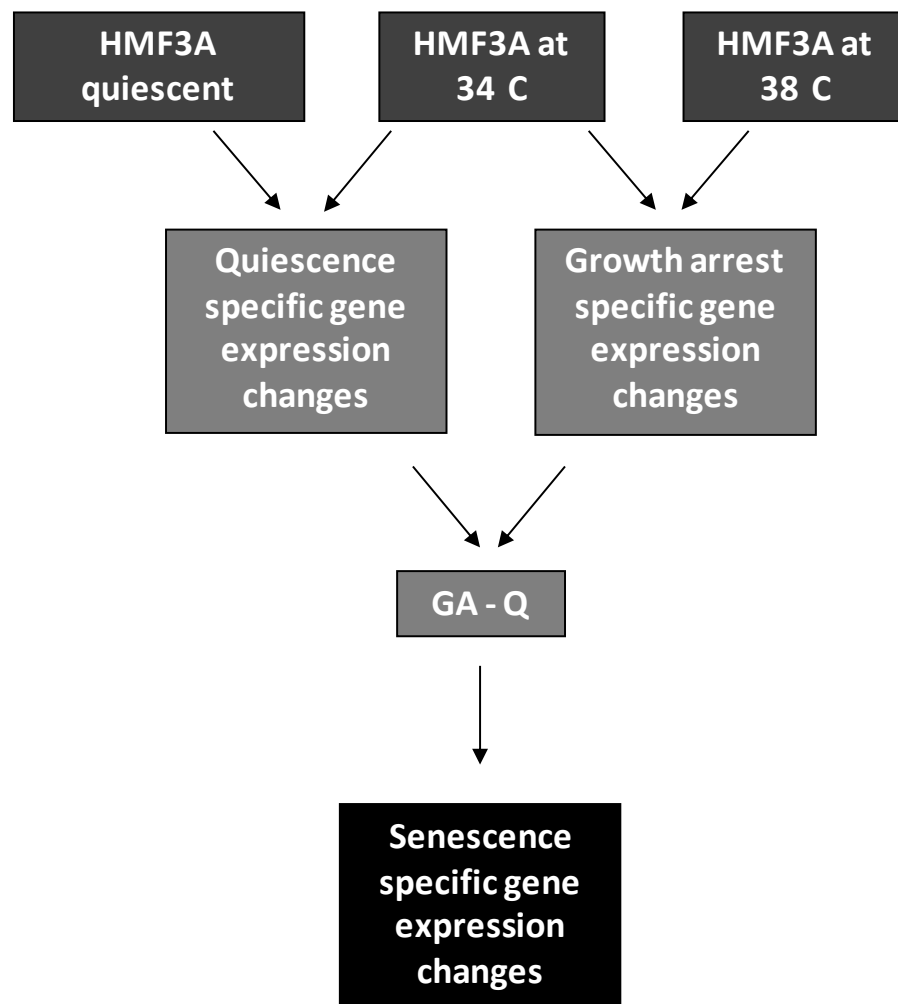


**Figure 6.1: microRNAs microarray profiling strategy**

Significant changes in miRNA expression between HMF3A<sup>EcoR</sup> cells incubated at 34°C and HMF3A<sup>EcoR</sup> cells incubated at 38°C for 7 days and changes that occur due to quiescence were identified. The quiescence specific signal was determined by comparing the signal from HMF3A<sup>EcoR</sup> cells incubated at 34°C with serum starved (0.5%FCS) HMF3A<sup>EcoR</sup> cells incubated at 34°C for a week. To obtain senescence specific changes, the growth arrest changes occurring also in quiescence were removed.



Dual hybridization was set-up to make pairwise comparison of the samples as seen in Table 6.1 to minimize inter chip errors and provide more reliable data. The triplicate samples were also labelled with Cy3 and Cy5 alternatively to normalize the differences in the dye incorporation.

#### 6.1.4 Quality Control of RNA Samples

The 260 nm/230 nm and 260 nm/280 nm ratio of each extracted RNA sample were analyzed by Nanodrop. The samples all had a 260/280 ratio above 1.8 which means that the samples were not contaminated by proteins. The 260/230 ratio was above 1.8 for approximately 50% of the samples leaving the other 50% of the samples with a slight trace of ethanol contamination present in the samples.

#### 6.1.5 miRNAs senescence specific differential expression

This analysis was designed to identify senescence-specific miR expression by determining which miRs are differentially expressed upon the shift from 34°C to 38°C but do not change significantly upon quiescence. Because I found that many of the up-regulated changes and particularly the NF- $\kappa$ B targets were also up-regulated by quiescence, my strategy was to take the quiescence expression in consideration but not eliminate the genes also modulated by quiescence from the results. That way, I had all the information necessary to choose targets.

Due to the prices of the arrays, it was impossible to incorporate the HMF3S at 34° versus 38°C to eliminate changes due to the temperature shift.

Chip	Cy3	Cy5
#1	34.0C #1	38.0C #1
#2	38.0C #2	34.0C #2
#3	34.0C #3	38.0C #3
#4	34.0C #1	Quiescent #1
#5	Quiescent #2	34.0C #2
#6	34.0C #3	Quiescent #3

**Table 6.1: Dual-hybridization analysis**

Dual hybridization was set-up to make pairwise comparison of the samples and to minimize inter chip errors and provide more reliable data. The triplicate samples were also labelled with Cy3 and Cy5 alternatively to normalize the differences in the dyes incorporation.

In the first step, the genes differentially expressed upon growth arrest were identified after filtering for low signals (at least  $> 32$ ). Expression results for the 86 remaining miRs for growth arrest and 64 for quiescence after filtering for low signal and for significant results (p-value at least  $< 0.1$ ) are displayed in table 6.2 and 6.3.

The Figure 6.2 represents the heat map of the 86 micro-RNAs differentially expressed with a mean p-value  $< 0.1$  upon growth arrest and the 64 micro-RNAs differentially expressed with a mean p-value  $< 0.1$  upon quiescence. This cut off value was suggested by LC Sciences for significant samples in this analysis even though it is much higher than the one used for the Affymetrix data.

The first three columns and the three last columns of each heat map represent the triplicate samples at  $34^{\circ}\text{C}$  against samples at  $38^{\circ}\text{C}$ . It is possible to note that the triplicate samples displayed the same colour changes upon growth arrest or quiescence which validates the reproducibility of the data even though column 2 shows slight inconsistency with the other two.

The expression changes upon both growth arrest and quiescence for the 86 miRs with a mean p-value  $< 0.1$  upon growth arrest were overlapped and the difference between growth arrest and quiescence differential was calculated.

Micro-RNAs were considered specifically differential upon growth arrest only if the difference between growth arrest and quiescence differentials was  $> 1$  or  $< -1$  in  $\log_2$  fold change (which corresponds to a two-fold difference in expression). In addition, the list was also filtered for the miRs, which exhibited changes in expression at least  $> 0.5$  or  $< -0.5$   $\log_2$  fold change upon growth arrest.

This gave a micro-RNA list of 33 micro-RNAs of which 18 were up-regulated upon growth arrest and 15 were down regulated.

The up and down-regulated micro-RNAs and their respective expression levels are shown in Tables 6.4 and 6.5.

			Group 34		Group 38		Log2 (38/34 )
No.	Reporter Name	p-value	Mean	StDev	Mean	StDev	
197	hsa-miR-20a	5.49E-04	2,566	203	925	76	-1.47
289	hsa-miR-320	1.17E-03	3,742	81	5,107	196	0.45
26	hsa-miR-106a	1.27E-03	1,605	164	703	43	-1.19
123	hsa-miR-15a	2.50E-03	756	166	167	28	-2.18
127	hsa-miR-16	3.29E-03	13,974	1,466	6,359	716	-1.14
237	hsa-miR-25	4.46E-03	3,615	390	1,705	207	-1.08
152	hsa-miR-18a	4.91E-03	507	42	109	19	-2.22
396	hsa-miR-455-3p	5.88E-03	364	67	940	137	1.37
697	hsa-miR-92a	6.11E-03	7,050	1,183	3,292	306	-1.10
130	hsa-miR-17	8.49E-03	1,932	366	879	99	-1.14
320	hsa-miR-34a	8.54E-03	55	21	723	112	3.71
101	hsa-miR-146a	1.13E-02	83	11	1,676	871	4.33
64	hsa-miR-128	1.70E-02	582	52	360	52	-0.69
617	hsa-miR-638	1.84E-02	2,531	496	5,921	1,287	1.23
125	hsa-miR-15b	1.89E-02	7,796	3,119	1,469	58	-2.41
112	hsa-miR-149*	1.92E-02	256	5	537	91	1.07
144	hsa-miR-185	1.93E-02	585	91	959	105	0.71
351	hsa-miR-376c	1.99E-02	115	16	492	168	2.10
62	hsa-miR-127-3p	2.18E-02	293	97	990	49	1.76
121	hsa-miR-155	2.23E-02	4,558	1,492	1,475	470	-1.63
256	hsa-miR-29a	2.37E-02	15,363	2,653	29,875	314	0.96
201	hsa-miR-21	2.61E-02	41,589	3,185	21,404	3,554	-0.96
16	hsa-let-7i	2.64E-02	12,627	742	9,856	889	-0.36
223	hsa-miR-221	2.64E-02	5,028	1,373	15,117	2,250	1.59
70	hsa-miR-130b	3.03E-02	410	98	184	47	-1.16
650	hsa-miR-708	3.07E-02	246	64	589	18	1.26
163	hsa-miR-193a-5p	3.66E-02	1,021	124	1,492	81	0.55
246	hsa-miR-27b	3.68E-02	4,034	713	2,491	401	-0.70
406	hsa-miR-487b	4.10E-02	380	57	565	75	0.57
276	hsa-miR-30b	4.16E-02	472	42	376	27	-0.33
373	hsa-miR-423-5p	4.45E-02	1,862	379	1,205	124	-0.63
175	hsa-miR-199a-3p	5.29E-02	6,741	557	9,064	1,287	0.43
274	hsa-miR-30a	6.32E-02	310	90	585	26	0.92
117	hsa-miR-152	6.34E-02	428	76	655	117	0.62
19	hsa-miR-100	8.02E-02	6,956	1,647	11,677	1,310	0.75
643	hsa-miR-663	8.87E-02	704	375	1,491	380	1.08
14	hsa-let-7g	9.04E-02	3,999	1,374	2,144	462	-0.90
700	hsa-miR-92b	9.11E-02	2,173	1,211	788	69	-1.46
30	hsa-miR-107	9.36E-02	1,277	333	2,025	396	0.66

285	hsa-miR-31	9.73E-02	4,350	1,582	8,595	680	0.98
Following transcripts are statistically significant but have low							
231	hsa-miR-23a*	1.69E-05	488	10	136	5	-1.84
199	hsa-miR-20b	1.38E-03	409	76	85	11	-2.27
135	hsa-miR-181b	1.47E-03	437	27	213	20	-1.04
258	hsa-miR-29b	3.69E-03	32	5	146	8	2.18
129	hsa-miR-16-2*	6.88E-03	29	3	14	2	-1.02
247	hsa-miR-27b*	8.93E-03	180	48	37	2	-2.27
497	hsa-miR-532-5p	1.09E-02	56	6	106	17	0.93
555	hsa-miR-584	1.24E-02	29	2	84	15	1.55
401	hsa-miR-485-3p	1.28E-02	105	9	165	19	0.65
400	hsa-miR-484	1.66E-02	159	19	98	13	-0.69
238	hsa-miR-25*	1.92E-02	121	57	30	8	-2.03
133	hsa-miR-181a*	2.05E-02	30	4	19	2	-0.69
370	hsa-miR-421	2.46E-02	62	14	28	7	-1.12
297	hsa-miR-329	2.64E-02	35	7	69	3	0.97
418	hsa-miR-495	2.74E-02	56	18	161	14	1.52
154	hsa-miR-18b	2.79E-02	101	6	42	11	-1.26
542	hsa-miR-574-3p	2.86E-02	60	8	180	56	1.59
544	hsa-miR-575	3.28E-02	40	4	119	35	1.57
379	hsa-miR-431	3.51E-02	28	6	52	10	0.87
119	hsa-miR-154	3.52E-02	35	8	78	10	1.14
415	hsa-miR-493	3.70E-02	22	4	37	6	0.80
305	hsa-miR-337-5p	3.82E-02	30	10	72	18	1.25
404	hsa-miR-486-5p	4.01E-02	18	4	31	6	0.80
286	hsa-miR-31*	4.01E-02	18	4	38	12	1.12
205	hsa-miR-212	4.20E-02	35	6	24	2	-0.54
203	hsa-miR-210	4.47E-02	47	3	123	40	1.40
46	hsa-miR-1229	4.49E-02	29	4	22	2	-0.44
100	hsa-miR-145*	5.19E-02	38	10	20	4	-0.95
72	hsa-miR-132	5.40E-02	283	117	100	16	-1.50
84	hsa-miR-138	5.60E-02	82	18	145	34	0.83
109	hsa-miR-148b	5.81E-02	31	2	26	2	-0.28
55	hsa-miR-125a-3p	5.86E-02	40	4	24	5	-0.74
229	hsa-miR-224	5.87E-02	135	46	65	17	-1.07
329	hsa-miR-362-5p	6.07E-02	37	2	43	2	0.19
76	hsa-miR-134	6.22E-02	384	34	302	34	-0.35
375	hsa-miR-424*	6.90E-02	129	52	50	4	-1.38
633	hsa-miR-654-3p	7.05E-02	40	2	84	27	1.06
139	hsa-miR-182	7.09E-02	29	8	47	9	0.72
381	hsa-miR-432	8.06E-02	130	56	264	11	1.02
300	hsa-miR-331-3p	8.20E-02	48	6	91	28	0.92
316	hsa-miR-342-3p	8.82E-02	58	18	33	6	-0.83

**Table 6.2: Raw microarray results for growth arrest**

Results microarray for the micro-RNAs transcripts with significant results (p-value > 0.1)

			Group 34		Group Q		Log2 (Q/34)
No.	Reporter Name	p-value	Mean	StDev	Mean	StDev	
617	hsa-miR-638	1.64E-04	2,102	147	6,888	367	1.71
101	hsa-miR-146a	2.36E-03	176	29	1,692	139	3.27
99	hsa-miR-145	4.10E-03	737	168	206	28	-1.84
246	hsa-miR-27b	5.07E-03	4,862	435	2,252	80	-1.11
117	hsa-miR-152	5.40E-03	840	74	508	43	-0.73
239	hsa-miR-26a	6.38E-03	8,256	271	9,925	332	0.27
130	hsa-miR-17	6.74E-03	1,622	129	1,118	61	-0.54
26	hsa-miR-106a	7.35E-03	1,509	117	1,051	62	-0.52
112	hsa-miR-149*	7.96E-03	312	101	1,363	312	2.13
16	hsa-let-7i	1.20E-02	12,578	82	10,889	295	-0.21
695	hsa-miR-923	1.24E-02	3,289	352	5,297	581	0.69
121	hsa-miR-155	1.38E-02	5,525	1,070	2,745	390	-1.01
197	hsa-miR-20a	1.62E-02	2,480	285	1,373	81	-0.85
135	hsa-miR-181b	1.64E-02	393	96	184	23	-1.10
95	hsa-miR-143	2.11E-02	625	229	185	41	-1.76
278	hsa-miR-30c	2.13E-02	1,248	109	1,746	25	0.48
234	hsa-miR-24	2.92E-02	6,275	1,048	3,507	633	-0.84
720	hsa-miR-99a	3.06E-02	1,522	216	2,359	314	0.63
123	hsa-miR-15a	3.38E-02	801	123	1,412	288	0.82
258	hsa-miR-29b	3.39E-02	71	34	482	278	2.76
244	hsa-miR-27a	4.25E-02	6,381	1,319	3,498	178	-0.87
643	hsa-miR-663	4.62E-02	588	299	2,069	266	1.81
199	hsa-miR-20b	6.04E-02	654	67	479	79	-0.45
232	hsa-miR-23b	6.70E-02	16,932	1,069	13,987	1,407	-0.28
223	hsa-miR-221	6.73E-02	5,695	1,882	10,960	700	0.94
127	hsa-miR-16	8.05E-02	11,327	1,359	14,836	1,851	0.39
276	hsa-miR-30b	8.52E-02	1,040	185	1,508	292	0.54
116	hsa-miR-151-5p	9.26E-02	2,192	202	1,432	328	-0.61
225	hsa-miR-222	9.78E-02	7,788	2,027	12,033	408	0.63
Following transcripts are statistically significant but have low signals							
401	hsa-miR-485-3p	1.77E-03	58	5	26	3	-1.16
100	hsa-miR-145*	2.62E-03	43	4	17	2	-1.35
247	hsa-miR-27b*	3.65E-03	117	16	44	6	-1.41
418	hsa-miR-495	6.60E-03	108	15	47	7	-1.20
357	hsa-miR-379*	8.13E-03	42	5	20	1	-1.10
224	hsa-miR-221*	1.06E-02	125	14	235	36	0.92
544	hsa-miR-575	1.10E-02	40	9	144	11	1.84
173	hsa-miR-197	1.12E-02	129	6	60	8	-1.09
368	hsa-miR-411*	1.50E-02	65	12	27	2	-1.28
8	hsa-let-7d*	1.74E-02	55	2	32	4	-0.79

76	hsa-miR-134	1.85E-02	189	24	105	17	-0.84
104	hsa-miR-146b-5p	2.20E-02	44	12	146	59	1.72
152	hsa-miR-18a	2.34E-02	277	53	131	30	-1.08
399	hsa-miR-483-5p	2.66E-02	26	15	108	36	2.03
29	hsa-miR-106b*	2.80E-02	22	2	33	5	0.60
229	hsa-miR-224	2.99E-02	313	73	134	12	-1.23
318	hsa-miR-345	3.04E-02	31	2	38	3	0.31
149	hsa-miR-187*	3.46E-02	28	18	169	70	2.59
658	hsa-miR-765	3.55E-02	18	4	35	3	0.96
406	hsa-miR-487b	3.83E-02	256	59	131	30	-0.96
231	hsa-miR-23a*	4.00E-02	272	36	119	31	-1.20
55	hsa-miR-125a-3p	4.51E-02	21	2	29	3	0.44
134	hsa-miR-181a-2*	4.62E-02	71	1	41	9	-0.80
255	hsa-miR-299-5p	5.18E-02	212	45	126	21	-0.74
297	hsa-miR-329	5.83E-02	63	16	34	3	-0.87
361	hsa-miR-382	6.21E-02	355	91	193	48	-0.88
375	hsa-miR-424*	6.36E-02	103	17	62	17	-0.73
431	hsa-miR-503	6.66E-02	55	9	37	7	-0.59
649	hsa-miR-7	7.71E-02	90	36	37	17	-1.26
381	hsa-miR-432	7.78E-02	84	24	46	10	-0.88
348	hsa-miR-376a	8.21E-02	41	9	25	7	-0.70
47	hsa-miR-1231	8.73E-02	23	6	74	34	1.66
60	hsa-miR-126	9.18E-02	34	8	66	24	0.96
356	hsa-miR-379	9.72E-02	433	55	235	79	-0.88

**Table 6.3: Raw microarray results for quiescence**

Results microarray for the micro-RNAs transcripts with significant results (p-value > 0.1)

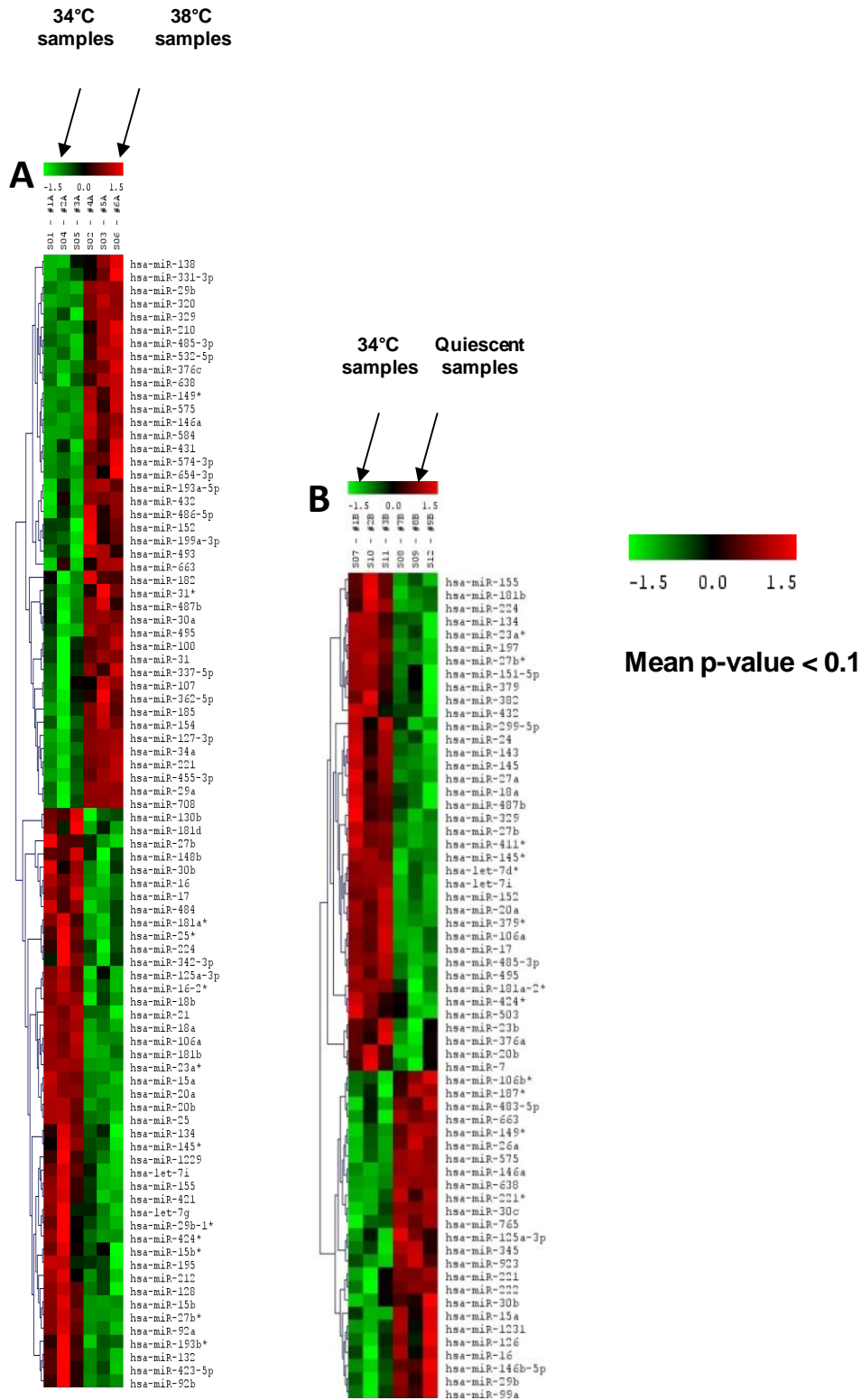


**Figure 6.2: Differential microRNAs upon growth arrest (A) and quiescence (B)**

Heat map of the 86 microRNAs differentially expressed with a mean p-value < 0.1 upon growth arrest (A) and the 64 microRNAs differentially expressed with a mean p-value < 0.1 upon quiescence (B). The first three columns and the three last columns of each heat map represent the triplicate samples at 34°C against samples at 38°C.



Reporter Name	LogFC GA	p-value	LogFC quiescence	p-value	Difference logFC
hsa-miR-146a	4.33	1.13E-02	3.27	2.36E-03	1.06
hsa-miR-34a	3.71	8.54E-03	-0.54	3.62E-01	4.25
hsa-miR-376c	2.10	1.99E-02	-1.05	1.34E-01	3.15
hsa-miR-127-3p	1.76	2.18E-02	-0.20	4.87E-01	1.96
hsa-miR-574-3p	1.59	2.86E-02	0.05	9.11E-01	1.53
hsa-miR-495	1.52	2.74E-02	-1.20	6.60E-03	2.72
hsa-miR-210	1.40	4.47E-02	0.26	3.75E-01	1.13
hsa-miR-455-3p	1.37	5.88E-03	0.02	9.58E-01	1.35
hsa-miR-708	1.26	3.07E-02	-0.09	9.02E-01	1.35
hsa-miR-154	1.14	3.52E-02	0.14	6.07E-01	1.00
hsa-miR-149*	1.07	1.92E-02	2.13	7.96E-03	-1.06
hsa-miR-654-3p	1.06	7.05E-02	-0.23	5.47E-01	1.28
hsa-miR-432	1.02	8.06E-02	-0.88	7.78E-02	1.91
hsa-miR-329	0.97	2.64E-02	-0.87	5.83E-02	1.84
hsa-miR-185	0.71	1.93E-02	-0.35	3.45E-01	1.06
hsa-miR-485-3p	0.65	1.28E-02	-1.16	1.77E-03	1.82
hsa-miR-152	0.62	6.34E-02	-0.73	5.40E-03	1.34
hsa-miR-487b	0.57	4.10E-02	-0.96	3.83E-02	1.54

The samples considered not significant (p-value>0.1) are shown in yellow

**Table 6.4: Up-regulated micro-RNAs upon senescence**

18 microRNAs were up-regulated upon growth arrest and this table represents their respective expression levels upon growth arrest and quiescence

Reporter Name	LogFC GA	p-value	LogFC quiescence	p-value	Difference logFC
hsa-miR-15b	-2.41	1.89E-02	-0.10	5.94E-01	-2.30
hsa-miR-20b	-2.27	1.38E-03	-0.45	6.04E-02	-1.82
hsa-miR-18a	-2.22	4.91E-03	-1.08	2.34E-02	-1.14
hsa-miR-15a	-2.18	2.50E-03	0.82	3.38E-02	-3.00
hsa-miR-29b-1*	-2.13	9.30E-02	-0.34	3.96E-01	-1.79
hsa-miR-25*	-2.03	1.92E-02	0.26	4.19E-01	-2.30
hsa-miR-132	-1.50	5.40E-02	-0.31	5.30E-01	-1.18
hsa-miR-15b*	-1.36	9.64E-02	0.43	5.16E-01	-1.79
hsa-miR-130b	-1.16	3.03E-02	0.02	9.51E-01	-1.17
hsa-miR-16	-1.14	3.29E-03	0.39	8.05E-02	-1.53
hsa-miR-16-2*	-1.02	6.88E-03	0.15	9.25E-01	-1.17
hsa-miR-195	-1.00	9.75E-02	1.51	3.53E-01	-2.51
hsa-miR-193b*	-0.82	9.54E-02	0.99	3.81E-01	-1.81
hsa-miR-125a-3p	-0.74	5.86E-02	0.44	4.51E-02	-1.18
hsa-miR-181a*	-0.69	2.05E-02	0.34	4.94E-01	-1.03

The samples considered not significant (p-value>0.1) are shown in yellow

**Table 6.5: Down-regulated microRNAs upon senescence**

15 microRNAs were up-regulated upon growth arrest and this table represents their respective expression levels upon growth arrest and quiescence

### 6.1.6 Up-regulated micro-RNAs

The microarray analysis permitted the designation of 18 micro-RNAs specifically up-regulated upon senescence; Table 6.4 shows them ranked by fold change for growth arrest. Some of the miRs were also up-regulated upon quiescence (miR-146a: 3.27 log<sub>2</sub> fold change- highest up-regulated) whereas others are down-regulated (miR-495: -1.2 log<sub>2</sub> fold change- highest down-regulated). It was particularly interesting that 34a was amongst the up-regulated miRs, exactly the way it had been described extensively in the last few years. MiR-34a has also been previously linked to cancer, apoptosis and growth arrest.

### 6.1.7 Down-regulated micro-RNAs

The microarray analysis permitted the designation of 15 micro-RNAs down-regulated upon senescence growth arrest some of which were also down-regulated upon quiescence (miR-18a: 1.08 log<sub>2</sub> fold change- highest down-regulated) whereas others were up-regulated (miR-195: 1.5 log<sub>2</sub> fold change- highest up-regulated) (table 6.5). MiR-372 and MiR-373 were absent from the chip I used which explain why they are absent from the differential results.

## **6.2 BIOLOGICAL VALIDATION BY GROWTH COMPLEMENTATION ASSAY IN THE HMF3A CELLS**

### 6.2.1 Objectives

The objectives of the biological validation were to confirm the involvement of the differentially expressed micro-RNAs in the senescence process and more specifically the down-regulated micro-RNAs. To address this issue, it was important to investigate whether the down regulation was essential to triggering the growth arrest or only a consequence. In theory, if the down-regulation of a miR was causal to senescence, its

up-regulation by ectopic expression should reverse senescence and not allow the growth arrest. The complementation using the CL3<sup>EcoR</sup> model was a great way to assess this biologically. Ultimately this should be also validated in primary cells. Since the LC Science chips were very expensive, I decided that it would be easier and more cost effective to simply validate them by ectopic expression since the miR-Vec were available.

## 6.2.2 Validation by ectopic expression

### 6.2.2.1 miR Vec clones

Agami and colleagues at NKI created a library of miRs cloned into a retroviral expression vector under the control of a CMV promoter (Voorhoeve, le Sage et al. 2006). Geneservice provides these clones as a micro-RNA library (MiR-Lib). The following miRs were purchased and used for the complementation assay and information about each miR was extracted from miRbase ([www.mirbase.org](http://www.mirbase.org)):

Mir-186\*: hsa-miR-186: A light dye bias has been found for this miR on the microarray which has to be taken into consideration as well as the p-value which was not within the filtering threshold applied which is why that micro-RNA was not in the Table 6.5. Nevertheless, since it was the most highly down-regulated micro-RNA, it was still selected for ectopic expression. This micro-RNA is also located within intron 8 of the ZRANB2 gene and does not form part of a miR cluster.

MiR-15b, miR-15b\*, mir-15a and miR-16: hsa-miR-15a and hsa-miR-15a/16: MiR-15 a, miR-15b and miR-16 are clustered together. There were only two clones available: miRVec hsa-miR-15a/16 or miRVec hsa-miR-15a. MiR-15a~16-1 cluster is found in the intron of a well-defined non-coding RNA gene, *DLEU2*.

MiR-20b: hsa-miR-20b: This is clustered with hsa-miR-106a, hsa-miR-18b, hsa-miR-19b-2, hsa-miR-92a-2 and hsa-miR-363. There are no overlapping transcripts with this miR.

MiR-18a: hsa-miR-18a: This miR is expressed as part of a cluster of intronic RNAs, including miR-17, miR-18a, miR-19a, miR-20a, miR-19b-1 and miR-92b. Due to the cloning method used to generate the miR-Vec clones and the close proximity within the cluster; miR-Vec hsa-miR-18a contains both miRs hsa-miR-17a and hsa-miR-19a in addition to hsa-miR-18a.

MiR-29b-1\*: hsa-miR-29b: It is clustered with miR-29a and is located within the transcript AC016831.7 within intron 2.

MiR-25\*: hsa-miR-25: This miR is clustered with miR-93 and 106b. The miR 106b-25 cluster consists of these three miRNAs and is located in the 13<sup>th</sup> intron of MCM7

MiR-132: Not available

MiR-130b: hsa-miR-130b: It is clustered with miR-301b. It overlaps with two transcripts in their intronic region: PPIL2 with its sense sequence and TOP3B with its antisense sequence.

MiR-195: hsa-miR-195: It overlaps with transcript AC027763.1 within intron 1. It is clustered with miR-497.

Mir-193b: hsa-miR-193b: Clustered with miR-365-1. It does not overlap with any transcript.

MiR-125a and miR-181a: These clones would not grow. After two attempts, they were put aside.

hsa-let-7a1 was also obtained as a negative control as its expression does not vary upon senescence or quiescence. Hsa-miR-7a1 miR-Vec clone contains Hsa-miR-let-7a1, Hsa-miR-let-7a2 and Hsa-miR-let-7a3. All three sequences correspond to the same identical Let-7a\* mature sequence. Let-7a does not overlap with any transcript and is clustered with Let-7-f-1 and Let-7-d.

Hsa-miR-373 and hsa-miR-372 clones were also obtained as controls since Voorhoeve *et al* (2006) have shown that they are able to immortalise BJ cells and overcome RAS induced premature senescence in conjunction with hTERT. Hsa-miR-372 miR-Vec clone contains both Hsa-miR-372 and Hsa-miR-371. Unfortunately, the microarray did not provide any information on these two miRs, probably because their expression signal was too weak.

Some additional potential candidates were also identified: miR-92b, miR-218, miR-128, miR-423-5p and Let-7g were selected for the complementation assay. These 5 micro-RNAs were originally identified in my first analysis of the micro-RNAs microarray and, although I later realised that this first analysis was wrong and produced the one described in this chapter, these micro-RNAs were obtained and tested.

MiR-218: hsa-miR-218: This miR overlaps with SLIT2 transcript within the intron 15. It isn't clustered.

MiR-92b\*: hsa-miR-92b: The Hsa-miR-92b miR-Vec clone contains only Hsa-miR-92a; No clone available within NKI library for Hsa-miR-92b. Hsa-miR-92a-1 is clustered with hsa-miR-17, hsa-miR-18a, hsa-miR-19a, hsa-miR-20a and hsa-miR-19b-1. This cluster does not overlap with any transcripts.

MiR-128: hsa-miR-128 mir-Vec clone contains both Hsa-miR-128 and Hsa-miR-128b (both corresponding to the same identical mature sequence) and miR-128 overlaps with the intronic region of ARPP21.

Let-7g: hsa-miR-Let7g miR-Vec is not clustered and overlaps with the transcript WDR82 within the intron 2.

MiR-423-5p: hsa-miR-423-5p miR-Vec clone contains both both Hsa-miR-423-5p and Hsa-miR-423. It also shows that miR-423-5p overlaps with the transcript AC104984.3 within intron 1.

#### 6.2.2.2 Sequencing of the MiRVec clones

The clones were sequenced to check the miR mature sequence. All clones contained the correct mature miR sequence.

#### 6.2.3 Complementation assay with the miR-Vec clones

Candidate miRs hsa-miR-186, hsa-miR-15a/16, hsa-miR-20b, hsa-miR-18a, hsa-miR-130b, hsa-miR-92b, hsa-miR-25, hsa-miR-218, hsa-miR-195, hsa-miR-193b, hsa-let-7a1, hsa-miR-373, hsa-miR-372, hsa-miR-92b, hsa-miR-218, hsa-miR-128, hsa-miR-423-5p and hsa-Let-7g were packaged into amphotropic viruses. pRS p21F RNAi constructs was used as a positive control and different mixes of the miR-Vec clones were used as negative controls. These different viral supernatants were applied to HMF3A cells and a selection of the infected cells was performed. The cells were then reseeded and shifted to 38°C for 3 weeks either in a 6-well plate format at 10,000 or 30,000 cells or in T-75 cm<sup>2</sup> format at  $1.2 \times 10^5$  or  $0.5 \times 10^5$ . The cells were stained after 3 weeks and the resulting colouration was scanned and the number of colonies counted.

#### 6.2.3.1 *MiR-18a, miR-130b, miR-372, miR-373 and Let7a*

The first step was to validate both the *Let7a* negative control and the *miR-373* and *miR-372* positive controls. In addition, two other miRs selected from the microarray were tested in this experiment: *miR-18a* and *miR-130b*.

The results show the number of colonies obtained after the same experiment was repeated in various formats. The variety of formats permitted me to assess which one would give the most consistent results: in 6-well plates with the cells seeded at 10,000 and 30,000 cells per well (Figure 6.3A), in 10 cm plates (data not shown) and in T-75 flasks with the cells seeded at  $1.2 \times 10^5$  (Figure 6.3B). All formats gave similar results although the flasks presented the less stressing option for the cells (healthier phenotype) and was slightly better for statistics due to the higher number of cells. It is possible to note that *Let-7a* was an excellent negative control and did not yield growing colonies under any of the conditions employed. In contrast, *miR-372* readily yielded densely growing colonies. *MiR-373* also abrogated growth arrest although not as efficiently.

The two other miRs tested here, namely *miR-18a* and *miR-130b* did bypass the growth arrest but not as efficiently as the *miR-372* control. Even though *miR-18a* and *miR-130b* did rescue in every single repeat experiment, colonies were much smaller than *miR-372* and *373*. *MiR-130b* was also tested in flasks reseeded at  $1.2 \times 10^5$  which showed the results: a low number of small colonies (Figure 6.4A). For this reason *miR-18a* and *miR-130b* were not pursued further.

#### 6.2.3.2 *MiR-92b, miR-15a, miR-16, miR-195 and miR-25*

*MiR-25*, *miR-15a*, *miR92b* and *miR-16* were tested alongside *miR-372* and *Let7a*. Once again, the format in which *miR-25* was tested was varied but they all gave consistent results: in 10 cm plates (data not shown), in 15cm plates (data not shown) and in T75 flasks seeded at both densities of  $1.2 \times 10^5$  (Figure 6.4A) and  $0.5 \times 10^5$  (Figure 6.4B).



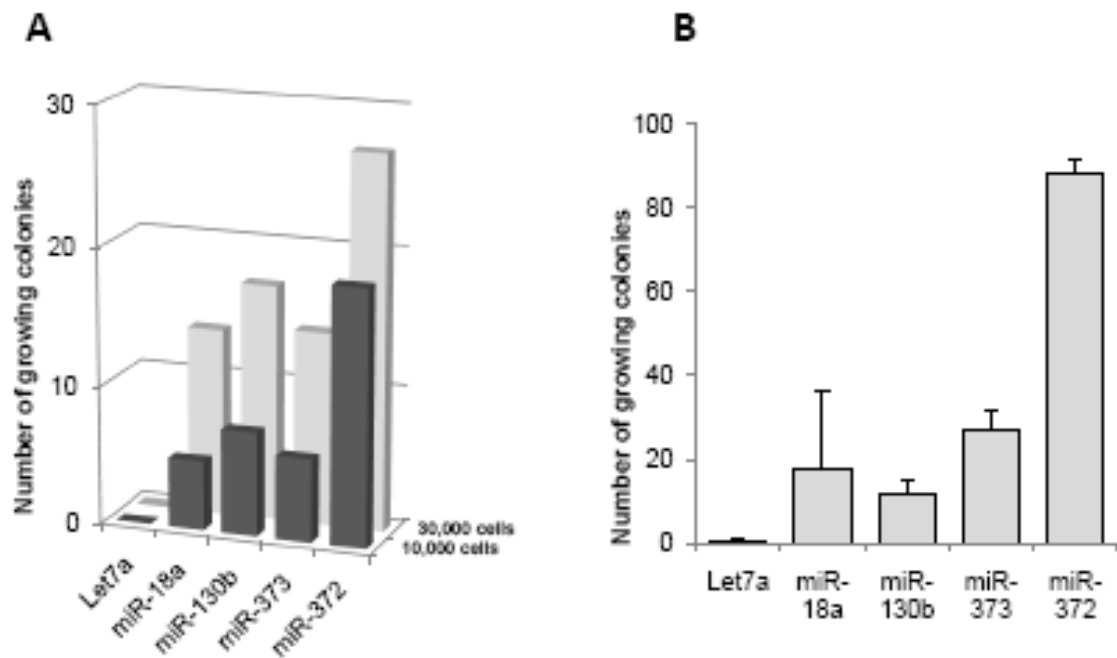


**Figure 6.3: Ectopic expression of miR-18a, miR-130b, miR-373 and miR-372**

HMF3A<sup>EcoR</sup> cells were infected in triplicate with retrovirus expressing the indicated miRs expression constructs and assayed for growth complementation at 38°C in 6-well plates (A) and in T-75cm<sup>2</sup> flasks at 1.2x10<sup>5</sup> (B). After 3 weeks the number of growing colonies was counted.

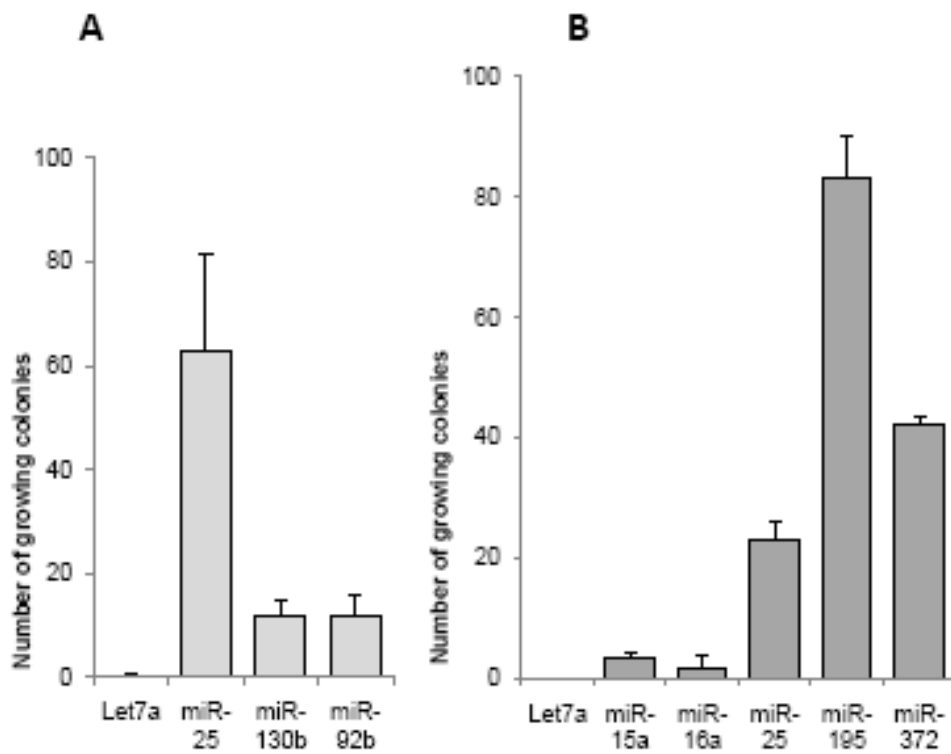


**Figure 6.4: Ectopic expression of miR-25, miR-92b, miR-195, miR-15a and miR-16a**

HMF3A<sup>EcoR</sup> cells were infected in triplicate with retrovirus expressing the indicated miRNAs expression constructs and assayed for growth complementation at 38°C in T-75cm<sup>2</sup> flasks at 1.2x10<sup>5</sup> (A) or at 0.5x10<sup>5</sup> (B). After 3 weeks the number of growing colonies was counted.

In each and every experiment, miR-25 gave strong rescue at levels almost comparable to miR-372. In comparison, miR-15a and miR-16 yielded no colonies and miR-92b yielded a low number of growing colonies (Figure 6.4A). MiR-195 produced a high number of densely growing colonies, even higher than miR-372 and miR-25 (Figure 6.4B).

In conclusion, miR-25 and miR-195 appeared to be good miR targets to study in this conditional cell system and were selected for further investigation. MiR-15a, miR-16 and miR-92b were not pursued further since they were unable to overcome growth arrest. These experiments were repeated with the same results.

#### *6.2.3.3 MiR-195, miR-218, miR-20b, miR-29b, miR-186 and miR-25*

In this experiment, the following miRs were examined (Figure 6.5): miR-15a, 16 and 195 were confirmed; miR-20b, 29b, 218, and 186 were also tested. The analysis was done in various different formats (data not shown) including T-75 flasks at  $0.5 \times 10^5$  (Figure 6.5).

All formats gave similar results: miR-20b and miR-29b gave weak rescue and were consequently not further pursued, miR-186, miR-25 and miR-193b yielded a low number of colonies but very large and densely growing and therefore were selected for further analysis and finally miR-218 and 195 gave a very strong rescue at a level above miR-372 and therefore were also selected for further analysis.

#### *6.2.3.4 MiR-128, miR-423-5p and Let7g*

The complementation assay was performed in various formats (data not shown) including in 6-well plates (Figure 6.6A) and in T-75 flask at the higher density (Figure 6.6B). The results show that miR-128 does not really rescue from growth arrest in a reproducible manner (Figure 6.6A and B). For these reasons, miR-128 was dropped from further investigation.

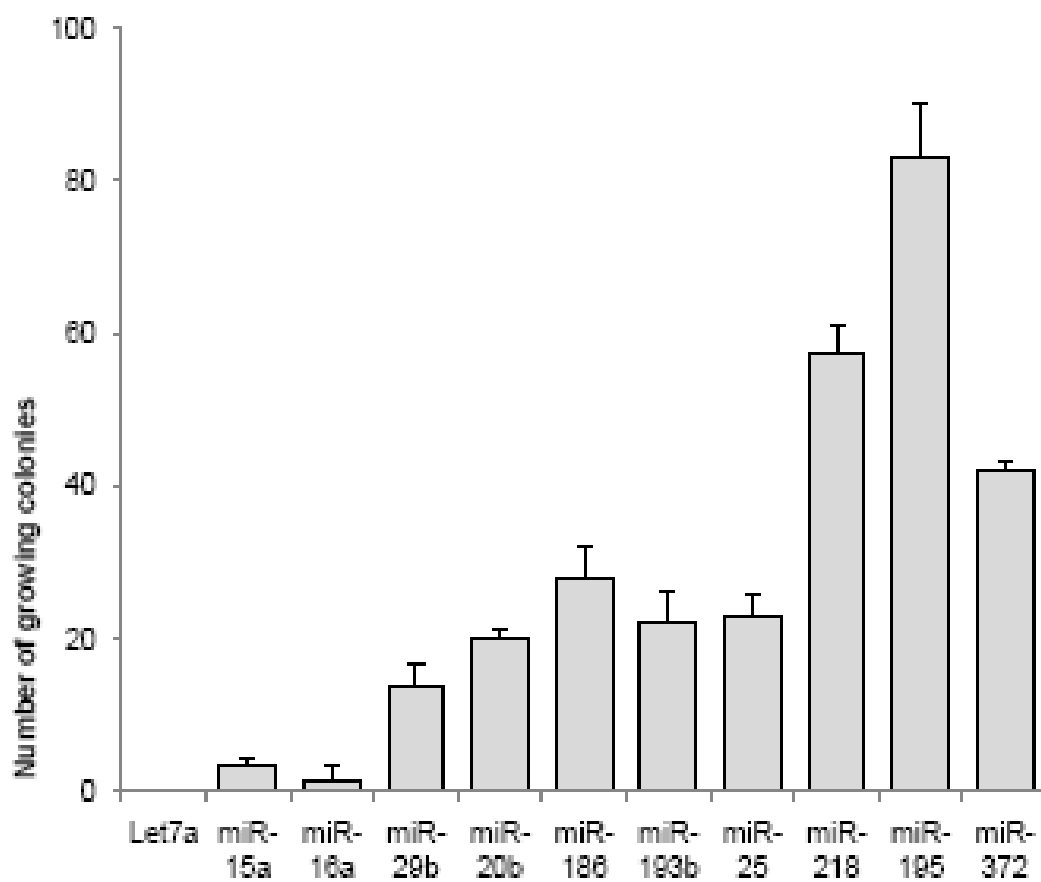


**Figure 6.5: Ectopic expression of miR-29b, miR-20b, miR-186, miR-193b and miR-218**

HMF3A<sup>EcoR</sup> cells were infected in triplicate with retrovirus expressing the indicated miRNAs expression constructs and assayed for growth complementation at 38°C in T-75cm<sup>2</sup> flasks at 0.5x10<sup>5</sup>. After 3 weeks the number of growing colonies were counted.

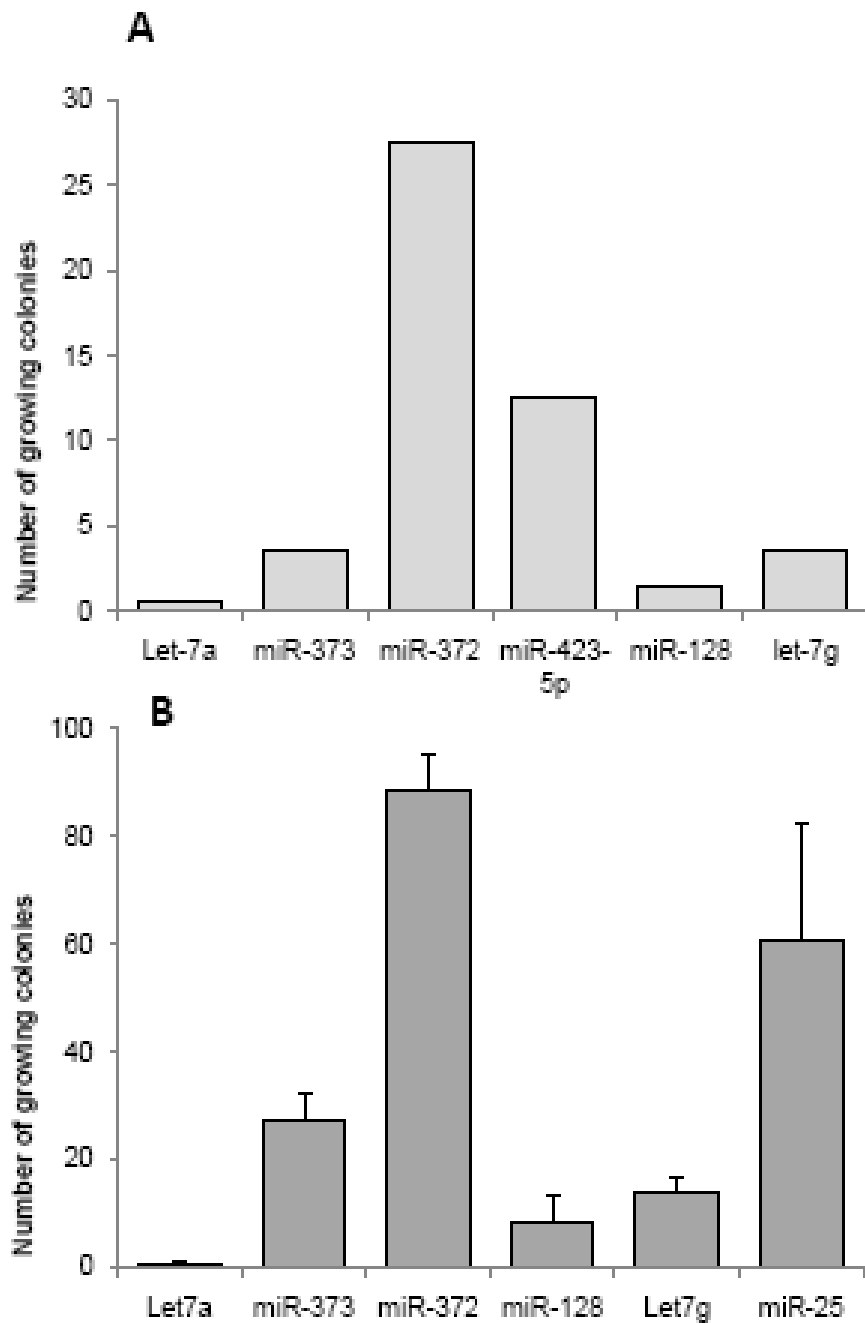


**Figure 6.6: Ectopic expression of miR-423-5p, miR-128 and Let-7g**

HMF3A<sup>EcoR</sup> cells were infected in triplicate with retrovirus expressing the indicated miRNAs expression constructs and assayed for growth complementation at 38°C in 6-well plates at 10,000 cells per well (A) or in T-75cm<sup>2</sup> flasks at 1.2x10<sup>5</sup> (B). After 3 weeks the numbers of growing colonies were counted.

The results show that Let-7g does not really rescue with a very low number of growing colonies similarly to miR-128. For these reasons, Let-7g was dropped for further investigation. Surprisingly, the results were very good for miR-423-5p which was able to rescue the cells from senescence in all experiments. MiR-423-5p ectopic expression was then further investigated along with miR-195, miR-218, miR-25 and miR-372 by complementation assay in additional experiments and in different format: In T-75 flasks seeded at  $0.5 \times 10^5$  (Figure 6.7A) and  $1 \times 10^5$  (Figure 6.7B) and in 10cm plates seeded at  $1 \times 10^5$  (Figure 6.7C). This showed that miR-423-5p rescued at a level comparable to miR-195, miR-25 and miR-218 in a reproducible manner and therefore was chosen for further analysis.

Two extra complementation assays were performed with the positive miRs: miR-423-5p, miR-195, miR-25, miR-218 and miR-186 in 6 well-plates (Figure 6.8A) and T-75 flasks (Figure 6.8B). The results confirmed that miR-423-5p, miR-195 and miR-218 yield the highest level of rescue comparable to miR-372 whereas miR-186, miR-25 and miR-193b were less efficient but produced larger colonies. All were selected for further analysis.

#### 6.2.4 Overlapping with the microarray data and the shRNA screen

##### 6.2.4.1 MiR-25

A MiR-25 target gene list can be produced from the website miRportal (<http://140.116.247.50:800/miRNA/web/index.jsp>) which integrates micro-RNA interacting targets from various prediction algorithms (MiRanda, TargetScan and miRtarget), biological pathway information (Kegg, biocarta and GenMap), and micro-RNA literature.

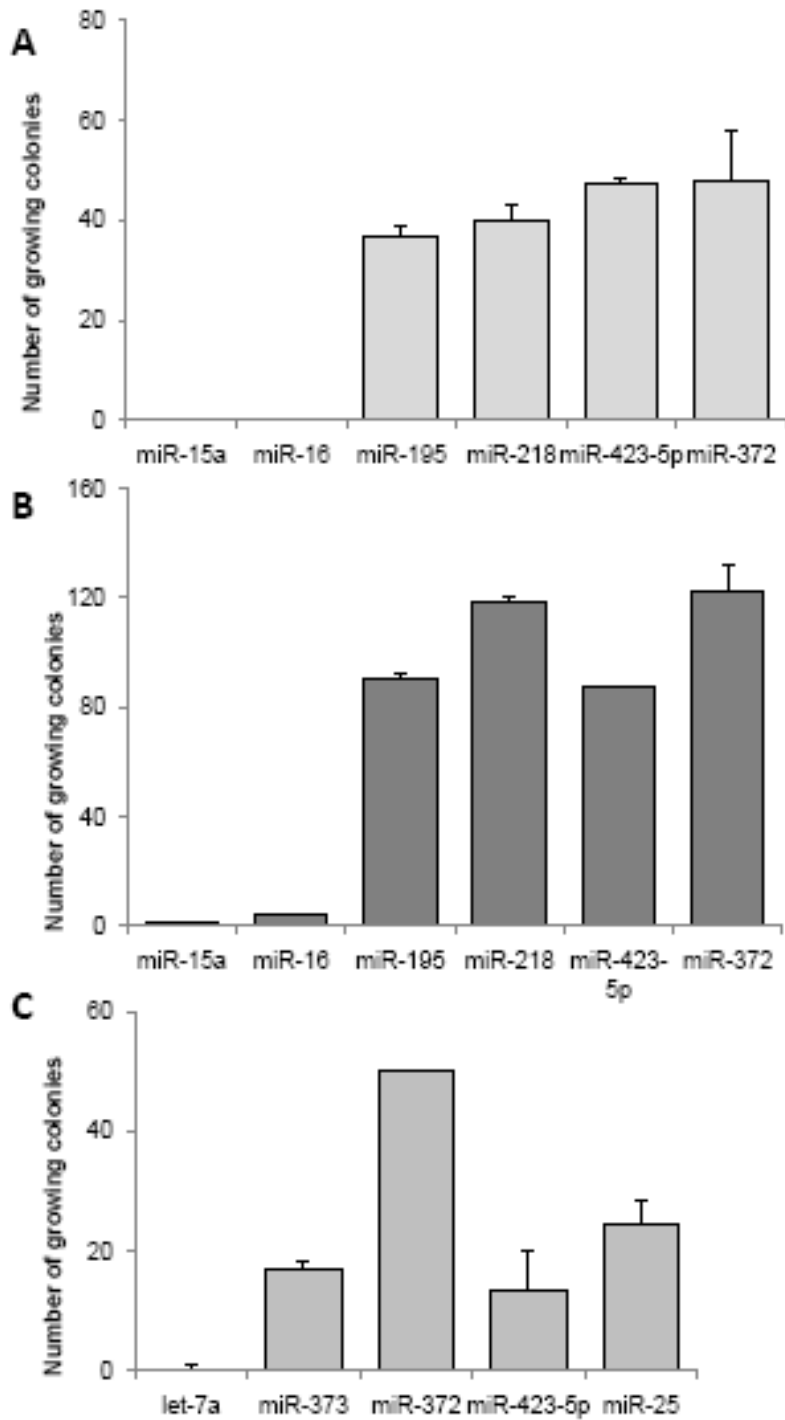


**Figure 6.7: Ectopic expression of miR-423-5p, miR-218 and miR-195**

HMF3A<sup>EcoR</sup> cells were infected in triplicate with retrovirus expressing the indicated miRNAs expression constructs and assayed for growth complementation at 38°C in T-75cm<sup>2</sup> flasks at 0.5x10<sup>5</sup> (A) or at 1x10<sup>5</sup> (B) or in 10 cm plates at 1x10<sup>5</sup> (C). After 3 weeks the number of growing colonies was counted.

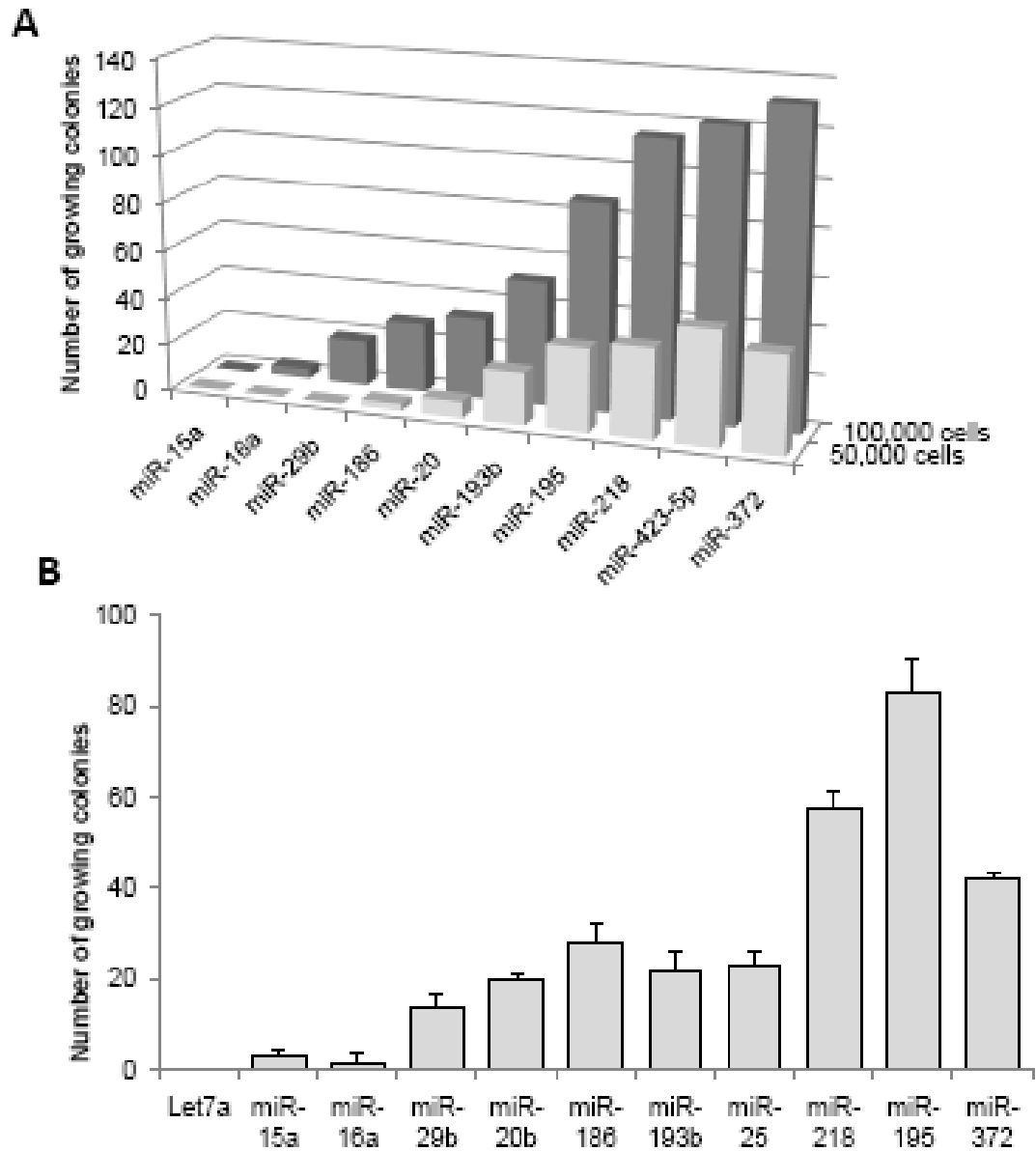


**Figure 6.8: Ectopic expression of miR-423-5p, miR-186, miR-20, miR-193b, miR-29b, miR-25, miR-218 and miR-195**

HMF3A<sup>EcoR</sup> cells were infected in triplicate with retrovirus expressing the indicated miRNAs expression constructs and assayed for growth complementation at 38°C in 6-well plates (A) or in T-75cm<sup>2</sup> flasks at 0.5x10<sup>5</sup> (B). After 3 weeks the number of growing colonies was counted.



The gene list for miR-25 mRNA targets was overlapped with the results of the microarray analysis. 69 of the differentially up-regulated genes were predicted targets of miR-25 including BTG2 and GRAMD3 which were shown to rescue the cells in the complementation assay in chapter 2. Two genes were both targets revealed in the shRNA screen in chapter 3 and predictive target of miR-25, namely LUZP1 and Rab23. Interestingly, LUZP1 was also up-regulated upon senescence.

#### *6.2.4.2 MiR-195*

The same analysis was performed for miR-195. The overlap of the mRNA target gene list provided by the website with the microarray data revealed 75 genes that were both predictive targets for miR-195 and also up-regulated upon senescence. This included the genes CCNE1 and GRAMD3, also a target of miR-25 (see above). 13 genes could be overlapped between the predictive miR-195 target gene list and the shRNA screen hit list. Interestingly, LUZP1 was one of them.

#### *6.2.4.3 MiR-218*

The same analysis was performed for miR-218. 92 genes were both predictive target for miR-218 and up-regulated upon senescence. This list included the genes CCNE1 which is also a target of miR-195 and SCN2A (see Chapter 4). Only one gene namely PPARGC1A could be overlapped between the miR-218 predictive target gene list and the shRNA screen hit list. There was no overlap between the three lists.

#### *6.2.4.4 MiR-193b*

The same analysis was performed with miR-193b. 12 genes were both predictive target for miR-193b and up-regulated upon senescence. Four genes namely PPARGC1A, GRM3, KCNJ2 and WDFY2 could be overlapped between the miR-193b predictive target gene list and the shRNA screen hit list. There was no overlap between the 3 lists.

#### *6.2.4.5 MiR-186*

The same analysis was performed with miR-186. 24 genes were both predictive target for miR-186 and up-regulated upon senescence. Only three genes namely IL2, PPP4R2 and TFG could be overlapped between the miR-186 predictive target gene list and the shRNA screen hit list. There was no overlap between the three lists.

#### *6.2.4.6 MiR-423-5p*

The miR-423-5p predicted target genes were examined. Only 10 genes were both predicted target of mR-423-5p and up-regulated upon senescence. There was no overlap with the shRNA screen results.

### **6.3 EXPRESSION PROFILING OF HMF3A CELLS IN WHICH GROWTH ARREST WAS OVERCOME BY ECTOPIC EXPRESSION OF MIRS**

#### 6.3.1 Objectives

To dissect the role of micro-RNAs in cellular senescence, it was critical to identify what were their downstream targets. Are they identical or different and what are their relationships to previously identified targets with different approaches?

In order to investigate further exactly how these micro-RNAs affect gene expression and furthermore which group of genes preferentially have their expression affected upon expression of which micro-RNA and also in order to overlay these results with the list of predicted target genes, a microarray profiling analysis of the mRNA from cells expressing the various micro-RNAs which abrogated the growth arrest was designed and performed.

### 6.3.2 Microarray Strategy

To minimise sources of technical variability, each experimental condition was analyzed using biological triplicates. Specifically, three cultures were processed in parallel and mRNA was extracted from each culture, as suggested by Lee and colleagues (Lee, Kuo et al. 2000). In addition, the cultures were all derived from the same batch of HMF3A cells. All cultures were developed by abrogating growth arrest upon miRNA expression.

To identify the changes in gene expression that occur upon ectopic expression of each selected micro-RNA, triplicate independent biological samples of RNA extracted from HMF3A<sup>EcoR</sup> cells growing at 38°C for 7 days and expressing the negative control Let7a or the relevant tested micro-RNAs, were analysed by expression profiling (Figure 6.9).

This data was then compared to the 8064 differential data set described in chapter 2. The log<sub>2</sub> FC of “Let7a vs miR-X” was calculated for each of the micro-RNAs and compared to the log<sub>2</sub> FC upon senescence.

To identify genes that were differential due to the miR ectopic expression, I proceeded in a similar way that was used for the whole genome microarray analysis described in Chapter 4. Genes were considered miR targets if they were both down-regulated upon expression of a certain miR (miR-X) compared to Let7a and the difference of Log Fold Change in the gene expression between “HMF3A<sup>EcoR</sup> 38 versus 34” and “Let7a versus miR-X” was >1 or < -1 (equivalent to a +2 or -2 times fold change).

In theory, if the genes were up-regulated upon senescence and also upon expression of a certain miR, this would suggest that the miR in question does not target that specific gene and therefore down-regulation of this gene is not essential to bypass senescence. Alternatively, if the gene is up-regulated upon senescence and down-regulated upon miRNA expression, it could be concluded that expression of this gene is probably important for the growth arrest.

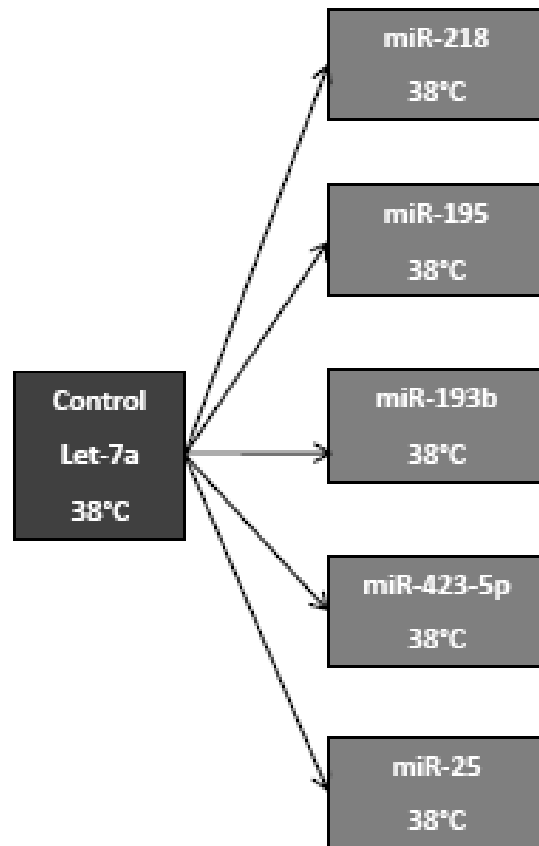


**Figure 6.9: Microarray profiling strategy of cells expressing miR-218, miR195, miR-193b, miR-423-5p and miR-25**

Triplicate independent biological samples of RNA extracted from HMF3A<sup>EcoR</sup> cells growing at 38°C for 7 days and expressing the negative control Let-7a or the relevant tested micro-RNAs were analysed by expression profiling

### 6.3.3 Microarray procedure

To perform the microarray procedure, total RNA was extracted from HMF3A<sup>EcoR</sup> cells incubated at 38°C and expressing Let7a (the reference RNA sample) or at 38°C but expressing each of the 5 miRs (miR-195, miR-423-5p, miR-25, miR-218 and miR-186). RNA was extracted from triplicate biological cultures using Trizol (Invitrogen), frozen and sent for analysis at the Memorial Sloan Kettering Cancer Centre/Ludwig Institute for Cancer Research Ltd in New York.

### 6.3.4 MiR-186

Out of 223 predicted targets actually present in the 8064 differential data set, 75 oligos corresponding to 51 genes (more than one oligo can represent the same gene) were actually down-regulated by miR-186 expression more than 0.5 Log<sub>2</sub> FC in the microarray results and 67 of these oligos corresponding to 42 genes were also differential (<-1 or >1, see above) between “HMF3A<sup>EcoR</sup> 38 versus 34” and “Let7a versus miR-X”.

Interestingly, a lot more genes were down regulated by the expression of miR-186 than the predictive target list. These could very well be secondary targets of miR-186. Among these are: BCL2L1, BTG2, GRAMD3, IL32, LTBP3, SGTB all of which have shown to rescue the cells when silenced. MiR-186 could very well be rescuing by silencing these genes.

### 6.3.5 MiR-195

Out of 631 predictive targets present in the 8064 differential data set, 159 oligos corresponding to 121 genes were actually down-regulated more than 0.5 Log<sub>2</sub> FC in the microarray results.

This list includes the genes BTG2, GRAMD3, LUZP1 and AK3L1, three of which have shown to rescue the cells when silenced with lenti-shmiRs. MiR-195 rescue could be partly due to the silencing of these genes.

Some genes were down regulated by the expression of miR-195 but are not in the predictive target list. Among these were CLCA2, IL32, LTBP3, SGTB and TXNIP, all of which have shown to rescue the cells when silenced. Rescue by miR-195 rescue could also very well be due to the silencing of these genes.

### 6.3.6 MiR-25

Out of 631 predictive targets present in the 8064 differential data set, 143 oligos corresponding to 98 genes were actually down-regulated more than a 0.5 Log<sub>2</sub> FC in the microarray results.

This list includes the genes BTG2, GRAMD3, LUZP1 and AK3L1, three of which have shown to rescue the cells when silenced with lenti-shmiRs.

Some genes were down regulated by the expression of miR-25 but do not appear in the predictive target list. Among these were RUNX1, BCL2L1, ATXN10, AK3L1, LTBP3, LUZP1, IL1 A and B, IL32, SCN2A, TXNIP.

### 6.3.7 MiR-218

Out of 476 predictive targets present in the 8064 differential data set, 142 oligos corresponding to 106 genes were actually down-regulated more than a 0.5 Log<sub>2</sub> FC. This includes SCN2A and AK3L1 which have shown to rescue the cells when silenced with lenti-shmiRs. MiR-218 rescue could be partly due to the silencing of these genes. Some genes were down regulated by the expression of miR-218 but are not in the predictive

target list. Among these were LUZP1, LTBP3, SGTB and CLCA2, GRAMD3 most of which were shown to rescue the cells when silenced.

#### 6.3.8 MiR-423-5p

Out of 59 predictive targets present in the 8064 differential data set, 13 oligos corresponding to 10 genes were actually down-regulated more than a 0.5 Log<sub>2</sub> FC. Two genes from this list, namely MAP1LC3A and MDX4, had their expression affected by all constructs that were able to bypass senescence except E1A. It is however important to note that this micro-RNA doesn't have as many predicted targets as for the others micro-RNAs studied here explaining the small gene-list that overlap with the prediction.

#### 6.3.9 MiR-372

Out of 261 predictive targets present in the 8064 differential data set, 59 oligos corresponding to 58 genes were actually down-regulated more than a 0.5 Log<sub>2</sub> FC. Interestingly, TXNIP and RUNX1 belong to this list. IL1 A and B, IL6, IL32, BCL2L1 and BTG2 were down-regulated by ectopic expression of miR-372 but do not appear on the predicted list. 337 genes are down-regulated by at least - 0.5 log<sub>2</sub> FC by all the 6 miRs including ADAMSTL1, BLNK, CLCA2, IKBKB, JAK1, MDM2, RUNX1 and SCN2A.

### **6.4 RAS INDUCED PREMATURE SENESCENCE**

#### 6.4.1 Objectives

Agami and colleagues have shown that expression of miR-372/373 in conjunction with hTERT overcomes RAS induced premature senescence (Voorhoeve, le Sage et al.

2006). The objectives were to test the 5 miRs plus miR-372 whose expression permitted the bypass of the growth arrest to see if their expression in primary fibroblasts could overcome RAS induced premature senescence.

#### 6.4.2 Strategy

5 down-regulated miRNAs plus miR-372 into primary BJ human fibroblasts in conjunction with hTERT by amphotropic retroviral infection. Cells were first selected for hygromycinB to select for transduction with hTERT and then selected with Blasticidin to isolate cells transduced with the miRNA. The cells were then challenged with inducible ER-RAS as it has been shown that expression of an activated oncogene such as RAS or RAF results in premature senescence in normal cells but transformation in most immortal cells (Elenbaas, Spirio et al. 2001; Serrano and Blasco 2001; Campisi 2005; Campisi and d'Adda di Fagagna 2007). Cells derived with hTERT alone undergo premature senescence upon challenge with these oncogenes (Morales, Holt et al. 1999) even if they are immortal as is the case in BJ cells.

This was the exact strategy used by Agami and colleagues to demonstrate that miR-372/373 immortalise human cells in conjunction with hTERT. Additional positive controls were also tested in a similar manner: WT SV40 LT, p21 shRNA, p53 shRNA, miR-372 as well as negative controls: hTERT + RAS alone or even RAS alone. Since it has been suggested that primary human fibroblast are immortalised more efficiently under low oxygen, these experiments were carried out under normal oxygen conditions to maintain stringency. An inducible version of RAS, ER-RAS (kindly provided by Dr. Jesus Gil), in which RAS expression can be turned on by adding 200nM 4OHT to the growth medium was used.



### 6.4.3 Procedure

Viral supernatants were prepared using Phoenix Ampho cells for each of the following constructs: miR-25, miR-372, miR-218, miR-193b, miR-423-5p, miR-195, WT SV40 LT, p53 shRNA, p21 shRNA. 20 µg of each of the miRs constructs were packaged whereas 10µg of the other constructs were packaged. 10µg of the ER-RAS construct was also packaged in Phoenix Ampho cells. hTERT viral supernatant was prepared from a stable TEFLYA cell line that produces hTERT virus (O'Hare, Bond et al. 2001).

BJ cells were infected with each of the above described constructs and hTERT as described in Table 6.6: 10ml viral supernatant for hTERT and 40ml of miR viral supernatant or 10ml for LT, p53 shRNA and p21 shRNA. 40ml of miR viral supernatant was used because it had been observed that the miR vectors produced low amounts of viruses. Each infection was performed as biological triplicates. The cells were then selected with hygromycin at 50 µg/ml (for hTERT alone), for at least 10 days, and then with blastocidin at 2.5 µg/ml (for miR cultures), for at least 8 days; for WT LT, p53 shRNA and p21 shRNA, cultures were selected with puromycin at 1µg/ml for at least 6 days. Control non-infected BJ cells subjected to puromycin (1µg/ml), blastocidin (2.5 µg/ml) or hygromycin (50 µg/ml) died in 4, 7 and 9 days respectively.

After selection, all cultures were infected with 10 ml of ER-RAS (Table 6.6) and selected with G418 at 0.75 mg/ ml for 10 days. Control non-infected BJ cells subjected to 0.75 mg per ml G418 died in 9 days. Immediately after infection with the ER-RAS virus, the cultures were transferred to phenol-red minus medium supplemented with charcoal stripped serum. Medium lacking phenol red was used because a lipophilic impurity contained in the phenol red has been described as a weak estrogen agonist (Berthois, Pourreau-Schneider et al. 1986). Activation was carried out by the addition of 200nM 4OHT. Due to lack of time, the growth assays upon activation of RAS were carried out by Ms. Katharina Wanek and will be presented in the following discussion.

Constructs to test	hTERT	RAS	Number of biological triplicate
none	No	Yes	3
none	Yes	Yes	3
P53 RNAi	Yes	Yes	3
P21 RNAi	Yes	Yes	3
WT LT	Yes	Yes	3
miR-372	Yes	Yes	3
miR-25	Yes	Yes	3
miR-218	Yes	Yes	3
miR-195	Yes	Yes	3
miR-193b	Yes	Yes	3
miR-423-5p	Yes	Yes	3

**Table 6.6: Layout of the primary BJ cells immortalization experiment**

Triplicate cultures of BJ primary cells were infected with the indicated constructs, hTERT and RAS as indicated above before being tested for immortalization by activating RAS.

## 6.5 DISCUSSION

### 6.5.1 Up-regulated micro-RNAs

Micro-RNAs inhibit gene expression by binding in the 3'UTR of target mRNAs with imperfect complementarity and preventing protein translation or promoting mRNA degradation. Much of the progress in understanding miRNA function to date has been from inhibition studies with antisense oligonucleotides (ASOs) or anti-miRNA oligonucleotides (AMOs). As miRNAs are small nucleic acids, only 19–24 nucleotides in length, ASO inhibition is considered the best and possibly the only practical approach for specific pharmacological inhibition of their function (Esau 2008). ASOs targeting mRNAs have been widely used to evaluate gene function *in vitro* and *in vivo* (Stepkowski, Qu et al. 2000; Zellweger, Miyake et al. 2001; Watts, Manchem et al. 2005; Lee, Dunham et al. 2006) and several antisense therapeutics are currently undergoing clinical trials .

More recently, modified AMOs were created with the dual purpose to stabilize their own structure and to improve their affinity for their targets. Locked nucleic acid (LNA), for example, give very strong duplex formation with their target sequences and they display excellent mismatch discrimination, hence avoiding off-target effects (Esau 2008; Mattes, Collison et al. 2008). A third generation of antisense oligonucleotides are phosphoramidate morpholino oligomers (PMO) in which the ribose ring is replaced with a morpholine ring (Spurgers, Sharkey et al. 2008). Krützfeldt *et al.* linked a cholesterol moiety to their AMOs and referred to these anti-miRNAs as antagomiRs. AntagomiRs should be >19 nucleotides in length to provide highest efficiency in silencing target miRNA (Krutzfeldt, Rajewsky et al. 2005). The putative therapeutic potentials of antagomiRs were recently demonstrated in treatment of lipid metabolic disease in animals (Esau, Davis et al. 2006). Another alternative class of AMOs is peptide nucleic acids (PNA), which are synthetic oligonucleotides with N-(2-aminoethyl)-glycine replacing ribose backbone (Fabani and Gait 2008). Finally, another

approach in silencing miRNA is the use of so-called micro-RNA sponge, a synthetic mRNA that contains multiple binding sites for a particular miRNA and that is transcribed from a plasmid containing a strong promoter (Mattes, Collison et al. 2008). In conclusion, different classes of AMO have been shown to be efficient in silencing miRNA and may be useful therapeutic tools.

In this case, it would have been interesting to validate the effect of the up-regulated micro-RNAs by inhibiting those individually using antagomiRs or LNAs. They can be introduced into cells using transfection or electroporation parameters similar to those used for siRNAs, and enable a study of miRNA biological effects. However since they can only be used in short term and since, the assay is a long-term one, and due to a lack of time and an obligation to prioritise, I focussed on the down-regulated miRs, as the effects of micro-RNAs are to silence gene expression; I expected that the down-regulated miRs would target genes up-regulated upon growth arrest and also targets identified from the shRNA screen. The 18 up-regulated miRs were still important and it was possible to note, notably, among the up-regulated targets, 34a which has described extensively in the last few years and been previously linked to cancer, apoptosis and growth arrest.

#### *6.5.1.1 MiR-34a*

MiR-34a expression has been found to be reduced in human epithelial ovarian cancers (EOC); moreover, miR-34 reconstitution in p53 mutant EOC cells resulted in reduced proliferation, motility, and invasion (Corney, Hwang et al. 2010). These are consistent with the data that miR-34a was up-regulated upon growth arrest. Ectopic expression of miR-34 has also been shown to induce apoptosis, cell-cycle arrest or senescence.

MiR-34a is a known direct transcriptional target of p53, so it is not surprising that when LT is inactivated and p53 activated upon temperature shift that miR-34a is also increased.

In a recent study, the expression of miRNAs in primary human TIG3 fibroblasts after constitutive activation of B-RAF was examined. Amongst the regulated miRNAs, both miR-34a and miR-146a were strongly induced upon senescence indicating that miR-34a was regulated independently of p53 during oncogene-induced senescence. Up-regulation of miR-34a was mediated by the ETS family transcription factor, ELK1 (Christoffersen, Shalgi et al. 2010). This totally corroborates the results of the microarray which placed miR-146a as the top up-regulated miR and miR-34a the second. Interestingly, miR-154, miR-376 and miR-495 are also up-regulated in both my and the Christoffersen study.

It has been shown that miR-34a regulates silent information regulator 1 (SIRT1) expression. MiR-34a inhibits SIRT1 expression through a miR-34a-binding site within the 3' UTR of SIRT1. This inhibition of SIRT1 leads to an increase in acetylated p53 and expression of p21 and PUMA, transcriptional targets of p53 that regulate the cell cycle and apoptosis, respectively (Yamakuchi, Ferlito et al. 2008). This is consistent with my finding that while miR-34a is up-regulated 3.71 log<sub>2</sub> FC upon senescence (Table 4.3), SIRT1 was down-regulated by 1.19 log<sub>2</sub> FC (chapter 2).

This also in agreement with my finding that SIRT1 ectopic expression bypassed senescence in CL3<sup>EcoR</sup> cells (See Chapter 4).

Additionally, in a recent study, cellular senescence was shown to be induced by nutlin-3a, an MDM2 inhibitor, in normal human fibroblasts. Nutlin-3a acts by up-regulating the expression of miR-34a, miR-34b, and miR-34c through the activation of p53 and the repression of ING2 (inhibitor of growth 2) (Kumamoto, Spillare et al. 2008).

#### *6.5.1.2 MiR-146a*

The most highly up-regulated miR is miR-146a with a Log<sub>2</sub> fold change of 4.33 which is more than 20 times the expression it has in growing cells. Recently, miR-146a expression has been shown to be up-regulated by IL-1 $\beta$  (Perry, Williams et al. 2009) which is one of the top up-regulated genes upon senescence (Chapter 4, Table 4.1B). MiR-146 has also been reported to be up-regulated by Breast cancer metastasis

suppressor 1 (BRMS1), a predominantly nuclear protein that differentially regulates expression of multiple genes, leading to growth arrest and suppression of metastasis (Hurst, Xie et al. 2009). The link between miR-146a up-regulation and growth arrest in the Hurst study is in agreement with my results. In addition, miR-146 was also found to be an NF- $\kappa$ B dependant gene (Taganov, Boldin et al. 2006) which is consistent with the activation of NF- $\kappa$ B signalling having a causative role in promoting cellular senescence. Interestingly, Bhaumik *et al* (Bhaumik, Scott et al. 2008) have suggested that miR-146a/b can act as a negative regulator of NF- $\kappa$ B activity in Breast Cancer cells. Taken together, these results suggest that there may be an autoregulation loop where NF- $\kappa$ B activates miR-146 which then suppresses NF $\kappa$ B activity.

### 6.5.2 Down-regulated micro-RNAs

Expression profiling indentified 15 micro-RNAs that were down-regulated upon senescence (Table 6.5). Many of them were up-regulated upon quiescence. These down-regulated micro-RNAs and their importance in the senescence process were, when available for ectopic expression, functionally analysed in the HMF3A cell system by constitutive expression and followed by growth complementation assay.

12 of these miRs plus an extra 6 miRs were chosen for ectopic expression in a complementation assay and some of them yielded large numbers of growing colonies by promoting cell growth namely miR-195, miR-25, miR-193b, miR-186, miR-218 and miR-423-5p.

#### 6.5.2.1 MiR-25

Replicative senescence was shown *in vitro* to be associated with the decrease of miR-15b and miR-25 among others in an HDF model. This decrease was shown to elicit the increase of MKK4 a pivotal upstream activator of c-Jun N-terminal kinase and p38 which are essential to the induction of cellular senescence (Marasa, Srikantan et al. 2009). This data is in accordance with my results that miR-25 is down-regulated upon

cellular senescence. Loss of miR-25 expression in the HMF3A cells could result in an increase of MKK4 leading to induction of senescence and thus ectopic expression of miR-25 would lead to down-regulation of MKK4. However, MKK4 (or MAP2K4) is not one of the predicted targets of miR-25 and is not present amongst the genes found to be up-regulated suggesting that in the HMF3A cells, modulation of MKK4 expression is unlikely to be the mechanism by which senescence is triggered.

Furthermore, miR-25 has also been reported down-regulated in ASM (Airway smooth muscle) cells exposed to IL-1 $\beta$  (Kuhn, Schlauch et al. 2010). This is consistent with my finding that IL-1 $\beta$  was one of the top up-regulated genes upon senescence and miR-25 was also down-regulated (Chapter 4, Table 4.1B) (Table 6.5). MiR-25 may be down-regulated by the increase in IL-1 $\beta$ . But, this would imply that miR-25 is downstream of the activation of the NF- $\kappa$ B pathway. I have shown here that miR-25 down-regulation was causal to senescence because it can be bypassed upon ectopic expression of miR-25. In addition, IL-1 $\alpha$  and IL-1 $\beta$  are both down-regulated by the expression of miR-25. Therefore, miR-25 cannot be considered as merely a consequence of the regulation of IL-1 $\beta$  upon senescence but as part of a pathway, maybe a negative loop of modulation necessary to activate the growth arrest.

The miR-106b-25 polycistron, which is located within the 3'UTR of the MCM7 transcript, was recently reported to exert potential proliferative, anti-apoptotic, cell cycle-promoting effects *in vitro* and tumourigenic activity *in vivo*. In this study, miRs-93 and -106b targeted and inhibited p21<sup>CIP1/WAF1/Sdi1</sup>, whereas miR-25 targeted and inhibited the pro-apoptotic factor Bim.

This polycistron was shown to be up-regulated progressively at successive stages of neoplasia, in association with genomic amplification and over-expression of MCM7 (Kan, Sato et al. 2009). This is accordance to my finding that miR-25 is down-regulated upon senescence (Table 6.5) and that its ectopic expression promotes cell growth (Figure 6.4 A and B, 6.5, 6.6B, 6.7C and 6.8B). In addition, MCM7 is also down-regulated upon

senescence by 1.4 log<sub>2</sub> FC in the HMF3A<sup>EcoR</sup> cells and becomes up-regulated when senescence is overcome probably resulting in an increase in miR-25 expression.

#### 6.5.2.2 *MiR-195*

MiR-195 expression has been linked in several studies to Cancer and tumorigenesis. In a recent study, cancer-specific miRNAs significantly altered in the circulation of breast cancer patients were detected and increased systemic miR-195 levels in breast cancer patients were reflected in breast tumours. Furthermore, circulating levels of miR-195 and Let7a were shown to decrease in cancer patients postoperatively, to levels comparable with control subjects, following curative tumour resection (Heneghan, Miller et al. 2010) suggesting that expression of miR-195 is strongly involved in the development and maintenance of Breast Cancers. This is in accordance with my findings that miR-195 is down-regulated upon senescence (Table 6.5) and that its ectopic expression promotes cell growth (Figure 6.4B, 6.5, 6.7A and B and 6.8 A and B).

Another study recently found that perturbation of the miRNA pathway function in human embryonic stem cells (hESCs) by RNA interference-mediated suppression of DICER and DROSHA, 2 proteins essential in the biogenesis of all miRs, attenuates cell proliferation. In this study, normal cell growth can be partially restored by introduction of the mature miR-195 and miR-372 which regulate two tumour suppressor genes: WEE1, a negative G2/M kinase modulator of the CycB/CDK complex and CDKN1A, which encodes p21<sup>CIP1/WAF1/Sdi1</sup>, the cyclin dependent kinase inhibitor. WEE 1 levels control the rate of hESC division, whereas p21<sup>CIP1/WAF1/Sdi1</sup> levels must be maintained at a low level for hESC division to proceed (Qi, Yu et al. 2009). These data support the result that introduction of miR-195 is sufficient to bypass senescence in HMF3A cells (Figure 6.4B, 6.5, 6.7A and B and 6.8 A and B). However, these results are contradictory to my results indicating that WEE1 was actually down-regulated upon senescence and gets up-regulated when senescence is overcome including with the ectopic expression of miR-195. This suggests that miR-195 may not directly target WEE1 and utilise a different pathway.



### 6.5.2.3 MiR-218

In a recent study, miR-218 expression was shown to be reduced significantly in gastric cancer tissues, in *H. pylori*-infected gastric mucosa, and in *H. pylori*-infected AGS cells. In the same study, over-expression of miR-218 inhibited cell proliferation and increased apoptosis *in vitro* (Gao, Zhang et al. 2010). Epidermal growth factor receptor co-amplified and over-expressed protein (ECOP), which regulates NF- $\kappa$ B transcriptional activity and is associated with apoptotic response. NF- $\kappa$ B transcriptional activation and the transcription of ECOP and cyclo-oxygenase-2 (COX2), a proliferative gene regulated by NF- $\kappa$ B, were all described to be targets of miR-218 (Gao, Zhang et al. 2010). This suggests that upon expression of miR-218, the NF- $\kappa$ B pathway, ECOP and COX2 expression should be down-regulated. In addition, COX2 expression had been previously described as linked with an increased risk of bladder cancer and prostate cancer (Kang, Kim et al. 2005) and its inhibition was shown to promote growth arrest in colon cancer cells and prostate cancer cells (Grosch, Tegeder et al. 2001; Narayanan, Narayanan et al. 2006). It would be, therefore, logical for COX2 to be down-regulated upon growth arrest.

MiR-218 was also shown to be involved in cervical carcinogenesis. Its expression was down-regulated in HPV-positive cell lines, cervical lesions and cancer tissues containing HPV-16 DNA compared to both C-33A and the normal cervix. It was also shown that the epithelial cell-specific marker LAMB3 is a target of miR-218 and that LAMB3 expression was increased in the presence of the HPV-16 E6 oncogene through miR-218 modulation (Martinez, Gardiner et al. 2008).

These results are completely contradictory with the data that miR-218 was down-regulated by  $-1 \log_2$  FC upon growth arrest (Table 6.5) and that its ectopic expression promoted cell growth (Table 4.6A, B and C). In addition, expression of miR-218 does not seem, in this case, to inhibit the NF- $\kappa$ B pathway as it is described in the Gao paper, as downstream targets of NF- $\kappa$ B such as IL-1A, IL1-B, IL-8, BMP2 and SOD2 are up-regulated in cells expressing miR-218 as shown in the microarray analysis. NF- $\kappa$ B pathway was activated upon growth arrest but not reversed by miR-218 expression and

neither ECOP nor COX2 (or PTGS2) nor LAMB3 expression varied upon growth arrest. This suggested that modulation of ECOP, COX2 and LAMB3 through miR-218 modulation was unlikely to be the mechanism by which senescence was triggered and that modulation of NF- $\kappa$ B was not essential for abrogation of the growth arrest through miR-218 expression.

#### *6.5.2.4 MiR-193b*

The literature is not clear with respect to the regulation of miR-193b expression. In one study, miR-193b was proposed to be up-regulated in Hepato-cellular cancer (HCC). In this study, HepG2 malignant hepatocytes were stably transfected with full-length HCV genome (Hep-394) or an empty vector (Hep-SWX) and micro-RNA expression profiling performed on both cell types. MiR-193b was shown to be over-expressed 5-fold in Hep-394 cells compared to the control and to target Mcl-1, an anti-apoptotic protein (Braconi, Huang et al. 2010).

In three other studies, however, miR-193b was reported to be down-regulated in cancer. One study looked at the miRNA expression profile in 10 pairs of endometrioid adenocarcinoma and adjacent non tumourous endometrium and found that miR-205, miR-449, and miR-429 were greatly enriched whereas miR-204, miR-99b, and miR-193b were greatly down-regulated in adenocarcinoma tissues (Wu, Lin et al. 2009). In another study, miR-193b was also down-regulated in clinical prostate cancer samples compared to benign prostatic hyperplasia. In this study, in addition, it was shown that expressing miR-193b in 22Rv1 cells using pre-miR-193b oligonucleotides caused a significant growth reduction ( $p < 0.001$ ) resulting from a decrease of cells in S-phase of the cell cycle ( $p < 0.01$ ). The authors even proposed that miR-193b could be an epigenetically silenced putative tumour suppressor in prostate cancer (Rauhala, Jalava et al. 2010). Expression of miR-193b was also shown to be down-regulated during breast cancer cell metastasis (Li, Yan et al. 2009). It is possible that the observed differences are due to the type of cancer, cell line/tissue and the context.

In our HMF3A cells, miR-193b shows a down-regulation upon senescence (Table 6.5) and its ectopic expression promotes cell growth and bypasses senescence (Figure 6.5 and 6.8A and B).

Since senescence bypass with miR-193b was weaker than with the other miRs, cells expressing miR-193b were not profiled by microarray analysis, so it was not determined what changes in expression were caused by miR-193b expression.

MCL-1, which was a proposed direct target of miR-193b in the Rauhala study, was not modulated upon growth arrest which suggests that its modulation is not the cause of neither the abrogation nor the trigger of growth arrest.

#### *6.5.2.5 MiR-186*

MiR-186 has been found to be significantly up-regulated in most pancreatic cancer tissues and cell lines, in conjunction with seven others miRs: miR-196a, miR-190, miR-186, miR-221, miR-222, miR-200b, miR-15b, and miR-95 (Zhang, Li et al. 2009). Levels of miR-186 and miR-150 were also reported to be higher in cancer epithelial cells than in normal cells. This study also showed that increased expression of miR-186 and miR-150 in cancer epithelial cells decreases P2X7 mRNA by activation of miR-186 and miR-150 instability sites located at the 3'-UTR-P2X7. Indeed, treatment with inhibitors of miR-186 and miR-150 increased P2X7 mRNA level (Zhou, Qi et al. 2008).

These results are in accordance to my findings that miR-186 expression is down-regulated upon senescence (Table 6.5) and that its ectopic expression bypasses the growth arrest (Table 6.5 and 6.8A and B). The levels of P2X7, however, do not vary upon senescence or upon rescue, which suggest that its expression does not play a major role in the senescence pathways.

#### *6.5.2.6 MiR-423-5p*

A recent study investigated the significance of miRNAs in patients with locally advanced head and neck squamous cell carcinoma and found miR-423, miR-106b, miR-20a, and miR-16 to be up-regulated and miR-10A to be down-regulated.(Hui,

Lenarduzzi et al. 2010) This is in accordance with my finding that miR-423 is down-regulated upon senescence (Table 6.5).

However, another study carried out to analyze the miRNA expression profile of 17 malignant mesothelioma samples using miRNA microarray has obtained contradictory results. Malignant mesothelioma (MM) is an aggressive cancer arising from mesothelial cells, mainly due to asbestos exposure. MiR-423 was found to be down-regulated in tumour samples compared with normal sample along with miR-34a (Guled, Lahti et al. 2009).

Although the miR-34a results are in accordance with my data, the miR-423-5p results are contradictory. However, after careful reading of the Guled paper, it was noted that at two different places miR-423 was replaced by miR-429 and thus it remains to be verified exactly which miRNA is down-regulated.

### 6.5.3 Expression profiling of HMF3A cells in which senescence has been bypassed by ectopic expression of miRs

An interesting fact is that when looking at the top up-regulated genes upon senescence, mostly, the genes were down-regulated upon rescue by abrogation of the pRb pathway, the p53 pathway or expression of miRs. However, some genes stood out because they were also up-regulated by the expression of 3 to 4 miRs namely miR-186, miR-195, miR-218 and miR-423. Among these are IL-1A, IL-1B (with 2 different oligos), BMP2, CEBPD, SOD2, IL-15RA, IL-6, CCL20, CSF2, RAB27B, BIRC3, DUSP6 all of which are either direct targets of NF- $\kappa$ B or linked to the activation of NF- $\kappa$ B. This suggests that the down-regulation of NF- $\kappa$ B may not be necessary in the rescue with the miRs miR-186, miR-195, miR-218 or miR-423. Therefore maybe these four micro-RNAs use a different pathway to bypass senescence than miR-25 or miR-372.

It is also interesting to note from the results of the microarrays with all miRs, that the miR-372 expressing cells expression pattern was very different to that of miR-186, miR-

25, miR-195, miR-423-5p and miR-218. For example, when looking at the list of the top genes down-regulated by miR-195 expression, it was possible to see a large majority of the targets expression were regulated identically by the others 4 miRs mentioned by were either up-regulated or not regulated by miR-372. It is also possible to note that among these first 100 targets several were actually NF- $\kappa$ B targets such as SOD2, SFS2, IL1A and B, CCL20, CEBPD, IL6 and IL8.

When overlapping all the miRs results, it was observed that ADAMTSL1 is a confirmed target of 4 miRs out of 6 and is down regulated by all 6 miRs. There are actually 337 genes that are down-regulated by all 6 miRs including CLCA2, IKBKB and MDM2.

#### 6.5.4 Expression of the miRs in 226L cells

226L8/13 cells correspond to human breast epithelial cells which have been immortalized by introducing into them the U19tsA58 LT and hTERT that were used to derive the HMF3A cells.

In an analogous manner to the HMF3A cells, these cells are immortal at 34°C but stop dividing upon inactivation of SV40 LT antigen at 38°C. These cells are used by Katharina Wanek for her thesis and she has prepared clones of these cells by stably infecting them with the murine ecotropic receptor and identified clone #7 cells as clonal cell line for identifying senescence pathways. These cells responded to abrogation of the p53 or pRb pathway in a similar manner to the one of the HMF3A, by bypassing the growth arrest.

After my results of the miRs expression with the HMF3A cells, it was interesting to test the same constructs in the mammary epithelial cell line to see if their action was only limited to fibroblasts. The 226L cells were transduced with the miRs-vectors miR-25, miR-218, miR-193b, miR-423-5p, miR-186, miR-186 as well as miR-372 and miR-373 as positive controls and miR-15a and Let7a as negative controls respectively. The cells

were selected for expression, then shifted to the non permissive temperature for 3 weeks and stained as for the HMF3A protocol.

The results obtained by Katharina Wanek (Figure 6.10) show similar results for all of the miRs tested apart from miR-193b and miR-186 which did not display any rescue. The positive controls miR-372 and miR-373 expression show very good cell growth with many growing (blue coloured) colonies and there is very little background in the negative controls, Let7a and miR-15a. MiR-373, surprisingly, works better than miR-372 in the 226L epithelial cells which is the opposite in the HMF3A fibroblasts. This variation could be due to the cell type.

The most efficient miR expression here seems to be miR-195 which corroborates my own results followed by miR-25, miR-218 and miR-423-5p. MiR-195 show less colonies than miR-373 but they are much darker and larger probably suggesting that they are growing faster. The reduced number of colonies is, however, not due to reduced infection since stably transduced cells were reseeded.

These results reinforce the idea that these 4 miRs are important effectors with a direct causality in the gene regulation changes that happen during senescence. It also means that miRs involvement in senescence is not limited to a certain cell type. There may be slight differences between epithelial cells and fibroblasts but the same sorts of miRs seem to be functional.

#### 6.5.5 RAS transformation of primary cells

This experiment is discussed here as it took months to optimise and for timescale reasons, the final growth assays were performed by Katharina Wanek.

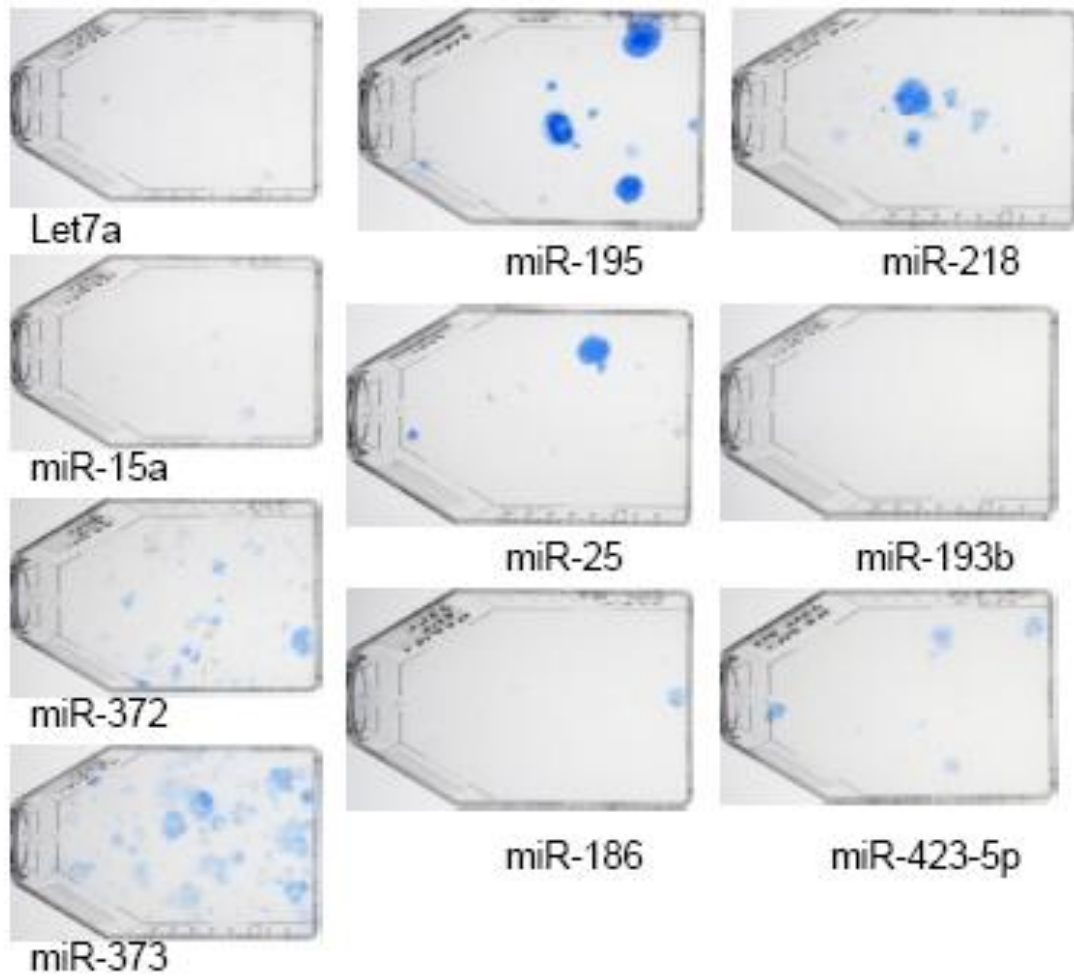


**Figure 6.10: Ectopic expression of micro-RNAs in human breast epithelial cells**

226L cells were infected in triplicate with retrovirus expressing the indicated miRs expression constructs and assayed for growth complementation at 38°C in T-75cm<sup>2</sup> flasks. After 3 weeks the flasks were stained and photographed.

In this experiment, miR-Vectors capable of ectopically expressing each of the 6 down-regulated miRNAs were introduced by retroviral delivery (Ampho) into primary BJ human fibroblasts in conjunction with hTERT. Cells were selected hTERT and the miRNAs before being transduced with inducible ER-RAS. Positive controls included WT LT, p21 shRNA, p53 shRNA and miR-372 and negative controls included hTERT + RAS alone or even RAS alone. The cells were then grown for 7 days in medium containing 200nM 4OHT as in to activate the expression of RAS. Then the cells were reseeded in 96 well plates in triplicate for the growth assay. The cells were counted at day 1, day 5 and day 7.

As the infection were already done in biological triplicate and the cell count was done in triplicate for each cell flask condition, there was 9 results per condition in total and the data looked surprisingly tight for a tissue culture results.

At day 5, it was already possible to see a large difference between p53 shRNA, WT LT and miR-372 positive control and the rest of the cells with about 70% more cells in average in these three cultures than the rest.

At day 7, the difference was even more pronounced. The curve with RAS alone remained flat and the cells became growth arrested and displayed a senescence like phenotype. This is in accordance with the Gil lab that kindly provided us with the ER-RAS construct that RAS expression causes premature senescence in BJ cells (Barradas, Anderton et al. 2009).

RAS + hTERT expressing cells registered a big decrease in their growth rate and looked arrested, however the numbers were higher than with RAS alone, suggesting that hTERT provides a boost to the cell growth. This is not surprising since hTERT immortalizes BJ cells.

Surprisingly, p21 shRNA expressing cells did not seem to grow at a better rate than hTERT + RAS expressing cells even though it is one of the best candidates for



bypassing senescence in the HMF3A cells. The p53 shRNA derived cells were resistant to the RAS effect and continued to divide.

In human, some studies have shown that inactivation of p21<sup>CIP1/WAF1/Sdi1</sup> alone was sufficient to bypass OIS (oncogene-induced senescence). A recent study showed that siRNA-mediated knockdown of p21<sup>CIP1/WAF1/Sdi1</sup> rescues from Ras-induced senescence in human mammary epithelial cells (HMECs) (Borgdorff, Leonart et al. 2010). This is in contradiction with my findings. In addition, inhibition of p21<sup>CIP1/WAF1/Sdi1</sup> expression in BJ foreskin human fibroblasts also resulted in RasG12V-resistant growth (Voorhoeve, le Sage et al. 2006). However, another study showed that, like in our case, inactivation of p21<sup>CIP1/WAF1/Sdi1</sup> alone in LF1 human lung fibroblasts could not bypass RasG12V-induced senescence unless p16<sup>INK4a</sup> was inactivated as well (Wei, Herbig et al. 2003).

In mice, my results are in accordance with the findings of the Serrano lab (Pantoja and Serrano 1999) that p21-deficient murine fibroblasts are not efficiently transformed by oncogenic Ras, and this is in contrast to p53<sup>-/-</sup> equivalent cells that are efficiently transformed, indicating that p21<sup>CIP1/WAF1/Sdi1</sup> is not essential for the anti-proliferative response induced by moderate levels of oncogenic Ras, and that p21-deficient fibroblasts are refractory to transformation. Regarding other cell types different than fibroblasts, it should be mentioned that there are conflictive reports about the susceptibility of p21-deficient keratinocytes to be transformed by oncogenic Ras (Missero, Di Cunto et al. 1996; Weinberg and Yuspa 1997). Missero reports that primary keratinocytes derived from p21<sup>CIP1/WAF1/Sdi1</sup> knockout mice, can be transformed with a ras oncogene while Weinberg reports the contrary. The mice were from different strains and I can hypothesize that the genetic context might be of importance. It can be concluded from this discordant results that p21<sup>CIP1/WAF1/Sdi1</sup> silencing is not always sufficient along with hTERT expression to overcome RAS induced premature senescence and that it is likely to depend upon the genetic context, the cell type, and the organism type.

It was surprising that p21<sup>CIP1/WAF1/Sdi1</sup><sup>-/-</sup> cells did not transform with RAS like in the Voorhoeve paper but underwent growth arrest. The p53 silenced cells, however, did transform with RAS indicating that even though in terms of abrogating growth arrest in the conditional immortal cells, p21<sup>CIP1/WAF1/Sdi1</sup><sup>-/-</sup> cells behaved the same as p53<sup>-/-</sup>, in case of the primary cells, they are not the same. This suggests that p53 has others targets in addition to p21<sup>CIP1/WAF1/Sdi1</sup>.

Ectopic expression of miR-372 overcame Ras induced senescence in conjunction with hTERT and resulted in the cells being transformed. This is in accordance with the data published by Voorhoeve *et al.*

Preliminary evidence suggests that only the miR-423-5p expressing cells continued dividing at a growth rate above hTERT reconstituted BJ cells. The remainder stopped dividing. Further experiments are now underway to confirm this finding.

Although miR-423-5p was the only micro-RNA able to overcome RAS induced premature senescence in BJ cells, it does not mean that it is more important than the other miRs in the senescence process but it follows a different pathway than the others, a pathway shared with p53 or LT. Indeed, p21<sup>CIP1/WAF1/Sdi1</sup> which is a very important effector in the senescence process could not overcome Ras induced senescence in these cells either (Brown, Wei et al. 1997; Wei and Sedivy 1999).

#### 6.5.6 Further work

An important question would be to determine what is causing the change in expression of the miRNAs. The regulation could be at the level of transcription or at the level of processing. For example, miR-25 belongs to the miR-106b-25 cluster of three miRNAs derived from the MCM7 transcript (Tanzer and Stadler 2004)( [www.miRbase.com](http://www.miRbase.com)); MCM7 is down-regulated >2 fold upon HMF3A growth arrest. In our HMF3A cells, miR-25 was down-regulated >2 fold whereas miR-106b and 93 were not significantly

down-regulated. Their processing might therefore be regulated differently. The regulation could also be at the level of transcription since miRNAs are transcribed by RNA Polymerase II and thus it will be important to identify the transcription factors involved. For example, Mcm7 expression has been proposed to be E2F dependent (Suzuki, Okuyama et al. 1998; Bruemmer, Yin et al. 2003) but I have also found it be modulated by p53 as well as p21<sup>CIP1/WAF1/Sdi1</sup> in the HMF3A cells upon growth arrest. So what regulates MCM7 expression in cellular senescence?

However, the main question would be to focus on the miR-423-5p. It was differential in the HMF3A upon growth arrest; its ectopic expression bypassed growth arrest. It also overrides Ras induced premature senescence in primary BJ cells. The next step could be to try to dissect the details of what makes the difference compared to the other miRNAs in the transformation of primary fibroblasts. It would be interesting as well to look at the gene expression and protein levels of members of the senescence pathway such as p53, p21<sup>CIP1/WAF1/Sdi1</sup>, pRb but also effectors of the NF- $\kappa$ B pathway in cells expressing miR-423-5p.

## **7 SUMMARY AND FINAL DISCUSSION**

Cellular senescence is an irreversible program of cell cycle arrest that normal cells undergo both *in vitro* and *in vivo* in response to a variety of intrinsic and extrinsic stimuli. Senescence is associated with organismal ageing as it promotes the disruption of tissue renewal and repair processes as well as the depletion of progenitor cell populations. Senescence also represents an important tumour suppressive mechanism that limits the growth capacity of potentially cancerous cells. Bypass of senescence therefore represents a mechanism by which cells can overcome finite proliferative potential, one of the six proposed hallmarks of cancer cells (Hanahan and Weinberg 2000).

In conjunction with hTERT, LT can immortalise many human cells including primary human fibroblasts by inactivating the p53-p21 and p16-pRB tumour suppressor pathways. Consequently, the generation of a thermolabile mutant of LT, U19tsA58, led to the development of a conditionally immortalised human mammary fibroblast cell model, HMF3A (O'Hare, Bond et al. 2001). HMF3A cells and its clonal derivative, CL3<sup>EcoR</sup> cells, grow at 34°C, but undergo an irreversible growth arrest within 5 days upon temperature shift to 38°C. Since telomerase remains constitutively active in these cells at both 34°C and 38°C, the growth of HMF3A cells is entirely dependent upon LT activity suppressing p53 and pRb activities.

Previously, Hardy *et al* (2005) have carried out a 6000 genes microarray analysis to identify changes that occur upon induction of irreversible growth arrest in the HMF3A cells and found that some of the changes in expression directly correlated with the transcriptional changes that are induced upon replicative senescence in normal human mammary fibroblasts.

Moreover, RNA interference and *in silico* analysis had indicated an important role for the p53, pRb and NF-κB signalling pathways in this process.

## 7.1 SUMMARY OF RESULTS

The main goal of this thesis was to profile the expression changes upon senescence in order to find new targets which would help to dissect the senescence pathways and then to analyse them in detail.

Since the cells growth-arrest in a synchronous manner, I have used Affymetrix expression profiling to identify the genes differentially expressed upon senescence. This identified 816 up- and 961 down-regulated genes whose expression was reversed when growth arrest was abrogated. Overlay of this data set with the meta-signatures of genes up-regulated in cancer showed that 50% of them were down-regulated upon senescence. Remarkably, 65 of the up- and 26 of the down-regulated genes are known downstream targets of NF- $\kappa$ B indicating that senescence may be associated with activation of the NF- $\kappa$ B pathway. Perturbation of this pathway by direct silencing of NF- $\kappa$ B subunits, by positive and negative upstream modulation, or by expressing the super repressor of NF- $\kappa$ B, can overcome growth arrest indicating that activation of NF- $\kappa$ B signalling has a causal role in promoting senescence.

Moreover, this activation of NF- $\kappa$ B upon senescence could also be the cause of the down-regulation of FOXM1 and E2F and consequently of their downstream targets that are critical for cell cycle progression particularly in the G2 phase.

At the same time, I also applied a retroviral shRNA screen covering ~10,000 genes to the same CL3<sup>EcoR</sup> cell model. Overlapping these results with the microarray data revealed particularly interesting targets, such as LTBP3, LAYN, SGTB, TMEM9B and ATXN10 which were both up-regulated upon senescence and able to bypass growth arrest when silenced by shRNA expression.

I also profiled micro-RNA expression. 15 of the top micro-RNAs down-regulated upon senescence were chosen for ectopic expression in the HMF3A cells. MiR-25, miR-423-5p, miR-218, miR-186, miR-193b and miR-195 upon ectopic expression were able to

bypass the growth arrest. Subsequently, these micro-RNAs were introduced into BJ human primary fibroblasts along with hTERT and activated RAS and miR-423-5p only was found to bypass RAS induced senescence.

In conclusion, my work has uncovered novel markers involved in senescence as well as identifying that both activation of p53-p21 and p16-pRB pathways results in activation of NF- $\kappa$ B signalling which promotes senescence. Both results lead to a better understanding of senescence and the underlying signalling pathways.

## **7.2 FUTURE DIRECTIONS**

Due to the time constraints and multiple aspects of the project, not all candidate genes identified by the different experimental approaches were functionally validated. Instead, a prioritisation of the identified targets was made and only a few were chosen for further investigation. For each of these targets, ectopic expression or silencing by RNAi was employed to complement the conditional growth of HMF3A<sup>EcoR</sup> or CL3<sup>EcoR</sup> cells. Upon confirmation of this activity, experimental analysis should be extended to primary human fibroblasts and other primary human cells, similarly to the experiment with the micro-RNAs. Since activities of each these genes may be impaired in different tumour types, expression could also be analysed in a variety of primary human tumours and cancer cell lines.

### **7.2.1 Saturation of shRNA screen in CL3<sup>EcoR</sup>**

The RNAi screen (see Chapter 3) should be performed on a much larger scale, as there was substantial evidence to suggest that the screen was performed under non-saturating conditions. Using a higher volume of virus and a higher concentration of antibiotics for selection could also ensure higher expression level of the inserts and perhaps the expression of shRNA that were not sufficiently expressed in our screen.

Although improvements in shRNA technology will be required to perform fully saturating loss-of-function screen, the development of multiple fully validated shRNA libraries coupled with the interrogation of a larger number of cell lines would permit saturating genetic screens.

### 7.2.2 Secondary shRNA screen

The primary shRNA screen uncovered 111 different genes and another 30 inserts corresponding to unidentified loci. Most of these targets were not investigated since they did not overlap with the microarray data. However, it is always possible that some targets could be activated without having their mRNA levels affected for example by loss of an upstream inhibitor.

To address this issue, a secondary screen should be performed (as suggested in Chapter 3) with the Lentiviral shMirs library on these 111 genes to functionally validate the primary screen and eliminate false positives. This would identify any genes whose expression or activation was causal to senescence.

### 7.2.3 Ectopic expression validation by protein analysis

Ectopic expression of genes found to be down-regulated upon senescence was not verified for all constructs and therefore it was not possible to conclude whether expression of HMGB2, DEPDC1, MELK and NEK2 would bypass senescence. It would be very valuable to find antibodies that can specifically identify protein expression for these genes and determine whether differential microarray expression correlates with differential expression at the protein level.

Similarly, for the shRNA silencing, it would be good practice to verify that silencing induces changes in the protein expression.

Alternatively, if these constructs do not give a satisfactory level of expression, other constructs could be designed and prepared for use in the CL3<sup>EcoR</sup> cells.

Despite any protein expression evidence, the possibility that LT-mediated negative regulation of cellular proteins may have occurred in the HMF3A system cannot be discounted. This is a particularly important point to consider when determining the effectiveness of expression knockdown by shRNAi; down-regulation of expression by shRNA was performed for TRIB2, GRAMD3, CDKN2A, RUNX1, BLCAP, SCN2A, CLCA2 and AK3L1 but the corresponding protein levels have not been assessed. Also, whilst the results of the shRNA screen were validated for 5 targets by using multiple shRNA constructs for each gene, again protein levels were not verified. By extension therefore, it is possible that stable proteins may not be identified by functional screens, such as RNAi screens. Therefore, it may be important to consider the utilisation of alternative strategies to specifically target protein activity such as short peptide inhibitors or dominant-negative peptides (for example, GSEs).

#### 7.2.4 FOXM1

FOXM1 was one of the most highly down-regulated gene upon senescence in the microarray data. This was also supported by our finding that constitutively active FOXM1 abrogated senescence in the CL3<sup>EcoR</sup> cells. Moreover, in another study, acute activation of NF- $\kappa$ B was shown to trigger growth arrest (Penzo, Massa et al. 2009) along with repression of FOXM1 and genes associated with transit through G2 phase. This makes FOXM1 a target of choice to study in understanding senescence pathways and the involvement of NF- $\kappa$ B signalling.

##### *7.2.4.1 Which spliceform is important?*

At the expression level, it would be interesting to find out exactly whether the 3 FOXM1 spliceforms are all down-regulated upon senescence and whether the level of



down-regulation is similar for all three. The aim would be to determine if FOXM1b and FOXM1c are both down-regulated in their expression. Since FoxM1a is potentially a natural dominant negative, it will be important to determine if it is also differentially expressed and how this affects the transcriptional activity of the other isoforms.

Similarly, finding which spliceform activity is required for the reversal of the growth arrest would bring light into the mechanism of action of FOXM1 in the senescence process. I have already shown that constitutively active FOXM1c can overcome senescence in CL3<sup>EcoR</sup> cells but if FOXM1b is also down-regulated upon senescence, I could attempt complementation with a constitutively active FOXM1b. Since FOXM1c contains exon A1 which is not present in FOXM1b, it is possible they have slightly different functional activities.

#### *7.2.4.2 Which kinases regulate the activation of FOXM1?*

I have found that senescence in HMF3A cells can be abrogated by the constitutively active FOXM1c but not the wild type protein. This indicates a requirement for activation of FOXM1. The N-terminus of FOXM1 contains an auto-repressor domain that inhibits transactivation by an intramolecular interaction with the C-terminal TAD. This repression can be relieved by phosphorylation of multiple cdk sites within the TAD by cyclinA/cdk2 or possibly by cyclinE/cdk2; PLK1 and PLK4 may also play a role.

Our expression profiling data indicates that cdk2 and cyclinE expression are unaffected upon growth arrest whereas cyclinA expression is down-regulated about 20 fold, PLK1 30 fold and PLK4 12 fold respectively.

To determine directly which of these kinases are important for activating FOXM1 for abrogating senescence, co-expressing each of these kinases with full length FOXM1 could be utilized

#### *7.2.4.3 What is the mechanism of action of FOXM1?*

To determine the mechanism of action of FOXM1, it is critical to identify what are the downstream targets and what is their relationship to genes found to be differentially expressed in HMF3A upon cell senescence by expression profiling?

I have already undertaken a highly sensitive expression profiling analysis of HMF3A cells when they undergo irreversible growth arrest. Expression profiling of cells rescued by activated FOXM1 could be performed and overlapped with our microarray data and the genes whose expression is maintained by expression of FOXM1 isoforms should be targets of FOXM1.

#### *7.2.4.4 What causes the decreased expression of FOXM1 in cell senescence?*

Another important question would be to determine what causes the down-regulation of FOXM1 upon cell senescence. Although it was recently suggested that that Stress-activated kinase p38 (p38<sup>SAPK</sup>) is capable of inhibiting FOXM1 expression (Adam et al, 2009), the transcription profiling data indicates that this unlikely to be the mechanism, since expression of the three isoforms  $\alpha$  (MAPK14),  $\beta$  (MAPK11) and  $\delta$  (MAPK13) of p38<sup>SAPK</sup> present in HMF3A cells, is unaffected upon growth arrest.

Previously it was suggested that in Basal Cell Carcinomas, FOXM1 was a downstream target of Gli1, which is transcriptionally up-regulated by Sonic hedgehog (Shh)-signalling (28). Gli1 is a member of the Gli family of three transcription factors Gli1, 2 and 3. Gli 1 and 2 are activators whereas Gli3 is a repressor. The expression profiling data shows that all three Gli proteins are expressed in proliferating HMF3A cells but upon growth arrest Gli2 and 3 are down-regulated whereas Gli1 may be slightly up-regulated. By expressing and silencing Gli 1, 2 or 3, it would be possible to directly determine their effect on FOXM1 expression.

### 7.3 FINAL REMARKS

Cellular senescence is closely associated with cancer development. Premature senescence induced following activation of oncogenes or inactivation of tumor suppressor genes (Courtois-Cox, Jones et al. 2008) is a potent anti-tumorigenic defense mechanism. It is also known that cellular transformation by activated *ras* requires cooperation from ‘immortalizing’ oncogenes that overcome the senescence response, such as those inactivating p53 (Land, Parada et al. 1983; Seger, Garcia-Cao et al. 2002). Recent studies have demonstrated that senescent cells can be detected in early-stage, premalignant lesions of lung, pancreas, skin and prostate in both human cancer patients and mouse tumor models (Narita and Lowe 2005; Sun, Yoshizuka et al. 2007).

In addition, I have shown in this study that nearly 50% of genes that were up-regulated in a study that analysed the meta-signatures of over-expressed genes upon neoplastic transformation and in undifferentiated cancer (Rhodes, Yu et al. 2004) were down-regulated upon senescence which further confirm the role of senescence as a barrier to cancer development.

The fact that senescent cells have been detected *in vivo* provides compelling evidence that cellular senescence represents a *bona fide* biological process acting as a protection against cancer development. (Braig, Lee et al. 2005; Chen, Trotman et al. 2005; Collado, Gil et al. 2005; Michaloglou, Vredeveld et al. 2005). This has profound implications for the study of both organismal ageing and tumorigenesis; for example, the genes identified here may not only represent novel markers of senescence, but may also have prognostic and/or diagnostic value in the context of tumorigenic treatment. Moreover, as there is accumulating evidence to suggest that the induction of senescence *in vivo* is critical to the efficacy of chemotherapeutic agents (Chang, Swift et al. 2002; Rebbaa, Zheng et al. 2003; Zheng, Wang et al. 2004), elucidation of the pathways critical regulating the finite proliferative potential of normal human cells will be important for the development of novel chemotherapeutic agents.

In contradiction, it has been demonstrated that senescent cells can also promote tumor progression in a paracrine fashion. Cells undergoing replicative senescence or oncogene-induced senescence secrete growth factors, inflammatory cytokines and chemokines, and extracellular matrix-degrading proteases that enhance the proliferation, invasion and angiogenesis of nearby premalignant tumor cells (Campisi and d'Adda di Fagagna 2007). This was further confirmed in this present study where many metalloproteinases, collagenases and other extra-cellular matrix degrading enzymes, secreted factors including interleukins and growth factor were up-regulated upon senescence.

As senescent cells accumulate with age, these observations could provide an explanation to the age-related increase in cancer incidence. In fact, senescence may be an example of antagonistic pleiotropy, acting as a tumor suppressor mechanism in the young but promoting tumor formation in the elderly.

## **8 REFERENCES**

- Acosta, J. C., A. O'Loughlen, et al. (2008). "Chemokine signaling via the CXCR2 receptor reinforces senescence." *Cell* **133**(6): 1006-1018.
- Adams, P. D. (2001). "Regulation of the retinoblastoma tumor suppressor protein by cyclin/cdks." *Biochim Biophys Acta* **1471**(3): M123-133.
- Adams, P. D. (2009). "Healing and hurting: molecular mechanisms, functions, and pathologies of cellular senescence." *Mol Cell* **36**(1): 2-14.
- Adler, A. S., M. Lin, et al. (2006). "Genetic regulators of large-scale transcriptional signatures in cancer." *Nat Genet* **38**(4): 421-430.
- Adler, A. S., S. Sinha, et al. (2007). "Motif module map reveals enforcement of aging by continual NF-kappaB activity." *Genes Dev* **21**(24): 3244-3257.
- Akao, Y., Y. Nakagawa, et al. (2006). "MicroRNAs 143 and 145 are possible common onco-microRNAs in human cancers." *Oncol Rep* **16**(4): 845-850.
- Alani, R. M., A. Z. Young, et al. (2001). "Id1 regulation of cellular senescence through transcriptional repression of p16/Ink4a." *Proc Natl Acad Sci U S A* **98**(14): 7812-7816.
- Alarcon-Vargas, D. and Z. Ronai (2002). "p53-Mdm2--the affair that never ends." *Carcinogenesis* **23**(4): 541-547.
- Albrechtsen, N., I. Dornreiter, et al. (1999). "Maintenance of genomic integrity by p53: complementary roles for activated and non-activated p53." *Oncogene* **18**(53): 7706-7717.
- Alcalay, M., L. Tomassoni, et al. (1998). "The promyelocytic leukemia gene product (PML) forms stable complexes with the retinoblastoma protein." *Mol Cell Biol* **18**(2): 1084-1093.

- Alcorta, D. A., Y. Xiong, et al. (1996). "Involvement of the cyclin-dependent kinase inhibitor p16 (INK4a) in replicative senescence of normal human fibroblasts." Proc Natl Acad Sci U S A **93**(24): 13742-13747.
- Ali, S. H. and J. A. DeCaprio (2001). "Cellular transformation by SV40 large T antigen: interaction with host proteins." Semin Cancer Biol **11**(1): 15-23.
- Alvarez-Salas, L. M., A. E. Cullinan, et al. (1998). "Inhibition of HPV-16 E6/E7 immortalization of normal keratinocytes by hairpin ribozymes." Proc Natl Acad Sci U S A **95**(3): 1189-1194.
- Alwine, J. C., S. I. Reed, et al. (1977). "Characterization of the autoregulation of simian virus 40 gene A." J Virol **24**(1): 22-27.
- Ambros, V. (2004). "The functions of animal microRNAs." Nature **431**(7006): 350-355.
- Appella, E. and C. W. Anderson (2001). "Post-translational modifications and activation of p53 by genotoxic stresses." Eur J Biochem **268**(10): 2764-2772.
- Aslanian, A., P. J. Iaquina, et al. (2004). "Repression of the Arf tumor suppressor by E2F3 is required for normal cell cycle kinetics." Genes Dev **18**(12): 1413-1422.
- Augert, A., C. Payre, et al. (2009). "The M-type receptor PLA2R regulates senescence through the p53 pathway." EMBO Rep **10**(3): 271-277.
- Avantaggiati, M. L., M. Carbone, et al. (1996). "The SV40 large T antigen and adenovirus E1a oncoproteins interact with distinct isoforms of the transcriptional co-activator, p300." EMBO J **15**(9): 2236-2248.
- Bammler, T., R. P. Beyer, et al. (2005). "Standardizing global gene expression analysis between laboratories and across platforms." Nat Methods **2**(5): 351-356.
- Bannister, A. J., P. Zegerman, et al. (2001). "Selective recognition of methylated lysine 9 on histone H3 by the HP1 chromo domain." Nature **410**(6824): 120-124.
- Barbeau, D., R. Charbonneau, et al. (1994). "Functional interactions within adenovirus E1A protein complexes." Oncogene **9**(2): 359-373.
- Barradas, M., E. Anderton, et al. (2009). "Histone demethylase JMJD3 contributes to epigenetic control of INK4a/ARF by oncogenic RAS." Genes Dev **23**(10): 1177-1182.
- Bartek, J., J. Bartkova, et al. (1996). "The retinoblastoma protein pathway and the restriction point." Curr Opin Cell Biol **8**(6): 805-814.
- Bartel, D. P. (2004). "MicroRNAs: genomics, biogenesis, mechanism, and function." Cell **116**(2): 281-297.
- Bartkova, J., N. Rezaei, et al. (2006). "Oncogene-induced senescence is part of the tumorigenesis barrier imposed by DNA damage checkpoints." Nature **444**(7119): 633-637.
- Basak, S., H. Kim, et al. (2007). "A fourth IkappaB protein within the NF-kappaB signaling module." Cell **128**(2): 369-381.
- Basak, S., V. F. Shih, et al. (2008). "Generation and activation of multiple dimeric transcription factors within the NF-kappaB signaling system." Mol Cell Biol **28**(10): 3139-3150.
- Bates, S., A. C. Phillips, et al. (1998). "p14ARF links the tumour suppressors RB and p53." Nature **395**(6698): 124-125.
- Beausejour, C. M., A. Krtolica, et al. (2003). "Reversal of human cellular senescence: roles of the p53 and p16 pathways." EMBO J **22**(16): 4212-4222.
- Bentwich, I., A. Avniel, et al. (2005). "Identification of hundreds of conserved and nonconserved human microRNAs." Nat Genet **37**(7): 766-770.

- Bernard, D., K. Gosselin, et al. (2004). "Involvement of Rel/nuclear factor-kappaB transcription factors in keratinocyte senescence." *Cancer Res* **64**(2): 472-481.
- Berns, K., E. M. Hijmans, et al. (2004). "A large-scale RNAi screen in human cells identifies new components of the p53 pathway." *Nature* **428**(6981): 431-437.
- Berry, D. E., Y. Lu, et al. (1996). "Retinoblastoma protein inhibits IFN-gamma induced apoptosis." *Oncogene* **12**(8): 1809-1819.
- Berthois, Y., N. Pourreau-Schneider, et al. (1986). "Estradiol membrane binding sites on human breast cancer cell lines. Use of a fluorescent estradiol conjugate to demonstrate plasma membrane binding systems." *J Steroid Biochem* **25**(6): 963-972.
- Bhaumik, D., G. K. Scott, et al. (2008). "Expression of microRNA-146 suppresses NF-kappaB activity with reduction of metastatic potential in breast cancer cells." *Oncogene* **27**(42): 5643-5647.
- Bialik, S. and A. Kimchi (2004). "DAP-kinase as a target for drug design in cancer and diseases associated with accelerated cell death." *Semin Cancer Biol* **14**(4): 283-294.
- Binet, R., D. Ythier, et al. (2009). "WNT16B is a new marker of cellular senescence that regulates p53 activity and the phosphoinositide 3-kinase/AKT pathway." *Cancer Res* **69**(24): 9183-9191.
- Blasco, M. A. (2005). "Telomeres and human disease: ageing, cancer and beyond." *Nat Rev Genet* **6**(8): 611-622.
- Blasco, M. A., H. W. Lee, et al. (1997). "Telomere shortening and tumor formation by mouse cells lacking telomerase RNA." *Cell* **91**(1): 25-34.
- Boden, D., O. Pusch, et al. (2004). "Enhanced gene silencing of HIV-1 specific siRNA using microRNA designed hairpins." *Nucleic Acids Res* **32**(3): 1154-1158.
- Bodnar, A. G., M. Ouellette, et al. (1998). "Extension of life-span by introduction of telomerase into normal human cells." *Science* **279**(5349): 349-352.
- Bolstad, B. M., R. A. Irizarry, et al. (2003). "A comparison of normalization methods for high density oligonucleotide array data based on variance and bias." *Bioinformatics* **19**(2): 185-193.
- Bond, J., C. Jones, et al. (2004). "Direct evidence from siRNA-directed "knock down" that p16(INK4a) is required for human fibroblast senescence and for limiting ras-induced epithelial cell proliferation." *Exp Cell Res* **292**(1): 151-156.
- Bonetto, F., M. Fanciulli, et al. (1999). "Interaction between the pRb2/p130 C-terminal domain and the N-terminal portion of cyclin D3." *J Cell Biochem* **75**(4): 698-709.
- Bonizzi, G., M. Bebien, et al. (2004). "Activation of IKKalpha target genes depends on recognition of specific kappaB binding sites by RelB:p52 dimers." *EMBO J* **23**(21): 4202-4210.
- Borgdorff, V., M. E. Leonart, et al. (2010). "Multiple microRNAs rescue from Ras-induced senescence by inhibiting p21(Waf1/Cip1)." *Oncogene* **29**(15): 2262-2271.
- Bos, J. L. (1989). "ras oncogenes in human cancer: a review." *Cancer Res* **49**(17): 4682-4689.
- Boulaire, J., A. Fotedar, et al. (2000). "The functions of the cdk-cyclin kinase inhibitor p21WAF1." *Pathol Biol (Paris)* **48**(3): 190-202.

- Bours, V., G. Franzoso, et al. (1993). "The oncoprotein Bcl-3 directly transactivates through kappa B motifs via association with DNA-binding p50B homodimers." Cell **72**(5): 729-739.
- Braconi, C., N. Huang, et al. (2010). "MicroRNA-dependent regulation of DNA methyltransferase-1 and tumor suppressor gene expression by interleukin-6 in human malignant cholangiocytes." Hepatology **51**(3): 881-890.
- Braig, M., S. Lee, et al. (2005). "Oncogene-induced senescence as an initial barrier in lymphoma development." Nature **436**(7051): 660-665.
- Braithwaite, A. W., B. F. Cheetham, et al. (1983). "Adenovirus-induced alterations of the cell growth cycle: a requirement for expression of E1A but not of E1B." J Virol **45**(1): 192-199.
- Brehm, A., E. A. Miska, et al. (1998). "Retinoblastoma protein recruits histone deacetylase to repress transcription." Nature **391**(6667): 597-601.
- Brennecke, J., D. R. Hipfner, et al. (2003). "bantam encodes a developmentally regulated microRNA that controls cell proliferation and regulates the proapoptotic gene hid in Drosophila." Cell **113**(1): 25-36.
- Brennecke, J., A. Stark, et al. (2005). "Principles of microRNA-target recognition." PLoS Biol **3**(3): e85.
- Brickman, J. M., M. Adam, et al. (1999). "Interactions between an HMG-1 protein and members of the Rel family." Proc Natl Acad Sci U S A **96**(19): 10679-10683.
- Brookes, S., J. Rowe, et al. (2002). "INK4a-deficient human diploid fibroblasts are resistant to RAS-induced senescence." EMBO J **21**(12): 2936-2945.
- Brown, D. R., S. Deb, et al. (1993). "The tumor suppressor p53 and the oncoprotein simian virus 40 T antigen bind to overlapping domains on the MDM2 protein." Mol Cell Biol **13**(11): 6849-6857.
- Brown, J. P., W. Wei, et al. (1997). "Bypass of senescence after disruption of p21CIP1/WAF1 gene in normal diploid human fibroblasts." Science **277**(5327): 831-834.
- Bruemmer, D., F. Yin, et al. (2003). "Rapamycin inhibits E2F-dependent expression of minichromosome maintenance proteins in vascular smooth muscle cells." Biochem Biophys Res Commun **303**(1): 251-258.
- Buchkovich, K., L. A. Duffy, et al. (1989). "The retinoblastoma protein is phosphorylated during specific phases of the cell cycle." Cell **58**(6): 1097-1105.
- Bulavin, D. V., C. Phillips, et al. (2004). "Inactivation of the Wip1 phosphatase inhibits mammary tumorigenesis through p38 MAPK-mediated activation of the p16(Ink4a)-p19(Arf) pathway." Nat Genet **36**(4): 343-350.
- Burkhart, B. A., D. A. Alcorta, et al. (1999). "Two posttranscriptional pathways that regulate p21(Cip1/Waf1/Sdi1) are identified by HPV16-E6 interaction and correlate with life span and cellular senescence." Exp Cell Res **247**(1): 168-175.
- Cahill, D. P., C. Lengauer, et al. (1998). "Mutations of mitotic checkpoint genes in human cancers." Nature **392**(6673): 300-303.
- Calin, G. A., C. D. Dumitru, et al. (2002). "Frequent deletions and down-regulation of micro- RNA genes miR15 and miR16 at 13q14 in chronic lymphocytic leukemia." Proc Natl Acad Sci U S A **99**(24): 15524-15529.
- Calin, G. A., C. Sevignani, et al. (2004). "Human microRNA genes are frequently located at fragile sites and genomic regions involved in cancers." Proc Natl Acad Sci U S A **101**(9): 2999-3004.

- Campisi, J. (2003). "Cancer and ageing: rival demons?" Nat Rev Cancer **3**(5): 339-349.
- Campisi, J. (2005). "Senescent cells, tumor suppression, and organismal aging: good citizens, bad neighbors." Cell **120**(4): 513-522.
- Campisi, J. and F. d'Adda di Fagagna (2007). "Cellular senescence: when bad things happen to good cells." Nat Rev Mol Cell Biol **8**(9): 729-740.
- Canela, A., J. Martin-Caballero, et al. (2004). "Constitutive expression of tert in thymocytes leads to increased incidence and dissemination of T-cell lymphoma in Lck-Tert mice." Mol Cell Biol **24**(10): 4275-4293.
- Canela, A., E. Vera, et al. (2007). "High-throughput telomere length quantification by FISH and its application to human population studies." Proc Natl Acad Sci U S A **104**(13): 5300-5305.
- Caporossi, D. and S. Bacchetti (1990). "Definition of adenovirus type 5 functions involved in the induction of chromosomal aberrations in human cells." J Gen Virol **71** ( Pt 4): 801-808.
- Carroll, R. B., L. Hager, et al. (1974). "Simian virus 40 T antigen binds to DNA." Proc Natl Acad Sci U S A **71**(9): 3754-3757.
- Carroll, R. B., A. Samad, et al. (1988). "RNA is covalently linked to SV40 large T antigen." Oncogene **2**(5): 437-444.
- Cartwright, P., H. Muller, et al. (1998). "E2F-6: a novel member of the E2F family is an inhibitor of E2F-dependent transcription." Oncogene **17**(5): 611-623.
- Cawthon, R. M., K. R. Smith, et al. (2003). "Association between telomere length in blood and mortality in people aged 60 years or older." Lancet **361**(9355): 393-395.
- Chan, H. M., M. Krstic-Demonacos, et al. (2001). "Acetylation control of the retinoblastoma tumour-suppressor protein." Nat Cell Biol **3**(7): 667-674.
- Chan, H. M., M. Narita, et al. (2005). "The p400 E1A-associated protein is a novel component of the p53 --> p21 senescence pathway." Genes Dev **19**(2): 196-201.
- Chang, B. D., E. V. Broude, et al. (1999). "A senescence-like phenotype distinguishes tumor cells that undergo terminal proliferation arrest after exposure to anticancer agents." Cancer Res **59**(15): 3761-3767.
- Chang, B. D., M. E. Swift, et al. (2002). "Molecular determinants of terminal growth arrest induced in tumor cells by a chemotherapeutic agent." Proc Natl Acad Sci U S A **99**(1): 389-394.
- Chang, B. D., K. Watanabe, et al. (2000). "Effects of p21Waf1/Cip1/Sdi1 on cellular gene expression: implications for carcinogenesis, senescence, and age-related diseases." Proc Natl Acad Sci U S A **97**(8): 4291-4296.
- Chang, T. H., F. A. Ray, et al. (1997). "Disregulation of mitotic checkpoints and regulatory proteins following acute expression of SV40 large T antigen in diploid human cells." Oncogene **14**(20): 2383-2393.
- Chen, C. Z., L. Li, et al. (2004). "MicroRNAs modulate hematopoietic lineage differentiation." Science **303**(5654): 83-86.
- Chen, J., P. K. Jackson, et al. (1995). "Separate domains of p21 involved in the inhibition of Cdk kinase and PCNA." Nature **374**(6520): 386-388.
- Chen, P. Y. and G. Meister (2005). "microRNA-guided posttranscriptional gene regulation." Biol Chem **386**(12): 1205-1218.



- Chen, Q. M., K. R. Prowse, et al. (2001). "Uncoupling the senescent phenotype from telomere shortening in hydrogen peroxide-treated fibroblasts." Exp Cell Res **265**(2): 294-303.
- Chen, T. T. and J. Y. Wang (2000). "Establishment of irreversible growth arrest in myogenic differentiation requires the RB LXCXE-binding function." Mol Cell Biol **20**(15): 5571-5580.
- Chen, Z., L. C. Trotman, et al. (2005). "Crucial role of p53-dependent cellular senescence in suppression of Pten-deficient tumorigenesis." Nature **436**(7051): 725-730.
- Chen, Z., W. Zhuo, et al. (2008). "Down-regulation of layilin, a novel hyaluronan receptor, via RNA interference, inhibits invasion and lymphatic metastasis of human lung A549 cells." Biotechnol Appl Biochem **50**(Pt 2): 89-96.
- Cheng, M., P. Olivier, et al. (1999). "The p21(Cip1) and p27(Kip1) CDK 'inhibitors' are essential activators of cyclin D-dependent kinases in murine fibroblasts." EMBO J **18**(6): 1571-1583.
- Chin, L., J. Pomerantz, et al. (1997). "Cooperative effects of INK4a and ras in melanoma susceptibility in vivo." Genes Dev **11**(21): 2822-2834.
- Chondrogianni, N., F. L. Stratford, et al. (2003). "Central role of the proteasome in senescence and survival of human fibroblasts: induction of a senescence-like phenotype upon its inhibition and resistance to stress upon its activation." J Biol Chem **278**(30): 28026-28037.
- Christoffersen, N. R., R. Shalgi, et al. (2010). "p53-independent upregulation of miR-34a during oncogene-induced senescence represses MYC." Cell Death Differ **17**(2): 236-245.
- Chuang, Y. T., L. W. Fang, et al. (2008). "The tumor suppressor death-associated protein kinase targets to TCR-stimulated NF-kappa B activation." J Immunol **180**(5): 3238-3249.
- Chung, E. J., Y. K. Sung, et al. (2002). "Gene expression profile analysis in human hepatocellular carcinoma by cDNA microarray." Mol Cells **14**(3): 382-387.
- Classon, M. and N. Dyson (2001). "p107 and p130: versatile proteins with interesting pockets." Exp Cell Res **264**(1): 135-147.
- Classon, M. and E. Harlow (2002). "The retinoblastoma tumour suppressor in development and cancer." Nat Rev Cancer **2**(12): 910-917.
- Claudio, P. P., A. De Luca, et al. (1996). "Functional analysis of pRb2/p130 interaction with cyclins." Cancer Res **56**(9): 2003-2008.
- Cleveland, J. L. and C. J. Sherr (2004). "Antagonism of Myc functions by Arf." Cancer Cell **6**(4): 309-311.
- Cobrinik, D., S. F. Dowdy, et al. (1992). "The retinoblastoma protein and the regulation of cell cycling." Trends Biochem Sci **17**(8): 312-315.
- Collado, M., M. A. Blasco, et al. (2007). "Cellular senescence in cancer and aging." Cell **130**(2): 223-233.
- Collado, M., J. Gil, et al. (2005). "Tumour biology: senescence in premalignant tumours." Nature **436**(7051): 642.
- Collado, M. and M. Serrano (2010). "Senescence in tumours: evidence from mice and humans." Nat Rev Cancer **10**(1): 51-57.
- Collins, K. and J. R. Mitchell (2002). "Telomerase in the human organism." Oncogene **21**(4): 564-579.

- Colman, M. S., C. A. Afshari, et al. (2000). "Regulation of p53 stability and activity in response to genotoxic stress." *Mutat Res* **462**(2-3): 179-188.
- Condorelli, G. and A. Giordano (1997). "Synergistic role of E1A-binding proteins and tissue-specific transcription factors in differentiation." *J Cell Biochem* **67**(4): 423-431.
- Condorelli, G. L., U. Testa, et al. (1995). "Modulation of retinoblastoma gene in normal adult hematopoiesis: peak expression and functional role in advanced erythroid differentiation." *Proc Natl Acad Sci U S A* **92**(11): 4808-4812.
- Conzen, S. D. and C. N. Cole (1995). "The three transforming regions of SV40 T antigen are required for immortalization of primary mouse embryo fibroblasts." *Oncogene* **11**(11): 2295-2302.
- Coppe, J. P., C. K. Patil, et al. (2008). "Senescence-associated secretory phenotypes reveal cell-nonautonomous functions of oncogenic RAS and the p53 tumor suppressor." *PLoS Biol* **6**(12): 2853-2868.
- Core, N., F. Joly, et al. (2004). "Disruption of E2F signaling suppresses the INK4a-induced proliferative defect in M33-deficient mice." *Oncogene* **23**(46): 7660-7668.
- Corney, D. C., C. I. Hwang, et al. (2010). "Frequent downregulation of miR-34 family in human ovarian cancers." *Clin Cancer Res* **16**(4): 1119-1128.
- Cosme-Blanco, W., M. F. Shen, et al. (2007). "Telomere dysfunction suppresses spontaneous tumorigenesis in vivo by initiating p53-dependent cellular senescence." *EMBO Rep* **8**(5): 497-503.
- Cotsiki, M., R. L. Lock, et al. (2004). "Simian virus 40 large T antigen targets the spindle assembly checkpoint protein Bub1." *Proc Natl Acad Sci U S A* **101**(4): 947-952.
- Counter, C. M., M. Meyerson, et al. (1998). "Telomerase activity is restored in human cells by ectopic expression of hTERT (hEST2), the catalytic subunit of telomerase." *Oncogene* **16**(9): 1217-1222.
- Courtois-Cox, S., S. M. Genter Williams, et al. (2006). "A negative feedback signaling network underlies oncogene-induced senescence." *Cancer Cell* **10**(6): 459-472.
- Courtois-Cox, S., S. L. Jones, et al. (2008). "Many roads lead to oncogene-induced senescence." *Oncogene* **27**(20): 2801-2809.
- Cristofalo, V. J. and M. Tresini (1998). "Defects in signal transduction during replicative senescence of diploid human fibroblasts in vitro." *Aging (Milano)* **10**(2): 151-152.
- Cui, J. W., Y. J. Li, et al. (2007). "Retroviral insertional activation of the Fli-3 locus in erythroleukemias encoding a cluster of microRNAs that convert Epo-induced differentiation to proliferation." *Blood* **110**(7): 2631-2640.
- Cziepluch, C., S. Lampel, et al. (2000). "H-1 parvovirus-associated replication bodies: a distinct virus-induced nuclear structure." *J Virol* **74**(10): 4807-4815.
- d'Adda di Fagagna, F., P. M. Reaper, et al. (2003). "A DNA damage checkpoint response in telomere-initiated senescence." *Nature* **426**(6963): 194-198.
- d'Adda di Fagagna, F., S. H. Teo, et al. (2004). "Functional links between telomeres and proteins of the DNA-damage response." *Genes Dev* **18**(15): 1781-1799.
- Dahiya, A., M. R. Gavin, et al. (2000). "Role of the LXCXE binding site in Rb function." *Mol Cell Biol* **20**(18): 6799-6805.

- Dankort, D., E. Filenova, et al. (2007). "A new mouse model to explore the initiation, progression, and therapy of BRAFV600E-induced lung tumors." Genes Dev **21**(4): 379-384.
- Davies, H., C. Hunter, et al. (2005). "Somatic mutations of the protein kinase gene family in human lung cancer." Cancer Res **65**(17): 7591-7595.
- Davies, R., R. Hicks, et al. (1993). "Human papillomavirus type 16 E7 associates with a histone H1 kinase and with p107 through sequences necessary for transformation." J Virol **67**(5): 2521-2528.
- de Bruin, A., B. Maiti, et al. (2003). "Identification and characterization of E2F7, a novel mammalian E2F family member capable of blocking cellular proliferation." J Biol Chem **278**(43): 42041-42049.
- de Lange, T. (2005). "Shelterin: the protein complex that shapes and safeguards human telomeres." Genes Dev **19**(18): 2100-2110.
- de Stanchina, E., M. E. McCurrach, et al. (1998). "E1A signaling to p53 involves the p19(ARF) tumor suppressor." Genes Dev **12**(15): 2434-2442.
- Debacq, C., J. M. Heraud, et al. (2005). "Reduced cell turnover in lymphocytic monkeys infected by human T-lymphotropic virus type 1." Oncogene **24**(51): 7514-7523.
- DeCaprio, J. A., J. W. Ludlow, et al. (1988). "SV40 large tumor antigen forms a specific complex with the product of the retinoblastoma susceptibility gene." Cell **54**(2): 275-283.
- DeCaprio, J. A., J. W. Ludlow, et al. (1989). "The product of the retinoblastoma susceptibility gene has properties of a cell cycle regulatory element." Cell **58**(6): 1085-1095.
- DeGregori, J., G. Leone, et al. (1997). "Distinct roles for E2F proteins in cell growth control and apoptosis." Proc Natl Acad Sci U S A **94**(14): 7245-7250.
- Deiss, L. P., E. Feinstein, et al. (1995). "Identification of a novel serine/threonine kinase and a novel 15-kD protein as potential mediators of the gamma interferon-induced cell death." Genes Dev **9**(1): 15-30.
- DeLeo, A. B., G. Jay, et al. (1979). "Detection of a transformation-related antigen in chemically induced sarcomas and other transformed cells of the mouse." Proc Natl Acad Sci U S A **76**(5): 2420-2424.
- Deppert, W., M. Haug, et al. (1987). "Modulation of p53 protein expression during cellular transformation with simian virus 40." Mol Cell Biol **7**(12): 4453-4463.
- Der, C. J., T. G. Krontiris, et al. (1982). "Transforming genes of human bladder and lung carcinoma cell lines are homologous to the ras genes of Harvey and Kirsten sarcoma viruses." Proc Natl Acad Sci U S A **79**(11): 3637-3640.
- Derynck, R., R. J. Akhurst, et al. (2001). "TGF-beta signaling in tumor suppression and cancer progression." Nat Genet **29**(2): 117-129.
- Dews, M., A. Homayouni, et al. (2006). "Augmentation of tumor angiogenesis by a Myc-activated microRNA cluster." Nat Genet **38**(9): 1060-1065.
- Di Leonardo, A., S. P. Linke, et al. (1994). "DNA damage triggers a prolonged p53-dependent G1 arrest and long-term induction of Cip1 in normal human fibroblasts." Genes Dev **8**(21): 2540-2551.
- Di Micco, P., M. Amitrano, et al. (2006). "Molecular and clinical conditions associated with venous thromboembolism in oncological patients." Exp Oncol **28**(3): 194-197.

- Dimri, G. P., E. Hara, et al. (1994). "Regulation of two E2F-related genes in presenescent and senescent human fibroblasts." J Biol Chem **269**(23): 16180-16186.
- Dimri, G. P., K. Itahana, et al. (2000). "Regulation of a senescence checkpoint response by the E2F1 transcription factor and p14(ARF) tumor suppressor." Mol Cell Biol **20**(1): 273-285.
- Dimri, G. P., X. Lee, et al. (1995). "A biomarker that identifies senescent human cells in culture and in aging skin in vivo." Proc Natl Acad Sci U S A **92**(20): 9363-9367.
- Dirac, A. M. and R. Bernards (2003). "Reversal of senescence in mouse fibroblasts through lentiviral suppression of p53." J Biol Chem **278**(14): 11731-11734.
- Dobrzanski, P., R. P. Ryseck, et al. (1995). "Specific inhibition of RelB/p52 transcriptional activity by the C-terminal domain of p100." Oncogene **10**(5): 1003-1007.
- Dodeller, F., M. Gottar, et al. (2008). "The lysosomal transmembrane protein 9B regulates the activity of inflammatory signaling pathways." J Biol Chem **283**(31): 21487-21494.
- Donehower, L. A., L. A. Godley, et al. (1995). "Deficiency of p53 accelerates mammary tumorigenesis in Wnt-1 transgenic mice and promotes chromosomal instability." Genes Dev **9**(7): 882-895.
- Donehower, L. A., M. Harvey, et al. (1992). "Mice deficient for p53 are developmentally normal but susceptible to spontaneous tumours." Nature **356**(6366): 215-221.
- Dornan, D., I. Wertz, et al. (2004). "The ubiquitin ligase COP1 is a critical negative regulator of p53." Nature **429**(6987): 86-92.
- Dorsman, J. C., B. M. Hagemeyer, et al. (1995). "The N-terminal region of the adenovirus type 5 E1A proteins can repress expression of cellular genes via two distinct but overlapping domains." J Virol **69**(5): 2962-2967.
- Doyle, S. L. and L. A. O'Neill (2006). "Toll-like receptors: from the discovery of NFkappaB to new insights into transcriptional regulations in innate immunity." Biochem Pharmacol **72**(9): 1102-1113.
- Draviam, V. M., F. Stegmeier, et al. (2007). "A functional genomic screen identifies a role for TAO1 kinase in spindle-checkpoint signalling." Nat Cell Biol **9**(5): 556-564.
- Duensing, S. and K. Munger (2002). "The human papillomavirus type 16 E6 and E7 oncoproteins independently induce numerical and structural chromosome instability." Cancer Res **62**(23): 7075-7082.
- Dumble, M., C. Gatz, et al. (2004). "Insights into aging obtained from p53 mutant mouse models." Ann N Y Acad Sci **1019**: 171-177.
- Dumble, M., L. Moore, et al. (2007). "The impact of altered p53 dosage on hematopoietic stem cell dynamics during aging." Blood **109**(4): 1736-1742.
- Dunaief, J. L., B. E. Strober, et al. (1994). "The retinoblastoma protein and BRG1 form a complex and cooperate to induce cell cycle arrest." Cell **79**(1): 119-130.
- Dyson, N., K. Buchkovich, et al. (1989). "The cellular 107K protein that binds to adenovirus E1A also associates with the large T antigens of SV40 and JC virus." Cell **58**(2): 249-255.
- Dyson, N. and E. Harlow (1992). "Adenovirus E1A targets key regulators of cell proliferation." Cancer Surv **12**: 161-195.

- Eckner, R. (1996). "p300 and CBP as transcriptional regulators and targets of oncogenic events." Biol Chem **377**(11): 685-688.
- Eckner, R., J. W. Ludlow, et al. (1996). "Association of p300 and CBP with simian virus 40 large T antigen." Mol Cell Biol **16**(7): 3454-3464.
- Ekloy, S., K. Funa, et al. (1993). "Lack of the latent transforming growth factor beta binding protein in malignant, but not benign prostatic tissue." Cancer Res **53**(13): 3193-3197.
- el-Deiry, W. S. (1998). "Regulation of p53 downstream genes." Semin Cancer Biol **8**(5): 345-357.
- el-Deiry, W. S., T. Tokino, et al. (1993). "WAF1, a potential mediator of p53 tumor suppression." Cell **75**(4): 817-825.
- Elenbaas, B., L. Spirio, et al. (2001). "Human breast cancer cells generated by oncogenic transformation of primary mammary epithelial cells." Genes Dev **15**(1): 50-65.
- Esau, C., S. Davis, et al. (2006). "miR-122 regulation of lipid metabolism revealed by in vivo antisense targeting." Cell Metab **3**(2): 87-98.
- Esau, C. C. (2008). "Inhibition of microRNA with antisense oligonucleotides." Methods **44**(1): 55-60.
- Esteller, M., S. Gonzalez, et al. (2001). "K-ras and p16 aberrations confer poor prognosis in human colorectal cancer." J Clin Oncol **19**(2): 299-304.
- Esteller, M., S. Tortola, et al. (2000). "Hypermethylation-associated inactivation of p14(ARF) is independent of p16(INK4a) methylation and p53 mutational status." Cancer Res **60**(1): 129-133.
- Evans, T., E. T. Rosenthal, et al. (1983). "Cyclin: a protein specified by maternal mRNA in sea urchin eggs that is destroyed at each cleavage division." Cell **33**(2): 389-396.
- Ewen, M. E., J. W. Ludlow, et al. (1989). "An N-terminal transformation-governing sequence of SV40 large T antigen contributes to the binding of both p110Rb and a second cellular protein, p120." Cell **58**(2): 257-267.
- Fabani, M. M. and M. J. Gait (2008). "miR-122 targeting with LNA/2'-O-methyl oligonucleotide mixmers, peptide nucleic acids (PNA), and PNA-peptide conjugates." RNA **14**(2): 336-346.
- Faha, B., M. E. Ewen, et al. (1992). "Interaction between human cyclin A and adenovirus E1A-associated p107 protein." Science **255**(5040): 87-90.
- Fakharzadeh, S. S., S. P. Trusko, et al. (1991). "Tumorigenic potential associated with enhanced expression of a gene that is amplified in a mouse tumor cell line." EMBO J **10**(6): 1565-1569.
- Ferbeyre, G., E. de Stanchina, et al. (2002). "Oncogenic ras and p53 cooperate to induce cellular senescence." Mol Cell Biol **22**(10): 3497-3508.
- Filippova, M., H. Song, et al. (2002). "The human papillomavirus 16 E6 protein binds to tumor necrosis factor (TNF) R1 and protects cells from TNF-induced apoptosis." J Biol Chem **277**(24): 21730-21739.
- Finkel, T., M. Serrano, et al. (2007). "The common biology of cancer and ageing." Nature **448**(7155): 767-774.
- Flemington, E. K., S. H. Speck, et al. (1993). "E2F-1-mediated transactivation is inhibited by complex formation with the retinoblastoma susceptibility gene product." Proc Natl Acad Sci U S A **90**(15): 6914-6918.

- Frame, S. and A. Balmain (2000). "Integration of positive and negative growth signals during ras pathway activation in vivo." Curr Opin Genet Dev **10**(1): 106-113.
- Franzoso, G., V. Bours, et al. (1992). "The candidate oncoprotein Bcl-3 is an antagonist of p50/NF-kappa B-mediated inhibition." Nature **359**(6393): 339-342.
- Friedman, S. R., W. de Jong, et al. (2007). "Harm reduction theory: users' culture, micro-social indigenous harm reduction, and the self-organization and outside-organizing of users' groups." Int J Drug Policy **18**(2): 107-117.
- Frippiat, C., Q. M. Chen, et al. (2001). "Subcytotoxic H<sub>2</sub>O<sub>2</sub> stress triggers a release of transforming growth factor-beta 1, which induces biomarkers of cellular senescence of human diploid fibroblasts." J Biol Chem **276**(4): 2531-2537.
- Frippiat, C., J. Dewelle, et al. (2002). "Signal transduction in H<sub>2</sub>O<sub>2</sub>-induced senescence-like phenotype in human diploid fibroblasts." Free Radic Biol Med **33**(10): 1334-1346.
- Frolov, M. V. and N. J. Dyson (2004). "Molecular mechanisms of E2F-dependent activation and pRB-mediated repression." J Cell Sci **117**(Pt 11): 2173-2181.
- Fujita, T., G. P. Nolan, et al. (1993). "The candidate proto-oncogene bcl-3 encodes a transcriptional coactivator that activates through NF-kappa B p50 homodimers." Genes Dev **7**(7B): 1354-1363.
- Fukasawa, K. and G. F. Vande Woude (1997). "Synergy between the Mos/mitogen-activated protein kinase pathway and loss of p53 function in transformation and chromosome instability." Mol Cell Biol **17**(1): 506-518.
- Gage, J. R., C. Meyers, et al. (1990). "The E7 proteins of the nononcogenic human papillomavirus type 6b (HPV-6b) and of the oncogenic HPV-16 differ in retinoblastoma protein binding and other properties." J Virol **64**(2): 723-730.
- Gao, C. P., Z. Y. Zhang, et al. (2010). "[Reduced expression of miR-218 and its significance in gastric cancer]." Zhonghua Zhong Liu Za Zhi **32**(4): 249-252.
- Gao, F., J. F. Ponte, et al. (2009). "hBub1 negatively regulates p53 mediated early cell death upon mitotic checkpoint activation." Cancer Biol Ther **8**(7): 548-556.
- Garcia-Cao, I., M. Garcia-Cao, et al. (2006). "Increased p53 activity does not accelerate telomere-driven ageing." EMBO Rep **7**(5): 546-552.
- Gartel, A. L., M. S. Serfas, et al. (1996). "p21 (WAF1/CIP1) expression is induced in newly nondividing cells in diverse epithelia and during differentiation of the Caco-2 intestinal cell line." Exp Cell Res **227**(2): 171-181.
- Gaubatz, S., J. G. Wood, et al. (1998). "Unusual proliferation arrest and transcriptional control properties of a newly discovered E2F family member, E2F-6." Proc Natl Acad Sci U S A **95**(16): 9190-9195.
- Gewin, L. and D. A. Galloway (2001). "E box-dependent activation of telomerase by human papillomavirus type 16 E6 does not require induction of c-myc." J Virol **75**(15): 7198-7201.
- Gil, J., D. Bernard, et al. (2004). "Polycomb CBX7 has a unifying role in cellular lifespan." Nat Cell Biol **6**(1): 67-72.
- Gilinger, G. and J. C. Alwine (1993). "Transcriptional activation by simian virus 40 large T antigen: requirements for simple promoter structures containing either TATA or initiator elements with variable upstream factor binding sites." J Virol **67**(11): 6682-6688.

- Gillison, M. L., W. M. Koch, et al. (2000). "Evidence for a causal association between human papillomavirus and a subset of head and neck cancers." J Natl Cancer Inst **92**(9): 709-720.
- Gilmore, T. D. (2006). "Introduction to NF-kappaB: players, pathways, perspectives." Oncogene **25**(51): 6680-6684.
- Gjoerup, O. V., J. Wu, et al. (2007). "Surveillance mechanism linking Bub1 loss to the p53 pathway." Proc Natl Acad Sci U S A **104**(20): 8334-8339.
- Gonos, E. S., J. S. Burns, et al. (1996). "Rat embryo fibroblasts immortalized with simian virus 40 large T antigen undergo senescence upon its inactivation." Mol Cell Biol **16**(9): 5127-5138.
- Gonzalez-Suarez, E., C. Geserick, et al. (2005). "Antagonistic effects of telomerase on cancer and aging in K5-mTert transgenic mice." Oncogene **24**(13): 2256-2270.
- Gonzalez-Suarez, E., E. Samper, et al. (2000). "Telomerase-deficient mice with short telomeres are resistant to skin tumorigenesis." Nat Genet **26**(1): 114-117.
- Goodman, R. H. and S. Smolik (2000). "CBP/p300 in cell growth, transformation, and development." Genes Dev **14**(13): 1553-1577.
- Gorman, S. D. and V. J. Cristofalo (1985). "Reinitiation of cellular DNA synthesis in BrdU-selected nondividing senescent WI-38 cells by simian virus 40 infection." J Cell Physiol **125**(1): 122-126.
- Gostissa, M., A. Hengstermann, et al. (1999). "Activation of p53 by conjugation to the ubiquitin-like protein SUMO-1." EMBO J **18**(22): 6462-6471.
- Greider, C. W. and E. H. Blackburn (1985). "Identification of a specific telomere terminal transferase activity in Tetrahymena extracts." Cell **43**(2 Pt 1): 405-413.
- Grobet, L., L. J. Martin, et al. (1997). "A deletion in the bovine myostatin gene causes the double-musled phenotype in cattle." Nat Genet **17**(1): 71-74.
- Grosch, S., I. Tegeder, et al. (2001). "COX-2 independent induction of cell cycle arrest and apoptosis in colon cancer cells by the selective COX-2 inhibitor celecoxib." FASEB J **15**(14): 2742-2744.
- Grossman, S. R., M. Perez, et al. (1998). "p300/MDM2 complexes participate in MDM2-mediated p53 degradation." Mol Cell **2**(4): 405-415.
- Groth, A., J. D. Weber, et al. (2000). "Oncogenic Ras induces p19ARF and growth arrest in mouse embryo fibroblasts lacking p21Cip1 and p27Kip1 without activating cyclin D-dependent kinases." J Biol Chem **275**(35): 27473-27480.
- Gruber, A. D. and B. U. Pauli (1999). "Tumorigenicity of human breast cancer is associated with loss of the Ca<sup>2+</sup>-activated chloride channel CLCA2." Cancer Res **59**(21): 5488-5491.
- Gruda, M. C., J. M. Zabolotny, et al. (1993). "Transcriptional activation by simian virus 40 large T antigen: interactions with multiple components of the transcription complex." Mol Cell Biol **13**(2): 961-969.
- Gruis, N. A., J. Weaver-Feldhaus, et al. (1995). "Genetic evidence in melanoma and bladder cancers that p16 and p53 function in separate pathways of tumor suppression." Am J Pathol **146**(5): 1199-1206.
- Gu, W., J. W. Schneider, et al. (1993). "Interaction of myogenic factors and the retinoblastoma protein mediates muscle cell commitment and differentiation." Cell **72**(3): 309-324.
- Guimaraes, D. P. and P. Hainaut (2002). "TP53: a key gene in human cancer." Biochimie **84**(1): 83-93.

- Guled, M., L. Lahti, et al. (2009). "CDKN2A, NF2, and JUN are dysregulated among other genes by miRNAs in malignant mesothelioma -A miRNA microarray analysis." Genes Chromosomes Cancer **48**(7): 615-623.
- Haas-Kogan, D. A., S. C. Kogan, et al. (1995). "Inhibition of apoptosis by the retinoblastoma gene product." EMBO J **14**(3): 461-472.
- Haddad, M. M., W. Xu, et al. (1999). "Activation of a cAMP pathway and induction of melanogenesis correlate with association of p16(INK4) and p27(KIP1) to CDKs, loss of E2F-binding activity, and premature senescence of human melanocytes." Exp Cell Res **253**(2): 561-572.
- Hahn, W. C. and R. A. Weinberg (2002). "Rules for making human tumor cells." N Engl J Med **347**(20): 1593-1603.
- Hainaut, P., T. Soussi, et al. (1997). "Database of p53 gene somatic mutations in human tumors and cell lines: updated compilation and future prospects." Nucleic Acids Res **25**(1): 151-157.
- Halazonetis, T. D., V. G. Gorgoulis, et al. (2008). "An oncogene-induced DNA damage model for cancer development." Science **319**(5868): 1352-1355.
- Hames, R. S. and A. M. Fry (2002). "Alternative splice variants of the human centrosome kinase Nek2 exhibit distinct patterns of expression in mitosis." Biochem J **361**(Pt 1): 77-85.
- Hanahan, D. and R. A. Weinberg (2000). "The hallmarks of cancer." Cell **100**(1): 57-70.
- Hanissian, S. H., B. Teng, et al. (2005). "Regulation of myeloid leukemia factor-1 interacting protein (MLF1IP) expression in glioblastoma." Brain Res **1047**(1): 56-64.
- Hannon, G. J., D. Demetrick, et al. (1993). "Isolation of the Rb-related p130 through its interaction with CDK2 and cyclins." Genes Dev **7**(12A): 2378-2391.
- Hansen, U., D. G. Tenen, et al. (1981). "T antigen repression of SV40 early transcription from two promoters." Cell **27**(3 Pt 2): 603-613.
- Hara, E., R. Smith, et al. (1996). "Regulation of p16CDKN2 expression and its implications for cell immortalization and senescence." Mol Cell Biol **16**(3): 859-867.
- Hardy, K., L. Mansfield, et al. (2005). "Transcriptional networks and cellular senescence in human mammary fibroblasts." Mol Biol Cell **16**(2): 943-953.
- Harley, C. B., A. B. Futcher, et al. (1990). "Telomeres shorten during ageing of human fibroblasts." Nature **345**(6274): 458-460.
- Harlow, E., P. Whyte, et al. (1986). "Association of adenovirus early-region 1A proteins with cellular polypeptides." Mol Cell Biol **6**(5): 1579-1589.
- Harper, J. W., G. R. Adami, et al. (1993). "The p21 Cdk-interacting protein Cip1 is a potent inhibitor of G1 cyclin-dependent kinases." Cell **75**(4): 805-816.
- Harvat, B. L., A. Wang, et al. (1998). "Up-regulation of p27Kip1, p21WAF1/Cip1 and p16Ink4a is associated with, but not sufficient for, induction of squamous differentiation." J Cell Sci **111** ( Pt 9): 1185-1196.
- Harvey, M., M. J. McArthur, et al. (1993). "Spontaneous and carcinogen-induced tumorigenesis in p53-deficient mice." Nat Genet **5**(3): 225-229.
- Hayden, M. S., A. P. West, et al. (2006). "NF-kappaB and the immune response." Oncogene **25**(51): 6758-6780.
- Hayflick, L. and P. S. Moorhead (1961). "The serial cultivation of human diploid cell strains." Exp Cell Res **25**: 585-621.



- Hayward, D. G., R. B. Clarke, et al. (2004). "The centrosomal kinase Nek2 displays elevated levels of protein expression in human breast cancer." Cancer Res **64**(20): 7370-7376.
- Hayward, D. G. and A. M. Fry (2006). "Nek2 kinase in chromosome instability and cancer." Cancer Lett **237**(2): 155-166.
- He, L., X. He, et al. (2007). "A microRNA component of the p53 tumour suppressor network." Nature **447**(7148): 1130-1134.
- He, L., J. M. Thomson, et al. (2005). "A microRNA polycistron as a potential human oncogene." Nature **435**(7043): 828-833.
- He, S., B. L. Cook, et al. (2000). "E2F is required to prevent inappropriate S-phase entry of mammalian cells." Mol Cell Biol **20**(1): 363-371.
- Heinrichs, S. and W. Deppert (2003). "Apoptosis or growth arrest: modulation of the cellular response to p53 by proliferative signals." Oncogene **22**(4): 555-571.
- Helenius, M., M. Hanninen, et al. (1996). "Aging-induced up-regulation of nuclear binding activities of oxidative stress responsive NF-kB transcription factor in mouse cardiac muscle." J Mol Cell Cardiol **28**(3): 487-498.
- Helin, K., E. Harlow, et al. (1993). "Inhibition of E2F-1 transactivation by direct binding of the retinoblastoma protein." Mol Cell Biol **13**(10): 6501-6508.
- Helt, A. M., J. O. Funk, et al. (2002). "Inactivation of both the retinoblastoma tumor suppressor and p21 by the human papillomavirus type 16 E7 oncoprotein is necessary to inhibit cell cycle arrest in human epithelial cells." J Virol **76**(20): 10559-10568.
- Hemann, M. T., K. L. Rudolph, et al. (2001). "Telomere dysfunction triggers developmentally regulated germ cell apoptosis." Mol Biol Cell **12**(7): 2023-2030.
- Heneghan, H. M., N. Miller, et al. (2010). "Systemic miRNA-195 differentiates breast cancer from other malignancies and is a potential biomarker for detecting noninvasive and early stage disease." Oncologist **15**(7): 673-682.
- Henning, W., G. Rohaly, et al. (1997). "MDM2 is a target of simian virus 40 in cellular transformation and during lytic infection." J Virol **71**(10): 7609-7618.
- Herbig, U., W. A. Jobling, et al. (2004). "Telomere shortening triggers senescence of human cells through a pathway involving ATM, p53, and p21(CIP1), but not p16(INK4a)." Mol Cell **14**(4): 501-513.
- Hilleman, M. R. (1998). "Discovery of simian virus 40 (SV40) and its relationship to poliomyelitis virus vaccines." Dev Biol Stand **94**: 183-190.
- Hoggard, N., B. Brintnell, et al. (1995). "Allelic imbalance on chromosome 1 in human breast cancer. II. Microsatellite repeat analysis." Genes Chromosomes Cancer **12**(1): 24-31.
- Holland, E. A., S. C. Beaton, et al. (1995). "Analysis of the p16 gene, CDKN2, in 17 Australian melanoma kindreds." Oncogene **11**(11): 2289-2294.
- Honda, R. and H. Yasuda (1999). "Association of p19(ARF) with Mdm2 inhibits ubiquitin ligase activity of Mdm2 for tumor suppressor p53." EMBO J **18**(1): 22-27.
- Hsieh, J. K., D. Yap, et al. (2002). "Novel function of the cyclin A binding site of E2F in regulating p53-induced apoptosis in response to DNA damage." Mol Cell Biol **22**(1): 78-93.

- Hu, G., J. Kim, et al. (2009). "A genome-wide RNAi screen identifies a new transcriptional module required for self-renewal." *Genes Dev* **23**(7): 837-848.
- Hu, Q. J., N. Dyson, et al. (1990). "The regions of the retinoblastoma protein needed for binding to adenovirus E1A or SV40 large T antigen are common sites for mutations." *EMBO J* **9**(4): 1147-1155.
- Huang, S., N. P. Wang, et al. (1990). "Two distinct and frequently mutated regions of retinoblastoma protein are required for binding to SV40 T antigen." *EMBO J* **9**(6): 1815-1822.
- Hui, A. B., M. Lenarduzzi, et al. (2010). "Comprehensive MicroRNA profiling for head and neck squamous cell carcinomas." *Clin Cancer Res* **16**(4): 1129-1139.
- Huibregtse, J. M., M. Scheffner, et al. (1991). "A cellular protein mediates association of p53 with the E6 oncoprotein of human papillomavirus types 16 or 18." *EMBO J* **10**(13): 4129-4135.
- Hurst, D. R., Y. Xie, et al. (2009). "Multiple forms of BRMS1 are differentially expressed in the MCF10 isogenic breast cancer progression model." *Clin Exp Metastasis* **26**(2): 89-96.
- Hussussian, C. J., J. P. Struewing, et al. (1994). "Germline p16 mutations in familial melanoma." *Nat Genet* **8**(1): 15-21.
- Iavarone, A., P. Garg, et al. (1994). "The helix-loop-helix protein Id-2 enhances cell proliferation and binds to the retinoblastoma protein." *Genes Dev* **8**(11): 1270-1284.
- Ikram, Z., T. Norton, et al. (1994). "The biological clock that measures the mitotic life-span of mouse embryo fibroblasts continues to function in the presence of simian virus 40 large tumor antigen." *Proc Natl Acad Sci U S A* **91**(14): 6448-6452.
- Imamura, T., H. Izumi, et al. (2001). "Interaction with p53 enhances binding of cisplatin-modified DNA by high mobility group 1 protein." *J Biol Chem* **276**(10): 7534-7540.
- Inoue, J., L. D. Kerr, et al. (1992). "I kappa B gamma, a 70 kd protein identical to the C-terminal half of p110 NF-kappa B: a new member of the I kappa B family." *Cell* **68**(6): 1109-1120.
- Inoue, K., R. Wen, et al. (2000). "Disruption of the ARF transcriptional activator DMP1 facilitates cell immortalization, Ras transformation, and tumorigenesis." *Genes Dev* **14**(14): 1797-1809.
- Inoue, K., F. Zindy, et al. (2001). "Dmp1 is haplo-insufficient for tumor suppression and modifies the frequencies of Arf and p53 mutations in Myc-induced lymphomas." *Genes Dev* **15**(22): 2934-2939.
- Iorio, M. V. and C. M. Croce (2009). "MicroRNAs in cancer: small molecules with a huge impact." *J Clin Oncol* **27**(34): 5848-5856.
- Iorio, M. V., M. Ferracin, et al. (2005). "MicroRNA gene expression deregulation in human breast cancer." *Cancer Res* **65**(16): 7065-7070.
- Irizarry, R. A., B. Hobbs, et al. (2003). "Exploration, normalization, and summaries of high density oligonucleotide array probe level data." *Biostatistics* **4**(2): 249-264.
- Irizarry, R. A., D. Warren, et al. (2005). "Multiple-laboratory comparison of microarray platforms." *Nat Methods* **2**(5): 345-350.
- Irwin, M. S. and W. G. Kaelin (2001). "p53 family update: p73 and p63 develop their own identities." *Cell Growth Differ* **12**(7): 337-349.

- Ishikawa, F. (1997). "Regulation mechanisms of mammalian telomerase. A review." Biochemistry (Mosc) **62**(11): 1332-1337.
- Itahana, K., Y. Zou, et al. (2003). "Control of the replicative life span of human fibroblasts by p16 and the polycomb protein Bmi-1." Mol Cell Biol **23**(1): 389-401.
- Ito, K., S. Adachi, et al. (2001). "N-Terminally extended human ubiquitin-conjugating enzymes (E2s) mediate the ubiquitination of RING-finger proteins, ARA54 and RNF8." Eur J Biochem **268**(9): 2725-2732.
- Jackson, A. L., S. R. Bartz, et al. (2003). "Expression profiling reveals off-target gene regulation by RNAi." Nat Biotechnol **21**(6): 635-637.
- Jacobs, J. J. and T. de Lange (2004). "Significant role for p16INK4a in p53-independent telomere-directed senescence." Curr Biol **14**(24): 2302-2308.
- Jacobs, J. J., P. Keblusek, et al. (2000). "Senescence bypass screen identifies TBX2, which represses Cdkn2a (p19(ARF)) and is amplified in a subset of human breast cancers." Nat Genet **26**(3): 291-299.
- Jacobs, J. J., K. Kieboom, et al. (1999). "The oncogene and Polycomb-group gene bmi-1 regulates cell proliferation and senescence through the ink4a locus." Nature **397**(6715): 164-168.
- Jacobs, M. D. and S. C. Harrison (1998). "Structure of an IkappaBalpha/NF-kappaB complex." Cell **95**(6): 749-758.
- Jarrard, D. F., S. Sarkar, et al. (1999). "p16/pRb pathway alterations are required for bypassing senescence in human prostate epithelial cells." Cancer Res **59**(12): 2957-2964.
- Jat, P. S. and P. A. Sharp (1989). "Cell lines established by a temperature-sensitive simian virus 40 large-T-antigen gene are growth restricted at the nonpermissive temperature." Mol Cell Biol **9**(4): 1672-1681.
- Jayaraman, L., N. C. Moorthy, et al. (1998). "High mobility group protein-1 (HMG-1) is a unique activator of p53." Genes Dev **12**(4): 462-472.
- Johnson, L., D. Greenbaum, et al. (1997). "K-ras is an essential gene in the mouse with partial functional overlap with N-ras." Genes Dev **11**(19): 2468-2481.
- Johnson, S. M., H. Grosshans, et al. (2005). "RAS is regulated by the let-7 microRNA family." Cell **120**(5): 635-647.
- Jones, S. N., A. E. Roe, et al. (1995). "Rescue of embryonic lethality in Mdm2-deficient mice by absence of p53." Nature **378**(6553): 206-208.
- Kaghad, M., H. Bonnet, et al. (1997). "Monoallelically expressed gene related to p53 at 1p36, a region frequently deleted in neuroblastoma and other human cancers." Cell **90**(4): 809-819.
- Kalderon, D., W. D. Richardson, et al. (1984). "Sequence requirements for nuclear location of simian virus 40 large-T antigen." Nature **311**(5981): 33-38.
- Kamijo, T., S. Bodner, et al. (1999). "Tumor spectrum in ARF-deficient mice." Cancer Res **59**(9): 2217-2222.
- Kamijo, T., J. D. Weber, et al. (1998). "Functional and physical interactions of the ARF tumor suppressor with p53 and Mdm2." Proc Natl Acad Sci U S A **95**(14): 8292-8297.
- Kamijo, T., F. Zindy, et al. (1997). "Tumor suppression at the mouse INK4a locus mediated by the alternative reading frame product p19ARF." Cell **91**(5): 649-659.

- Kan, T., F. Sato, et al. (2009). "The miR-106b-25 polycistron, activated by genomic amplification, functions as an oncogene by suppressing p21 and Bim." Gastroenterology **136**(5): 1689-1700.
- Kanehira, M., Y. Harada, et al. (2007). "Involvement of upregulation of DEPDC1 (DEP domain containing 1) in bladder carcinogenesis." Oncogene **26**(44): 6448-6455.
- Kang, S., Y. B. Kim, et al. (2005). "Polymorphism in the nuclear factor kappa-B binding promoter region of cyclooxygenase-2 is associated with an increased risk of bladder cancer." Cancer Lett **217**(1): 11-16.
- Kao, J., K. Salari, et al. (2009). "Molecular profiling of breast cancer cell lines defines relevant tumor models and provides a resource for cancer gene discovery." PLoS One **4**(7): e6146.
- Karin, M. (1999). "How NF-kappaB is activated: the role of the IkappaB kinase (IKK) complex." Oncogene **18**(49): 6867-6874.
- Karin, M. and Y. Ben-Neriah (2000). "Phosphorylation meets ubiquitination: the control of NF-[kappa]B activity." Annu Rev Immunol **18**: 621-663.
- Karlseder, J., D. Broccoli, et al. (1999). "p53- and ATM-dependent apoptosis induced by telomeres lacking TRF2." Science **283**(5406): 1321-1325.
- Katakura, Y. (2006). "Molecular basis for the cellular senescence program and its application to anticancer therapy." Biosci Biotechnol Biochem **70**(5): 1076-1081.
- Katz, M. E. and F. McCormick (1997). "Signal transduction from multiple Ras effectors." Curr Opin Genet Dev **7**(1): 75-79.
- Kawakubo, H., J. L. Carey, et al. (2004). "Expression of the NF-kappaB-responsive gene BTG2 is aberrantly regulated in breast cancer." Oncogene **23**(50): 8310-8319.
- Keeshan, K., Y. He, et al. (2006). "Tribbles homolog 2 inactivates C/EBPalpha and causes acute myelogenous leukemia." Cancer Cell **10**(5): 401-411.
- Kennedy, B. K., D. A. Barbie, et al. (2000). "Nuclear organization of DNA replication in primary mammalian cells." Genes Dev **14**(22): 2855-2868.
- Kerzee, J. K. and K. S. Ramos (2000). "Activation of c-Ha-ras by benzo(a)pyrene in vascular smooth muscle cells involves redox stress and aryl hydrocarbon receptor." Mol Pharmacol **58**(1): 152-158.
- Kilbey, A., K. Blyth, et al. (2007). "Runx2 disruption promotes immortalization and confers resistance to oncogene-induced senescence in primary murine fibroblasts." Cancer Res **67**(23): 11263-11271.
- Kim, V. N. (2005). "MicroRNA biogenesis: coordinated cropping and dicing." Nat Rev Mol Cell Biol **6**(5): 376-385.
- Kimchi, A., X. F. Wang, et al. (1988). "Absence of TGF-beta receptors and growth inhibitory responses in retinoblastoma cells." Science **240**(4849): 196-199.
- Kiyono, T., S. A. Foster, et al. (1998). "Both Rb/p16INK4a inactivation and telomerase activity are required to immortalize human epithelial cells." Nature **396**(6706): 84-88.
- Knudsen, E. S. and J. Y. Wang (1996). "Differential regulation of retinoblastoma protein function by specific Cdk phosphorylation sites." J Biol Chem **271**(14): 8313-8320.
- Knudson, A. G., Jr. (1971). "Mutation and cancer: statistical study of retinoblastoma." Proc Natl Acad Sci U S A **68**(4): 820-823.

- Koli, K., J. Saharinen, et al. (2001). "Novel non-TGF-beta-binding splice variant of LTBP-4 in human cells and tissues provides means to decrease TGF-beta deposition." *J Cell Sci* **114**(Pt 15): 2869-2878.
- Kriete, A., K. L. Mayo, et al. (2008). "Cell autonomous expression of inflammatory genes in biologically aged fibroblasts associated with elevated NF-kappaB activity." *Immun Ageing* **5**: 5.
- Krtolica, A. and J. Campisi (2002). "Cancer and aging: a model for the cancer promoting effects of the aging stroma." *Int J Biochem Cell Biol* **34**(11): 1401-1414.
- Krutzfeldt, J., N. Rajewsky, et al. (2005). "Silencing of microRNAs in vivo with 'antagomirs'." *Nature* **438**(7068): 685-689.
- Kuhn, A. R., K. Schlauch, et al. (2010). "MicroRNA expression in human airway smooth muscle cells: role of miR-25 in regulation of airway smooth muscle phenotype." *Am J Respir Cell Mol Biol* **42**(4): 506-513.
- Kuilman, T., C. Michaloglou, et al. (2008). "Oncogene-induced senescence relayed by an interleukin-dependent inflammatory network." *Cell* **133**(6): 1019-1031.
- Kuilman, T. and D. S. Peeper (2009). "Senescence-messaging secretome: SMS-ing cellular stress." *Nat Rev Cancer* **9**(2): 81-94.
- Kumamoto, K., E. A. Spillare, et al. (2008). "Nutlin-3a activates p53 to both down-regulate inhibitor of growth 2 and up-regulate mir-34a, mir-34b, and mir-34c expression, and induce senescence." *Cancer Res* **68**(9): 3193-3203.
- Kumar, M. S., J. Lu, et al. (2007). "Impaired microRNA processing enhances cellular transformation and tumorigenesis." *Nat Genet* **39**(5): 673-677.
- Kurochkin, I. V., N. Yonemitsu, et al. (2001). "ALEX1, a novel human armadillo repeat protein that is expressed differentially in normal tissues and carcinomas." *Biochem Biophys Res Commun* **280**(1): 340-347.
- Kusenda, B., M. Mraz, et al. (2006). "MicroRNA biogenesis, functionality and cancer relevance." *Biomed Pap Med Fac Univ Palacky Olomouc Czech Repub* **150**(2): 205-215.
- LaBaer, J., M. D. Garrett, et al. (1997). "New functional activities for the p21 family of CDK inhibitors." *Genes Dev* **11**(7): 847-862.
- Lachner, M., D. O'Carroll, et al. (2001). "Methylation of histone H3 lysine 9 creates a binding site for HP1 proteins." *Nature* **410**(6824): 116-120.
- Lagos-Quintana, M., R. Rauhut, et al. (2001). "Identification of novel genes coding for small expressed RNAs." *Science* **294**(5543): 853-858.
- Lagos-Quintana, M., R. Rauhut, et al. (2002). "Identification of tissue-specific microRNAs from mouse." *Curr Biol* **12**(9): 735-739.
- Lai, A., B. K. Kennedy, et al. (2001). "RBP1 recruits the mSIN3-histone deacetylase complex to the pocket of retinoblastoma tumor suppressor family proteins found in limited discrete regions of the nucleus at growth arrest." *Mol Cell Biol* **21**(8): 2918-2932.
- Land, H., A. C. Chen, et al. (1986). "Behavior of myc and ras oncogenes in transformation of rat embryo fibroblasts." *Mol Cell Biol* **6**(6): 1917-1925.
- Land, H., L. F. Parada, et al. (1983). "Tumorigenic conversion of primary embryo fibroblasts requires at least two cooperating oncogenes." *Nature* **304**(5927): 596-602.
- Lane, D. P. (1992). "Cancer. p53, guardian of the genome." *Nature* **358**(6381): 15-16.

- Lane, D. P. and L. V. Crawford (1979). "T antigen is bound to a host protein in SV40-transformed cells." *Nature* **278**(5701): 261-263.
- Langley, E., M. Pearson, et al. (2002). "Human SIR2 deacetylates p53 and antagonizes PML/p53-induced cellular senescence." *EMBO J* **21**(10): 2383-2396.
- Laoukili, J., M. Alvarez-Fernandez, et al. (2008). "FoxM1 is degraded at mitotic exit in a Cdh1-dependent manner." *Cell Cycle* **7**(17): 2720-2726.
- Laoukili, J., M. R. Kooistra, et al. (2005). "FoxM1 is required for execution of the mitotic programme and chromosome stability." *Nat Cell Biol* **7**(2): 126-136.
- Laoukili, J., M. Stahl, et al. (2007). "FoxM1: at the crossroads of ageing and cancer." *Biochim Biophys Acta* **1775**(1): 92-102.
- Larkin, J. E., B. C. Frank, et al. (2005). "Independence and reproducibility across microarray platforms." *Nat Methods* **2**(5): 337-344.
- Lau, N. C., L. P. Lim, et al. (2001). "An abundant class of tiny RNAs with probable regulatory roles in *Caenorhabditis elegans*." *Science* **294**(5543): 858-862.
- Lee, E. Y., C. Y. Chang, et al. (1992). "Mice deficient for Rb are nonviable and show defects in neurogenesis and haematopoiesis." *Nature* **359**(6393): 288-294.
- Lee, J. O., A. A. Russo, et al. (1998). "Structure of the retinoblastoma tumour-suppressor pocket domain bound to a peptide from HPV E7." *Nature* **391**(6670): 859-865.
- Lee, L. K., B. M. Dunham, et al. (2006). "Cellular dynamics of antisense oligonucleotides and short interfering RNAs." *Ann N Y Acad Sci* **1082**: 47-51.
- Lee, M. L., F. C. Kuo, et al. (2000). "Importance of replication in microarray gene expression studies: statistical methods and evidence from repetitive cDNA hybridizations." *Proc Natl Acad Sci U S A* **97**(18): 9834-9839.
- Lee, R. C., R. L. Feinbaum, et al. (1993). "The *C. elegans* heterochronic gene *lin-4* encodes small RNAs with antisense complementarity to *lin-14*." *Cell* **75**(5): 843-854.
- Lee, W. H., J. Y. Shew, et al. (1987). "The retinoblastoma susceptibility gene encodes a nuclear phosphoprotein associated with DNA binding activity." *Nature* **329**(6140): 642-645.
- Levrero, M., V. De Laurenzi, et al. (2000). "The p53/p63/p73 family of transcription factors: overlapping and distinct functions." *J Cell Sci* **113** ( Pt 10): 1661-1670.
- Li, Q. and I. M. Verma (2002). "NF-kappaB regulation in the immune system." *Nat Rev Immunol* **2**(10): 725-734.
- Li, R., S. Waga, et al. (1994). "Differential effects by the p21 CDK inhibitor on PCNA-dependent DNA replication and repair." *Nature* **371**(6497): 534-537.
- Li, X., J. K. Cowell, et al. (2004). "CLCA2 tumour suppressor gene in 1p31 is epigenetically regulated in breast cancer." *Oncogene* **23**(7): 1474-1480.
- Li, X. F., P. J. Yan, et al. (2009). "Downregulation of miR-193b contributes to enhance urokinase-type plasminogen activator (uPA) expression and tumor progression and invasion in human breast cancer." *Oncogene* **28**(44): 3937-3948.
- Lill, N. L., S. R. Grossman, et al. (1997). "Binding and modulation of p53 by p300/CBP coactivators." *Nature* **387**(6635): 823-827.
- Lim, L. P., N. C. Lau, et al. (2003). "The microRNAs of *Caenorhabditis elegans*." *Genes Dev* **17**(8): 991-1008.

- Lin, A. W., M. Barradas, et al. (1998). "Premature senescence involving p53 and p16 is activated in response to constitutive MEK/MAPK mitogenic signaling." Genes Dev **12**(19): 3008-3019.
- Lin, M. L., J. H. Park, et al. (2007). "Involvement of maternal embryonic leucine zipper kinase (MELK) in mammary carcinogenesis through interaction with Bcl-G, a pro-apoptotic member of the Bcl-2 family." Breast Cancer Res **9**(1): R17.
- Lindstrom, M. S. and K. G. Wiman (2003). "Myc and E2F1 induce p53 through p14ARF-independent mechanisms in human fibroblasts." Oncogene **22**(32): 4993-5005.
- Linggi, B., C. Muller-Tidow, et al. (2002). "The t(8;21) fusion protein, AML1 ETO, specifically represses the transcription of the p14(ARF) tumor suppressor in acute myeloid leukemia." Nat Med **8**(7): 743-750.
- Linzer, D. I. and A. J. Levine (1979). "Characterization of a 54K dalton cellular SV40 tumor antigen present in SV40-transformed cells and uninfected embryonal carcinoma cells." Cell **17**(1): 43-52.
- Lipinski, M. M. and T. Jacks (1999). "The retinoblastoma gene family in differentiation and development." Oncogene **18**(55): 7873-7882.
- Liu, C. G., G. A. Calin, et al. (2004). "An oligonucleotide microchip for genome-wide microRNA profiling in human and mouse tissues." Proc Natl Acad Sci U S A **101**(26): 9740-9744.
- Liu, L., N. J. Lassam, et al. (1995). "Germline p16INK4A mutation and protein dysfunction in a family with inherited melanoma." Oncogene **11**(2): 405-412.
- Lockyer, P. J., S. Kupzig, et al. (2001). "CAPRI regulates Ca(2+)-dependent inactivation of the Ras-MAPK pathway." Curr Biol **11**(12): 981-986.
- Lohrum, M. A. and K. H. Vousden (2000). "Regulation and function of the p53-related proteins: same family, different rules." Trends Cell Biol **10**(5): 197-202.
- Lowe, S. W. and H. E. Ruley (1993). "Stabilization of the p53 tumor suppressor is induced by adenovirus 5 E1A and accompanies apoptosis." Genes Dev **7**(4): 535-545.
- Lowe, S. W. and C. J. Sherr (2003). "Tumor suppression by Ink4a-Arf: progress and puzzles." Curr Opin Genet Dev **13**(1): 77-83.
- Lu, T. and T. Finkel (2008). "Free radicals and senescence." Exp Cell Res **314**(9): 1918-1922.
- Lu, W., R. Pochampally, et al. (2000). "Nuclear exclusion of p53 in a subset of tumors requires MDM2 function." Oncogene **19**(2): 232-240.
- Ludlow, J. W., J. A. DeCaprio, et al. (1989). "SV40 large T antigen binds preferentially to an underphosphorylated member of the retinoblastoma susceptibility gene product family." Cell **56**(1): 57-65.
- Ludlow, J. W., J. Shon, et al. (1990). "The retinoblastoma susceptibility gene product undergoes cell cycle-dependent dephosphorylation and binding to and release from SV40 large T." Cell **60**(3): 387-396.
- Lukas, J., D. Parry, et al. (1995). "Retinoblastoma-protein-dependent cell-cycle inhibition by the tumour suppressor p16." Nature **375**(6531): 503-506.
- Luo, R. X., A. A. Postigo, et al. (1998). "Rb interacts with histone deacetylase to repress transcription." Cell **92**(4): 463-473.
- Ma, L. and R. A. Weinberg (2008). "MicroRNAs in malignant progression." Cell Cycle **7**(5): 570-572.

- Ma, R. Y., T. H. Tong, et al. (2005). "Raf/MEK/MAPK signaling stimulates the nuclear translocation and transactivating activity of FOXM1c." *J Cell Sci* **118**(Pt 4): 795-806.
- Macip, S., M. Igarashi, et al. (2003). "Influence of induced reactive oxygen species in p53-mediated cell fate decisions." *Mol Cell Biol* **23**(23): 8576-8585.
- Macip, S., M. Igarashi, et al. (2002). "Inhibition of p21-mediated ROS accumulation can rescue p21-induced senescence." *EMBO J* **21**(9): 2180-2188.
- Maeda, T., R. M. Hobbs, et al. (2005). "Role of the proto-oncogene Pokemon in cellular transformation and ARF repression." *Nature* **433**(7023): 278-285.
- Maier, B., W. Gluba, et al. (2004). "Modulation of mammalian life span by the short isoform of p53." *Genes Dev* **18**(3): 306-319.
- Maione, R., G. M. Fimia, et al. (1994). "Retinoblastoma antioncogene is involved in the inhibition of myogenesis by polyomavirus large T antigen." *Cell Growth Differ* **5**(2): 231-237.
- Mantovani, F. and L. Banks (2001). "The human papillomavirus E6 protein and its contribution to malignant progression." *Oncogene* **20**(54): 7874-7887.
- Mao, L., A. Merlo, et al. (1995). "A novel p16INK4A transcript." *Cancer Res* **55**(14): 2995-2997.
- Marasa, B. S., S. Srikantan, et al. (2009). "Increased MKK4 abundance with replicative senescence is linked to the joint reduction of multiple microRNAs." *Sci Signal* **2**(94): ra69.
- Marie, S. K., O. K. Okamoto, et al. (2008). "Maternal embryonic leucine zipper kinase transcript abundance correlates with malignancy grade in human astrocytomas." *Int J Cancer* **122**(4): 807-815.
- Martens, U. M., E. A. Chavez, et al. (2000). "Accumulation of short telomeres in human fibroblasts prior to replicative senescence." *Exp Cell Res* **256**(1): 291-299.
- Martin, D. W., M. A. Subler, et al. (1993). "p53 and SV40 T antigen bind to the same region overlapping the conserved domain of the TATA-binding protein." *Biochem Biophys Res Commun* **195**(1): 428-434.
- Martin, K. J., E. Graner, et al. (2001). "High-sensitivity array analysis of gene expression for the early detection of disseminated breast tumor cells in peripheral blood." *Proc Natl Acad Sci U S A* **98**(5): 2646-2651.
- Martinez, I., A. S. Gardiner, et al. (2008). "Human papillomavirus type 16 reduces the expression of microRNA-218 in cervical carcinoma cells." *Oncogene* **27**(18): 2575-2582.
- Marz, P., A. Probst, et al. (2004). "Ataxin-10, the spinocerebellar ataxia type 10 neurodegenerative disorder protein, is essential for survival of cerebellar neurons." *J Biol Chem* **279**(34): 35542-35550.
- Maser, R. S. and R. A. DePinho (2002). "Connecting chromosomes, crisis, and cancer." *Science* **297**(5581): 565-569.
- Massague, J. (1990). "Transforming growth factor-alpha. A model for membrane-anchored growth factors." *J Biol Chem* **265**(35): 21393-21396.
- Massimi, P. and L. Banks (2000). "Differential phosphorylation of the HPV-16 E7 oncoprotein during the cell cycle." *Virology* **276**(2): 388-394.
- Matsuda, A., Y. Suzuki, et al. (2003). "Large-scale identification and characterization of human genes that activate NF-kappaB and MAPK signaling pathways." *Oncogene* **22**(21): 3307-3318.



- Matsumoto, N., N. Yoneda-Kato, et al. (2000). "Elevated MLF1 expression correlates with malignant progression from myelodysplastic syndrome." *Leukemia* **14**(10): 1757-1765.
- Mattes, J., A. Collison, et al. (2008). "Emerging role of microRNAs in disease pathogenesis and strategies for therapeutic modulation." *Curr Opin Mol Ther* **10**(2): 150-157.
- Mayol, X., X. Grana, et al. (1993). "Cloning of a new member of the retinoblastoma gene family (pRb2) which binds to the E1A transforming domain." *Oncogene* **8**(9): 2561-2566.
- Mayr, C., M. T. Hemann, et al. (2007). "Disrupting the pairing between let-7 and Hmga2 enhances oncogenic transformation." *Science* **315**(5818): 1576-1579.
- McConnell, B. B., M. Starborg, et al. (1998). "Inhibitors of cyclin-dependent kinases induce features of replicative senescence in early passage human diploid fibroblasts." *Curr Biol* **8**(6): 351-354.
- McMahon, M. and D. Woods (2001). "Regulation of the p53 pathway by Ras, the plot thickens." *Biochim Biophys Acta* **1471**(2): M63-71.
- McPherron, A. C. and S. J. Lee (1997). "Double muscling in cattle due to mutations in the myostatin gene." *Proc Natl Acad Sci U S A* **94**(23): 12457-12461.
- Mertens-Talcott, S. U., S. Chintharlapalli, et al. (2007). "The oncogenic microRNA-27a targets genes that regulate specificity protein transcription factors and the G2-M checkpoint in MDA-MB-231 breast cancer cells." *Cancer Res* **67**(22): 11001-11011.
- Michael, D. and M. Oren (2002). "The p53 and Mdm2 families in cancer." *Curr Opin Genet Dev* **12**(1): 53-59.
- Michaloglou, C., L. C. Vredevel, et al. (2005). "BRAF<sup>V600E</sup>-associated senescence-like cell cycle arrest of human naevi." *Nature* **436**(7051): 720-724.
- Millis, A. J., H. M. McCue, et al. (1992). "Metalloproteinase and TIMP-1 gene expression during replicative senescence." *Exp Gerontol* **27**(4): 425-428.
- Missero, C., F. Di Cunto, et al. (1996). "The absence of p21<sup>Cip1</sup>/WAF1 alters keratinocyte growth and differentiation and promotes ras-tumor progression." *Genes Dev* **10**(23): 3065-3075.
- Mitchell, P. J., C. Wang, et al. (1987). "Positive and negative regulation of transcription in vitro: enhancer-binding protein AP-2 is inhibited by SV40 T antigen." *Cell* **50**(6): 847-861.
- Mizoi, T., H. Ohtani, et al. (1993). "Immunoelectron microscopic localization of transforming growth factor beta 1 and latent transforming growth factor beta 1 binding protein in human gastrointestinal carcinomas: qualitative difference between cancer cells and stromal cells." *Cancer Res* **53**(1): 183-190.
- Mohr, S., G. D. Leikauf, et al. (2002). "Microarrays as cancer keys: an array of possibilities." *J Clin Oncol* **20**(14): 3165-3175.
- Momand, J., D. Jung, et al. (1998). "The MDM2 gene amplification database." *Nucleic Acids Res* **26**(15): 3453-3459.
- Montes de Oca Luna, R., D. S. Wagner, et al. (1995). "Rescue of early embryonic lethality in mdm2-deficient mice by deletion of p53." *Nature* **378**(6553): 203-206.
- Mooi, W. J. and D. S. Peeper (2006). "Oncogene-induced cell senescence--halting on the road to cancer." *N Engl J Med* **355**(10): 1037-1046.

- Morales, C. P., S. E. Holt, et al. (1999). "Absence of cancer-associated changes in human fibroblasts immortalized with telomerase." *Nat Genet* **21**(1): 115-118.
- Moran, E. (1988). "A region of SV40 large T antigen can substitute for a transforming domain of the adenovirus E1A products." *Nature* **334**(6178): 168-170.
- Moran, E. (1993). "Interaction of adenoviral proteins with pRB and p53." *FASEB J* **7**(10): 880-885.
- Morris, E. J. and N. J. Dyson (2001). "Retinoblastoma protein partners." *Adv Cancer Res* **82**: 1-54.
- Motoda, L., M. Osato, et al. (2007). "Runx1 protects hematopoietic stem/progenitor cells from oncogenic insult." *Stem Cells* **25**(12): 2976-2986.
- Moyzis, R. K., J. M. Buckingham, et al. (1988). "A highly conserved repetitive DNA sequence, (TTAGGG)<sub>n</sub>, present at the telomeres of human chromosomes." *Proc Natl Acad Sci U S A* **85**(18): 6622-6626.
- Mraz, M., S. Pospisilova, et al. (2009). "MicroRNAs in chronic lymphocytic leukemia pathogenesis and disease subtypes." *Leuk Lymphoma* **50**(3): 506-509.
- Munger, K., B. A. Werness, et al. (1989). "Complex formation of human papillomavirus E7 proteins with the retinoblastoma tumor suppressor gene product." *EMBO J* **8**(13): 4099-4105.
- Munro, J., F. J. Stott, et al. (1999). "Role of the alternative INK4A proteins in human keratinocyte senescence: evidence for the specific inactivation of p16INK4A upon immortalization." *Cancer Res* **59**(11): 2516-2521.
- Muntoni, A. and R. R. Reddel (2005). "The first molecular details of ALT in human tumor cells." *Hum Mol Genet* **14 Spec No. 2**: R191-196.
- Murphree, A. L. and W. F. Benedict (1984). "Retinoblastoma: clues to human oncogenesis." *Science* **223**(4640): 1028-1033.
- Murphy, M., J. Ahn, et al. (1999). "Transcriptional repression by wild-type p53 utilizes histone deacetylases, mediated by interaction with mSin3a." *Genes Dev* **13**(19): 2490-2501.
- Myatt, S. S. and E. W. Lam (2007). "The emerging roles of forkhead box (Fox) proteins in cancer." *Nat Rev Cancer* **7**(11): 847-859.
- Mymryk, J. S. and S. T. Bayley (1994). "Multiple pathways for activation of E2A expression in human KB cells by the 243R E1A protein of adenovirus type 5." *Virus Res* **33**(1): 89-97.
- Nabel, G. J. and I. M. Verma (1993). "Proposed NF-kappa B/I kappa B family nomenclature." *Genes Dev* **7**(11): 2063.
- Nagai, H., M. Negrini, et al. (1995). "Detection and cloning of a common region of loss of heterozygosity at chromosome 1p in breast cancer." *Cancer Res* **55**(8): 1752-1757.
- Naiki, T., E. Saijou, et al. (2007). "TRB2, a mouse Tribbles ortholog, suppresses adipocyte differentiation by inhibiting AKT and C/EBPbeta." *J Biol Chem* **282**(33): 24075-24082.
- Nakano, I., M. Masterman-Smith, et al. (2008). "Maternal embryonic leucine zipper kinase is a key regulator of the proliferation of malignant brain tumors, including brain tumor stem cells." *J Neurosci Res* **86**(1): 48-60.
- Narayanan, B. A., N. K. Narayanan, et al. (2006). "RNA interference-mediated cyclooxygenase-2 inhibition prevents prostate cancer cell growth and induces

- differentiation: modulation of neuronal protein synaptophysin, cyclin D1, and androgen receptor." *Mol Cancer Ther* **5**(5): 1117-1125.
- Narita, M. and S. W. Lowe (2005). "Senescence comes of age." *Nat Med* **11**(9): 920-922.
- Narita, M., S. Nunez, et al. (2003). "Rb-mediated heterochromatin formation and silencing of E2F target genes during cellular senescence." *Cell* **113**(6): 703-716.
- Nelson, D. A., N. A. Krucher, et al. (1997). "High molecular weight protein phosphatase type 1 dephosphorylates the retinoblastoma protein." *J Biol Chem* **272**(7): 4528-4535.
- Nevels, M., S. Rubenwolf, et al. (1997). "The adenovirus E4orf6 protein can promote E1A/E1B-induced focus formation by interfering with p53 tumor suppressor function." *Proc Natl Acad Sci U S A* **94**(4): 1206-1211.
- Nevins, J. R. (2001). "The Rb/E2F pathway and cancer." *Hum Mol Genet* **10**(7): 699-703.
- Nielsen, S. J., R. Schneider, et al. (2001). "Rb targets histone H3 methylation and HP1 to promoters." *Nature* **412**(6846): 561-565.
- Nip, J., D. K. Strom, et al. (2001). "E2F-1 induces the stabilization of p53 but blocks p53-mediated transactivation." *Oncogene* **20**(8): 910-920.
- Noda, A., Y. Ning, et al. (1994). "Cloning of senescent cell-derived inhibitors of DNA synthesis using an expression screen." *Exp Cell Res* **211**(1): 90-98.
- O'Donnell, K. A., E. A. Wentzel, et al. (2005). "c-Myc-regulated microRNAs modulate E2F1 expression." *Nature* **435**(7043): 839-843.
- O'Hare, M. J., J. Bond, et al. (2001). "Conditional immortalization of freshly isolated human mammary fibroblasts and endothelial cells." *Proc Natl Acad Sci U S A* **98**(2): 646-651.
- Ogami, M., Y. Ikura, et al. (2004). "Telomere shortening in human coronary artery diseases." *Arterioscler Thromb Vasc Biol* **24**(3): 546-550.
- Oh, S. T., S. Kyo, et al. (2001). "Telomerase activation by human papillomavirus type 16 E6 protein: induction of human telomerase reverse transcriptase expression through Myc and GC-rich Sp1 binding sites." *J Virol* **75**(12): 5559-5566.
- Ohtani, N., Z. Zebedee, et al. (2001). "Opposing effects of Ets and Id proteins on p16INK4a expression during cellular senescence." *Nature* **409**(6823): 1067-1070.
- Oklu, R. and R. Hesketh (2000). "The latent transforming growth factor beta binding protein (LTBP) family." *Biochem J* **352 Pt 3**: 601-610.
- Oren, M. and A. J. Levine (1981). "Immunoselection of simian virus 40 large T antigen messenger rnas from transformed cells." *Virology* **113**(2): 790-793.
- Orjalo, A. V., D. Bhaumik, et al. (2009). "Cell surface-bound IL-1alpha is an upstream regulator of the senescence-associated IL-6/IL-8 cytokine network." *Proc Natl Acad Sci U S A* **106**(40): 17031-17036.
- Ortega, S., M. Malumbres, et al. (2002). "Cyclin D-dependent kinases, INK4 inhibitors and cancer." *Biochim Biophys Acta* **1602**(1): 73-87.
- Osada, M., M. Ohba, et al. (1998). "Cloning and functional analysis of human p51, which structurally and functionally resembles p53." *Nat Med* **4**(7): 839-843.
- Ossovskaya, V. S., I. A. Mazo, et al. (1996). "Use of genetic suppressor elements to dissect distinct biological effects of separate p53 domains." *Proc Natl Acad Sci U S A* **93**(19): 10309-10314.

- Otterson, G. A., R. A. Kratzke, et al. (1994). "Absence of p16INK4 protein is restricted to the subset of lung cancer lines that retains wildtype RB." *Oncogene* **9**(11): 3375-3378.
- Paddison, P. J. (2008). "RNA interference in mammalian cell systems." *Curr Top Microbiol Immunol* **320**: 1-19.
- Paddison, P. J., J. M. Silva, et al. (2004). "A resource for large-scale RNA-interference-based screens in mammals." *Nature* **428**(6981): 427-431.
- Palmero, I., C. Pantoja, et al. (1998). "p19ARF links the tumour suppressor p53 to Ras." *Nature* **395**(6698): 125-126.
- Panossian, L. A., V. R. Porter, et al. (2003). "Telomere shortening in T cells correlates with Alzheimer's disease status." *Neurobiol Aging* **24**(1): 77-84.
- Pantoja, C. and M. Serrano (1999). "Murine fibroblasts lacking p21 undergo senescence and are resistant to transformation by oncogenic Ras." *Oncogene* **18**(35): 4974-4982.
- Parada, L. F., C. J. Tabin, et al. (1982). "Human EJ bladder carcinoma oncogene is homologue of Harvey sarcoma virus ras gene." *Nature* **297**(5866): 474-478.
- Parisi, T., A. Pollice, et al. (2002). "Transcriptional regulation of the human tumor suppressor p14(ARF) by E2F1, E2F2, E2F3, and Sp1-like factors." *Biochem Biophys Res Commun* **291**(5): 1138-1145.
- Park, H. J., Z. Wang, et al. (2008). "An N-terminal inhibitory domain modulates activity of FoxM1 during cell cycle." *Oncogene* **27**(12): 1696-1704.
- Park, I. K., S. J. Morrison, et al. (2004). "Bmi1, stem cells, and senescence regulation." *J Clin Invest* **113**(2): 175-179.
- Parrinello, S., E. Samper, et al. (2003). "Oxygen sensitivity severely limits the replicative lifespan of murine fibroblasts." *Nat Cell Biol* **5**(8): 741-747.
- Parsons, D. W., S. Jones, et al. (2008). "An integrated genomic analysis of human glioblastoma multiforme." *Science* **321**(5897): 1807-1812.
- Pascal, T., F. Debacq-Chainiaux, et al. (2005). "Comparison of replicative senescence and stress-induced premature senescence combining differential display and low-density DNA arrays." *FEBS Lett* **579**(17): 3651-3659.
- Passos, J. F., G. Nelson, et al. (2010). "Feedback between p21 and reactive oxygen production is necessary for cell senescence." *Mol Syst Biol* **6**: 347.
- Passos, J. F., G. Saretzki, et al. (2007). "Mitochondrial dysfunction accounts for the stochastic heterogeneity in telomere-dependent senescence." *PLoS Biol* **5**(5): e110.
- Passos, J. F., G. Saretzki, et al. (2007). "DNA damage in telomeres and mitochondria during cellular senescence: is there a connection?" *Nucleic Acids Res* **35**(22): 7505-7513.
- Pavel, S., N. P. Smit, et al. (2003). "Homozygous germline mutation of CDKN2A/p16 and glucose-6-phosphate dehydrogenase deficiency in a multiple melanoma case." *Melanoma Res* **13**(2): 171-178.
- Pearson, M., R. Carbone, et al. (2000). "PML regulates p53 acetylation and premature senescence induced by oncogenic Ras." *Nature* **406**(6792): 207-210.
- Pedoux, R., S. Sengupta, et al. (2005). "ING2 regulates the onset of replicative senescence by induction of p300-dependent p53 acetylation." *Mol Cell Biol* **25**(15): 6639-6648.

- Penttinen, C., J. Saharinen, et al. (2002). "Secretion of human latent TGF-beta-binding protein-3 (LTBP-3) is dependent on co-expression of TGF-beta." J Cell Sci **115**(Pt 17): 3457-3468.
- Penzo, M., P. E. Massa, et al. (2009). "Sustained NF-kappaB activation produces a short-term cell proliferation block in conjunction with repressing effectors of cell cycle progression controlled by E2F or FoxM1." J Cell Physiol **218**(1): 215-227.
- Perricaudet, M., J. M. le Moullec, et al. (1980). "Structure of two adenovirus type 12 transforming polypeptides and their evolutionary implications." Nature **288**(5787): 174-176.
- Perry, M. M., A. E. Williams, et al. (2009). "Divergent intracellular pathways regulate interleukin-1beta-induced miR-146a and miR-146b expression and chemokine release in human alveolar epithelial cells." FEBS Lett **583**(20): 3349-3355.
- Phillips, A. C. and K. H. Vousden (2001). "E2F-1 induced apoptosis." Apoptosis **6**(3): 173-182.
- Piedimonte, G., A. F. Borghetti, et al. (1982). "Effect of cell density on growth rate and amino acid transport in simian virus 40-transformed 3T3 cells." Cancer Res **42**(11): 4690-4693.
- Place, R. F., L. C. Li, et al. (2008). "MicroRNA-373 induces expression of genes with complementary promoter sequences." Proc Natl Acad Sci U S A **105**(5): 1608-1613.
- Poliseno, L., L. Pitto, et al. (2008). "The proto-oncogene LRF is under post-transcriptional control of MiR-20a: implications for senescence." PLoS One **3**(7): e2542.
- Polyak, K., Y. Xia, et al. (1997). "A model for p53-induced apoptosis." Nature **389**(6648): 300-305.
- Pomerantz, J., N. Schreiber-Agus, et al. (1998). "The Ink4a tumor suppressor gene product, p19Arf, interacts with MDM2 and neutralizes MDM2's inhibition of p53." Cell **92**(6): 713-723.
- Powell, A. J., A. J. Darmon, et al. (1999). "Different functions are required for initiation and maintenance of immortalization of rat embryo fibroblasts by SV40 large T antigen." Oncogene **18**(51): 7343-7350.
- Poy, M. N., L. Eliasson, et al. (2004). "A pancreatic islet-specific microRNA regulates insulin secretion." Nature **432**(7014): 226-230.
- Prives, C. (1998). "Signaling to p53: breaking the MDM2-p53 circuit." Cell **95**(1): 5-8.
- Qi, J., J. Y. Yu, et al. (2009). "microRNAs regulate human embryonic stem cell division." Cell Cycle **8**(22): 3729-3741.
- Quartin, R. S., C. N. Cole, et al. (1994). "The amino-terminal functions of the simian virus 40 large T antigen are required to overcome wild-type p53-mediated growth arrest of cells." J Virol **68**(3): 1334-1341.
- Quelle, D. E., F. Zindy, et al. (1995). "Alternative reading frames of the INK4a tumor suppressor gene encode two unrelated proteins capable of inducing cell cycle arrest." Cell **83**(6): 993-1000.
- Rai, R., A. Phadnis, et al. (2008). "Differential regulation of centrosome integrity by DNA damage response proteins." Cell Cycle **7**(14): 2225-2233.
- Ramaswamy, S. and C. M. Perou (2003). "DNA microarrays in breast cancer: the promise of personalised medicine." Lancet **361**(9369): 1576-1577.

- Ramsey, M. R. and N. E. Sharpless (2006). "ROS as a tumour suppressor?" Nat Cell Biol **8**(11): 1213-1215.
- Rao, L., M. Debbas, et al. (1992). "The adenovirus E1A proteins induce apoptosis, which is inhibited by the E1B 19-kDa and Bcl-2 proteins." Proc Natl Acad Sci U S A **89**(16): 7742-7746.
- Rapp, L. and J. J. Chen (1998). "The papillomavirus E6 proteins." Biochim Biophys Acta **1378**(1): F1-19.
- Rauhala, H. E., S. E. Jalava, et al. (2010). "miR-193b is an epigenetically regulated putative tumor suppressor in prostate cancer." Int J Cancer **127**(6): 1363-1372.
- Rayman, J. B., Y. Takahashi, et al. (2002). "E2F mediates cell cycle-dependent transcriptional repression in vivo by recruitment of an HDAC1/mSin3B corepressor complex." Genes Dev **16**(8): 933-947.
- Rebbaa, A., X. Zheng, et al. (2003). "Caspase inhibition switches doxorubicin-induced apoptosis to senescence." Oncogene **22**(18): 2805-2811.
- Reinhart, B. J., E. G. Weinstein, et al. (2002). "MicroRNAs in plants." Genes Dev **16**(13): 1616-1626.
- Reynolds, A., D. Leake, et al. (2004). "Rational siRNA design for RNA interference." Nat Biotechnol **22**(3): 326-330.
- Rheinwald, J. G., W. C. Hahn, et al. (2002). "A two-stage, p16(INK4A)- and p53-dependent keratinocyte senescence mechanism that limits replicative potential independent of telomere status." Mol Cell Biol **22**(14): 5157-5172.
- Rhoades, M. W., B. J. Reinhart, et al. (2002). "Prediction of plant microRNA targets." Cell **110**(4): 513-520.
- Rhodes, D. R., J. Yu, et al. (2004). "Large-scale meta-analysis of cancer microarray data identifies common transcriptional profiles of neoplastic transformation and progression." Proc Natl Acad Sci U S A **101**(25): 9309-9314.
- Rice, P. W. and C. N. Cole (1993). "Efficient transcriptional activation of many simple modular promoters by simian virus 40 large T antigen." J Virol **67**(11): 6689-6697.
- Roberts, J. M. (1999). "Evolving ideas about cyclins." Cell **98**(2): 129-132.
- Rodier, F., J. P. Coppe, et al. (2009). "Persistent DNA damage signalling triggers senescence-associated inflammatory cytokine secretion." Nat Cell Biol **11**(8): 973-979.
- Rodriguez, A., S. Griffiths-Jones, et al. (2004). "Identification of mammalian microRNA host genes and transcription units." Genome Res **14**(10A): 1902-1910.
- Rogoff, H. A., M. T. Pickering, et al. (2002). "E2F1 induces phosphorylation of p53 that is coincident with p53 accumulation and apoptosis." Mol Cell Biol **22**(15): 5308-5318.
- Rowland, B. D., S. G. Denisov, et al. (2002). "E2F transcriptional repressor complexes are critical downstream targets of p19(ARF)/p53-induced proliferative arrest." Cancer Cell **2**(1): 55-65.
- Rushton, J. J., D. Jiang, et al. (1997). "Simian virus 40 T antigen can regulate p53-mediated transcription independent of binding p53." J Virol **71**(7): 5620-5623.
- Saffer, J. D., S. P. Jackson, et al. (1990). "SV40 stimulates expression of the transacting factor Sp1 at the mRNA level." Genes Dev **4**(4): 659-666.

- Salminen, A., J. Ojala, et al. (2008). "Interaction of aging-associated signaling cascades: inhibition of NF-kappaB signaling by longevity factors FoxOs and SIRT1." Cell Mol Life Sci **65**(7-8): 1049-1058.
- Sang, L., H. A. Collier, et al. (2008). "Control of the reversibility of cellular quiescence by the transcriptional repressor HES1." Science **321**(5892): 1095-1100.
- Saretzki, G. (2003). "Telomerase inhibition as cancer therapy." Cancer Lett **194**(2): 209-219.
- Sato, F., N. Harpaz, et al. (2002). "Hypermethylation of the p14(ARF) gene in ulcerative colitis-associated colorectal carcinogenesis." Cancer Res **62**(4): 1148-1151.
- Scheffner, M., J. M. Huibregtse, et al. (1993). "The HPV-16 E6 and E6-AP complex functions as a ubiquitin-protein ligase in the ubiquitination of p53." Cell **75**(3): 495-505.
- Scheffner, M., R. Knippers, et al. (1989). "RNA unwinding activity of SV40 large T antigen." Cell **57**(6): 955-963.
- Scheffner, M., K. Munger, et al. (1992). "Targeted degradation of the retinoblastoma protein by human papillomavirus E7-E6 fusion proteins." EMBO J **11**(7): 2425-2431.
- Scheidereit, C. (2006). "IkappaB kinase complexes: gateways to NF-kappaB activation and transcription." Oncogene **25**(51): 6685-6705.
- Schmale, H. and C. Bamberger (1997). "A novel protein with strong homology to the tumor suppressor p53." Oncogene **15**(11): 1363-1367.
- Schmitt, C. A., J. S. Fridman, et al. (2002). "A senescence program controlled by p53 and p16INK4a contributes to the outcome of cancer therapy." Cell **109**(3): 335-346.
- Schwarz, E., U. K. Freese, et al. (1985). "Structure and transcription of human papillomavirus sequences in cervical carcinoma cells." Nature **314**(6006): 111-114.
- Schwarze, S. R., Y. Shi, et al. (2001). "Role of cyclin-dependent kinase inhibitors in the growth arrest at senescence in human prostate epithelial and uroepithelial cells." Oncogene **20**(57): 8184-8192.
- Sebastian, T., R. Malik, et al. (2005). "C/EBPbeta cooperates with RB:E2F to implement Ras(V12)-induced cellular senescence." EMBO J **24**(18): 3301-3312.
- Seger, Y. R., M. Garcia-Cao, et al. (2002). "Transformation of normal human cells in the absence of telomerase activation." Cancer Cell **2**(5): 401-413.
- Sellers, W. R. and W. G. Kaelin, Jr. (1997). "Role of the retinoblastoma protein in the pathogenesis of human cancer." J Clin Oncol **15**(11): 3301-3312.
- Semizarov, D., L. Frost, et al. (2003). "Specificity of short interfering RNA determined through gene expression signatures." Proc Natl Acad Sci U S A **100**(11): 6347-6352.
- Sen, R. and D. Baltimore (1986). "Inducibility of kappa immunoglobulin enhancer-binding protein Nf-kappa B by a posttranslational mechanism." Cell **47**(6): 921-928.
- Senfleben, U., Y. Cao, et al. (2001). "Activation by IKKalpha of a second, evolutionary conserved, NF-kappa B signaling pathway." Science **293**(5534): 1495-1499.
- Serrano, M. (1997). "The tumor suppressor protein p16INK4a." Exp Cell Res **237**(1): 7-13.

- Serrano, M. and M. A. Blasco (2001). "Putting the stress on senescence." Curr Opin Cell Biol **13**(6): 748-753.
- Serrano, M., G. J. Hannon, et al. (1993). "A new regulatory motif in cell-cycle control causing specific inhibition of cyclin D/CDK4." Nature **366**(6456): 704-707.
- Serrano, M., H. Lee, et al. (1996). "Role of the INK4a locus in tumor suppression and cell mortality." Cell **85**(1): 27-37.
- Serrano, M., A. W. Lin, et al. (1997). "Oncogenic ras provokes premature cell senescence associated with accumulation of p53 and p16INK4a." Cell **88**(5): 593-602.
- Shapiro, G. I., J. E. Park, et al. (1995). "Multiple mechanisms of p16INK4A inactivation in non-small cell lung cancer cell lines." Cancer Res **55**(24): 6200-6209.
- Sharpless, N. E. and R. A. DePinho (2005). "Cancer: crime and punishment." Nature **436**(7051): 636-637.
- Shay, J. W., O. M. Pereira-Smith, et al. (1991). "A role for both RB and p53 in the regulation of human cellular senescence." Exp Cell Res **196**(1): 33-39.
- Shelton, D. N., E. Chang, et al. (1999). "Microarray analysis of replicative senescence." Curr Biol **9**(17): 939-945.
- Sherr, C. J. (1996). "Cancer cell cycles." Science **274**(5293): 1672-1677.
- Sherr, C. J. (2000). "Cell cycle control and cancer." Harvey Lect **96**: 73-92.
- Sherr, C. J. (2001). "The INK4a/ARF network in tumour suppression." Nat Rev Mol Cell Biol **2**(10): 731-737.
- Sherr, C. J. and R. A. DePinho (2000). "Cellular senescence: mitotic clock or culture shock?" Cell **102**(4): 407-410.
- Sherr, C. J. and J. M. Roberts (1999). "CDK inhibitors: positive and negative regulators of G1-phase progression." Genes Dev **13**(12): 1501-1512.
- Sherr, C. J. and J. D. Weber (2000). "The ARF/p53 pathway." Curr Opin Genet Dev **10**(1): 94-99.
- Shivji, M. K., S. J. Grey, et al. (1994). "Cip1 inhibits DNA replication but not PCNA-dependent nucleotide excision-repair." Curr Biol **4**(12): 1062-1068.
- Shohat, G., G. Shani, et al. (2002). "The DAP-kinase family of proteins: study of a novel group of calcium-regulated death-promoting kinases." Biochim Biophys Acta **1600**(1-2): 45-50.
- Shvarts, A., T. R. Brummelkamp, et al. (2002). "A senescence rescue screen identifies BCL6 as an inhibitor of anti-proliferative p19(ARF)-p53 signaling." Genes Dev **16**(6): 681-686.
- Silberstein, G. B. and C. W. Daniel (1987). "Reversible inhibition of mammary gland growth by transforming growth factor-beta." Science **237**(4812): 291-293.
- Sionov, R. V. and Y. Haupt (1999). "The cellular response to p53: the decision between life and death." Oncogene **18**(45): 6145-6157.
- Slack, R. S., I. S. Skerjanc, et al. (1995). "Cells differentiating into neuroectoderm undergo apoptosis in the absence of functional retinoblastoma family proteins." J Cell Biol **129**(3): 779-788.
- Smogorzewska, A. and T. de Lange (2002). "Different telomere damage signaling pathways in human and mouse cells." EMBO J **21**(16): 4338-4348.
- Sossey-Alaoui, K., E. Kitamura, et al. (2001). "Fine mapping of the PTGFR gene to 1p31 region and mutation analysis in human breast cancer." Int J Mol Med **7**(5): 543-546.



- Soule, H. R. and J. S. Butel (1979). "Subcellular Localization of simian virus 40 large tumor antigen." J Virol **30**(2): 523-532.
- Soussi, T. and P. May (1996). "Structural aspects of the p53 protein in relation to gene evolution: a second look." J Mol Biol **260**(5): 623-637.
- Spurgers, K. B., C. M. Sharkey, et al. (2008). "Oligonucleotide antiviral therapeutics: antisense and RNA interference for highly pathogenic RNA viruses." Antiviral Res **78**(1): 26-36.
- Stansel, R. M., T. de Lange, et al. (2001). "T-loop assembly in vitro involves binding of TRF2 near the 3' telomeric overhang." EMBO J **20**(19): 5532-5540.
- Stein, G. H., L. F. Drullinger, et al. (1999). "Differential roles for cyclin-dependent kinase inhibitors p21 and p16 in the mechanisms of senescence and differentiation in human fibroblasts." Mol Cell Biol **19**(3): 2109-2117.
- Stepkowski, S. M., X. Qu, et al. (2000). "Inhibition of C-raf expression by antisense oligonucleotides extends heart allograft survival in rats." Transplantation **70**(4): 656-661.
- Stewart, S. A. and R. A. Weinberg (2006). "Telomeres: cancer to human aging." Annu Rev Cell Dev Biol **22**: 531-557.
- Stros, M., T. Ozaki, et al. (2002). "HMGB1 and HMGB2 cell-specifically down-regulate the p53- and p73-dependent sequence-specific transactivation from the human Bax gene promoter." J Biol Chem **277**(9): 7157-7164.
- Su, G., T. Roberts, et al. (1999). "TTC4, a novel human gene containing the tetratricopeptide repeat and mapping to the region of chromosome 1p31 that is frequently deleted in sporadic breast cancer." Genomics **55**(2): 157-163.
- Sun, P., N. Yoshizuka, et al. (2007). "PRAK is essential for ras-induced senescence and tumor suppression." Cell **128**(2): 295-308.
- Sun, W., K. Zhang, et al. (2004). "Identification of differentially expressed genes in human lung squamous cell carcinoma using suppression subtractive hybridization." Cancer Lett **212**(1): 83-93.
- Suzuki, M., S. Okuyama, et al. (1998). "A novel E2F binding protein with Myc-type HLH motif stimulates E2F-dependent transcription by forming a heterodimer." Oncogene **17**(7): 853-865.
- Taganov, K. D., M. P. Boldin, et al. (2006). "NF-kappaB-dependent induction of microRNA miR-146, an inhibitor targeted to signaling proteins of innate immune responses." Proc Natl Acad Sci U S A **103**(33): 12481-12486.
- Takahashi, Y., J. B. Rayman, et al. (2000). "Analysis of promoter binding by the E2F and pRB families in vivo: distinct E2F proteins mediate activation and repression." Genes Dev **14**(7): 804-816.
- Tam, W. and J. E. Dahlberg (2006). "miR-155/BIC as an oncogenic microRNA." Genes Chromosomes Cancer **45**(2): 211-212.
- Tang, J., G. M. Gordon, et al. (2002). "The helix-loop-helix protein id-1 delays onset of replicative senescence in human endothelial cells." Lab Invest **82**(8): 1073-1079.
- Tanzer, A. and P. F. Stadler (2004). "Molecular evolution of a microRNA cluster." J Mol Biol **339**(2): 327-335.
- Tao, W. and A. J. Levine (1999). "Nucleocytoplasmic shuttling of oncoprotein Hdm2 is required for Hdm2-mediated degradation of p53." Proc Natl Acad Sci U S A **96**(6): 3077-3080.

- Tao, W. and A. J. Levine (1999). "P19(ARF) stabilizes p53 by blocking nucleocytoplasmic shuttling of Mdm2." Proc Natl Acad Sci U S A **96**(12): 6937-6941.
- Taubert, S., C. Gorrini, et al. (2004). "E2F-dependent histone acetylation and recruitment of the Tip60 acetyltransferase complex to chromatin in late G1." Mol Cell Biol **24**(10): 4546-4556.
- Tavazoie, S. F., C. Alarcon, et al. (2008). "Endogenous human microRNAs that suppress breast cancer metastasis." Nature **451**(7175): 147-152.
- Taylor, W. R. and G. R. Stark (2001). "Regulation of the G2/M transition by p53." Oncogene **20**(15): 1803-1815.
- Tazawa, H., N. Tsuchiya, et al. (2007). "Tumor-suppressive miR-34a induces senescence-like growth arrest through modulation of the E2F pathway in human colon cancer cells." Proc Natl Acad Sci U S A **104**(39): 15472-15477.
- te Poele, R. H., A. L. Okorokov, et al. (2002). "DNA damage is able to induce senescence in tumor cells in vitro and in vivo." Cancer Res **62**(6): 1876-1883.
- Teh, M. T., S. T. Wong, et al. (2002). "FOXM1 is a downstream target of Gli1 in basal cell carcinomas." Cancer Res **62**(16): 4773-4780.
- Tergaonkar, V. (2006). "NFkappaB pathway: a good signaling paradigm and therapeutic target." Int J Biochem Cell Biol **38**(10): 1647-1653.
- Thomas, D. M., S. A. Carty, et al. (2001). "The retinoblastoma protein acts as a transcriptional coactivator required for osteogenic differentiation." Mol Cell **8**(2): 303-316.
- Thomas, M., D. Pim, et al. (1999). "The role of the E6-p53 interaction in the molecular pathogenesis of HPV." Oncogene **18**(53): 7690-7700.
- Tjian, R. and A. Robbins (1979). "Enzymatic activities associated with a purified simian virus 40 T antigen-related protein." Proc Natl Acad Sci U S A **76**(2): 610-614.
- Tobaben, S., P. Thakur, et al. (2001). "A trimeric protein complex functions as a synaptic chaperone machine." Neuron **31**(6): 987-999.
- Tolbert, D., X. Lu, et al. (2002). "p19(ARF) is dispensable for oncogenic stress-induced p53-mediated apoptosis and tumor suppression in vivo." Mol Cell Biol **22**(1): 370-377.
- Trentin, J. J., Y. Yabe, et al. (1962). "The quest for human cancer viruses." Science **137**: 835-841.
- Trimarchi, J. M., B. Fairchild, et al. (1998). "E2F-6, a member of the E2F family that can behave as a transcriptional repressor." Proc Natl Acad Sci U S A **95**(6): 2850-2855.
- Trimarchi, J. M., B. Fairchild, et al. (2001). "The E2F6 transcription factor is a component of the mammalian Bmi1-containing polycomb complex." Proc Natl Acad Sci U S A **98**(4): 1519-1524.
- Tsukamoto, K., N. Ito, et al. (1998). "Allelic loss on chromosome 1p is associated with progression and lymph node metastasis of primary breast carcinoma." Cancer **82**(2): 317-322.
- Tyner, S. D., S. Venkatachalam, et al. (2002). "p53 mutant mice that display early ageing-associated phenotypes." Nature **415**(6867): 45-53.
- van 't Veer, L. J., H. Dai, et al. (2002). "Gene expression profiling predicts clinical outcome of breast cancer." Nature **415**(6871): 530-536.

- van der Lugt, N. M., J. Domen, et al. (1994). "Posterior transformation, neurological abnormalities, and severe hematopoietic defects in mice with a targeted deletion of the bmi-1 proto-oncogene." Genes Dev **8**(7): 757-769.
- Vasudevan, S. A., H. V. Russell, et al. (2007). "Neuroblastoma-derived secretory protein messenger RNA levels correlate with high-risk neuroblastoma." J Pediatr Surg **42**(1): 148-152.
- Vaziri, N. D., Z. Ni, et al. (1998). "Upregulation of renal and vascular nitric oxide synthase in young spontaneously hypertensive rats." Hypertension **31**(6): 1248-1254.
- Veldman, T., I. Horikawa, et al. (2001). "Transcriptional activation of the telomerase hTERT gene by human papillomavirus type 16 E6 oncoprotein." J Virol **75**(9): 4467-4472.
- Vijg, J. (2000). "The science of aging and the need for a mechanistic approach." Mech Ageing Dev **114**(1): 1-3.
- Vijg, J., R. A. Busuttill, et al. (2005). "Aging and genome maintenance." Ann N Y Acad Sci **1055**: 35-47.
- Vogelstein, B., D. Lane, et al. (2000). "Surfing the p53 network." Nature **408**(6810): 307-310.
- Volinia, S., G. A. Calin, et al. (2006). "A microRNA expression signature of human solid tumors defines cancer gene targets." Proc Natl Acad Sci U S A **103**(7): 2257-2261.
- von Zglinicki, T., G. Saretzki, et al. (2005). "Human cell senescence as a DNA damage response." Mech Ageing Dev **126**(1): 111-117.
- Vooijs, M. and A. Berns (1999). "Developmental defects and tumor predisposition in Rb mutant mice." Oncogene **18**(38): 5293-5303.
- Voorhoeve, P. M., C. le Sage, et al. (2006). "A genetic screen implicates miRNA-372 and miRNA-373 as oncogenes in testicular germ cell tumors." Cell **124**(6): 1169-1181.
- Vousden, K. H. and X. Lu (2002). "Live or let die: the cell's response to p53." Nat Rev Cancer **2**(8): 594-604.
- Vousden, K. H., B. Vojtesek, et al. (1993). "HPV-16 E7 or adenovirus E1A can overcome the growth arrest of cells immortalized with a temperature-sensitive p53." Oncogene **8**(6): 1697-1702.
- Wagner, M., B. Hampel, et al. (2001). "Replicative senescence of human endothelial cells in vitro involves G1 arrest, polyploidization and senescence-associated apoptosis." Exp Gerontol **36**(8): 1327-1347.
- Wagner, W., P. Horn, et al. (2008). "Replicative senescence of mesenchymal stem cells: a continuous and organized process." PLoS One **3**(5): e2213.
- Wajapeyee, N., R. W. Serra, et al. (2008). "Oncogenic BRAF induces senescence and apoptosis through pathways mediated by the secreted protein IGFBP7." Cell **132**(3): 363-374.
- Walia, V., M. Ding, et al. (2009). "hCLCA2 Is a p53-Inducible Inhibitor of Breast Cancer Cell Proliferation." Cancer Res **69**(16): 6624-6632.
- Wang, H., Q. Zhang, et al. (2003). "hSGT interacts with the N-terminal region of myostatin." Biochem Biophys Res Commun **311**(4): 877-883.

- Wang, H. G., E. Moran, et al. (1995). "E1A promotes association between p300 and pRB in multimeric complexes required for normal biological activity." J Virol **69**(12): 7917-7924.
- Wang, I. C., Y. J. Chen, et al. (2005). "Forkhead box M1 regulates the transcriptional network of genes essential for mitotic progression and genes encoding the SCF (Skp2-Cks1) ubiquitin ligase." Mol Cell Biol **25**(24): 10875-10894.
- Wang, J., N. K. Jacob, et al. (2009). "RelA/p65 functions to maintain cellular senescence by regulating genomic stability and DNA repair." EMBO Rep **10**(11): 1272-1278.
- Wang, R. H., K. Sengupta, et al. (2008). "Impaired DNA damage response, genome instability, and tumorigenesis in SIRT1 mutant mice." Cancer Cell **14**(4): 312-323.
- Wang, W., J. X. Chen, et al. (2002). "Sequential activation of the MEK-extracellular signal-regulated kinase and MKK3/6-p38 mitogen-activated protein kinase pathways mediates oncogenic ras-induced premature senescence." Mol Cell Biol **22**(10): 3389-3403.
- Wang, Y. and M. You (2001). "Alternative splicing of the K-ras gene in mouse tissues and cell lines." Exp Lung Res **27**(3): 255-267.
- Waragai, M., S. Nagamitsu, et al. (2006). "Ataxin 10 induces neuritogenesis via interaction with G-protein beta2 subunit." J Neurosci Res **83**(7): 1170-1178.
- Watts, L. M., V. P. Manchem, et al. (2005). "Reduction of hepatic and adipose tissue glucocorticoid receptor expression with antisense oligonucleotides improves hyperglycemia and hyperlipidemia in diabetic rodents without causing systemic glucocorticoid antagonism." Diabetes **54**(6): 1846-1853.
- Weber, J. D., J. R. Jeffers, et al. (2000). "p53-independent functions of the p19(ARF) tumor suppressor." Genes Dev **14**(18): 2358-2365.
- Weber, J. D., L. J. Taylor, et al. (1999). "Nucleolar Arf sequesters Mdm2 and activates p53." Nat Cell Biol **1**(1): 20-26.
- Webley, K., J. A. Bond, et al. (2000). "Posttranslational modifications of p53 in replicative senescence overlapping but distinct from those induced by DNA damage." Mol Cell Biol **20**(8): 2803-2808.
- Wei, S. and J. M. Sedivy (1999). "Expression of catalytically active telomerase does not prevent premature senescence caused by overexpression of oncogenic Ha-Ras in normal human fibroblasts." Cancer Res **59**(7): 1539-1543.
- Wei, W., R. M. Hemmer, et al. (2001). "Role of p14(ARF) in replicative and induced senescence of human fibroblasts." Mol Cell Biol **21**(20): 6748-6757.
- Wei, W., U. Herbig, et al. (2003). "Loss of retinoblastoma but not p16 function allows bypass of replicative senescence in human fibroblasts." EMBO Rep **4**(11): 1061-1066.
- Weinberg, R. A. (1995). "The retinoblastoma protein and cell cycle control." Cell **81**(3): 323-330.
- Weinberg, W. C. and S. H. Yuspa (1997). "An antibody to p53 recognizes soluble keratins in epidermal keratinocyte cultures under differentiating, but not proliferating, conditions." J Invest Dermatol **109**(4): 611-612.
- Weinrich, S. L., R. Pruzan, et al. (1997). "Reconstitution of human telomerase with the template RNA component hTR and the catalytic protein subunit hTRT." Nat Genet **17**(4): 498-502.

- Wellinger, R. J. and D. Sen (1997). "The DNA structures at the ends of eukaryotic chromosomes." Eur J Cancer **33**(5): 735-749.
- West, M. D., O. M. Pereira-Smith, et al. (1989). "Replicative senescence of human skin fibroblasts correlates with a loss of regulation and overexpression of collagenase activity." Exp Cell Res **184**(1): 138-147.
- Westbrook, T. F., F. Stegmeier, et al. (2005). "Dissecting cancer pathways and vulnerabilities with RNAi." Cold Spring Harb Symp Quant Biol **70**: 435-444.
- White, E., S. K. Chiou, et al. (1994). "Control of p53-dependent apoptosis by E1B, Bcl-2, and Ha-ras proteins." Cold Spring Harb Symp Quant Biol **59**: 395-402.
- White, E., P. Sabbatini, et al. (1992). "The 19-kilodalton adenovirus E1B transforming protein inhibits programmed cell death and prevents cytolysis by tumor necrosis factor alpha." Mol Cell Biol **12**(6): 2570-2580.
- Whitfield, M. L., G. Sherlock, et al. (2002). "Identification of genes periodically expressed in the human cell cycle and their expression in tumors." Mol Biol Cell **13**(6): 1977-2000.
- Whyte, P., K. J. Buchkovich, et al. (1988). "Association between an oncogene and an anti-oncogene: the adenovirus E1A proteins bind to the retinoblastoma gene product." Nature **334**(6178): 124-129.
- Whyte, P., N. M. Williamson, et al. (1989). "Cellular targets for transformation by the adenovirus E1A proteins." Cell **56**(1): 67-75.
- Wierstra, I. and J. Alves (2007). "FOXO1, a typical proliferation-associated transcription factor." Biol Chem **388**(12): 1257-1274.
- Wilfred, B. R., W. X. Wang, et al. (2007). "Energizing miRNA research: a review of the role of miRNAs in lipid metabolism, with a prediction that miR-103/107 regulates human metabolic pathways." Mol Genet Metab **91**(3): 209-217.
- Williams, G. L., T. M. Roberts, et al. (2007). "Bub1: escapades in a cellular world." Cell Cycle **6**(14): 1699-1704.
- Wolyniec, K., S. Wotton, et al. (2009). "RUNX1 and its fusion oncoprotein derivative, RUNX1-ETO, induce senescence-like growth arrest independently of replicative stress." Oncogene **28**(27): 2502-2512.
- Woods, D. B. and K. H. Vousden (2001). "Regulation of p53 function." Exp Cell Res **264**(1): 56-66.
- Wotton, S. F., K. Blyth, et al. (2004). "RUNX1 transformation of primary embryonic fibroblasts is revealed in the absence of p53." Oncogene **23**(32): 5476-5486.
- Wu, S. J., F. H. Liu, et al. (2001). "Different combinations of the heat-shock cognate protein 70 (hsc70) C-terminal functional groups are utilized to interact with distinct tetratricopeptide repeat-containing proteins." Biochem J **359**(Pt 2): 419-426.
- Wu, W., Z. Lin, et al. (2009). "Expression profile of mammalian microRNAs in endometrioid adenocarcinoma." Eur J Cancer Prev **18**(1): 50-55.
- Xiao, Z. X., J. Chen, et al. (1995). "Interaction between the retinoblastoma protein and the oncoprotein MDM2." Nature **375**(6533): 694-698.
- Yamakuchi, M., M. Ferlito, et al. (2008). "miR-34a repression of SIRT1 regulates apoptosis." Proc Natl Acad Sci U S A **105**(36): 13421-13426.
- Yan, D., X. Zhou, et al. (2009). "MicroRNA-34a inhibits uveal melanoma cell proliferation and migration through downregulation of c-Met." Invest Ophthalmol Vis Sci **50**(4): 1559-1565.

- Yang, A., M. Kaghad, et al. (2002). "On the shoulders of giants: p63, p73 and the rise of p53." Trends Genet **18**(2): 90-95.
- Yang, A., M. Kaghad, et al. (1998). "p63, a p53 homolog at 3q27-29, encodes multiple products with transactivating, death-inducing, and dominant-negative activities." Mol Cell **2**(3): 305-316.
- Yao, J., L. Duan, et al. (2007). "Overexpression of BLCAP induces S phase arrest and apoptosis independent of p53 and NF-kappaB in human tongue carcinoma : BLCAP overexpression induces S phase arrest and apoptosis." Mol Cell Biochem **297**(1-2): 81-92.
- Yeung, F., J. E. Hoberg, et al. (2004). "Modulation of NF-kappaB-dependent transcription and cell survival by the SIRT1 deacetylase." EMBO J **23**(12): 2369-2380.
- Yew, P. R., X. Liu, et al. (1994). "Adenovirus E1B oncoprotein tethers a transcriptional repression domain to p53." Genes Dev **8**(2): 190-202.
- Yoneda-Kato, N. and J. Y. Kato (2008). "Shuttling imbalance of MLF1 results in p53 instability and increases susceptibility to oncogenic transformation." Mol Cell Biol **28**(1): 422-434.
- Yoneda-Kato, N., K. Tomoda, et al. (2005). "Myeloid leukemia factor 1 regulates p53 by suppressing COP1 via COP9 signalosome subunit 3." EMBO J **24**(9): 1739-1749.
- Yoon, I. K., H. K. Kim, et al. (2004). "Exploration of replicative senescence-associated genes in human dermal fibroblasts by cDNA microarray technology." Exp Gerontol **39**(9): 1369-1378.
- Young, A. P. and G. D. Longmore (2004). "Ras protects Rb family null fibroblasts from cell death: a role for AP-1." J Biol Chem **279**(12): 10931-10938.
- Zellweger, T., H. Miyake, et al. (2001). "Chemosensitization of human renal cell cancer using antisense oligonucleotides targeting the antiapoptotic gene clusterin." Neoplasia **3**(4): 360-367.
- Zender, L., W. Xue, et al. (2008). "An oncogenomics-based in vivo RNAi screen identifies tumor suppressors in liver cancer." Cell **135**(5): 852-864.
- Zhang, H. S., A. A. Postigo, et al. (1999). "Active transcriptional repression by the Rb-E2F complex mediates G1 arrest triggered by p16INK4a, TGFbeta, and contact inhibition." Cell **97**(1): 53-61.
- Zhang, S., R. Binari, et al. (2010). "A genomewide RNA interference screen for modifiers of aggregates formation by mutant Huntingtin in *Drosophila*." Genetics **184**(4): 1165-1179.
- Zhang, Y., M. Li, et al. (2009). "Profiling of 95 microRNAs in pancreatic cancer cell lines and surgical specimens by real-time PCR analysis." World J Surg **33**(4): 698-709.
- Zhang, Y., Y. Xiong, et al. (1998). "ARF promotes MDM2 degradation and stabilizes p53: ARF-INK4a locus deletion impairs both the Rb and p53 tumor suppression pathways." Cell **92**(6): 725-734.
- Zhao, J. J., J. Yang, et al. (2009). "Identification of miRNAs associated with tumorigenesis of retinoblastoma by miRNA microarray analysis." Childs Nerv Syst **25**(1): 13-20.

- Zheng, W., H. Wang, et al. (2004). "Regulation of cellular senescence and p16(INK4a) expression by Id1 and E47 proteins in human diploid fibroblast." J Biol Chem **279**(30): 31524-31532.
- Zhou, L., X. Qi, et al. (2008). "MicroRNAs miR-186 and miR-150 down-regulate expression of the pro-apoptotic purinergic P2X7 receptor by activation of instability sites at the 3'-untranslated region of the gene that decrease steady-state levels of the transcript." J Biol Chem **283**(42): 28274-28286.
- Zhu, J., D. Woods, et al. (1998). "Senescence of human fibroblasts induced by oncogenic Raf." Genes Dev **12**(19): 2997-3007.
- Zhu, J. W., D. DeRyckere, et al. (1999). "A role for E2F1 in the induction of ARF, p53, and apoptosis during thymic negative selection." Cell Growth Differ **10**(12): 829-838.
- Zhu, J. Y., P. W. Rice, et al. (1991). "Mapping the transcriptional transactivation function of simian virus 40 large T antigen." J Virol **65**(6): 2778-2790.
- Zhu, L., S. van den Heuvel, et al. (1993). "Inhibition of cell proliferation by p107, a relative of the retinoblastoma protein." Genes Dev **7**(7A): 1111-1125.
- Zimmers, T. A., M. V. Davies, et al. (2002). "Induction of cachexia in mice by systemically administered myostatin." Science **296**(5572): 1486-1488.
- Zindy, F., C. M. Eischen, et al. (1998). "Myc signaling via the ARF tumor suppressor regulates p53-dependent apoptosis and immortalization." Genes Dev **12**(15): 2424-2433.
- Zindy, F., H. Soares, et al. (1997). "Expression of INK4 inhibitors of cyclin D-dependent kinases during mouse brain development." Cell Growth Differ **8**(11): 1139-1150.
- Zuo, L., J. Weger, et al. (1996). "Germline mutations in the p16INK4a binding domain of CDK4 in familial melanoma." Nat Genet **12**(1): 97-99.
- Zuo, Z., M. Zhao, et al. (2006). "Functional analysis of bladder cancer-related protein gene: a putative cervical cancer tumor suppressor gene in cervical carcinoma." Tumour Biol **27**(4): 221-226.
- zur Hausen, H. (2001). "Cervical carcinoma and human papillomavirus: on the road to preventing a major human cancer." J Natl Cancer Inst **93**(4): 252-253.